

Materials Horizons: From Nature to Nanomaterials

Vimal Katiyar

Amit Kumar

Neha Mulchandani *Editors*

Advances in Sustainable Polymers

Synthesis, Fabrication and Characterization

 Springer

Materials Horizons: From Nature to Nanomaterials

Series Editor

Vijay Kumar Thakur, School of Aerospace, Transport and Manufacturing,
Cranfield University, Cranfield, UK

Materials are an indispensable part of human civilization since the inception of life on earth. With the passage of time, innumerable new materials have been explored as well as developed and the search for new innovative materials continues briskly. Keeping in mind the immense perspectives of various classes of materials, this series aims at providing a comprehensive collection of works across the breadth of materials research at cutting-edge interface of materials science with physics, chemistry, biology and engineering.

This series covers a galaxy of materials ranging from natural materials to nanomaterials. Some of the topics include but not limited to: biological materials, biomimetic materials, ceramics, composites, coatings, functional materials, glasses, inorganic materials, inorganic-organic hybrids, metals, membranes, magnetic materials, manufacturing of materials, nanomaterials, organic materials and pigments to name a few. The series provides most timely and comprehensive information on advanced synthesis, processing, characterization, manufacturing and applications in a broad range of interdisciplinary fields in science, engineering and technology.

This series accepts both authored and edited works, including textbooks, monographs, reference works, and professional books. The books in this series will provide a deep insight into the state-of-art of Materials Horizons and serve students, academic, government and industrial scientists involved in all aspects of materials research.

More information about this series at <http://www.springer.com/series/16122>

Vimal Katiyar · Amit Kumar ·
Neha Mulchandani
Editors

Advances in Sustainable Polymers

Synthesis, Fabrication and Characterization

 Springer

Editors

Vimal Katiyar
Department of Chemical Engineering
Indian Institute of Technology Guwahati
Guwahati, Assam, India

Amit Kumar
Department of Chemical Engineering
Indian Institute of Technology Guwahati
Guwahati, Assam, India

Neha Mulchandani
Department of Chemical Engineering
Indian Institute of Technology Guwahati
Guwahati, Assam, India

ISSN 2524-5384

ISSN 2524-5392 (electronic)

Materials Horizons: From Nature to Nanomaterials

ISBN 978-981-15-1250-6

ISBN 978-981-15-1251-3 (eBook)

<https://doi.org/10.1007/978-981-15-1251-3>

© Springer Nature Singapore Pte Ltd. 2020

This work is subject to copyright. All rights are reserved by the Publisher, whether the whole or part of the material is concerned, specifically the rights of translation, reprinting, reuse of illustrations, recitation, broadcasting, reproduction on microfilms or in any other physical way, and transmission or information storage and retrieval, electronic adaptation, computer software, or by similar or dissimilar methodology now known or hereafter developed.

The use of general descriptive names, registered names, trademarks, service marks, etc. in this publication does not imply, even in the absence of a specific statement, that such names are exempt from the relevant protective laws and regulations and therefore free for general use.

The publisher, the authors and the editors are safe to assume that the advice and information in this book are believed to be true and accurate at the date of publication. Neither the publisher nor the authors or the editors give a warranty, expressed or implied, with respect to the material contained herein or for any errors or omissions that may have been made. The publisher remains neutral with regard to jurisdictional claims in published maps and institutional affiliations.

This Springer imprint is published by the registered company Springer Nature Singapore Pte Ltd. The registered company address is: 152 Beach Road, #21-01/04 Gateway East, Singapore 189721, Singapore

Inspired from

&

Dedicated to

Dr. Swaminathan Sivaram

Preface

This book throws light on sustainable polymers from the perspective of researchers constantly looking for alternatives to conventional petroleum-based plastics in order to reduce global environmental impact. There has been significant development in the area of sustainable polymers. This book focuses on the vital elements of sustainable polymers for applications ranging from commodity to biomedicine. This book consists of 17 chapters which describe existing technologies for sustainable polymers and their synthesis mechanisms along with their future prospects eventually connecting a pathway between the contemporary environment and sustainable future.

Chapter 1 begins by describing various strategies for synthesizing biomedical-grade polymers. Developing materials for biomedical applications necessitates choosing appropriate methods of synthesis and post-synthesis techniques to overcome the clinical drawbacks associated with several conventional materials. Medical-grade polymers are often employed for the applications *in vivo* along with certain medical devices that remain in contact with the body. In this context, the chapter underscores the methods of polymerization for synthesizing various polymers and the effect of reaction route on the properties of the polymers. Additionally, biodegradable and non-biodegradable polymers and their uses in medical applications are elaborated along with the effect of various factors on the properties of the polymers. Furthermore, there is a discussion on the existing medical-grade polymers have been featured from the perspective of their extraordinary characteristics.

Chapter 2 deals with sustainable routes towards the synthesis of poly(ϵ -caprolactone) (PCL), which is a biodegradable polymer. The conventional reaction pathways to the production of PCL are demonstrated with a focus on alternative methods such as biomass sources and microbial synthesis. This is followed by providing a glimpse of the prospects of sustainable routes in chemical industries.

Chapter 3 deciphers the utilization of greenhouse gas “carbon dioxide” in developing polymers or their precursors. The potential of carbon dioxide as a monomer has been extricated by detailing several pathways for synthesizing polymers with carbon dioxide in their backbone. Further, the chapter brings to light existing technologies to make polymers from carbon dioxide along with the

challenges it faces. Exploration of such unique strategies in making polymers would build a route towards a sustainable future.

Chapter 4 discusses the production, characterization and applications of biodegradable polyhydroxy-alkanoates (PHAs). The chapter begins by providing a historical overview of PHAs and its essential properties. The production of PHAs from microorganisms using various extraction techniques is highlighted. This is followed by the characterization techniques adopted for the analysis of PHAs and determination of their biodegradability. The noteworthy applications of PHAs in the medical, agricultural and industrial sectors are manifested along with addressing the challenges in PHA production.

Chapter 5 presents the concept of alternating copolymers based on amino acids and peptides. The chapter focuses on recent developments in amino acid and peptide-based alternating architectures, their interesting properties and applications as bio-inspired nanomaterials, in inclusion chemistry, catalysis, sensing, tissue engineering, molecular electronics, molecular separation technology, etc.

The fabrication methods for sutures are discussed in Chapter 6 with their stimuli-responsive aspects. The chapter begins by introducing the characteristics of a suture followed by the classification and selection of an ideal suture material along with the fabrication techniques. The chapter also focuses on biodegradable sutures based on resorbable polymers and composites which are extended to various stimuli-responsive sutures and their applications in vivo supported by several case studies.

Chapter 7 highlights thermo-responsive polymers and concerns associated with their biocompatible nature to be utilized in biological applications. The chapter strategically describes various polymerization techniques for the synthesis of thermo-responsive biocompatible polymers with a special emphasis on Lower Critical Solution Temperature (LCST) of most polymers. The nature of repeating units of the polymer is stated to govern the thermo-responsive behavior along with the biocompatible nature of the polymers.

Chapter 8 reports the use of Ionic Liquids (IL) as solvents in Reversible Addition-Fragmentation chain Transfer (RAFT) process which is applied for the polymerization of methacrylates. The polymerization kinetics of methacrylates in IL is also presented along with the recovery and reuse of IL with the aim of improving the sustainability of the reaction process.

The usage of cellulose derivatives such as cellulose acetate, cyanoethyl cellulose and ethyl cellulose is employed in the creation of electrically and optically functional materials as described in Chapter 9. The chapter further highlights the series of investigations carried out for improvement of dielectric constant, birefringence control and dual mechanochromism for possible industrial applications.

Chapter 10 focuses on the spatio-selective surface modification of individual compartments yielding a novel type of shape-shifted microcylinders via surface-selective click chemistry in conjunction with surface-initiated Atom Transfer Radical Polymerization (ATRP). Further, the discussion has been extended to the microparticles with fully orthogonal surface patches that take advantage of a combination of chemically orthogonal polylactide-based polymers and their

fabrication via electro hydrodynamic co-jetting to yield rarely reported multifunctional microparticles. The potential of micro particles in controlled drug delivery has been delineated.

Chapter 11 outlines the development of cellulose nanocrystals from biomass sources such as lignocellulosic sources and algal and bacterial sources. Further, various techniques are highlighted for the extraction of cellulose nanocrystals including acid hydrolysis, enzymatic hydrolysis, mechanical and oxidation methods, combined processes, followed by their purification and fractionation. Moreover, the composites based on cellulose nanocrystals and their mechanical and rheological properties are discussed along with the surface modification strategies with the aim of obtaining improved overall properties.

The development of biodegradable nanocomposite foams is outlined in Chapter 12 which reports the use of poly (lactic acid) (PLA) as the matrix material. A brief discussion on different techniques of fabrication, their economic viability and industrial feasibility in regard to the polymeric foams has been made along with the effect of nanofillers on the properties of the foam. Further, the effect of nanofillers on the degradation of PLA has been remarked. The tailor-made properties of PLA-based nanocomposite foams may be employed in various aspects of research.

Chapter 13 details the preparation and characterization techniques for micro- and nanocrystalline cellulose using chemical, bacterial and mechanical methods. This is followed by a discussion on natural fibres and degradable green composites along with different mechanisms of biodegradation. An overview of structure-property correlations of biodegradable co-polyester composites has been presented for their possible applications in smart packaging, functional coating on films and flexible conducting materials along with the biomedical applications.

The most widely reported bio-based polyester is poly (L-lactic acid) (PLLA) known for its mechanical properties and biodegradable nature. However, its slow crystallization rate and lower crystallinity are known to hinder commercial use. Chapter 14 reports the usage of silk nanocrystal (SNC) in the PLLA matrix to overcome the potential drawbacks of PLLA. In this context, extensive crystallization studies are conducted using differential scanning calorimetry (DSC) and small- and wide-angle X-ray scattering (SWAXS) to identify the effect of SNC on the crystallizability of PLLA.

Chapter 15 focuses on the fabrication of smart textiles from stereocomplex poly (lactic acid) (PLA) nanocomposite nanofibers. The incorporation of various organic and inorganic nanofillers such as cellulose nanocrystals, silk nanocrystals titanium dioxide, clay nanoparticles and zinc oxide into the matrix of biodegradable stereocomplex PLA is underlined with the aim of extracting the advantages of both types of fillers in developing smart textiles with biodegradable characteristics.

The life cycle assessment (LCA) of the most extensively studied polysaccharide, i.e. chitosan, is presented in Chapter 16. The chapter deals with the purpose, methods and variants of LCA, featuring the history of chitosan along with the different routes of fabrication and related approaches from available resources for tailor-made properties including various design parameters, environmental impacts, product formulation steps, use of different agents and others. Additionally, the

chapter presents the importance of chitosan in day-to-day life along with its environmental impact on various applications such as food packaging films, edible coatings, flocculants and adhesives.

Chapter 17 addresses the trends and advances in the biodegradation of conventional plastics such as polyethylene terephthalate (PET), polyethylene (PE) and polystyrene (PS) under different environmental conditions by incorporating enzymes and microbes for disintegration and assimilation of plastics. The chapter thus aims at providing a broader aspect of conventional plastic biodegradation, its degradation mechanisms and an overview on viable bioremediation of plastic waste along with the discussion on the current status of techniques used for degradation, characterizing degraded plastics and factors affecting their biodegradation.

Guwahati, Assam, India

Vimal Katiyar
Amit Kumar
Neha Mulchandani

Acknowledgements

Had the Fourth International Symposium on Advances in Sustainable Polymers (ASP 17) not been commended, this book would not have been penned. We owe our deepest gratitude to all the eminent scientists, academicians and researchers who disseminated a vast pool of knowledge to the audience of ASP 17 organized at the Indian Institute of Technology Guwahati (IITG), Assam, India. This book comprises the scientific literature in the area of sustainable polymers which aims at providing the readers with the holistic view of sustainable polymers which are most needed alternatives to the petroleum-based polymers. We sincerely thank the contributors for their efforts in making this book possible.

The editors would like to express their sense of indebtedness towards Dr. Swaminathan Sivaram, Indian Institute of Science Education and Research (IISER), Pune, India, for his pioneering work in the area of polymer chemistry and science. The editors would like to dedicate this book to him for his renowned research contribution in the field of sustainable polymer chemistry.

Guwahati, Assam, India

Vimal Katiyar
Amit Kumar
Neha Mulchandani

About Fourth International Symposium on Advances in Sustainable Polymers (ASP 17): From 08–11 January 2018 organized by IIT Guwahati

Centre of Excellence for Sustainable Polymers (CoE-SusPol), Department of Chemical Engineering, successfully organized the Fourth International Symposium on Advances in Sustainable Polymers (ASP-17) during 8–11 January 2018 with the aim of promoting various biodegradable plastic-based technologies in line with the global emphasis on environmental protection and sustainable growth. During this scientific gathering, many distinguished professors and senior scientists, researchers, policymakers, from across the country, senior officials of various industries including Reliance Industries Limited, Indian Oil Corporation Limited, Oil India Limited, Bharat Petroleum Corporation Limited, Numaligarh Refinery Limited, Brahmaputra Chemicals and Petrochemicals Limited, etc. including delegates representing the USA, Canada, Japan, Taiwan, Czech Republic, Singapore, Nepal, Thailand, Germany, Australia and other countries attended this symposium.

Serving as one platform which brought together all the stakeholders including academia and industry, the four days of symposium comprise four plenary sessions, three Bilateral Symposium sessions and multiple technical sessions. The Bilateral Symposium sessions included: Indo-Japan Bilateral Symposium, Indo-Taiwan Bilateral Symposium and Indo-Nepal Bilateral Symposium. On the sideline of the symposium, one-day IIT Guwahati and Kyoto Institute of Technology, Japan, Technical Session was also organized. Experts from more than fifteen countries delivered lectures on different aspects of sustainable polymers and allied areas. The pre- and post-symposium workshops on polymer processing and 3D printing, molecular modelling and simulation of sustainable polymers for young scientists and PhD scholars were also successfully conducted. The symposium began with the opening remarks of Prof. Ashok Misra, Former Director, IIT Bombay, who graced the occasion as the distinguished guest, while Professor Emeritus Yoshiharu Kimura, Kyoto Institute of Technology, Japan, was the chief guest in the inaugural session.

It concluded with a total of 111 paper presentations and 81 poster presentations from researchers covering a wide range of applications relating to the advances made in the field of sustainable polymers. The symposium also witnessed the congregation of interactive dialogues and expert talks by eminent scientists from

across the globe with Prof. Ramani Narayan, Michigan State University, USA; Prof. Kohei Oda, KIT, Japan; Prof. Amar K. Mohanty, University of Guelph, ON, Canada; Arup K. SenGupta, Lehigh University, Bethlehem, USA; Prof. S. Sivaram, Former Director, NCL Pune to name a few.

The symposium provided ample opportunities for the researchers across the world in sharing and gathering knowledge on various aspects of sustainable polymers starting from overviewing the current research activities and global trends on sustainable polymers (bio-based and biodegradable plastics) and bio-based materials to promote these activities in their countries. The highlight of the symposium being the signing of MoU between IITG and Ming Chi University of Technology, Taiwan, and IIT Guwahati and Tomas Bata University in Zlín, Czech Republic. The session chair was Dr. Henry H. Chen, Counsellor and Director, Science and Technology Division (TECC) of Taiwan in India. Dr. Vimal Katiyar served as an organizing chair for ASP 17. The fifth edition of ASP series was organized in Japan in October 2019. Further, IIT Guwahati is indeed very thankful to the North East Council (NEC), Government of India, for providing all the supports to accelerate this initiative.

The conference was supported by the North Eastern Council, Govt. of India (NEC), Science and Engineering Research Board (SERB), Department of Science and Technology (DST), Govt. of India, Department of Chemicals and Petrochemicals (DCPC), Ministry of Chemicals and Fertilizers, Govt. of India, CSIR, and the Oil India Limited, Reliance Industries Limited, Indian Oil Corporation Limited, etc., which were the major sponsors.

Prof. Vimal Katiyar
Chair, ASP 17
Coordinator, CoE-SusPol, IIT Guwahati
Email: vkatiyar@iitg.ac.in

Contents

1	Synthesis Strategies for Biomedical Grade Polymers	1
	Neha Mulchandani and Vimal Katiyar	
2	Sustainable Routes for Synthesis of Poly(ϵ-Caprolactone): Prospects in Chemical Industries	21
	Munmi Das, Bishnupada Mandal and Vimal Katiyar	
3	Polymers from Carbon Dioxide—A Route Towards a Sustainable Future	35
	Neha Mulchandani and Vimal Katiyar	
4	Production, Characterization, and Applications of Biodegradable Polymer: Polyhydroxyalkanoates	51
	Sushobhan Pradhan, Pritam Kumar Dikshit and Vijayanand S. Moholkar	
5	Alternating Copolymers Based on Amino Acids and Peptides	95
	Ishita Mukherjee, Krishna Gopal Goswami and Priyadarsi De	
6	Fabrication of Stimuli-Responsive Polymers and their Composites: Candidates for Resorbable Sutures	121
	Deepshikha Das, Neha Mulchandani, Amit Kumar and Vimal Katiyar	
7	Biocompatible Thermoresponsive Polymers: Property and Synthesis	145
	Varnakumar Gayathri, Nagaraju Pentela and Debasis Samanta	
8	Reversible Addition-Fragmentation Chain Transfer (RAFT) Polymerization in Ionic Liquids: A Sustainable Process	183
	Arunjunai R. S. Santha Kumar and Nikhil K. Singha	
9	Creation of Electrically and Optically Functional Materials from Cellulose Derivatives via Simple Modification and Orientation Control	195
	Yoshikuni Teramoto and Kazuma Miyagi	

10 Biocompatible Anisotropic Designer Particles	217
T. T. Aiswarya and Sampa Saha	
11 Development of Biomass-Derived Cellulose Nanocrystals and its Composites	237
Kona Mondal, Neha Mulchandani, Somashree Mondal and Vimal Katiyar	
12 Biodegradable Nanocomposite Foams: Processing, Structure, and Properties	271
Shasanka Sekhar Borkotoky, Tabli Ghosh and Vimal Katiyar	
13 Biodegradable Copolyester-Based Natural Fibers–Polymer Composites: Morphological, Mechanical, and Degradation Behavior	289
Jyoti Giri and Rameshwar Adhikari	
14 DSC and SWAXS Studies on the Effects of Silk Nanocrystals on Crystallization of Poly(L-Lactic Acid)	321
Amit Kumar Pandey, Pham Thi Ngoc Diep, Rahul Patwa, Vimal Katiyar, Sono Sasaki and Shinichi Sakurai	
15 Mimicking Smart Textile by Fabricating Stereocomplex Poly(Lactic Acid) Nanocomposite Fibers	341
Doli Hazarika, Amit Kumar and Vimal Katiyar	
16 Life Cycle Assessment of Chitosan	363
Tabli Ghosh and Vimal Katiyar	
17 Recent Trends and Advances in the Biodegradation of Conventional Plastics	389
Naba Kumar Kalita, Ajay Kalamdhad and Vimal Katiyar	

Editors and Contributors

About the Editors

Vimal Katiyar is a Professor in the Department of Chemical Engineering, Indian Institute of Technology (IIT) Guwahati, India. He has done his M. Tech and PhD in Chemical Engineering from IIT Kanpur and IIT Bombay respectively, and post-doctoral work in Riso National Laboratory for Sustainable Energy, DTU, Denmark. His current research interests include the synthetic and biodegradable polymers, polymer processing, biothermosets, nanobiocomposites and fuel cells. Dr Katiyar has more than 100 research publications in reputed journals, and has authored numerous book chapters and conference papers, and holds 22 published patents.

Amit Kumar is an Associate Professor in the Department of Chemical Engineering, IIT Guwahati. He has done his B.Tech and PhD from IIT Kharagpur and the University of Delaware respectively. His research interests include molecular modeling and simulation, polymers and polymer nanocomposites, gas adsorption, transport and separation. He has authored 3 book chapters and more than 30 research papers in reputed journals and conferences.

Neha Mulchandani is a research scholar in the Department of Chemical Engineering, IIT Guwahati. Her work focuses on developing carbon dioxide derived lactone based copolymers and composites for potential applications.

Contributors

Rameshwar Adhikari Central Department of Chemistry, Research Centre for Applied Science and Technology, Tribhuvan University, Kathmandu, Nepal

T. T. Aiswarya Department of Materials Science and Engineering, Indian Institute of Technology Delhi, New Delhi, India

Shasanka Sekhar Borkotoky Department of Chemical Engineering, Indian Institute of Technology Guwahati, Guwahati, Assam, India

Deepshikha Das Department of Chemical Engineering, Indian Institute of Technology Guwahati, Guwahati, Assam, India

Munmi Das Department of Chemical Engineering, Indian Institute of Technology Guwahati, Guwahati, Assam, India

Priyadarsi De Department of Chemical Sciences, Polymer Research Centre and Centre for Advanced Functional Materials, Indian Institute of Science Education and Research Kolkata, Mohanpur, Nadia, West Bengal, India

Pham Thi Ngoc Diep Department of Biobased Materials Science, Kyoto Institute of Technology, Kyoto, Japan

Pritam Kumar Dikshit The Energy and Resources Institute (TERI), New Delhi, India

Varnakumar Gayathri Polymer Science and Technology Department, CSIR-Central Leather Research Institute, Chennai, India

Tabli Ghosh Department of Chemical Engineering, Indian Institute of Technology Guwahati, Guwahati, Assam, India

Jyoti Giri Central Department of Chemistry, Department of Chemistry, Tri-Chandra Multiple Campus, Tribhuvan University, Kathmandu, Nepal

Krishna Gopal Goswami Department of Chemical Sciences, Polymer Research Centre and Centre for Advanced Functional Materials, Indian Institute of Science Education and Research Kolkata, Mohanpur, Nadia, West Bengal, India

Doli Hazarika Department of Chemical Engineering, Indian Institute of Technology Guwahati, Guwahati, Assam, India

Ajay Kalamdhad Department of Civil Engineering, Indian Institute of Technology Guwahati, Guwahati, Assam, India

Naba Kumar Kalita Department of Chemical Engineering, Indian Institute of Technology Guwahati, Guwahati, Assam, India

Vimal Katiyar Department of Chemical Engineering, Indian Institute of Technology Guwahati, Guwahati, Assam, India

Amit Kumar Department of Chemical Engineering, Indian Institute of Technology Guwahati, Guwahati, Assam, India

Bishnupada Mandal Department of Chemical Engineering, Indian Institute of Technology Guwahati, Guwahati, Assam, India

Kazuma Miyagi Department of Applied Life Science, Faculty of Applied Biological Sciences, Gifu University, Gifu, Japan

Vijayanand S. Moholkar Department of Chemical Engineering, Indian Institute of Technology Guwahati, Guwahati, Assam, India

Kona Mondal Department of Chemical Engineering, Indian Institute of Technology Guwahati, Guwahati, Assam, India

Somashree Mondal Department of Chemical Engineering, Indian Institute of Technology Guwahati, Guwahati, Assam, India

Ishita Mukherjee Department of Chemical Sciences, Polymer Research Centre and Centre for Advanced Functional Materials, Indian Institute of Science Education and Research Kolkata, Mohanpur, Nadia, West Bengal, India

Neha Mulchandani Department of Chemical Engineering, Indian Institute of Technology Guwahati, Guwahati, Assam, India

Amit Kumar Pandey Department of Biobased Materials Science, Kyoto Institute of Technology, Kyoto, Japan

Rahul Patwa Department of Chemical Engineering, Indian Institute of Technology Guwahati, Guwahati, Assam, India

Nagaraju Pentela Polymer Science and Technology Department, CSIR-Central Leather Research Institute, Chennai, India

Sushobhan Pradhan School of Chemical Engineering, Oklahoma State University, Stillwater, OK, USA

Sampa Saha Department of Materials Science and Engineering, Indian Institute of Technology Delhi, New Delhi, India

Shinichi Sakurai Department of Biobased Materials Science, Kyoto Institute of Technology, Kyoto, Japan

Debasis Samanta Polymer Science and Technology Department, CSIR-Central Leather Research Institute, Chennai, India

Arunjunai R. S. Santha Kumar Rubber Technology Centre, Indian Institute of Technology Kharagpur, Kharagpur, West Bengal, India

Sono Sasaki Department of Biobased Materials Science, Kyoto Institute of Technology, Kyoto, Japan

Nikhil K. Singha Rubber Technology Centre, Indian Institute of Technology Kharagpur, Kharagpur, West Bengal, India

Yoshikuni Teramoto Division of Forest and Biomaterials Science, Graduate School of Agriculture, Kyoto University, Kyoto, Japan

Abbreviations

[BMIM]Cl	1-butyl-3-methylimidazolium chloride
[BMIM]HSO ₄	1-butyl-3-methylimidazolium hydrogen sulfate
[BMIM]OAc	1-butyl-3-methylimidazolium acetate
[EMIM]DEP	1-ethyl-3-methylimidazolium diethylphosphonate
[M]	Monomer concentration
¹³ C NMR	Carbon-13 nuclear magnetic resonance
¹ H NMR	Proton nuclear magnetic resonance
AA	Acrylic acid
AAm	Poly(acrylamide)
ABCN	1,1'-azobis-(cyclohexanocarbonitrile)
ABS	Acrylonitrile butadiene styrene
ADMO	(<i>N</i> -acryloyl-2,2-dimethyl-1,3-oxazolidine)
AFM	Atomic force microscopy
AgNP	Silver nanoparticle
Aib	2-aminoisobutylic acid
AIBN	2,2'-azobisisobutyronitrile
AIBN	2,2'-azobisisobutyronitrile
AIBN	Azobisisobutyronitrile
AN	Acrylonitrile
APEG	α -acryloyl- ω -methoxy-poly(ethyleneglycol)
APS	Ammonium persulfate
ATRP	Atom transfer radical polymerization
BC	Bacterial nanocellulose
BCBS	Biodegradable composite-based sutures
BDB	Benzyl dithiobenzoate
BF	Bamboo flour
BHK	Baby hamster kidney
BMA	Butyl methacrylate
BMDO	5,6-benzo-2-methylene-1,3-dioxepane
BMIM[BF ₄]	3-butyl-1-methyl imidazolium tetrafluoroborate

BMIM[PF6]	3-butyl-1-methyl imidazolium hexafluorophosphate
BPA	Bisphenol A
BPBS	Biodegradable polymer based suture
bpy	2,2'-bipyridine
BSPA	Benzylsulfanylthiocarbonylsulfanylpropionic acid
BSPA	3-(benzyl sulfanylthiocarbonylsulfanyl)-propionic acid
C/L	Casting and leaching
C ₂ NVP	3-ethyl-1-vinyl-2-pyrrolidone
CA	Cellulose acetate
CBA	Chemical blowing agents
CBHs	Cellobiohydrolases
CD	Carbidopa
CDB	Cumyldithiobenzoate
CDTB	Cyanopentanoic acid dithiobenzoate
CDW	Cell dry weight
CeO ₂	Cerium oxide
CFA	Chemical foaming agent
ChLC	Cholesteric liquid crystal
CHO	Cyclohexene oxide
CLRP	Controlled living radical polymerization
CLSM	Confocal laser scanning microscopy
CMC	Critical micelle concentration
Cm-CyEC	CyEC ester derivatives
CMPC	Cyanomethyl methyl(4-pyridyl)carbomodithioate
CNC	Cellulose nanocrystals
CNF	Cellulose nanofibrils
CNT	Carbon Nanotubes
CO	Carbon monoxide
CO ₂	Carbon dioxide
COD	Chemical oxygen demand
CPADB	4-cyano-4-((phenylcarbonothioyl)thio)pentanoic acid
CPBDT	2-cyano-2-propyl benzodithioate
CPCB	Central pollution control board
Cpdtc	2-cyano-2-propyl dodecyl trithiocarbonate
CPL	Circular polarized light
CPM	Complex participation model
CROP	Cationic ring-opening polymerization
CSN	Crystalline silk nano disc
CTA	Chain transfer agent
CyEC	Cyanoethyl cellulose
Đ	Dispersity of the polymer
DBTTC	Dibenzyltrithiocarbonate
DCM	Dichloromethane
DEA	2-(1,3-dioxan-2-yloxy)ethyl acrylate

DE-ATRP	Deactivation enhanced atom transfer radical polymerization
DEGEA	Diethylene glycol ethyl ether acrylate
DHHA/PDHHA	Dihydroxyhexyl acrylate/poly(dihydroxyhexyl acrylate)
DKA	Diabetic ketoacidosis
DLS	Dynamic light scattering
DMA	N,N'-dimethylacrylamide
DMA	n,n-dimethylacrylamide
DMDEA	2-(5,5-dimethyl-1,3-dioxan-2-yloxy) ethyl acrylate
DMF	Dimethylformamide
DMF	N,N-dimethyl formamide
DMF	N,N'-dimethylformamide
DMF	n,n-dimethylformamide
DMF	Dimethyl formamide
DMSO	Dimethyl sulfoxide
DNA	Deoxyribonucleic acid
DODAB	Dimethyldioctadecylammonium bromide
Diox	1,4-dioxane
DOX	Doxorubicin
DP	Degree of polymerization
DSC	Differential scanning calorimetry
DT	Dithioester
DTG	Differential thermogravimetric analysis
DTT	Dithiothreitol
EBiB	Ethyl 2-bromoisobutyrate
EC	Ethyl cellulose
EDTA	Ethylenediaminetetraacetic acid
EGDMA	Ethylene glycol dimethacrylate
EHDC	Electrohydrodynamic co-jetting
EIPPMMA	4-(1-ethyl-1H-imidazo[4,5-f][1,10]phenanthroline-2-yl) phenyl methacrylate]
EMIM[EtOSO ₃]	3-ethyl-1-methyl imidazolium ethyl sulphate
EO	Ethylene oxide
EP	European pharmacopoeia
EPDM	Ethylene propylene diene monomer
EPI	Epichlorohydrin
EVOH	Ethylene vinyl alcohol
FAO	Food and agriculture organization
FDA	Food and drug administration
FESEM	Field emission scanning electron microscopy
FITC	Fluorescein isothiocyanate
FMA	Furfuryl methacrylate
FRP	Free-radical copolymerization
FRP	Free radical polymerization
FTIR	Fourier transform infrared spectroscopy

GA	Gum arabic
GCF	Green cell [®] foam
GC-MS	Gas chromatography coupled with mass spectrometer
GHG	Greenhouse gas
GMA	Glycidyl methacrylate
GPC	Gel permeation chromatography
GRAS	Generally recognized as safe
H ₂ O	Water
HA	Hydroxyapatite
HAP/HA	Hydroxyapatite
HAs	Hydroxyalkanoates
HBP	Hyperbranched polyester
HBr	Hydrobromic acid
HCl	Hydrogen chloride
HCW	Hot compressed water
HD	Hexamethylene diisocyanate
HDPE	High density polyethylene
HEA	2-hydroxyethyl acrylate
HEBM	High energy bead milling
HEMA	2-hydroxyethyl methacrylate
HMF	5-hydroxymethyl furfural
HMTETA	Hexamethyltriethylenetetramine
HPC	Hydroxypropylcellulose
HPLC	High-pressure liquid chromatography
HPMC	Hydroxypropyl methylcellulose
HV	Heat vulcanizing
IAS	Invasive alien species
ICI	Imperial Chemical Industries
IL	Ionic liquid
ISO	International Organization for Standardization
K ₂ S ₂ O ₈	Potassium persulfate
k _{app}	Apparent kinetic rate constant
KOH	Potassium hydroxide
LbL	Layer by layer
LCA	Life cycle assessment
LCC	Life cycle costing
LCI	Life cycle inventory
LCIA	Life cycle impact assessment
lcl	Long-chain-length
LCST	Lower critical solution temperature
LD	Levodopa
LDH	Lactate dehydrogenase
LDPE	Low-density polyethylene
Leu	L-leucine

leu	D-leucine
LGO	Levoglucosenone
LiBr	Lithium bromide
LPS	Lipopolysaccharide
MA	Methyl acrylate
MAA	Methacrylic acid
MADIX	Macromolecular design by interchange of xanthate
MALDI-TOF	Matrix-assisted laser detection ionization–time-of-flight
MALDI-TOF	Matrix-assisted laser desorption/ionization time-of-flight
MALDI-ToF	Matrix-assisted laser desorption/ionization—time-of-flight mass spectroscopy
MBA	N,N'-methylenebisacrylamide
MC	Modified chitosan
MCC	Microcrystalline cellulose
mcl	Medium-chain-length
MDO	2-methylene-1,3-dioxepane
MDR	Melt draw ratio
Me ₄ Cyclam	1,4,8,11-tetramethyl-1,4,8,11-tetraazacyclotetradecane
Me ₆ TREN	Tris [2-(dimethylamino)ethyl]amine
MEO ₂ AM	Diethylene glycol acrylamide
MEO ₂ MA	Poly(2-(2-methoxyethoxy)ethyl methacrylate)
MEO ₂ MAM	Diethylene glycol methacrylamide
MeO ₂ VAc	Oligo (ethylene glycol) vinyl acetate
MePEGMA	Poly(ethylene glycol) methyl ether methacrylate
MFR	Melt flow rate
MG	Modified gum arabic
Mg ₈ Si ₁₂ O ₃₀ (OH) ₄ (H ₂ O) 4·8H ₂ O	Sepiolite
MHEX	s-(1-methyl-4-hydroxyethyl acetate) o-ethyl xanthate
MMA	Methyl methacrylate
MMT	Montmorillonite
Mn	Number average molecular weight
Mn,GPC	Molar mass of polymer obtained from GPC
Mn,Theo	Theoretical molar mass of polymer
mol. wt	Molecular weight
MPC	2-methacryloyloxyethyl phosphorylcholine
mPEG	Methoxy poly(ethylene glycol)
Mw	Weight average molecular weight
MWCNT	Multiwalled carbon nanotube
MWD	Molecular weight distribution
MWNT	Multi wall carbon nano-tubes
NaBr	Sodium bromide
NaClO	Sodium hypochlorite

$\text{Na}_h(\text{Mg}_{3-h}\text{Li}^h)$	Laponite
$\text{Si}_4\text{O}_{10}(\text{OH})_{2-n}\text{H}_2\text{O}$	Montmorillonite
$\text{Na}_m(\text{Al}_{2-m}\text{Mg}_m)$	Sodium hydroxide
$\text{Si}_4\text{O}_{10}(\text{OH})_{2-n}\text{H}_2\text{O}$	<i>N</i> -carboxyanhydride
NaOH	Nanocrystalline cellulose
NCA	Nitroxide mediated polymerization
NCC	<i>N</i> -methyl pyrrolidinone
NMP	Nuclear magnetic resonance
NMPy	Natural rubber latex
NMR	<i>N</i> -vinylpyrrolidone
NRL	Oligoethyleneglycol
NVP	Oligo(ethylene glycol) acrylate
OEG	Oligo(ethylene glycol) methyl ether methacrylate
OEGA	Oligo(ethylene glycol) methyl ether amines
OEGMA	Oligo(2-ethyl-2-oxazoline)acrylate
OEGMEAs	Optical microscopy
OEtOxA	Poly(oligoethylene glycol methyl ether acrylate)
OM	Poly-(oligoethylene glycol methyl ether methacrylate)
P(OEG-A)	Poly(triphenyl-4-vinylbenzylphosphonium chloride)
P(OEG-MA)	Poly(3- <i>n</i> -butyl-1-vinylimidazolium bromide)
P[VBTP][Cl]	Poly(2-vinylpyridine)
P[VBuIm][Br]	Polyamide
P2VP	Poly(acrylic acid)
PA	Poly(<i>n</i> -acryloyl-2,2-dimethyl-1,3-oxazolidine)
PAA	Poly(acryloyl glucosamine)
PADMO	Polyacrylamide
PAGA	Poly(acrylonitrile)
PAM	Poly(butylacrylate)
PAN	Physical blowing agents
PBA	Polybutylene adipate- <i>co</i> -terephthalate
PhyBA	Poly butyl methacrylate
PBAT	Phosphate-buffer-solution
PBMA	Polybutylene succinate
PBS	Polycarbonate
PBS	Poly(cyclohexene carbonate)
PC	Poly(ϵ -caprolactone)
PCHC	Polycaprolactonedimethacrylate
PCL	Polydispersity index
PCLDMA	Poly(D-lactic acid)
PDI	Pyridylsulfide
PDLA	Polyethylene
PDS	
PE	

PEA	Poly(ethyl acrylate)
PEEK	Polyaryletheretherketone
PEG	Poly(ethylene glycol)
PEGMA	Poly(ethylene glycol) methacrylate
PEGMEMA	Poly(ethylene glycol) methyl ether methacrylate
PEI	Polyethyleneimine
PEO	Poly(ethylene oxide)
PET	Poly(ethylene terephthalate)
PEtOx	Poly(n-ethyl oxazoline)
PFMA	Poly furfuryl methacrylate
PFP(M)A	Pentafluorophenyl(meth)acrylate
PFPA	Pentafluorophenyl acrylate
PGA	Poly(glycolic acid)
PHA	Polyhydroxyalkanoates
PHAs	Poly(hydroxyalkanoates)
PHB	Poly(3-hydroxybutyrate)
PHBV	Poly(3-hydroxybutyrate-co-3-hydroxyvalerate)
PHEA	Poly(2-hydroxyethyl acrylate)
PHHxHO	Poly(3-hydroxyhexanoate-co-3-hydroxyoctanoate)
PHMPA	Poly((n-2-hydroxypropyl)-methacrylamide)
PLA	Poly(lactic acid)
PLACNs	PLA-based nanocomposites
PLGA	Poly(lactic-co-glycolic acid)
PLL	Poly(l-lysine)
PLLA	Poly(L-lactic acid)
PMA	Poly(methyl acrylate)
PMMA	Poly(methyl methacrylate)
PMPC	Poly(2-methacryloyloxyethyl phosphorylcholine)
PMVE	Poly(methyl vinyl ether)
PNASME	Poly(n-acryloylsarcosine methyl ester)
PNIPAAm	Poly(n-isopropylacrylamide)
PNIPAM	Poly(n-isopropylacrylamide)
POE	Poly(oxoethylene)
POEGMA	Poly[oligo(ethylene glycol) methyl ether methacrylate]
poly(A-Pro-OMe)	Poly(n-acryloyl-l-prolinemethylester)
POME	Palm oil mill effluent
PP	Poly(propylene)
PPEGMAxTTC	Poly[poly(ethylene glycol) methyl ether methacrylate]-trithiocarbonate
PPG	Poly(propylene glycol)
PPGMA	Poly(propylene glycol) methacrylate
PP-g-MA	Maleic anhydrides grafted polypropylene
PPh ₃	Triphenylphosphine
PPNCl	Bis-triphenylphosphine iminium chloride
PPG	poly(propylene glycol)

PPO	Poly(phenylene oxide)
PPP	Poly(p-phenylene)
PS	Polystyrene
PTFE	Polytetrafluoroethylene
PTmmCF ₃	Tris(m,m-di-trifluoromethylphenyl) phosphine
PToME	Triphenylphosphine
PTpOME	Tris-(<i>p</i> -methoxyphenyl)-phosphine
PTT	Polytrimethylene terephthalate
PU	polyurethanes
PUR	Polyurethane
Pus	Polyurethanes
PVA	Poly(vinyl alcohol)
PVAc	Polyvinyl acetate
PVAVAc	Poly(vinyl alcohol- <i>co</i> -vinyl acetate)
PVC	Polyvinyl chloride
PVCa	Poly(n-vinyl caprolactam)
PVDF	Poly(vinylidene fluoride)
PVOH	Polyvinyl alcohol
PVP	Polyvinylpyrrolidone
PVPhol	Poly(vinylphenol)
PVPip	Poly(n-vinylpiperidone)
RAFT	Reversible addition-fragmentation chain transfer
REPA	Resource and environmental profile analysis
RNA	Ribonucleic acid
ROP	Ring-opening polymerization
RPM	Revolutions per minute
RT	Room temperature
RTV	Room temperature vulcanizing
SBC	Sulfonated bamboo-derived carbon
SBR	Sequencing batch reactor
scl	Short-chain-length
SCMC	Sodium carboxymethyl cellulose
SDS	Sodium dodecyl sulfate
SEC	Size exclusion chromatography
SEM	Scanning electron microscopy
SETAC	Society of Environmental Toxicology and Chemistry
SLCA	Social life cycle assessment
SNC	Silk nanocrystal
sPLA	Stereocomplex PLA
SR	Silicone rubber
SSD	Solid-state drawing
SWAX	Small- and wide-angle X-ray scattering
SWCNTs	Single-walled carbon nanotubes
TA	Tannic acid
TEAC	Triethyl ammonium chloride

TEM	Transmission electron microscopy
TEMPO	(2,2,6,6-tetramethylpiperidin-1-yl)oxidanyl
T _g	Glass transition temperature
TGA	Thermogravimetric analysis
THF	Tetrahydrofuran
TiO ₂	Titanium oxide
TIPS	Thermally induced phase separation
T _m	Melting temperature
TMC-306	Tetramethylene dicarboxylic dibenzoyl hydrazide
TON	Turnover number
TPA	Triphenylamine
TPP	Tripolyphosphate
TPUs	Thermoplastic PUs
TsOH	p-toluenesulfonic acid
UCST	Upper critical solution temperature
UHMWPE	Ultra-high-molecular weight polyethylene
UNEP	United nations environment programme
USFDA	US Food and Drug Administration
USP	US pharmacopeia
UV	Ultraviolet
VAc	Vinylacetate
VCL	Vinylcaprolactam
VFA	Volatile fatty acid
VOC	Volatile organic content
VP	Vinyl pyridine
WAXD	Wide-angle X-ray diffraction
XPS	X-ray photoelectron spectroscopy
XRD	X-ray powder diffraction
XRD	X-ray diffraction
ZnO	Zinc oxide nanoparticles

Chapter 1

Synthesis Strategies for Biomedical Grade Polymers



Neha Mulchandani and Vimal Katiyar

Abstract Developing materials for biomedical applications necessitates choosing the appropriate methods of synthesis and post synthesis techniques to overcome the clinical drawbacks associated with several conventional materials. Medical grade polymers are often employed for the applications in vivo along with certain medical devices that remain in contact with the body. However, several factors affect the biocompatibility of the polymers along with their degradation inside the body. Tailoring the routes of polymerization may serve as an effective strategy to overcome the current scenario. In this regard, the current chapter highlights the methods of polymerization for synthesizing various polymers and the effect of reaction route on the properties of the polymers. Additionally, the biodegradable and non-biodegradable polymers and their uses in medical applications have been elaborated along with the effect of the various factors on the properties of the polymers. Further, the discussion has been narrowed down to depict some of the commercially available polymers in medical applications with their extraordinary characteristics.

Keywords Biomedical · Polymers · Synthesis · Non-biodegradable · Biodegradable

1 Introduction

The natural polymers such as cellulose, cotton and silk have been utilized by the man since the ancient ages for multiple purposes. Natural polymers have also been employed for various biomedical applications such as wound healing and sutures as they resemble the biological tissues [1]. Over the years, the concept of synthetic polymers was evolved. The natural and synthetic polymers may be biodegradable or non-biodegradable depending on their chemical structure. The polymers have been exploited for solving the most common therapeutic problems ranging from cardiovascular diseases, dental, soft tissue prostheses and skeletal replacement to

N. Mulchandani · V. Katiyar (✉)
Department of Chemical Engineering, Indian Institute of Technology Guwahati, Kamrup,
Guwahati, Assam 781039, India
e-mail: vkatiyar@iitg.ac.in

sensory and neural systems [2]. Synthetic polymers explored for human therapy may be regarded as toxic materials as a result of the impurities or low-molecular weight compounds leaching out from the material into the body fluids. In the past few decades, extensive studies have been carried out pertaining to the adaptability of foreign materials into the living systems and severe concerns of synthetic plastics have been witnessed [3]. Considering the functional duration of the therapeutic materials, the biomedical polymers may be classified as prosthetic systems and temporary aids. The prosthetic systems may be regarded as materials that are used to replace the diseased tissues or organs and must remain functional during the life of the person which usually consist of the biostable compounds. On the other hand, temporary aids are required for a shorter duration which usually varies with the healing time. The examples of temporary aids may be sutures, staples, wound dressings, bone fixation devices (plates, nails, screws, pins), artificial skin, etc. [4, 5]. Additionally, the use of polymers is also witnessed in extracorporeal applications including tubing, catheters, ocular devices, dialysis membranes, etc. The quality of human life has been enhanced due to the extending functionality of the human body systems (due to the action of biomedical implants) beyond their expected lifespan. The U.S. Food and Drug Administration (FDA) defines the medical device as a medical instrument/in vitro reagent/implant/apparatus or a similar entity that is utilized in the diagnosis, treatment or prevention of a disease or that which affects the structure of the body function and which is incapable of achieving its own intended function [6]. While developing materials for medical applications, it is essential to determine the compatibility, toxicity and side effects of the material which may depend on several factors. The polymerization mechanism can govern the factors affecting the compatibility of the material in vivo, and thus, the reaction pathways may be tailored to design materials for the intended use. In this context, the current chapter focuses on the polymerization mechanisms involved in synthesizing the polymers followed by the discussion on several biodegradable and non-biodegradable polymers for various medical applications. The commercially existing polymers are also highlighted along with the material considerations for medical applications.

2 Methods of Polymerization

Polymers may be referred to as long-chain compounds or macromolecules which are composed of several short-chain monomers. Polymers are usually organic in nature apart from a few exceptions. The concept of addition and condensation polymerization, the two well-known methods of polymerization was given by Carothers in 1929. Addition polymerization may be referred to the reaction wherein the short-chain monomers combine to form the long-chain polymers without the elimination of any by-products. On the other hand, condensation polymerization involves the elimination of smaller molecules (usually water) upon reaction of two or more types of monomers to yield the long-chain polymers (the exception being polyurethane) [7]. The addition and condensation methods are based on the structure/composition of the

polymers. In case of addition polymerization, the structural formula of the repeating unit is same as that of the monomeric units which is not true for condensation polymers. Further, the classification of polymers according to their mechanism of growth (mechanism of polymerization) may be done as: chain-growth polymerization and step-growth polymerization.

2.1 Chain-Growth Polymerization

In this mechanism, the monomers are added to the site of the growing polymer, and the reaction proceeds by the formation of the growth centre. The polymers formed through chain-growth mechanism include polypropylene (PP), polyvinyl chloride (PVC), polyethylene (PE), teflon, polymethyl methacrylate (PMMA), etc., which involve the unsaturated monomers as the precursors.

2.1.1 Free Radical Polymerization

The polymerization proceeds through the initiation (decomposition of an initiator into free radicals under the influence of external factors), followed by propagation (growth of the chain) which is finally terminated by the combination or disproportion [8].

2.1.2 Ionic Polymerization

Ionic initiators are employed in this kind of polymerization. Here, the initiator transfers its charge to the monomer thereby making it reactive and leading to the chain growth. This kind of polymerization usually takes place in the presence of a solvent. This may be further classified into anionic and cationic polymerization depending on the ionic nature of the initiator. Styrene-based monomers may undergo anionic polymerization [9], and the olefinic monomers may be polymerized through cationic pathways [10].

2.1.3 Coordination Insertion Polymerization

The organometallic catalysts are used for this kind of polymerization to occur. The polymerization of the most widely used synthetic polymers such as PP and PE involves the use of heterogeneous catalysts (Ziegler–Natta) which are usually the aluminium cocatalysts or titanium tetrachloride. These catalysts impart linearity to the polymers along with the ability to yield high-molecular weight polymers [11].



Scheme 1 Formation of polyurethane

2.2 Step-Growth Polymerization

The step-growth polymerization occurs when the monomers consist of two or more functional groups present as end groups. The presence of more than two end groups leads to the formation of branched or cross-linked structures leading to the formation of thermosetting polymers. Unlike chain-growth polymerization, the molecular weight of the polymer depends on the conversion of the monomer in case of step-growth polymerization as the degree of polymerization (D_p) will increase with the increased conversion of monomer. The polymers usually formed through step-growth mechanism include polyamides (PA) and polyurethanes (PU). For instance, in the case of PU, the isocyanate and hydroxyl groups react to form the urethane linkage as shown in Scheme 1. The structure of PU resembles to that of condensation polymer; however, there is no elimination of other molecules [12].

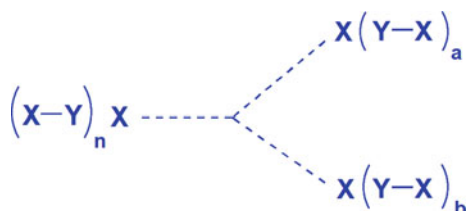
2.3 Branched Polymers

The branched polymers may also be synthesized by employing the chain-growth or step-growth means. The synthesis of branched polymers using the step-growth mechanism is described below:

2.3.1 Star Polymers

The condensation of X-Y monomer usually leads to the formation of star polymer. This reaction proceeds with the functional monomer containing functional groups of X or Y. The reaction mechanism is shown in Scheme 2 [13].

Scheme 2 Star polymer obtained from X-Y monomer



2.3.2 Dendrimers

The polymers that are highly branched and follow a regular geometric pattern are known as dendrimers. These are found to have excellent rheological properties and are made by either divergent or convergent methods. The regions of the dendrimer molecules include the core, interior and outer periphery. Multiple steps are involved in the synthesis of dendrimers. Further, the dendrimers like star polymers have been developed with novel architecture which are capable of reaching the high-molecular weight in few steps [14].

The various synthesis routes described above have been used in synthesizing different polymers for targeted applications. The commercial aspect is essential when synthesizing polymers on a commercial scale without compromising on the desired properties such as toxicity, biocompatibility, duration of usage and post implantation effects for biomedical purposes. In order to meet the criteria for the medical applications, the variation in the synthesis parameters such as the type of initiators, catalysts, solvents and additives along with the sterilization mechanisms must be carefully made. Several natural and synthetic polymers are already in use in various medical applications, of which a few are described in the subsequent sections.

3 Biodegradable and Non-biodegradable Polymers

Compared to the conventional materials used in biomedical applications such as metals, ceramics and glasses, the polymers offer a wide range of flexibility to develop materials with a variety of structures along with the desired physical, chemical, mechanical and biomimetic properties. The polymers may be classified as degradable and non-degradable and both the classes of polymers have been extensively explored for various biomedical uses. The schematic diagram depicting the various biodegradable and non-biodegradable polymers for biomedical applications is shown in Fig. 1.

3.1 *Non-biodegradable Polymers and their Medical Uses*

Several non-biodegradable polymers such as PP, PE, PA, polyethers and polytetrafluoroethylene (PTFE)/teflon are employed in medical applications. PE and PP (olefins) are known to be hydrophobic materials with inert nature. They have been explored in making tubings for blood supply and heart valve, respectively [15, 16]. The use of ultra-high-molecular weight PE (UHMWPE) has been reported for artificial joints [17]. Also, the use of PP in hernia repair is noticeable; however, it is also known to disrupt the surrounding tissue over a period of time [18]. Therefore, several warnings have been laid on the usage of the material in certain medical applications. Further,

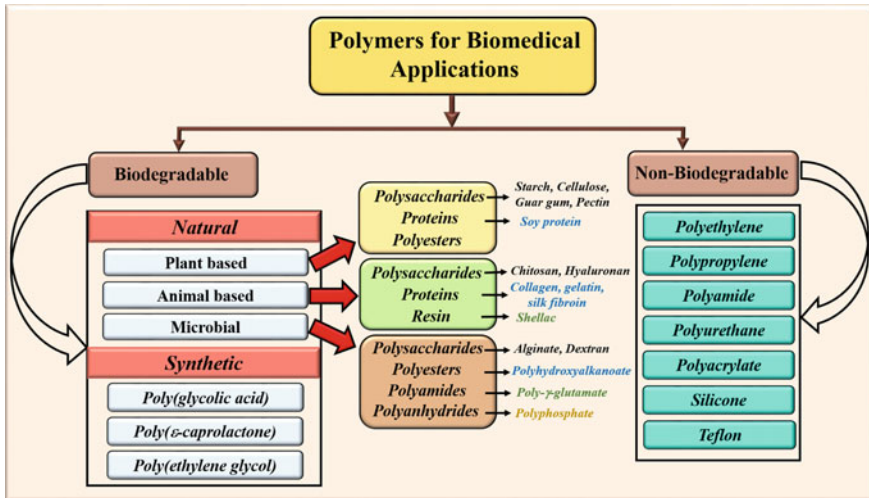


Fig. 1 Biodegradable and non-biodegradable polymers for medical applications

Nylon 6 and Nylon 6, 6 are the most commonly employed polyamides on a commercial scale. Due to the ability of nylon to be formed into fibres, it has been used as a reinforcing agent in biomedical applications such as hard tissue engineering [19, 20]. Teflon is known to be a hydrophobic and non-degradable material which has noticed application in vascular grafts [21]. Additionally, PMMA has witnessed a widespread use in orthopaedics and dental applications. They have also been used as hydrogels for haemocompatible coatings along with the contact lenses [22].

3.2 Biodegradable Polymers and their Medical Uses

3.2.1 Natural

The polymers derived from natural sources which are biodegradable in nature have also been exploited for their use in medical applications. Various natural biodegradable polymers include chitosan, collagen, starch, alginates, polyhydroxyalkanoates (PHA), etc.

Collagen: The naturally occurring collagen is a fibrous protein which is present in all mammals and provides structural stability to the tendons, ligaments, bones, teeth, blood vessels, etc. [23]. Collagen exists as a triple-helix structure which is formed by the three polypeptide chains [24]. It is available in different forms ranging from type I to type X. The most abundant form of collagen is type I which is present in tendons, bones, skin and cornea; whereas, type II collagen is present in cartilage, intervertebral discs and hyaline cartilage. Type III collagen is present naturally in blood vessels, skin, internal organs, etc., and type IV is present in membranes surrounding

the cells. Type V collagen is similar to type I in terms of its chain structure; however, it does not contain the fibrillary structure [25]. Due to the biocompatible and non-toxic nature of collagen and its ability to be processed into various forms, it has been utilized in various biomedical applications including surgical sutures, wound dressings, treatment of scars, etc. Additionally, collagen is used for the drug delivery systems, tissue engineering scaffolds, vascular grafts, tissue sealants, dental implants, implant coatings, substitutes for bone grafting, etc. The prediction of the degradation rate of collagen *in vivo* is difficult as it can be degraded both by enzymatic and hydrolytic means [26, 27].

Chitosan: Chitosan is the deacetylated derivative of chitin with D-glucosamine repeating units. The degree of crystallinity of chitosan is dependent on the degree of deacetylation. It is soluble only in acidic media. It is a biocompatible and non-toxic material along with possessing fungistatic, haemostatic, anti-tumoural and wound healing properties [28]. Chitosan has been widely used in drug delivery and tissue engineering applications. The degradation of chitosan *in vivo* often occurs by enzymatic hydrolysis. Also, the degree of deacetylation affects the degradation of chitosan. For instance, the material with a higher degree of deacetylation retards the degradation; whereas, that with a lower degree of deacetylation enhances the rate of degradation. Much rapid degradation of chitosan may occur by derivatizing it with other side chains which may possibly lead to the alteration in the chain packing, thereby increasing the amorphous region [29–31].

Polyhydroxyalkanoates: PHAs are the polyesters derived from bacteria or microbes, viz. *A. eutrophus*, *R. rubrum*, *Rb. spaeroides* [32, 33]. These are biocompatible and biodegradable materials and also explored for various biomedical applications. Poly(hydroxybutyrate) (PHB) is a class of PHA which is one of the most widely studied material as it has the properties similar to that of PE and PP. It is a thermoplastic, hydrophobic material which can be melt processed. The glass transition temperature (T_g) of PHB is $\sim 9^\circ\text{C}$ with T_m being 177°C which is near to its degradation temperature. PHB degrades into crotonic acid, and the processing of PBH is thus difficult as compared to other materials. Due to this reason, it has been blended with other polymers such as PVC, polyvinyl acetate (PVAc), poly(ethylene oxide) (PEO) and polysaccharides to improve its processability. PHAs degrade into CO_2 and water in the time frame of ~ 6 months, and the degradation (enzymatic) of these polymers usually depends on several factors such as temperature, pH and composition. PHB has been utilized in several medical and surgical devices along with sutures, drug delivery systems, bone plates, other absorbable materials, etc. [34, 35]. Furthermore, the copolymer of hydroxybutyrate and hydroxyvalerate (PHBV) has been used in orthopaedic applications while exploiting its piezoelectric properties [36, 37].

3.2.2 Synthetic

Poly(glycolic acid): Poly(glycolic acid) (PGA) is hydrophilic, linear aliphatic polyester with a high melting point ($225\text{--}230^\circ\text{C}$) [38]. The degradation of PGA

is usually encountered by bulk erosion through ester hydrolysis [39, 40]. The degradation of PGA may be regarded as biphasic, with the hydrolysis of its amorphous region followed by the crystalline region. The use of PGA has been widely explored in sutures, wherein the degradation may occur between 1 and 3 months. Further, varying the pH may also affect the hydrolysis of PGA along with the crystallinity which may be considered as the controlling factor [41, 42].

Poly(lactic acid): Poly(lactic acid) (PLA) is also a linear aliphatic polyester. However, the presence of an extra methyl group in PLA (as compared to PGA) imparts hydrophobicity to it and leads to the increased solubility in organic solvents due to the presence of more amorphous regions [43]. The two enantiomeric forms of PLA are well-known, viz. poly(D-lactic acid) (PDLA) and poly(L-lactic acid) (PLLA) which are due to the presence of a chiral centre [44, 45]. The degradation of PLA leads to the formation of lactic acid which is naturally present in the human body. Hence, PLA is regarded as biocompatible; however, an increase in the lactic acid concentration in vivo may lead to the inflammatory reactions resulting in tissue necrosis [46, 47]. Due to its relatively slower rate of degradation, PLLA has been explored widely for orthopaedic fixation devices such as bone plates, pins and screws which require the implant stability for a longer duration unlike sutures. The tumorigenicity of PLLA plates ($20 \times 10 \times 1$ mm) was evaluated by Nakamura et al. along with medical grade PE plates as controls. The plates were implanted in vivo into male Wistar rats and the tumorigenicity was evaluated for 2 years. The tumours (mesenchymal malignant) observed were nearly similar in case of both PLLA and PE plates, and it was found that the shape of PLLA plates was intact after 2 years with small holes on their surface as determined from scanning electron microscopy (SEM). Thus, the comparison of PLLA with medical grade PE suggests the application and potential of PLLA in orthopaedic applications [48].

Poly(lactic-co-glycolic acid): In order to control the physical and mechanical properties of the material, copolymerization is considered to be an effective strategy. In that context, poly(lactic-co-glycolic acid) (PLGA) which is a copolymer of PLA and PGA has received a considerable interest in various biomedical applications including sutures [49–51]. Furthermore, the degradation rate of PLGA is highly dependent on the individual comonomers and usually those with the equimolar ratios are more susceptible to hydrolysis. However, the drawback of copolymerization may be the “autocatalysis” which would lead to the heterogeneous degradation thereby creating a differential rate of degradation and affecting the desired properties [52, 53].

Poly(ϵ -caprolactone): Yet, another biodegradable polymer widely explored for biomedical applications is poly(ϵ -caprolactone) (PCL). PCL is found to be in a rubbery state at room temperature ($T_g \sim -60$ °C) with the lower melting point ($T_m \sim 60$ °C). It has been studied alone as well as in combination with other polymers, i.e. blending, [54] copolymerization [55], grafting [56], etc., which has led to the formation of copolymers/blends with tailored properties for targeted applications [57]. The degradation of PCL also occurs in two steps; however, its rate of degradation is much slower than that of PLA. The degradation rate of PCL may further be enhanced upon copolymerization with DL-lactide [58]. Tailoring the rate of degradation by copolymerizing with other suitable polymers may significantly expand its applicability in

various fields such as orthopaedic fixation devices and scaffolds for bone regeneration. [59]. Additionally, the degradation rate is governed by the molecular weight, crystallinity and molecular architecture which are the parameters important to be considered while developing materials for biomedical applications [60]. PCL has been used as a controlled release agent in various domains due to its high permeability [61, 62].

Polyanhydrides: Belonging to the class of hydrolytically unstable polymers, polyanhydrides are highly reactive materials which may exist in the aromatic or aliphatic form or the combination of these. These materials are explored for the controlled drug release applications; however, at elevated temperature, these polymers may react with the drug thereby becoming unstable [63, 64]. These are usually brittle materials but the copolymerization may be an effective strategy to increase their mechanical properties. For instance, the copolymers of 1,6-bis(carboxyphenoxy) hexane and methacrylated sebacic acid are found to have the mechanical properties similar to that of the cortical and trabecular bone along with biocompatible nature. Thus, these materials may be potential candidates for orthopaedic applications [65].

Furthermore, the functionalizable biomedical polymers received a great interest in medical uses due to their ability to carry the bioactive agents and release them at the targeted site. The biodegradable polymer after releasing the bioactive agent would undergo degradation inside the body and be eliminated by the metabolic pathways. Considering the importance of functionalized polymers, Lenz and Guerin prepared the polymers (polyesters and polyamides) based on aspartic acid and malic acid to be used as synthetic drug carriers. The developed polymers were designated to be non-toxic in nature and may be utilized effectively in vivo [66]. The biomedical applications of a few biomedical polymers, copolymers and their composites are given in Table 1.

Table 1 Biomedical applications of biodegradable polymers, copolymers and their composites

Polymer/copolymer/composite	Biomedical application	Reference(s)
Chitosan	Biological adhesive	[67]
Alginate	Tissue engineering and surgical tissue adhesion	[68, 69]
Gelatin	Wound healing	[70]
PLA-PGA	Orthopaedic	[71]
PLA/chitosan/keratin	Bone tissue engineering	[72]
PHBV/PLA	Sutures	[73]
PEEK	Surgical implants, orthopaedics and oral implants	[74–76]
PHA	Tissue engineering	[77]

(continued)

Table 1 (continued)

Polymer/copolymer/composite	Biomedical application	Reference(s)
PMMA	Drug delivery and bone cements	[78, 79]
PCL	Drug delivery	[80]
PLGA	Biosensors	[81]
PLA/starch/PCL	Drug delivery	[82]
PU	Urinary catheters and stents	[83, 84]
nano-HA (hydroxyapatite)/collagen/PLA	Bone scaffold	[85]

4 Considerations for Biomedical Applications

4.1 Selection of Initiator and Catalyst

Tin octoate and various tin alkoxides have been tested widely for in vitro and in vivo applications. Tin alkoxides have been explored in the synthesis of block and star-shaped copolymers. A notified difference has been observed in the toxicity between Sn^{2+} and Sn^{4+} as the cell growth is restricted in case of alkoxide initiators (Sn^{4+}). Reducing the amount of tin content, while using alkoxide initiators, is crucial for the biomedical applications. The commercial medical polymers have been restricted to the limit of 20 ppm of residual tin by Food and Drug Administration (FDA), and beyond this, the materials would usually be regarded as toxic. In spite of the immense work reported on the lab-scale development of polymers using such initiators, their large-scale reaction has been very limited. With the aim of exploiting such systems for the industrial production, a large-scale polymerization (50 g) of PCL has been reported by Stjerndahl et al. using 1-di-*n*-butyl-stanna-2,5-dioxacyclopentane as an initiator. The reaction of the polymer with 1,2-ethanedithiol resulted in the residual amount of tin content of ~23 ppm which was close to the limit set by FDA [86].

The conventional metal-based catalysts reported for the ROP of ϵ -caprolactone although lead to the formation of polyesters with controlled molecular weight, these catalysts may impart toxicity and add to the environmental pollution. Due to these reasons, the application of such materials is restricted for biomedical applications. Various other organocatalysts have been explored for the ROP of ϵ -caprolactone, but they also lead to the toxicity issues along with several other drawbacks. In this regard, the enzymatic synthesis of PCL has been reported by Duchiron et al. wherein they utilized natural amino acids as initiators, viz. cysteine (Cys) and methionine (Met). The functional group (thiol) present in Cys permits the grafting, branching and cross-linking; whereas, the functional group of Met (thioether) permits the control over the thermal resistance of the polymer (by sulphonation). Strategically, the direct polymerization of ϵ -caprolactone was carried out using amino acids with and without the functional groups. The reaction carried out with amino acids in the presence of the functional groups led to the enhanced conversion and solubility in the reaction

medium and improved affinity with the catalyst binding sites. The resultant polymer chains consisted mainly of PCL homopolymers and such a polymerization reaction is ought to be an efficient strategy for the development of functionalized polymers with tailored macromolecular architecture for biomedical applications [87].

PCL, which is found to have substantial potential in various biomedical applications such as wound healing, controlled drug delivery, prostheses [88] often employs the utilization of metal-based catalysts. The lanthanide-based catalysts are non-toxic and may be considered as suitable materials for synthesizing polymers directly for biomedical applications. Barbier-Baudry et al. have proposed a mechanism for the synthesis of PCL by microwave irradiation using lanthanide halides. As compared to the conventional methods of synthesis, microwave-assisted synthesis may aid in synthesizing PCL with higher selectivity and yield, shorter reaction time along with improved purity of the products. This would serve as an efficient and economical method for the solvent-free synthesis of PCL with controlled molecular weight without involving the purification step of catalyst. Such a polymerization procedure may be economically viable for the commercial production of PCL for biomedical applications [89].

4.2 Sterilization Techniques

In order to use the polymers as medical devices, their sterilization (destruction of living species on the surface) is an essential criterion. The properties of the medical devices/implants must remain intact post sterilization, i.e. the surface or the bulk properties along with biocompatibility must not be affected by the sterilization procedures (gamma irradiation, plasma treatment, steam autoclaving, etc.) [90]. The sterilization of such devices using carbon dioxide (CO₂) has also been explored at mild conditions [91, 92]. As liquid CO₂ (obtained by compressing beyond its critical point, 304.2 K and 7.38 MPa) is economically viable as compared to supercritical CO₂, Jimenez et al. reported the biocompatibility of medical grade with liquid CO₂ by testing the mechanical properties of the biomaterials before and after sterilizing with CO₂ (single cycle). The commercial polymers used by them were low density polyethylene (LDPE), high density polyethylene (HDPE), UHMWPE, polystyrene (PS), PU, silicon rubber (SI), PMMA, poly(ethylene terephthalate) (PET), natural rubber latex (NRL), ethylene propylene diene monomer (EPDM), polycarbonate (PC), acrylonitrile-butadiene-styrene (ABS), poly(vinylidene fluoride) (PVDF), poly(phenylene oxide) (PPO), nylon (PA), PVC, acetal and teflon. The mechanical tests were performed after exposing the polymers to CO₂ at 6.5 MPa (ambient temperature). The decrease in the tensile strength for ABS, PVC, PMMA and PC was significant; whereas, a slight decrease was observed in case of PET. An increase in Young's modulus was observed for PVC and PS which may be attributed to the increased crystallinity, and a decrease in modulus was evident for PMMA which may be accounted for the induced plasticization effect. A compromise in the bulk strength was found in case of amorphous polymers, and therefore, such polymers were found

types are used as medical adhesives. Further, stannous octoate is the most widely adapted catalyst (for medical applications) in case of two-component-type RTV. It has been reported that the medical grade RTV SR upon vulcanization with stannous octoate and implanting in the body does not exhibit any reaction; whereas, the SR vulcanized with catalysts such as dibutyl tin dilaurate exhibits (used in industrial application) severe reaction with the tissues of the body [99]. This clearly suggests the disagreement of the industrial grade silicone for medical applications. On the other hand, the medical grade HV-type rubbers available are Silastic 370, Silastic 372 and Silastic 373 [100]. These materials usually incorporate silica as the filler which is essential for the rubber hardening. In case of medical grade SR, dichlorobenzoyl peroxide is used as a vulcanizing agent unlike sulphur which is used for the vulcanization of organic rubber [101, 102]. Thus, the medical grade SRs are synthesized by the alternative strategies (unlike industrial) for biomedical applications/therapy.

5.2 Polyaryletheretherketones

Polyaryletheretherketone (PEEK) is a chemically inert material which is insoluble in almost all solvents at ambient conditions. For the biomedical applications, the inertness and insolubility are advantageous; however, these properties render the polymer difficult to be manufactured. The synthesis of PEEK requires high temperature (300 °C) which may be carried out in the presence of diphenyl sulphone or benzophenone solvents [103, 104]. Electrophilic and nucleophilic routes have been used for manufacturing of PEEK. PEEK produced from the electrophilic routes is thermally unstable and requires endcapping for being processed and usually leads to the formation of a gel while processing at high temperatures. The PEEK production from the nucleophilic routes has thus gained little commercial interest. On the other hand, nucleophilic route has gained much interest as it provides a straightforward path to the production of PEEK [105]. In order to synthesize high-molecular weight PEEK, very high temperature is required (>300 °C). PEEK was commercialized by ICI as “Vitrex PEEK” in 1987 which involved the use of difluorobenzophenone to control the molecular weight. The T_g of PEEK is ~143 °C and its T_m is ~343 °C due to which it remains in the glassy state at room temperature. Further, the utilization of PEEK was witnessed for the long-term implant applications after the development of PEEK-OPTIMA by ICI in 1998. Since then, several grades of PEEK were commercially made available with different trade names. The implantable PEEK materials have been highlighted in Table 2. PEEK-OPTIMA is commercially available in three grades, viz. general purpose grade, medium-flow grade and easy-flow grade which are designated as OPTIMA LT1, OPTIMA LT2 and OPTIMA LT3, respectively. The medical grade PEEK polymers are found to have the melting temperature ~340 °C along with possessing well melt stability [106]. The conventional methods of plastic processing are employed for the processing of medical grade PEEK including injection moulding, extrusion, compression moulding, etc. It is noteworthy to mention that the synthetic route may probably alter the biocompatibility of PEEK, and therefore,

Table 2 Commercially available PEEK materials for implant applications

Sr. No.	PEEK trade name	Commercial producer	References
1.	OPTIMA	Invibio Ltd., the UK	[109]
2.	Zeniva	Solvay, LLC	[110]
3.	Keta-Spire	Solvay, LLC	[111]
4.	OXPEKK	Oxford Performance Materials, CT	[112]
5.	VESTAKEEP I	Evonik, Germany	[113]
6.	Victrex	Victrex, the UK	[114]

care must be taken to choose the manufacturing route while developing materials for medical applications. Furthermore, PEEK has also been utilized in combination with reinforcing agents such as carbon fibres for orthopaedic and spinal implant applications [107, 108].

6 Summary

The various biodegradable and non-biodegradable polymers with their applications in the medical field have been discussed in the chapter. The effect of the catalyst, initiator and sterilization techniques on the properties of the polymers has been demonstrated which suggests that developing medical grade polymers by tailored routes may be an efficient strategy. Further, the potential of polymers in medical applications is witnessed through the range of commercially available grades of PEEK and silicone rubbers. It may be inferred that tailoring the reaction pathway may lead to multiple advantages while developing polymers for intended medical applications.

References

1. Mogoşanu GD, Grumezescu AM (2014) Natural and synthetic polymers for wounds and burns dressing. *Int J Pharm* 463:127–136. <https://doi.org/10.1016/j.ijpharm.2013.12.015>
2. Sionkowska A (2011) Current research on the blends of natural and synthetic polymers as new biomaterials: review. *Prog Polym Sci* 36:1254–1276. <https://doi.org/10.1016/j.progpolymsci.2011.05.003>
3. Helmus MN, Gibbons DF, Cebon D (2008) Biocompatibility: meeting a key functional requirement of next-generation medical devices. *Toxicol Pathol* 36:70–80. <https://doi.org/10.1177/0192623307310949>
4. Vert M (1989) Bioresorbable polymers for temporary therapeutic applications. *Die Angewandte Makromolekulare Chemie* 166:155–168. <https://doi.org/10.1002/apmc.1989.051660111>
5. Alarie Y, Anderson RC (1981) Toxicologic classification of thermal decomposition products of synthetic and natural polymers. *Toxicol Appl Pharmacol* 57:181–188. [https://doi.org/10.1016/0041-008X\(81\)90278-7](https://doi.org/10.1016/0041-008X(81)90278-7)

6. Teo AJT, Mishra A, Park I, Kim Y-J, Park W-T, Yoon Y-J (2016) Polymeric biomaterials for medical implants and devices. *ACS Biomater Sci Eng* 2:454–472. <https://doi.org/10.1021/acsbiomaterials.5b00429>
7. Flory PJ (1946) Fundamental principles of condensation polymerization. *Chem Rev* 39:137–197. <https://doi.org/10.1021/cr60122a003>
8. Hawker CJ (1994) Molecular weight control by a “living” free-radical polymerization process. *J Am Chem Soc* 116:11185–11186. <https://doi.org/10.1021/ja00103a055>
9. Worsfold DJ, Bywater S (1960) Anionic polymerization of styrene. *Can J Chem* 38:1891–1900. <https://doi.org/10.1139/v60-254>
10. Kennedy JP (1999) Living cationic polymerization of olefins. How did the discovery come about? *J Polym Sci Part A Polym Chem* 37:2285–2293. [https://doi.org/10.1002/\(sici\)1099-0518\(19990715\)37:14%3c2285:aid-pola1%3e3.0.co;2-p](https://doi.org/10.1002/(sici)1099-0518(19990715)37:14%3c2285:aid-pola1%3e3.0.co;2-p)
11. Ito S, Kanazawa M, Munakata K, Kuroda J-i, Okumura Y, Nozaki K (2011) Coordination–insertion copolymerization of allyl monomers with ethylene. *J Am Chem Soc* 133:1232–1235. <https://doi.org/10.1021/ja1092216>
12. Spindler R, Frechet JMJ (1993) Synthesis and characterization of hyperbranched polyurethanes prepared from blocked isocyanate monomers by step-growth polymerization. *Macromolecules* 26:4809–4813. <https://doi.org/10.1021/ma00070a013>
13. Pearson DS, Helfand E (1984) Viscoelastic properties of star-shaped polymers. *Macromolecules* 17:888–895. <https://doi.org/10.1021/ma00134a060>
14. Trollsås M, Hedrick JL (1998) Dendrimer-like star polymers. *J Am Chem Soc* 120:4644–4651. <https://doi.org/10.1021/ja973678w>
15. Hardin CA (1954) Experimental repair of ureters by polyethylene tubing and ureteral and vessel grafts. *JAMA Surg* 68:57–61. <https://doi.org/10.1001/archsurg.1954.01260050059007>
16. Thornton MA, Howard IC, Patterson EA (1997) Three-dimensional stress analysis of polypropylene leaflets for prosthetic heart valves. *Med Eng Phys* 19:588–597. [https://doi.org/10.1016/S1350-4533\(96\)00042-2](https://doi.org/10.1016/S1350-4533(96)00042-2)
17. Chiesa R, Tanzi MC, Alfonsi S, Paracchini L, Moscatelli M, Cigada A (2000) Enhanced wear performance of highly crosslinked UHMWPE for artificial joints. *J Biomed Mater Res* 50:381–387. [https://doi.org/10.1002/\(sici\)1097-4636\(20000605\)50:3%3c381:aid-jbm12%3e3.0.co;2-p](https://doi.org/10.1002/(sici)1097-4636(20000605)50:3%3c381:aid-jbm12%3e3.0.co;2-p)
18. Cobb WS, Kercher KW, Heniford BT (2005) the argument for lightweight polypropylene mesh in hernia repair. *Surg Innov* 12:63–69. <https://doi.org/10.1177/155335060501200109>
19. Pant HR, Kim HJ, Bhatt LR, Joshi MK, Kim EK, Kim JI, Abdal-hay A, Hui KS, Kim CS (2013) Chitin butyrate coated electrospun nylon-6 fibers for biomedical applications. *Appl Surf Sci* 285:538–544. <https://doi.org/10.1016/j.apsusc.2013.08.089>
20. Panthi G, Barakat NAM, Risal P, Yousef A, Pant B, Unnithan AR, Kim HY (2013) Preparation and characterization of nylon-6/gelatin composite nanofibers via electrospinning for biomedical applications. *Fibers Polym* 14:718–723. <https://doi.org/10.1007/s12221-013-0718-y>
21. Liekweg WG Jr, Greenfield LJ (1977) Vascular prosthetic infections: collected experience and results of treatment. *Surgery* 81:335–342. <https://doi.org/10.5555/uri:pii:0039606077902392>
22. Yasuda H, Bumgarner MO, Marsh HC, Yamanashi BS, Devito DP, Wolbarsht ML, Reed JW, Bessler M, Landers MB III, Hercules DM, Carver J (1975) Ultrathin coating by plasma polymerization applied to corneal contact lens. *J Biomed Mater Res* 9:629–643. <https://doi.org/10.1002/jbm.820090609>
23. Pauling L, Corey RB (1951) The structure of fibrous proteins of the collagen-gelatin group. *Proc Natl Acad Sci USA* 37:272–281. <https://doi.org/10.1073/pnas.37.5.272>
24. Brodsky B, Persikov AV (2005) Molecular structure of the collagen triple helix. *Advances in protein chemistry*. Academic Press, pp 301–339. [https://doi.org/10.1016/S0065-3233\(05\)70009-7](https://doi.org/10.1016/S0065-3233(05)70009-7)
25. Bornstein P, Sage H (1980) Structurally distinct collagen types. *Annu Rev Biochem* 49:957–1003. <https://doi.org/10.1146/annurev.bi.49.070180.004521>

26. Cen L, Liu W, Cui L, Zhang W, Cao Y (2008) Collagen tissue engineering: development of novel biomaterials and applications. *Pediatr Res* 63:492. <https://doi.org/10.1203/PDR.0b013e31816c5bc3>
27. Friess W (1998) Collagen—biomaterial for drug delivery. Dedicated to Professor Dr. Eberhard Nürnberg, Friedrich-Alexander-Universität Erlangen-Nürnberg, on the occasion of his 70th birthday. *Eur J Pharm Biopharm* 45:113–136. [https://doi.org/10.1016/S0939-6411\(98\)00017-4](https://doi.org/10.1016/S0939-6411(98)00017-4)
28. Kean T, Thanou M (2010) Biodegradation, biodistribution and toxicity of chitosan. *Adv Drug Deliv Rev* 62:3–11. <https://doi.org/10.1016/j.addr.2009.09.004>
29. Hirai A, Odani H, Nakajima A (1991) Determination of degree of deacetylation of chitosan by ¹H NMR spectroscopy. *Polym Bull* 26:87–94. <https://doi.org/10.1007/bf00299352>
30. Huang M, Khor E, Lim L-Y (2004) Uptake and cytotoxicity of chitosan molecules and nanoparticles: effects of molecular weight and degree of deacetylation. *Pharm Res* 21:344–353. <https://doi.org/10.1023/B:PHAM.0000016249.52831.a5>
31. Mima S, Miya M, Iwamoto R, Yoshikawa S (1983) Highly deacetylated chitosan and its properties. *J Appl Polym Sci* 28:1909–1917. <https://doi.org/10.1002/app.1983.070280607>
32. Haywood GW, Anderson AJ, Dawes EA (1989) The importance of PHB-synthase substrate specificity in polyhydroxyalkanoate synthesis by *Alcaligenes eutrophus*. *FEMS Microbiol Lett* 57:1–6. <https://doi.org/10.1111/j.1574-6968.1989.tb03210.x>
33. Anderson AJ, Dawes EA (1990) Occurrence, metabolism, metabolic role, and industrial uses of bacterial polyhydroxyalkanoates. *Microbiol Rev* 54:450–472
34. Quagliano Javier C, Miyazaki Silvia S (2002) Microbial production of the biodegradable polyester poly-3-hydroxybutyrate (PHB) from *Azotobacter chroococcum* 6B: relation between PHB molecular weight, thermal stability and tensile strength. In: Durieux A, Simon JP (eds) *Applied microbiology*. Springer Netherlands, Dordrecht, pp 135–140. https://doi.org/10.1007/0-306-46888-3_9
35. Ikada Y, Tsuji H (2000) Biodegradable polyesters for medical and ecological applications. *Macromol Rapid Commun* 21:117–132. [https://doi.org/10.1002/\(sici\)1521-3927\(20000201\)21:3%3c117:aid-marc117%3e3.0.co;2-x](https://doi.org/10.1002/(sici)1521-3927(20000201)21:3%3c117:aid-marc117%3e3.0.co;2-x)
36. Gorodzha SN, Muslimov AR, Syromotina DS, Timin AS, Tsvetkov NY, Lepik KV, Petrova AV, Surmeneva MA, Gorin DA, Sukhorukov GB, Surmenev RA (2017) A comparison study between electrospun polycaprolactone and piezoelectric poly(3-hydroxybutyrate-co-3-hydroxyvalerate) scaffolds for bone tissue engineering. *Colloids Surf B* 160:48–59. <https://doi.org/10.1016/j.colsurfb.2017.09.004>
37. Zinn M, Weilenmann H-U, Hany R, Schmid M, Egli T (2003) Tailored synthesis of poly([R]-3-hydroxybutyrate-co-3-hydroxyvalerate) (PHB/HV) in *Ralstonia eutropha* DSM 428. *Acta Biotechnol* 23:309–316. <https://doi.org/10.1002/abio.200390039>
38. Ma PX, Langer R (2011) Degradation, structure and properties of fibrous nonwoven poly(glycolic acid) scaffolds for tissue engineering. *MRS Proc* 394:99. <https://doi.org/10.1557/PROC-394-99>
39. Lee K-B, Yoon KR, Woo SI, Choi IS (2003) Surface modification of poly(glycolic acid) (PGA) for biomedical applications. *J Pharm Sci* 92:933–937. <https://doi.org/10.1002/jps.10556>
40. Fv Burkersroda, Schedl L, Göpferich A (2002) Why degradable polymers undergo surface erosion or bulk erosion. *Biomaterials* 23:4221–4231. [https://doi.org/10.1016/S0142-9612\(02\)00170-9](https://doi.org/10.1016/S0142-9612(02)00170-9)
41. Chu CC (1981) Hydrolytic degradation of polyglycolic acid: Tensile strength and crystallinity study. *J Appl Polym Sci* 26:1727–1734. <https://doi.org/10.1002/app.1981.070260527>
42. Chu CC (1981) The in-vitro degradation of poly(glycolic acid) sutures—effect of pH. *J Biomed Mater Res* 15:795–804. <https://doi.org/10.1002/jbm.820150604>
43. Vert M, Schwarch G, Coudane J (1995) Present and future of PLA polymers. *J Macromol Sci Part A* 32:787–796. <https://doi.org/10.1080/10601329508010289>
44. Van Wouwe P, Dusselier M, Vanleeuw E, Sels B (2016) Lactide synthesis and chirality control for polylactic acid production. *ChemSusChem* 9:907–921. <https://doi.org/10.1002/cssc.201501695>

45. Ho R-M, Chiang Y-W, Tsai C-C, Lin C-C, Ko B-T, Huang B-H (2004) Three-dimensionally packed nanohelical phase in chiral block copolymers. *J Am Chem Soc* 126:2704–2705. <https://doi.org/10.1021/ja039627i>
46. Hakkarainen M (2002) Aliphatic polyesters: abiotic and biotic degradation and degradation products. *degradable aliphatic polyesters*. Springer, Berlin, pp 113–138. https://doi.org/10.1007/3-540-45734-8_4
47. Miller RA, Brady JM, Cutright DE (1977) Degradation rates of oral resorbable implants (polylactates and polyglycolates): Rate modification with changes in PLA/PGA copolymer ratios. *J Biomed Mater Res* 11:711–719. <https://doi.org/10.1002/jbm.820110507>
48. Nakamura T, Shimizu Y, Okumura N, Matsui T, Hyon S-H, Shimamoto T (1994) Tumorigenicity of poly-L-lactide (PLLA) plates compared with medical-grade polyethylene. *J Biomed Mater Res* 28:17–25. <https://doi.org/10.1002/jbm.820280104>
49. Lee HS, Park SH, Lee JH, Jeong BY, Ahn SK, Choi YM, Choi DJ, Chang JH (2013) Antimicrobial and biodegradable PLGA medical sutures with natural grapefruit seed extracts. *Mater Lett* 95:40–43. <https://doi.org/10.1016/j.matlet.2012.12.090>
50. Haghghat F, Ravandi SAH (2014) Mechanical properties and in vitro degradation of PLGA suture manufactured via electrospinning. *Fibers Polym* 15:71–77. <https://doi.org/10.1007/s12221-014-0071-9>
51. Weldon CB, Tsui JH, Shankarappa SA, Nguyen VT, Ma M, Anderson DG, Kohane DS (2012) Electrospun drug-eluting sutures for local anesthesia. *J Control Release* 161:903–909. <https://doi.org/10.1016/j.jconrel.2012.05.021>
52. Ford Versypt AN, Pack DW, Braatz RD (2013) Mathematical modeling of drug delivery from autocatalytically degradable PLGA microspheres—a review. *J Control Release* 165:29–37. <https://doi.org/10.1016/j.jconrel.2012.10.015>
53. Siepmann J, Elkharraz K, Siepmann F, Klose D (2005) How autocatalysis accelerates drug release from PLGA-Based microparticles: a quantitative treatment. *Biomacromolecules* 6:2312–2319. <https://doi.org/10.1021/bm050228k>
54. Patrício T, Bártolo P (2013) Thermal stability of PCL/PLA blends produced by physical blending process. *Procedia Eng* 59:292–297. <https://doi.org/10.1016/j.proeng.2013.05.124>
55. Piao L, Dai Z, Deng M, Chen X, Jing X (2003) Synthesis and characterization of PCL/PEG/PCL triblock copolymers by using calcium catalyst. *Polymer* 44:2025–2031. [https://doi.org/10.1016/S0032-3861\(03\)00087-9](https://doi.org/10.1016/S0032-3861(03)00087-9)
56. Chen L, Ni Y, Bian X, Qiu X, Zhuang X, Chen X, Jing X (2005) A novel approach to grafting polymerization of ϵ -caprolactone onto starch granules. *Carbohydr Polym* 60:103–109. <https://doi.org/10.1016/j.carbpol.2004.11.028>
57. Zhang L, Xiong C, Deng X (1995) Biodegradable polyester blends for biomedical application. *J Appl Polym Sci* 56:103–112. <https://doi.org/10.1002/app.1995.070560114>
58. Fukushima K, Feijoo JL, Yang M-C (2013) Comparison of abiotic and biotic degradation of PDLLA, PCL and partially miscible PDLLA/PCL blend. *Eur Polymer J* 49:706–717. <https://doi.org/10.1016/j.eurpolymj.2012.12.011>
59. Fu S, Guo G, Gong C, Zeng S, Liang H, Luo F, Zhang X, Zhao X, Wei Y, Qian Z (2009) Injectable biodegradable thermosensitive hydrogel composite for orthopedic tissue engineering. 1. Preparation and characterization of nanohydroxyapatite/poly(ethylene glycol)–poly(ϵ -caprolactone)–poly(ethylene glycol) hydrogel nanocomposites. *J Phys Chem B* 113:16518–16525. <https://doi.org/10.1021/jp907974d>
60. Lam CXF, Savalani MM, Teoh S-H, Huttmacher DW (2008) Dynamics of invitro polymer degradation of polycaprolactone-based scaffolds: accelerated versus simulated physiological conditions. *Biomed Mater* 3:034108. <https://doi.org/10.1088/1748-6041/3/3/034108>
61. Karuppuswamy P, Reddy Venugopal J, Navaneethan B, Luwang Laiva A, Ramakrishna S (2015) Polycaprolactone nanofibers for the controlled release of tetracycline hydrochloride. *Mater Lett* 141:180–186. <https://doi.org/10.1016/j.matlet.2014.11.044>
62. Ahmed F, Discher DE (2004) Self-porating polymersomes of PEG–PLA and PEG–PCL: hydrolysis-triggered controlled release vesicles. *J Control Release* 96:37–53. <https://doi.org/10.1016/j.jconrel.2003.12.021>

63. Berkland C, Kipper MJ, Narasimhan B, Kim K, Pack DW (2004) Microsphere size, precipitation kinetics and drug distribution control drug release from biodegradable polyanhydride microspheres. *J Control Release* 94:129–141. <https://doi.org/10.1016/j.jconrel.2003.09.011>
64. Leong KW, Brott BC, Langer R (1985) Bioerodible polyanhydrides as drug-carrier matrices. I: Characterization, degradation, and release characteristics. *J Biomed Mater Res* 19:941–955. <https://doi.org/10.1002/jbm.820190806>
65. *Molecules* (Basel, Switzerland). <https://doi.org/10.3390/molecules23020290>
66. Lenz RW, Guerin P (1983) Functional polyesters and polyamides for medical applications of biodegradable polymers. In: Chiellini E, Giusti P (eds) *Polymers in medicine: biomedical and pharmacological applications*. Springer, US, pp 219–230. https://doi.org/10.1007/978-1-4615-7643-3_16
67. Ono K, Saito Y, Yura H, Ishikawa K, Kurita A, Akaie T, Ishihara M (2000) Photocrosslinkable chitosan as a biological adhesive. *J Biomed Mater Res* 49:289–295. [https://doi.org/10.1002/\(sici\)1097-4636\(200002\)49:2%3c289:aid-jbm18%3e3.0.co;2-m](https://doi.org/10.1002/(sici)1097-4636(200002)49:2%3c289:aid-jbm18%3e3.0.co;2-m)
68. Cho WJ, Oh SH, Lee JH (2010) Alginate film as a novel post-surgical tissue adhesion barrier. *J Biomater Sci Polym Ed* 21:701–713. <https://doi.org/10.1163/156856209X435835>
69. Jeong SI, Krebs MD, Bonino CA, Khan SA, Alsberg E (2010) Electrospun alginate nanofibers with controlled cell adhesion for tissue engineering. *Macromol Biosci* 10:934–943. <https://doi.org/10.1002/mabi.201000046>
70. Tucci MG, Ricotti G, Mattioli-Belmonte M, Gabbanelli F, Lucarini G, Orlando F, Viticchi C, Bigi A, Panzavolta S, Roveri N, Morganti G, Muzzarelli RAA (2001) Chitosan and gelatin as engineered dressing for wound repair. *J Bioactive Compat Polym* 16:145–157. <https://doi.org/10.1106/NYTK-W829-UWC1-PMLW>
71. Athanasiou KA, Agrawal CM, Barber FA, Burkhart SS (1998) Orthopaedic applications for PLA-PGA biodegradable polymers. *Arthroscopy J Arthroscop Rel Surg* 14:726–737. [https://doi.org/10.1016/S0749-8063\(98\)70099-4](https://doi.org/10.1016/S0749-8063(98)70099-4)
72. Tanase CE, Spiridon I (2014) PLA/chitosan/keratin composites for biomedical applications. *Mater Sci Eng C* 40:242–247. <https://doi.org/10.1016/j.msec.2014.03.054>
73. He Y, Hu Z, Ren M, Ding C, Chen P, Gu Q, Wu Q (2014) Evaluation of PHBHHx and PHBV/PLA fibers used as medical sutures. *J Mater Sci Mater Med* 25:561–571. <https://doi.org/10.1007/s10856-013-5073-4>
74. Scolozzi P, Martinez A, Jaques B (2007) Complex orbito-fronto-temporal reconstruction using computer-designed PEEK implant. *J Craniofacial Surg* 18:224–228. <https://doi.org/10.1097/01.scs.0000249359.56417.7e>
75. Wiesli MG, Özcan M (2015) High-performance polymers and their potential application as medical and oral implant materials: a review. *Implant Dent* 24:448–457. <https://doi.org/10.1097/id.0000000000000285>
76. Horák Z, Pokorný D, Fulín P, Slouf M, Jahoda D, Sosna A (2010) Polyetheretherketone (PEEK). Part I: Prospects for use in orthopaedics and traumatology. *Acta Chir Orthop Traumatol Cech* 77:463–469
77. Williams SF, Martin DP, Horowitz DM, Peoples OP (1999) PHA applications: addressing the price performance issue: I. Tissue engineering. *Int J Biol Macromol* 25:111–121. [https://doi.org/10.1016/S0141-8130\(99\)00022-7](https://doi.org/10.1016/S0141-8130(99)00022-7)
78. Perni S, Caserta S, Pasquino R, Jones SA, Prokopovich P (2019) Prolonged antimicrobial activity of PMMA bone cement with embedded gentamicin-releasing silica nanocarriers. *ACS Appl Bio Mater*. <https://doi.org/10.1021/acsabm.8b00752>
79. Redolfi Riva E, Desii A, Sartini S, La Motta C, Mazzolai B, Mattoli V (2013) PMMA/polysaccharides nanofilm loaded with adenosine deaminase inhibitor for targeted anti-inflammatory drug delivery. *Langmuir* 29:13190–13197. <https://doi.org/10.1021/la402229k>
80. Holländer J, Genina N, Jukarainen H, Khajeheian M, Rosling A, Mäkilä E, Sandler N (2016) Three-dimensional printed PCL-based implantable prototypes of medical devices for controlled drug delivery. *J Pharm Sci* 105:2665–2676. <https://doi.org/10.1016/j.xphs.2015.12.012>

81. Hickey T, Kreutzer D, Burgess DJ, Moussy F (2002) In vivo evaluation of a dexamethasone/PLGA microsphere system designed to suppress the inflammatory tissue response to implantable medical devices. *J Biomed Mater Res* 61:180–187. <https://doi.org/10.1002/jbm.10016>
82. Davoodi S, Oliaei E, Davachi SM, Hejazi I, Seyfi J, Heidari BS, Ebrahimi H (2016) Preparation and characterization of interface-modified PLA/starch/PCL ternary blends using PLLA/triclosan antibacterial nanoparticles for medical applications. *RSC Adv* 6:39870–39882. <https://doi.org/10.1039/C6RA07667J>
83. Robert M, Boularan AM, El Sandid M, Grasset D (1997) Double-J ureteric stent encrustations: clinical study on crystal formation on polyurethane stents. *Urol Int* 58:100–104. <https://doi.org/10.1159/000282959>
84. Park JH, Cho YW, Kwon IC, Jeong SY, Bae YH (2002) Assessment of PEO/PTMO multiblock copolymer/segmented polyurethane blends as coating materials for urinary catheters: in vitro bacterial adhesion and encrustation behavior. *Biomaterials* 23:3991–4000. [https://doi.org/10.1016/S0142-9612\(02\)00144-8](https://doi.org/10.1016/S0142-9612(02)00144-8)
85. Liao SS, Cui FZ, Zhang W, Feng QL (2004) Hierarchically biomimetic bone scaffold materials: nano-HA/collagen/PLA composite. *J Biomed Mater Res B Appl Biomater* 69B:158–165. <https://doi.org/10.1002/jbm.b.20035>
86. Stjern Dahl A, Wistrand AF, Albertsson A-C (2007) Industrial utilization of tin-initiated resorbable polymers: synthesis on a large scale with a low amount of initiator residue. *Biomacromol* 8:937–940. <https://doi.org/10.1021/bm0611331>
87. Duchiron SW, Pollet E (2018) Enzymatic synthesis of amino acids endcapped polycaprolactone: a green route towards functional polyesters. *Molecules* 23. <https://doi.org/10.3390/molecules23020290>
88. Simioni AR, Vaccari C, Re MI, Tedesco AC (2008) PHBHV/PCL microspheres as biodegradable drug delivery systems (DDS) for photodynamic therapy (PDT). *J Mater Sci* 43:580–584. <https://doi.org/10.1007/s10853-007-1652-4>
89. Barbier-Baudry D, Brachais L, Cretu A, Gattin R, Loupy A, Stuerger D (2003) Synthesis of polycaprolactone by microwave irradiation—an interesting route to synthesize this polymer via green chemistry. *Environ Chem Lett* 1:19–23. <https://doi.org/10.1007/s10311-002-0005-4>
90. An YH, Alvi FI, Kang Q, Laberge M, Drews MJ, Zhang J, Matthews MA, Arciola CR (2005) Effects of sterilization on implant mechanical property and biocompatibility. *Int J Artif Organs* 28:1126–1137
91. Spilimbergo S, Bertuccio A (2003) Non-thermal bacterial inactivation with dense CO₂. *Biotechnol Bioeng* 84:627–638. <https://doi.org/10.1002/bit.10783>
92. Dillow AK, Dehghani F, Hrkach JS, Foster NR, Langer R (1999) Bacterial inactivation by using near- and supercritical carbon dioxide. *Proc Natl Acad Sci* 96:10344–10348. <https://doi.org/10.1073/pnas.96.18.10344>
93. Jiménez A, Thompson GL, Matthews MA, Davis TA, Crocker K, Lyons JS, Trapotsis A (2007) Compatibility of medical-grade polymers with dense CO₂. *J Supercrit Fluids* 42:366–372. <https://doi.org/10.1016/j.supflu.2007.05.002>
94. Braley S (1968) The silicones as subdermal engineering materials. *Ann N Y Acad Sci* 146:148–157. <https://doi.org/10.1111/j.1749-6632.1968.tb20279.x>
95. Wang Q, Gao W, Xie Z (2003) Highly thermally conductive room-temperature-vulcanized silicone rubber and silicone grease. *J Appl Polym Sci* 89:2397–2399. <https://doi.org/10.1002/app.12363>
96. Chen D, Yi S, Wu W, Zhong Y, Liao J, Huang C, Shi W (2010) Synthesis and characterization of novel room temperature vulcanized (RTV) silicone rubbers using vinyl-POSS derivatives as cross linking agents. *Polymer* 51:3867–3878. <https://doi.org/10.1016/j.polymer.2010.06.028>
97. Poplawski ME, Brown B, Lae Rho K, Yong Yun S, Jung Lee H, Sig Cha G, Paeng K-J (1997) One-component room temperature vulcanizing-type silicone rubber-based sodium-selective membrane electrodes. *Analytica Chimica Acta* 355:249–257. [https://doi.org/10.1016/S0003-2670\(97\)00482-0](https://doi.org/10.1016/S0003-2670(97)00482-0)

98. Yoon IJ, Lee DK, Nam H, Cha GS, Strong TD, Brown RB (1999) Ion sensors using one-component room temperature vulcanized silicone rubber matrices. *J Electroanal Chem* 464:135–142. [https://doi.org/10.1016/S0022-0728\(99\)00010-8](https://doi.org/10.1016/S0022-0728(99)00010-8)
99. Braden M, Elliott JC (1966) Characterization of the setting process of silicone dental rubbers. *J Dent Res* 45:1016–1023. <https://doi.org/10.1177/00220345660450040101>
100. Gifford GH Jr, Merrill EW, Morgan MS (1976) In vivo tissue reactivity of radiation-cured silicone rubber implants. *J Biomed Mater Res* 10:857–865. <https://doi.org/10.1002/jbm.820100605>
101. Morrison NJ, Porter M (1984) Temperature effects on the stability of intermediates and crosslinks in sulfur vulcanization. *Rubber Chem Technol* 57:63–85. <https://doi.org/10.5254/1.3536002>
102. Saville B, Watson AA (1967) Structural characterization of sulfur-vulcanized rubber networks. *Rubber Chem Technol* 40:100–148. <https://doi.org/10.5254/1.3539039>
103. Shibata M, Cao J, Yosomiya R (1997) Synthesis and properties of the block copolymers of poly(ether ether ketone) and the poly(aryl ether sulfone) containing biphenylene moiety. *Polymer* 38:3103–3108. [https://doi.org/10.1016/S0032-3861\(96\)00869-5](https://doi.org/10.1016/S0032-3861(96)00869-5)
104. Cao J, Su W, Wu Z, Kitayama T, Hatada K (1994) Synthesis and properties of poly(ether ether ketone)-poly(ether sulfone) block copolymers. *Polymer* 35:3549–3556. [https://doi.org/10.1016/0032-3861\(94\)90922-9](https://doi.org/10.1016/0032-3861(94)90922-9)
105. Klein DJ, Korleski JE, Harris FW (2001) Synthesis of polyphenylquinoxaline copolymers via aromatic nucleophilic substitution reactions of an A-B quinoxaline monomer. *J Polym Sci Part A Polym Chem* 39:2037–2042. <https://doi.org/10.1002/pola.1179>
106. Panayotov IV, Orti V, Cuisinier F, Yachouh J (2016) Polyetheretherketone (PEEK) for medical applications. *J Mater Sci Mater Med* 27:118. <https://doi.org/10.1007/s10856-016-5731-4>
107. Steinberg EL, Rath E, Shlaifer A, Chechik O, Maman E, Salai M (2013) Carbon fiber reinforced PEEK Optima—a composite material biomechanical properties and wear/debris characteristics of CF-PEEK composites for orthopedic trauma implants. *J Mech Behav Biomed Mater* 17:221–228. <https://doi.org/10.1016/j.jmbbm.2012.09.013>
108. Kurtz SM, Devine JN (2007) PEEK biomaterials in trauma, orthopedic, and spinal implants. *Biomaterials* 28:4845–4869. <https://doi.org/10.1016/j.biomaterials.2007.07.013>
109. Cowie RM, Briscoe A, Fisher J, Jennings LM (2016) PEEK-OPTIMA™ as an alternative to cobalt chrome in the femoral component of total knee replacement: a preliminary study. *Proc Inst Mech Eng [H]* 230:1008–1015. <https://doi.org/10.1177/0954411916667410>
110. Torstrick FB, Evans NT, Stevens HY, Gall K, Guldborg RE (2016) Do surface porosity and pore size influence mechanical properties and cellular response to PEEK? *Clin Orthop Rel Res* 474:2373–2383. <https://doi.org/10.1007/s11999-016-4833-0>
111. Mishra TK, Kumar A, Verma V, Pandey KN, Kumar V (2012) PEEK composites reinforced with zirconia nanofiller. *Compo Sci Technol* 72:1627–1631. <https://doi.org/10.1016/j.compscitech.2012.06.019>
112. Berretta S, Evans K, Ghita O (2018) Additive manufacture of PEEK cranial implants: manufacturing considerations versus accuracy and mechanical performance. *Mater Des* 139:141–152. <https://doi.org/10.1016/j.matdes.2017.10.078>
113. Schwitalla AD, Abou-Emara M, Spintig T, Lackmann J, Müller WD (2015) Finite element analysis of the biomechanical effects of PEEK dental implants on the peri-implant bone. *J Biomech* 48:1–7. <https://doi.org/10.1016/j.jbiomech.2014.11.017>
114. Searle OB, Pfeiffer RH (1985) Victrex® poly(ethersulfone) (PES) and Victrex® poly(etheretherketone) (PEEK). *Polym Eng Sci* 25:474–476. <https://doi.org/10.1002/pen.760250808>

Chapter 2

Sustainable Routes for Synthesis of Poly(ϵ -Caprolactone): Prospects in Chemical Industries



Munmi Das, Bishnupada Mandal and Vimal Katiyar

Abstract Environmental concerns associated with the hazardous and toxic petroleum resources have created an imperative need to fabricate new biodegradable materials having practically identical properties as that of the present polymeric materials at a comparable expense. The selection and utilization of agricultural products, such as biomass are regarded as an intriguing and sustainable method to lessen surplus farm wastes and further transformation to other value-added products making itself the most attractive replacement of fossil resources. Plastics are habitually stained by food and other organic matter, which makes their recycling unrealistic and inadmissible. Contrary to that, biodegradable polymers are naturally recycled by biological process, i.e., enzymatic activity of microorganisms such as bacteria, fungi and algae, and the breaking down of polymer chains occurs by chemical hydrolysis when disposed to the bioactive environment. Recently, biosynthetic pathway utilizing ring-opening polymerization (ROP) of biomass-derived ϵ -caprolactone has grasped recognition because of mild reaction requirements, recyclability and ease of processing. Thus, this polymerization can be considered as a sustainable and environment-friendly green chemistry approach to develop bio-derived biodegradable poly(ϵ -caprolactone).

Keywords Sustainable · Bio-derived · Biomass · Poly(ϵ -caprolactone) · Ring-opening polymerization · Lactones

1 Introduction

Poly(ϵ -caprolactone): Petroleum-based biodegradable polyester Poly(ϵ -caprolactone) (PCL) is one of the first polymers to be synthesized in the early 1930s by the Carothers group, but was soon replaced by quicker resorbable polymers [1, 2]. PCL is well known for its inherent biodegradable and biocompatible nature, which directs its use in the food packaging industry, drug delivery systems, resorbable sutures and in tissue engineering [3]. The production route of PCL is

M. Das · B. Mandal · V. Katiyar (✉)

Department of Chemical Engineering, Indian Institute of Technology Guwahati, Guwahati, Kamrup, Assam 781039, India
e-mail: vkatiyar@iitg.ac.in

© Springer Nature Singapore Pte Ltd. 2020

V. Katiyar et al. (eds.), *Advances in Sustainable Polymers*, Materials Horizons: From Nature to Nanomaterials, https://doi.org/10.1007/978-981-15-1251-3_2

comparatively economical in comparison with counterpart aliphatic polyesters, hence its use in the development of biomedical devices is highly beneficial. PCL is a linear, aliphatic semicrystalline biodegradable thermoplastic polyester consisting of hexanoate repeating units, obtained by ring-opening polymerization (ROP) of ϵ -caprolactone (obtained from crude oil through chemical conversion) [4]. Figure 1 illustrates different synthetic routes to obtain poly(ϵ -caprolactone). PCL can be achieved as a result of (a) condensation of 6-hydroxycaproic acid, (b) ROP of ϵ -caprolactone or (c) radical ROP of 2-methylene-1,3-dioxepane. Of all these three techniques, ring-opening polymerization is the widely studied one [5].

Over the last two decades, PCL has regained attention into the biomaterials domain of tissue engineering with the advantage of having satisfactory viscoelastic and rheological properties over other aliphatic polyesters and has become a suitable material for manufacturing large range of implants [6, 7].

PCL is one of the hydrophobic industrially accessible biodegradable polymers with low melting point range (58–64 °C), good chemical and oil resistance, lower viscosity and easily processable thermal properties. It has a glass transition temperature (T_g) of -60 °C, indicating the semicrystalline nature of PCL which empowers easy moldability at relatively low temperatures [8, 9]. The properties of PCL, such as poor mechanical property, low glass transition temperature and melting point, can be improved by blending or by cross-linking with other materials with superior properties to make it suitable for large-scale industrial applications and also to manipulate the rate of microcapsulated drug release [10–12]. However, PCL possesses inherent rubbery characteristics with a comparatively higher elongation at break of nearly 600% and acts as a good toughening material when used alone or enhancing the

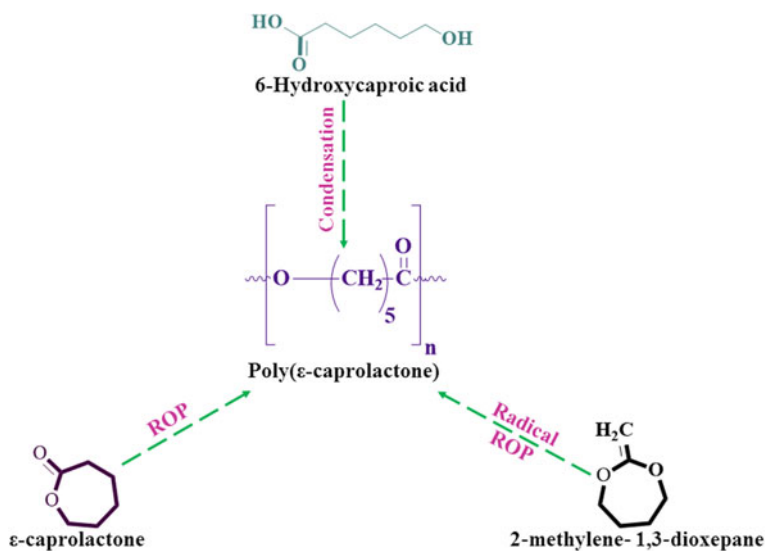


Fig. 1 Different routes to synthesize poly(ϵ -caprolactone)

Table 1 Solubility parameters of PCL in different solvents at room temperature [16]

Solvent	Chloroform	DCM	Benzene	Cyclohexanone	Acetone	Acetonitrile	DMF	Alcohol
Solubility	Good	Good	Good	Good	Low	Low	Low	Insoluble

property of blends [13]. The dissolution of PCL in different solvents is dependent on the temperature (Table 1); for example, it is slightly soluble in acetone at room temperature, but the solubility can be improved by increasing the temperature to 50 °C.

Although the biodegradation and hydrolysis rate of PCL depends on its molecular weight, environmental conditions and degree of crystallinity, there are numerous microbes and fungi capable of completely degrading PCL [9, 14]. Abiotic degradation was studied in phosphate buffer and biotic degradation in soil, lake and seawater, sewage, sludge and in compost [15]. The amorphous phase of PCL is first degraded during the biodegradation process, which causes an increase in the degree of crystallinity, without a remarkable change in the molecular weight. Cleavage of ester bonds occurs in the next stage resulting in the weight loss of PCL. The polymer degrades at high temperature by chain-end scission while random chain scission is observed at low temperatures [14].

2 Ring-Opening Polymerization of ϵ -Caprolactone

Lactone polymerization is mostly performed in bulk or solution than in emulsion or dispersion [17]. Bulk polymerization reactions are carried out at high temperatures between 100 and 150 °C, while solution polymerization is carried out below room temperature (25 °C) to avoid side reactions (inter- and intramolecular transesterification) [18]. Conventional step-growth polymerization leads to the production of polyesters with excess monomer residues and side-products, making ring-opening polymerization the widely used route, especially using anionic and covalent initiators. The use of alkali-metal alkyls and alkoxides leads to rapid and quantitative polymerizations, but a few transesterification reactions are also observed leading to a broadened molecular weight distribution (MWD) [19, 20].

Ring-opening polymerization (ROP) of lactones and associated monomers is the most efficient method of composing biocompatible and biodegradable aliphatic polymeric polyester materials. ROP enables a higher degree of control in terms of molecular weight and molecular weight distribution (M_w/M_n) compared to step-growth processes, i.e., polycondensation reactions. Original polymer topologies can also be obtained, primarily via ROP of monomers that contain prochiral centers using stereochemistry. The use of suitable initiators and catalysts promotes the monomer activation and controls the rate of ROP. The driving force for the polymerization in ROP processes depends on the reactivity and nature of the cyclic ester. It is therefore compulsory to select strongly active initiators and catalysts to achieve highly

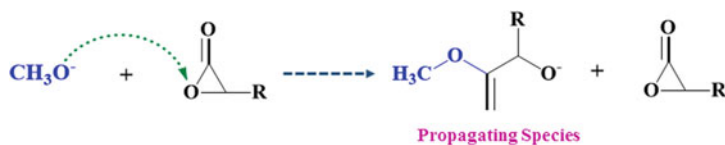


Fig. 2 Reaction scheme depicting acyl-oxygen scission of lactone

stable lactones [21–23]. Many organometallic compounds, such as oxides, carboxylates and alkoxides are considered to be effective initiators of controlled polyester synthesis using ROP of lactones, and the polymerization mechanism is dependent on the chosen initiator [24, 25]. Stannous octoate, also known as tin(II) octoate is extensively used as a catalyst in the ROP of ϵ -caprolactone, and the molecular weight of PCL could also be tuned utilizing low molecular weight alcohols [26]. ROP of ϵ -caprolactone can be achieved either by anionic, cationic, free radical, zwitterionic, monomer activated or coordination–insertion reaction mechanism. Anionic and coordination–insertion ring opening, however, are the most common mechanisms as they contribute to achieve high molecular weight polyesters [18, 27, 28].

2.1 Anionic Ring-Opening Polymerization

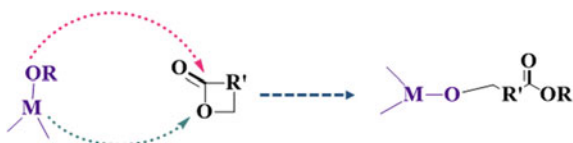
Alkali metals and their complexes with crown ethers are examples of effective initiators used in anionic polymerization. This type of polymerization can be carried out either through a living or non-living mechanism, depending on the parameters of the reaction such as type of initiators and monomers. The initiation of the reaction takes place with the nucleophilic attack of a negatively charged initiator on the alkyl-oxygen or the carbon of the carbonyl group leading to the development of linear polyester [29–34].

The polymerization of β -lactones can be done by using potassium methoxide and potassium tert-butoxide complexes with 18-crown-6 as initiators. In the polymerization of ϵ -caprolactone or lactide, the reaction is initiated by the acyl-oxygen scission, resulting in the formation of an alkoxide ion as a propagating species (Fig. 2). However, if ϵ -CL is polymerized using potassium tert-butoxide, a considerable amount of cyclic oligomers is formed due to the backbiting reaction, and this production of oligomers can be reduced by using lithium tert-butoxide in an apolar solvent [32].

2.2 Coordination–Insertion Polymerization

Coordination–insertion polymerization is extensively used to develop aliphatic polyesters of well-defined structure. This polymerization technique mostly uses various aluminum and tin alkoxides and carboxylates with vacant ‘d’ orbitals acting

Fig. 3 Lactone polymerization using coordination–insertion mechanism



as corresponding coordination initiators. These initiators are effective in producing stereoregular polymers with narrow molecular weight distribution along with well-defined end-groups. In coordination–insertion polymerization (Fig. 3), the monomer is inserted into the initiator's metal–oxygen bond via acyl–oxygen scission [35–37]. ROP of lactones in the presence of these organometallic initiators results in both inter- and intramolecular transesterification reactions, thereby leading to increased polydispersity of the polyesters [38, 39].

These transesterification reactions are dependent on the factors such as temperature, reaction time, concentration of initiator or catalyst and nature of the monomer (lactone/lactide) used [40, 41]. The rate of ROP is affected in high temperatures because of the disintegration of some catalyst or initiators thereby expanding the side reactions. Moreover, the extent of these side reactions also increases with the increasing flexibility of the polymer backbone [42]. Initiators such as tin (II) carboxylates and oxides and tin (IV) alkoxides are widely used in the ROP of caprolactone [43]. As mentioned earlier, due to the better solubility in lactones and most of the organic solvents, stannous octoate is extensively used to catalyze/initiate ROP of lactones [44]. Also, the production of high molecular weight PCL with a PDI less than 2 was observed using tin (IV) alkoxide [45]. Some other initiators used for ROP are aluminum alkoxides, lanthanide alkoxides, etc. [46, 47]. There are also reports of using enzymes and lipozyme IM 20, as a catalyst in the polymerization reaction between 15-hydroxypentadecanoic and 16-hydroxyhexadecanoic acids to obtain macrocyclic mono- and oligolactones [48].

3 Caprolactone from Biomass

Considering the environmental concerns of using toxic and harmful petroleum-based products, the prospects of using agricultural residues to synthesize caprolactone provide an opportunity to eliminate and regenerate value-added products, thereby improving the process economy and making it a renewable, less-costly and sustainable approach [49]. Thaore et al. evaluated a bio-based synthetic pathway to develop caprolactone from corn stover, a biomass residue. In their study, they also revealed the energy and material balances, cost efficiency of the process and the depletion of greenhouse gas (GHG) emissions. The reaction conditions and energy requirement involving the transformation of corn stover to caprolactone were integrated and optimized using simulation study in Aspen PlusTM [50].

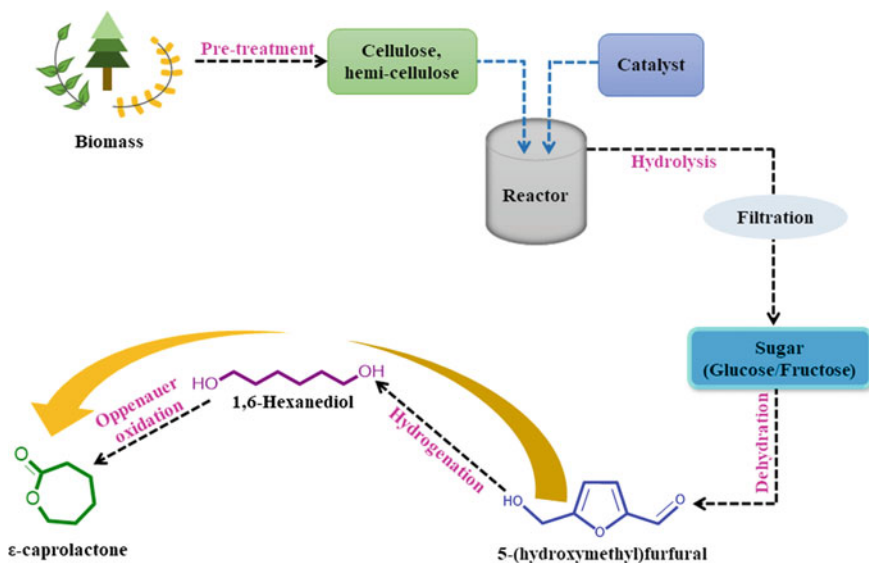


Fig. 4 Biosynthetic pathway demonstrating the isolation and extraction of ϵ -caprolactone from biomass

Moliner et al. developed a class of unsaturated chiral γ -lactones from levoglucosenone (LGO), a pyrolysis product of acid-treated cellulose with superior optical properties discovering application in the preparation of medicines, aromatizers and antivirals [51]. Figure 4 illustrates the biosynthetic pathway to prepare caprolactone from biomass. The intermediate products in this reaction series are fructose, 5-hydroxymethyl furfural (HMF) and 1,6-Hexanediol. HMF is obtained as a result of dehydration of fructose catalyzed by ammonium salts such as triethyl ammonium chloride (TEAC) at high temperatures [52].

3.1 Extraction of Hydroxymethylfurfural from Biomass

The evolution in the field of renewable non-conventional biomass energy captivated comprehensive recognition because of the fast depletion of non-renewable conventional fossil resources keeping environmental integrity in focus. Solid waste lignocellulosic biomass materials such as tree trunks, barks, leaves, rice straw, rice husk, wheat straw, wheat husk, corn stover and corncob, coconut shell and palm shell, cassava pulp and sugarcane bagasse are the most copious biomass materials obtained as agricultural residue, arboricultural residue and available around the globe. Lignin, cellulose and hemicellulose are the main building blocks of these types of biomass materials, and these building block substituents can deliver green value-added chemicals and renewable transportation fuels by incorporating various technologies. The

bio-based green compounds obtained by transforming this biomass consist of the latent property of producing bio-based plastics and valuable fine chemicals [53].

5-Hydroxymethylfurfural (HMF) is one of such fine chemicals which is obtained from hexose after the acid-catalyzed dehydration reaction, and it has various applications which deliberates its property of platform chemical during the synthesis of bio-fuels and valuable intermediate chemicals [54]. It is an important organic compound which produces bio-based plastics, valuable chemicals and transportation fuels. The manufacturing of HMF is done using edible glucose and fructose which suppresses the food source while the focus is now shifting toward the use of lignocellulosic biomass materials as a raw material such as sugarcane bagasse. The experimental studies were performed on sugarcane bagasse by maintaining the operating temperature at 200 and 300 °C to study the temperature effect and reaction time of 3–30 min to yield HMF from batch reactor consisting of slurry mixed with 10 ml of water and 1.2 g of solids. Among these experimental insights, the maximum yield of HMF is obtained at temperature 270 °C and at time 10 min. This study revealed that the yield of HMF decreases as the reaction temperature goes beyond 300 °C and the time of reaction longer than 30 min, and this happens because of intensified decomposition of HMF and its polymerization to yield formic acid and char accordingly [55]. Regular methods to convert biomass into HMF are described below.

Hydrolysis using Hot Compressed Water Hydrolysis reaction of cellulose and hemicellulose delivers sugar and furan-based chemicals at numerous conditions [56]. Hydrolysis for biomass conversion using hot compressed water (HCW) got wide range of interest among thermochemical degradation methods [57]. In this technique, wet biomass can be directly processed under several operating conditions which avoids the tedious pretreatment of biomass. Watanabe et al. carried out the process of hydrolysis using HCW for glucose adding H₂SO₄ and NaOH solutions for catalytic study. They reported the results as the acid catalyst H₂SO₄ encouraged the HMF production and base catalyst NaOH encouraged the isomerization of glucose into fructose [58]. Chareonlimkun et al. experimented co-hydrolysis/dehydration reaction for sugarcane bagasse, rice husk and corncob using HCW adding TiO₂, ZrO₂ and TiO₂–ZrO₂ as catalyst at the temperature range of 473–673 K. The results show the highest yields of furfural and 5-HMF with other by-products, viz. glucose, fructose, xylose and 1,6-anhydroglucose [59].

Microwave Radiation The microwave radiations were discovered in 1947 and continuously got the interest of researchers and were developed over a period of time. Operating wavelengths for microwave ovens are either 12.2 cm and 2.45 GHz or 32.8 cm and 915 MHz; the electromagnetic field generated by microwave radiations in these conditions produces energy effective homogeneous heating. Production of 5-HMF from sugars and polysaccharides using microwave radiation in homogeneous and heterogeneous heating environment gives high selectivity with low conversion. In this study, conditions were optimized where fructose and 9 mol% HCl combine with potassium bromide (KBr) in water–acetonitrile mixture of ratio 1:2 volume/volume heated at 160 °C for 1 min produces 91% of 5-HMF [60]. Riisager et al. conducted



Fig. 5 Synthesis of methyl-ε-caprolactone from p-cresol [63]

experiments to study the influence of different parameters which affects the above-mentioned scheme. They deliberately calculated the influence of temperature, pH, microwave power and residence time on 5-HMF yield. When diluted fructose of 27 wt% added with 0.01 M HCl undergoes microwave radiation at 200 °C for 1 s, it delivers 52% fructose conversion with 33% 5-HMF yield. If the reaction takes place for 60 s, the fructose conversion will be 95% which will yield 53% 5-HMF [61].

Carbonization and Sulfonation For the production of HMF from waste biomass, a strategic technique is followed where carbon is sulfonated and used as a catalyst. The novel technique of sulfonated bamboo-derived carbon (SBC) is ready as a one-pot synchronized carbonization and sulfonation method where the sulfonating agent used is p-toluene sulfonic acid. This technique uses single step process rather than going for uneconomical two step carbonization followed by sulfonation. The catalysts prepared by this method help in yielding the 92.1% HMF by dehydration of fructose [62].

4 Caprolactone from Petroleum Resources

While not much work is reported to synthesize caprolactone from petroleum-derived components, Lundberg et al. explained a techno-economic analysis involving the production of methyl-ε-caprolactone from p-cresol, extracted conventionally from coal tar. According to their conceptual study, the conversion of p-cresol to methyl-ε-CL will take place mainly in two steps, (a) hydrogenation of cresol to form methyl-cyclohexanone followed by purification of ketone and (b) Baeyer–Villiger oxidation to obtain methyl-ε-CL as shown in Fig. 5.

5 Microbial Synthesis of Caprolactone

Researchers have been trying to use isolated enzymes from microorganisms as a catalyst in the biotransformation of cyclohexanone into ε-caprolactone for nearly three decades. It has been concluded in a study that the fungus *Fusarium oxysporum* f. sp. *ciceri* NCIM 1282, possessing redox activity is competent enough to take part in biotransformation reaction with remarkable activity and selectivity. Following this,

Mandal et al. used whole cell of this fungus to produce ϵ -caprolactone from cyclohexanone in high selectivity (99+%). The inherent redox activity of *F. oxysporum* converted cyclohexanone to cyclohexanol initially followed by caprolactone formation [64]. Also in 2005, Xie et al. reported the microbial synthesis of 4-Hydroxy-6-methyl-2-pyrone, also known as triacetic acid lactone (TAL) with the highest concentration and a yield of 6%, from glucose by utilizing TAL-synthesizing enzyme activity of *S. cerevisiae*, which was cultured in a fermented-controlled condition expressing mutant Y1572F 6-MSAS [65].

6 Future Prospects in Chemical Industries

The inherent properties of poly(ϵ -caprolactone) such as hydrophobicity, higher molecular weight and flexibility empower its application as a blending material to improve properties of PCL copolymers. PCL is also used extensively as a preliminary component for the synthesis of other polymers, for example, polyurethanes (PUs) and thermoplastic PUs (TPUs), thereby making it a competitive commodity in the polymer market today. The blends and copolymers of PCL have gained attention as they are capable of developing novel polymers suitable for remarkable biomedical applications. However, with an increase in the consumption of this polymer, there also lies a question in replacing its synthesis route by a sustainable approach to make it more environment-friendly and less expensive.

Moreover, in today's scenario, the environmental concerns related to the use of petroleum-based resources, in terms of waste management and disposal, pose a serious threat to human society and the atmosphere. The use of biomass as a source not only will reduce the consumption of depleting petroleum resources but also will provide a greener and economic approach to obtain important monomers from biomass. Various strategies are formulated to acquire efficient and sustainable bio-based plastics from biomass nowadays which could be recycled, reused and utilized in packaging and biomedical applications. The study on the production of ϵ -caprolactone from bioresources has not yet been implemented experimentally, but it can be presumed that this pathway will lead to an inexpensive and sustainable approach that eliminates waste disposal and environmental concerns.

References

1. Van Natta FJ, Hill JW, Carothers WH (1934) Studies of polymerization and ring formation. XXIII. ϵ -caprolactone and its polymers. *J Am Chem Soc* 56:455–457. <https://doi.org/10.1021/ja01317a053>
2. Woodruff MA, Hutmacher DW (2010) The return of a forgotten polymer—polycaprolactone in the 21st Century. *Prog Polym Sci* 35:1217–1256. <https://doi.org/10.1016/j.progpolymsci.2010.04.002>

3. Vroman I, Tighzert L (2009) Biodegradable polymers. *Materials (Basel)* 2:307–344. <https://doi.org/10.3390/ma2020307>
4. Nair LS, Laurencin CT (2007) Biodegradable polymers as biomaterials. *Prog Polym Sci* 32:762–798. <https://doi.org/10.1016/j.progpolymsci.2007.05.017>
5. Labet M, Thielemans W (2009) Synthesis of polycaprolactone: a review. *Chem Soc Rev* 38:3484–3504. <https://doi.org/10.1039/b820162p>
6. Zein I, Hutmacher DW, Tan KC, Teoh SH (2002) Fused deposition modeling of novel scaffold architectures for tissue engineering applications. *Biomaterials* 23:1169–1185. [https://doi.org/10.1016/S0142-9612\(01\)00232-0](https://doi.org/10.1016/S0142-9612(01)00232-0)
7. Luciani A, Coccoli V, Orsi S, Ambrosio L, Netti PA (2008) PCL microspheres based functional scaffolds by bottom-up approach with predefined microstructural properties and release profiles. *Biomaterials* 29:4800–4807. <https://doi.org/10.1016/j.biomaterials.2008.09.007>
8. Hayashi T (1994) Biodegradable polymers for biomedical uses. *Prog Polym Sci* 19:663–702. [https://doi.org/10.1016/0079-6700\(94\)90030-2](https://doi.org/10.1016/0079-6700(94)90030-2)
9. Chandra R, Rustgi R (1998) Biodegradable polymers. *Prog Polym Sci* 23:1273–1335. [https://doi.org/10.1016/S0079-6700\(97\)00039-7](https://doi.org/10.1016/S0079-6700(97)00039-7)
10. Averous L, Moro L, Dole P, Fringant C (2000) Properties of thermoplastic blends: starch—polycaprolactone. *Polymer* 41:4157–4167. [https://doi.org/10.1016/S0032-3861\(99\)00636-9](https://doi.org/10.1016/S0032-3861(99)00636-9)
11. Bordes P, Pollet E, Avérous L (2009) Nano-biocomposites: biodegradable polyester/nanoclay systems. *Prog Polym Sci* 34:125–155. <https://doi.org/10.1016/j.progpolymsci.2008.10.002>
12. Koenig MF, Huang SJ (1994) Evaluation of crosslinked poly (caprolactone) as a biodegradable, hydrophobic coating. *Polym Degrad and Stabil* 45:139–144. [https://doi.org/10.1016/0141-3910\(94\)90189-9](https://doi.org/10.1016/0141-3910(94)90189-9)
13. Guarino V, Gentile G, Sorrentino L, Ambrosio L (2017) Polycaprolactone: synthesis, properties, and applications. *Encycl Polym Sci Technol*. <https://doi.org/10.1002/0471440264.pst658>
14. Labet M, Thielemans W (2009) Synthesis of polycaprolactone: a review. *Chem Soc Rev* 38(12):3484–3504. <https://doi.org/10.1039/b820162p>
15. Tokiwa Y, Suzuki T (2014) Purification and some properties of polyethylene adipate-degrading enzyme produced by *Penicillium* sp. Strain 14–3. *Agric Biol Chem* 1369:265–274. <https://doi.org/10.1080/00021369.1977.10862486>
16. Hedrick JL, Dubois P, Coulembier O, Dege P (2006) From controlled ring-opening polymerization to biodegradable aliphatic polyester: especially poly (β -malic acid) derivatives. *Prog Polym Sci* 31:723–747. <https://doi.org/10.1016/j.progpolymsci.2006.08.004>
17. Sosnowski S, Gadzinowski M, Slomkowski S (1996) Poly (L,L-lactide) microspheres by ring-opening polymerization. *Macromolecules* 29:4556–4564. <https://doi.org/10.1021/ma951542h>
18. Albertsson A, Varma IK (2003) Recent developments in ring opening polymerization of lactones for biomedical applications. *Biomacromol* 4(6):1466–1486. <https://doi.org/10.1021/bm034247a>
19. Okamoto Y (1991) Cationic ring-opening polymerization of lactones in the presence of alcohol. *Makromol Chem, Macromol Symp* 42/43(1):117–133. <https://doi.org/10.1002/masy.19910420109>
20. Jedliński Z, Wafach W, Kurcok P, Adamus G (1991) Polymerization of lactones, 12. Polymerization of L-dilactide and L,D-dilactide in the presence of potassium methoxide. *Makromol Chem* 192:2051–2057. <https://doi.org/10.1002/macp.1991.021920914>
21. Ajellal N, Carpentier J, Guillaume C, Guillaume SM, Helou M, Poirier V, Sarazin Y, Trifonov A (2010) Metal-catalyzed immortal ring-opening polymerization of lactones, lactides and cyclic carbonates. (Perspective) *Dalton Trans* 39:8363–8376. <https://doi.org/10.1039/c001226b>
22. Dove AP (2008) Controlled ring-opening polymerisation of cyclic esters : polymer blocks in self-assembled nanostructures. *Chem Commun* 6446–6470. <https://doi.org/10.1039/b813059k>
23. Kamber NE, Jeong W, Waymouth RM, Pratt RC, Lohmeijer BGG, Hedrick JL (2007) Organocatalytic ring-opening polymerization. *Chem Rev* 107:5813–5840. <https://doi.org/10.1021/cr068415b>
24. Mecerreyes D, Je R (1999) Feature Article From living to controlled aluminium alkoxide mediated ring—opening polymerization of (di) lactones, a powerful tool for the macromolecular

- engineering of aliphatic polyesters. *Macromol Chem Phys* 200:2581–2590. [https://doi.org/10.1002/\(SICI\)1521-3935\(19991201\)200:12%3c2581:AID-MACP2581%3e3.0.CO;2-P](https://doi.org/10.1002/(SICI)1521-3935(19991201)200:12%3c2581:AID-MACP2581%3e3.0.CO;2-P)
25. Mecerreyes D, Jérôme R, Dubois P (1999) Novel macromolecular architectures based on aliphatic polyesters: relevance of the “coordination-insertion” ring-opening polymerization. In *Macromolecular architectures*, Adv Polym Sci 147:1–59. Springer-Berlin, Heidelberg
 26. Storey RF, Taylor AE (1998) Effect of stannous octoate on the composition, molecular weight, and molecular weight distribution of ethylene glycol-initiated poly (ϵ -Caprolactone). *J Macromol Sci Part A Pure Appl Chem* 35(5):723–750. <https://doi.org/10.1080/10601329808002008>
 27. Liverani L, Boccaccini A (2016) Versatile production of poly(epsilon-caprolactone) fibers by electrospinning using benign solvents. *Nanomaterials* 6(4):75. <https://doi.org/10.3390/nano6040075>
 28. Löfgren A, Albertsson A, Dubois P, Jérôme R (1995) Recent advances in ring—opening polymerization of lactones and related compounds. *J Macromol Sci, Pure Appl Chem* 35(3):379–418. <https://doi.org/10.1080/15321799508014594>
 29. Ageyeva T, Sibikin I, Kocsis JK (2018) Polymers and related composites via anionic ring-opening polymerization of lactams: recent developments and future trends. *Polymers* 10(4):357. <https://doi.org/10.3390/polym10040357>
 30. Kurcok P, Penczek J, Franek J, Jedliński Z (1992) Anionic polymerization of lactones. 14. Anionic block copolymerization of δ -valerolactone and L-lactide initiated with potassium methoxide. *Macromolecules*, 25(9):2285–2289. <https://doi.org/10.1021/ma00035a001>
 31. Jedliński Z, Kurcok P, Walach W, Janeczok H, Radecka I (1993) Polymerization of lactones, synthesis of ethylene glycol-L-lactide block copolymers. *Makromol Chem* 194:1681–1689. <https://doi.org/10.1002/macp.1993.021940616>
 32. Jedliński Z, Kowalczyk M, Kurcok P (1991) What is the real mechanism of anionic polymerization of β -Lactones by potassium alkoxides? A critical approach. *Macromolecules* 24:1218–1219. <https://doi.org/10.1021/ma00005a042>
 33. Rulkens R, Lough AJ, Manners I (1994) anionic ring-opening oligomerization and polymerization of silicon-bridged [I] ferrocenophanes: characterization of short-chain models for poly(ferrocenylsilane) high polymers. *J Am Chem Soc* 116:797–798. <https://doi.org/10.1021/ja00081a062>
 34. Furuta A, Okada K, Fukuyama T (2017) Efficient anionic ring opening polymerization of ethylene oxide under microfluidic conditions. *Bull Chem Soc Jpn* 90:838–842. <https://doi.org/10.1246/bcsj.20170073>
 35. Kowalski A, Duda A, Penczek S (1998) Kinetics and mechanism of cyclic esters polymerization initiated with tin (II) octoate, 1. Polymerization of ϵ -caprolactone. *Macromol Rapid Commun* 19(11):567–572
 36. Kricheldorf HR, Kreiser-Saunders I, Boettcher C (1995) Poly lactones: 31. Sn (II) octoate-initiated polymerization of L-lactide: a mechanistic study. *Polymer* 36(6):1253–1259. [https://doi.org/10.1016/0032-3861\(95\)93928-f](https://doi.org/10.1016/0032-3861(95)93928-f)
 37. In't Veld PJ, Vclner EM, Van De Witte P, Hamhuis J, Dijkstra PJ, Feijen J (1997) Melt block copolymerization of ϵ -caprolactone and L-lactide. *J Polym Sci, Part A: Polym Chem* 35(2):219–226. [https://doi.org/10.1002/\(SICI\)1099-0518\(19970130\)35:2](https://doi.org/10.1002/(SICI)1099-0518(19970130)35:2)
 38. Schwach G, Coudane J, Engel R, Vert M (1997) More about the polymerization of lactides in the presence of stannous octoate. *J Polym Sci, Part A: Polym Chem* 35(16):3431–3440. [https://doi.org/10.1002/\(SICI\)1099-0518\(19971130\)35:16](https://doi.org/10.1002/(SICI)1099-0518(19971130)35:16)
 39. Zhang X, MacDonald DA, Goosen MF, McAuley KB (1994) Mechanism of lactide polymerization in the presence of stannous octoate: the effect of hydroxy and carboxylic acid substances. *J Polym Sci, Part A: Polym Chem* 32(15):2965–2970. <https://doi.org/10.1002/pola.1994.080321519>
 40. Tian D, Dubois P, Jérôme R (1997) Macromolecular engineering of poly lactones and poly lactides. 23. Synthesis and characterization of biodegradable and biocompatible homopolymers and block copolymers based on 1,4,8-trioxo[4.6]spiro-9-undecanone. *Macromolecules* 30:1947–1954. <https://doi.org/10.1021/ma961614k>

41. Libiszowski J, Kowalski A, Duda A, Penczek S, Studies M (2002) Kinetics and mechanism of cyclic esters polymerization initiated with covalent metal carboxylates, 5. End-group studies in the model ϵ -caprolactone and L,L-dilactide/Tin (II) and zinc octoate/butyl alcohol systems. *Macromol Chem Phys* 203(10–11):1694–1701. [https://doi.org/10.1002/1521-3935\(200207\)203:10/11%3c1694](https://doi.org/10.1002/1521-3935(200207)203:10/11%3c1694)
42. Kricheldorf HR, Kreiser-saunders I, Stricker A (2000) Poly lactones 48. SnOct2-initiated polymerizations of lactide: a mechanistic study. *Macromolecules* 33:702–709. <https://doi.org/10.1021/ma991181w>
43. Kricheldorf HR, Kreiser-Saunders I (2000) Poly lactones 49: Bu₄Sn-initiated polymerizations of ϵ -caprolactone. *Polymer* 41(11):3957–3963. [https://doi.org/10.1016/S0032-3861\(99\)00606-0](https://doi.org/10.1016/S0032-3861(99)00606-0)
44. Nijenhuis AJ, Grijpma DW, Pennings AJ (1992) Lewis acid catalyzed polymerization of L-lactide. Kinetics and mechanism of the bulk polymerization. *Macromolecules* 25(24):6419–6424. <https://doi.org/10.1021/ma00050a006>
45. Von Schenck H, Ryner M, Albertsson A, Svensson M (2002) Ring-opening polymerization of lactones and lactides with Sn (IV) and Al (III) initiators. *Macromolecules* 35:1556–1562. <https://doi.org/10.1021/ma011653i>
46. Ko B, Lin C (1999) Efficient “living” and “immortal” polymerization of lactones and diblock copolymer of ϵ -CL and δ -VL catalyzed by aluminum alkoxides. *Macromolecules* 32(25):8296–8300. <https://doi.org/10.1021/ma991055s>
47. Ropson N, Dubois P, Jérôme R, Teyssié P (1995) Macromolecular engineering of poly lactones and poly lactides. 20. Effect of monomer, solvent, and initiator on the ring-opening polymerization as initiated with aluminum alkoxides. *Macromolecules* 28:7589–7598. <https://doi.org/10.1021/ma00127a002>
48. Antczak U, Antczak T, Galas E (1991) Enzymatic lactonization of 15-hydroxypentadecanoic and 16-hydroxyhexadecanoic acids to macrocyclic lactones. *Enzyme Microb Technol* 13:589–593. [https://doi.org/10.1016/0141-0229\(91\)90095-R](https://doi.org/10.1016/0141-0229(91)90095-R)
49. Hillmyer MA (2017) The promise of plastics from plants. *Science* 358(6365):868–870. <https://doi.org/10.1126/science.aao6711>
50. Thaire V, Chadwick D, Shah N (2018) Chemical engineering research and design sustainable production of chemical intermediates for nylon manufacture: a techno-economic analysis for renewable production of caprolactone. *Chem Eng Res Des* 135:140–152. <https://doi.org/10.1016/j.cherd.2018.05.026>
51. Moliner M (2014) State of the art of Lewis acid-containing zeolites: lessons from fine chemistry to new biomass transformation processes. *Dalton Trans* 43:4197–4208. <https://doi.org/10.1039/c3dt52293h>
52. Cao Q, Guo X, Guan J, Mu X, Zhang D (2011) Applied catalysis A: general a process for efficient conversion of fructose into 5-hydroxymethylfurfural in ammonium salts. *Appl Catal A, Gen* 403:98–103. <https://doi.org/10.1016/j.apcata.2011.06.018>
53. Yuriy RL, Chheda JN, Dumesic JA (2006) Phase modifiers promote efficient production of hydroxymethylfurfural from fructose. *Science* 312:1933–1937. <https://doi.org/10.1126/science.1126337>
54. Liu B, Zhang Z, Kent Z (2013) Microwave-assisted catalytic conversion of cellulose into 5-hydroxymethylfurfural in ionic liquids. *Chem Eng J* 215–216:517–521. <https://doi.org/10.1016/j.cej.2012.11.019>
55. Agustina D, Kumagai S, Nonaka M, Sasaki K (2013) Production of 5-hydroxymethyl furfural from sugarcane bagasse under hot compressed water. *Procedia Earth Planet Sci* 6:441–447. <https://doi.org/10.1016/j.proeps.2013.01.058>
56. Karimi K, Kheradmandinia S, Taherzadeh MJ (2006) Conversion of rice straw to sugars by dilute-acid hydrolysis. *Biomass Bioenergy* 30:247–253. <https://doi.org/10.1016/j.biombioe.2005.11.015>
57. Kumagai A, Lee S, Endo T (2016) Evaluation of the effect of hot-compressed water treatment on enzymatic hydrolysis of lignocellulosic nanofibrils with different lignin content using a quartz crystal microbalance. *Biotechnol Bioeng* 113(7):1441–1447. <https://doi.org/10.1002/bit.25911>

58. Watanabe M, Aizawa Y, Iida T, Aida TM, Levy C, Sue K, Inomata H (2005) Glucose reactions with acid and base catalysts in hot compressed water at 473 K. *Carbohydr Res* 340:1925–1930. <https://doi.org/10.1016/j.carres.2005.06.017>
59. Chareonlimkun A, Champreda V, Shotipruk A, Laosiripojana N (2010) Bioresource technology catalytic conversion of sugarcane bagasse, rice husk and corncob in the presence water (HCW) condition. *Bioresour Technol* 101:4179–4186. <https://doi.org/10.1016/j.biortech.2010.01.037>
60. Delbecq F, Len C (2018) Recent advances in the microwave-assisted production of hydroxymethylfurfural by hydrolysis of cellulose derivatives—a review. *Molecules* 23:1973. <https://doi.org/10.3390/molecules23081973>
61. Hansen TS, Woodley JM, Riisager A (2009) Efficient microwave-assisted synthesis of 5-hydroxymethylfurfural from concentrated aqueous fructose. *Carbohydr Res* 344:2568–2572. <https://doi.org/10.1016/j.carres.2009.09.036>
62. Shen Z, Yu X, Chen J (2016) Production of 5-hydroxymethylfurfural from fructose catalyzed by sulfonated bamboo-derived carbon prepared by simultaneous carbonization and sulfonation. *BioResources* 11(2):3094–3109
63. Lundberg DJ, Lundberg DJ, Hillmyer MA, Dauenhauer PJ (2018) Techno-economic analysis of a chemical process to manufacture methyl- ϵ -caprolactone from cresols. *ACS Sustain Chem Eng* 6:15316–15324. <https://doi.org/10.1021/acssuschemeng.8b03774>
64. Mandal D, Ahmad A, Khan MI, Kumar R (2002) Biocatalytic transformation of cyclohexanone by *Fusarium* sp. *J Mol Catal A: Chem* 181:237–241
65. Xie D, Shao Z, Achkar J, Zha W, Frost JW (2005) Microbial synthesis of triacetic acid lactone. *Biotechnol Bioeng* 93(4):727–736. <https://doi.org/10.1002/bit.20759>

Chapter 3

Polymers from Carbon Dioxide—A Route Towards a Sustainable Future



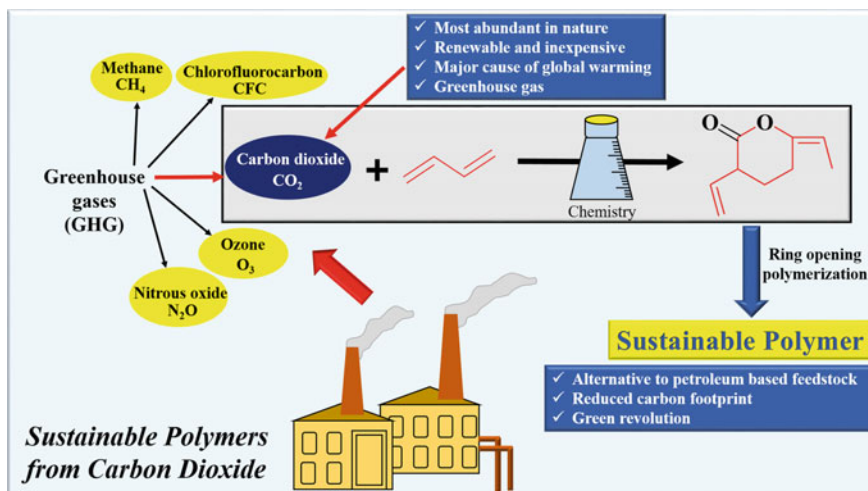
Neha Mulchandani and Vimal Katiyar

Abstract Carbon dioxide, which is one of the major causes of global warming, has posed alarmed issues with constant rising levels. It is, therefore, important to look forward into its alternate uses and reduce the global environmental impact. Various strategies for utilizing the greenhouse gas into possible-end products have been explored considering its abundant, non-toxic and renewable nature. However, the low reactivity of carbon dioxide has restricted its use in large-scale applications. The current chapter highlights the reaction mechanisms for fixing carbon dioxide into useful polymers and the challenges associated with it. The potential of carbon dioxide as a monomer along with the role of catalyst has been discussed. The existing technologies for developing polymers from carbon dioxide along with the future scope and applications have been portrayed. An emphasis has been laid on developing biodegradable polymers using greenhouse gas as the precursor with possible chemical routes and their limitations. The concept of sustainable polymers has been focused in terms of utilizing the greenhouse gas as precursor for developing the polymers with high yields using industrially viable approaches.

Graphical Abstract

N. Mulchandani · V. Katiyar (✉)
Department of Chemical Engineering, Indian Institute of Technology Guwahati, Kamrup,
Guwahati, Assam 781039, India
e-mail: vkatiyar@iitg.ac.in

© Springer Nature Singapore Pte Ltd. 2020
V. Katiyar et al. (eds.), *Advances in Sustainable Polymers*, Materials Horizons: From
Nature to Nanomaterials, https://doi.org/10.1007/978-981-15-1251-3_3



Keywords Carbon dioxide · Polymers · Greenhouse gas · Sustainable · Copolymerization

1 Introduction

Carbon dioxide (CO_2) is a greenhouse gas which is available in abundant amount in the atmosphere. The average lifetime of CO_2 molecule may be considered to be of the order of ten years before it is dissolved into the oceans [1]. CO_2 is not only available in the large amount in the atmosphere but is also regenerative in nature as it gets integrated with the natural cycle. The constant rise in the CO_2 levels has led the researchers to focus towards the mitigation [2] or finding alternate uses of this greenhouse gas in order to reduce the global environmental impact [3–6]. In order to reduce the greenhouse gas from further accumulating in environment, the strategy of capturing CO_2 has been adopted by several researchers. However, converting CO_2 into useful end products is preferred over storing it because of its non-toxic, renewable and inexpensive nature [7–11]. One such possibility is exploring its potential in developing monomers/precursors which would be utilized for the synthesis of polymers [12, 13]. Conventional polymers are usually derived from petroleum-based feedstock which is available in limited amount on the planet. At the current rate of consumption of petroleum-based feedstock, these resources are predicted to be exhausted by the next century [14–17]. Additionally, burning of fossil fuel leads to the accumulation of CO_2 in the atmosphere at a rate which is significantly higher than its usage by green plants during photosynthesis [18]. Thus, finding the alternatives for the petroleum-based resources is a prime concern of the present age [19, 20]. Considering this situation, using CO_2 as a precursor in the synthesis of polymers would not only reduce the human dependence on the fossil fuels but would also

reduce the accumulations of the potential greenhouse gas in the atmosphere along with developing polymers from a greener route. This strategy may aid in combating the ongoing environmental issues. The interesting properties of CO₂ at supercritical conditions, i.e. the viscosity and surface tension of CO₂ being comparable to that of gases while its solubility parameter, density and dielectric constant being comparable to that of liquids have witnessed its exploration in replacing the organic solvents [21–23]. However, it is difficult to fix CO₂ in the chemistry of polymerization due to its low reactivity and usually requires extreme conditions of temperature and pressure for its reaction. Catalysis is perhaps, one of the best solutions to overcome the thermodynamic stability of the most abundant C1 resource [24–26]. The current chapter describes the potential of the carbon dioxide as a monomer in synthesizing polymers/precursors for polymers and the mechanism involved therein. The possible exploitation of CO₂ for the effective synthesis of polycarbonate, polylactone, poly(limonene oxide), etc., have been discussed followed by the existing technologies for the commercial production of polymers from CO₂. The challenges associated with the existing technologies have been briefly described along with the future directions to it.

2 Carbon Dioxide: Potential as a Monomer

One of the most fascinating discoveries is the synthesis of aliphatic polycarbonate by the ring-opening copolymerization of CO₂ with epoxides. Epoxides are the cyclic ethers containing a three-atom ring, and their high reactivity is accounted for their strained ring structure which is due to the equilateral triangle formed by the ring. It is known that catalyst plays a crucial role in fixing CO₂ in the backbone of polymers. Additionally, the catalyst lays an essential effect on the yield, properties and applications of the polymers that are produced. In view of this, Trott et al. have reported the important findings in the field of catalysis for the ring-opening polymerization of CO₂ and epoxide [27].

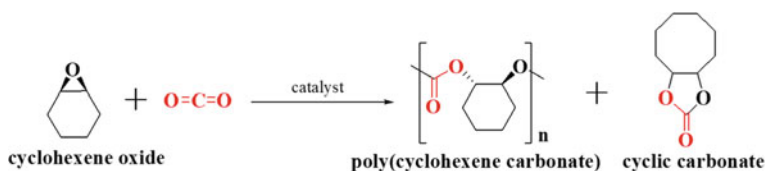
2.1 CO₂/Epoxide Copolymerization

The copolymerization of CO₂ with epoxide was successfully carried out by Inoue and co-workers in 1969 using organometallic catalysts [28]. They reported the synthesis of high molecular weight polycarbonates by alternating copolymerization of CO₂ with propylene oxide. Polycarbonates have been conventionally manufactured industrially by using bisphenol A (BPA) and phosgene precursors which are known for their harmful (during foetal development) [29] and toxic natures [30], respectively. Polycarbonates have been used substantially in food packaging, and the researchers have found that BPA tends to hydrolyze and release from the food packages causing an increased exposure to human health [31]. This has led the scientists to focus

towards developing plastics that are devoid of BPA [32]. In the work reported by Inoue et al., various organometallic catalysts were tested for the copolymerization of CO₂ and propylene oxide to yield polypropylene oxide. Among various catalyst systems, diethylzinc/water (1:1) system was found to be the most effective which yielded the methanol insoluble copolymer at 20–50 atm CO₂ pressure and 80 °C. Owing to its high efficiency, the same catalyst system was chosen for the copolymerization of CO₂ with other epoxides such as ethylene oxide, isobutylene oxide, styrene oxide and epichlorohydrin which were found to be soluble in methylene chloride. Their study led to the development of polypropylene carbonate with high molecular weight ($\overline{Mn}(\text{osm.}) = 115,000$). Further extending the copolymerization of CO₂/epoxide, the authors studied the copolymerization of CO₂ with 1,2-epoxycyclohexane (cyclohexene oxide, CHO) and 1,4-epoxycyclohexane [33]. In order to conduct the copolymerization, the catalyst and monomer (epoxide) were incorporated into the autoclave equipped with a magnetic stirrer which was followed by adding CO₂. The reaction was conducted at room temperature with CO₂ pressure of ~50 atm. To the reaction mixture, benzene was added to dilute it, followed by washing with HCl and water and subjecting it to freeze drying. They found that the diethylzinc/water system did not result in the copolymerization or homopolymerization of 1,4-epoxycyclohexane, whereas the catalyst system worked efficiently for 1,2-epoxycyclohexane suggesting the anionic character of copolymerization. Thermogravimetric analysis (TGA) was conducted, and the synthesized copolymer was found to degrade around 300 °C. Further, an important aspect of stereochemistry was highlighted with a focus on the existence of *cis* and *trans* isomers of 1,2-epoxycyclohexane. They concluded that the carbon atom configuration where ROP of epoxide took place (at the site of attack), the cleavage of C–O bond led to the inversion and yielded the product with *trans* configuration. However, the drawback of the Inoue's process was the formation of cyclic carbonate as a by-product which resulted from the back-biting of the growing polymer chain. The heterogeneous nature of the catalyst resulted in the lack of control of the active-site which possibly led to the formation of copolymers with high polyether content. Since the breakthrough achieved by Inoue's group, the researchers began to direct their efforts towards improving the efficiency and selectivity of catalysts and its derivatives.

Mechanism

Darensbourg et al. had prepared zinc(II) phenoxides as homogenous catalysts with available active sites for the copolymerization of CHO and CO₂ to obtain poly(cyclohexene carbonate) (PCHC) with high molecular weight (Scheme 1) [34].



Scheme 1 Synthesis of poly(cyclohexene carbonate) from cyclohexene oxide

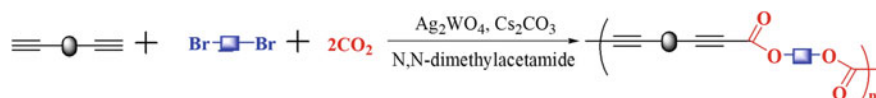
Table 1 Parameters for the reaction of CO₂ with epoxides

Copolymer system	Catalyst	p (CO ₂) (bar)	T (°C)	t (h)	References
CO ₂ + PPO	ZnEt ₂ /H ₂ O	20–50	80	48	[35]
CO ₂ + CHO	ZnEt ₂ /H ₂ O	~50	RT	45	[12]
CO ₂ + CHO	Zn(II) phenoxides	~55	90	69	[34]
CO ₂ + CHO	Zn-fluoroalkyl	~57	60–172	24	[36]

The reaction was carried out at 90 °C under 800 psi of CO₂ for 69 h (Table 1). They obtained high conversion of cyclohexene oxide to the final polymer with high turnover (more than 350 g polymer/g Zn). This was followed by the development of CO₂ soluble Zn-based catalyst for the synthesis of polycarbonates by Super et al. [21]. They synthesized fluoroalkyl monoester by using maleic anhydride, tridecafluorooctanol, solution of triethylamine in toluene reagents followed by its purification and its reaction with zinc oxide in order to form Zn-fluoroalkyl catalyst. They further utilized the catalyst for the reaction of CHO with CO₂ at ~850 psi of CO₂ (its vapour pressure). They fixed the catalyst to monomer ratio and varied the temperature for synthesizing the series of polymers. The maximum yield of the polymer (440 g polymer/g Zn) was achieved at 110 °C. Further, a series of reactions were carried out with varying the pressure (1000–5000 psig) and fixing the temperature and time to 110 °C and 24 h, respectively. The maximum conversion and selectivity were achieved at 2000 psig pressure being ~75% and ~55%, respectively.

2.2 CO₂/Alkyne Copolymerization

Copolymerization of CO₂ with alkynes involves the carbon–carbon triple bonds as the building blocks for the reaction. This is a unique technique developed to yield poly(alkanoate)s with high weight average molecular weight ($M_w \sim 31,400$). The reaction of CO₂ with alkyl dihalides and diynes in presence of Ag₂WO₄ catalyst, Cs₂CO₃ additive along with *N,N*-dimethylacetamide (Scheme 2) was reported by Song et al. which resulted in poly(alkanoates) with high yields (~95%) possessing superior thermal and chemical stability [37]. The reactions were conducted at very mild conditions (80 °C, 12 h). Such efficient and robust reaction resulting in high yield of the final product may be considered as an industrially viable process. Furthermore, the reaction of CO₂ with alkyl dihalide and triphenylamine (TPA) containing



Scheme 2 Polymerization reaction of dienes, alkyl halide and CO₂ in presence of Ag₂WO₄ and Cs₂CO₃

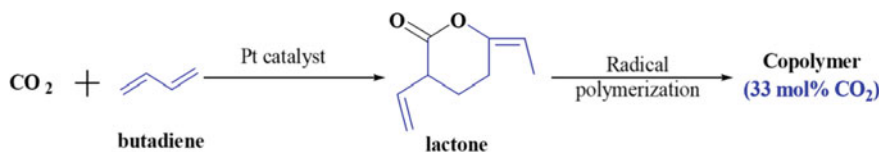
diyne led to the formation of telechelic polymer via step-growth polymerization. The synthesized telechelic polymer can be used for the synthesis of high molecular weight functional polymers by continuously adding alkyl dihalide in presence of catalyst and CO_2 . The direct conversion of CO_2 into useful end products such as poly(alkanoate)s reports the potential of the greenhouse gas in useful chemical reactions under mild conditions. The synthesized poly(alkanoates) may be considered as polyesters due to their structure and may be hydrolyzed under alkaline environment at ambient conditions in few minutes which makes them as promising materials for biomedical as well as engineering applications. In this regard, utilization of CO_2 for the development of end product that is biodegradable lays a significant impact and may be a solution to the current environmental issues.

Mechanism

See Scheme 2.

2.3 CO_2 /Olefin Copolymerization

The copolymerization of CO_2 with olefins has been a subject of broad interest; however, it is restricted by the propagation step which is endothermic; and on several occasions, homopolymerization of olefin takes place due to the reaction failure. In this regard, Nakano et al. have adopted a unique strategy to overcome the barriers associated in the reaction by using a lactone intermediate. The copolymerization of CO_2 with 1,3-butadiene led to the formation of 3-ethylidene-6-vinyltetrahydro-2H-pyran-2-one (lactone) which was followed by the homopolymerization of lactone [38] as shown in Scheme 3. The synthesized copolymers consisted of 33 mol% CO_2 which was consistent with the theoretical values. Furthermore, they extended their research to develop one-pot copolymerization process of CO_2 and butadiene along with one-pot terpolymerization process which was considered to be a sustainable and scalable process. They had used a mixture of dienes such as butadiene, isoprene and 1,3-pentadiene by varying their molar ratios and reacted with CO_2 in presence of palladium acetylacetonate, triisopropylphosphine and ethylene carbonate at 80 °C. The reaction time was varied from 3 to 20 h for the mixture of dienes. Furthermore, the synthesized lactones were subjected to polymerization in presence of 1-1'-azobis (cyclohexane-1-carbonitrile) and zinc chloride which resulted in the formation of terpolymers, i.e. (CO_2 /butadiene/isoprene and CO_2 /butadiene/1,3-pentadiene) with molecular weights (M_n) 5,500 and 16,000 and yields of 46% and 35%, respectively.



Scheme 3 Copolymerization of CO_2 with butadiene by radical polymerization

Additionally, the glass transition temperature of these polymers was found to be 63 °C and 33 °C, respectively. The authors concluded that their process had the potential to be utilized on a large scale in order to synthesize the synthetic polymers via a green and sustainable route.

Mechanism

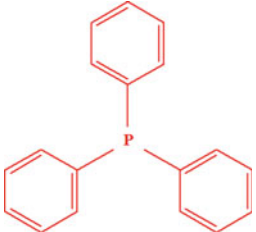
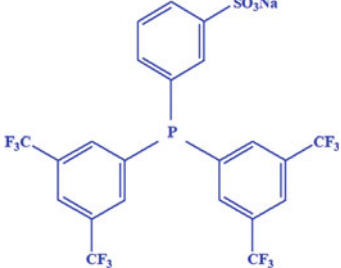
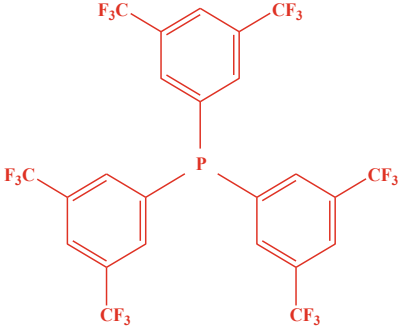
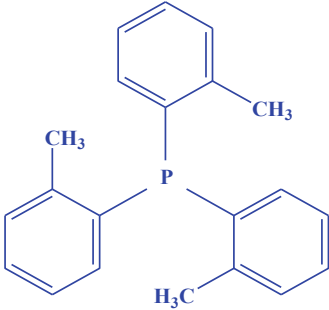
The selective telomerization of 1,3-butadiene with CO₂ was carried out by Balbino et al. to develop lactones [39]. The catalyst used was Pd/phosphine along with *p*-hydroquinone, *N,N*-diisopropylethylamine and acetonitrile as solvent. They used a series of phosphines as shown in Table 2 to be used as ligands for the Pd catalyst. They carried out the reactions at 30 bar pressure of CO₂ and 70 °C for 5 h. The major products obtained were lactones and dimers. They also found that the telomerization reaction did not take place in the absence of phosphate ligand. The turnover number (TON) obtained by using PTpOME was 4500 with 96% selectivity yielding δ -lactone. The reaction was deactivated after 5 h by 1,3-dialkylimidazolium ionic liquids.

2.4 CO₂/Diol Copolymerization

The direct copolymerization of CO₂ with diols was attempted by Kadokawa et al. by taking into consideration the conventional processes which usually require high cost or hazardous chemicals for the production of polycarbonates. The reaction of CO₂ with *p*- and *m*-xylene glycols was carried out in presence of condensing agents to yield poly(xylylene carbonate) [40]. Furthermore, the direct copolymerization of CO₂ with 1,4-butanediol was carried out by Tamura et al. wherein the catalyst used for the reaction was cerium oxide (CeO₂) in presence of 2-cyanopyridine as a promotor [41]. They carried out the reactions in an autoclave wherein they inserted the catalyst, promotor along with 1,4-butanediol. They purged the reactor with CO₂ (1 MPa) thrice followed by pressurizing the autoclave with CO₂ (5 MPa) at room temperature. Later, they heated the autoclave to 433 K (CO₂ pressure: 12 MPa) under constant stirring followed by immersing in water bath to achieve cooling. The mixture of THF and 1-hexanol was used as solvents which were added to the liquid phase. The resulting co-oligomers were precipitated followed by filtration and analysed by gas chromatography coupled with mass spectrometer (GC-MS), nuclear magnetic resonance (NMR), size exclusion chromatography (SEC), high-pressure liquid chromatography (HPLC) and matrix-assisted laser detection ionization-time of flight (MALDI-TOF). The reaction possibly takes place in the following steps which is shown in Scheme 4.

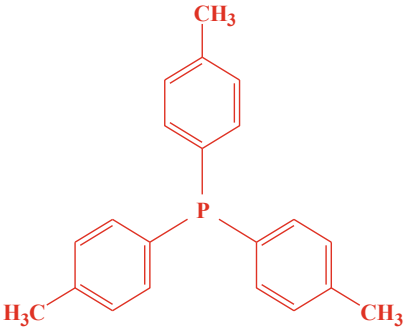
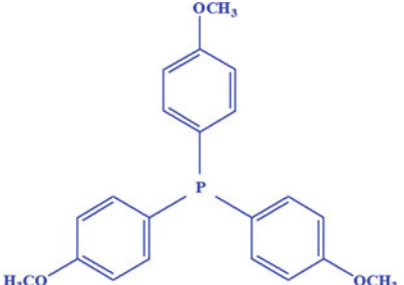
1. 1,4-butanediol adsorbs on the surface of CeO₂ resulting in alkoxides.
2. CO₂ is inserted into the alkoxide and species resulting in the formation of carbonates.
3. The nucleophilic attack of oxygen (present in alkoxide) to the carbonates leads to the formation of carbonate.

Table 2 Phosphines used as ligands for the Pd catalyst

Sr. no.	Ligands	Structure
1.	PPh ₃ [Triphenylphosphine]	
2.	Dan2phos	
3.	PTmmCF ₃ [tris(m,m-di-trifluoromethylphenyl) phosphine]	
4.	PToME [triphenylphosphine]	

(continued)

Table 2 (continued)

Sr. no.	Ligands	Structure
5.	PTpME	
6.	PTpOME [tris-(<i>p</i> -methoxyphenyl)-phosphine]	

- The water (H₂O) produced in the above step is removed by the hydration of 2-cyanopyridine to 2-picolinamide in presence of CeO₂.
- The reaction of carbonate with the co-oligomer results in the formation of polytetramethylene carbonate.

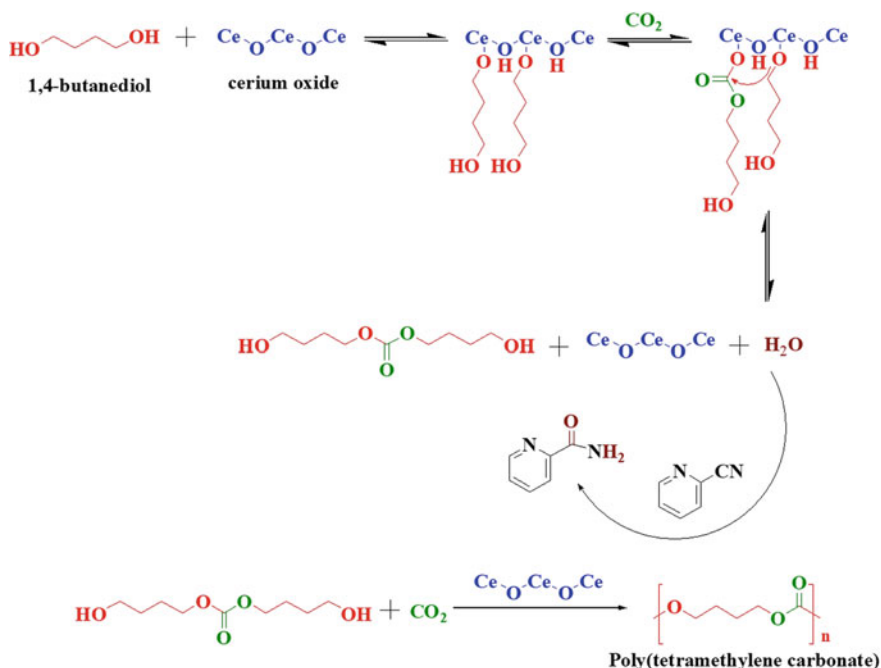
Mechanism

See Scheme 4.

2.5 Other Methods

2.5.1 Polymethacrylates from CO₂

It is possible to obtain five-membered cyclic carbonates by the reaction of CO₂ with epoxides under mild conditions. However, these reactions suffer from the drawbacks of the multiple steps required to transform CO₂. For instance, poly(methacrylates)

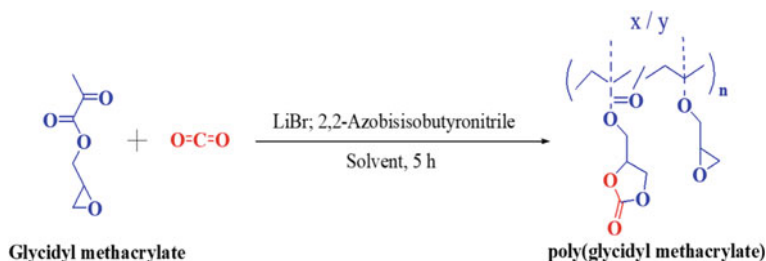


Scheme 4 Polytetramethylene carbonate formed by the reaction of 1,4-butanediol, cerium oxide and CO₂

(utilizing CO₂) are usually prepared by two-step reaction and require an additional purification process along with high reaction time. To overcome these drawbacks, Ochiai et al. proposed a single-step reaction for the radical polymerization of glycidyl methacrylate (GMA) along with CO₂ fixation [42]. They carried out the radical polymerization of GMA under CO₂ environment (1 atm) and lithium bromide (LiBr) and 2,2-azobisisobutyronitrile (AIBN). They conducted the reactions in *N*-methyl pyrrolidinone (NMPy), *N,N*-dimethyl formamide (DMF), 1,4-dioxane (Diox) and dimethyl sulfoxide (DMSO) solvents. The poor solubility of LiBr in Diox resulted in the negligible fixation of CO₂. The reactions carried out in presence of NMPy at lower temperature led to the decrease in the CO₂ incorporation ratio as well as the yield which may be due to the polymerization reaction occurring much faster than that of CO₂ fixation. It was found that the LiBr could control the carbonation degree. The trials had been made by employing benzoyl peroxide as an initiator which was not effective possibly due to the lower conversion of the moieties with double bond or side reactions (may be speculated as the colour of obtained after the polymerization was red). The typical reaction scheme for the radical polymerization of GMA along with CO₂ fixation is shown in Scheme 5.

Mechanism

See Scheme 5.



Scheme 5 Synthesis of poly(glycidyl methacrylate) from CO₂

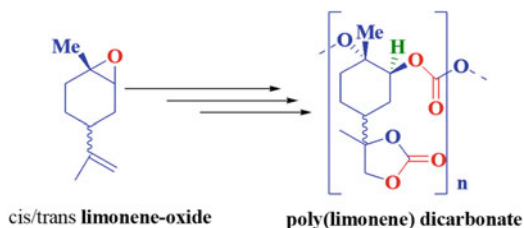
2.5.2 Bioderived Epoxides from CO₂

Although several epoxides have been explored for the reaction with CO₂, not much focus has been laid on the bioderived epoxides. D-limonene is the cyclic monoterpene which is usually extracted from the orange peel. Limonene oxide is available in abundant amount which is structurally similar to cyclohexene oxide and has low cost. The alternating copolymerization of limonene oxide and CO₂ was reported by Byrne et al. under mild conditions to yield polycarbonates [43]. The copolymerization was carried out using β-diiminate zinc acetate as catalyst. They observed that the catalyst led to the formation of regioregular polycarbonate with high selectivity of trans isomer at 25 °C and 100 psi pressure of CO₂. The resulting copolymer was found to have a narrow molecular weight distribution with >99% carbon linkage. Furthermore, Kindermann et al. reported the reaction of limonene oxide with CO₂ in presence of Al(III) complex catalyst to develop poly(limonene) dicarbonate [44]. They mixed limonene oxide (cis/trans mixture), bis-triphenylphosphine iminium chloride (PPNCl) and catalyst and placed inside the stainless steel reactor followed by purging with CO₂ thrice. The reactor pressure was increased to 15 bar with temperature 45 °C, and the reaction was carried out for 48 h. The resulting material was poly(limonene carbonate) which was dissolved in dichloromethane and oxidized at 0 °C using 3-chloroperbenzoic acid for 12 h to form poly(limonene-8,9-oxide carbonate). Further, PPNCl was used as a nucleophile to copolymerize the epoxide with CO₂. They were able to obtain the polycarbonates with glass transition (T_g) as high as 180 °C and high molecular weight (1.3–15.1 kg/mol) through sequential approach. The reaction mechanism is shown in Scheme 6. The developed polycarbonates find applications as precursors for the coating materials, and formation of polymer blends with tailored properties.

Mechanism

See Scheme 6.

Scheme 6 Poly(limonene) dicarbonate from cis/trans limonene oxide



3 Existing Technologies for Making Polymers from CO₂

Novomer Inc. (USA) founded by Geoffrey Coates (Cornell University graduate) has initiated the production of polyols (copolymers resulting from epoxides and CO₂) which have the applications in light-weight polyurethane foams. The Novomer technology may also be adopted by Ford Motor Co. to use polyols in the cushions of the automobile seats. This will indeed lay a great impact on the society [45]. Also, the industrial production of poly(propylene carbonate) has been witnessed in China which aims at producing poly(propylene carbonate) (average mol wt. of tens of thousands) by using diethylzinc-glycerol system (Nd(CCl₃COO)₃) [46]. Norner™, a Norway-based company has also actively been involved in the development of CO₂-based polycarbonates. It has been able to design a continuous process for the production of polycarbonates and is aiming towards developing pilot scale process and commercialization of the product [47]. Researchers from Rutgers University have established a startup “RENEWCO₂” which is the outcome of the project carried out under Prof. Charles Dismukes. They have developed an electrochemical method to convert CO₂ and water into polymers using the nickel and phosphorous-based catalysts [48]. A German-based company “Covestro” headed by Markus Steilemann has developed CO₂-based polyols which are used to make the synthetic sports flooring. They have made a novel CO₂-based binder for sports flooring which has been installed at the Crefelder Hockey and Tennis Club which is one of the leading hockey facilities in Germany. These CO₂-based materials are replacing ~20% of fossil fuels that are required for the production of polymers [49].

4 Current Challenges and Future Scope

Utilization of CO₂ as a feedstock for the development of sustainable polymers could be a possible approach in reducing the human dependence on the non-renewable resources that are currently being utilized for the production of plastics. The resulting polymers by fixing CO₂ may serve as good candidates for replacing the conventional plastics due to their attractive properties such as biodegradability and biocompatibility. CO₂-based polymers may also be explored in biomedical applications such as implants. The most widely explored polycarbonate from CO₂ is quite similar

to the currently used thermoplastics in terms of its characteristics such as being processed by the conventional moulding techniques. Due to its easy processability, it has obtained a commercial acceptance. However, the lower glass transition temperature of these materials restricts their usage in certain applications and thus blending with conventional polymers such as polyethylene (PE) and polypropylene (PP) may serve as an effective strategy in achieving optimum properties for end-use applications. Nevertheless, the complete potential of these materials is yet to be explored as the technological development is still at an early stage. Additionally, the other polymers/copolymers such as poly(methacrylates), poly(lactones) and poly(methacrylates) require insights into the chemistry to scale up the process to a commercial level. These methods, if developed may bring a global transformation in terms of replacement of various petroleum-based precursors and thus reduce the global environmental impact. Furthermore, the cost of the polymers plays an important role in commercialization of the product. It requires a great deal of scientific effort in lowering the cost of the CO₂-based polymers in order to compete with the existing fossil-based polymers. Thus, it can be said that the development of CO₂-derived polymers has given a pathway for adopting a renewable and non-toxic route in order to save the planet from further worsening but the complete revolution towards sustainability would require cost-effective strategies.

References

1. Revelle R, Suess HE (1957) Carbon dioxide exchange between atmosphere and ocean and the question of an increase of atmospheric CO₂ during the past decades. *Tellus* 9:18–27. <https://doi.org/10.1111/j.2153-3490.1957.tb01849.x>
2. Packer M (2009) Algal capture of carbon dioxide; biomass generation as a tool for greenhouse gas mitigation with reference to New Zealand energy strategy and policy. *Energy Policy* 37:3428–3437. <https://doi.org/10.1016/j.enpol.2008.12.025>
3. Olah GA, Goepfert A, Prakash GKS (2009) Chemical recycling of carbon dioxide to methanol and dimethyl ether: from greenhouse gas to renewable, environmentally carbon neutral fuels and synthetic hydrocarbons. *J Org Chem C* 74:487–498. <https://doi.org/10.1021/jo801260f>
4. Zhang Y, Xia J, Song J, Zhang J, Ni X, Jian Z (2019) Combination of ethylene, 1,3-butadiene, and carbon dioxide into ester-functionalized polyethylenes via palladium-catalyzed coupling and insertion polymerization. *Macromolecules* 52:2504–2512. <https://doi.org/10.1021/acs.macromol.9b00195>
5. Gray ML, Champagne KJ, Fauth D, Baltrus JP, Pennline H (2008) Performance of immobilized tertiary amine solid sorbents for the capture of carbon dioxide. *Int J Greenhouse Gas Cont* 2:3–8. [https://doi.org/10.1016/S1750-5836\(07\)00088-6](https://doi.org/10.1016/S1750-5836(07)00088-6)
6. Riduan SN, Zhang Y (2010) Recent developments in carbon dioxide utilization under mild conditions. *Dalton Trans* 39:3347–3357. <https://doi.org/10.1039/B920163G>
7. ElMekawy A, Hegab HM, Mohanakrishna G, Elbaz AF, Bulut M, Pant D (2016) Technological advances in CO₂ conversion electro-biorefinery: a step toward commercialization. *Biores Technol* 215:357–370. <https://doi.org/10.1016/j.biortech.2016.03.023>
8. Islam Mozumder MS, Garcia-Gonzalez L, Wever HD, Volcke EIP (2015) Poly(3-hydroxybutyrate) (PHB) production from CO₂: model development and process optimization. *Biochem Eng J* 98:107–116. <https://doi.org/10.1016/j.bej.2015.02.031>
9. Qin Y, Sheng X, Liu S, Ren G, Wang X, Wang F (2015) Recent advances in carbon dioxide based copolymers. *J CO₂ Util* 11:3–9. <https://doi.org/10.1016/j.jcou.2014.10.003>

10. Albo J, Alvarez-Guerra M, Castaño P, Irabien A (2015) Towards the electrochemical conversion of carbon dioxide into methanol. *Green Chem* 17:2304–2324. <https://doi.org/10.1039/C4GC02453B>
11. Sun X, Zhu Q, Kang X, Liu H, Qian Q, Zhang Z, Han B (2016) Molybdenum-Bismuth bimetallic chalcogenide nanosheets for highly efficient electro catalytic reduction of carbon dioxide to methanol. *Angew Chem* 55:6771–6775. <https://doi.org/10.1002/anie.201603034>
12. Inoue S, Koinuma H, Tsuruta T (1969) Copolymerization of carbon dioxide and epoxide. *J Polym Sci B* 7:287–292. <https://doi.org/10.1002/pol.1969.110070408>
13. Vogdanis L, Heitz W (1986) Carbon dioxide as a monomer, 3. The polymerization of ethylene carbonate. *Makromol Chem Rapid Comm* 7:543–547. <https://doi.org/10.1002/marc.1986.030070901>
14. Okada M (2002) Chemical syntheses of biodegradable polymers. *Prog Polym Sci* 27:87–133. [https://doi.org/10.1016/S0079-6700\(01\)00039-9](https://doi.org/10.1016/S0079-6700(01)00039-9)
15. Danner H, Braun R (1999) Biotechnology for the production of commodity chemicals from biomass. *Chem Soc Rev* 28:395–405. <https://doi.org/10.1039/A806968I>
16. Alagi P, Hong SC (2015) Vegetable oil-based polyols for sustainable polyurethanes. *Macromol Res* 23:1079–1086. <https://doi.org/10.1007/s13233-015-3154-6>
17. Zhang C, Garrison TF, Madbouly SA, Kessler MR (2017) Recent advances in vegetable oil-based polymers and their composites. *Prog Polym Sci* 71:91–143. <https://doi.org/10.1016/j.progpolymsci.2016.12.009>
18. Cui Y, Tang X, Huang X, Chen Y (2003) Synthesis of the star-shaped copolymer of ϵ -caprolactone and l-lactide from a cyclotriphosphazene core. *Biomacromol* 4:1491–1494. <https://doi.org/10.1021/bm034237+>
19. Mooney BP (2009) The second green revolution? Production of plant-based biodegradable plastics. *Biochem J* 418:219–232. <https://doi.org/10.1042/BJ20081769>
20. Fortman JL, Chhabra S, Mukhopadhyay A, Chou H, Lee TS, Steen E, Keasling JD (2008) Biofuel alternatives to ethanol: pumping the microbial well. *Trends Biotechnol* 26:375–381. <https://doi.org/10.1016/j.tibtech.2008.03.008>
21. Super M, Berluche E, Costello C, Beckman E (1997) Copolymerization of 1,2-epoxycyclohexane and carbon dioxide using carbon dioxide as both reactant and solvent. *Macromolecules* 30:368–372. <https://doi.org/10.1021/ma960755j>
22. Gao Z, Zhao H, Li Z, Tan X, Lu X (2012) Photosynthetic production of ethanol from carbon dioxide in genetically engineered cyanobacteria. *Energy Environ Sci* 5:9857–9865. <https://doi.org/10.1039/C2EE22675H>
23. Riduan SN, Zhang Y, Ying JY (2009) Conversion of carbon dioxide into methanol with silanes over N-heterocyclic carbene catalysts. *Angew Chem* 48:3322–3325. <https://doi.org/10.1002/anie.200806058>
24. Darensbourg DJ, Holtcamp MW (1996) Catalysts for the reactions of epoxides and carbon dioxide. *Coordin Chem Rev* 153:155–174. [https://doi.org/10.1016/0010-8545\(95\)01232-X](https://doi.org/10.1016/0010-8545(95)01232-X)
25. Ang RR, Sin LT, Bee ST, Tee TT, Kadhum AAH, Rahmat AR, Wasmi BA (2015) A review of copolymerization of green house gas carbon dioxide and oxiranes to produce polycarbonate. *J Clean Prod* 102:1–17. <https://doi.org/10.1016/j.jclepro.2015.04.026>
26. Zhang H, Liu B, Ding H, Chen J, Duan Z (2017) Polycarbonates derived from propylene oxide, CO₂, and 4-vinyl cyclohexene oxides terpolymerization catalyzed by bifunctional salcyCoIIIINO₃ complex and its post-polymerization modification. *Polymer* 129:5–11. <https://doi.org/10.1016/j.polymer.2017.09.033>
27. Trott G, Saini PK, Williams CK (2016) Catalysts for CO₂/epoxide ring-opening copolymerization. *Philos Trans A Math Phys Eng Sci* 374:20150085. <https://doi.org/10.1098/rsta.2015.0085>
28. Inoue S, Koinuma H, Tsuruta T (1969) Copolymerization of carbon dioxide and epoxide with organometallic compounds. *Makromol Chem* 130:210–220. <https://doi.org/10.1002/macp.1969.021300112>
29. Wang P, Park JH, Sayed M, Chang TS, Moran A, Chen S, Pyo SH (2018) Sustainable synthesis and characterization of a bisphenol A-free polycarbonate from a six-membered dicyclic carbonate. *Polym Chem* 9:3798–3807. <https://doi.org/10.1039/C8PY00676H>

30. Woo BG, Choi KY, Song KH, Lee SH (2001) Melt polymerization of bisphenol-A and diphenyl carbonate in a semibatch reactor. *J Appl Polym Sci* 80:1253–1266. <https://doi.org/10.1002/app.1211>
31. Yang CZ, Yaniger SI, Jordan VC, Klein DJ, Bittner GD (2011) Most plastic products release estrogenic chemicals: a potential health problem that can be solved. *Environ Health Perspect* 119:989–996. <https://doi.org/10.1289/ehp.1003220>
32. Xu J, Feng E, Song J (2014) Renaissance of aliphatic polycarbonates: new techniques and biomedical applications. *J Appl Polym Sci* 131. <https://doi.org/10.1002/app.39822>
33. Inoue S, Koinuma H, Yokoo Y, Tsuruta T (1971) Stereochemistry of copolymerization of carbon dioxide with epoxy cyclohexane. *Die Makromolekulare Chemie* 143:97–104
34. Darensbourg DJ, Holtcamp MW (1995) Catalytic activity of zinc(II) phenoxides which possess readily accessible coordination sites. copolymerization and terpolymerization of epoxides and carbon dioxide. *Macromolecules* 28:7577–7579. <https://doi.org/10.1021/ma00126a043>
35. Inoue S, Kobayashi M, Koinuma H, Tsuruta T (1972) Reactivities of some organozinc initiators for copolymerization of carbon dioxide and propylene oxide. *Makromol Chem* 155:61–73. <https://doi.org/10.1002/macp.1972.021550107>
36. Super M, Beckman EJ (1998) Copolymerization of CO₂ and cyclohexene oxide. *Macromol Symp* 127:89–108. <https://doi.org/10.1021/acs.macromol.8b01651>
37. Song B, He B, Qin A, Tang BZ (2018) Direct polymerization of carbon dioxide, diynes, and alkyl dihalides under mild reaction conditions. *Macromolecules* 51:42–48. <https://doi.org/10.1021/acs.macromol.7b02109>
38. Nakano R, Ito S, Nozaki K (2014) Copolymerization of carbon dioxide and butadiene via a lactone intermediate. *Nat Chem* 6:325. <https://doi.org/10.1038/nchem.1882>
39. Balbino JM, Dupont J, Bayón JC (2018) Telomerization of 1,3-Butadiene with Carbon Dioxide: a highly efficient process for δ -lactone generation. *ChemCatChem* 10:206–210. <https://doi.org/10.1002/cctc.201701058>
40. Kadokawa J, Habu H, Fukamachi S, Karasu M, Tagaya H, Chiba K (1998) Direct polycondensation of carbon dioxide with xylylene glycols: a new method for the synthesis of polycarbonates. *Macromol Rapid Commun* 19:657–660. [https://doi.org/10.1002/\(SICI\)1521-3927\(19981201\)19:12%3c657:AID-MARC657%3e3.0.CO;2-R](https://doi.org/10.1002/(SICI)1521-3927(19981201)19:12%3c657:AID-MARC657%3e3.0.CO;2-R)
41. Tamura M, Ito K, Honda M, Nakagawa Y, Sugimoto H, Tomishige K (2016) Direct Copolymerization of CO₂ and Diols. *Sci Rep* 6:24038. <https://doi.org/10.1038/srep24038>
42. Ochiai B, Hatano Y, Endo T (2008) fixing carbon dioxide concurrently with radical polymerization for utilizing carbon dioxide by low-energy cost. *Macromolecules* 41:9937–9939. <https://doi.org/10.1021/ma801960q>
43. Byrne CM, Allen SD, Lobkovsky EB, Coates GW (2004) Alternating copolymerization of limonene oxide and carbon dioxide. *J Am Chem Soc* 126:11404–11405. <https://doi.org/10.1021/ja0472580>
44. Kindermann N, Cristófol V, Kleij AW (2017) Access to biorenewable polycarbonates with unusual glass-transition temperature (T_g) modulation. *ACS Catal* 7:3860–3863. <https://doi.org/10.1021/acscatal.7b00770>
45. Kemp TJ (2006) Carbon dioxide as a polymer feedstock. *Sci Prog* 97:249–260. <https://doi.org/10.3184/003685014x14092298279136>
46. Sugimoto H, Inoue S (2006) Recent progress in the synthesis of polymers based on carbon dioxide. *Pure Appl Chem* 78:1823. <https://doi.org/10.1351/pac200678101823>
47. Barreto C, Hansen E, Fredriksen S (2012) Novel solventless purification of poly(propylene carbonate): Tailoring the composition and thermal properties of PPC. *Polym Degrad Stab* 97:893–904. <https://doi.org/10.1016/j.polymdegradstab.2012.03.033>
48. Calvinho KUD, Laursen AB, Yap KMK, Goetjen TA, Hwang S, Murali N, Meija-Sosa B, Lubarski A, Teeluck KM, Hall ES, Garfunkel E, Greenblatt M, Dismukes GC (2018) Selective CO₂ reduction to C₃ and C₄ oxyhydrocarbons on nickel phosphides at overpotentials as low as 10 mV. *Energy Environ Sci* 11:2550–2559. <https://doi.org/10.1039/C8EE00936H>
49. The Chemical Engineer (2016) Covestro uses captured CO₂ to produce plastics. *The Chemical Engineer*. Available: <https://www.thechemicalengineer.com/news/covestro-uses-captured-co2-to-produce-plastics/>

Chapter 4

Production, Characterization, and Applications of Biodegradable Polymer: Polyhydroxyalkanoates



Sushobhan Pradhan , Pritam Kumar Dikshit 
and Vijayanand S. Moholkar 

Abstract The usage of petroleum-based polymers by the human beings has enhanced the quality and comfort of life in the recent decades. These polymers are extremely persistent in the environment, and none of the conventional techniques can effectively degrade such polymers. A remedy to this issue is the application of biodegradable polymers from different organic sources. Biodegradable polymers are comprised of monomers that are linked with one another through various functional groups with unstable links in the backbone. During degradation, these polymers are broken down into molecules that are degradable by conventional biological techniques. Biodegradable polymers have been synthesized from four different sources: agro-resources, microorganisms, biotechnological renewable sources, and classical chemical synthesis. Polyhydroxyalkanoates (PHAs) are one of the prime substitutes for conventional plastics because they are derived from renewable feedstock by fermentation and are completely biodegradable upon disposal. The fermentation route for the synthesis of PHAs is one of the best substitutes for petroleum-derived polymers. PHAs have excellent physical characteristics, such as low toxicity and high molecular weight, and they can be naturally produced from several carbon sources using numerous microorganisms. Moreover, they possess mechanical and physical properties similar to synthetic plastics such as polyethylene and polypropylene like tensile strength and melting point, etc. More than 300 different types of bacteria, including both gram-positive and gram-negative strains, produce PHAs. In order to reduce the production cost of PHAs, several inexpensive substrates, such as whey, malt, soy and starch waste, palm oil, beet, and cane molasses, are being used. In the

S. Pradhan

School of Chemical Engineering, Oklahoma State University, Stillwater, OK 74078, USA

e-mail: sushobhan.pradhan@okstate.edu

P. K. Dikshit

The Energy and Resources Institute (TERI), Darbari Seth Block, IHC Complex, Lodhi Road, New Delhi 110003, India

e-mail: biotech.pritam@gmail.com

V. S. Moholkar (✉)

Department of Chemical Engineering, Indian Institute of Technology Guwahati, Guwahati 781039, Assam, India

e-mail: vmoholkar@iitg.ac.in

© Springer Nature Singapore Pte Ltd. 2020

V. Katiyar et al. (eds.), *Advances in Sustainable Polymers*, Materials Horizons: From Nature to Nanomaterials, https://doi.org/10.1007/978-981-15-1251-3_4

recent past, several invasive weed biomasses have been used in the microbial fermentation process for the production of PHAs. This invasive alien species (IAS) is non-native to an ecosystem and when introduced outside its natural habitats, affects the native biodiversity in almost every ecosystem. Hence, the production of Poly(3-hydroxybutyrate) (PHB) using these invasive weeds is a brand new technology for the production of biodegradable polymers. Various blends like copolymers have been developed to improve the cost, performance, and physical properties of PHAs. Several PHA nanocomposites have been developed to enhance mechanical properties. PHAs degrade into carbon dioxide and water under aerobic conditions and to methane under anaerobic conditions without any harmful products. These biopolymers can also be degraded either by thermal mode or by enzymatic hydrolysis. The last two decades have seen a shift from bio-stable materials to biodegradable (i.e., hydrolytically and enzymatically) materials for medical and related applications. Initially, PHAs were used in the packaging industry, but their importance was later shifted to the medical industry, pharmacological, and agricultural sectors. This chapter addresses the synthesis and benefits of PHAs over petroleum-derived polymers, their biodegradable characteristics, and applications in several sectors.

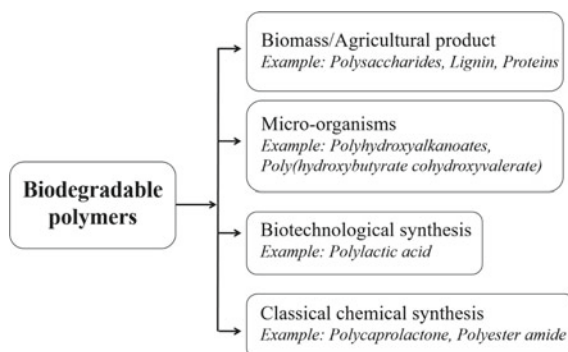
Keywords Biodegradable polymer · Polyhydroxyalkanoates · Fermentation · Microorganism · Copolymers · Carbon substrate

1 Introduction

The world has witnessed the consumption and side effects of fossil fuel derivatives for the last two centuries. This extensive usage of petrochemical derived polymers is accountable for worldwide ecological imbalance in several sectors: the plant kingdom, aquatic and terrestrial life, food chains, and stability of the earth's atmosphere [1]. These polymers are extremely persistent in nature, and an alarming accumulation of such plastics have caused problems in safe disposal, recycling, landfilling of waste, bio- or photo-degradation, and incineration. Therefore, the demand for biodegradable polymers has become an urgent need of the hour. Biodegradable polymers consist of monomers that are linked with each other through various functional groups having unstable links in the backbone. Several biologically accepted molecules form in the course of the degradation process of these polymers. Biopolymers are usually developed from four different sources: biomass/agricultural products, microorganisms, biotechnologically renewal sources, and chemically synthesis route. A schematic of various types of biodegradable polymers has been illustrated with examples in Fig. 1 [2].

Among several categories of biodegradable polymers, polyhydroxyalkanoates (PHAs) are one of the most promising alternatives to replace the petroleum-derived polymers because of their excellent physical properties. They resolve the problem of the accumulation of conventional non-biodegradable polymers. These polymers are commonly produced by a wide variety of microbial routes. They can be degraded

Fig. 1 Classification of biodegradable polymers



under both aerobic conditions (with water) and anaerobic conditions (methane and water). PHAs are the polyesters, which consists of various repeated chains of hydroxyalkanoates (HAs) with different side chains. It is reported that more than 150 types of (R)-3-hydroxy fatty acids have been identified as part of the PHA family [3]. Because of biodegradability and biocompatibility characteristics, PHAs are of interest for potential research and its commercialization. Saturated, unsaturated, branched, and substituted alkyl groups [4] can replace the monomer unit *R* group in PHAs. Polyhydroxybutyrate (PHB) is the most common and simplest polymer of PHAs family. These polymers are produced intracellularly with an excess of carbon source and essential elements required for growth like carbon, oxygen, nitrogen, phosphorus, sulfur, hydrogen, etc. in a limiting condition. Despite the several advantages of PHA over petroleum-derived polymers, the high cost of production of PHA limits its extensive use and makes it inefficient in replacing the conventional plastics. Procurement of pure carbon sources, sterilization of equipment to prevent contamination and pathogenic activity, lower production capacity of fermentation reactors, and the requirement of pure solvents during the extraction process enhance the cost of production [5]. Therefore, in order to reduce production, the cost use of waste organics like industrial sludge, agricultural and food waste, lignocellulosic biomass will play a vital role. Moreover, recently researchers have been focusing on the preparation of mixed cultures (or recombinant microbial strains) compared to refined cultures, which is commercially viable [6]. A typical flowsheet has been illustrated in Fig. 2 to analyze several pathways for the production of PHAs, which includes both conventional and economical routes. This chapter provides a systematic study about PHA-producing microbes and potential carbon substrates, metabolic pathways for their production, extraction and characterization of PHAs, its biodegradability nature, and applications in several sectors.

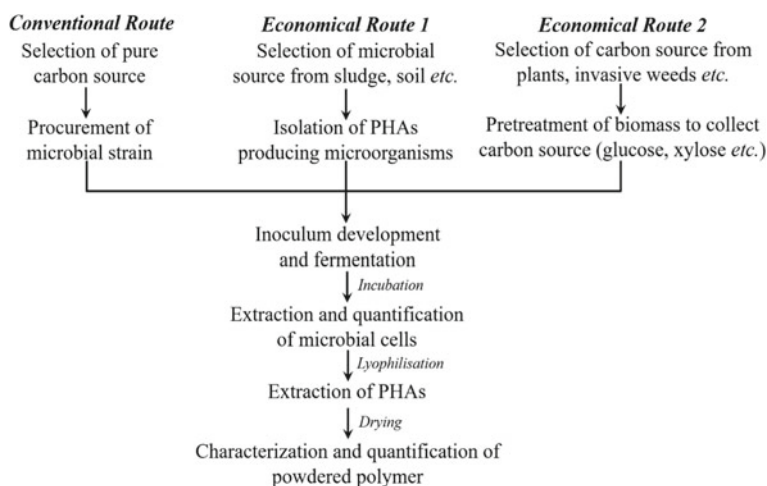


Fig. 2 Pathways for the production of PHAs

1.1 Historical Overview

Maurice Lemoigne first synthesized polyhydroxyalkanoates (PHAs) in 1923, using a gram-positive bacteria *Bacillus megaterium* as a carbon storage compound [7, 8]. He described the biodegradable polymer as an ether-insoluble lipid in a French journal. During the period of 1923–1951, he published 27 articles and postulated that PHB can be produced by a variety of microorganisms [9]. In 1958, Wilkinson Macre observed that by increasing the concentration of carbon sources like glucose and nutrient elements like nitrogen, accumulation of *B. megaterium* granules increased [10]. Later on, researchers synthesized P(3HB) using several microorganisms of bacteria genera like *Pseudomonas*, *Azotobacter*, *Hydrogenomonas*, *Chromatium*, a cyanobacterium, and many others during 1959–1973 [11]. In 1974, Wallen et al. first reported that PHA can be synthesized by extracting the carbon source from activated sludge [12]. Later, numerous compounds of PHAs were developed by several microorganisms using different carbon sources. In 1990s, *Alcaligenes eutrophus* was used for production of PHB, which accumulated up to 75% of dry cell weight [13]. The bacterium was later renamed as *Ralstonia eutropha*, which was again retitled to *Wautersia eutropha*. At present, *R. eutropha* is one of the most promising microorganisms that have been discovered for efficient production of PHAs from several carbon sources.

1.2 General Structure and Classification of Polyhydroxyalkanoates (PHAs)

PHAs are polyesters of HAs and the general structure formula is given in Fig. 3a

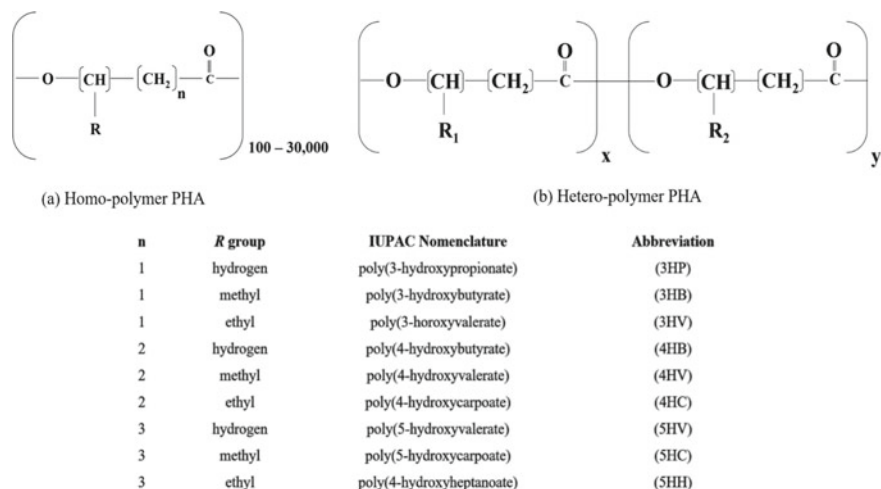


Fig. 3 Structure of polyhydroxyalkanoates (PHAs)

with its IUPAC nomenclature. In Fig. 3a, the commonly used polymers are shown by varying the pendant group R . Generally, based on the monomer units, the PHAs are classified into three different categories. Short-chain-length (*scl*) PHAs are composed of monomers with 3–5 (C_3 – C_5) carbon atoms. Carbon numbers ranged from 6 to 14 (C_6 – C_{14}) are categorized as medium-chain-length (*mcl*) PHAs. Similarly, the long-chain-length (*lcl*) PHAs have carbon atoms greater than 14 ($>C_{14}$). The most commonly produced PHAs are *scl*-PHAs that possess a tensile strength as high as polypropylene. Most *mcl*-PHAs are elastomeric and semi-crystalline in nature. *lcl*-PHAs are very infrequent and are the least studied materials among all types of PHAs [14]. Depending upon the type of monomer present in the PHAs, it can be divided into two types: homo-polymer PHA and hetero-polymer PHAs. If the monomer unit consists of one type of 3-hydroxy fatty acid, then it is called as homo-polymer PHA. Hetero-polymer PHA contains more than one type of fatty acid of varying chain length [15]. A schematic of hetero-polymer or copolymer PHA has been shown in Fig. 3b. The polymers can be biosynthesized by a wide range of microbes (i.e., gram-positive and gram-negative bacteria) as an intracellular carbon source and energy storage compounds.

1.3 Physical Properties of PHA

The physical properties of *scl*-PHAs and *mcl*-PHAs are given in Table 1 [3, 5, 16]. It can be observed that different *scl*-PHAs and *mcl*-PHAs show a wide distribution ranging from wooden fibers to petroleum-based polymers (i.e., polyethylene

Table 1 Comparative physical properties analysis of *scl*-PHA and *mcl*-PHA

	<i>scl</i> -PHA	<i>mcl</i> -PHA
Melting point T_m ($^{\circ}\text{C}$)	~180	~60
Glass transition temperature T_g ($^{\circ}\text{C}$)	~ 0	~ -40
Tensile strength (MPa)	Lower	Higher
Average molecular weight	Higher	Lower
Crystallinity (%)	70	40
Tensile strength	Higher	Lower
Extension to breakage	Lower	Higher
Elasticity	Lower (brittle)	Higher

and polypropylene). The *mcl*-PHAs have lower glass transition temperatures, crystallinity, molar mass, and tensile strength compared to *scl*-PHA. They also have a wide range of melting temperatures varying from 170 to 180 $^{\circ}\text{C}$ and high elongation at break compared to *scl*-PHA. *mcl*-PHAs are flexible and elastomeric, but *scl*-PHAs are stiff and brittle in nature [14, 17].

Similarly, Table 2 shows major physical properties of PHAs, polypropylene, HDPE, and LDPE [18–20]. The PHAs possess similar material properties as polypropylene, whereas polypropylene has better mechanical properties compared to PHAs. In addition, it can be observed that the physical properties can be altered by introducing a co-monomer into the polymer backbone.

Table 2 Physical properties of PHB, P(3HB-*co*-3HV), polypropylene, HDPE, LDPE

	P(3HB)	P(3HB- <i>co</i> -3HV)	Polypropylene	HDPE	LDPE
Melting point T_m ($^{\circ}\text{C}$)	162–181	64–171	160–169	130–137	105–125
Glass transition temperature T_g ($^{\circ}\text{C}$)	-4 to 18	-13 to 10	-14 to -6	-125 to -90	-125 to -90
Tensile strength (MPa)	19–44	1.8–51	28–40	20–40	7–17
Tensile Young's modulus	1.2–4	0.14–8.7	1.1–2	0.7–1.4	0.14–0.3
Elongation at break (%)	0.8–4.5	1–970	20–75	100–1000	200–900
Density	1.18–1.26	1.18–1.26	0.90–0.91	0.95–0.97	0.92–0.93
Crystallinity (%)	50–80	53–56	50	79.8–81	43

2 Production of PHAs

Biologically derived polymers have created significant impacts on petroleum-derived polymers in terms of the green synthesis method and environmental friendly applications. Biotechnological production of PHA is carried out via two routes: (1) microbial fermentation method and (2) plant-based production system. Significant research has been carried out toward bacterial production of PHAs in recent years, and substantial efforts are in progress to improve the production process [21, 22]. The worldwide production of bio-based polymers is expected to reach 17 million tons (~3 times higher) by the end of 2020 in comparison to 5.1 million tons in 2013 [23].

2.1 PHA-Producing Microorganisms

The biopolymers, PHAs, are synthesized by microorganisms as an intracellular product for storage of carbon and energy under nutrient-limited conditions [24]. In the presence of excess carbon source and limitation of nitrogen, phosphorus or oxygen in the growth media facilitates microorganisms to synthesize PHAs as an energy reserve material [25]. In 1926, French scientist Lemoigne first discovered poly (3-hydroxybutyrate) (PHB) in *B. megaterium* cells [26]. Since the discovery of PHB, more than 90 various bacterial genera and up to 300 species (both gram-positive and gram-negative) have been recognized as PHAs producers in both aerobic and anaerobic conditions [27, 28]. However, *Cupriavidus necator*, formerly known as *A. eutrophus* or *R. eutropha*, is one the most widely used strain for the production of PHAs. This was the first bacterial species used in the industrial production of P(3HB-co-3HV) copolymer by Imperial Chemical Industries (ICI) [23]. Types of PHAs depend on the bacterial strain used for the production process, and the production can reach up to a level of 90% dry cell weight depending on the microorganism used. PHAs production process categorizes bacteria community into two groups. In the first group, the PHAs are not accumulated as growth associated product, and they are often produced as energy reserve materials upon depletion of phosphorus, magnesium, nitrogen, or oxygen in the medium. For example, the bacteria such as *R. eutropha*, *P. oleovorans*, and *P. putida* belong to this group, whereas the second group does not require any nutrient limitation to accumulate PHAs, and these are accumulated during growth phase [29]. Recombinant *Escherichia coli* belongs to the second group [30]. The list of PHA-producing genera reported in the literature is provided in Table 3 [31]. From the past several years, PHAs have been known to be an intracellular product, as it accumulates in the cytoplasm of bacterial cells. However, Sabirova et al. reported extracellular production of PHAs using a genetically modified *Alcanivorax borkumensis* SK2 strain [32].

In addition to several wild-type PHA producer strains, certain efforts have also been made to design genetically recombinant strains with improved features for PHAs production. Introduction of appropriate genes into non-PHA-producing strains such

Table 3 List of genera known to be the producer of PHAs

<i>Acidovorax</i>	<i>Clostridium</i>	<i>Leptothrix</i>	<i>Rhodobacter</i>
<i>Acinetobacter</i>	<i>Comamonas</i>	<i>Methanomonas</i>	<i>Rhodococcus</i>
<i>Actinobacillus</i>	<i>Corynebacterium</i>	<i>Methylobacterium</i>	<i>Rhodopseudomonas</i>
<i>Actinomycetes</i>	<i>Cupriavidus</i>	<i>Methylocystis</i>	<i>Rhodospirillum</i>
<i>Aeromonas</i>	<i>Cyanobacterium</i>	<i>Methylomonas</i>	<i>Rubrivivax</i>
<i>Alcaligenes</i>	<i>Defluviicoccus</i>	<i>Methylosinus</i>	<i>Saccharophagus</i>
<i>Allochromatium</i>	<i>Delftia</i>	<i>Methylovibrio</i>	<i>Shinorhizobium</i>
<i>Anabaena</i>	<i>Derxia</i>	<i>Micrococcus</i>	<i>Sphaerotilus</i>
<i>Aphanothece</i>	<i>Ectothiorhodospira</i>	<i>Microcoleus</i>	<i>Spirillum</i>
<i>Aquaspirillum</i>	<i>Erwinia</i>	<i>Microcystis</i>	<i>Spirulina</i>
<i>Asticcaulus</i>	<i>Escherichia</i>	<i>Microlunatus</i>	<i>Staphylococcus</i>
<i>Azomonas</i>	<i>Ferrobacillus</i>	<i>Moraxella</i>	<i>Streptomyces</i>
<i>Azospirillum</i>	<i>Gamphospheria</i>	<i>Mycoplanaa</i>	<i>Synechococcus</i>
<i>Azotobacter</i>	<i>Gloeocapsa</i>	<i>Nitrobacter</i>	<i>Syntrophomonas</i>
<i>Bacillus</i>	<i>Gleothece</i>	<i>Nitrococcus</i>	<i>Thiobacillus</i>
<i>Beggiatoa</i>	<i>Haemophilus</i>	<i>Nocardia</i>	<i>Thiococcus</i>
<i>Beijerinckia</i>	<i>Haloarcula</i>	<i>Nostoc</i>	<i>Thiocystis</i>
<i>Beneckea</i>	<i>Halobacterium</i>	<i>Oceanospirillum</i>	<i>Thiodictyon</i>
<i>Brachymonas</i>	<i>Haloferax</i>	<i>Oscillatoria</i>	<i>Thiopedia</i>
<i>Bradyrhizobium</i>	<i>Halomonas</i>	<i>Paracoccus</i>	<i>Thiosphaera</i>
<i>Burkholderia</i>	<i>Haloquadratum</i>	<i>Paucispirillum</i>	<i>Vibrio</i>
<i>Caryophanon</i>	<i>Haloterrigena</i>	<i>Pedomicrobium</i>	<i>Wautersia (Cupriavidus)</i>
<i>Caulobacter</i>	<i>Hydrogenophaga</i>	<i>Photobacterium</i>	<i>Xanthobacter</i>
<i>Chloroflexus</i>	<i>Hyphomicrobium</i>	<i>Protomonas</i>	<i>Zoogloea</i>
<i>Chlorogloea</i>	<i>Klebsiella</i>	<i>Pseudomonas</i>	
<i>Chromatium</i>	<i>Lamprocystis</i>	<i>Ralstonia</i>	
<i>Chromobacterium</i>	<i>Lampropedia</i>	<i>Rhizobium</i>	

as *E. coli* can enable the microorganism to synthesize biopolymers. Wang et al. reported an accumulation of 90% P(3HB) by using genetically modified *E. coli* strain [33]. Several studies also reported a successful integration of PHA-producing gene from various microorganisms such as *C. necator*, *Pseudomonas aeruginosa*, *Alcaligenes latus*, *Thiocapsa pfennigii*, and *Streptomyces aureofaciens*, into a *E. coli* strain [23]. These recombinant strains hold several advantages over the wild type of PHA-producing strains in terms of higher production capacity and diversity in the substrate selection.

Apart from using pure cultures of wild or recombinant strains, several studies also reported the use of the mixed microbial culture as an effective technique for PHA production. Different microorganisms belonging to several groups carry out

PHA synthesis in the mixed culture. The major advantages of using mixed cultures in comparison with pure cultures are reduction in process costs, exclusion of sterilization process, and minimum control requirements. The other advantage of mixed culture is its ability to utilize a wide range of substrates, including agro-industrial wastes. Ashby et al. observed an increase in PHA content and maximum substrate (glycerol) utilization through mixed cultures of *Pseudomonas corrugate* and *Pseudomonas oleovorans* [34]. Mixed cultures also proved favorable for PHA production using effluent from the starch and wood mill industry [35, 36]. However, low PHA content and less volumetric productivity (cell mass) are the major drawbacks of using mixed cultures in the PHA production process. These limitations can be surmounted by strain development and improving fermentation methods.

2.1.1 Metabolic Pathways

Three major pathways such as fatty acid β -oxidation, de novo fatty acid synthesis, and carbohydrates biosynthesis associated with the metabolism of PHA are depicted in Fig. 4 [37]. Microorganisms that follow the de novo biosynthesis pathway utilize glucose, gluconate, or acetate as carbon source, while fatty acids are utilized as carbon source in a β -oxidation pathway [38]. The enzymes responsible for PHA synthesis and their respective coding genes are the same in different bacteria. PhaA, PhaB, and

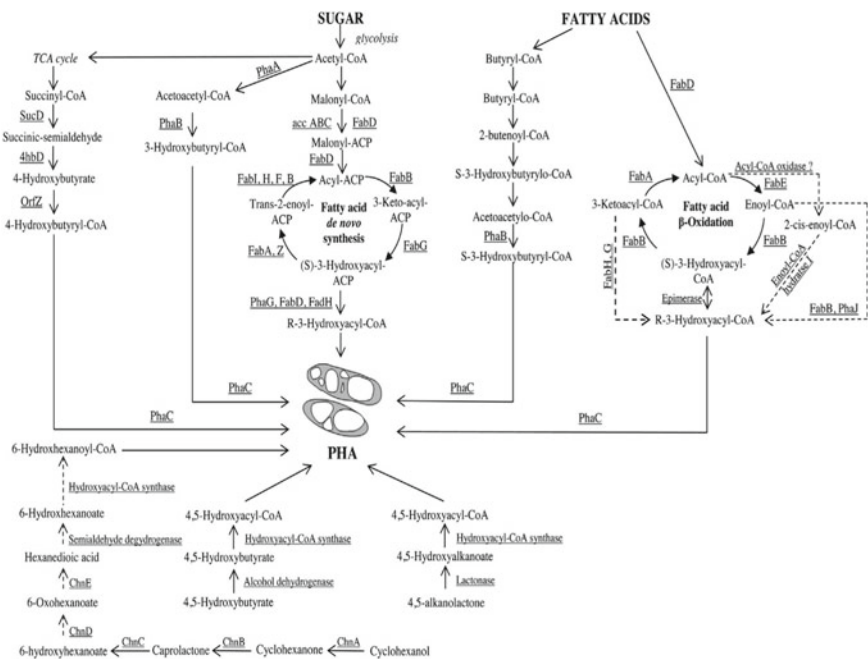


Fig. 4 Metabolic pathways of PHA synthesis

PhaC are some of the essential coding genes synthesizing β -ketothiolase, acetoacetyl-CoA reductase, and PHA synthase enzymes, respectively. At the same time, few other secondary genes required for PHA formation are PhaE, PhaF, PhaZ, and PhaP. Most of the bacteria such as *C. necator*, *Aeromonas hydrophila*, or *Pseudomonas stutzeri* follow the common three-step pathway for PHA biosynthesis using acetyl CoA as the precursor. Acetyl CoA, the end product of carbohydrate metabolism, is further converted into acetoacetyl CoA followed by 3-hydroxybutyryl CoA, the substrate for PHA synthesis. Fatty acid β -oxidation and de novo fatty acid synthesis are the two other pathways for PHA synthesis apart from the above-mentioned pathway. Maximum amount of PHA is reported to be produced from a fatty acid synthesis pathway [37]. The produced polymer composition is directly related to the substrate composition used for the growth of the microorganisms. Short-chain volatile fatty acids are reported to be the most suitable substrates for the PHA production by bacteria [39].

2.2 Substrates for PHAs Production

Appropriate substrate selection improves biomass yield, reduces fermentation cost, and aids in an easy separation of product from fermentation mixture. Selection of carbon source for PHA production primarily depends on the microorganisms used in the fermentation process. The substrate for PHAs production varies from simple commercial sugars (glucose, sucrose, glycerol, etc.) to innumerable waste products including industrial, agricultural, and food waste. All together, the substrates for PHAs production can be divided into three different categories: (i) simple sugars (monosaccharides), (ii) triacylglycerol, and (iii) hydrocarbons [40]. Most of the microorganisms favor the usage of simple sugars as their carbon source, while others use triacylglycerol and hydrocarbons as their carbon sources for PHA biosynthesis. The structural composition of PHAs varies with the use of different carbon sources and microorganisms, which subsequently affects its further applications. For example, several PHA-producing *Pseudomonas* species have the capability of incorporating functional groups such as phenyl, phenoxy, halogens, branched alkyls, olefin, and esters into the PHAs chain when they are grown over substrates containing the respective functional groups [41]. Kim et al. investigated the effect of using 36 various carboxylic acids containing carbon substrates on the PHA production by *Pseudomonas putida* KCTC 2407. Physical properties of PHAs can be significantly improved by incorporating suitable functional group into PHA chain. These groups can be further modified by chemical reactions to extend the potential applications of PHA as biodegradable polymers and possible applications in the medical sector. Table 4 represents production of PHAs using various carbon sources as a substrate. More details about the substrates can be found in the following sections [13, 35, 36, 42–93].

Table 4 Production of PHAs from various feedstocks

Carbon source/waste feedstock	Microorganisms	Fermentation mode	PHA content (%)	Reference
<i>Commercial sugars</i>				
Glucose	<i>Bacillus cereus</i>	Batch	47.9	[57]
	<i>Pseudomonas mendocina</i> NK-01	Shake flask (batch)	51.2	[89]
	<i>Pseudomonas stutzeri</i> 1317	Batch	52	[63]
	<i>Pseudomonas putida</i> Δ gcd (recombinant)	Fed-batch	67.1	[77]
	<i>Escherichia coli</i> (mutant)	Batch	11.9	[88]
	<i>Pseudomonas aeruginosa</i> ATCC 9027	Batch	10.8	[81]
	<i>Ralstonia. Eutropha</i>	Fed-batch	73.8	[13]
	<i>Escherichia coli</i> K24KP (recombinant)	Aerobic batch	37.2	[42]
Sucrose	<i>Cupriavidus necator</i> (recombinant)	Fed-batch	74.3	[43]
	<i>Alcaligenes latus</i>	Fed-batch	50.0	[90]
Glycerol	<i>Escherichia coli</i> K24KL (recombinant)	Fed-batch	63	[73]
	<i>Cupriavidus necator</i> DSM 545	Fed-batch	62	[50]
	<i>Shimwellia blattae</i> (recombinant)	Two-step fed-batch	30.7	[83]
<i>Starch</i>				
Starch	<i>Bacillus cereus</i> CFR06	Batch	48	[62]
Starch	<i>Azotobacter chroococcum</i>	Batch	46	[67]
Cornstarch (extruded)	<i>Haloferax mediterranei</i>	Repeated fed-batch	24.2	[64]
Corn starch (extruded)	<i>Haloferax mediterranei</i>	Fed-batch	50.8	[55]

(continued)

Table 4 (continued)

Carbon source/waste feedstock	Microorganisms	Fermentation mode	PHA content (%)	Reference
Potato starch	<i>Ralstonia eutropha</i>	Fed-batch	55	[60]
<i>Industrial waste</i>				
Crude glycerol	<i>Pandoraea</i> sp. MA03	Batch	63.6	[56]
Crude glycerol	Mixed microbial consortia	Batch	47	[72]
Crude glycerol	Mixed microbial culture	Batch	59	[59]
Wood mill effluent	Two different cultures	Aerobic batch	29	[35]
Starch industry wastewater	Mixed cultures	Sequencing batch	60–65	[36]
Palm oil mill effluent	<i>Comamonas</i> sp. EB172	Fed-batch	59	[93]
Olive oil mill effluent	<i>Lampropedia arbour</i> and <i>Candidatus Meganema perideroedes</i>	Anaerobic fermentation and aerobic batch sequencing	–	[44]
Kraft cellulose mill effluent	<i>Sphingopyxis chilensis</i> S37 and <i>Wautersia</i> sp.	Batch	–	[86]
Paper mill waste	<i>Plasticicumulans acidivorans</i>	Sequencing batch	77	[65]
Paper mill waste	<i>Deftuviicoccus vanus/Candidatus Competibacter phosphatis</i>	Aerobic/anaerobic process	42	[46]
<i>Food wastes</i>				
Extruded rice bran: extruded corn starch (1:8)	<i>Haloferax mediterranei</i>	Repeated fed-batch	55.6	[64]
Wheat bran	<i>Halomonas boliviensis</i> LC1	Batch	34	[87]
Molasses	<i>Escherichia coli</i> (recombinant)	Batch	75.5	[82]
Crude palm kernel oil	<i>Burkholderia</i> sp. USM (JCM 15050) (recombinant)	Fed-batch	66	[54]

(continued)

Table 4 (continued)

Carbon source/waste feedstock	Microorganisms	Fermentation mode	PHA content (%)	Reference
Crude palm kernel oil	<i>Cupriavidus necator</i> (recombinant)	Fed-batch	66	[69]
Palm kernel oil	<i>Cupriavidus necator</i> (recombinant)	Fed-batch	79	[48]
Whey	<i>Haloferax mediterranei</i>	Fed-batch	66	[68]
Whey	<i>Haloferax mediterranei</i>	Batch	53	[75]
Whey	<i>Thermus thermophiles</i> HB8	Batch	35.6	[76]
Whey permeate	<i>Cupriavidus necator</i> mRePT	Batch	25	[79]
Soy bean and rapeseed oil	<i>Cupriavidus necator</i> H16	Two-stage batch	57	[85]
Waste frying rapeseed oil	<i>Cupriavidus necator</i> H16	Batch	67.9	[74]
Waste frying sunflower oil	<i>Cupriavidus necator</i> H16	Batch	52.4	[74]
Corn oil	<i>Psuedomonas</i> species	Batch	35.63	[53]
Sugarcane vinasse	<i>Haloferax mediterranei</i>	Batch	70	[47]
Malt waste	<i>Alcaligenus eutrophus</i> DSM1124	Batch	70	[92]
Soy waste	<i>Alcaligenus eutrophus</i> DSM1124	Batch	32.57	[92]
Restaurant waste	Recombinant <i>E. coli</i> pnDTM2	Batch	45	[58]
Restaurant waste	<i>Cupriavidus necator</i> H16	Continuous feeding	87	[61]
<i>Lignocellulosic biomass</i>				
Wheat straw	<i>Burkholderia sacchari</i> DSM 17165	Fed-batch	72	[51]
Rice straw	<i>Bacillus firmus</i> NII 0830	Batch	89	[84]

(continued)

Table 4 (continued)

Carbon source/waste feedstock	Microorganisms	Fermentation mode	PHA content (%)	Reference
Sugarcane bagasse	<i>Burkholderia</i> sp	Fed-batch	48	[71]
Sugarcane bagasse	<i>Cupriavidus necator</i>	Batch	57	[91]
<i>Parthenium hysterophorus</i> and <i>Eichhornia crassipes</i>	<i>Ralstonia eutropha</i>	Batch	8.1–21.6	[80]
<i>Wastewater</i>				
Cassava starch wastewater	<i>Bacillus tequilensis</i> MSU 112	Sequencing batch	79.2	[52]
Cassava starch wastewater	<i>Cupriavidus</i> sp. K KU38	Batch	61.6	[78]
Brewery wastewater	Activated sludge consortium	Stirred batch reactor	39	[45]
Food processing wastewater effluent	Activated sludge consortium	Batch	60.7	[66]
Olive oil mill wastewater	Wastewater microbes	Stirred batch reactor	11.3	[49]
Tomato wastewater	Activated sludge consortium	Batch	20	[70]

2.2.1 Commercial Substrates

Carbohydrates are mainly classified into three groups including monosaccharides, disaccharides, and polysaccharides. Monosaccharide carbohydrates are a simple sugar that cannot be hydrolyzed further, whereas disaccharides and polysaccharides can be hydrolyzed to form monosaccharides. PHA-producing microorganisms can directly utilize monosaccharides and disaccharides for PHA production, while polysaccharides need to be hydrolyzed to simple sugars prior to the fermentation. Starch, hemicellulose, and cellulose belong to the polysaccharides category.

The simplest sugar, glucose, is the most widely used carbon source for PHA production. Several wild types of strains such as *R. eutropha*, *Bacillus cereus*, *P. aeruginosa*, and genetically modified strains of *E. coli*, *P. putida* have been used for PHA production using glucose as substrate. Kim et al. reported 73.8% PHA accumulation by using *R. eutropha* strain in a fed-batch process applying glucose as the carbon source [13]. In another study, Poblete-Castro et al. adopted various fed-batch strategies to improve *mcl*-PHAs production from glucose using metabolically engineered *P. putida* strains [77].

The other substrate for PHA production is sucrose, a disaccharide composed of two monosaccharides, glucose, and fructose linked via a glycoside linkage. *R. eutropha* (renamed as *C. necator*), the most widely used microorganism in PHA production cannot utilize sucrose as a carbon source directly [94]. However, other wild strains such as *Azotobacter vinelandii*, *A. latus*, and *Hydrogenophaga pseudoflava* have been identified to produce PHA by utilizing sucrose directly [95, 96]. These microorganisms hydrolyze sucrose into glucose the wild type of strains, several recombinant strains are also reported for the direct utilization of sucrose as a carbon source. Zhang et al. reported PHA production in a recombinant *Klebsiella aerogenes* by inserting a PHA synthesis gene from *R. eutropha* [97]. In another study, sucrose-utilizing gene from *Mannheimia succiniciproducens* was introduced into *R. eutropha*, which enabled the cells to utilize sucrose for PHA production [94]. The recombinant *R. eutropha* produced approximately $0.0046 \text{ g L}^{-1} \text{ h}^{-1}$ of PHA in a 5-L batch fermenter with sucrose as a substrate.

Glycerol, one of the important commercial chemicals, has been used as a substrate for the production of various fine chemicals, which includes lactic acid, 1,3-propanediol, dihydroxyacetone, ethanol, biohydrogen, etc. Some of the recent studies also focused on the production of PHA from pure glycerol. Using pure glycerol as substrate, 63 and 30.7% PHA content are accumulated with the help of recombinant *E. coli* and *Shimwellia blattae* strains, respectively [73, 83].

Even though utmost efforts have been taken to compete with the petrochemical plastics, biopolymers are still unattractive due to their higher production cost and inferior material properties. Production cost is one of the main constraints in commercialization of biopolymer as compared to conventional polymers. The major fraction of production cost is associated with the carbon substrates, and the cost of the substrate has been reported to contribute about 28–50% of the total production cost [98, 99]. To make the PHA production process economical, worldwide research has been focused on the utilization of several waste materials as carbon source [100]. Wastes or by-products obtained from the biodiesel industry, palm oil industry, paper mill, food waste, agricultural sector, animal wastes, and many more wastes have been explored as a potential carbon substrate for PHA production. More details about the substrates and PHA production processes are described in the subsequent sections.

2.2.2 Starch

Starch is a polymeric carbohydrate consisting of glucose monomers joined by glycosidic linkage. Several plants such as rice, wheat, potatoes, cassava, and maize are known to be the producers of starch. However, many bacterial strains lack the ability to produce α -amylase, the key enzyme responsible for starch hydrolysis. Therefore, α -amylase synthesis gene from external source is essential for starch hydrolysis and to use it as carbon source for PHA production. Along with saccharified waste potato starch, the *R. eutropha* strain resulted a biomass yield of 179 g/L with PHAs content 55% (w/w) of CDW in a fed-batch process [60]. In another study, Chen et al. reported 50.8% (w/w) PHA accumulation in *H. mediterranei* using an enzymatic

extruded cornstarch as a substrate in a fed-batch operation [55]. In these studies, saccharification of starch was carried out by the enzymes from an external source (i.e., commercial enzymes) prior to the main PHA production process. Halami et al. isolated α -amylase producing native *B. cereus* CFR06 strains from soil sample, which could accumulate about 48% of PHA after 72 h of fermentation in a starch-containing medium [62]. These studies clearly indicate a higher production of PHA using starchy food wastes as the substrates with minimal or no pre-saccharification process.

2.2.3 Industrial Wastes

Effective utilization of industrial wastes for value-added products are considered as an economical solution to reduce production cost, while simultaneously addressing the environmental issues. Waste from biodiesel industry and effluents from palm oil, paper, olive, and wood industry have been used as a substrate for the PHA production using various microbial strains. More details about the industrial wastes, microorganisms used and PHA content are listed in Table 4.

Nowadays, biodiesel is considered as one of the major alternative green fuels for petroleum diesel. The global biodiesel production is expected to reach 32 billion liters (8.2 billion gallons) by the end of the year 2020. This would concurrently produce 2.6 million tons (5.9 billion gallons) of crude glycerol, a major by-product from biodiesel industry [101]. On the weight basis, approximately 1 kg of crude glycerol is produced as a by-product for every 9 kg of biodiesel. The effective utilization of enormous quantity of crude glycerol for PHA production is a viable solution to trim down the production cost of both biodiesel and biopolymers. Freches and Lemos reported a final PHA content of 59% from acclimatized mixed microbial cultures using crude glycerol as substrate in a sequencing batch reactor (SBR) [59]. de Paula et al. reported PHA production from biodiesel-derived crude glycerol by newly isolated *Pandoraea* sp. from Atlantic rainforest in Brazil [56]. PHA accumulation by this strain ranged from 49.0 to 63.6% CDW using crude glycerol as substrate, which reported to be higher than the pure glycerol. Presence of NaCl contaminants in crude glycerol enhanced biopolymer accumulation in *Pandoraea* species.

Effluents from wood mill, palm mill, olive oil mill, paper mill, etc. are rich in organic sources, which are further converted to value-added chemicals including PHA. Palm oil mill effluent (POME), rich in carbohydrate, protein, lipids, nitrogenous compounds, and minerals, provides nutritious support for bacterial growth concurrently degrading the waste to reduce its environmental hazard [102]. Zakaria et al. isolated eleven potential PHA-producing strains from the treated palm oil wastewater [93]. Among the isolated strains, *Comamonas* sp. accumulated highest PHA content (44%) and they exhibited a wide range of substrate utilization. Hassan et al. recommended a two-stage process for the PHA production from POME [103]. In the first stage, production of acids, particularly acetic and propionic acids was carried out in the anaerobic process, which was subsequently converted to PHA using *Rhodobacter sphaeroides* at the second stage. This study also reported inhibition effect of formic acid in PHA production process and a decrease in PHA content

from 67 to 18% was noticed with an increase in formic acid concentration. A three-stage treatment (anaerobic and aerobic) of olive oil mill effluent for PHA production was investigated using activated sludge, dominated with *Lamprospedia arbour* and *Candidatus Meganema perideroedes* species [44]. Volatile fatty acid (VFA) content, the most direct precursor for PHA production, was increased from 18 to 32% at the first stage (anaerobic) of the process. Similarly, Jiang et al. reported that the PHA production from the organic-rich paper mill effluent in a three-stage process [65]. The conversion of paper mill effluent to VFA is carried out in the first stage, followed by the enrichment of PHA-producing bacteria, and later maximizing their storage capacity at the second and the third stages of the process, respectively. This process accumulated maximum PHA content up to 77% of cell dry weight within 5 h of enrichment process. Similarly, Bengtsson et al. reported a three-stage process for PHA accumulation (42%) using glycogen accumulating organisms, and observed a total PHA yield 0.10 kg per kg of influent soluble chemical oxygen demand [46]. Further, the optimization of process and purification of the final product is required to make the process more economical and feasible for an industrial-scale production.

2.2.4 Food Wastes

Food wastes are one of the major form of wastes generated worldwide, starting from harvesting of the crop to the end of life [104]. Food and Agriculture Organization (FAO) estimated that one-third of the world food production is lost or wasted during this process. It was reported that approximately 89 million tons of food waste are produced by the EU-28 Member States in 2012 [105, 106]. Many developing countries are observing significant increase in the quantity of food waste in recent years due to the increasing population growth, increase in food consumption, and lack of proper treatment process. A sustainable, economic, and efficient alternative for the conversion of these surplus food wastes to several value-added products can simultaneously reduce environmental pollution and health risk hazard caused by the perishable food waste. These food wastes are rich in proteins, carbohydrates (e.g., cellulose, hemicellulose, starch, and sugars), minerals, oils and fats, which can be used as a substrate for microbial or enzymatic processes. The exploitation of food waste for the production of several value-added products (lactic acid, biohydrogen, ethanol, and biogas) has been reported in past several years. PHA, another value-added product produced from various food wastes using microbes, is summarized in Table 4. These wastes include rice or wheat bran, molasses, whey, palm kernel oil, soy waste, malt waste, restaurant waste, waste frying oils, etc.

Whey, the major by-product from cheese-making process, has been extensively studied for the production of PHA. Whey is a rich source of lactose, proteins, fats, vitamins, and other essential nutrients that does not require any extensive pre-treatment step for the use in the fermentation process conducted by microorganism [107]. Most of the studies reported the use of recombinant *E. coli* for the production of PHA, as the wild microbial strains have limited ability to utilize lactose directly. Studies reported the use of *Haloferax mediterranei*, *Thermus thermophilus* HB8, and

C. necator for whey fermentation, and the final PHA content varied from 25 to 66% [68, 75, 76, 79].

Recently, various plant oils from household and industry have also used as an economic substrate for PHA production. Oils produced from industries such as palm oil [54], soybean oil [85], sunflower oil [108], olive oil [53], and from household such as waste frying rapeseed and sunflower oil [74, 85] are successfully tested for the production of PHA. These oils are devoid of costly pre-treatment processes, and they can be directly added to the fermentation media as carbon source for the production of PHA. A study by Taniguchi et al. reported the conversion of various waste edible oils and fats for the production of PHA using *R. eutropha* H16 strain [85]. A highest PHA yield of 83%, and final cell dry weight 6.8 g/L were observed from this study with the use of palm oil with lard as carbon sources. Production of copolymer poly(3-hydroxybutyrate-co-3-hydroxyvalerate) (PHBV) occurred instead of pure PHB when tallow was used as the carbon source. In another study, Obruca et al. reported the utilization of waste frying oils (rapeseed, palm, sunflower) as a carbon source in fermentation using *C. necator* H16 microbial strain [74]. The cell dry weight and PHB content using these substrates varied in the range from 10.8 to 11.9 g/L and from 52.4 to 67.9%, with a higher PHB production level from waste frying rapeseed oil. Other than whey and oils, studies also reported the use of several other food wastes such as molasses, wheat bran, rice bran, malt waste, soy waste, sugarcane vinasse, and restaurant waste as an economical carbon source for the production of PHA. Nielsen et al. have given a detailed review of the utilization of various food wastes for the production of PHA [109].

2.2.5 Agricultural Waste and Lignocellulosic Biomass

In recent years, agricultural wastes and its coproducts have become the major contributor of waste into the environment, and its annual global production has reached 16 million metric tons [110]. Stubble burning of these lignocellulosic wastes such as sugarcane bagasse, rice straw, rice husk, corn stover, wheat straw, and wood chips is the major source of environmental pollution in many agrarian countries. Cellulose (40–50%), hemicellulose (25–30%), and lignin (15–20%) are the three major constituents of lignocellulosic biomass, with some amount of extractives such as ash, proteins, pectins [111, 112]. Cellulose is a homo-polymer, consisting of a linear chain of D-glucose linked with a β -1,4 glycosidic bond, whereas pentose sugars (xylose, arabinose), hexose sugars (glucose, galactose, mannose), glucuronic acid, and uronic acids are the major components of hemicellulose. Lignin is a complex polymer of aromatic ring compounds (sinapyl, coniferyl, and p-coumaryl alcohols) that provide mechanical strength to the plant cell wall. Pre-treatment of biomass partially removes the hemicellulose and lignin fractions, which also decreases the cellulose crystallinity and improves the porosity of biomass for accessibility of enzymes or acids to hydrolysis [113]. Hydrolysis of biomass releases hexose and pentose sugars, which are subsequently used in fermentation for production of various value-added products.

Sindhu et al. reported the utilization of hemicellulosic rich, acid hydrolyzed rice straw hydrolysate for the production of PHB using *Bacillus firmus* NII 0830 strain [84]. Acid hydrolysis was carried out in the presence of 2% (w/w) H_2SO_4 for the release of pentose sugar. The bacterium accumulated 1.697 g/L of PHB with a final cell mass 1.9 g/L, after 90 h of fermentation using pentose hydrolysate without any prior detoxification. Another study by Cesario et al., used wheat straw hydrolysate in batch and fed-batch fermentation, which resulted in a PHB production of 0.7 and 0.72 g of PHB/g of CDW, respectively [51]. The microorganism *Burkholderia sacchari* DSM 17165 has the ability to utilize both C_6 and C_5 carbon sugars (i.e., glucose, xylose, and arabinose) in hydrolysate for the PHA production. Sugarcane bagasse is one of the other abundant agricultural wastes used in the PHB production using *Burkholderia* sp and *C. necator* microbial strain [71, 91]. Apart from the agricultural waste, limited studies also explored the possible utilization of invasive weeds as potential feedstock for the production of PHA. In one of our studies, we selected two different invasive weeds such as *Eichhornia crassipes* and *Parthenium hysterophorus* as substrates for PHB production using *R. eutropha* strain [80]. Biomasses were hydrolyzed using dilute acid pre-treatment (1% v/v H_2SO_4) and enzymatic hydrolysis (cellulase and cellobiase) process for obtaining pentose and hexose-rich hydrolyzates. These hydrolyzates were further fermented separately using *R. eutropha* strain, and the PHB content in dry cell mass varied in the range of 8.1–21.6% w/w with yield 6.85×10^{-3} – 36.41×10^{-3} w/w of raw biomass. Significant variation in thermal properties of the produced polymers derived from two different hydrolyzates was noticed. Higher maximum thermal degradation observed for PHB derived from hexose-rich hydrolyzate, whereas the pentose-rich hydrolyzate derived PHB showed higher glass transition temperature.

Further research on effective utilization of other invasive weeds and mixed lignocellulosic feedstock for biopolymer production need to be carried out. Combination of suitable pre-treatment techniques can increase the fermentable sugars production, which can be further used for higher PHA yield.

2.2.6 Wastewater

The production of PHA using cassava starch, brewery, and wastewater obtained from food processing industry has gained much attention in recent years due to the use of mixed microbial culture and open reactors despite a costly sterilization process. The treatment of wastewater for removing impurities and organic content with a simultaneous production of biopolymers is an efficient solution to address the problems of environmental pollution. Chaleomrum et al. investigated the potential of cassava starch wastewater for PHA production using *Bacillus tequilensis* in a sequencing batch reactor (SBR) [52]. The effect of different inlet COD concentrations in cassava starch wastewater on the treatment efficiency and the PHA production was determined. Highest PHA production (79.2%) was reported with a COD concentration of 4000 mg/L, while the maximum COD removal efficiency (94.8%) was at

5000 mg/L COD. The PHA accumulation of 58 and 43% (w/w) was reported using swine wastewater and paper and pulp wastewater, respectively [114, 115].

3 PHAs Extraction from Microorganism

PHAs are intracellular polymers, i.e., they are stored inside the extracted cells post-fermentation cycle. Therefore, extraction of these polymers is often complex and expensive. Many researchers have developed various economical methodologies for extraction of the intracellular PHAs. Before performing any extraction technique, the cells are harvested after fermentation by centrifugation at low temperature (~ 10 °C). The centrifugation should be performed at lower temperature to prevent damage/disruption to the cells. The biomass should be freeze dried or lyophilized prior to performing the extraction of PHAs.

3.1 Solvent Extraction

The solvent extraction method is commonly used for recovery of PHAs from microbial cells; it is divided into two phases. First, the breakage of cellular membrane is done by solubilization of PHA molecules. Several researchers observed that solvent containing at least one hydrogen and one chlorine atoms provide best recovery of PHA with high purity. Using solvents like 1,2-propandiol, or glycerol formal, or diethyl succinate, or butyrolactone, 79–90% of PHB recovery can be achieved with purity ranging from of 99.1 to 100% [116]. The cellular debris can be removed by suitable filter papers to get dissolved PHA solution. Then, the soluble PHA is subjected to precipitation in the form of granules using non-solvent such as alcohols and hexane. Repeating the precipitation step up to three times yields maximum amount of PHAs precipitate [117]. The precipitated PHB can further be dried at room temperature or in vacuum oven to evaporate all the residual solvents to get PHB in powder form.

3.2 Digestion Method

For extraction of PHAs, the digestion method is a potential alternative to solvent extraction, which can be achieved by either enzymatic or chemical reactions. Applications of surfactants like sodium dodecyl sulfate (SDS) not only disrupt the cellular membrane but also break the membrane to make micelles and phospholipids [116]. The surfactant (betaine) and chelate aqueous system help in solubilization of protein and non-polymeric cellular materials [118]. After solubilization of all non-PHA

components, the PHA molecules are released to the solution surrounded by the surfactants. The chemical digestion method is achieved by addition of chemicals such as sodium hypochlorite followed by addition of chloroform. After addition of sodium hypochlorite, the entire solution is stabilized into three phases. The first or upper phase is the hypochlorite solution, the second or middle phase consists of cellular debris, and the third or bottom phase is the PHA dissolved in the chloroform. The chloroform soluble phase is separated by filtration which can be further precipitated by addition of non-solvent solution [119]. Similarly, the enzymatic digestion for extraction of PHA is achieved by proteolytic enzyme digestion, which minimized the degradation of HB polymer [120]. Similarly, Kathiraser et al. reported the performance of the enzymatic degradation of PHAs cells using *Alcalase* enzyme, SDS, and EDTA and obtained a purity of 92.6% [121].

3.3 Mechanical Disruption

Cellular disruption of bacterial cells using mechanical agitation method is a very widely used technique for extraction of PHAs as it is economically viable possessing lesser chance of degradation to PHA polymers. It is an environmentally friendly method because no chemicals are required and contamination of PHA polymer can be minimized. This method can be categorized into two categories such as solid shear and liquid shear methods. The extraction method using bead mill includes solid shear method, and high-pressure homogenization includes liquid shear method [116, 122]. The bead mill is comprised of a vertical cylinder-grinding chamber where the microbial cells are allowed to enter at the base and flow through the annular space between the rotor and the stator exiting at the top. The heat generated during the homogenization process is minimized by cooling water supply in the jacket around the chamber [116]. The efficiency of cells disruption is a strong function of bead loading, agitation speed, cell concentration, residence time distribution, bead diameter, and geometry of loading chamber, etc. For large-scale PHA cell disruption, high-pressure homogenization is one of the most effective mechanical methods for extraction. This extraction process involves homogenization under high-pressure via an adjustable and restricted orifice discharge valve. This extraction process depends on operating pressure, number of passes, valve design, and operating temperature [122]. However, this process is not efficient for low biomass concentrations inside the homogenizer [122].

3.4 Supercritical Fluid Extraction

Usage of supercritical fluids is one of the latest technologies for extraction of PHAs because of its physical properties such as high density, low viscosity, and less toxicity. Because of lower viscosity with almost negligible surface tension, the speed

of percolation is very high resulting in better diffusion of fluid for extraction process compared to liquid solvents [123]. A wide range of supercritical fluids such as carbon dioxide (CO₂), ammonia (NH₃), and methanol (CH₃OH) can be used for recovery of PHAs. Hejazi et al. reported that the application of supercritical CO₂ in addition to methanol results in 89% recovery of PHB polymer from microbial cells obtained from *R. eutropha*. As reported by Williams et al., extraction of PHAs using supercritical fluid results in recovery of 100% pure PHA, which is 150 times less contaminated compared to PHAs produced from other methods [124].

3.5 Aqueous Two-Phase Extraction

Aqueous two-phase extraction method is one of the potential alternatives for extraction of PHAs using microorganism such as *B. flexus*. Aqueous two-phase systems are observed when two immiscible phases coexists. Such scenario is observed when the two polymers show chemical incompatibilities in nature and are present at low concentrations. Similar aqueous phase can also be observed when one of the polymers and inorganic phase are present at low concentration at the same time. During the extraction process, enzymatic hydrolysis of *B. flexus* cells is done followed by introducing polymer-salt two-phase system to recover PHAs. During this process, high molecular PHAs are obtained with purity of around 97% [122]. This method of PHA extraction is relatively less time consuming along with lesser cost and lesser energy consumption. In some cases, the two phases are observed as water and non-volatile phase. The isolation, purification, and recovery of PHA are done by water phase. The cellular debris can be recovered from the bottom layer as it settles down during extraction process. This method is an environmentally viable and effective non-solvent method for isolation of PHA from bacterial cells [123].

3.6 Ultrasound-Assisted Extraction

Ultrasound-assisted cell disruption is a new potential alternative for the extraction of PHA. The ultrasound waves are very effective for the rupture of cell walls/membranes, emulsification, and homogenizing, as it focuses on a localized volume [80]. It employs the instantaneous sinusoidal movement of a soundwave in a liquid medium. During sonication process, formation of microbubbles takes place, which leads to the generation of cavitation phenomena. Cavitation process or phenomena is controlled by two forces, viz. pressure force and inertial force, under the influence of pressure variation induced by ultrasound acting simultaneously on the radial motion of the bubble. The dominant force between these two forces governs the expansion of the bubble in the rarefaction half cycle, which is governed by the amplitude of the ultrasound wave. During the compression half cycle, the

inertial force dominates over pressure force resulting in the compression of the bubble. This phenomenon continues until the bubble is compressed to extremely small size (minimum radius or maximum compression). Further variation in any force will result in transient collapse of the bubble. Temperature and pressure can reach up to ~5000 K and ~50 MPa, respectively, during the transient collapse [125]. As the bubble collapses during cavitation, it generates high-energy (temperature and pressure) concentration in a very small (nano) spatial and temporary scale [126]. The transient collapse of bubbles leads to chemical (generation of free radicals) and physical (shockwaves and micro-turbulence) effects [127]. During the cavitation process, the sonic/vibrational energy is converted into mechanical energy due to conservation of momentum, resulting in generation of high-pressure shockwave causing the cell disruption.

4 Characterization of PHA

A number of PHA homo-polymer and copolymers have been developed through different microbial process in order to fulfill the research gap for biodegradable polymers for the last five decades. To understand the chemical compositions, crystallinity, glass transition temperature, thermal properties, mechanical properties, molecular weight, etc. of PHAs, physical, and chemical characterizations are very important for their quantification and identification and are discussed in the following subsections.

4.1 Nuclear Magnetic Resonance (NMR) Spectroscopy

NMR spectroscopy helps to identify the functional groups and quantifies of PHA content present in the polymer chain by observing magnetic field around the nucleus of the atom. The chemical shifts for methyl, methylene, and methine groups are observed in the range of 1.25–1.28, 2.17–2.65, and 5.25–5.26 ppm, respectively, for ^1H NMR of *scl*-PHA (e.g., polyhydroxybutyrate). Similarly, for ^{13}C NMR the corresponding chemical shifts are observed in the range of 19.95–21.4, 31.09–41.3, and 67.8–68.5 ppm, respectively. The $-\text{C}=\text{O}$ group is observed in ^{13}C NMR, which is in the range of 169.31–170 ppm [128–130]. For *mcl*-PHAs (e.g., P(3HB-*co*-3HV)) the methyl, methylene, and methine groups are detected at 1.26–1.6, 2.3–2.7, and 5.2–5.25 ppm, respectively. For detection of $-\text{C}=\text{O}$ group, the chemical shift observed in ^{13}C NMR is in the range of 169.1–169.5 ppm [131–133]. A summary of the NMR characterization results for both *scl*-PHA and *mcl*-PHA is presented in Table 5.

Table 5 Summary of functional groups observed from NMR and FTIR analysis for *scl*-PHA and *mcl*-PHAs

Group or moiety	Chemical Shift (ppm)		Group or moiety	Wave number (cm ⁻¹)
	¹ H NMR	¹³ C NMR		
– CH	5.2–5.26	67.8–68.5	– CH	2962–2853
– CH ₂	2.17–2.7	31.09–41.3	– C = O	1742–1709
– CH ₃	1.25–1.6	19.95–21.4	– C–O or –C–C	1300–1000
– C=O		169.1–169.5	– OH	3460–3407

4.2 Fourier Transform Infrared (FTIR) Spectroscopy

FTIR spectroscopy is used to identify the organic functional groups present in PHAs by measuring absorption of infrared radiation as a function of wavenumber. For both *scl*-PHA and *mcl*-PHAs (including copolymer), the range of wavenumber shifts for different moieties is in the similar range. The absorption of hydroxyl groups (–OH) is observed in the range of 3460 to 3407 cm⁻¹ for wide range of PHAs [134, 135]. The major strong bands are observed for carbonyl (–C=O) and unsaturated ester (–COO) groups and are within the range of 1742–1709 cm⁻¹ [128, 136]. The coupling of –C–O and –C–C intense stretches are observed in the range of 1300–1000 cm⁻¹. For methine (–CH) group, mild stretch vibrations have been observed in the range of 2962–2853 cm⁻¹ [121]. The details of wavenumber shifts ranges for all types of functional groups present in different types of PHAs are summarized in Table 5.

4.3 X-Ray Powder Diffraction (XRD) Analysis

X-ray powder diffraction measurement helps to understand the crystalline nature and morphology of PHAs. In the XRD profile of PHAs, two strong intense peaks are observed around $2\theta = 13^\circ$ and 17° having miller indices of (020) and (110), respectively, suggesting the α -PHB crystal and orthorhombic unit cells appeared on the plane. Relatively weaker reflections are observed at around $2\theta = 21^\circ$ and 22° , which corresponds to miller indices of (101) and (111), respectively for α -PHB crystal. Other similar weaker reflections are observed at $2\theta = 26^\circ$ and 27° showing (130) and (040) reflections, respectively [128, 137, 138]. Senhorini et al. reported that the crystallinity (χ_c) of PHAs can be calculated by measuring the area of crystalline and amorphous peaks. The empirical formula is stated as follows:

$$\chi_c = \frac{A_t - A_a}{A_t} \times 100 \quad (1)$$

where A_t and A_a are the areas under crystalline and amorphous peaks [139]. Bhaskaran et al. reported a comparative study for crystallinity (χ_c) of PHAs synthesized from palm oil in which the χ_c of PHAs are observed in the range of 34–52% [135]. Therefore, from the observation of peaks and calculation of χ_c of different PHA samples, it can be concluded that the PHAs are partially crystalline in nature.

Similarly, the apparent crystal size (D_{hkl}) of PHA samples can be determined by Scherrer's equation, which is stated as follows:

$$D_{hkl} = \frac{K\lambda}{\beta_0 \cos \theta} \quad (2)$$

where K is the geometrical shape factor, β_0 is the half width (radian unit) of the reflections corrected for instrumental broadening, θ is the peak position, and λ is the wavelength (nm) [140]. Mottin et al. reported that the average sizes for PHB film, nanofibers, and crystals are observed in the range of 19–79 nm. [137].

4.4 Differential Scanning Calorimetry (DSC)

The thermal properties of PHAs such as melting point, glass transition temperature, and crystalline temperature on heating and cooling can be obtained from differential scanning calorimetry (DSC) analysis. Apart from these properties, the crystallinity (χ_c) of PHAs can be calculated from DSC curve by measuring the melting enthalpy or heat of melting (H_f). The degree of crystallinity can be estimated by the following equation:

$$\chi_c(\text{Percentage}) = \frac{H_f}{H_{100\%}} \times 100 \quad (3)$$

where $H_{100\%}$ is the fusion enthalpy of 100% crystal PHB, which is 146 J/g [141]. The crystallinity of PHB obtained from soy waste and commercial PHB is in the range of 46–53% [142], whereas the corresponding value for PHB copolymer, e.g., P(3HB-co-3HV) lies within 39–47% [141]. The crystallinity range is similar to the values obtained from XRD analysis confirming the partial crystalline nature of PHAs. The melting point range of PHB obtained from molasses, corn steep liquor, and soy waste using different microorganisms (i.e., *C. necator* and *B. megaterium*) are around 169–177 °C. The crystalline temperature on heating (T_{hc}) and cooling (T_{cc}) and glass transition temperature (T_g) for corresponding PHBs is in the range of 40–48, 86–114, and -1 – 1 °C, respectively [142, 143]. It has also been reported that the melting point and glass transition temperatures of PHA copolymers decrease with increase in 4HB (hydroxybutyrate) and HH (hydroxyhexanoate) content over 3HB content. Cheng et al. reported that for co-polyester P(3HB)(4HB), as the 4HB content increases from 0 to 40%; the melting point was decreases from 173 to 51 °C, the glass transition temperature decreases from -6 to -20 °C, and the crystallinity decreases form 59

to 0.5%. Such variations in thermal properties are due to destruction of crystalline structure of PHB, which not only affect the surface free energy, but also change the biocompatibility nature of the polymers. In addition to this, the differences in crystallinity and molecular weight of different polymer matrices result change in the aforementioned thermal properties [144, 145].

4.5 Thermogravimetric and Differential Thermogravimetric Analysis (TGA and DTG)

Thermogravimetric analysis or thermal gravimetric analysis (TGA) is an analytical technique that helps to analyze the thermal properties such as thermal stability, resistance, and rate of degradation that are measured as a function of temperature or as a function of time. The decomposition of PHAs can be categorized into three different phases. The first phase or initial phase of mass loss results due to evaporation of physically adsorbed impurities and solvents during the fermentation process. The second stage of mass loss is the major degradation step, which occurs after the melting point of a particular PHA polymer. In this stage, the β -chain scission process results in cleavage of $-C-O$ and $-C=O$ bonds in ester functional group with the formation of crotonic acid. During this heating process, the crystalline regions are destroyed and depolymerization of hemicellulose results in rapid mass loss of PHAs [80]. The third and final degradation stage occurs after residual mass left in the PHA sample, in which the rate of mass loss is negligible. Several researchers have assessed the thermal stability by analyzing the quantitative details of weight loss (e.g., 5% mass loss) with respect to temperature. The temperature at 5% mass loss of PHB obtained from recombinant *A. hydrophila* was in the range of 226–235 °C. The corresponding mass loss for copolymers such as P(3HB-*co*-4HB-*co*-3HH_x), P(3HB-*co*-3HV), P(3HB-*co*-3HH_x), P(3HB-3HV-3HH_x), and P(3HB-*co*-3H4MV) lies within 247–306 °C, respectively [146–150]. The temperature details of PHAs at 5% mass loss with their compositions are given in Table 6 [146–150]. Therefore, it can be concluded that the incorporation of various monomers such as 4HB, 3HH, 3HV, and 3H4MV provides more thermal stability to the polymer as it has shown higher thermal degradation temperature. The rate of mass loss of PHAs with respect to temperature is measured by differential thermogravimetric (DTG) analysis which is obtained from the first derivative of the weight loss curve, and it indicates the thermal stability with respect to temperature at which maximum degradation occurs in the polymer matrix. He et al. studied the DTG analysis of three different types of PHAs such as PHB, P(HB 70 mol%: HV 30 mol%), P(HB 85 mol%: HH_x 15 mol%) in which the maximum degradation temperatures are observed at 349, 352, and 359 °C, respectively. They observed that copolymers (e.g., P(HB-HV) and P(HB-HH_x)) have higher thermal degradation temperatures relative to homo-polymer PHAs such as PHB, and hence, the thermal stability of such polyesters improves by increasing the number of structural hydrocarbon units [151].

Table 6 TGA analysis of 5% mass loss temperature ($T_5\%$) of different types of PHA

Type of copolymer	Composition of PHAs (mol%)	$T_5\%$ mass loss ($^{\circ}\text{C}$)	Name of the strain
P(3HB)	3HB: 100	226–235	Recombinant <i>A. hydrophila</i>
P(3HB-co-4HB-co-3HH _x)	3HB: 73.8, 4HB: 5.1, HH: 21.2	257	Recombinant <i>A. hydrophila</i>
P(3HB-co-3HV)	3HB: 80, 3HV: 20	247–253	<i>Alcaligenes eutropha</i>
P(3HB-co-3HH _x)	3HB: 57%, 3HH: 43%	285	Recombinant <i>Cupriavidus necator</i>
P(3HB-3HV-3HH _x)	HB: 5.4, HV: 9.9, HH: 86.7	273	Recombinant <i>A. hydrophila</i>
P(3HB-co-3H4MV)	3HB: 81, 3H4MV: 19	306	<i>Burkholderia</i> sp.

4.6 Gel Permeation Chromatography (GPC)

Gel permeation chromatography (GPC) is primarily used for analysis of biological, polymeric and macromolecule samples to estimate weight-average molecular weight (M_w) and number average molecular weight (M_n). The polydispersity index (M_w/M_n) which is a measure of molecular mass distribution is defined as the ratio of average molecular average to the number average molecular weight. The two types of molecular weights and polydispersity index are shown in Table 7, for a wide range of PHA samples. From Table 7, it can be observed that the weight-average molecular weight (M_w) of several homo- and hetero-polymers lies in between 9 and 16×10^5 Da [146, 148–150, 152]. The PHA copolymer containing HH_x monomer unit poses lesser molecular weight compared to P(3HB). The lower molecular weight of such copolymers is due to the higher accumulation of PHA synthase (bulkier monomer like HH_x) containing both soluble bound and granule bound PHA synthase [149]. Mizuno et al. have studied the time-dependent change of molecular weight of PHAs

Table 7 Molecular weight analysis of several PHAs

Type of PHA sample	M_w (10^5 Da)	M_n (10^5 Da)	M_w/M_n
P(3HB)	9–16	1.66–8.4	1.7–2.9
P(3HB-co-32 mol% 3HH _x)	3.47	2.24	1.55
P(4HB)	8.54	4.87	1.75
P(HV)	10.56	8.15	1.3
P(3HB-co-77 mol% 3HV)	9.24	1.59	5.8
P(3HB- 6.6 mol% 4HB- 19.5 mol% 3HH _x)	7.61	5.54	1.37
P(3HB-5.4 mol% 3HV- 9.9 mol% 3HH _x)	3.73	1.71	2.17

by extracting the cultured cells at different time intervals. It is observed that weight-average molecular weight drastically decreases from 19.3×10^5 Da to 1.46×10^5 Da between 14 and 72 h of cell cultivation. Such rapid reduction of molecular weight is because of depolymerization of intracellular PHA at late stationary growth phase for a particular microorganism [153]. Since higher molecular weight PHAs are useful for several domestic and industrial applications; therefore, the reduction in molecular weight of such polymers should be avoided by optimizing the culture time period.

4.7 Mechanical Properties (Tensile Strength, Young's Modulus, and Elongation at Break)

The principal mechanical properties of polymers that govern response of the polymer to mechanical forces are: tensile strength, Young's modulus, and percentage elongation. In this section, mechanical properties of several types of PHAs have been discussed. A comparative study between different types of PHAs (e.g., *scf*-PHA, *mcl*-PHA, and copolymer) and petroleum-derived polymer has also been summarized in Table 8, to understand the mechanical viability of PHA [117, 148, 149, 154]. From Table 8, it can be observed that for P(3HB-*co*-HHx) polymers, there is a sharp decrease in both tensile strength and Young's modulus. Therefore, it suggests that as the monomer fraction of HHx increases from 32 to 70 mol%, the polymer become more brittle and stiff. All the P(3HB-*co*-HHx) polymers have elongation at break up to 107% indicating a better elasticity compared to polyethylene and polypropylene. Based on the mechanical properties observed, it can be inferred that the P(3HB-*co*-HHx) polymers are gluey and sticky [149]. Similarly, the P(3HB-*co*-3HV) polymer possesses much better mechanical properties (in all the three cases) compared to the simple polymer like P(3HB), whereas it possesses better stiffness (i.e., Young's modulus) compared to polyethylene and polypropylene. The copolymer P(3HB-*co*-3HV-*co*-4HB) with 34% 3HV and 55% 4HB have similar stiffness compared to polypropylene and HDPE, whereas the copolymer with 3% 3HV and 93% 4HB have comparable elasticity like polypropylene, HDPE, and LDPE [154]. Zhao et al. study the mechanical properties of terpolyester such as P(3HB-*co*-3HV-*co*-3HHx), by varying the mol% of HV and HHx. They observed that with varying HHx concentration from 10 to 13%, the elongation at break varies from 277 to 481%, with a reduction in Young's modulus from 319 MPa to 110 MPa, respectively. Therefore, the introduction of HHx decreases the mechanical strength and improves the stiffness/flexibility of PHAs [148].

Table 8 Comparative study for mechanical properties of PHAs and petroleum-derived polymers

Polymer sample	Young's modulus (MPa)	Elongation at break (%)	Tensile strength (MPa)
P(3HB)	3.5	0.4–5	40–43
P(3HB-co-32% #HH _x)	101	856	8
P(3HB-co-43% #HH _x)	75	481	5
P(3HB-co-56% #HH _x)	12	368	1
P(3HB-co-60% #HH _x)	3	424	1
P(3HB-co-70% #HH _x)	1	1075	1
P(3HB-co-3% 3HV)	2900	–	38
P(3HB-co-9% 3HV)	1620	37	190
P(3HB-co-14% 3HV)	1500	35	150
P(3HB-co-20% 3HV)	1450	32	120
P(3HB-co-25% 3HV)	1370	30	70
P(3HB-co-40% 3HV-co-50% 4HB)	503	4	9
P(3HB-co-34% 3HV-co-55% 4HB)	618	3	10
P(3HB-co-23% 3HV-co-66% 4HB)	392	5	9
P(3HB-co-12% 3HV-co-76% 4HB)	142	9	4
P(3HB-co-6% 3HV-co-84% 4HB)	118	300	9
P(3HB-co-3% 3HV-co-93% 4HB)	127	430	14
P(3HB-co-5% 3HV-co-3HH _x)	63	123	2
P(3HB-co-3HV-co-12% 3HH _x)	135	108	5
P(3HB-co-1% 3HV-co-10.7% 3HH _x)	319	277	10
P(3HB-co-2.4% 3HV-co-13.4% 3HH _x)	110	481	8
P(3HB-co-5.4% 3HV-co-11.7% 3HH _x)	291	340	16
Polypropylene	590	435	27
High-density polyethylene	640	576	19
Low-density polyethylene	50–156	126–700	13–79

5 Biodegradability of PHAs

The ultimate advantage of PHAs that distinguishes it from other biopolymers is due to its biodegradability and biocompatibility characteristics. These polymers can be degraded under both aerobic and anaerobic environments [155]. The final products after the degradation of PHA are carbon dioxide and water in aerobic environments, whereas the end products during anaerobic degradation are carbon dioxide, methane, and water [156]. Moreover, they can also be degraded via thermal degradation, enzymatic hydrolysis, using microbial depolymerases, and by enzymatic and non-enzymatic hydrolysis in animal tissues [155]. The biopolymer is made up of 100% organic and bio-based resources having multiple degradable options. The carbon cycle of biopolymers is shown in Fig. 5 to have a better understanding on life cycle of biopolymers [157]. The degradation period ranges from few months in anaerobic condition and up to few years in brackish water. However, the rate of degradation can be accelerated under the application of UV light. As reported by Lee et al., it takes 6, 75, and 350 weeks for PHB to degrade in anaerobic condition, soil, and saline water, respectively [158]. During the degradation process, the microorganisms develop extracellular PHA depolymerases resulting in the conversion of PHAs into water-soluble oligomers and monomers as a carbon source. Similarly, the PHA-producing microorganisms hold the capability to degrade the PHA intracellularly. The PHA depolymerase break the polymer to hydroxyalkanoic acid [159]. It is biocompatible showing no lethal effect on animals for biomedical applications [124]. There are some generalized concepts, i.e., physical and chemical properties on which the biodegradability nature of PHA depends. The rate of biodegradation decreases with increase in melting point, stereo-regularity, and crystallinity of the polymer, whereas low molecular weight PHAs are prone to biodegradation. Biodegradation



Fig. 5 Carbon cycle of biopolymers

of PHA depends on several factors such as temperature, pressure, moisture, surface area, pH, and microbial effect in disposal environment [156]. Mergaert et al. studied the effect of temperature on biodegradation of simple PHA and its copolymer [160]. They noticed that for PHB, the weight loss was observed at 40 °C, which is higher compared to 28 °C for P(3HB-*co*-20% 3HV), because of the increase in microbial activity. Similarly, at higher temperature the rate of degradation for P(3HB-*co*-3HV) was very fast compared to PHB. It has also been observed that, with an increase in HV content in the copolymer, the rate of degradation increases [160].

6 Application of PHAs

The applications of PHAs have attracted not only the researchers but also the industries because of its competitive physical properties such as mechanical properties, crystallinity, and melting point with polyethylene and polypropylene. In this section, applications of PHAs in medical, agricultural, and industrial sector are discussed.

6.1 Medical Sector

The PHAs having higher mechanical strength are extensively used for preparation of medical scaffold in the form of screws, pins, etc. These PHAs are durable, harmless and help in the stem cell growth, and cartilage repair [161]. The PHAs can be used for enhancing the mechanical strength of bone tissues by copolymerizing with hydroxyapatite. Scaffolds made from PHBV coated with collagen are used to repair injured spinal cord. The fabrication of fibers and tubes into P(3HB)-*co*-HHx is used for curing Achilles tendon injury observed in rats. Because of biodegradability characteristics, PHAs can be easily placed inside the body as a carrier for controlled drug release [162]. PHAs such as P(3HB) and P(HB-*co*-HV) are used for healing the wounds of domestic animals. Due to promising mechanical properties, P(4HB) can be used to prepare suture, clinical meshes, etc. In spite of several medical applications, preparation of pure PHAs through industrially viable method must be developed to increase the demand for PHAs in medical sector [163]. The poly(ester urethane) based on poly(3-hydroxyhexanoate-*co*-3-hydroxyoctanoate) (PHHxHO) in the synthesis is more hydrophobic and used for synthesis of wound remedial and hemostatic materials. The graft copolymers contains poly(methyl methacrylate) as backbone and PHB as side chain. These graft polymers are commercially used as orthopedic application in the form of acrylic bone cement [164]. Similarly, PHAs such as PHB and PHBV help in activation of blood enzymes. These phenomena are achieved by reducing the concentration of LPS endotoxins from 100 to 120 U/g to 20 U/g using bacteria such as *A. eutrophus* and a recombinant strain of *E. coli* [165]. The nonwoven PHB sheets are used in preparation of effective superficial conduits for treatment of peripheral nerve and spinal cord injuries. For diseases like hernias

and gastrointestinal tract, PHB is proposed for repairing the soft tissues. However, all the applications are verified on animals like rats. Similarly, P(3HB-co-3HV) membranes are used for treatment of jaw bone defects and in growing the height of the rat mandible [166]. PHAs have also shown potential applications in diagnostic and therapeutic disease treatments. 3-HB has been commercially used for the preparation of low-cost point-of-care device for treatment of diabetic ketoacidosis (DKA) to help hyperglycemic patients. Moreover, 3-HB monomer is useful to maintain blood levels for the epilepsy and neurodegenerative disorders [167]. Some of the PHAs are used for anti-microbial treatment, e.g., 3-hydroxy-n-phenylalkanoic acid is used to counter-attack the universal strains like *Listeria monocytogenes*, which has the ability to grow at both extremely high and low temperatures and low pH [168].

6.2 Agricultural Sector

The PHA nanocomposites are used as plastic mulch in the cultivated land to prevent the growth of weeds and suppress the evaporation from the soil. They act as a protective layer to preserve the vital ingredients in the soil. It not only reduces the labor cost but also helps in ecofriendly recycling process [169]. The PHAs act as bacteria inoculants to improve nitrogen fixation in plant kingdom using strains such as *Azospirillum*. The plant growth is observed to be very consistent (irrespective of carriers) having intracellular PHA with *Azospirillum brasilense* strain [155]. The strain shows a greater permanence to withstand UV radiation, heat, osmotic pressure, etc. PHAs help in applying control release fertilizers by embedding pesticides in PHA polymer (e.g., P(3HB-3HV)) matrix to control the pest activity in farmer's crop fields. The copolymer gradually degrades by bacteria, microscopic algae, and fungi. However, it is essential to optimize the polymer to pesticide ratio and regulate the application of pesticide to obtain best mechanism to prevent pest activity [14, 155]. PHAs can also be used to act as a carrier to prevent herbicidal action to destroy invasive weeds from soil. Loading the chemicals like Zellek Super on poly(3HB-co-3HV) as carrier is one of the most effective methods during tillering phase on plants. Release of such pesticides in a controlled way helps in diminishing its adverse effect on human health, environment, and ecology [155].

6.3 Industrial Sector

The P(3HB-co-3HV) is thermoplastic copolymer which is being used by BIOPOL® for preparation of coat papers and paper boards, electrical appliances packaging, fishing nets and ropes, and several types of containers for storage of shampoo, razors, and motor oil. Another biopolymer produced by Nodax™ company synthesizes copolymer using P(3HB) and small amount of *mcl*-PHA. These polymers are available in the forms of foams, fibers, latex, and films [155]. PHAs have been applied

for renewable biofuel production by hydrolysis of PHAs followed by esterification that produces 3-hydroxyalkanoates methyl esters. These biofuels have similar energy content compared to bioethanol. Because of high glass transition temperature (T_m), PHB has limited applications in packaging industries. However, the glass transition temperature can be increased by incorporating hydroxyvalerate, which extends its application in packaging industry [170]. PHAs are also being used as toners for printing purposes and adhesives for coating applications [171].

7 Challenges in PHAs Production

Because of similar properties like petroleum-derived polymers and biodegradability characteristics, PHAs have acquired much consideration toward several academia research groups and industries. However, many factors limit its production for several manufacturing industries. It is estimated that PHAs are approximately 15 times more expensive than the conventional polymers [23]. The cost of PHAs production increases due to the carbon source substrates used for microbial growth. The usage of pure carbon sources such as glucose, fructose, and xylose constitutes significant amount of production cost to PHAs as their price is increasing very fast. Therefore, extraction of carbon sources from activated sludge, industrial waste, and food waste (rice, whey, malt, etc.) would be helpful in reducing the substrate cost. Similarly, with the advancement of technologies, the production of petroleum resources such as crude oil and shale gas increases significantly, and hence, the production cost of petroleum-derived plastics is not going to increase drastically in near future [172]. Hence, lowering the PHA cost is still a crucial challenge for industries. As it can be observed from the above-mentioned sections, the structure and physical properties of different types of PHAs (i.e., *scl*-PHA, *mcl*-PHA, and copolymers) are not similar and lie in a wide range of values. Therefore, it affects the economic situation of PHA-producing industries.

Apart from the basic challenges mentioned above, there exist a few technical challenges associated with the production process. The major limitation is the determination of optimized growth conditions of bacteria and production of microbial cells. Lower fermentation time results in reduction of PHAs yield, whereas higher fermentation time results in degradation of physical properties (as mentioned in Sect. 4.7). The entire synthesis process is extremely tedious and time consuming (takes several weeks to complete), which includes inoculum preparation, fermentation growth, lyophilization, extraction of PHA, and drying. One apparent limitation of the bioprocessing industries includes operation through batch process or non-continuous process, and fed-batch systems during synthesis process. This results in consumption of fresh water and additional energy requirements for sterilization process [172]. The conversion of PHA from its carbon source is another vital challenge for synthesis of PHA. Conversion of the substrates to PHA varies from 10 to 89% depending on the type of strains and carbon sources used [4]; however, the conversion of polyethylene and polypropylene can be achieved close to 100% from its

monomer. It can be noted that the 89% conversion of substrate to PHA is extremely difficult to attain and can be achieved under certain rigorous conditions and only for few particular types of PHA. Another critical factor that affects the economics is the oxygen limitation during high cell density culture. Supplying enough oxygen to obtain aerobic condition can increase the running cost of PHA production [158, 173]. Since PHA is an intracellular polymer, the extraction method results in additional costs of production. The solvent extraction of PHA leads to the accumulation of harmful wastes in the environment causing disposal and recycling issues. Moreover, the extraction methods such as digestion method are very expensive [23], whereas mechanical methods have abundant energy requirements for breakage of cell wall for releasing the PHA polymer. Thus, combination of latest mechanical method like ultrasonication with the usage of reduced amount of solvent like chloroform could be an effective alternative in terms of energy requirements for extraction of intracellular polymers [128].

8 Conclusion

This chapter has attempted to present a comprehensive discussion on various facets of microbial production (both upstream and downstream) and characterization of the biodegradable polymer of PHA. In addition, different aspects of biodegradation of PHAs, applications of PHA in several sectors, and challenges in commercial scale PHA production have also been discussed. PHAs were first synthesized in 1923 and since then, particularly after 1959, the developments in the preparation of *scl*-PHA, *mcl*-PHA, and copolymers have been quite phenomenal. From the properties of PHAs, it can be inferred that PHAs are one of the potential alternatives to substitute the conventional petroleum-derived polymers (e.g., HDPE, LDPE, and polypropylene). Approximately 90 various bacterial genera and up to 300 microorganism species were found to be PHA producers in both aerobic and anaerobic conditions. Carbon substrates such as commercial sugars, starch, industrial and food waste, biomass, and wastewater help in production of PHAs, along with different microorganisms, having PHA content in a wide range of 10–89%. These biopolymers are intracellular in nature, and therefore, several extraction methods have been proposed in this chapter to obtain pure form of PHA. Characterization techniques such as NMR and FTIR help in detection of functional groups present in PHA after extraction process. ^1H NMR helps in detecting $-\text{CH}$, $-\text{CH}_2$, and $-\text{CH}_3$ functional groups, whereas ^{13}C NMR helps in detection of additional $-\text{C}=\text{O}$ moiety in the form of chemical shifts. However, all the moieties can be observed in FTIR analysis by measuring absorbance as a function of wavenumbers. The crystalline nature of PHAs can be studied using various characterization techniques like XRD and DSC analytical tools. The crystallinity of PHA can be determined by measuring the area under the crystalline and amorphous region or using Scherrer's equation from XRD diffractogram. From DSC curve, the crystallinity can be measured from melting enthalpy of PHA samples. It has been observed that the PHAs are partially crystalline in nature

having crystallinity in the range of 34–53%. The properties such as melting point, crystallinity, tensile strength, and Young's modulus can be varied to a wide range by copolymerization of PHA depending upon the requirements and applications. The TGA and DTG analysis have shown that better thermal properties can be achieved by synthesizing copolymers of PHAs compared to simple PHB polymers. These polymers have excellent biodegradability and biocompatibility characteristics depending on several factors such as temperature, pressure, moisture, surface area, and pH of the disposal environment. They can be degraded in a few months to a few years in both aerobic and anaerobic conditions to carbon dioxide, methane, and water. However, cost of production, duration of fermentation process, and selection of ecofriendly extraction mechanisms are a few major challenges in commercial synthesis of PHA. It is anticipated that with advancement in basic research aimed at cheaper carbon sources and high yielding strains, commercialization of PHAs can be realized in near future.

References

1. de Paula FC, de Paula CB, Contiero J (2018) Prospective biodegradable plastics from biomass conversion processes. *Biofuels: state of development*:245–271 <https://doi.org/10.5772/intechopen.75111>
2. Anne B (2011) Environmental-friendly biodegradable polymers and composites. *Integrated waste management-volume I*. InTechOpen <https://doi.org/10.5772/16541>
3. Roy I, Visakh P (2014) Polyhydroxyalkanoate (PHA) based blends, composites and nanocomposites. *R Soc Chem*. <https://doi.org/10.1039/9781782622314>
4. Tan G-YA, Chen C-L, Li L, Ge L, Wang L, Razaad IMN, Li Y, Zhao L, Mo Y, Wang J-Y (2014) Start a research on biopolymer polyhydroxyalkanoate (PHA): a review. *Polymers* 6:706–754. <https://doi.org/10.3390/polym6030706>
5. Chan CM, Vandi L-J, Pratt S, Halley P, Richardson D, Werker A, Laycock B (2018) Composites of wood and biodegradable thermoplastics: a review. *Polym Rev* 58:444–494. <https://doi.org/10.1080/15583724.2017.1380039>
6. Amache R, Sukan A, Safari M, Roy I, Keshavarz T (2013) Advances in PHAs production. *Chem Eng Trans* 32:931–936. <https://doi.org/10.3303/CET1332156>
7. Huang JC, Shetty AS, Wang MS (1990) Biodegradable plastics: a review. *Adv Polym Technol* 10:23–30. <https://doi.org/10.1002/adv.1990.060100103>
8. Girdhar A, Bhatia M, Nagpal S, Kanampalliwar A, Tiwari A (2013) Process parameters for influencing polyhydroxyalkanoate producing bacterial factories: an overview. *J Pet Environ Biotechnol* 4:2. <https://doi.org/10.4172/2157-7463.1000155>
9. Chodak I (2008) Polyhydroxyalkanoates: origin, properties and applications. *Monomers, polymers and composites from renewable resources*. Elsevier, pp 451–477 <https://doi.org/10.1016/b978-0-08-045316-3.00022-3>
10. Alves MI, Macagnan KL, Rodrigues AA, de Assis DA, Torres MM, de Oliveira PD, Furlan L, Vendruscolo CT, Moreira AdS (2017) Poly (3-hydroxybutyrate)-P (3HB): review of production process technology. *Ind Biotechnol* 13:192–208. <https://doi.org/10.1089/ind.2017.0013>
11. Braunegg G, Lefebvre G, Genser KF (1998) Polyhydroxyalkanoates, biopolyesters from renewable resources: physiological and engineering aspects. *J Biotech* 65:127–161. [https://doi.org/10.1016/S0168-1656\(98\)00126-6](https://doi.org/10.1016/S0168-1656(98)00126-6)
12. Wallen LL, Rohwedder WK (1974) Poly-. beta.-hydroxyalkanoate from activated sludge. *Environ Sci Technol* 8:576–579. <https://doi.org/10.1021/es60091a007>

13. Kim BS, Lee SC, Lee SY, Chang HN, Chang YK, Woo SI (1994) Production of poly (3-hydroxybutyric acid) by fed-batch culture of *Alcaligenes eutrophus* with glucose concentration control. *Biotechnol Bioeng* 43:892–898. <https://doi.org/10.1002/bit.260430908>
14. Abdullah AA-A (2015) Microbial-based polyhydroxyalkanoates. *Smithers Rapra*
15. Sharma PK, Munir RI, Blunt W, Dartiailh C, Cheng J, Charles TC, Levin DB (2017) Synthesis and physical properties of polyhydroxyalkanoate polymers with different monomer compositions by recombinant *Pseudomonas putida* LS46 Expressing a Novel PHA synthase (PhaC116) enzyme. *Appl Sci* 7:242. <https://doi.org/10.3390/app7030242>
16. Ghaemy M, Haj MM, Tabaraki R (2000) Study of crystallinity of high-density polyethylene by inverse gas chromatography. 9:117–124
17. Koller M, Niebelschütz H, Braunegg G (2013) Strategies for recovery and purification of poly [(R)-3-hydroxyalkanoates](PHA) biopolyesters from surrounding biomass. *Eng Life Sci* 13:549–562. <https://doi.org/10.1002/elsc.201300021>
18. Koller M (2018) Biodegradable and biocompatible polyhydroxy-alkanoates (PHA): auspicious microbial macromolecules for pharmaceutical and therapeutic applications. *Molecules* 23:362. <https://doi.org/10.3390/molecules23020362>
19. Poirier Y, Nawrath C, Somerville C (1995) Production of polyhydroxyalkanoates, a family of biodegradable plastics and elastomers, in bacteria and plants. *Nature Biotechnol* 13:142
20. Sheu D-S, Lee C-Y (2004) Altering the substrate specificity of polyhydroxyalkanoate synthase I derived from *Pseudomonas putida* GPo1 by localized semirandom mutagenesis. *J Bacteriol* 186:4177–4184. <https://doi.org/10.1128/JB.186.13.4177-4184.2004>
21. Braunegg G, Bona R, Koller M (2004) Sustainable polymer production. *Polym Plast Technol Eng* 43:1779–1793. <https://doi.org/10.1081/PPT-200040130>
22. Khanna S, Srivastava AK (2005) Recent advances in microbial polyhydroxyalkanoates. *Process Biochem* 40:607–619. <https://doi.org/10.1016/j.procbio.2004.01.053>
23. Możejko-Ciesielska J, Kiewisz R (2016) Bacterial polyhydroxyalkanoates: still fabulous? *Microbiol Res* 192:271–282. <https://doi.org/10.1016/j.micres.2016.07.010>
24. Poli A, Di Donato P, Abbamondi GR, Nicolaus B (2011) Synthesis, production, and biotechnological applications of exopolysaccharides and polyhydroxyalkanoates by archaea. *Archaea* 2011 <https://doi.org/10.1155/2011/693253>
25. Shang L, Jiang M, Chang HN (2003) Poly (3-hydroxybutyrate) synthesis in fed-batch culture of *Ralstonia eutropha* with phosphate limitation under different glucose concentrations. *Biotechnol Lett* 25:1415–1419. <https://doi.org/10.1023/A:1025047410699>
26. Lemoigne M (1926) Produits de Deshydratation et de Polymerisation de L'acide β -Oxybutyrique. *Bull Soc Chim Biol* 8:770–782
27. Kim HW, Chung MG, Rhee YH (2007) Biosynthesis, modification, and biodegradation of bacterial medium-chain-length polyhydroxyalkanoates. *J Microbiol* 45:87–97
28. Zinn M, Witholt B, Egli T (2001) Occurrence, synthesis and medical application of bacterial polyhydroxyalkanoate. *Adv Drug Deliv Rev* 53:5–21. [https://doi.org/10.1016/S0169-409X\(01\)00218-6](https://doi.org/10.1016/S0169-409X(01)00218-6)
29. Muhammadi Shabina, Afzal M, Hameed S (2015) Bacterial polyhydroxyalkanoates-eco-friendly next generation plastic: production, biocompatibility, biodegradation, physical properties and applications. *Green Chem Lett Rev* 8:56–77. <https://doi.org/10.1080/17518253.2015.1109715>
30. Nitschke M, Costa SG, Contiero J (2011) Rhamnolipids and PHAs: recent reports on *Pseudomonas*-derived molecules of increasing industrial interest. *Process Biochem* 46:621–630. <https://doi.org/10.1016/j.procbio.2010.12.012>
31. Sathya A, Sivasubramanian V, Santhiagu A, Sebastian C, Sivashankar R (2018) Production of polyhydroxyalkanoates from renewable sources using bacteria. *J Polym Environ*:1–18 <https://doi.org/10.1007/s10924-018-1259-7>
32. Sabirova JS, Ferrer M, Lünsdorf H, Wray V, Kalscheuer R, Steinbüchel A, Timmis KN, Golyshin PN (2006) Mutation in a “tesB-like” hydroxyacyl-coenzyme A-specific thioesterase gene causes hyperproduction of extracellular polyhydroxyalkanoates by *Alcanivorax borkumensis* SK2. *J Bacteriol* 188:8452–8459. <https://doi.org/10.1128/JB.01321-06>

33. Wang Q, Yu H, Xia Y, Kang Z, Qi Q (2009) Complete PHB mobilization in *Escherichia coli* enhances the stress tolerance: a potential biotechnological application. *Microb Cell Fact* 8:47. <https://doi.org/10.1186/1475-2859-8-47>
34. Ashby RD, Solaiman DK, Foglia TA (2005) Synthesis of short-/medium-chain-length poly (hydroxyalkanoate) blends by mixed culture fermentation of glycerol. *Biomacromol* 6:2106–2112. <https://doi.org/10.1021/bm058005h>
35. Ben M, Mato T, Lopez A, Vila M, Kennes C, Veiga MC (2011) Bioplastic production using wood mill effluents as feedstock. *Water Sci Technol* 63:1196–1202. <https://doi.org/10.2166/wst.2011.358>
36. De Grazia G, Quadri L, Majone M, Morgan-Sagastume F, Werker A (2017) Influence of temperature on mixed microbial culture polyhydroxyalkanoate production while treating a starch industry wastewater. *J Environ Chem Eng* 5:5067–5075. <https://doi.org/10.1016/j.jece.2017.09.041>
37. Luengo JM, García B, Sandoval A, Naharro G, Olivera ER (2003) Bioplastics from microorganisms. *Curr Opin Microbiol* 6:251–260 [https://doi.org/10.1016/s1369-5274\(03\)00040-7](https://doi.org/10.1016/s1369-5274(03)00040-7)
38. Huijberts G, Eggink G, De Waard P, Huisman GW, Witholt B (1992) *Pseudomonas putida* KT2442 cultivated on glucose accumulates poly (3-hydroxyalkanoates) consisting of saturated and unsaturated monomers. *Appl Environ Microbiol* 58:536–544
39. Inoue D, Suzuki Y, Uchida T, Morohoshi J, Sei K (2016) Polyhydroxyalkanoate production potential of heterotrophic bacteria in activated sludge. *J Biosci Bioeng* 121:47–51. <https://doi.org/10.1016/j.jbiosc.2015.04.022>
40. Jiang G, Hill D, Kowalczyk M, Johnston B, Adamus G, Irorere V, Radecka I (2016) Carbon sources for polyhydroxyalkanoates and an integrated biorefinery. *Int J Mol Sci* 17:1157. <https://doi.org/10.3390/ijms17071157>
41. Kim YB, Rhee YH (2000) Evaluation of various carbon substrates for the biosynthesis of polyhydroxyalkanoates bearing functional groups by *Pseudomonas putida*. *Int J Biol Macromol* 28:23–29. [https://doi.org/10.1016/S0141-8130\(00\)00150-1](https://doi.org/10.1016/S0141-8130(00)00150-1)
42. de Almeida A, Giordano AM, Nikel PI, Pettinari MJ (2010) Effects of aeration on the synthesis of poly (3-hydroxybutyrate) from glycerol and glucose in recombinant *Escherichia coli*. *Appl Environ Microbiol* 76:2036–2040. <https://doi.org/10.1128/AEM.02706-09>
43. Arikawa H, Matsumoto K, Fujiki T (2017) Polyhydroxyalkanoate production from sucrose by *Cupriavidus necator* strains harboring csc genes from *Escherichia coli* W. *Appl Microbiol Biotechnol* 101:7497–7507. <https://doi.org/10.1007/s00253-017-8470-7>
44. Beccari M, Bertin L, Dionisi D, Fava F, Lampis S, Majone M, Valentino F, Vallini G, Villano M (2009) Exploiting olive oil mill effluents as a renewable resource for production of biodegradable polymers through a combined anaerobic-aerobic process. *J Chem Technol Biotechnol* 84:901–908. <https://doi.org/10.1002/jctb.2173>
45. Ben M, Kennes C, Veiga MC (2016) Optimization of polyhydroxyalkanoate storage using mixed cultures and brewery wastewater. *J Chem Technol Biotechnol* 91:2817–2826. <https://doi.org/10.1002/jctb.4891>
46. Bengtsson S, Werker A, Welander T (2008) Production of polyhydroxyalkanoates by glycogen accumulating organisms treating a paper mill wastewater. *Water Sci Technol* 58:323–330. <https://doi.org/10.2166/wst.2008.381>
47. Bhattacharyya A, Pramanik A, Maji SK, Halder S, Mukhopadhyay UK, Mukherjee J (2012) Utilization of vinasse for production of poly-3-(hydroxybutyrate-co-hydroxyvalerate) by *Haloflex mediterranei*. *AMB Express* 2:34. <https://doi.org/10.1186/2191-0855-2-34>
48. Bhubalan K, Lee W-H, Loo C-Y, Yamamoto T, Tsuge T, Doi Y, Sudesh K (2008) Controlled biosynthesis and characterization of poly (3-hydroxybutyrate-co-3-hydroxyvalerate-co-3-hydroxyhexanoate) from mixtures of palm kernel oil and 3HV-precursors. *Polym Degrad Stab* 93:17–23 <https://doi.org/10.1016/j.polymdegradstab.2007.11.004>
49. Campanari S, Augelletti F, Rossetti S, Sciubba F, Villano M, Majone M (2017) Enhancing a multi-stage process for olive oil mill wastewater valorization towards polyhydroxyalkanoates and biogas production. *Chem Eng J* 317:280–289. <https://doi.org/10.1016/j.cej.2017.02.094>

50. Cavalheiro JM, de Almeida MCM, Grandfils C, Da Fonseca M (2009) Poly (3-hydroxybutyrate) production by *Cupriavidus necator* using waste glycerol. *Process Biochem* 44:509–515. <https://doi.org/10.1016/j.procbio.2009.01.008>
51. Cesário MT, Raposo RS, de Almeida MCM, van Keulen F, Ferreira BS, da Fonseca MMR (2014) Enhanced bioproduction of poly-3-hydroxybutyrate from wheat straw lignocellulosic hydrolysates. *N Biotechnol* 31:104–113. <https://doi.org/10.1016/j.nbt.2013.10.004>
52. Chaleomrum N, Chookietwattana K, Dararat S (2014) Production of PHA from cassava starch wastewater in sequencing batch reactor treatment system. *APCBEE Procedia* 8:167–172. <https://doi.org/10.1016/j.apcb.2014.03.021>
53. Chaudhry WN, Jamil N, Ali I, Ayaz MH, Hasnain S (2011) Screening for polyhydroxyalkanoate (PHA)-producing bacterial strains and comparison of PHA production from various inexpensive carbon sources. *Ann Microbiol* 61:623–629. <https://doi.org/10.1007/s13213-010-0181-6>
54. Chee JY, Lau NS, Samian MR, Tsuge T, Sudesh K (2012) Expression of *Aeromonas caviae* polyhydroxyalkanoate synthase gene in *Burkholderia* sp. USM (JCM15050) enables the biosynthesis of SCL-MCL PHA from palm oil products. *J Appl Microbiol* 112:45–54. <https://doi.org/10.1111/j.1365-2672.2011.05189>
55. Chen CW, Don T-M, Yen H-F (2006) Enzymatic extruded starch as a carbon source for the production of poly (3-hydroxybutyrate-co-3-hydroxyvalerate) by *Haloferax mediterranei*. *Process Biochem* 41:2289–2296. <https://doi.org/10.1016/j.procbio.2006.05.026>
56. de Paula FC, Kakazu S, de Paula CBC, Gomez JGC, Contiero J (2017) Polyhydroxyalkanoate production from crude glycerol by newly isolated *Pandoraea* sp. *J King Saud Univ Sci* 29:166–173. <https://doi.org/10.1016/j.jksus.2016.07.002>
57. Devi AB, Nachiyar CV, Kaviyarsi T, Samrot AV (2015) Characterization of polyhydroxybutyrate synthesized by *Bacillus cereus*. *Int J Pharm Pharm Sci* 7:140–144
58. Eshtaya MK, Nor 'Aini AR, Hassan MA (2013) Bioconversion of restaurant waste into Polyhydroxybutyrate (PHB) by recombinant *E. coli* through anaerobic digestion. *Int J Environ Waste Manag* 11:27–37 <https://doi.org/10.1504/ijewm.2013.050521>
59. Freches A, Lemos PC (2017) Microbial selection strategies for polyhydroxyalkanoates production from crude glycerol: effect of OLR and cycle length. *N Biotechnol* 39:22–28
60. Haas R, Jin B, Zepf FT (2008) Production of poly (3-hydroxybutyrate) from waste potato starch. *Biosci Biotechnol Biochem* 72:253–256. <https://doi.org/10.1016/j.nbt.2017.05.011>
61. Hafuka A, Sakaida K, Satoh H, Takahashi M, Watanabe Y, Okabe S (2011) Effect of feeding regimens on polyhydroxybutyrate production from food wastes by *Cupriavidus necator*. *Bioresour Technol* 102:3551–3553. <https://doi.org/10.1016/j.biortech.2010.09.018>
62. Halami PM (2008) Production of polyhydroxyalkanoate from starch by the native isolate *Bacillus cereus* CFR06. *World J Microbiol Biotechnol* 24:805–812. <https://doi.org/10.1007/s11274-007-9543-z>
63. He W, Tian W, Zhang G, Chen G-Q, Zhang Z (1998) Production of novel polyhydroxyalkanoates by *Pseudomonas stutzeri* 1317 from glucose and soybean oil. *FEMS Microbiol Lett* 169:45–49. <https://doi.org/10.1111/j.1574-6968.1998.tb13297.x>
64. Huang T-Y, Duan K-J, Huang S-Y, Chen CW (2006) Production of polyhydroxyalkanoates from inexpensive extruded rice bran and starch by *Haloferax mediterranei*. *J Ind Microbiol Biotechnol* 33:701–706. <https://doi.org/10.1007/s10295-006-0098-z>
65. Jiang Y, Marang L, Tamis J, van Loosdrecht MC, Dijkman H, Kleerebezem R (2012) Waste to resource: converting paper mill wastewater to bioplastic. *Water Res* 46:5517–5530. <https://doi.org/10.1016/j.watres.2012.07.028>
66. Khardenavis AA, Kumar MS, Mudliar SN, Chakrabarti T (2007) Biotechnological conversion of agro-industrial wastewaters into biodegradable plastic, poly β -hydroxybutyrate. *Bioresour Technol* 98:3579–3584. <https://doi.org/10.1016/j.biortech.2006.11.024>
67. Kim BS (2000) Production of poly (3-hydroxybutyrate) from inexpensive substrates. *Enzyme Microb Technol* 27:774–777. [https://doi.org/10.1016/S0141-0229\(00\)00299-4](https://doi.org/10.1016/S0141-0229(00)00299-4)
68. Koller M (2015) Recycling of waste streams of the biotechnological poly (hydroxyalkanoate) production by *Haloferax mediterranei* on whey. *Int J Polym Sci* 2015 <https://doi.org/10.1155/2015/370164>

69. Lau N-S, Sudesh K (2012) Revelation of the ability of *Burkholderia* sp. USM (JCM 15050) PHA synthase to polymerize 4-hydroxybutyrate monomer. *AMB express* 2:41 <https://doi.org/10.1186/2191-0855-2-41>
70. Liu H-Y, Hall PV, Darby JL, Coats ER, Green PG, Thompson DE, Loge FJ (2008) Production of polyhydroxyalkanoate during treatment of tomato cannery wastewater. *Water Environ Res* 80:367–372. <https://doi.org/10.2175/106143007X221535>
71. Lopes MSG, Gomez JGC, Taciro MK, Mendonça TT, Silva LF (2014) Polyhydroxyalkanoate biosynthesis and simultaneous removal of organic inhibitors from sugarcane bagasse hydrolysate by *Burkholderia* sp. *J Ind Microbiol Biotechnol* 41:1353–1363. <https://doi.org/10.1007/s10295-014-1485-5>
72. Moita R, Freches A, Lemos P (2014) Crude glycerol as feedstock for polyhydroxyalkanoates production by mixed microbial cultures. *Water Res* 58:9–20. <https://doi.org/10.1016/j.watres.2014.03.066>
73. Nikel PI, Giordano AM, de Almeida A, Godoy MS, Pettinari MJ (2010) Elimination of D-lactate synthesis increases poly (3-hydroxybutyrate) and ethanol synthesis from glycerol and affects cofactor distribution in recombinant *Escherichia coli*. *Appl Environ Microbiol* 76:7400–7406. <https://doi.org/10.1128/AEM.02067-10>
74. Obruca S, Petrik S, Benesova P, Svoboda Z, Eremka L, Marova I (2014) Utilization of oil extracted from spent coffee grounds for sustainable production of polyhydroxyalkanoates. *Appl Microbiol Biotechnol* 98:5883–5890. <https://doi.org/10.1007/s00253-014-5653-3>
75. Pais J, Serafim LS, Freitas F, Reis MA (2016) Conversion of cheese whey into poly (3-hydroxybutyrate-co-3-hydroxyvalerate) by *Haloferax mediterranei*. *N Biotechnol* 33:224–230. <https://doi.org/10.1016/j.nbt.2015.06.001>
76. Pantazaki AA, Papanephytous CP, Pritsa AG, Liakopoulou-Kyriakides M, Kyriakidis DA (2009) Production of polyhydroxyalkanoates from whey by *Thermus thermophilus* HB8. *Process Biochem* 44:847–853. <https://doi.org/10.1016/j.procbio.2009.04.002>
77. Poblete-Castro I, Rodriguez AL, Lam CMC, Kessler W (2013) Improved production of medium-chain-length Polyhydroxyalkanoates in glucose-based fed-batch cultivations of metabolically engineered *Pseudomonas putida* strains. *J Microbiol Biotechnol*
78. Poomipuk N, Reungsang A, Plangklang P (2014) Poly- β -hydroxyalkanoates production from cassava starch hydrolysate by *Cupriavidus* sp. KKU38. *Int J Biol Macromol* 65:51–64. <https://doi.org/10.1016/j.jbiomac.2014.01.002>
79. Povo S, Toffano P, Basaglia M, Casella S (2010) Polyhydroxyalkanoates production by engineered *Cupriavidus necator* from waste material containing lactose. *Bioresour Technol* 101:7902–7907. <https://doi.org/10.1016/j.biortech.2010.05.029>
80. Pradhan S, Borah AJ, Poddar MK, Dikshit PK, Rohidas L, Moholkar VS (2017) Microbial Production, Ultrasound-Assisted Extraction and Characterization of Biopolymer Polyhydroxybutyrate (PHB) from Terrestrial (*P. hysterophorus*) and Aquatic (*E. crassipes*) Invasive Weeds. *Bioresour Technol* 242:304–310. <https://doi.org/10.1016/j.biortech.2017.03.117>
81. Rojas-Rosas O, Villafañá-Rojas J, López-Dellamary FA, Nungaray-Arellano J, González-Reynoso O (2007) Production and characterization of polyhydroxyalkanoates in *Pseudomonas aeruginosa* ATCC 9027 from glucose, an unrelated carbon source. *Can J Microbiol* 53:840–851. <https://doi.org/10.1139/W07-023>
82. Saranya V, Shenbagarathai R (2011) Production and characterization of PHA from recombinant *E. coli* harbouring phaC1 gene of indigenous *Pseudomonas* sp. LDC-5 using molasses. *Braz J Microbiol* 42:1109–1118. <https://doi.org/10.1590/S1517-838220110003000032>
83. Sato S, Maruyama H, Fujiki T, Matsumoto K (2015) Regulation of 3-hydroxyhexanoate composition in PHB synthesized by recombinant *Cupriavidus necator* H16 from plant oil by using butyrate as a co-substrate. *J Biosci Bioeng* 120:246–251. <https://doi.org/10.1016/j.jbiosc.2015.01.016>
84. Sindhu R, Silviya N, Binod P, Pandey A (2013) Pentose-rich hydrolysate from acid pretreated rice straw as a carbon source for the production of poly-3-hydroxybutyrate. *Biochem Eng J* 78:67–72. <https://doi.org/10.1016/j.bej.2012.12.015>

85. Taniguchi I, Kagotani K, Kimura Y (2003) Microbial production of poly (hydroxyalkanoate) s from waste edible oils. *Green Chem* 5:545–548. <https://doi.org/10.1039/B304800B>
86. Tobella LM, Bunster M, Pooley A, Becerra J, Godoy F, Martínez MA (2005) Biosynthesis of poly- β -hydroxyalkanoates by *Sphingopyxis chilensis* S37 and *Wautersia* sp. PZK cultured in cellulose pulp mill effluents containing 2, 4, 6-trichlorophenol. *J Ind Microbiol Biotechnol* 32:397–401. <https://doi.org/10.1007/s10295-005-0011-1>
87. Van-Thuoc D, Quillaguaman J, Mamo G, Mattiasson B (2008) Utilization of agricultural residues for poly (3-hydroxybutyrate) production by *Halomonas boliviensis* LC1. *J Appl Microbiol* 104:420–428. <https://doi.org/10.1111/j.1365-2672.2007.03553.x>
88. Wang Q, Tappel RC, Zhu C, Nomura CT (2012) Development of a new strategy for production of medium-chain-length polyhydroxyalkanoates by recombinant *Escherichia coli* via inexpensive non-fatty acid feedstocks. *Appl Environ Microbiol* 78:519–527. <https://doi.org/10.1128/AEM.07020-11>
89. Wang Y, Zhao F, Fan X, Wang S, Song C (2016) Enhancement of medium-chain-length polyhydroxyalkanoates biosynthesis from glucose by metabolic engineering in *Pseudomonas mendocina*. *Biotechnol Lett* 38:313–320. <https://doi.org/10.1007/s10529-015-1980-4>
90. Yamane T, Fukunaga M, Lee YW (1996) Increased PHB productivity by high-cell-density fed-batch culture of *Alcaligenes latus*, a growth-associated PHB producer. *Biotechnol Bioeng* 50:197–202 [https://doi.org/10.1002/\(sici\)1097-0290\(19960420\)50:2%3c197::aid-bit8%3e3.0.co;2-h](https://doi.org/10.1002/(sici)1097-0290(19960420)50:2%3c197::aid-bit8%3e3.0.co;2-h)
91. Yu J, Stahl H (2008) Microbial utilization and biopolyester synthesis of bagasse hydrolysates. *Bioresour Technol* 99:8042–8048. <https://doi.org/10.1016/j.biortech.2008.03.071>
92. Yu P, Chua H, Huang A, Lo W, Chen G (1998) Conversion of food industrial wastes into bioplastics. *Appl Biochem Biotechnol* 70:603–614. <https://doi.org/10.1007/BF02920172>
93. Zakaria MR, Tabatabaei M, Ghazali FM, Abd-Aziz S, Shirai Y, Hassan MA (2010) Polyhydroxyalkanoate production from anaerobically treated palm oil mill effluent by new bacterial strain *Comamonas* sp. EB172. *World J Microbiol Biotechnol* 26:767–774. <https://doi.org/10.1007/s11274-009-0232-y>
94. Park SJ, Jang YA, Noh W, Oh YH, Lee H, David Y, Baylon MG, Shin J, Yang JE, Choi SY (2015) Metabolic engineering of *Ralstonia eutropha* for the production of polyhydroxyalkanoates from sucrose. *Biotechnol Bioeng* 112:638–643. <https://doi.org/10.1002/bit.25469>
95. Grothe E, Moo-Young M, Chisti Y (1999) Fermentation optimization for the production of poly (β -hydroxybutyric acid) microbial thermoplastic. *Enzym Microb Technol* 25:132–141. [https://doi.org/10.1016/S0141-0229\(99\)00023-X](https://doi.org/10.1016/S0141-0229(99)00023-X)
96. Tanamool V, Imai T, Danvirutai P, Kaewkannetra P (2010) Screening, identification and production of polyhydroxyalkanoates (PHAs) by sucrose utilizing microbes isolated from soil environments. *J Biotechnol* 150:361. <https://doi.org/10.1016/j.jbiotec.2010.09.419>
97. Zhang H, Obias V, Gonyer K, Dennis D (1994) Production of polyhydroxyalkanoates in sucrose-utilizing recombinant *Escherichia coli* and *Klebsiella* strains. *Appl Environ Microbiol* 60:1198–1205
98. Obruca S, Benesova P, Marsalek L, Marova I (2015) Use of lignocellulosic materials for PHA production. *Chem Biochem Eng Q* 29:135–144. <https://doi.org/10.15255/CABEQ.2014.2253>
99. Strong PJ, Laycock B, Mahamud SNS, Jensen PD, Lant PA, Tyson G, Pratt S (2016) The opportunity for high-performance biomaterials from methane. *Microorganisms* 4:11. <https://doi.org/10.3390/microorganisms4010011>
100. Alavi S, Thomas S, Sandeep K, Kalarikkal N, Varghese J, Yaragalla S (2014) *Polymers for packaging applications*. CRC Press
101. Ren21 R (2016) Global status report. REN21 secretariat, Paris. United Nations Environment Program, Paris, France, p 272
102. Wu TY, Mohammad AW, Jahim JM, Anuar N (2009) A holistic approach to managing palm oil mill effluent (POME): biotechnological advances in the sustainable reuse of POME. *Biotechnol Adv* 27:40–52. <https://doi.org/10.1016/j.biotechadv.2008.08.005>

103. Hassan MA, Shirai Y, Kusubayashi N, Karim MIA, Nakanishi K, Hashimoto K (1996) Effect of organic acid profiles during anaerobic treatment of palm oil mill effluent on the production of polyhydroxyalkanoates by *Rhodobacter sphaeroides*. J Ferment Bioeng 82:151–156. [https://doi.org/10.1016/0922-338X\(96\)85038-0](https://doi.org/10.1016/0922-338X(96)85038-0)
104. Parfitt J, Barthel M, Macnaughton S (2010) Food waste within food supply chains: quantification and potential for change to 2050. Philos Trans R Soc Lond B Biol Sci 365:3065–3081. <https://doi.org/10.1098/rstb.2010.0126>
105. Braguglia CM, Gallipoli A, Gianico A, Pagliaccia P (2017) Anaerobic bioconversion of food waste into energy: a critical review. Bioresour Technol 248:37–56. <https://doi.org/10.1016/j.biortech.2017.06.145>
106. Lucifero N (2016) Food Loss and Waste in the EU Law between sustainability of well-being and the implications on food system and on environment. Agric Agric Sci Procedia 8:282–289. <https://doi.org/10.1016/j.aaspro.2016.02.022>
107. Gomez JG, Méndez BS, Nickel PI, Pettinari MJ, Prieto MA, Silva LF (2011) Making green polymers even greener: towards sustainable production of poly (hydroxy-alkanoates) from agroindustrial by-products. Advances in applied biotechnology. InTechOpen <https://doi.org/10.5772/31847>
108. Kimura H, Takahashi T, Hiraka H, Iwama M, Takeishi M (1999) Effective biosynthesis of poly (3-hydroxybutyrate) from plant oils by Chromobacterium sp. Polym J 31:210
109. Nielsen C, Rahman A, Rehman AU, Walsh MK, Miller CD (2017) Food waste conversion to microbial polyhydroxyalkanoates. Microb Biotechnol 10:1338–1352. <https://doi.org/10.1111/1751-7915.12776>
110. Solaiman DK, Ashby RD, Foglia TA, Marmer WN (2006) Conversion of agricultural feedstock and coproducts into poly (hydroxyalkanoates). Appl Microbiol Biotechnol 71:783–789. <https://doi.org/10.1007/s00253-006-0451-1>
111. Gray KA, Zhao L, Emptage M (2006) Bioethanol. Curr Opin Chem Biol 10:141–146. <https://doi.org/10.1016/j.cbpa.2006.02.035>
112. Seidl PR, Goulart AK (2016) Pretreatment processes for lignocellulosic biomass conversion to biofuels and bioproducts. Curr Opin Green Sustainable Chem 2:48–53. <https://doi.org/10.1016/j.cogsc.2016.09.003>
113. Zhang Y-HP, Berson E, Sarkanen S, Dale BE (2009) Sessions 3 and 8: pretreatment and biomass recalcitrance: fundamentals and progress. Appl Biochem Biotechnol 153:80–83. <https://doi.org/10.1007/s12010-009-8610-3>
114. Ryu HW, Cho KS, Goodrich PR, Park C-H (2008) Production of polyhydroxyalkanoates by *Azotobacter vinelandii* UWD using swine wastewater: effect of supplementing glucose, yeast extract, and inorganic salts. Biotechnol Bioprocess Eng 13:651–658. <https://doi.org/10.1007/s12257-008-0072-x>
115. Yan S, Tyagi R, Surampalli R (2006) Polyhydroxyalkanoates (PHA) production using wastewater as carbon source and activated sludge as microorganisms. Water Sci Technol 53:175–180
116. Jacquelin N, Lo C-W, Wei Y-H, Wu H-S, Wang SS (2008) Isolation and purification of bacterial poly (3-hydroxyalkanoates). Biochem Eng J 39:15–27. <https://doi.org/10.1016/j.bej.2007.11.029>
117. Chanprateep S, Buasri K, Muangwong A, Utiswannahakul P (2010) Biosynthesis and biocompatibility of biodegradable poly (3-hydroxybutyrate-co-4-hydroxybutyrate). Polym Degrad Stab 95:2003–2012. <https://doi.org/10.1016/j.polydegradstab.2010.07.014>
118. Chen Y, Chen J, Yu C, Du G, Lun S (1999) Recovery of poly-3-hydroxybutyrate from Alcaligenes eutrophus by surfactant-chelate aqueous system. Process Biochem 34:153–157. [https://doi.org/10.1016/S0032-9592\(98\)00082-X](https://doi.org/10.1016/S0032-9592(98)00082-X)
119. Hahn SK, Chang YK, Kim BS, Chang HN (1994) Optimization of microbial poly (3-hydroxybutyrate) recover using dispersions of sodium hypochlorite solution and chloroform. Biotechnol Bioeng 44:256–261. <https://doi.org/10.1002/bit.260440215>
120. Holmes PA, Lim GB (1990) Separation process. Google Patents

121. Kathiraser Y, Aroua MK, Ramachandran KB, Tan IKP (2007) Chemical characterization of medium-chain-length polyhydroxyalkanoates (PHAs) recovered by enzymatic treatment and ultrafiltration. *J Chem Technol Biotechnol* 82:847–855. <https://doi.org/10.1002/jctb.1751>
122. Kunasundari B, Sudesh K (2011) Isolation and recovery of microbial polyhydroxyalkanoates. *Express Polym Lett* 5:620–634
123. Raza ZA, Abid S, Banat IM (2018) Polyhydroxyalkanoates: characteristics, production, recent developments and applications. *Int Biodeterior Biodegradation* 126:45–56. <https://doi.org/10.1016/j.ibiod.2017.10.001>
124. Verlinden RA, Hill DJ, Kenward M, Williams CD, Radecka I (2007) Bacterial synthesis of biodegradable polyhydroxyalkanoates. *J Appl Microbiol* 102:1437–1449. <https://doi.org/10.1111/j.1365-2672.2007.03335.x>
125. Ranjan A, Singh S, Malani RS, Moholkar VS (2016) Ultrasound-assisted bioalcohol synthesis: review and analysis. *RSC Adv* 6:65541–65562. <https://doi.org/10.1039/C6RA11580B>
126. Poddar MK, Pradhan S, Moholkar VS, Arjmand M, Sundararaj U (2018) Ultrasound-assisted synthesis and characterization of polymethyl methacrylate/reduced graphene oxide nanocomposites. *AIChE J* 64:673–687. <https://doi.org/10.1002/aic.15936>
127. Malani RS, Pradhan S, Goyal A, Moholkar VS (2016) Ultrasound-Assisted Interesterification of Waste cooking Oil with Heterogeneous Catalyst. In: LAMSYS 2016, Satish Dhawan Space Centre (SDSC), ISRO, Sriharikota
128. Pradhan S, Dikshit PK, Moholkar VS (2018) Production, ultrasonic extraction, and characterization of poly (3-hydroxybutyrate)(PHB) using *Bacillus megaterium* and *Cupriavidus necator*. *Polym Adv Technol* 29:2392–2400. <https://doi.org/10.1002/pat.4351>
129. Vrábel P, Hronský V, Fričová O, Koval'aková M, Chodák I, Alexy P (2014) Solid State ¹³C NMR Study of Modified Polyhydroxybutyrate. *Acta Phys Pol, A* 126:419–420. <https://doi.org/10.12693/APhysPolA.126.419>
130. Zhu C, Nomura CT, Perrotta JA, Stipanovic AJ, Nakas JP (2010) Production and characterization of poly-3-hydroxybutyrate from biodiesel-glycerol by *Burkholderia cepacia* ATCC 17759. *Biotechnol Prog* 26:424–430. <https://doi.org/10.1002/btpr.355>
131. Shang L, Yim SC, Park HG, Chang HN (2004) Sequential Feeding of Glucose and Valerate in a Fed-Batch Culture of *Ralstonia eutropha* for Production of Poly (hydroxybutyrate-co-hydroxyvalerate) with High 3-Hydroxyvalerate Fraction. *Biotechnol Progr* 20:140–144
132. Bhati R, Mallick N (2012) Production and characterization of poly (3-hydroxybutyrate-co-3-hydroxyvalerate) co-polymer by a N₂-fixing cyanobacterium, *Nostoc muscorum* Agardh. *J Chem Technol Biotechnol* 87:505–512
133. Gumel AM, Annuar MSM, Heidelberg T (2012) Biosynthesis and characterization of polyhydroxyalkanoates copolymers produced by *Pseudomonas putida* Bet001 isolated from palm oil mill effluent. *PLoS ONE* 7:e45214
134. Cyrus VP, Soledad CM, Analía V (2009) Biocomposites based on renewable resource: acetylated and non acetylated cellulose cardboard coated with polyhydroxybutyrate. *Polymer* 50:6274–6280
135. Baskaran M, Hashim R, Said N, Raffi SM, Balakrishnan K, Sudesh K, Sulaiman O, Arai T, Kosugi A, Mori Y (2012) Properties of binderless particleboard from oil palm trunk with addition of polyhydroxyalkanoates. *Compos Part B: Eng* 43:1109–1116
136. Mousavioun P, Doherty WO, George G (2010) Thermal stability and miscibility of poly (hydroxybutyrate) and soda lignin blends. *Ind Crop Prod* 32:656–661
137. Mottin AC, Ayres E, Oréface RL, Câmara JJD (2016) What changes in poly (3-hydroxybutyrate)(PHB) when processed as electrospun nanofibers or thermo-compression molded film? *Mat Res* 19:57–66
138. Sun X, Guo L, Sato H, Ozaki Y, Yan S, Takahashi I (2011) A study on the crystallization behavior of poly (β-hydroxybutyrate) thin films on si wafers. *Polymer* 52:3865–3870
139. Senhorini GA, Zawadzki SF, Farago PV, Zanin SM, Marques FA (2012) Microparticles of poly (hydroxybutyrate-co-hydroxyvalerate) loaded with andiroba oil: preparation and characterization. *Mater Sci Eng, C* 32:1121–1126

140. Canetti M, Urso M, Sadocco P (1999) Influence of the morphology and of the supermolecular structure on the enzymatic degradation of bacterial poly (3-hydroxybutyrate). *Polymer* 40:2587–2594
141. Chen L, Wang M (2002) Production and evaluation of biodegradable composites based on PHB-PHV copolymer. *Biomaterials* 23:2631–2639
142. Oliveira FC, Dias ML, Castilho LR, Freire DM (2007) Characterization of poly (3-hydroxybutyrate) produced by *Cupriavidus necator* in solid-state fermentation. *Bioresour Technol* 98:633–638
143. Chaijamrus S, Udpuay N (2008) Production and characterization of polyhydroxybutyrate from molasses and corn steep liquor produced by *Bacillus megaterium* ATCC 6748. *Agric Eng Int X*:1–12
144. Cheng S-T, Chen Z-F, Chen G-Q (2008) The expression of cross-linked elastin by rabbit blood vessel smooth muscle cells cultured in polyhydroxyalkanoate scaffolds. *Biomaterials* 29:4187–4194. <https://doi.org/10.1016/j.biomaterials.2008.07.022>
145. Pradhan S, Dikshit PK, Moholkar VS (2018) Production and characterization of biodegradable polymer poly (3-hydroxybutyrate) using ultrasound assisted extraction. In: Abstracts of papers of the American Chemical Society, Boston, MA. Amer Chemical Soc 1155 16th St, NW, Washington, DC 20036 USA. https://scholar.google.com/scholar?hl=en&as_sdt=0,37&cluster=12756667527516586406
146. Xie WP, Chen G-Q (2008) Production and characterization of terpolyester poly (3-hydroxybutyrate-co-4-hydroxybutyrate-co-3-hydroxyhexanoate) by recombinant *Aeromonas hydrophila* 4AK4 harboring genes phaPCJ. *Biochem Eng J* 38:384–389. <https://doi.org/10.1016/j.bej.2007.08.002>
147. Carrasco F, Dionisi D, Martinelli A, Majone M (2006) Thermal stability of polyhydroxyalkanoates. *J Appl Polym Sci* 100:2111–2121. <https://doi.org/10.1002/app.23586>
148. Zhao W, Chen G-Q (2007) Production and characterization of terpolyester poly (3-hydroxybutyrate-co-3-hydroxyvalerate-co-3-hydroxyhexanoate) by recombinant *Aeromonas hydrophila* 4AK4 harboring genes phaAB. *Process Biochem* 42:1342–1347. <https://doi.org/10.1016/j.procbio.2007.07.006>
149. Wong Y-M, Brigham CJ, Rha C, Sinskey AJ, Sudesh K (2012) Biosynthesis and characterization of polyhydroxyalkanoate containing high 3-hydroxyhexanoate monomer fraction from crude palm kernel oil by recombinant *Cupriavidus necator*. *Bioresour Technol* 121:320–327. <https://doi.org/10.1016/j.biortech.2012.07.015>
150. Lau N-S, Tsuge T, Sudesh K (2011) Formation of new polyhydroxyalkanoate containing 3-hydroxy-4-methylvalerate monomer in *Burkholderia* sp. *Appl Microbiol Biotechnol* 89:1599–1609. <https://doi.org/10.1007/s00253-011-3097-6>
151. He JD, Cheung MK, Yu PH, Chen GQ (2001) Thermal analyses of poly (3-hydroxybutyrate), poly (3-hydroxybutyrate-co-3-hydroxyvalerate), and poly (3-hydroxybutyrate-co-3-hydroxyhexanoate). *J Appl Polym Sci* 82:90–98. <https://doi.org/10.1002/app.1827>
152. Wong AL, Chua H, Yu PHF (2000) Microbial production of polyhydroxyalkanoates by bacteria isolated from oil wastes. In: Twenty-First Symposium on Biotechnology for Fuels and Chemicals. Springer, pp 843–857
153. Mizuno K, Ohta A, Hyakutake M, Ichinomiya Y, Tsuge T (2010) Isolation of polyhydroxyalkanoate-producing bacteria from a polluted soil and characterization of the isolated strain *Bacillus cereus* YB-4. *Polym Degrad Stab* 95:1335–1339. <https://doi.org/10.1016/j.polymdegradstab.2010.01.033>
154. Chanprateep S (2010) Current trends in biodegradable polyhydroxyalkanoates. *J Biosci Bioeng* 110:621–632. <https://doi.org/10.1016/j.jbiosc.2010.07.014>
155. Philip S, Keshavarz T, Roy I (2007) Polyhydroxyalkanoates: biodegradable polymers with a range of applications. *J Chem Technol Biotechnol* 82:233–247. <https://doi.org/10.1002/jctb.1667>
156. Ojumu T, Yu J, Solomon B (2004) Production of polyhydroxyalkanoates, a bacterial biodegradable polymers. *Afr J Biotechnol* 3:18–24

157. Bharti S, Swetha G (2016) Need for bioplastics and role of biopolymer PHB: a short review. *J Pet Environ Biotechnol* 7:272. <https://doi.org/10.4172/2157-7463.1000272>
158. Lee SY (1996) Bacterial polyhydroxyalkanoates. *Biotechnol Bioeng* 49:1–14 [https://doi.org/10.1002/\(sici\)1097-0290\(19960105\)49:1%3c1::aid-bit1%3e3.0.co;2-p](https://doi.org/10.1002/(sici)1097-0290(19960105)49:1%3c1::aid-bit1%3e3.0.co;2-p)
159. Anjum A, Zuber M, Zia KM, Noreen A, Anjum MN, Tabasum S (2016) Microbial production of polyhydroxyalkanoates (PHAs) and its copolymers: a review of recent advancements. *Int J Biol Macromol* 89:161–174. <https://doi.org/10.1016/j.ijbiomac.2016.04.069>
160. Mergaert J, Anderson C, Wouters A, Swings J, Kersters K (1992) Biodegradation of polyhydroxyalkanoates. *FEMS Microbiol Rev* 9:317–321
161. Ray S, Kalia VC (2017) Biomedical applications of polyhydroxyalkanoates. *Indian J Microbiol* 57:261–269. <https://doi.org/10.1007/s12088-017-0651-7>
162. Butt FI, Muhammad N, Hamid A, Moniruzzaman M, Sharif F (2018) Recent progress in the utilization of biosynthesized polyhydroxyalkanoates for biomedical applications-review. *Int J Biol Macromol* 120:1294–1305. <https://doi.org/10.1016/j.ijbiomac.2018.09.002>
163. Brigham CJ, Sinskey AJ (2012) Applications of polyhydroxyalkanoates in the medical industry. *Int J Biotechnol Wellness Ind* 1:52–60. <https://doi.org/10.6000/1927-3037.2012.01.01.03>
164. Kai D, Loh XJ (2013) Polyhydroxyalkanoates: chemical modifications toward biomedical applications. *ACS Sustain Chem Eng* 2:106–119. <https://doi.org/10.1021/sc400340p>
165. Sevastianov V, Perova N, Shishatskaya E, Kalacheva G, Volova T (2003) Production of purified polyhydroxyalkanoates (PHAs) for applications in contact with blood. *J Biomater Sci Polym Ed* 14:1029–1042. <https://doi.org/10.1163/156856203769231547>
166. Valappil SP, Misra SK, Boccaccini AR, Roy I (2006) Biomedical applications of polyhydroxyalkanoates, an overview of animal testing and in vivo responses. *Expert Rev Med Devices* 3:853–868. <https://doi.org/10.1586/17434440.3.6.853>
167. Li Z, Loh XJ (2015) Water soluble polyhydroxyalkanoates: future materials for therapeutic applications. *Chem Soc Rev* 44:2865–2879. <https://doi.org/10.1039/c5cs00089k>
168. Chen G-Q (2009) A microbial polyhydroxyalkanoates (PHA) based bio-and materials industry. *Chem Soc Rev* 38:2434–2446. <https://doi.org/10.1039/b812677c>
169. Ivanov V, Stabnikov V, Ahmed Z, Dobrenko S, Saliuk A (2015) Production and applications of crude polyhydroxyalkanoate-containing bioplastic from the organic fraction of municipal solid waste. *Int J Environ Sci Technol* 12:725–738. <https://doi.org/10.1007/s13762-014-0505-3>
170. Gumel A, Annuar M, Chisti Y (2013) Recent advances in the production, recovery and applications of polyhydroxyalkanoates. *J Polym Environ* 21:580–605. <https://doi.org/10.1007/s10924-012-0527-1>
171. Kynadi AS, Suchithra TV (2014) Polyhydroxyalkanoates: biodegradable plastics for environmental conservation. *Industrial and Environmental Biotechnology*. Studium Press (India) Pvt. Ltd., pp 1–15 <https://doi.org/10.13140/rg.2.1.4642.5682>
172. Wang Y, Yin J, Chen G-Q (2014) Polyhydroxyalkanoates, challenges and opportunities. *Curr Opin Biotechnol* 30:59–65. <https://doi.org/10.1016/j.copbio.2014.06.001>
173. Choi J, Lee SY (1999) Factors affecting the economics of polyhydroxyalkanoate production by bacterial fermentation. *Appl Microbiol Biotechnol* 51:13–21. <https://doi.org/10.1007/s002530051>

Chapter 5

Alternating Copolymers Based on Amino Acids and Peptides



Ishita Mukherjee, Krishna Gopal Goswami and Priyadarsi De

Abstract Controlling the monomer sequence along the polymer chain leads to the development of a special class of synthetic copolymers, and they are known as alternating copolymers when the two comonomers are placed in a regular exchanging fashion. The monomer sequence control plays an important role to regulate the different bulk properties such as conductivity, rigidity, biodegradability, as well as mimic the properties of the sequence defined biopolymers like DNA, RNA, enzymes, and proteins. Very recently, different synthetic strategies have been explored to mimic the monomer sequences in synthetic polymeric materials. An enormous combination of several desired functionalities has been attached with the electron donor styrene, stilbene or electron acceptor maleic anhydride or *N*-substituted maleimide moieties to produce strictly alternating backbone and their properties have been extensively investigated. Nowadays, functionalities like amino acids and peptides, essential and fundamental components of protein biopolymers and alive entities extending from bacteria to humans with a variety of enormities from nano to macro dimension, are widely used to design an extensive range of block or random copolymers with significant assets and applications, as they can play critical responsibility in both functional and structural levels. The multifaceted biological features of these moieties help to generate bioactive and biocompatible materials. However, the properties associated with their alternating architecture have not been broadly studied. By providing a quick look on different types of alternating copolymers, in this book chapter, we aim to focus on recent developments of amino acid and peptide-based alternating architectures, their interesting properties and applications as bioinspired nanomaterials, in inclusion chemistry, catalysis, sensing, tissue engineering, molecular electronics, molecular separation technology, and so on.

Keywords Alternating copolymers · Amino acids and peptides · Biopolymers · Building block

Authors Ishita Mukherjee and Krishna Gopal Goswami are contributed equally to this work.

I. Mukherjee · K. G. Goswami · P. De (✉)

Department of Chemical Sciences, Polymer Research Centre and Centre for Advanced Functional Materials, Indian Institute of Science Education and Research Kolkata, Mohanpur, Nadia, West Bengal 741246, India
e-mail: p_de@iiserkol.ac.in

© Springer Nature Singapore Pte Ltd. 2020

V. Katiyar et al. (eds.), *Advances in Sustainable Polymers*, Materials Horizons: From Nature to Nanomaterials, https://doi.org/10.1007/978-981-15-1251-3_5

1 Introduction

The field of macromolecular architecture and its applications has been extensively explored over the last two decades particularly in the devise of complex macromolecular designs with significant advances [1, 2]. Copolymers, a long macromolecular chain comprised of at least two monomers of unlike chemical nature, can be usually classified as random or statistical copolymers, block or segmented copolymers, graft copolymers, star polymers, alternating copolymers, periodic copolymers [3], gradient copolymers [4], and aperiodic copolymers [5] relying on various distributions of monomers along the chain (Fig. 1) [6]. One of the principal objectives in the field of precise macromolecular chemistry is to regulate the sequential arrangement of monomers in the as-prepared polymer chains [7, 8]. Sequence modulation in polymer materials is of tremendous interest as the polymer properties rely both on the monomer constitution and their arrays which critically determine higher-order polymer conformation in addition to polymeric bulk properties and applications [9, 10], as witnessed in various existing biopolymers, for instance, proteins, DNA, and RNA [11]. This molecular facet appears vital for adjusting subnanometric features like molecular recognition, biocatalysis, molecular encoding of information, and therefore emerging novel generations of polymeric materials after learning from biopolymers [12]. Consequently, an extensive array of the novel sequence defined polymer-based nanomaterials have been newly emerged via iterative [13, 14], step-growth [15], chain-growth, template [16], multiblock [17, 18] chain shuttling mechanism to yield periodic pattern or kinetic strategies [19, 20].

In this regard, an alternating copolymer is a special class of sequence defined polymers where two comonomers are arranged in a regular exchanging fashion [21], leading to $r_1 r_2 = 0$ where r_1 and r_2 denote the ratio of the rate constant of homopropagation to cross-propagation [22]. Copolymerizations of electron donor styrene (also

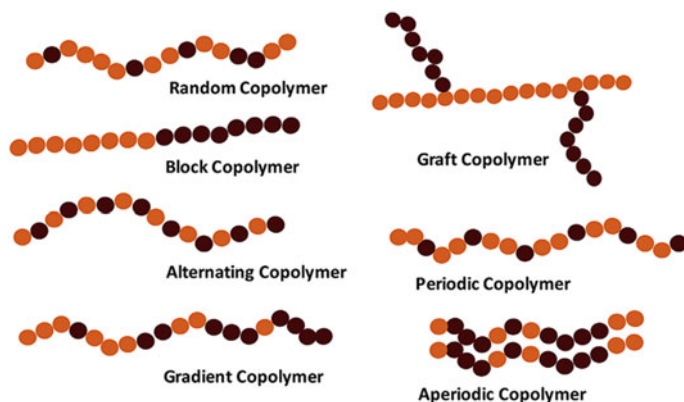


Fig. 1 Various types of copolymers from two different monomers. Reprinted with permission from Ref. [23]. Copyright (2017) Elsevier

stilbene) with electron acceptor maleimide or maleic anhydride are mostly used to produce strictly alternating backbone [23]. The phenyl ring of styrene can be functionalized with desired functionalities, and also various *N*-substituted maleimide moieties can be used to prepare varieties of strictly alternating copolymers. Several emerging applications like nanoelectronics, photonics, biotechnologies, and alternative energies are generated from these novel structures [24].

Amino acids and peptides, the major building block of protein biopolymers, are the natural key ingredients to facilitate life [25]. These molecules have engrossed immense attention over the last few decades as their bioactive, biodegradable, and biocompatible nature leads to potential biomedical applications [26, 27]. Amino acids and peptides offer an exciting platform for the fabrication of nanoscale biocompatible materials as a promising alternative of synthetic compounds through self-assembly or co-assembly of two or more kinds of building blocks ensuing progressively more complex nano-assemblies with distinctly different features comparing to the basic mono-structures [28, 29]. Recently, an extensive range of block or random copolymers with significant properties has been designed with amino acid or peptide-based building block with significant possessions and applications [30, 31], though the properties associated with their alternating architecture have not been broadly studied. This chapter summarizes the recent developments of amino acid and peptide-based alternating constructions by presenting an overall discussion on different types of alternating copolymers with their interesting applicative side as catalyst, bioinspired nanomaterials, tissue engineering scaffold, in inclusion chemistry, molecular electronics, molecular separation technology, etc.

2 Different Synthetic Strategies

Monomer sequence control in polymers can be achieved via numerous synthetic strategies which include both biological (e.g., DNA templates) and synthetic chemistry concepts to countenance the synthesis of macromolecules with diverse chemical structures [12]. The simplest examples of such controlled sequence arrangements are the alternating copolymers, composed of two monomer units [10]. The copolymerization of electron-rich styrene with electron-accepting maleic anhydride or *N*-substituted maleimide representing such monomer pairs has been extensively investigated since the early 1940s [32]. The successful synthesis of the alternating copolymers from these monomers was attained in conventional free-radical copolymerization (FRP) using 2,2'-azobisisobutyronitrile (AIBN) as the initiator [33, 34]. Apart from common organic solvents, for instance, tetrahydrofuran (THF) and *N,N'*-dimethylformamide (DMF), supercritical carbon dioxide (CO₂) was also used to accomplish an ultrahigh molecular weight alternating copolymer from styrene and maleic anhydride. By increasing the free volume and segmental motion of the copolymer chain, CO₂ restricts its precipitation from the solvent leading to the emergence of a high molecular weight polymeric structure [35]. As reported in the literature, UV irradiation was also efficiently incorporated for preparing alternating copolymers at

room temperature [36]. Though traditional free-radical polymerization has been conveniently implemented to fabricate alternating copolymers, it suffers from some limitations while the amount of in feed maleic anhydride is less than 50 mol% resulting in a mixed assemblage of copolymer and homopolymer [23]. A strong compositional drift was reported for two random copolymer samples where the resultant polymer chains were rich in maleic anhydride and styrene content at low and high masses, respectively [37]. Nevertheless, if one starts with imbalanced monomer ratio with low maleic anhydride content, the polymerization will begin as an alternate copolymerization till the entire maleic anhydride is incorporated. After that, the excess styrene will be homopolymerized ensuing the in situ formation of a block copolymer composed of a poly(styrene-*alt*-maleic anhydride) block and a polystyrene segment [38].

Successful utilization of both nitroxide mediated polymerization (NMP) and reversible addition-fragmentation chain transfer (RAFT) polymerization for styrene and maleic anhydride system was reported in the literature. Hawker and coworkers have investigated the controlled copolymerization of maleic anhydride via NMP resulting in the occurrence of a unique, single-step production of functionalized block copolymers from a 9:1 amalgamation of styrene and maleic anhydride [39]. Wang et al. described an effective strategy to prepare poly(styrene-*co*-maleic anhydride)/SiO₂ hybrid composites by NMP which permits a facile control over the molecular weight distributions and architecture of grafted copolymers onto solid surfaces [40]. Williams and coworkers have reported the successful fabrication of alternate copolymers from nucleobase-enclosed styrene monomers with maleic anhydride through the RAFT polymerization process using hexafluoroisopropanol as the solvent [41]. Several other reports are there where RAFT has been found fruitful for synthesizing alternating copolymers [42, 43]. Other than NMP and RAFT polymerization, atom transfer radical polymerization (ATRP) can also be effectively employed to copolymerize styrene and *N*-substituted maleimides [44, 45]. Based on it, Lutz and coworkers have presented a sequence-modulation tactic to tune conventional alternating behaviors by time-dependent introduction of small amounts of ultra-reactive maleimide monomer during the controlled polymerization of an excess of styrene monomer leading to the local functionalization of polymer chains [19, 46]. However, ATRP seems incompatible with styrene and maleic anhydride comonomers, owing to the interaction between maleic anhydride and the copper complex as used for such polymerization process. Apart from this, Heuts et al. successfully employed catalytic chain transfer polymerization to synthesize styrene-maleic anhydride copolymers in presence of low spin [bis(difluoroboryl) dimethylglyoximate] cobalt(II) complex [47].

Still, so far, the above discussion was mainly focused on the alternating copolymerization of styrene and maleic anhydride or *N*-substituted maleimide monomers. There are many other examples where different structural units have been utilized to prepare alternating polymer networks. Coates and coworkers have optimized the ring-opening alternate copolymerization of succinic anhydride with propylene oxide to synthesize a fresh array of semicrystalline polyesters [48]. A catalyst driven sequence

control strategy was developed by Thomas et al. to produce highly alternating copolymers from a combination of enantiomerically pure but dissimilar monomers [49]. The successful synthesis of alternating polyacetylene was recently reported by He and coworkers through the regioselective anionic polymerization of butadiene derivatives [50]. Literature reports also revealed the usefulness of condensation polymerization to formulate the alternating structures [51]. Tsuji and Arakawa have recently employed this process to synthesize alternating stereocopolymer, poly (L-lactic acid-*alt*-D-lactic acid) from chiral hydroxyalkanoic acids [52]. Generally speaking, continuous efforts are still made to design artificial polymeric structures with controlled sequence which may open up numerous opportunities to switch the structure–property relationship in tomorrow’s polymer science. Figure 2 schematically represents different synthetic procedure to synthesize alternating copolymer architectures.

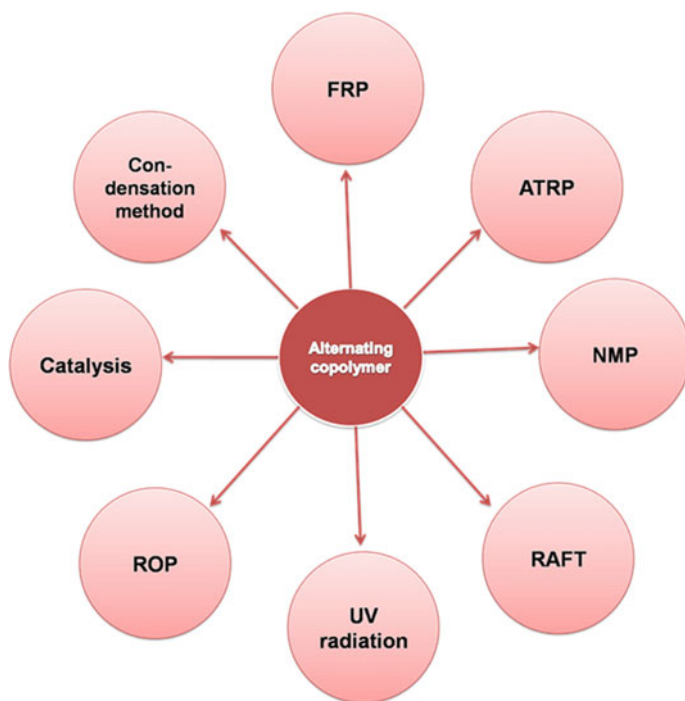


Fig. 2 Schematic illustration of the different synthetic strategies of alternating copolymers

3 Mechanistic Models on Styrene–Maleic Anhydride Radical Copolymerization

There has been a resurgence of attention in the study of styrene–maleic anhydride copolymerization from a mechanistic point of view as it shows a strong tendency to form alternating structures. Numerous studies have been endorsed to ascertain the underlying reason behind this alternating tendency which has been argued very much in the literature [38]. Several models are demonstrated to rationalize this alternation behavior. The earlier Mayo-Lewis model recommended the dependence of the propagation rate constant on both the terminal radical and the arriving monomer [53]. Though it could be successfully utilized to relate the copolymer composition with monomer feed composition, it suffers limitation to justify the correlation of rate constant versus monomer feed composition [23, 54]. Another model is the penultimate unit model (PUM) which could be incorporated to account for the deviation from Mayo-Lewis model [55]. Apart from the terminal radical, the rate constant of monomer addition also depends on the penultimate monomer unit as depicted in this model [56, 57]. The third model is the complex participation model (CPM) which could be employed to elucidate both the copolymerization kinetics and the copolymer composition in addition to monomer sequence distribution [38]. As the styrene monomer is an electron-rich monomer, it is susceptible to form charge-transfer complexes via the interaction with the electron-poor maleic anhydride monomer that has been confirmed by spectroscopic evidences [58, 59]. Based on this, the CPM model has been established, which suggests the participation of single monomer as well as the charge-transfer complex in the copolymerization [60, 61]. Nevertheless, there are still some doubts about the involvement of charge-transfer complexes in the copolymerization as evidenced by literature [62]. The underlying mechanism of the alternating behavior is still a topic of discussion and continuous efforts are made to find out the exact reason behind this copolymerization.

4 Recent Development of Alternating Copolymers Containing Amino Acids and Peptides

Over the last few decades, amino acids and peptides are widely used to design an extensive range of copolymers containing two or more amino acids at the side chain [31] or main chain peptide [63]. Primary synthesis and conformational investigation of alternating poly(γ -benzyl D, L-glutamates) [64] and alternating copolypeptide, poly(Lys-Phe) [65] are already reported in the literature long before. Primarily, the copolymer sequencing toward alternating, block or random orientations is presented and regulated by relative reactivity ratios of two diverse amino acid-based monomers. Further, information on sequencing was dictated by matrix-assisted laser desorption/ionization time-of-flight (MALDI-TOF) mass spectroscopy. As dictated by Gross and coworkers, the evident selectivity of several protease enzymes for

addition of either L-Et-Leu or L-(Et)₂-Glu to propagate chain ends with extreme sequencing leading to alternating, random, and block orientations was estimated from relative reactivity ratios, which was calculated during protease-catalyzed co-oligomerizations of γ -ethyl-L-glutamate (L-(Et)₂-Glu) with L-leucine ethyl ester (L-Et-Leu) monomer (Fig. 3) [66].

Various molecular techniques like solid-phase peptide synthesis, native chemical ligation, Staudinger ligation, *N*-carboxyanhydride (NCA) polymerization, and genetic engineering are adopted facilitating the rapid, adaptable, and orthogonal synthesis of main chain peptide-based materials [23]. The amino acid sequence in a peptide can be regulated by the genetic engineering method, though several limitations are associated with this technique like more laborious technique than others, significantly lower yield, use of natural amino acids only unless additional efforts are applied [67, 68]. The molecular devices required for the assembly of precisely designed sequence defined materials are especially genetic engineering, ring-opening polymerization (ROP), and solid-phase peptide synthesis leading to a fruitful transition from fundamental research to industrial application.

Rationally designed cyclic alternating polypeptide facilitates the production of a novel organic nanotubes with specified internal diameter and surface characteristics having potential applications in several industries and educations like chemistry, biochemistry, and material sciences, which includes mimicking biological channels and porous structures, investigating physical and chemical properties of restricted molecules, controlling properties and expansion of inorganic and metallic clusters, or designing novel optical and electronic devices [69]. An eight-residue cyclic peptide with an alternate sequence *cyclo*[-(D-Ala-Glu-D-Ala-Gln)₂-] was considered as a subunit with the postulation of cyclic peptide with an even sequence of alternating D- and L-amino acids. A low-energy flat ring-shaped orientation can be adopted by them with all approximately perpendicular backbone amide functionalities to the plane of the adopted β -sheet structure resulting backbone-backbone intermolecular hydrogen bonding (Fig. 4). The alternating D- and L-sequence results from the peptide side chain necessarily lying at the outside of the ensemble to prepare the most wanted hollow tube structure at the core.

Recently, a unique alternating peptide peptoid copolymer was prepared via one-pot Ugi four-component reaction polymerization of dipeptides in aqueous solution involving a primary amine, an aldehyde, an isocyanide, and a carboxylic acid. Thus,

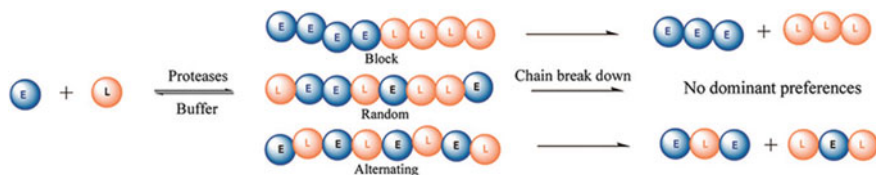


Fig. 3 Possible sequence selectivity of proteases during oligomerization reaction of γ -ethyl-L-glutamate (E) with L-leucine ethyl ester (L) monomer. Reprinted with permission from Ref. [66]. Copyright (2008) American Chemical Society

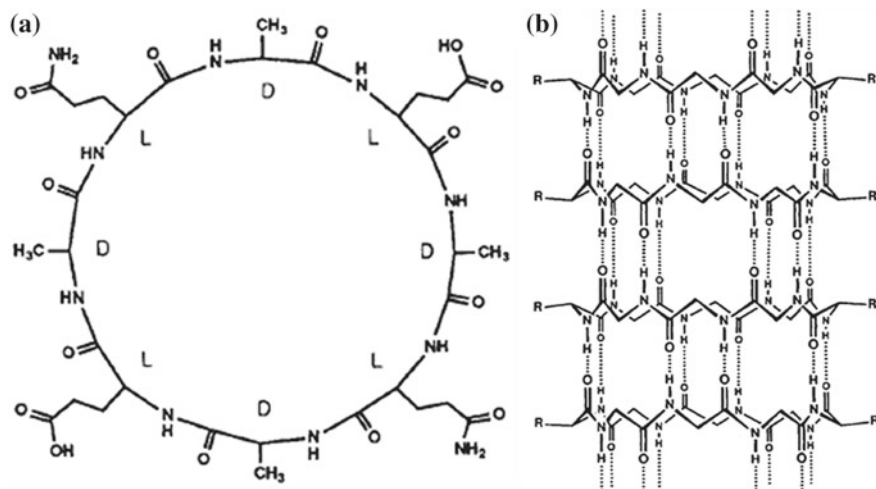


Fig. 4 **a** A two-dimensional representation of the chemical structure of the peptide subunit (D or L refers to the amino acid chirality). **b** Peptide subunits are shown in a self-assembled tubular configuration emphasizing the antiparallel stacking and the extensive network of intermolecular hydrogen bonding interactions (for clarity only backbone structure is presented). Reprinted with permission from Ref. [69]. Copyright (2013) Nature Chemistry

a quasi-quantitative pathway of α -amido amide compounds with high atomic efficiency has been developed due to potential biomedical applications of polypeptides and polypeptoids, analogous to *N*-substituted amino acids [70]. Despite the simplest dipeptide, glycyl-glycine (Gly-Gly), for a trial reaction, the amino acid sequence on the final structure of the peptide-*alt*-peptoid copolymers was highlighted by choosing several dipeptides like glycyl-alanine (Gly-Ala) and L-alanyl-glycine (Ala-Gly) (Fig. 5a). A great attention has been paid on those water-soluble peptide-based alter-

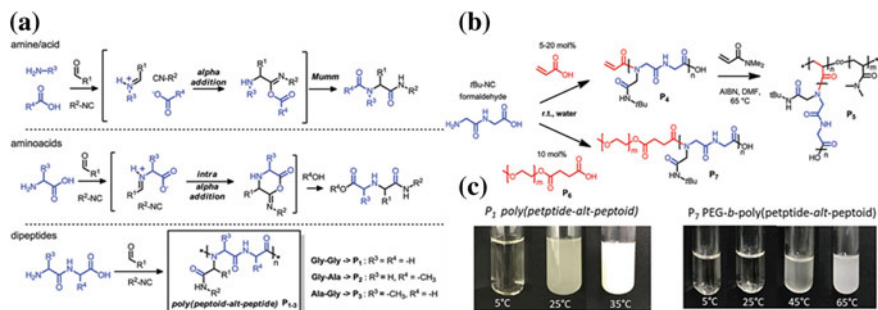


Fig. 5 **a** Synthesis based on Ugi four-component reaction, **b** synthesis of the poly(peptide-*alt*-peptoid) macromonomer as well as the corresponding graft and block copolymers with acrylic acid and *N,N'*-dimethylacrylamide (DMA), and **c** their thermo-responsive properties in aqueous solution. Reprinted with permission from Ref. [70]. Copyright (2017) The Royal Society of Chemistry

nating copolymers and their derivatives with acrylic acid, graft copolymerization with *N,N'*-dimethylacrylamide (DMA) by free-radical polymerization or modification with carboxylic acid terminated polyethylene glycol (PEG), due to their significant thermoresponsive properties exhibiting a range of lower critical solution temperature (LCST) leading to several biomedical applications (Fig. 5b, c).

Another interesting example of amino acid-based alternate architecture is MAX1, a sequence defined peptide containing 20 amino acids [71]. It is fully soluble in aqueous media, adopts random coil conformation, and can transfer to β -hairpin conformation to facilitate a targeted self-assembly structure into a rigid cross-linked hydrogel by applying exogenous stimulus like pH [34], temperature [72], ionic strength [73] of cell growth media. Kretsinger et al. demonstrated the cytocompatibility of the hydrogel toward NIH 3T3 murine fibroblasts generated from MAX1 including alternating sequence of lysine and valine residues oriented on two β -strands edges. They can be crinkled and self-assembled under treatment of buffered concentrated saline solution, i.e., cell growth media (Fig. 6) [74]. Cytotoxicity was measured in a qualitative pathway using a live/dead cell viability analysis. Here, calcein-AM hydrolysis in live cells produced a green fluorescent signal while ethidium homodimer generated a red fluorescent signal only in dead cells. The non-cytotoxicity of the hydrogel surface was exhibited by Fig. 7, where that cell viability on the hydrogel surface was comparable to that of the control TCTP surface. Due to non-toxic nature toward fibroblasts cells, porosity, biocompatibility, supportive properties to cell adhesion both in presence and absence of serum protein and proliferation, the hydrogel meets the preliminary mechanical and cytocompatibility requirement to act as an attractive candidate of tissue engineering scaffold.

Selectivity of pH-triggered supramolecular polymerization can be regulated by amino acid-based alternating peptide. In neutral buffer, self-assembly of phenylalanine-lysine (FK)- and phenylalanine-glutamic acid (FE)-composed

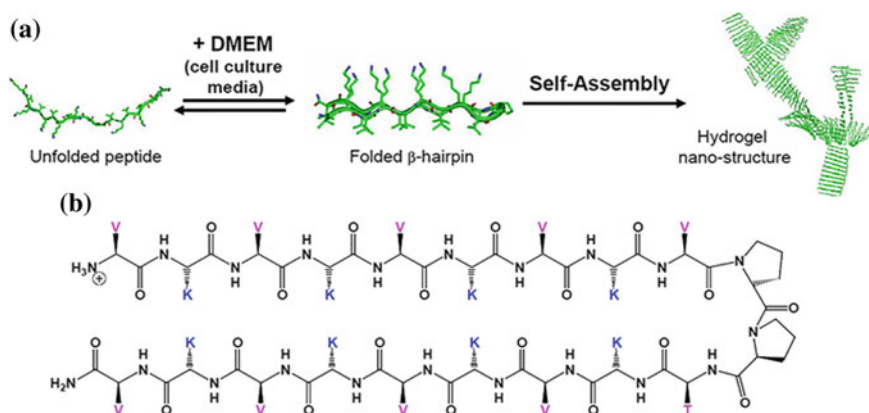


Fig. 6 **a** Model for the folding and self-assembly of MAX1. **b** Folded sequence of MAX1. Reprinted with permission from Ref. [74]. Copyright (2005) Elsevier

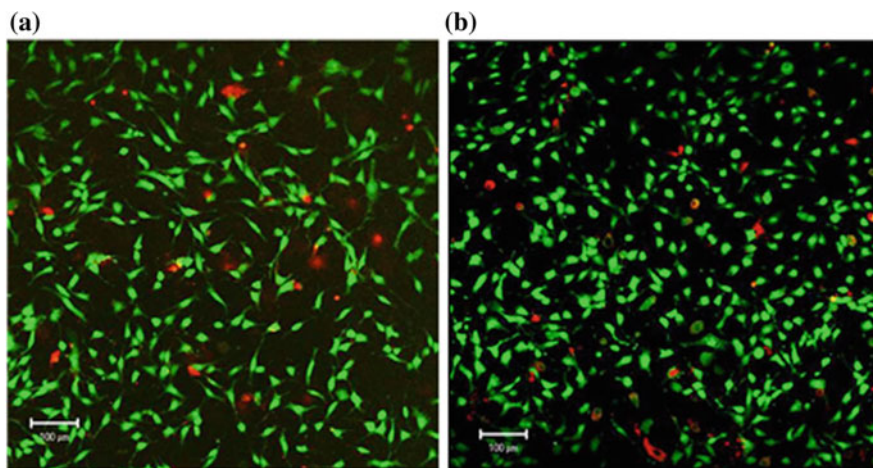


Fig. 7 Live/dead cytotoxicity assay on 40,000 cells/cm² murine NIH 3T3 cells 5 h after introduction onto **a** 2 wt% MAX1 hydrogels or **b** TCTP control plates. Viable cells fluoresce green and compromised cells fluoresce red. Scale bar represents 100 μm. Reprinted with permission from Ref. [74]. Copyright (2005) Elsevier

amphiphilic alternating dendron shaped peptides 1 and 2 can happen to generate a distinct 1–2 copolymers. pH can control the selective turn off of the negative or positive charges on the oppositely charged comonomers [75], hence leading to selective homopolymerization based on stimuli-responsive opposite comonomer release phenomenon. This was the first report of a supramolecular polymerization in solution with the ability to reversible switch over between three differential compositions: homopolymer of 1 (pH > 10), copolymer of 1–2 (neutral pH) and homopolymer of 2 (pH < 4) were postulated (Fig. 8) [76].

Conformational properties of amino acid-based alternating copolymers are regulated by salt effect and pH, though the consequence is somewhat different from amino acid-based statistical copolymers due to differential basic architecture. As reported in the literature, the alternating copoly(L-leucyl-L-lysine), however, does not exhibit coil to α -helix conformational switching like its statistical analog. But the precise alternating arrangement along the polymeric chain could result in a β -sheet orientation composed of hydrophilic and hydrophobic residues at two terminal sides. In the hydrophilic end, salt addition or pH enhancement could neutralize the repulsion among the positively charged amino groups of lysine side chains [77]. Different anions present in the salts are postulated to generate coil to β -sheet conformation of alternate amino acid-based architecture through different mechanism. ClO_4^- , specifically, bind to the positively charged side chain group, whereas β -structural orientation is dictated by SO_4^{2-} due to the intermolecular hydrophobic interactions between the leucyl residues of adjacent chains and ionic interactions between one

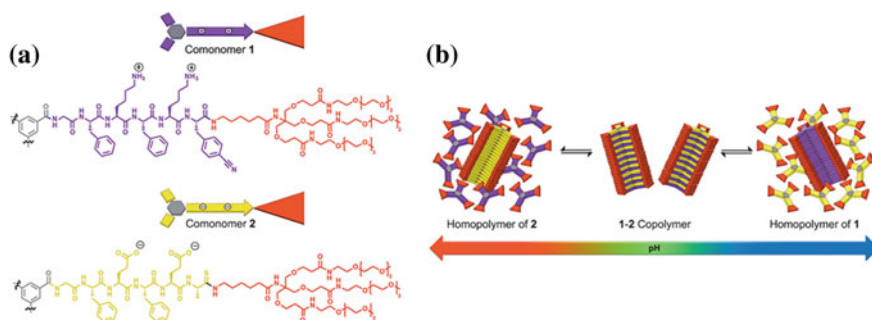


Fig. 8 **a** Chemical structures of the C_3 -symmetric dendritic peptide comonomers 1 and 2; **b** their pH-regulated supramolecular polymerization into homopolymer of 1 and 2, at high and low pH, respectively, and 1–2 copolymer at neutral pH. Reprinted with permission from Ref. [76]. Copyright (2015) WILEY

SO_4^{2-} and two NH_3^+ groups of two neighboring polymers. Hence, the absence of specific binding capacity toward polycation by SO_4^{2-} unlike ClO_4^- dominantly regulates the mechanistic pathway.

The pH-induced conformational transition of an alternating amphiphilic peptide with an amino acid sequence Phe-(Leu-Glu)₈ can regulate the structural control of peptide-gold nanoparticles, where the surface of the nanoparticle is covered by the peptide chain [78]. The sequence defined alternating amphiphilic peptide surface adopts a α -helical conformation along with a substantial extent of a random coil and β -sheet arrangements under basic condition, whereas β -sheet structure was the dominant orientation for the peptide material under acidic environment. These conformational changes lead to morphological differentiation of the peptide coated gold nanoparticle assembly from globular to nanosheet structure by changing pH leading to intermolecular hydrogen bonding among the surface peptide (Fig. 9). The core gold nanoparticles could be fixed to the β -sheet assembly of the surface peptides, generating a useful system for new molecular tools with quantized properties.

Alanine and lysine containing sequence defined peptides $(AKA_3KA)_2$ (AK_2) produce an alternating architecture with flexible PEG moiety. Hence, a multiblock polymeric fusion material has been developed to imitate the molecular structure and design of natural elastin. The peptide $(AKA_3KA)_2$ (AK_2) is an essential structural component of the cross-linking structural biomolecules like proteins, e.g., mechanically active tissues to provide elastic property. Natural elastin-like mechanical strength could be introduced to a peptide-polymer hybrid hydrogel synthesized by covalently cross-linked alternating copolymers composed by hexamethylene diisocyanate and lysine side chains in the peptidic blocks (Fig. 10) [79]. Furthermore, PEG was substituted by an amphiphilic ABA block copolymer composed of PEG end blocks and a poly(propylene oxide) (PPO) center block, known as pluronics (F127). These types of copolymers can self-assemble into micelles leading to various conformational and assembly characteristics of AK_2 peptide under various environments (Fig. 11) [80]. Helical property and thermal stability of F127 micelles connected

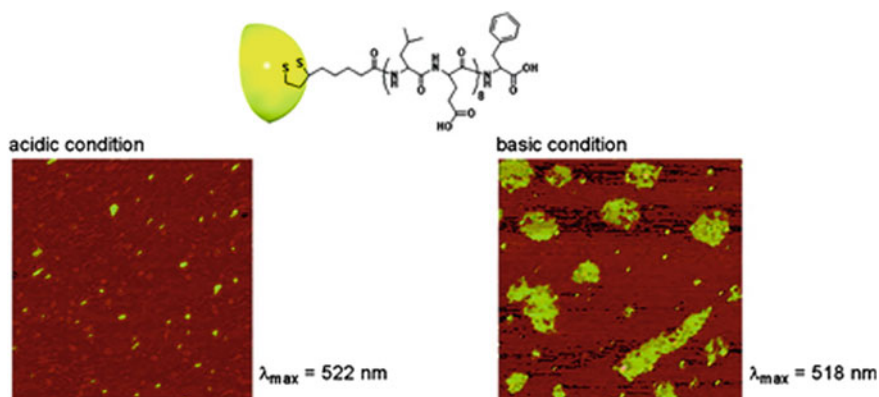


Fig. 9 Morphological changes of the alternating amphiphilic peptide, Phe-(Leu-Glu)₈ coated gold nanoparticle assembly from the globular to nanosheet structure by changing pH. Reprinted with permission from Ref. [78]. Copyright (2008) American Chemical Society

peptide materials are improved significantly as compared to the free peptide.

In contrast, amino acid-based alternating approach has opened a new dimension to develop a series of interesting, novel, biodegradable, and biocompatible materials called polyesteramides (PEAs) having potential applications in agricultural fields, drug delivery system, and tissue engineering scaffold. The potential thermal and mechanical properties of PEAs were introduced by the biodegradability of polyesters, substantial thermomechanical activities, and hydrogen bond-forming ability of polyamide functionality. The ring-opening bulk polymerization of morpholine-2,5-diones is an established technique for synthesizing alternating PEAs, called polydepsipeptides, which consist of alternating monomer units from α -amino acids like aspartic acid or lysine and α -hydroxy acids [81, 82]. Hence, a wide variety of polydepsipeptides could be prepared with different functionality and reactivity [83]. Copoly(L-lactide-depsipeptide)s [84] or poly(L-lactide)-polydepsipeptide block copolymers [85] are produced by the copolymerization of morpholine-2,5-diones with L-lactide which can be utilized for drug-loaded microspheres generation. This method has some limitations to the production of polyesteramides from α -amino acids and α -hydroxy acids as such cyclic compounds are difficult to synthesize from bulky monomers. A direct reaction between cyclic esters and amino acids can also generate PEAs. Melt polymerization of ϵ -caprolactone with 6-aminocaproic acid or 11-aminoundecanoic acid has been reported to prepare desired PEAs where the tensile strength is dictated by the amino acid portions in the primary mixture [86, 87]. Bulk copolymerization of ϵ -caprolactone and shorter amino acid, β -alanine, with extensive properties and biomedical applications are recently explored which is schematically represented in Fig. 12 [88].

Stereocomplexation can be achieved by using amino acid-based alternating strategies with potential applications in biomedical hydrogels and micelle or vesicle type microspheres for drug delivery systems [89, 90]. 12-mer sequence defined alternating

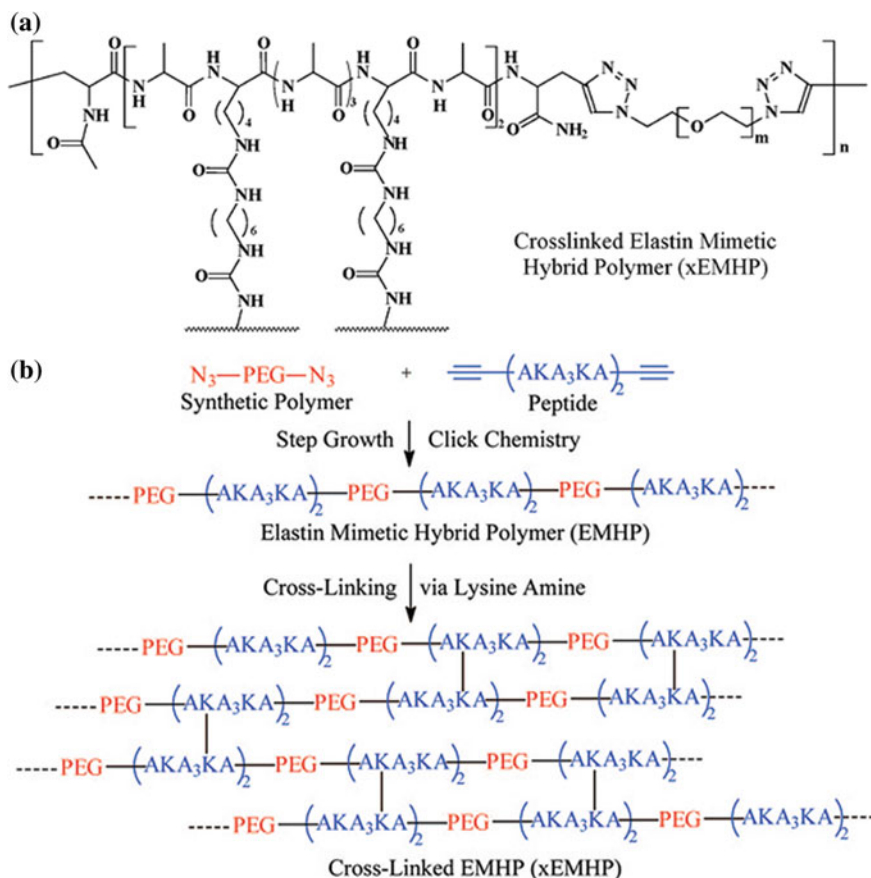


Fig. 10 a Chemical structure and b schematic representation of synthesis of covalently cross-linked elastin-mimetic hybrid polymer. Reprinted with permission from Ref. [79]. Copyright (2009) American Chemical Society

architecture composed of L-leucine (Leu) or D-leucine (leu) and 2-aminoisobutylic acid (Aib) produced a helical conformation of peptide chain and from the *N*-terminal residue, a poly(sarcosine) block was incorporated as expressed in Fig. 13 [91]. The molecular assembly from the mixtures of those block amphiphilic polypeptides transforming from planar sheet to vesicle upon heating is explained by stereocomplexation between right-handed and left-handed helical structure in hydrophobic core area of the sheet conformation [92, 93]. Right-handed helical amphiphilic peptide-based material was introduced to second-generation dendrimer at its eight terminal positions as a hydrophobic block, therefore leading to the supramolecular assembly as a consequence of stereocomplexation.

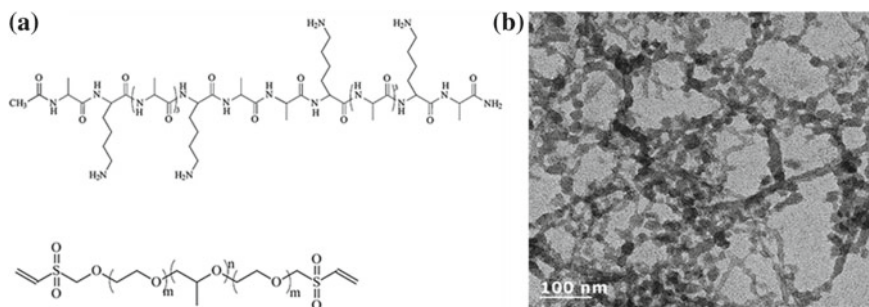
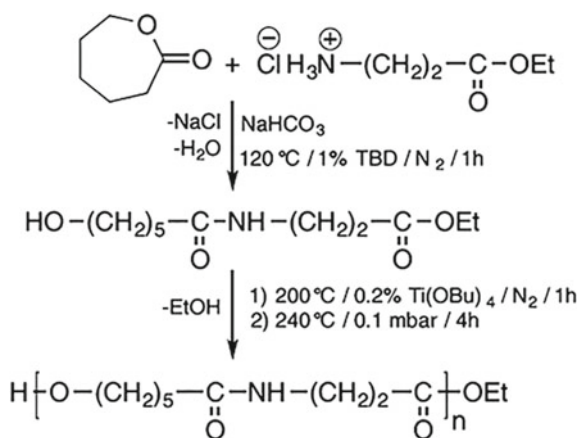


Fig. 11 **a** Chemical structure of alanine-rich, lysine-containing peptide with a sequence of Ac-(AKA₃KA)₂-NH₂ (AK₂, top) and vinylsulfone terminated pluronic F127, **b** transmission electron micrographs of peptide/F127 hybrid. Reprinted with permission from Ref. [80]. Copyright (2011) WILEY

Fig. 12 Synthesis of alternating copolymer from ϵ -caprolactone and β -alanine. Reprinted with permission from Ref. [88]. Copyright (2014) Elsevier



Collective H-bonding and hydrophobic interactions lead to the generation of multiblock nanoparticle possessing elastin-mimetic property consisting an alternating sequence of poly(acrylic acid) (PAA) and alkyne-terminated, valine and glycine-rich peptide, (VPGVG)₂ (VG2) via the step-growth polymerization with potential application as pH-responsive drug delivery systems [94]. Biomedical applications of amino acid-based alternating polymers are further extended in several fields like bone repair, which is sluggish and complex physiological practice, biosensing applications [95], e.g., peptide-mimetic alternating copolymers (PMACs), synthesized by the copolymerization of ϵ -Z-lysine with hexamethylene diisocyanate (HDI), acted as an antibacterial delivery vehicle to transfer growth factors which were used to control bone repairing process [96].

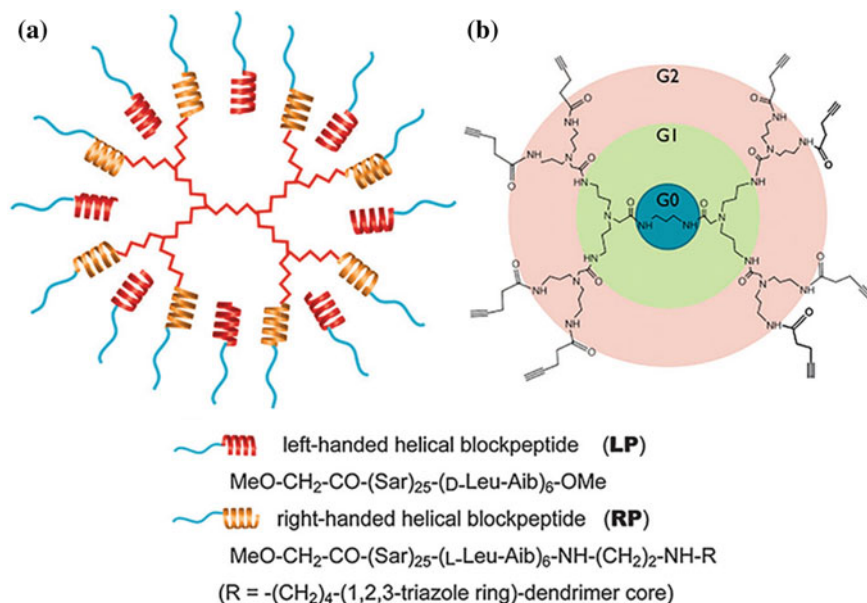


Fig. 13 The diagrams of molecular design: **a** the cartoon-like diagram of a co-assembling second-generation dendrimer template bearing amphiphilic right-handed block peptides (yellow helix) with amphiphilic left-handed block peptides (red helix), **b** the schematic diagram of the second-generation dendrimer core emphasized on the generation number. Reprinted with permission from Ref. [91]. Copyright (2012) The Royal Society of Chemistry

A novel and interesting traditional fluorophore-free water-soluble dual pH- and thermoresponsive fluorescent poly(styrene-*alt*-maleimide) skeleton-based copolymer was recently explored by our group through amino acid-based sequence-controlled copolymerization [43]. The thermoresponsive properties originated from the diethylene oxide side chain attached to maleimide moiety and the pH-responsiveness instigated from the deprotected leucine-appended styrene backbone. Thus, pH/thermoresponsive fluorescence activity in water was observed due to “through-space” π - π interaction between the benzene ring and the neighboring carbonyl group of the maleimide unit. This leucine containing alternating copolymer was further explored for speedy, selective, and sensitive detection of a well-known explosive nitro compound, picric acid (PA), in a 100% aqueous medium utilizing their nonfluorophore fluorescence property through determination of fluorescence quenching efficiency expressed in Fig. 14 [97].

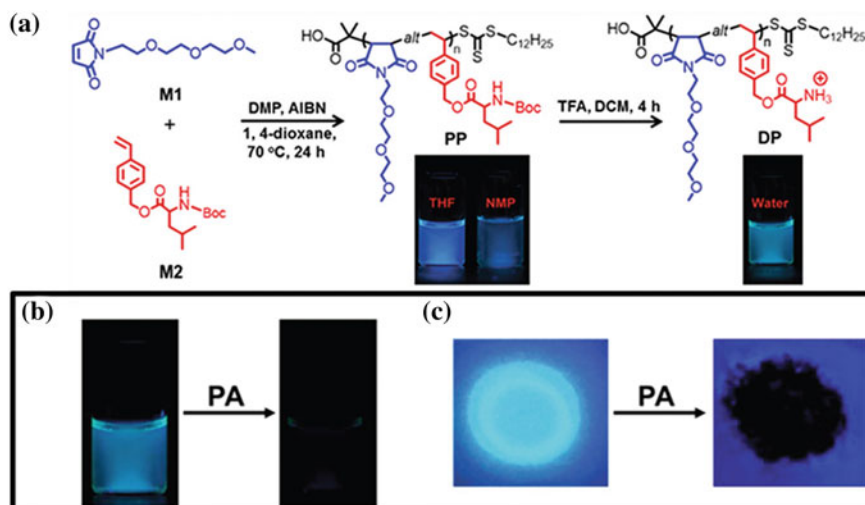


Fig. 14 a Synthesis of Boc-protected alternating copolymer (PP) and its subsequent deprotection under acidic conditions to afford the target macromolecular probe, deprotected polymer (DP). Fluorescence images of PP in tetrahydrofuran (THF) and *N*-methyl-2-pyrrolidone (NMP) and DP in water upon excitation with UV light at 366 nm. Naked-eye observation of fluorescence quenching under UV light: **b** in the solution state upon the addition of picric acid (PA) to the aqueous sensor solution, and **c** in the solid state upon adsorption of the PA solution on the sensor spot on a TLC plate. Reprinted with permission from Ref. [97]. Copyright (2017) The Royal Society of Chemistry

5 General Applications Originated from Alternating Architectures

Several applicative sides such as catalysis, molecular recognition, generation of biodegradable materials have been opened up from the alternating sequence-controlled polymeric architectures leading to the generation of microstructural periodicity, single-chain functional group distributions, and complicated macromolecular architectures [98]. Poly(styrene-*alt*-maleic anhydride) backbone supported copolymers displayed a selective detection for definite dialkylammonium ions or other size-specific complexations via inclusion complex formation where the crown ether moiety was formed by cyclo copolymerization [99]. Again, heterogeneous solid acid catalytic activity in organic transformation [100]; a new, recyclable, highly active Pd modified heterogeneous catalyst for Suzuki and Sonogashira cross-coupling reactions under “green” condition [101]; preparation of surfactant-free modified latexes [102]; fuel cell application [33]; drug release application [103]; fluorescence “OFF–ON” response to several selective metal ions and solution pH [42]; nanotube self-assembly behavior [104]; guest molecules entrapment, release properties along with multiple end group modified dendritic side chains [105]; generation of polyhedral oligomeric silsesquioxane (POSS)-based organic–inorganic hybrid materials having alternating architecture with enhanced thermal properties [106],

self-assembly behavior in aqueous solution [107], unusual fluorescence behavior in solid and solution state [34]; preparation of well-defined polyelectrolyte with complex microstructure [108] were explored from the same alternating skeleton with selective modification of side chain functionality attached to styrene or maleic anhydride/maleimide. Sequence control copolymer microstructure like their amorphous, crystalline or semicrystalline nature can finely tune the material properties with potential applications [109].

Synthesis of alternating copolymers with the cluster of bulky functional groups snatched a great attention as impenetrable well-designed clusters presenting in many biological organisms exhibited a crucial role in biological detection procedures susceptible of many applications [110]. Interactions with biomolecules can be exhibited by multivalent dendritic structures through introducing into the polymeric materials. Sterically crowded alternating polymer backbones based on functionalized stilbenes and maleic anhydride/functionalized maleimides lead to the generation of new anionic polyelectrolytes with tunable charge densities [111] with variable solution properties like dissociation or aggregation behavior [112]. A 2,3,4,5,6-pentafluorostyrene (PFS)-based alternating copolymer bearing $-\text{NH}_2$ and $-\text{SO}_3^-$ functional groups was originated as a capable organocatalyst for a Henry reaction between benzaldehyde and nitromethane [113]. Nanoporosity originates from the *tert*-butyl group deprotection of alternating copolymer containing *tert*-butyl carboxylate-functionalized stilbene or styrene and *N*-phenylmaleimide resulting in carbon dioxide capture properties [114]. Nitrogen adsorption/desorption applications can also be promoted by the hypercross-linked alternating sequence [115]. An interesting class of toothbrush like alternating graft copolymers with biocompatible PEG or polycaprolactone (PCL) can act as a potent drug carrier [116]. A novel approach, amphiphilic alternating copolymer brush (AACPB) opens a new dimension in applications like self-assembly [117], lithium salt-induced microphase separation, high-temperature ionic conductivity [118], and so on. The alternating copolymers consisting an anhydride functionality and a carbon-to-carbon double bond like twisted 1,3-butadiene in each replicate were conveniently applied for the polymer-surface alteration by several post-polymerization reactions, thermosetting and successive degradation process [119]. Low cytotoxicity and high serum compatibility of sugar responsive polymersomes with alternating architectures facilitated the application as elegant insulin delivery carriers and the glucose level in the surroundings controlled the release properties [120]. Recently, a potential application for sterically stabilized nanoparticles in the area of foam stabilization was explored by styrene and *N*-phenylmaleimide-based alternating architectures [121].

Nowadays, amino acids or peptide functionalized alternating architectures have attained a significant interest as those units can self-assemble into ordered nanostructures like the assembly of diphenylalanine leads to the core detection motif of Alzheimer's β -amyloid [122]. Well-defined nanotube with potential self-assembly application is reported from peptide functionalized alternating copolymer of poly(2,3-dihydroxy butylene-*alt*-butylene di-thioether) (P(DHB-*a*-BDT)) [123]. The application of the peptide-based alternating polymers in various technological

utilizations, self-organization properties, piezoelectric devices, energy storage components, devices with light-emitting properties, superhydrophobic surfaces for self-cleaning, metal-organic frameworks, composite strengthening, ultra-sensitive sensing devices, 3D hydrogel scaffolds for inorganic ultra-structures, tissue engineering, and drug delivery purposes is investigated extensively [124].

6 Conclusions

The generation of huge and assorted collections of alternating copolymers has developed an exciting and creative area of progressive polymer sciences, where several novel functionalities could be oriented along the polymer backbone leading to an innovative functional polymer structure. In this chapter, we presented an overall discussion on different types of alternating copolymers, different synthetic strategies, mechanism, their interesting properties, and several applications along with the recent developments of amino acid and peptide-based alternating constructions. Peptide-based substances present an outstanding platform for the development of tissue engineering scaffold, targeted drug delivery systems, inclusion chemistry, molecular recognition and as substrates for regenerative medicine with the demand for several newly emergent technologies. Though a large number of synthetic strategies like solid-phase synthesis, ring-opening polymerization, NCA polymerization etc. are available for the production of these materials, defined regulation of the amino acid sequence in higher molecular weight peptides can only be generated by genetic engineering method. But several drawbacks associated with this method like lower yield, more laborious technique than others have led to additional, more fascinating approaches like side chain modifications of styrene and malimide units through amino acids [43, 97]. Hence, several modified molecular tools involving amino acid sequence in the main chain and side chains are adopted for the creation of these alternating peptide-based compounds with potential applicative sides. However, the evolution and bridging between fundamental research and industry applications still remain elusive. Those peptide composed materials have the extensive and prospective viewpoints including self-assemblies that not only acquire unique chemical and physical properties, but also responsive nature, functional self-healing or wound-healing capacity, and catalytic activities. However, both the academic and industrial sector must realize and should construct an attempt to bridge the gap existing between fundamental research and industrial applications.

Acknowledgements I. M. and K. G. G. acknowledge Council of Scientific and Industrial Research (CSIR), Government of India, India, for their research fellowships.

References

1. Matyjaszewski K (2005) Macromolecular engineering: from rational design through precise macromolecular synthesis and processing to targeted macroscopic material properties. *Prog Polym Sci* 30:858–875. <https://doi.org/10.1016/j.progpolymsci.2005.06.004>
2. (a) Pyun J, Zhou XZ, Drockenmuller E, Hawker CJ (2003) Macromolecules of controlled architecture. *J Mat Chem* 13:2653–2660. <https://doi.org/10.1039/b304682f>; (b) Bernaerts KV, Du Prez FE (2006) Dual/heterofunctional initiators for the combination of mechanistically distinct polymerization techniques. *Prog Polym Sci* 31:671–722. <https://doi.org/10.1016/j.progpolymsci.2006.08.007>; (c) Lutz J-F (2007) 1,3-dipolar cycloadditions of azides and alkynes: a universal ligation tool in polymer and materials science. *Angew Chem Int Ed* 46:1018–1025. <https://doi.org/10.1002/anie.200604050>; (d) McCormick CL, Sumerlin BS, Lokitz BS, Stempka JE (2008) RAFT-synthesized diblock and triblock copolymers: thermally-induced supramolecular assembly in aqueous media. *Soft Matter* 4:1760–1773. <https://doi.org/10.1039/b719577j>; (e) Moad G, Rizzardo E, Thang SH (2008) Radical addition–fragmentation chemistry in polymer synthesis. *Polymer* 49:1079–1131. <https://doi.org/10.1016/j.polymer.2007.11.020>
3. Yokota K (1999) Periodic copolymers. *Prog Polym Sci* 24:517–563. [https://doi.org/10.1016/S0079-6700\(99\)00010-6](https://doi.org/10.1016/S0079-6700(99)00010-6)
4. Matyjaszewski K, Ziegler MJ, Arehart SV, Greszta D, Pakula T (2000) Gradient copolymers by atom transfer radical copolymerization. *J Phys Org Chem* 13:775–786. [https://doi.org/10.1002/1099-1395\(200012\)13:12%3c775:AID-POC314%3e3.0.CO;2-D](https://doi.org/10.1002/1099-1395(200012)13:12%3c775:AID-POC314%3e3.0.CO;2-D)
5. Lutz J-F (2014) Aperiodic copolymers. *ACS Macro Lett* 3:1020–1023. <https://doi.org/10.1021/mz5004823>
6. Badi N, Chan-Seng D, Lutz J-F (2013) Microstructure control: an underestimated parameter in recent polymer design. *Macromol Chem Phys* 214:135–142. <https://doi.org/10.1002/macp.201200475>
7. Lutz J-F (2010) A controlled sequence of events. *Nat Chem* 2:84–85. <https://doi.org/10.1038/nchem.530>
8. Badi N, Lutz J-F (2009) Sequence control in polymer synthesis. *Chem Soc Rev* 38:3383–3390. <https://doi.org/10.1039/B806413J>
9. Ouchi M, Badi N, Lutz J-F, Sawamoto M (2011) Single-chain technology using discrete synthetic macromolecules. *Nat Chem* 3:917–924. <https://doi.org/10.1038/nchem.1175>
10. Lutz J-F (2010) Sequence-controlled polymerizations: the next Holy Grail in polymer science? *Polym Chem* 1:55–62. <https://doi.org/10.1039/B9PY00329K>
11. Schmidt BVKJ, Fechner N, Falkenhagen J, Lutz J-F (2011) Controlled folding of synthetic polymer chains through the formation of positionable covalent bridges. *Nat Chem* 3:234–238. <https://doi.org/10.1038/nchem.964>
12. Lutz J-F, Ouchi M, Liu DR, Sawamoto M (2013) Sequence-controlled polymers. *Science* 341:628–636. <https://doi.org/10.1126/science.1238149>
13. Espeel P, Carrette LLG, Bury K, Capenberghs S, Martins JC, Du Prez FE, Madder A (2013) Multifunctionalized sequence-defined oligomers from a single building block. *Angew Chem Int Ed* 52:13261–13264. <https://doi.org/10.1002/anie.201307439>
14. Solleder SC, Meier MAR (2014) Sequence control in polymer chemistry through the Passerini three-component reaction. *Angew Chem Int Ed* 53:711–714. <https://doi.org/10.1002/anie.201308960>
15. Satoh K, Ozawa S, Mizutani M, Nagai K, Kamigaito M (2010) Sequence-regulated vinyl copolymers by metal-catalysed step-growth radical polymerization. *Nat Commun* 1:1–6. <https://doi.org/10.1038/ncomms1004>
16. Niu J, Hili R, Liu DR (2013) Enzyme-free translation of DNA into sequence-defined synthetic polymers structurally unrelated to nucleic acids. *Nat Chem* 5:282–292. <https://doi.org/10.1038/nchem.1577>

17. Zhang Q, Collins J, Anastasaki A, Wallis R, Mitchell DA, Becer CR, Haddleton DM (2013) Sequence-controlled multi-block glycopolymers to inhibit DC-SIGN-gp120 binding. *Angew Chem* 125:4531–4535. <https://doi.org/10.1002/ange.201300068>
18. Gody G, Maschmeyer T, Zetterlund PB, Perrier S (2013) Rapid and quantitative one-pot synthesis of sequence-controlled polymers by radical polymerization. *Nat Commun* 4:2505 (1–9). <https://doi.org/10.1038/ncomms3505>
19. Pfeifer S, Lutz J-F (2007) A facile procedure for controlling monomer sequence distribution in radical chain polymerizations. *J Am Chem Soc* 129:9542–9543. <https://doi.org/10.1021/ja0717616>
20. Satoh K, Matsuda M, Nagai K, Kamigaito M (2010) A AB-sequence living radical chain copolymerization of naturally occurring limonene with maleimide: an end-to-end sequence-regulated copolymer. *J Am Chem Soc* 132:10003–10005. <https://doi.org/10.1021/ja1042353>
21. IUPAC (1997) Compendium of chemical terminology (the “Gold Book”), 2nd edn. Blackwell Scientific Publications, Oxford
22. Odian G (2004) Principles of polymerization. Wiley, Hoboken, NJ
23. Huang J, Turner SR (2017) Recent advances in alternating copolymers: the synthesis, modification, and applications of precision polymers. *Polymer* 116:572–586. <https://doi.org/10.1016/j.polymer.2017.01.020>
24. Berthet M-A, Zarafshani Z, Pfeifer S, Lutz J-F (2010) Facile synthesis of functional periodic copolymers: a step toward polymer-based molecular arrays. *Macromolecules* 43:44–50. <https://doi.org/10.1021/ma902075q>
25. Ramakers BEI, van Hest JCM, Lowik DWPM (2014) Molecular tools for the construction of peptide-based materials. *Chem Soc Rev* 43:2743–2756. <https://doi.org/10.1039/C3CS60362H>
26. Deng C, Wu J, Cheng R, Meng F, Klok H-A, Zhong Z (2014) Functional polypeptide and hybrid materials: precision synthesis *via* α -amino acid *N*-carboxyanhydride polymerization and emerging biomedical applications. *Prog Polym Sci* 39:330–364. <https://doi.org/10.1016/j.progpolymsci.2013.10.008>
27. Secker C, Brosnan SM, Luxenhofer R, Schlaad H (2015) Poly(α -peptoid)s revisited: synthesis, properties, and use as biomaterial. *Macromol Biosci* 15:881–891. <https://doi.org/10.1002/mabi.201500023>
28. Sedman VL, Chen X, Allen S, Roberts CJ, Korolkov VV, Tendler SJB (2013) Tuning the mechanical properties of self-assembled mixed-peptide tubes. *J Microsc* 249:165–172. <https://doi.org/10.1111/jmi.12005>
29. Orbach R, Mironi-Harpaz I, Adler-Abramovich L, Mossou E, Mitchell EP, Forsyth VT, Gazit E, Seliktar D (2012) The rheological and structural properties of fmoc-peptide-based hydrogels: the effect of aromatic molecular architecture on self-assembly and physical characteristics. *Langmuir* 28:2015–2022. <https://doi.org/10.1021/la204426q>
30. Bauri K, Pant S, Roy SG, De P (2013) Dual pH and temperature responsive helical copolymer libraries with pendant chiral leucine moieties. *Polym Chem* 4:4052–4060. <https://doi.org/10.1039/C3PY00434A>
31. Kumar S, Acharya R, Chatterji U, De P (2013) Side-chain amino-acid-based pH-responsive self-assembled block copolymers for drug delivery and gene transfer. *Langmuir* 29:15375–15385. <https://doi.org/10.1021/la403819g>
32. Alfrey T, Lavin E (1945) The copolymerization of styrene and maleic anhydride. *J Am Chem Soc* 67:2044–2045. <https://doi.org/10.1021/ja01227a502>
33. Oishi A, Matsuoka H, Yasuda T, Watanabe M (2009) Novel styrene/*N*-phenylmaleimide alternating copolymers with pendant sulfonimide acid groups for polymer electrolyte fuel cell applications. *J Mater Chem* 19:514–521. <https://doi.org/10.1039/B815390F>
34. Mohamed MG, Hsu K-C, Hong J-L, Kuo S-W (2016) Unexpected fluorescence from maleimide-containing polyhedral oligomeric silsesquioxanes: nanoparticle and sequence distribution analyses of polystyrene-based alternating copolymers. *Polym Chem* 7:135–145. <https://doi.org/10.1039/C5PY01537E>

35. Qiu G-M, Zhu B-K, Xu Y-Y, Geckeler KE (2006) Synthesis of ultrahigh molecular weight poly(styrene-*alt*-maleic anhydride) in supercritical carbon dioxide. *Macromolecules* 39:3231–3237. <https://doi.org/10.1021/ma052520q>
36. Wu D-C, Hong C-Y, Pan C-Y, He W-D (2003) Study on controlled radical alternating copolymerization of styrene with maleic anhydride under UV irradiation. *Polym Int* 52:98–103. <https://doi.org/10.1002/pi.1039>
37. Montaudo MS (2001) Determination of the compositional distribution and compositional drift in styrene/maleic anhydride copolymers. *Macromolecules* 34:2792–2797. <https://doi.org/10.1021/ma0010231>
38. Klumperman B (2010) Mechanistic considerations on styrene–maleic anhydride copolymerization reactions. *Polym Chem* 1:558–562. <https://doi.org/10.1039/B9PY00341J>
39. Benoit D, Hawker CJ, Huang EE, Lin Z, Russell TP (2000) One-step formation of functionalized block copolymers. *Macromolecules* 33:1505–1507. <https://doi.org/10.1021/ma991721p>
40. Wang Y, Shen Y, Pei X, Zhang S, Liu H, Ren J (2008) In situ synthesis of poly(styrene-*co*-maleic anhydride)/SiO₂ hybrid composites *via* “grafting onto” strategy based on nitroxide-mediated radical polymerization. *React Funct Polym* 68:1225–1230. <https://doi.org/10.1016/j.reactfunctpolym.2008.05.003>
41. Williams EGL, Fairbanks B, Moad G, Mulder RJ, Rizzardo E, Thang SH (2015) Preparation of 1:1 alternating, nucleobase-containing copolymers for use in sequence-controlled polymerization. *Polym Chem* 6:228–232. <https://doi.org/10.1039/C4PY01247J>
42. Wang S, Wu B, Liu F, Gao Y, Zhang W (2015) A well-defined alternating copolymer based on a salicylaldehyde Schiff base for highly sensitive zinc(II) detection and pH sensing in aqueous solution. *Polym Chem* 6:1127–1136. <https://doi.org/10.1039/C4PY01298D>
43. Saha B, Bauri K, Bag A, Ghorai PK, De P (2016) Conventional fluorophore-free dual pH- and thermo-responsive luminescent alternating copolymer. *Polym Chem* 7:6895–6900. <https://doi.org/10.1039/C6PY01738J>
44. Wenyan H, Huili P, Bibiao J, Qiang R, Guangqun Z, Lizhi K, Dongliang Z, Jianhai C (2011) Preparation of heat-resistant branched poly(styrene-*alt*-NPMI) by ATRP with divinylbenzene as the branching agent. *J Appl Polym Sci* 119:977–982. <https://doi.org/10.1002/app.32814>
45. Chen GQ, Wu ZQ, Wu JR, Li ZC, Li FM (2000) Synthesis of alternating copolymers of *n*-substituted maleimides with styrene *via* atom transfer radical polymerization. *Macromolecules* 33:232–234. <https://doi.org/10.1021/ma991047b>
46. Lutz J-F, Schmidt BVKJ, Pfeifer S (2011) Tailored polymer microstructures prepared by atom transfer radical copolymerization of styrene and *n*-substituted maleimides. *Macromol Rapid Commun* 32:127–135. <https://doi.org/10.1002/marc.201000664>
47. Sanders GC, Duchateau R, Lin CY, Coote ML, Heuts JPA (2012) End-functional styrene–maleic anhydride copolymers *via* catalytic chain transfer polymerization. *Macromolecules* 45:5923–5933. <https://doi.org/10.1021/ma301161u>
48. Longo JM, DiCiccio AM, Coates GW (2014) Poly(propylene succinate): a new polymer stereocomplex. *J Am Chem Soc* 136:15897–15900. <https://doi.org/10.1021/ja509440g>
49. Kramer JW, Treitler DS, Dunn EW, Castro PM, Roisnel T, Thomas CM, Coates GW (2009) Polymerization of enantiopure monomers using syndiospecific catalysts: a new approach to sequence control in polymer synthesis. *J Am Chem Soc* 131:16042–16044. <https://doi.org/10.1021/ja9075327>
50. Li J, He J (2015) Synthesis of sequence-regulated polymers: alternating polyacetylene through regioselective anionic polymerization of butadiene derivatives. *ACS Macro Lett* 4:372–376. <https://doi.org/10.1021/acsmacrolett.5b00125>
51. Stayshich RM, Meyer TY (2008) Preparation and microstructural analysis of poly(lactic-*alt*-glycolic acid). *J Polym Sci Part A Polym Chem* 46:4704–4711. <https://doi.org/10.1002/pola.22801>
52. Tsuji H, Arakawa Y (2018) Synthesis, properties, and crystallization of the alternating stereocopolymer poly(L-lactic acid-*alt*-D-lactic acid) [syndiotactic poly(lactic acid)] and its blend with isotactic poly(lactic acid). *Polym Chem* 9:2446–2457. <https://doi.org/10.1039/C8PY00391B>

53. Mayo FR, Lewis FM (1944) Copolymerization. I. A basis for comparing the behavior of monomers in copolymerization; the copolymerization of styrene and methyl methacrylate. *J Am Chem Soc* 66:1594–1601. <https://doi.org/10.1021/ja01237a052>
54. Fukuda T, Ma Y-D, Kubo K, Inagaki H (1991) Penultimate-unit effects in free-radical copolymerization. *Macromolecules* 24:370–375. <https://doi.org/10.1021/ma00002a005>
55. Sanayei RA, O'Driscoll KF, Klumperman B (1994) Pulsed laser copolymerization of styrene and maleic anhydride. *Macromolecules* 27:5577–5582. <https://doi.org/10.1021/ma00098a010>
56. Fukuda T, Kubo K, Ma Y-D (1992) Kinetics of free radical copolymerization. *Prog Polym Sci* 17:875–916. [https://doi.org/10.1016/0079-6700\(92\)90012-N](https://doi.org/10.1016/0079-6700(92)90012-N)
57. Jones SA, Prementine GS, Tirrell DA (1985) Model copolymerization reactions. Direct observation of a “penultimate effect” in a model styrene-acrylonitrile copolymerization. *J Am Chem Soc* 107:5275–5276. <https://doi.org/10.1021/ja00304a042>
58. Tsuchida E, Tomono T (1971) Discussion on the mechanism of alternating copolymerization of styrene and maleic anhydride. *Makromol Chem* 141:265–298. <https://doi.org/10.1002/macp.1971.021410122>
59. Zhao Y, Li H, Liu P, Liu H, Jiang J, Xi F (2002) Reactivity ratios of free monomers and their charge-transfer complex in the copolymerization of *N*-butyl maleimide and styrene. *J Appl Polym Sci* 83:3007–3012. <https://doi.org/10.1002/app.2330>
60. Dodgson K, Ebdon JR (1977) On the role of monomer—monomer donor—acceptor complexes in the free-radical copolymerisation of styrene and maleic anhydride. *Eur Polym J* 13:791–797. [https://doi.org/10.1016/0014-3057\(77\)90024-6](https://doi.org/10.1016/0014-3057(77)90024-6)
61. Deb PC, Meyerhoff G (1985) Study on kinetics of copolymerization of styrene and maleic anhydride in methyl ethyl ketone. *Polymer* 26:629–635. [https://doi.org/10.1016/0032-3861\(85\)90166-1](https://doi.org/10.1016/0032-3861(85)90166-1)
62. Hall HK, Padias AB (2001) “Charge transfer” polymerization—and the absence thereof! *J Polym Sci Part A Polym Chem* 39:2069–2077. <https://doi.org/10.1002/pola.1183>
63. Haldar U, Pan A, Mukherjee I, De P (2016) POSS semitelechelic A β _{17–19} peptide initiated helical polypeptides and their structural diversity in aqueous medium. *Polym Chem* 7:6231–6240. <https://doi.org/10.1039/C6PY01399F>
64. Heitz F, Spach G (1971) Synthesis and conformational study of alternating poly(γ -benzyl D,L-glutamates). *Macromolecules* 4:429–432. <https://doi.org/10.1021/ma60022a011>
65. Seipke G, Arfmann H-A, Wagner KG (1974) Synthesis and properties of alternating poly(Lys-Phe) and comparison with the random copolymer poly(Lys⁵¹, Phe⁴⁹). *Biopolymers* 13:1621–1633. <https://doi.org/10.1002/bip.1974.360130809>
66. Li G, Raman VK, Xie W, Gross RA (2008) Protease-catalyzed co-oligomerizations of L-leucine ethyl ester with L-glutamic acid diethyl ester: sequence and chain length distributions. *Macromolecules* 41:7003–7012. <https://doi.org/10.1021/ma800946d>
67. DiMarco RL, Heilshorn SC (2012) Multifunctional materials through modular protein engineering. *Adv Mater* 24:3923–3940. <https://doi.org/10.1002/adma.201200051>
68. Garanger E, Lecommandoux S (2012) Towards bioactive nanovehicles based on protein polymers. *Angew Chem Int Ed* 51:3060–3062. <https://doi.org/10.1002/anie.201107734>
69. Ghadiri MR, Granja JR, Milligan RA, McRee DE, Khazanovich N (1993) Self-assembling organic nanotubes based on a cyclic peptide architecture. *Nature* 366:324–327. <https://doi.org/10.1038/366324a0>
70. Al Samad A, De Winter J, Gerbaux P, Jerome C, Debuigne A (2017) Unique alternating peptide-peptoid copolymers from dipeptides *via* a Ugi reaction in water. *Chem Commun* 53:12240–12243. <https://doi.org/10.1039/C7CC06463B>
71. Schneider JP, Pochan DJ, Ozbas B, Rajagopal K, Pakstis L, Kretsinger J (2002) Responsive hydrogels from the intramolecular folding and self-assembly of a designed peptide. *J Am Chem Soc* 124:15030–15037. <https://doi.org/10.1021/ja027993g>
72. Pochan DJ, Schneider JP, Kretsinger J, Ozbas B, Rajagopal K, Haines L (2003) Thermally reversible hydrogels via intramolecular folding and consequent self-assembly of a de novo designed peptide. *J Am Chem Soc* 125:11802–11803. <https://doi.org/10.1021/ja0353154>

73. Ozbas B, Kretsinger J, Rajagopal K, Schneider JP, Pochan DJ (2004) Salt-triggered peptide folding and consequent self-assembly into hydrogels with tunable modulus. *Macromolecules* 37:7331–7337. <https://doi.org/10.1021/ma0491762>
74. Kretsinger JK, Haines LA, Ozbas B, Pochan DJ, Schneider JP (2005) Cytocompatibility of self-assembled β -hairpin peptide hydrogel surfaces. *Biomaterials* 26:5177–5186. <https://doi.org/10.1016/j.biomaterials.2005.01.029>
75. Frisch H, Besenius P (2015) pH-Switchable self-assembled materials. *Macromol Rapid Commun* 36:346–363. <https://doi.org/10.1002/marc.201400623>
76. Frisch H, Nie Y, Raunser S, Besenius P (2015) pH-Regulated selectivity in supramolecular polymerizations: switching between co- and homopolymers. *Chem Eur J* 21:3304–3309. <https://doi.org/10.1002/chem.201406281>
77. Ebert G, Kuroyanagi Y (1982) Salt effect on the conformation of an alternating copolymer of L-leucine and L-lysine. *Polymer* 23:1154–1158. [https://doi.org/10.1016/0032-3861\(82\)90370-6](https://doi.org/10.1016/0032-3861(82)90370-6)
78. Higuchi M, Nagata K, Abiko S, Tanaka M, Kinoshita T (2008) Stimuli induced structural changes of gold nanoparticle assemblies having sequential alternating amphiphilic peptides at the surface. *Langmuir* 24:13359–13363. <https://doi.org/10.1021/la802527n>
79. Grieshaber SE, Farran AJE, Lin-Gibson S, Kiick KL, Jia X (2009) Synthesis and characterization of elastin-mimetic hybrid polymers with multiblock, alternating molecular architecture and elastomeric properties. *Macromolecules* 42:2532–2541. <https://doi.org/10.1021/ma802791z>
80. Grieshaber SE, Nie T, Yan C, Zhong S, Teller SS, Clifton RJ, Pochan DJ, Kiick KL, Jia X (2011) Assembly properties of an alanine-rich, lysine-containing peptide and the formation of peptide/polymer hybrid hydrogels. *Macromol Chem Phys* 212:229–239. <https://doi.org/10.1002/macp.201000446>
81. Kricheldorf HR, Hauser K (2001) Poly lactones, 45. Homo- and copolymerizations of 3-methylmorpholine-2,5-dione initiated with a cyclic tin alkoxide. *Macromol Chem Phys* 202:1219–1226. [https://doi.org/10.1002/1521-3935\(20010401\)202:7%3c1219:AID-MACP1219%3e3.0.CO;2-U](https://doi.org/10.1002/1521-3935(20010401)202:7%3c1219:AID-MACP1219%3e3.0.CO;2-U)
82. Feng Y, Guo J (2009) Biodegradable polydepsipeptides. *Int J Mol Sci* 10:589–615. <https://doi.org/10.3390/ijms10020589>
83. Franz N, Klok H-A (2010) Synthesis of functional polydepsipeptides *via* direct ring-opening polymerization and post-polymerization modification. *Macromol Chem Phys* 211:809–820. <https://doi.org/10.1002/macp.200900521>
84. Ouchi T, Hamada A, Ohya Y (1999) Biodegradable microspheres having reactive groups prepared from L-lactic acid-depsipeptide copolymers. *Macromol Chem Phys* 200:436–441. [https://doi.org/10.1002/\(SICI\)1521-3935\(19990201\)200:2%3c436:AID-MACP436%3e3.0.CO;2-6](https://doi.org/10.1002/(SICI)1521-3935(19990201)200:2%3c436:AID-MACP436%3e3.0.CO;2-6)
85. Ouchi T, Toyohara M, Arimura H, Ohya Y (2002) Preparation of poly(L-lactide)-based microspheres having a cationic or anionic surface using biodegradable surfactants. *Biomacromolecules* 3:885–888. <https://doi.org/10.1021/bm0200231>
86. He Y, Du YR, Liu XB (2011) Synthesis, characterization and properties of polyesteramides based on ϵ -caprolactone and 6-aminocaproic acid. *Adv Mat Res* 287–290:1538–1547. <https://doi.org/10.4028/www.scientific.net/AMR.287-290.1538>
87. Qian Z, He Y, Zou Y, Li S, Liu X (2004) Structure and property study of degradable polyesteramide fibres: processing and alkaline degradation behaviour. *Polym Degrad Stab* 83:127–132. [https://doi.org/10.1016/S0141-3910\(03\)00233-7](https://doi.org/10.1016/S0141-3910(03)00233-7)
88. Ali Mohamed A, Salhi S, Abid S, El Gharbi R, Fradet A (2014) Random and quasi-alternating polyesteramides deriving from ϵ -caprolactone and β -alanine. *Eur Polym J* 53:160–170. <https://doi.org/10.1016/j.eurpolymj.2014.01.023>
89. Tsuji H (2016) Poly(lactic acid) stereocomplexes: a decade of progress. *Adv Drug Deliv Rev* 107:97–135. <https://doi.org/10.1016/j.addr.2016.04.017>
90. Tsuji H, Sato S, Masaki N, Arakawa Y, Kuzuya A, Ohya Y (2018) Synthesis, stereocomplex crystallization and homo-crystallization of enantiomeric poly(lactic acid-co-alanine)s with ester and amide linkages. *Polym Chem* 9:565–575. <https://doi.org/10.1039/C7PY02024D>

91. Matsui H, Ueda M, Makino A, Kimura S (2012) Molecular assembly composed of a dendrimer template and block polypeptides through stereocomplex formation. *Chem Commun* 48:6181–6183. <https://doi.org/10.1039/C2CC30926B>
92. Ueda M, Makino A, Imai T, Sugiyama J, Kimura S (2011) Transformation of peptide nanotubes into a vesicle via fusion driven by stereo-complex formation. *Chem Commun* 47:3204–3206. <https://doi.org/10.1039/C0CC04209A>
93. Ueda M, Makino A, Imai T, Sugiyama J, Kimura S (2011) Tubulation on peptide vesicles by phase-separation of a binary mixture of amphiphilic right-handed and left-handed helical peptides. *Soft Matter* 7:4143–4146. <https://doi.org/10.1039/C0SM01308K>
94. Grieshaber SE, Paik BA, Bai S, Kiick KL, Jia X (2013) Nanoparticle formation from hybrid, multiblock copolymers of poly(acrylic acid) and a VPGVG peptide. *Soft Matter* 9:1589–1599. <https://doi.org/10.1039/C2SM27496E>
95. Graña-Suárez L, Verboom W, Buckle T, Rood M, van Leeuwen FWB, Huskens J (2016) Loading and release of fluorescent oligoarginine peptides into/from pH-responsive anionic supramolecular nanoparticles. *J Mater Chem B* 4:4025–4032. <https://doi.org/10.1039/C6TB00933F>
96. Zhou C, Yuan Y, Zhou P, Wang F, Hong Y, Wang N, Xu S, Du J (2017) Highly effective antibacterial vesicles based on peptide-mimetic alternating copolymers for bone repair. *Biomacromolecules* 18:4154–4162. <https://doi.org/10.1021/acs.biomac.7b01209>
97. Bauri K, Saha B, Mahanti J, De P (2017) A nonconjugated macromolecular luminogen for speedy, selective and sensitive detection of picric acid in water. *Polym Chem* 8:7180–7187. <https://doi.org/10.1039/C7PY01579H>
98. Srichan S, Chan-Seng D, Lutz J-F (2012) Influence of strong electron-donor monomers in sequence-controlled polymerizations. *ACS Macro Lett* 1:589–592. <https://doi.org/10.1021/mz3001513>
99. Jia Y-G, Liu L-Y, Lei B, Li J, Zhu XX (2011) Crown ether cavity-containing copolymers *via* controlled alternating cyclocopolymerization. *Macromolecules* 44:6311–6317. <https://doi.org/10.1021/ma201247d>
100. Heravi MM, Hashemi E, Beheshtiha YS, Kamjou K, Toolabi M, Hosseintash N (2014) Solvent-free multicomponent reactions using the novel *N*-sulfonic acid modified poly(styrene-maleic anhydride) as a solid acid catalyst. *J Mol Catal A-Chem* 392:173–180. <https://doi.org/10.1016/j.molcata.2014.04.024>
101. Heravi MM, Hashemi E, Beheshtiha YS, Ahmadi S, Hosseinejad T (2014) PdCl₂ on modified poly(styrene-*co*-maleic anhydride): a highly active and recyclable catalyst for the Suzuki–Miyaura and Sonogashira reactions. *J Mol Catal A-Chem* 394:74–82. <https://doi.org/10.1016/j.molcata.2014.07.001>
102. Soer WJ, Ming W, Klumperman B, Koning C, van Benthem R (2006) Surfactant-free artificial latexes from modified styrene–maleic anhydride (SMA) copolymers. *Polymer* 47:7621–7627. <https://doi.org/10.1016/j.polymer.2006.09.007>
103. Baranello MP, Bauer L, Benoit DSW (2014) Poly(styrene-*alt*-maleic anhydride)-based diblock copolymer micelles exhibit versatile hydrophobic drug loading, drug-dependent release, and internalization by multidrug resistant ovarian cancer cells. *Biomacromolecules* 15:2629–2641. <https://doi.org/10.1021/bm500468d>
104. Lazzara TD, van de Ven TGM, Whitehead MA (2008) Nanotube self-assembly of a styrene and maleimide alternating copolymer. *Macromolecules* 41:6747–6751. <https://doi.org/10.1021/ma800926a>
105. Wang Z, Gao M, Sun J, Liang D, Jia X (2013) Photoresponsive dendronized copolymers of styrene and maleic anhydride pendant with poly(amidoamine) dendrons as side groups. *Macromolecules* 46:1723–1731. <https://doi.org/10.1021/ma302358t>
106. Zhang Z, Hong L, Gao Y, Zhang W (2014) One-pot synthesis of POSS-containing alternating copolymers by RAFT polymerization and their microphase-separated nanostructures. *Polym Chem* 5:4534–4541. <https://doi.org/10.1039/C4PY00302K>
107. Zhang Z, Hong L, Li J, Liu F, Cai H, Gao Y, Zhang W (2015) One-pot synthesis of well-defined amphiphilic alternating copolymer brushes based on POSS and their self-assembly in aqueous solution. *RSC Adv* 5:21580–21587. <https://doi.org/10.1039/C4RA15492D>

108. Srichan S, Oswald L, Zamfir M, Lutz J-F (2012) Precision polyelectrolytes. *Chem Commun* 48:1517–1519. <https://doi.org/10.1039/C1CC14823K>
109. Srichan S, Kayunkid N, Oswald L, Lotz B, Lutz J-F (2014) Synthesis and characterization of sequence-controlled semicrystalline comb copolymers: influence of primary structure on materials properties. *Macromolecules* 47:1570–1577. <https://doi.org/10.1021/ma4023179>
110. Baradel N, Gok O, Zamfir M, Sanyal A, Lutz J-F (2013) Sequence-controlled polymerization using dendritic macromonomers: precise chain-positioning of bulky functional clusters. *Chem Commun* 49:7280–7282. <https://doi.org/10.1039/C3CC43501F>
111. Li Y, Mao M, Matolyak LE, Turner SR (2012) Sterically crowded anionic polyelectrolytes with tunable charge densities based on stilbene-containing copolymers. *ACS Macro Lett* 1:257–260. <https://doi.org/10.1021/mz200061w>
112. Li Y, Savage AM, Zhou X, Turner SR, Davis RM (2013) Solution properties of stilbene-containing sterically crowded alternating polyanions. *J Polym Sci Part B Polym Phys* 51:1565–1570. <https://doi.org/10.1002/polb.23370>
113. O’Shea J-P, Solovyeva V, Guo X, Zhao J, Hadjichristidis N, Rodionov VO (2014) Sequence-controlled copolymers of 2,3,4,5-pentafluorostyrene: mechanistic insight and application to organocatalysis. *Polym Chem* 5:698–701. <https://doi.org/10.1039/C3PY01368E>
114. Huang J, Zhou X, Lamprou A, Maya F, Svec F, Turner SR (2015) Nanoporous polymers from cross-linked polymer precursors *via* tert-butyl group deprotection and their carbon dioxide capture properties. *Chem Mater* 27:7388–7394. <https://doi.org/10.1021/acs.chemmater.5b03114>
115. Zhou X, Huang J, Barr KW, Lin Z, Maya F, Abbott LJ, Colina CM, Svec F, Turner SR (2015) Nanoporous hypercrosslinked polymers containing T_g enhancing comonomers. *Polymer* 59:42–48. <https://doi.org/10.1016/j.polymer.2014.12.065>
116. Tang D, Jiang X, Liu H, Li C, Zhao Y (2014) Synthesis and properties of heterografted toothbrush-like copolymers with alternating PEG and PCL grafts and tunable RAFT-generated segments. *Polym Chem* 5:4679–4692. <https://doi.org/10.1039/C4PY00332B>
117. Ping J, Gu K, Zhou S, Pan H, Shen Z, Fan X-H (2016) Hierarchically self-assembled amphiphilic alternating copolymer brush containing side-chain cholesteryl units. *Macromolecules* 49:5993–6000. <https://doi.org/10.1021/acs.macromol.6b01043>
118. Ping J, Pan Y, Pan H, Wu B, Zhou H, Shen Z, Fan X-H (2015) Microphase separation and high ionic conductivity at high temperatures of lithium salt-doped amphiphilic alternating copolymer brush with rigid side chains. *Macromolecules* 48:8557–8564. <https://doi.org/10.1021/acs.macromol.5b01678>
119. Tsujii A, Namba M, Okamura H, Matsumoto A (2014) Radical alternating copolymerization of twisted 1,3-butadienes with maleic anhydride as a new approach for degradable thermosetting resin. *Macromolecules* 47:6619–6626. <https://doi.org/10.1021/ma501555n>
120. Kim H, Kang YJ, Jeong ES, Kang S, Kim KT (2012) Glucose-responsive disassembly of polymersomes of sequence-specific boroxole-containing block copolymers under physiologically relevant conditions. *ACS Macro Lett* 1:1194–1198. <https://doi.org/10.1021/mz3004192>
121. Yang P, Mykhaylyk OO, Jones ER, Armes SP (2016) RAFT dispersion alternating copolymerization of styrene with *N*-phenylmaleimide: morphology control and application as an aqueous foam stabilizer. *Macromolecules* 49:6731–6742. <https://doi.org/10.1021/acs.macromol.6b01563>
122. Reches M, Gazit E (2003) Casting metal nanowires within discrete self-assembled peptide nanotubes. *Science* 300:625–627. <https://doi.org/10.1126/science.1082387>
123. Chen J, Yu C, Shi Z, Yu S, Lu Z, Jiang W, Zhang M, He W, Zhou Y, Yan D (2015) Ultrathin alternating copolymer nanotubes with readily tunable surface functionalities. *Angew Chem* 127:3692–3696. <https://doi.org/10.1002/ange.201408290>
124. Adler-Abramovich L, Gazit E (2014) The physical properties of supramolecular peptide assemblies: from building block association to technological applications. *Chem Soc Rev* 43:6881–6893. <https://doi.org/10.1039/C4CS00164H>

Chapter 6

Fabrication of Stimuli-Responsive Polymers and their Composites: Candidates for Resorbable Sutures



Deepshikha Das, Neha Mulchandani, Amit Kumar and Vimal Katiyar

Abstract Sutures are known to facilitate wound healing and recently, a significant attention has been laid on the development of different classes of materials, their properties to enhance tissue approximation and wound closure. The advancements in the suture technology have introduced different types of sutures such as barbed sutures, antimicrobial sutures, drug-eluting sutures. The biostable and bioresorbable materials have received importance in augmentation and proper growth of the tissues due to their extraordinary characteristics. Furthermore, the biodegradable polymeric sutures have been explored for suture applications due to their efficiency, both in terms of property and application. In this regard, the current chapter highlights the various biodegradable polymers as possible candidates for sutures along with their essential properties and applications. Moreover, the utilization of different biofillers for fabricating sutures along with various fabrication techniques is discussed. Additionally, an impact is laid on the development of ‘stimuli-responsive sutures’ in order to tailor the behavior of the suture for subjected applications by using external agents or stimulus. These materials respond to small changes that can be both physical and chemical environment. Electric field, magnetic field, radiation are some of the stimulants that can be used based on the polymer used and nature of the application (cell adhesion, nerve regeneration, drug delivery, degradation control, antimicrobial, etc.) of suture. Magnetic responsive composite materials possess fine tuning properties which find their potential in biomedical, cell guidance and controlled drug release study (hyperthermia effect). A good understanding in terms of application and physical phenomena is portrayed which would help in developing the stimuli-responsive materials and devices in the biomedical field.

Keywords Biodegradable polymers · Composites · Bioresorbable · Stimuli-responsive sutures

D. Das · N. Mulchandani · A. Kumar · V. Katiyar (✉)
Department of Chemical Engineering, Indian Institute of Technology Guwahati, Guwahati,
Kamrup, Assam 781039, India
e-mail: vkatiyar@iitg.ac.in

© Springer Nature Singapore Pte Ltd. 2020
V. Katiyar et al. (eds.), *Advances in Sustainable Polymers*, Materials Horizons: From Nature to Nanomaterials, https://doi.org/10.1007/978-981-15-1251-3_6

1 Introduction

The development of biomaterials in today's era is one of the significant research challenges evolving in the areas of medicine and tissue engineering. Based on their behavior in the living tissue, these materials are divided into biodegradable and bio-absorbable materials. Biodegradable polymer-based materials are nowadays becoming an obvious choice for preparation of biomaterials for their degradable behavior, compatibility with living system and non-toxic nature. The biodegradable polymers degrade into the host and are removed thereafter, whereas the importance of the resorbable biopolymers eliminates this process and gets metabolized therein. Biodegradable polymers are in use for various versatile applications such as packaging, cosmetics, textile applications and one of the most prominent emerging fields is biomedical. Till date, a number of polymers have been explored for their biodegradable nature and compatibility with most of the living tissues. The most important among these are polyglycolic acid (PGA), polylactic acid (PLA), poly(ϵ -caprolactone) (PCL) and copolymers of different biodegradable polymers [1].

The biodegradable and bio-absorbable polymers used for the biomedical applications must possess essential properties for their safe medical use. The removal of the implant post-healing often requires re-surgery which may be painful. The materials used as implants must therefore absorb inside the body, possess good mechanical strength, easy processability, controllable surface nature and retention of strength during in vivo and in vitro analysis. Such properties have therefore promoted these classes of materials as one of the prime replacement for the conventional orthopaedics transplants, tissue engineering substance, drug delivery application, surgical applications, etc. [2].

Recently, the use of biodegradable polymers as surgical sutures has been commercially increased. These materials are replacing the conventional suture materials almost in all the different surgical cases. However, different modifications have been carried out by different groups in order to improve the properties of suture apart from only the mechanical support such as fabrication of composites, variation in the spinning technique, coating the surface of the suture. In order to get the controllable performance of suture under external fields and tailor the properties like antibacterial activity, cell adhesion stimuli-responsive materials are studied in the form of matrix or filler. Electric field, magnetic field, pH, chemical environment are the stimulus studied majorly. In this chapter, a detailed survey of biodegradable polymeric materials as sutures and the scope of stimuli-responsive sutures and their fabrication are discussed [3].

2 Suture

Suture is a biomedical device which is used to ligate blood vessels by upholding tissues together to expedite wound healing. It has both natural and synthetic origins.

Physicians have used suture to close wounds for at least 4000 years [4]. The wound closure implies eradication of dead space, evenly distributed tension along deep suture lines, maintenance of tissue tensile strength and approximation of the closure. Although there are various developed materials for wound closure management such as staples, screws, tape, and adhesive, sutures are found to be the most widely used ones. Sutures have witnessed enormous growth since the past two decades. Sutures are considered to be the largest group of biomaterials which constitute a huge market exceeding \$1.3 billion annually [5]. A significant growth of surgical sutures features in the case of healthcare industry, for both absorbable and non-absorbable suture-based products. Since the early times, different plant- (cotton, silk) and animal-based (animal gut, horse hair), metal- and steel-based sutures have been utilized. Recently, various synthetic biomaterials such as polydioxanone, polyglycolic acid (PGA) are being used as suture materials. Sutures provide the flexibility and stability during wound management which are usually the shortcomings observed in other wound healing products. Different kinds of sutures may be fabricated such as absorbable, antimicrobial, barbed, coated sutures based on the targeted applications [6]. Roberts et al. in the year 1983 reported a comparative study between PGA sutures and traditional catgut in 190 patients undergoing episiotomy. They found edema disease was significantly reduced in case of PGA-based suture compared to the catgut suture [7]. In the year 1988, Singhal et al. reviewed emerging trends on sutures and its biodegradability based on PGA and its copolymers [8]. In the year 2006, Li and Yuan studied about the progress on synthetic-based absorbable polymeric sutures [9]. A general comparative study was made upon closure materials for vascular devices by Hon et al. in the year 2009. They focused on the mechanism of sutures and their potential in serving homeostasis [10].

2.1 Characteristics of Suture

The ideal properties of suture for fulfilling the increasing demands of wound-closure issues are described below:

- It must be biocompatible, biodegradable and bioresorbable.
- It must have adequate mechanical strength and impart flexibility.
- It must have knot-pull strength and straight-pull strength and knot security [11].
- It must evoke inflammatory response.
- It must have an acceptable shelf life.
- It must have permeability and help in healing process.
- It should be non-toxic and should not support bacterial growth.
- It should be easily handled.
- It must have slow absorption rate with the healing of the wound.

3 Classification of Suture Materials

Sutures are originally made from natural and synthetic polymers. It can be classified into different categories based on their nature of degradation, size, texture and structure, and commercial surgery notation.

Filament Structure	Texture	Degradation	Size
Monofilament	Smooth	Absorbable	US Pharmacopeia (USP),
Multifilament	Barbed	Non-absorbable	European Pharmacopeia (EP)
Pseudo-filament			

On the basis of the structure and number of strands, sutures may be classified as monofilament, multifilament, and pseudo-filament [12].

Monofilament sutures: These are single-stranded materials. These impart less resistance while passing through tissues and are also less prone to infection. These are easily tied down and must be handled carefully. Because of their simple structure, these can lead to breakage of the suture strand.

Multifilament sutures: These are comprised of many strands of filaments twisted and braided together. The multifilament sutures render much higher mechanical property with appropriate flexibility and pliability than the monofilament ones. These are sometimes coated to enhance handling properties and are applicable in intestinal procedures. These are called as *pseudo-filament sutures*.

The sutures for wound closures may further be categorized on the basis of their texture and surface design as follows:

Barbed sutures: These sutures generally contain spikes on their surfaces for deep wound closures and possess sharp projections or barbs which help in anchoring of the sutures to tissues in a linear fashion, thereby eliminating the need to knot. The barbed sutures have widened their applications in complex reconstructive surgical procedures.

Smooth sutures: The smooth sutures are tightly knotted around the tissues of bones. These correspond to the response to inflammation and bacterial growth. These are not recommended for minimally invasive surgeries.

On the basis of nature of degradation, sutures may be classified as:

Absorbable sutures: These sutures undergo rapid degradation in tensile strength within 60 days. These are used to hold wound edges temporarily. These are prepared from animal origin and synthetic polymers. These can also be coated for easy handling and visibility in the tissue. The natural-based sutures are absorbed by body enzymes, and the synthetic polymers are hydrolyzed by breaking the polymer chains.

Non-absorbable sutures: These sutures are not digested by enzymes or hydrolyzed into the living tissue. These are made up of non-biodegradable materials which remain repressed within the host tissue. There is a need for postoperative removal. These comprises of single or multiple filaments. The fiber strand conforms to the USP for

its size and composition. These are of different types, coated or uncoated, dyed, etc., to enhance visibility.

There are different standards to select size of suture for surgery. One of such standard is 'US Pharmacopeia' (USP), according which the size of the suture indicates the diameter denoted by the number of zeroes. The number of zeroes is inversely proportional to the strand diameter. The smaller the diameter, the lesser is the strength of the suture [5].

Sr. No.	Size	Use	Diameter (mm) (natural)
1.	7-0 or smaller	Ophthalmology	0.070–0.099
2.	6-0	Blood vessels	0.100–0.149
3.	5-0	Face, neck, blood vessels	0.150–0.199
4.	4-0	Mucosa, neck, hands, limbs, tendons, blood vessels	0.200–0.249
5.	3-0	Limbs, trunk, gut, blood vessels	0.300–0.339
6.	2-0	Trunk, fascia, viscera, blood vessels	0.400–0.399
7.	0 or larger	Orthopedics	0.400–0.499

3.1 Selection of Suture

The ability of the sutures to facilitate wound healing directly correlates to the size and tensile property of the suturing material. The tensile strength of any suture material should also balance the tensile strength of the healing tissues. The tensile strength of the knot denotes the force in pounds which the suture strand resists before it breaks when tied a knot. The size of the suture signifies the diameter, which is denoted by the number of zeroes. The number of zero's is inversely proportional to the diameter of the suture. For example, size 5-0 or 00000 is smaller in diameter than size 4-0 or 0000. The smaller the diameter, the lesser is the strength of the suture. The selection of any suture material takes into account the layers of wound closure, tension around the wound and location of the suture [4].

- Suture must be selected on the basis of strength retention and finely structured material which also correspond to the strength of tissue.
- In case of slow healing tissues, non-absorbable sutures and in the case of fast healing tissues, absorbable sutures must be used.
- When the foreign bodies prevail in the contaminated tissues, multifilament sutures must be avoided and monofilament should be used.
- In the case of cosmetic surgeries, monofilament materials such as polypropylene, PP, and nylon are used for the proper closure and recovery of tissues.

- In the presence of fluids such as in urinary tracts, monofilament materials are used to prevent from causing stone formation and precipitation.

3.2 Fabrication of Sutures

The suture material can be synthesized by fiber spinning process. The ingredient can be directly from nature (cotton, catgut etc.), synthesized polymers (degradable, non-degradable), or metallic. The spinning process involves two steps, i.e., conversion of polymers into fibers such as extrusion or spinning of fibers and further post-spinning, i.e., drawing of fibers and heat treatment. Different spinning methods are selected based on the nature of material and thermal stability of materials. Post-treatments are conducted in order to achieve better properties or tailored surface nature [13].

The major steps involved in the fiber production are:

- Spinning
- Drawing
- Post-treatment.

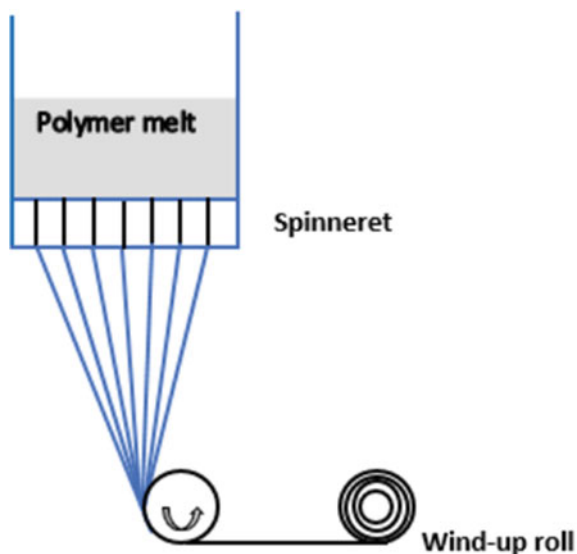
The spinning techniques may be classified as:

- Melt spinning
- Solvent spinning
 - Dry spinning
 - Wet spinning
 - Dry-jet wet spinning
- Electrospinning.

Melt spinning technique:

The *melt spinning process* is the primitive method used for the production of fibers which is a solvent-free process and based on simple extrusion process. It is the most eco-friendly route used for the fiber fabrication. The schematic of the melt spinneret is shown in Fig. 1. The polymers having degradation temperature much higher than their melting temperature may be subjected to melt spinning in order to be spun into fibers. The production speeds are normally high. The polymer melting point and its solubility in organic/inorganic solvents are to be known when using this technique. This method is mainly used for the polymers such as polyesters, polyamides, polyolefins. After melting at higher temperatures, the melt is forced to pass through the spinneret at high pressure around 10–20 MPa and temperature. The molten strands are then cooled while it solidifies. One of the characteristic of the melt spinning is that the strands are extruded from the melt which are solidified by exchange of heat within the medium. Eling et al. 1982 fabricated poly (L-lactic acid), PLLA-based melt spun fiber at 185 °C and used hot furnace for the thermal

Fig. 1 Schematic of melt spinneret



treatment which led to the production of PLLA fiber with 0.5 GPa tensile strength was achieved [14]. Charuchinda et al. studied the effect of spinning temperature, drawing speed, polymer properties on the melt spinning of PCL. Increase in the drawing ratio, spinning temperature led to the reduction of the fiber diameter, whereas increase in the drawing ratio led to the increase the strength of melt spun fiber [15].

Solvent spinning technique:

The solution spinning, although complex, is suitable for the polymers which do not meet the requirements for melt spinning and such polymers may be spun if they are dissolved in a suitable solvent. The polymer then dissolved, swells, and forms a completely homogeneous solution. The polymers prepared by this process can be directly spun without intermediate processing such as polyacrylonitrile (PAN). The spinning pressures are usually 0.5–4 MPa, which is less than that in melt. The polymers with a very high molecular mass, i.e., M_w around 250,000 can also be spun which is not the case in melt spinning because the limiting viscosity at zero shear η_0 and the spinning pressure increases in proportion to $M_w^{3.4}$. In the solution spinning, the effect of molecular mass on viscosity can be compensated by appropriate dilution [16]. However, the concentration used should not be low since this will affect less polymer throughput and increase the cost of solvent recovery. This is classified into as (a) dry spinning technique and (b) wet spinning technique.

Dry spinning technique:

In the *dry spinning* process, the polymer solution is spun in the presence of hot gas where the temperature is higher than the normal boiling point of the solvent. The

evaporation of the solvent by the drying gas along the spinning path is determined mainly by its rate of diffusion through the strand, which decreases with the solidification rate. Solidification occurs because of the decrease in solvent concentration and the associated increase in viscosity. In this process, the strand bears a residual solvent content of 5–25 wt%. This is desirable because it plasticizes, thereby facilitating the subsequent drawing of the filament. The residual solvent is removed later in the process. The spin–draw ratio is based on the extrusion rate of the spinning solution [17]. The schematic of the dry spinning process is shown in Fig. 2. Gogolewski and Pennings 1985 fabricated nylon-6 filaments from nylon-6 solution using solvent mixture of formic acid and chloroform followed by hot drawing in the temperature range 200–240 °C and the strength of fiber was reported to be 1 GPa [18]. PLLA fiber of high strength was drawn by dry spinning followed by hot drawing by Leenslag and Pennings [19] with 2.1 GPa tenacity and 16 GPa modulus.

Wet spinning technique:

In the *wet spinning* process, the polymer is dissolved in a nonvolatile solvent which necessitates a subsequent reverse reaction. In this process, the polymer solution is spun into a liquid coagulating bath. The heat exchange within the spinning medium is not responsible for solidification of the strand. Instead, solidification results due to coagulation caused by phase separation which is induced by a component of the spin bath which is incompatible with the polymer which is a non-solvent [20]. Um et al. [21], utilized wet spinning technique to fabricate silk fibroin filaments using formic acid solvent and methanol coagulation bath. With decrease in the drawing ratio, the fracture stress decreased and the elongation increased for the fibers [21].

Fig. 2 Schematic of dry spinning

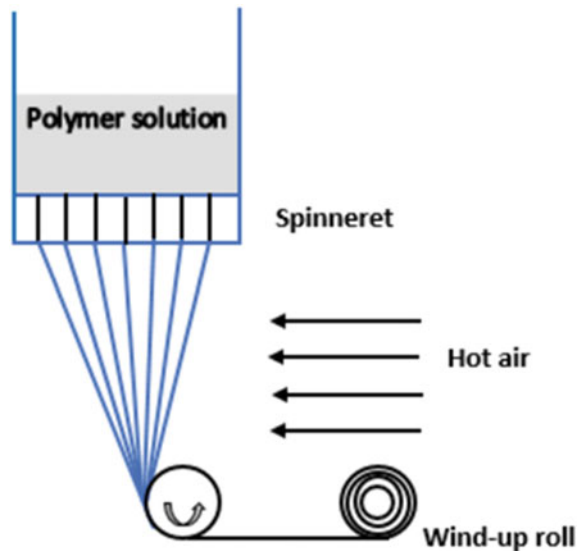
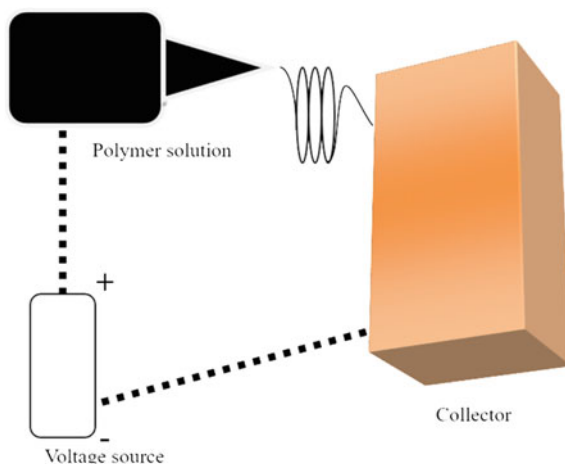


Fig. 3 Schematic of electrospinning



In the *electrospinning* process, the polymer solution or melt is drawn to continuous fiber with diameter ranging from few microns to nanometers which is shown in Fig. 3. It is processed under the influence of an electric field. Voltage difference, solution viscosity, nozzle type, etc., influence the fiber property [20]. Hu et al., 2014, fabricated different polymer-based electro-spun fibers for drug delivery application with variety of surface properties [22]. Matthews et al., 2001, fabricated collagen nanofiber by electrospinning technique. Acid soluble collagen was used and voltage difference was 15–30 kV. The fibers were applied for tissue engineering application [23].

4 Biodegradable Suture

Biodegradable Polymers

The biodegradable polymers have been sparked by the recent advances in the fields of biomedical, packaging, textiles, etc. Biodegradable polymers break down into stable end products under physiological conditions. When a neat polymer, blended product or composite is obtained completely from renewable resources, it may be considered a green polymeric material [24]. Biodegradable polymers can be either natural or synthetic. Natural polymers such as protein, polysaccharide, and nucleic acid are degraded in the biological systems by oxidation and hydrolysis [25]. For the synthetic polymers, enzymatic degradation is witnessed, wherein the microbes utilize the carbon backbone as a carbon source when is required. This technique offers a solution to biodegradable waste management. However, the emerging research and interest have focused the attention of biodegradable polymers for biomedical applications owing to their biocompatibility (in some cases) [26]. In the terms of biocompatibility, biopolymers offer an alternative to traditional biodegradable materials and non-biodegradable polymers. The polymeric biomaterials can be broadly classified

as enzymatically degradable and hydrolytically degradable polymers. Bioabsorbable polymers can be blended to improve their overall functional properties. These are processed to fabricate different objects such as fibers, films, screws, plates, sutures which are cost-effective too. The fundamental aspects of biodegradability are

- The effect of polymer structure on biodegradation.
- The effective relationship between degradation and absorption.

The polymer structure on biodegradation is important to understand the correct approach for the production of composites, the properties of the biopolymers and how well they recombine with the natural polymers such as polypeptides, polysaccharides, polynucleotides, fibers, etc. Biodegradable polymers, mostly used for biomedical applications in tissue engineering, should have parallel rate of absorption and curing. It depends on the location of the tissue or organ in the human body. These should maintain the desired strength, modulus and function until the tissues are completely cured by minimizing unwanted side effects. The synthetic polymers, on the other hand, remain in the host after their practical functions are lost. Although, for most of the biodegradable polymers, the complete decomposition rate is much slower than the curing rate of bio-tissues, the products are likely to reside in the cured tissues even after the therapy. The rate depends on many factors which includes the chemical composition of the main chain and side groups, the state of aggregation, extent of crystallinity, hydrophilic–hydrophobic balance, surface area, and morphological behavior of the polymer material. It is also strongly affected by the primary and higher order structure, solid-state structures of the polymer. The polymer surface area also becomes the main factor for biodegradability. A polymer having both hydrophobic and hydrophilic characteristic serves better for biodegradation by hydrolysis reactions [1]. Sir John Charnley successfully made the first clinical application of biomaterial which dates back 50 years ago, poly(methyl methacrylate) (PMMA), an acrylic cement which was used to attach a femoral head prosthesis [27].

4.1 Biodegradable Polymer-Based Suture (BPBS)

Generally, the sutures are made from natural and synthetic origins. The synthetic polymers possess acceptable mechanical strength and their rate of degradation along with the shape can be easily modified. Their hydrophobic surfaces and cell recognition signals can be easily tuned. The polymers which are derived from natural resources are likely to possess the advantage of cell support and cell proliferation. These kind of natural polymers bear poor mechanical properties and are costly when the supply is limited [28]. The natural sutures are usually made of catgut or reconstituted collagen, cotton, silk. The two naturally absorbable sutures (types) available in the market are catgut and regenerated collagen. Catgut is available as plain catgut (untreated) and chromic gut (tanned by chromium trioxide). Since 1930s, catgut has been used as the staple absorbable suture material, whereas silk and cotton are used

as non-absorbable materials. These sutures are noted for their toughness and tenacity. The basic constituent of catgut is collagen and is the major structural protein found in all multicellular organisms. These sutures are coated with glycerin to eliminate the requirement of alcohol packing. During the early 1970s, absorbable synthetic polymer PGA was developed and its copolymer is commercially available as a suture material. The absorbable sutures are established to behave favorably both in vitro and in vivo [29]. Owing to their controlled manufacturing processes and reproducible properties, these kinds of biomaterials have received a great deal of interest in the biomedical field [30]. The advantage of synthetic absorbable sutures is their reproducibility and degradability within a biological environment which enables them to minimize undesirable reactions in the tissues after the sutures discontinued their function. These synthetic-based sutures have replaced the natural ones for the wound-closure management. A braided suture marketed as Vicryl[®] is a copolymer of (glycolic acid/lactic acid), GA/LA mol/mol composition. Further, a homopolymer of GA is a braided suture commercially available with the trade name Dexon[®]. The most susceptible monofilament suture till date is Maxon[®], which is a segmented block copolymer of glycolide and ϵ -CL. Another commercial suture named as Panacryl[®] is a copolymer with a high LA/GA ratio [31]. The copolymers of linear aliphatic polyesters like PLA, PGA which are also biodegradable in nature are frequently used in tissue engineering [32] and as in vivo degradable surgical sutures which achieved (US Food and Drug Administration) FDA recognition for medical use. The other linear polyesters which are also used in tissue engineering applications are polyhydroxybutyrate (PHB), PCL. PCL though possessing a slower degradation rate which is not desirable for most of the biomedical applications but, it finds its usefulness in long-term implants, controlled drug delivery applications. It has also appeared as a perfect candidate for fabricating suture and scaffold materials [3]. Some absorbable natural- and synthetic-based sutures are highlighted in Table 1.

Furthermore, some of the non-absorbable polymer sutures marketed are

- Polyamide (Ethicon)
- Tantalum (B. Braun)
- Polyethylene/Polypropylene (Ethicon)
- Poly-but-ester.

4.2 Biodegradable Composite-Based Sutures (BCBS)

Biodegradable polymers have several shortcomings like low thermal stability, mechanical strength, brittleness which are detrimental for the applicability of the polymer. For the biomedical applications, the biocompatibility, strength sustainability under buffer solution, mineralization, mechanical strength and processability of the polymers are essential to be modified by using suitable reinforcement. Different reinforcements like hydroxyapatite, silicates, carbon nanotubes are incorporated into the biodegradable polymers in order to fabricate bionanocomposites for biomedical

Table 1 Commercially available sutures from natural and synthetic polymers

Natural polymers			
Sr. No.	Name of polymer	Trade name	Year of manufacture
1.	Bovine origin	Catgut plain	Sixteenth century
2.	Collagen/intestines of sheep	Surgical catgut	1880 (Ethicon)
3.	Collagen	Chromic gut	1950–1960 (Ethicon)
Synthetic polymers			
1.	Polyvinyl alcohol	HS-PVA braids	1931
2.	PGA	Dexon [®]	1970
3.	PGA	Medifit [®]	1974
4.	PGA/PLLA(glycolide-L-lactide)	Polyglactin 910 (Vicryl [®])	1974
5.	Poly(glycolide-L-lactide)	Polysorb [®]	1981
6.	Polydioxanone (PDS)	PDS II [®]	1981
7.	Poly(glycolide-ε-caprolactone)	Polyglecapron 25, (Monocryl [®])	1992

applications like tissue engineering, orthopaedic implants, suture. Some of the nano-based material used for fabrication of composite materials maybe given as follows [33]:

Hydroxyapatite (HAP): Hydroxyapatite ($\text{Ca}_{10}(\text{PO}_4)_6(\text{OH})_2$), which is both osteoconductive and biocompatible, is used mainly for bone tissue applications as it is a major mineral component of the bones consisting of 69 wt% of the hard tissues [34]. It is both naturally available in bones and teeth and can be synthesized to promote bone growth, tissue repair with a Ca/P range of 1.50–1.67. In case of PLA/hydroxyapatite composites, where hydroxyapatite serves as the filler, the alkaline part of it neutralizes the acidic neutralization of the PLA matrix to make it bio-functional. The recent research proved that nano-sized HAP (n-HAP) due to its huge surface area showed prominent increase in protein adsorption and osteoblast adhesion than the micro-sized ceramic HAP [35]. In the year 1992, Verheyen et al. investigated the mechanical behavior of the L-lactide/HAP biocomposite for applications in orthopaedics surgery. Gupta et al. in the year 2017 fabricated high molecular weight stereocomplex PLA (sPLA)/n-HAP bionanocomposites for orthopaedic implants [36].

Carbon nanotubes (CNT): These can be of single sheet (single-walled carbon nanotubes) (SWCNTs) and multi-walled sheets (multi-walled carbon nanotubes) (MWCNTs). Because of their regular structure and excellent electrical and mechanical properties, it can find application in sensors, biomedical and electronic devices [37]. It serves as a structural reinforcing agent for biomedical applications. Incorporation of SWCNTs enhances the bioactivity of the composite material. Cheng et al. prepared CNT/PLGA composite by solvent-casting/particle-leaching method for scaffold fabrication [38]. Also, Pan et al. prepared PCL/MWCNT composite by solvent-casting method and found the increase of cell adhesion [39].

Chitosan: Chitosan is a linear polymer which is obtained from the parent origin chitin and is widely available in nature such as in certain fungi and crustaceans. It is biocompatible, biodegradable and also possesses inherent antimicrobial property which makes it a good candidate for biomedical applications. Chitosan promotes wound healing and protects the cell from infection. It enhances vascularisation and also endothelial cell proliferation. Besides, the repairing nature of the chitosan, it can also be used as gels for therapeutic delivery to the local wound. Kashiwazaki et al. in the year 2009 prepared HAP/chitosan composite by co-precipitation method. These were used for fabrication of scaffolds in the rat model [40].

Cellulose: Cellulose is a naturally occurring filler which is most abundant in nature. It has hydroxyl functional groups on its surface which helps in even mixing for the preparation of the composite. It can be easily modified and helps in enhancing the properties of the material. Jiang et al. have used cellulose nanocrystals which directly acted as a nucleating agent in the PLLA/PDLA blend matrix that improved crystallizability of the material [41].

Silk: It is a fibrous protein which is known for its biocompatibility, ease of functionalization, flexible morphology and better mechanical properties. It is a viable candidate for various tissue engineering, wound healing applications. It shows promising in vivo response. Patwa et al. in the year 2018 prepared magnetic silk/PLA composite by electrospinning method and studied the cytocompatibility which is effective for cancer therapy [42].

Silver nanoparticles: It is known for its disinfectant and antimicrobial property. It is capable of releasing silver ions and serves as an antibacterial agent. It has a high surface area which enhances its inhibitory property. Simone et al. prepared novel silver treated suture and studied its antibacterial effect for the prevention of surgical infections [43].

4.3 Advantages of BCBS Over BPBS

- The incorporation of fillers like CNT, hydroxyapatite can improve the mechanical strength of BCBS compared to the polymer.
- Collagen, peptides, etc., can improve bioresorbability of BCBS over BPBS.
- Different magnetic materials and electrically conducting filler loaded BCBS can be tuned for particular applications using external stimulus.
- Different composite-based sutures can be utilized for drug carrier system more effectively as compared to the polymer system.
- The degradation behavior, especially the mechanical strength retention under in vivo and in vitro condition, is improved for the composite.
- The surface property of BPBS can be tuned by using suitable modification and thus biocompatibility and cell adhesion are controlled.
- In some cases, incorporation of fillers into polymeric system can improve the bone growth as compared to the pure polymer.

5 Stimuli-Responsive Polymers

A Brief Introduction

Polymers that respond to external stimulus exhibit dramatic changes in their properties in the presence of different environment such as pH, solvents, salts, light, electrical, and electromagnetic radiation. These changes may include conformation, surface, hydrophilic, and hydrophobic behavior and solubility. These kinds of polymers behave intelligently in varied applications such as in biomedical, micromechanical, biosensors, commodity, and packaging applications. The emerging interests in the stimuli-responsive polymers have endured since decades and an ample amount of work have been carried out to develop macromolecules to be crafted into smart materials. In the living cells, the macromolecules regulate their functions which respond to changes in environment locally and these biopolymers control all the major natural processes. The initial motive using such material was to develop biomaterials only for smart therapeutic delivery methods. Recently, many synthetic polymers have been explored that are responsive to various stimuli and can be considered as biomimetic leading to the development of smart applications in tissue engineering and wound healing applications. The responsive behavior to an external stimulus is a nonlinear behavior [44]. There are different aspects of stimuli such as to attune the response by integrating different responsive elements for the case of biodegradable macromolecules. Applications of these smart polymers in the targeted-delivery of therapeutics, tissue engineering, bio-separations and sensors have been studied diversely, and innumerable publications are evident in this area. Additionally, to achieve the macromolecular assemblies (combining two or more chemical, physical, biological stimuli-responsive materials) with stimuli-responsive characteristics, different controlled polymerization techniques have been reported such as reversible addition-fragmentation chain transfer polymerization (RAFT), atom transfer radical polymerization (ATRP), nitroxide-mediated radical polymerization (NMRP) and ring-opening metathesis polymerization (ROMP).

In the present days, researchers are exploring different stimulus like magnetic field, electric field, ultraviolet, pH, ultrasonication and chemical environment to enhance the development of suture-based stimuli-responsive materials. A schematic representation of the external stimulus affecting the properties of the polymers is shown in Fig. 4. The fabrication of such multi-stimuli-responsive polymers is synthetically challenging but is of active interest for their application in various biomedical fields [45]. The development of these kinds of materials to tune the properties of the end product can be helpful to fabricate custom-designed materials. The knowledge of structure-property relationship is necessary for further development and designing of new functional materials. Some of the stimuli components are highlighted below.

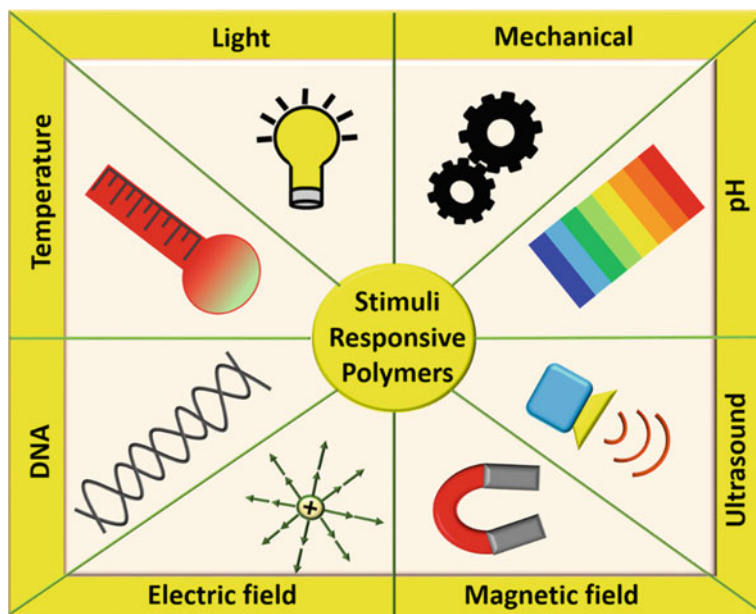


Fig. 4 Different external stimuli that affect the properties of the polymers

5.1 Magnetic Field Responsive Polymers

These kinds of polymer materials respond to the changes in the magnetic fields. These provide exciting applications in biomedical applications such as in controlled drug delivery. Based on the polymer matrix, magneto-active polymers can be divided into magneto-active elastomers and magneto-active gels. Magnetic field responsive materials can form different materials such as magnetic cellulose, magnetic hydroxyapatite, magnetic carbon fibers. Different types of direct and alternating fields are used based on the application of magnetic-based stimuli-responsive materials in cell adhesion, antimicrobial activity and drug delivery applications. De Santis et al. designed 3D PCL-magnetic HAP-based scaffolds that showed enhancement in cell growth and histocompatibility in both in vitro and in vivo studies [46]. The incorporation of magnetic material increased the cell population by 2.2 fold higher than normal PCL-based scaffold. Patwa et al. 2018 successfully synthesized Fe-doped crystalline silk nano-disks (CSNs) by co-precipitation method. The polylactide/CSNs scaffolds were prepared using electrospinning method. Under static magnetic field, this scaffold showed remarkable increase in cell growth of BHK-21 by 27% for aligned PLA composite and 40% for nonaligned PLA composite. In the presence of alternative field, magnetic materials generate heat which is called as 'hyperthermia' in order to control targeted release of drug and regulate antimicrobial activity. To obtain the desired temperature for hyperthermia effect which is 42 °C, the magnetic field frequency and strength were kept at 293 kHz and 12.57 kA/m respectively. The

drug-loaded composite scaffold showed 63% reduction in cell viability. In the post-hyperthermia effect, the cancer cells failed to resist higher temperature, resulting in reduced cell counts irrespective of the presence or absence of drug. Using magnetized CSNs disk in reinforced PLA-based scaffold, it showed cytocompatibility under magnetic effect which are capable of destroying cancer cells depicting hyperthermia [42]. In the similar fashion, Chertok et al. in the year 2008 used iron oxide nanoparticles for targeted drug delivery toward brain tumor under magnetic field [47]. Similarly, Fuchigami et al. in the year 2012 used porous iron/platinum capsules for targeted drug delivery for cancer therapy under the guidance of magnetic field [48].

5.2 *Electric Field Responsive Polymers*

These polymers that respond to the electric field and undergo change in their properties are termed as electric field responsive polymers. Such materials convert electrical energy into mechanical energy which are applicable in biomechanics, actuators, chemical separations and controlled drug delivery. The electric field can act as a stimulus for different biomedical applications like nerve regeneration, drug delivery. In the presence of electric field, there is a variant in cell growth from cathode to anode which can help in nerve regeneration where conductive composites and blends are utilized as nerve conduit. Jeong et al. in the year 2008 fabricated the blends of polyaniline (PANI)/poly(L-lactide-co- ϵ -caprolactone) PLCL doped with camphorsulfonic acid using electrospinning process. They found the conductivity value around 0.0138 S cm^{-1} for 30:70 v/v of the blend. There was a significant enhancement in the cell adhesion in the blends (PACL) than that in the neat PLCL fibers. These were considered as potential candidates for studying the effect of electric field to improve desirable cell activity for tissue engineering applications. These blends were also used for modeling of the system to study the effect of electric field on the mitochondrial activity of the NIH-3T3 cells. In case of higher loading, i.e., at 20 mA, the cell culture showed enhancement in the activity on the blends [49]. Wei et al. in the year 2007 fabricated electroactive polymer using aniline and oligopeptide. They used PC12 neuronal-like cell lines to check the neurotrophic cell growth and found significant cell adhesion and proliferation [50]. Huang et al. in the year 2008 synthesized multiblock copolymer using PLA and aniline pentamer by group-shielding approach and fabricated scaffold pertaining better mechanical strength, excellent electroactivity, and biodegradability. The copolymer showed improved cell adhesion and proliferation in the in vitro studies. Under the effect of electric field, the copolymer also showed enhancement in cell differentiation of rat neuronal pheochromocytoma PC12 cells. This copolymer possessed the properties in vivo as nerve regeneration scaffold materials in tissue engineering applications [51]. Similarly, Hu et al. in the year 2008 fabricated electrically active cell using chitosan and aniline pentamer [52]. In the similar way, Rivers et al. synthesized biodegradable,

conducting blend using pyrrole and thiophene via degradable polyester for tissue engineering application [53].

5.3 Temperature and pH Responsive Polymers

The thermal nature of the environment also acts as stimulus for some applications where polymer and composites are thermosensitive. The change in temperature alters the solubility of the components. It is specially observed for the colloid systems [54]. Peng et al. synthesized PEG-based random copolymer having thermosensitivity. Change in sol–gel behavior was reported at 25–39 °C from %T value because of lower critical solubility temperature change. Thermo-responsive gels and hydrogels incorporated with drug can be controlled by varying temperature. In some of the cases, activity of enzyme can be controlled by altering temperature. Shape memory polymers are also utilized as stimuli-responsive materials for fabrication of biomedical devices. Property of this kind of polymers also can be controlled by varying temperature [55].

Biodegradable polymer-based gel characteristics are based on the nature of the polymer, cross-linker as well as physical condition like pH and temperature. Marsano et al. showed that network formation between chitosan and polyvinylpyrrolidone is dependent on different pH condition. It swells around pH = 4, whereas shrinks at pH = 9 [56]. Dai et al. well described how pH can be used as stimulus for drug delivery in different gel, micelle and copolymer systems [57]. Yan et al. noticed that pH can alter surface wettability between oil to water for surface treated fabrics. Fabric showed super hydrophobicity at pH = 7, however, noticed to have hydrophilic nature at pH = 12 [58]. Efficiency of chitosan-based drug carrier under pH change also investigated by Hua et al. Chitosan-based conjugate graft copolymer was prepared in two steps. First chitosan–lilial conjugate was synthesized using DMF solvent and then graft polymerization was conducted with carboxyl terminated PNIPAM. It was observed that lilial was not released from chitosan core at neutral pH up to 72 h, whereas 70% of lilial was released after 30 h at 4.5 pH [59]. Zhang et al. 2007 investigated release behavior of anticancer drug Paclitaxel which is water insoluble in nature using P (N-isopropylacrylamide-co-acrylic acid) block and a biocompatible hydrophobic polycaprolactone (PCL) block polymer. Faster drug release was reported at higher temperature and lower pH [60].

5.4 Chemical Environment, Photo Effect, Sonication and Other Stimulus

Chemical environment of living system is different and based on the components as well as pH. This also can act as stimulus for targeted applications such as glucose-rich

condition can be treated using glucose oxidase-based conjugate systems. Glucose oxidase and polyacrylic acid-based hydrogels are found to be active and glucose responsive [61].

The activity of some of the polymers can be controlled by the enzymatic action. The blood clotting and hydrolysis of peptide have been investigated by different groups under different enzymatic conditions. Effect of protease enzyme on *E. coli* cells was investigated by Ulijin et al. by entrapping in a protein–gelatin mixture hydrogel. It was observed that transglutaminase enzymes are only active in the calcium ion's environment, and exposure to Ca^{2+} can also enhance enzymatic crosslinking [62]. Similarly, other chemical environments like antigen, thiol can act as stimulus for different targeted applications.

The photoresponsive polymers can vary their property when subjected to irradiation of light. This can control the efficiency of some of the biomedical applications like tissue engineering, protein bioactivity and drug delivery. Also, UV and near-infrared irradiations have been utilized to different drug delivery investigations by different groups.

Ultrasound also utilized as stimulus by different groups for controlled drug release studies. It gives local shock which can disrupt the shell of drug-loaded system and based on the amplitude, controlled release can be done.

Stimulus and Suture Application

Incorporation of stimuli-responsive ingredients in the form of biodegradable polymer or reinforcement for targeted environment application, suture is a lucrative area of research. Drug-coated suture can be applicable for both external healing and internal wound healing. Drug-loaded gels which are responsive to external stimulus can be utilized in order to control the release depending on the nature and location of wound. In the above-mentioned section, magnetic guidance of cell adhesion, hyperthermia controlled antibacterial, and drug delivery were discussed. The similar can be utilized for suture application which will serve both holding of stitches and control recovery based on application. Electro-spun fibers having conductive nature are utilized for nerve regeneration. These sutures also can serve the purpose for eye injury or any internal organ malfunction case. Orthopaedic application of suture has huge range of utilization of stimulus responsive suture. Bone growth, cell proliferation, biocompatibility, bioresorbability all can be controlled using suitable polymer-reinforcement composition under stimulus like pH, enzyme. Thus, control of behavior of biomedical application of suture has a huge importance for simplification and more effective medical treatment. Researchers across the world are investigating in various routes to fabricate smart suture or stimuli-responsive suture which are capable of addressing various wound healing issues based on the application and need.

6 Resorbable Sutures: In Vitro and In Vivo Studies

In vitro studies involve the examination of biological entities outside the living body, whereas the in vivo studies involve the examination of the entities within the living organisms and cells. Cell adhesion, cytotoxicity, bone regeneration, load bearing capacity under simulated body fluid, etc., are need to be studied for both in vitro and in vivo technique prior to implementation of any biomedical devices. The properties of suture also require in vivo and in vitro activity along with mechanical, surface property, etc. In the year 1992, Verheyen et al. fabricated PLLA/hydroxyapatite (HA) composites using in situ polycondensation of L-lactic acid in the presence of HA. The monomer to catalyst ratio was varied during the polycondensation. Tensile strength was 136.5 MPa in 600 M/I ratio and 30 wt% of HA. In vitro studies showed degradation in molecular weight with time in phosphate-buffered solution (PBS). In case of both in vitro and in vivo studies, all materials were found to retain their initial weight after six months [36].

Similarly, Kim et al. in the year 2006, fabricated poly(lactide-co-glycolide)/hydroxyapatite composite scaffold using gas foaming and particulate leaching (GF/PL) method. Commercial HAP was used for this particular work. PLGA/HAP/NaCl was mixed in a ratio of 1:1:9 loaded into a disk mold and compressed and exposed to high pressure CO₂ gas. NaCl was leached out using distilled water. In vivo analysis showed that HAP enhanced the cell growth and the GF/PL scaffold exhibited enhanced bone regeneration when compared to the SC/PL scaffold [63].

Okada et al. in the year 1990 reported in vivo and in vitro studies of the commercial suture. Collagen and pepsin were added to PBS solution for in vitro analysis. The results indicated the hydrolysis from surface of suture, wherein the fiber diameter decreased upon hydrolysis. The degradation of suture was found to accelerate in the presence of enzyme. In case of in vitro analysis, no cellular infiltration was noticed [64].

In the year 2007, Im et al. prepared poly(p-dioxanone) (PDO) and its copolymer by conjugate spinning method. The method used was conventional bulk ROP. The suture retained about 70 and 55% of its original linear tensile strength after two and four weeks of incubation. Strength retention percentage decreased with time in the in vivo degradation test. It was completely absorbed after 180–210 days of implantation, which was slightly faster than some of the commercially available PDO sutures [65].

Makela et al. [66] reported the in vitro study of the strong bio-absorbable self-reinforced/PLLA sutures (SR/PLLA) to investigate the mechanical properties in comparison with polyglyconate (Maxon[®]) and polydioxanone (PDS) sutures. PLLA was melt spun with die exit diameter of 1.5 mm and hot drawn with an oven temperature of 120 and 140 °C and drawing ratio of 7. The filament diameter was 0.3–0.7 mm which was found to increase with the density. The crystallinity of the suture was found to be 64–71%. The highest elongation found was ~62% for 0.3 and 0.5 mm sutures. The thicker sutures were found to fail at their knots [66].

Lee et al. prepared poly(lactic-co-glycolic acid) (PLGA) particles by loading dexamethasone (DEX, a model drug) using water–oil emulsion technique. They modified the surface of the DEX/PLGA particles using plasma treatment followed by dispersing in polyethyleneimine (PEI) to enhance its hydrophilicity. They used the absorbable braided suture (composition: 10% lactide, 90% glycolide) for immobilizing the PEI/DEX/PLGA particles onto the surface of the sutures to develop functional suture absorbable sutures [67]. The *in vitro* studies showed that the particles remained on the surface of the suture along with the sustained release of DEX during 4 weeks. They developed technique did not alter the mechanical properties of the suture. Thus, an indigenous strategy was developed to fabricate drug-eluting sutures which may be potential candidates for wound healing at the surgical sites along with anti-inflammatory response.

Being aware of the hydrolysis of the absorbable sutures resulting from the chain scission in the amorphous regions and hypothesizing that the rate of hydrolysis of suture would be directly dependent on the temperature, Cannizzo et al. evaluated the absorbable sutures, i.e., Monocryl and Maxon[®] used in fish surgery [68]. They maintained the sutures in the filtered water over a period of 8 weeks at 4, 25 and 37 °C temperature. In case of Monocryl, the tensile strength decreased after 2 weeks at 25 °C which was not the case at 4 °C. There was no decrease in tensile strength in case of Maxon[®] at 4 and 25 °C. Further, the Monocryl suture was found to disintegrate after 4 weeks at 37 °C and the tensile strength of Maxon[®] was decreased over a period of 6 weeks. It was concluded that the tensile strength of absorbable sutures was found to reduce slowly at ambient temperature as compared to that of the body temperature. Thus, such sutures when used for the fish surgery would be retained for a longer duration as the fishes usually reside in the water below 25 °C.

7 Future Perspectives

The utilization of novel resorbable copolymers and composite systems has a noteworthy development in various biomedical fields; however, the study of such materials needs to be extensively carried out for the development of sutures for targeted surgical sites. Different stimuli like magnetic, electric field, pH are found to govern the properties of biomaterials for drug delivery, cell adhesion, nerve regeneration applications which can be implemented by fabricating stimuli-responsive sutures. The drug-loaded gels and hydrogels can be used as a novel coating for synthetic- and natural-based sutures for wound healing, antimicrobial activity and drug delivery. Thus, the fabrication of stimuli-responsive polymers and composites can address both the mechanical support for wound healing as well can effectively serve for the recovery of wound under controlled conditions. The use of novel biodegradable polymer, protein, peptide in combination with different nanomaterial under various stimuli may also be explored and novel formulations may be developed for the targeted wound healing supported by essential *in vitro* and *in vivo* studies.

References

1. Hayashi T (1994) Biodegradable polymers for biomedical uses. *Prog Polym Sci* 19(4):663–702. [https://doi.org/10.1016/0079-6700\(94\)90030-2](https://doi.org/10.1016/0079-6700(94)90030-2)
2. Törmälä P, Pohjonen T, Rokkanen P (1998) Bioabsorbable polymers: materials technology and surgical applications. *Proc Inst Mech Eng H* 212(2):101–111. <https://doi.org/10.1243/0954411981533872>
3. Pillai CKS, Sharma CP (2010) Absorbable polymeric surgical sutures: chemistry, production, properties, biodegradability, and performance. *J Biomater Appl* 25(4):291–366. <https://doi.org/10.1177/0885328210384890>
4. Chu CC, Von Fraunhofer JA, Greisler HP (1996) Wound closure biomaterials and devices. CRC Press, Boca Raton
5. Moy RL, Waldman B, Hein DW (1992) A review of sutures and suturing techniques. *J Dermatol Surg Oncol* 18(9):785–795. <https://doi.org/10.1111/j.1524-4725.1992.tb03036.x>
6. Dennis C, Sethu S, Nayak S, Mohan L, Morsi Y, Manivasagam G (2016) Suture materials—current and emerging trends. *J Biomed Mater Res A* 104(6):1544–1559. <https://doi.org/10.1002/jbm.a.35683>
7. Roberts ADG, Hart DM (1983) Polyglycolic acid and catgut sutures, with and without oral proteolytic enzymes, in the healing of episiotomies. *BJOG* 90(7):650–653. <https://doi.org/10.1111/j.1471-0528.1983.tb09284.x>
8. Singhal JP, Singh H, Ray AR (1988) Absorbable suture materials: preparation and properties. *Polym Rev* 28(3–4):475–502. <https://doi.org/10.1080/15583728808085383>
9. Li J, Yuan XY (2006) Research progresses on synthetic absorbable sutures. *J Tianjin Polytech Univ* 25:18–21
10. Hon LQ, Ganeshan A, Thomas SM, Warakaulle D, Jagdish J, Uberoi R (2009) Vascular closure devices: a comparative overview. *Curr Probl Diagn Radiol* 38(1): 33–43. <https://doi.org/10.1067/j.cpradiol.2008.02.002>
11. Eling B, Gogolewski S, Pennings AJ (1982). Biodegradable materials of poly(L-lactic acid): 1. Melt-spun and solution-spun fibres. *Polymer* 23(11):1587–1593. [https://doi.org/10.1016/0032-3861\(82\)90176-8](https://doi.org/10.1016/0032-3861(82)90176-8)
12. Dunn DL (2005) Wound closer manual. Ethicon, Inc., Johnson and Johnson Company
13. Stibal W, Schwarz R, Kemp U, Bender K, Weger F, Stein M (2000) Fibers 3. General production technology, Ullmann's encyclopedia of industrial chemistry
14. Eling B, Gogolewski S, Pennings AJ (1982) Biodegradable materials of poly (l-lactic acid): 1. Melt-spun and solution-spun fibres. *Polymer* 23(11):1587–1593. [https://doi.org/10.1016/0032-3861\(82\),90176-8](https://doi.org/10.1016/0032-3861(82),90176-8)
15. Charuchinda A, Molloy R, Siripitayananon J, Molloy N, Sriyai M (2003) Factors influencing the small-scale melt spinning of poly (ϵ -caprolactone) monofilament fibres. *Polym Int* 52(7):1175–1181. <https://doi.org/10.1002/pi.1234>
16. Ziabicki A (1976) Fundamentals of fibre formation. Wiley-Interscience, New York
17. Gupta B, Revagade N, Hilborn J (2007) Poly (lactic acid) fiber: an overview. *ProgPolymSci* 32(4):455–482. <https://doi.org/10.1016/j.progpolymsci.2007.01.005>
18. Gogolewski S, Pennings AJ (1985) High-modulus fibres of nylon-6 prepared by a dry-spinning method. *Polymer* 26(9):1394–1400. [https://doi.org/10.1016/0032-386\(85\)90317-9](https://doi.org/10.1016/0032-386(85)90317-9)
19. Leenslag JW, Pennings AJ (1987) High-strength poly (l-lactide) fibres by a dry-spinning/hot-drawing process. *Polymer* 28(10):1695–1702. [https://doi.org/10.1016/0032-3861\(87\),90012-7](https://doi.org/10.1016/0032-3861(87),90012-7)
20. Greiner A, Wendorff JH (2007) Electrospinning: a fascinating method for the preparation of ultrathin fibers. *Angew Chemi Int Ed* 46(30):5670–5703. <https://doi.org/10.1002/anie.200604646>
21. Um IC, Ki CS, Kweon H, Lee KG, Ihm DW, Park YH (2004) Wet spinning of silk polymer: II. Effect of drawing on the structural characteristics and properties of filament. *Int J Biol Macromol* 34(1–2): 107–119. <https://doi.org/10.1016/j.ijbiomac.2004.03.011>

22. Hu X, Liu S, Zhou G, Huang Y, Xie Z, Jing X (2014) Electrospinning of polymeric nanofibers for drug delivery applications. *J Control Release* 185:12–21. <https://doi.org/10.1016/j.jconrel.2014.04.018>
23. Matthews JA, Wnek GE, Simpson DG, Bowlin GL (2002) Electrospinning of collagen nanofibers. *Biomacromol* 3(2):232–238. <https://doi.org/10.1021/bm015533u>
24. Mohanty AK, Misra M, Hinrichsen GI (2000) Biofibres, biodegradable polymers and biocomposites: an overview. *Macromol Mater Eng* 276(1):1–24. [https://doi.org/10.1002/\(SICI\)1439-2054\(20000301\)276:1%3C1:A](https://doi.org/10.1002/(SICI)1439-2054(20000301)276:1%3C1:A)
25. Kyrikou I, Briassoulis D (2007) Biodegradation of agricultural plastic films: a critical review. *J Polym Environ* 15(2):125–150. <https://doi.org/10.1007/s10924-007-0063-6>
26. Amass W, Amass A, Tighe B (1998) A review of biodegradable polymers: uses, current developments in the synthesis and characterization of biodegradable polyesters, blends of biodegradable polymers and recent advances in biodegradation studies. *Polym Int* 47(2):89–144. [https://doi.org/10.1002/\(SICI\)1097-0126\(199810\)47:2%3C89:AID-PI86%3E3.0.CO;2-F](https://doi.org/10.1002/(SICI)1097-0126(199810)47:2%3C89:AID-PI86%3E3.0.CO;2-F)
27. Charnley J (1960) Anchorage of the femoral head prosthesis to the shaft of the femur. *J Bone Joint Surg. British* 42(1):28–30
28. Kalia S, Dufresne A, Cherian B M, Kaith BS, Avérous L, Njuguna J, Nassiopoulos E (2011) Cellulose-based bio-and nanocomposites: a review. *Int J Polym Sci* 1–35. <https://doi.org/10.1155/2011/837875>
29. Benicewicz BC, Hopper PK (1991) Polymers for absorbable surgical sutures—Part II. *J Bioact Compat Polym* 6:64–94. <https://doi.org/10.1177/088391159100600106>
30. Chen FM, Liu X (2016) Advancing biomaterials of human origin for tissue engineering. *Prog Polym Sci* 53:86–168. <https://doi.org/10.1016/j.progpolymsci.2015.02.004>
31. Bennett RG (1988) Selection of wound closure materials. *J Am Acad Dermatol* 18(4):619–637. [https://doi.org/10.1016/S0190-9622\(88\)70083-3](https://doi.org/10.1016/S0190-9622(88)70083-3)
32. B Kim, Atala A (2001) *Encyclopedia of materials: science and technology*
33. Song R, Murphy M, Li C, Ting K, Soo C, Zheng Z (2018) Current development of biodegradable polymeric materials for biomedical applications. *Drug Des Dev Ther* 12:3117–3145. <https://doi.org/10.2147/DDDT.S165440>
34. Palmer LC, Newcomb CJ, Kaltz SR, Spoerke ED, Stupp SI (2008) Biomimetic systems for hydroxyapatite mineralization inspired by bone and enamel. *Chem Rev* 108(11):4754–4783. <https://doi.org/10.1021/cr8004422>
35. Siddiqui H, Pickering K, Mucalo M (2018) A review on the use of hydroxyapatite-carbonaceous structure composites in bone replacement materials for strengthening purposes. *Materials* 11(10):1813. <https://doi.org/10.3390/ma11101813>
36. Verheyen CCPM, De Wijn JR, Van Blitterswijk CA, De Groot K (1992) Evaluation of hydroxylapatite/poly(l-lactide) composites: mechanical behavior. *J Biomed Mater Res* 26(10):1277–1296. <https://doi.org/10.1002/jbm.820261003>
37. Saifuddin N, Raziah AZ, Junizah AR (2012) Carbon nanotubes: a review on structure and their interaction with proteins. *J Chem* 2013:1–18. <https://doi.org/10.1155/2013/676815>
38. Cheng Q, Rutledge K, Jabbarzadeh E (2013) Carbon nanotube–poly (lactide-co-glycolide) composite scaffolds for bone tissue engineering applications. *Ann Biomed Eng* 41(5):904–916. <https://doi.org/10.1007/s10439-012-0728-8>
39. Pan L, Pei X, He R, Wan Q, Wang J (2012) Multiwall carbon nanotubes/polycaprolactone composites for bone tissue engineering application. *Colloids Surf B* 93:226–234. <https://doi.org/10.1016/j.colsurfb.2012.01.011>
40. Kashiwazaki H, Kishiya Y, Matsuda A, Yamaguchi K, Iizuka T, Tanaka J, Inoue N (2009) Fabrication of porous chitosan/hydroxyapatite nanocomposites: their mechanical and biological properties. *Biomater Eng* 19(2–3):133–140. <https://doi.org/10.3233/BME-2009-0572>
41. Gupta A, Katiyar V (2017) Cellulose functionalized high molecular weight stereocomplex polylactic acid biocomposite films with improved gas barrier, thermomechanical properties. *ACS Sustain Chem Eng* 5(8):6835–6844. <https://doi.org/10.1021/acssuschemeng.7b01059>
42. Patwa R, Kumar A, Katiyar V (2018) Crystallization kinetics, morphology, and hydrolytic degradation of novel bio-based poly (lactic acid)/crystalline silk nano-discs nanobiocomposites. *J Appl Polym Sci* 135(33):46590. <https://doi.org/10.1002/app.46590>

43. De Simone S, Gallo AL, Paladini F, Sannino A, Pollini M (2014) Development of silver nano-coatings on silk sutures as a novel approach against surgical infections. *J Mater Sci Mater Med* 25(9):2205–2214. <https://doi.org/10.1007/s10856-014-5262-9>
44. Galaev IY, Mattiasson B (1999) ‘Smart’ polymers and what they could do in biotechnology and medicine. *Trends Biotechnol* 17(8):335–340. [https://doi.org/10.1016/S0167-7799\(99\)01345-1](https://doi.org/10.1016/S0167-7799(99)01345-1)
45. De las Heras Alarcón C, Pennadam S, Alexander C (2005) Stimuli responsive polymers for biomedical applications. *Chem Soc Rev* 34(3):276–285. <https://doi.org/10.1039/b406727d>
46. De Santis R, Russo A, Gloria A, D’Amora U, Russo T, Panseri S, Wilde CJ (2015) Towards the design of 3D fiber-deposited poly (-caprolactone)/iron-doped hydroxyapatite nanocomposite magnetic scaffolds for bone regeneration. *J Biomed Nanotechnol* 11(7):1236–1246. <https://doi.org/10.1166/jbn.2015.2065>
47. Chertok B, Moffat BA, David AE, Yu F, Bergemann C, Ross BD, Yang VC (2008) Iron oxide nanoparticles as a drug delivery vehicle for MRI monitored magnetic targeting of brain tumors. *Biomaterials* 29(4):487–496. <https://doi.org/10.1016/j.biomaterials.2007.08.050>
48. Fuchigami T, Kawamura R, Kitamoto Y, Nakagawa M, Namiki Y (2012) A magnetically guided anti-cancer drug delivery system using porous FePt capsules. *Biomaterials* 33(5):1682–1687. <https://doi.org/10.1016/j.biomaterials.2011.11.016>
49. Jeong SI, Jun ID, Choi MJ, Nho YC, Lee YM, Shin H (2008) Development of electroactive and elastic nanofibers that contain polyaniline and poly(L-lactide-co-ε-caprolactone) for the control of cell adhesion. *Macromol Biosci* 8(7):627–637. <https://doi.org/10.1002/mabi.200800005>
50. Guo Y, Li M, Mylonakis A, Han J, MacDiarmid AG, Chen X, Wei Y (2007) Electroactive oligoaniline-containing self-assembled monolayers for tissue engineering applications. *Biomacromol* 8(10):3025–3034. <https://doi.org/10.1021/bm070266z>
51. Huang L, Zhuang X, Hu J, Lang L, Zhang P, Wang Y, Jing X (2008) Synthesis of biodegradable and electroactive multiblock polylactide and aniline pentamer copolymer for tissue engineering applications. *Biomacromol* 9(3):850–858. <https://doi.org/10.1021/bm7011828>
52. Hu J, Huang L, Zhuang X, Zhang P, Lang L, Chen X, Jing X (2008) Electroactive aniline pentamer cross-linking chitosan for stimulation growth of electrically sensitive cells. *Biomacromol* 9(10):2637–2644. <https://doi.org/10.1021/bm800705t>
53. Rivers TJ, Hudson TW, Schmidt CE (2002) Synthesis of a novel, biodegradable electrically conducting polymer for biomedical applications. *Adv Funct Mater* 12(1):33–37. [https://doi.org/10.1002/1616-3028\(20020101\)12:1%3C33::AID-ADFM33%3E3.0.CO;2-E](https://doi.org/10.1002/1616-3028(20020101)12:1%3C33::AID-ADFM33%3E3.0.CO;2-E)
54. Hirokawa Y, Tanaka T (1984) Volume phase transition in a non-ionic gel. *AIP Conf Proc* 107(1):203–208. <https://doi.org/10.1063/1.34300>
55. Peng B, Grishkewich N, Yao Z, Han X, Liu H, Tam KC (2012) Self-assembly behavior of thermoresponsive oligo (ethylene glycol) methacrylates random copolymer. *ACS Macro Lett* 1(5):632–635. <https://doi.org/10.1021/mz300135x>
56. Marsano E, Bianchi E, Vicini S, Compagnino L, Sionkowska A, Skopińska J, Wiśniewski M (2005) Stimuli responsive gels based on interpenetrating network of chitosan and poly (vinylpyrrolidone). *Polymer* 46(5):1595–1600. <https://doi.org/10.1016/j.polymer.2004.12.017>
57. Dai S, Ravi P, Tam KC (2008) pH-responsive polymers: synthesis, properties and applications. *Soft Matter* 4(3):435–449. <https://doi.org/10.1039/B714741D>
58. Yan T, Chen X, Zhang T, Yu J, Jiang X, Hu W, Jiao F (2018) A magnetic pH-induced textile fabric with switchable wettability for intelligent oil/water separation. *Chem Eng J* 347:52–63. <https://doi.org/10.1016/j.cej.2018.04.021>
59. Hua D, Jiang J, Kuang L, Jiang J, Zheng W, Liang H (2011) Smart chitosan-based stimuli-responsive nanocarriers for the controlled delivery of hydrophobic pharmaceuticals. *Macromolecules* 44(6):1298–1302. <https://doi.org/10.1021/ma102568p>
60. Zhang L, Guo R, Yang M, Jiang X, Liu B (2007) Thermo and pH dual-responsive nanoparticles for anti-cancer drug delivery. *Adv Mater* 19(19):2988–2992. <https://doi.org/10.1002/adma.200601817>
61. Roy D, Cambre JN, Sumerlin BS (2010) Future perspectives and recent advances in stimuli-responsive materials. *Prog Polym Sci* 35(1–2):278–301. <https://doi.org/10.1016/j.progpolymsci.2009.10.008>

62. Toledano S, Williams RJ, Jayawarna V, Ulijn RV (2006) Enzyme-triggered self-assembly of peptide hydrogels via reversed hydrolysis. *J Am Chem Soc* 128(4):1070–1071. <https://doi.org/10.1021/ja056549l>
63. Kim SS, Park MS, Jeon O, Choi CY, Kim BS (2006) Poly (lactide-co-glycolide)/hydroxyapatite composite scaffolds for bone tissue engineering. *Biomaterials* 27(8):1399–1409. <https://doi.org/10.1016/j.biomaterials.2005.08.016>
64. Okada T, Hayashi T, Ikada Y (1992) Degradation of collagen suture in vitro and in vivo. *Biomaterials* 13(7):448–454. [https://doi.org/10.1016/0142-9612\(92\)90165-K](https://doi.org/10.1016/0142-9612(92)90165-K)
65. Im JN, Kim JK, Kim HK, In CH, Lee KY, Park WH (2007) In vitro and in vivo degradation behaviors of synthetic absorbable bicomponent monofilament suture prepared with poly (p-dioxanone) and its copolymer. *Polym Degrad Stab* 92(4):667–674. <https://doi.org/10.1016/j.polymdegradstab.2006.12.011>
66. Mäkelä P, Pohjonen T, Törmälä P, Waris T, Ashammakhi N (2002) Strength retention properties of self-reinforced poly l-lactide (SR-PLLA) sutures compared with polyglyconate (Maxon®) and polydioxanone (PDS) sutures. An in vitro study. *Biomaterials* 23(12):2587–2592. [https://doi.org/10.1016/S0142-9612\(01\)00396-9](https://doi.org/10.1016/S0142-9612(01)00396-9)
67. Lee DH, Kwon TY, Kim KH, Kwon ST, Cho DH, Jang SH, Son JS, Lee KB (2014) Anti-inflammatory drug releasing absorbable surgical sutures using poly (lactic-co-glycolic acid) particle carriers. *Polym Bull* 71(8):1933–1946. <https://doi.org/10.1007/s00289-014-1164-8>
68. Cannizzo SA, Roe SC, Harms CA, Stoskopf MK (2016) Effect of water temperature on the hydrolysis of two absorbable sutures used in fish surgery. *Facets* 1(1):44–54. <https://doi.org/10.1139/facets-2016-0006>

Chapter 7

Biocompatible Thermoresponsive Polymers: Property and Synthesis



Varnakumar Gayathri, Nagaraju Pentela and Debasis Samanta

Abstract Thermoresponsive polymers are responsive to slight changes in temperatures. In many cases, particularly with *N*-isopropylacrylamide group as repeating unit, the temperature at which the change takes place falls in physiological range. Hence, such polymers can be used for biological applications, even though biocompatibility is major issue in many cases. There is no universal solution to this; however, copolymerization is one strategy to address the issue. Choice of polymerization process also emerges as critical standpoint in several cases. In this chapter, such issues have been discussed with special emphasis on lower critical solution temperature (LCST) of most polymers. In certain cases, polymers with upper critical solution temperature (UCST) have been described briefly. Finally, the description along with schematic representation of preparation of various biocompatible thermoresponsive polymers using various controlled living radical polymerization techniques has been presented with references (total 86 references).

Keywords Thermoresponsive · Biocompatible · RAFT · ATRP polymers

Abbreviations

PVCa	poly(<i>n</i> -vinyl caprolactam)
PMVE	poly(methyl vinyl ether)
PEtOx	poly(<i>n</i> -ethyl oxazoline)
CLRP	controlled living radical polymerization
ATRP	atom transfer radical polymerization
RAFT	reversible addition-fragmentation chain transfer polymerization
NMP	nitroxide mediated polymerization

V. Gayathri · N. Pentela · D. Samanta (✉)

Polymer Science and Technology Department, CSIR-Central Leather Research Institute, Chennai, India

e-mail: debasis@clri.res.in

© Springer Nature Singapore Pte Ltd. 2020

V. Katiyar et al. (eds.), *Advances in Sustainable Polymers*, Materials Horizons: From Nature to Nanomaterials, https://doi.org/10.1007/978-981-15-1251-3_7

145

LCST	lower critical solution temperature
UCST	upper critical solution temperature
PDI	polydispersity index
NIPAM/NIPAAm/NIPAm/NIPAAM	N-isopropylacrylamide
PNIPAM/PNIPAAm/ PNIPAm/PNIPAAM	poly(n-isopropylacrylamide)
PLL	poly(l-lysine)
VP	vinyl pyridine
PAM	polyacrylamide
PHB	poly[(r)-3-hydroxybutyrate]
HMTETA	hexamethyltriethylenetetramine
PS	polystyrene
EBiB	ethyl 2-bromoisobutyrate
DCM	dichloromethane
DMF	n,n-dimethylformamide
PEG	polyethylene glycol
PCL	polycaprolactone
PCLDMA	polycaprolactonedimethacrylate
Me ₆ TREN	tris [2-(dimethylamino)ethyl]amine
DMSO	dimethyl sulfoxide
PPO	poly(propylene oxide)
MPC	2-methacryloyloxyethyl phosphorylcholine
PMPC	poly(2-methacryloyloxyethyl phosphorylcholine)
bpy	2,2'-bipyridine
Me ₄ Cyclam	1,4,8,11-tetramethyl-1,4,8,11- tetraazacyclotetradecane
TsOH	ρ-toluenesulfonic acid
DEA	2-(1,3-dioxan-2-yloxy)ethyl acrylate
DMDEA	2-(5,5-dimethyl-1,3-dioxan-2-yloxy) ethyl acrylate
OEGA	oligo(ethylene glycol) acrylate
DE-ATRP	deactivation enhanced atom transfer radical polymerization
PEGMEMA	poly(ethylene glycol) methyl ether methacrylate
PPGMA	poly(propylene glycol) methacrylate
EGDMA	ethylene glycol dimethacrylate
poly(A-Pro-OMe)	poly(n-acryloyl-l-prolinemethylester)
BDB	benzyl dithiobenzoate
CTA	chain transfer agent
DMA	n,n-dimethylacrylamide
AIBN	azobisisobutyronitrile
ADMO	(n-acryloyl-2,2-dimethyl-1,3- oxazolidine)

PADMO	poly(n-acryloyl-2,2-dimethyl-1,3-oxazolidine)
HEMA	2-hydroxyethyl methacrylate
BSPA	benzylsulfanylthiocarbonylsulfanyl propionic acid
PAGA	poly(acryloyl glucosamine)
EIPPMMA	4-(1-ethyl-1H-imidazo[4,5-f][1,10]phenanthroline-2-yl) phenyl methacrylate]
PVPhol	poly(vinylphenol)
FITC	fluorescein isothiocyanate
PDS	pyridylsulfide
DTT	dithiothreitol
OEG	oligoethyleneglycol
VCL	vinylcaprolactam
AA	acrylic acid
DODAB	dimethyldioctadecylammonium bromide
DBTTC	dibenzyltrithiocarbonate
EGDMA	ethyleneglycoldimethacrylate
MBA	N,N'-methylenebisacrylamide
PHMPA	poly((n-2-hydroxypropyl)-methacrylamide)
P(OEG-A)	poly(oligoethylene glycol methyl ether acrylate)
P(OEG-MA)	poly-(oligoethylene glycol methyl ether methacrylate)
CDTB	cyanopentanoic acid dithiobenzoate
BSPA	3-(benzyl sulfanylthio carbonylsulfanyl)-propionic acid
CDB	cumyldithiobenzoate
PPEGMAxTTC	poly[poly(ethylene glycol) methyl ether methacrylate]-trithiocarbonate
DT	dithioester
MEO ₂ MA	poly(2-(2-methoxyethoxy)ethyl methacrylate)
PVPip	poly(n-vinylpiperidone)
VAc	vinylacetate
LDH	lactate dehydrogenase
PNASME	poly(n-acryloylsarcosine methyl ester)
C ₂ NVP	3-ethyl-1-vinyl-2-pyrrolidone
NVP	n-vinylpyrrolidone
MHEX	s-(1-methyl-4-hydroxyethyl acetate) o-ethyl xanthate

Mw	molecular weight
MADIX	Macromolecular design by interchange of xanthate
MeO ₂ VAc	oligo (ethylene glycol) vinyl acetate
ABCN	1,1'-azobis-(cyclohexanocarbonitrile)
BMDO	5,6-benzo-2-methylene-1,3-dioxepane
MDO	2-methylene-1,3-dioxepane
TEMPO	(2,2,6,6-tetramethylpiperidin-1-yl)oxidanyl
MePEGMA	poly(ethylene glycol) methyl ether methacrylate
AN	acrylonitrile
HEA	2-hydroxyethyl acrylate
FRP	free radical polymerization
DEGEA	diethylene glycol ethyl ether acrylate
DHHA/PDHHA	dihydroxyhexyl acrylate/poly(dihydroxyhexyl acrylate)
MA	methyl acrylate
OEGMA	oligo(ethylene glycol) methyl ether methacrylate
POEGMA	poly[oligo(ethylene glycol) methyl ether methacrylate]
OEGMEAs	oligo(ethylene glycol) methyl ether amines
CPADB	4-cyano-4-((phenylcarbonothioyl)thio)pentanoic acid
PFP(M)A	pentafluorophenyl(meth)acrylate
PFFA	pentafluorophenyl acrylate
MEO ₂ MAM	diethylene glycol methacrylamide
MEO ₂ AM	diethylene glycol acrylamide
mPEG	methoxy poly(ethylene glycol)
AAM/AM	acrylamide
APEG	α -acryloyl- ω -methoxypoly(ethyleneglycol)
CMC	critical micelle concentration
DOX	doxorubicin
PVP	polyvinylpyrrolidone
CMPC	cyanomethyl methyl(4-pyridyl)carbamodithioate
LbL	layer by layer
OEtOxA	oligo(2-ethyl-2-oxazoline)acrylate
TA	tannic acid

CROP	cationic ring-opening polymerization
P[VBTP][Cl]	poly(triphenyl-4-vinylbenzylphosphonium chloride)
P[VBuIm][Br]	poly(3- <i>n</i> -butyl-1-vinylimidazolium bromide)
P2VP	poly(2-vinylpyridine)
PHEA	poly(2-hydroxyethyl acrylate)
PEA	poly(ethyl acrylate)
PEGMA	poly(ethylene glycol) methacrylate
Hex	Hexylamine

1 Introduction

Responsive polymers or smart polymers are categorized under the class of “smart materials” which undergo unique reversible changes/transitions with respect to chemical, physical, or biological external stimuli. Conventional external stimuli associated with responsive polymers are temperature, electromagnetic radiation, electric field, ionic strength, mechanical stress, pH, chemical agents, enzyme substrates, etc. The reversible changes associated with the physical or chemical external stimuli may cause change in conformation, shape, hydrophilic–hydrophobic behavior in aqueous medium, solubility, and molecular assembly [1]. These reversible changes arise as a consequence of involvements of secondary forces like hydrogen bonding and hydrophobic interactions between polymer moiety and solvent, van der Waals forces, and electrostatic interaction [2, 3]. Responsive polymers can further be distinguished based on the external stimuli, and it can restrict to a single stimulus or more than one stimulus to acquire desirable properties. Exterior to different responsive polymers, thermoresponsive polymers have been extensively studied which can be elucidated as smart polymers which experience volume phase transition in aqueous medium at a definite temperature to emerge a change in solubility. Thermoresponsive polymers can be segregated into two different categories according to critical parameters such as lower critical solution temperature (LCST) and upper critical solution temperature (UCST) (shown in Fig. 1 [4, 5]).

Polymeric systems associated with LCST (Fig. 2) undergo coil-to-globule transition as results of phase separation from hydrophilic to hydrophobic at LCST in aqueous medium. The driving force for any polymeric system to show phase separation at LCST is enthalpy (ΔH) and entropy (ΔS). Below the LCST, the interactions between hydrophilic moiety of a polymeric system and water molecule result in negative enthalpy and negative entropy which is vital for a given system to be miscible in a given solvent. So below the LCST, these polymers will form a hydrogen bond with the water molecule to provoke complete solubility in water medium. Above the LCST, an elevation in entropy is caused which stimulates the breaking of hydrogen

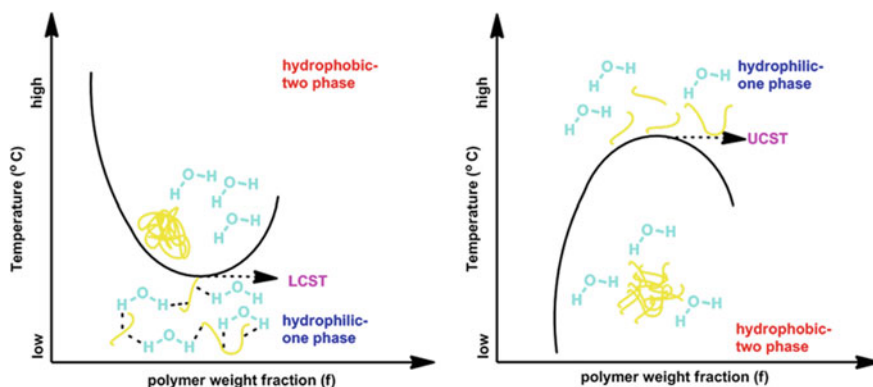


Fig. 1 Phase diagrams of thermoresponsive polymers with LCST and UCST property [1]

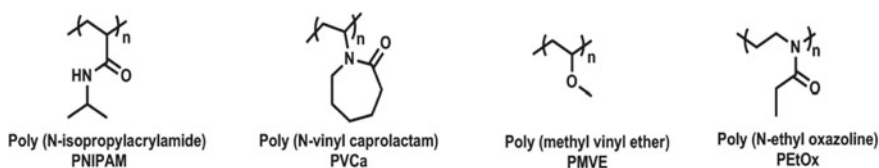


Fig. 2 Examples of thermoresponsive polymers

bond and increases the interaction between hydrophobic groups within the polymeric system causing the phase separation in aqueous medium [1, 4, 6]. The perfect balance between hydrophobic and hydrophilic moieties within the polymeric system provides LCST nature for these responsive polymers. Thus by disturbing the balance between hydrophilic–hydrophobic moieties, LCST of the responsive polymers can be altered. Addition of copolymer will affect the interactions of hydrophilic moiety with water molecule, and interaction between the hydrophobic groups within polymeric system will result in altering of LCST property [7–9]. In polymeric systems, the ability of the hydrophilic unit to form hydrogen bond with the water molecule is increased during the addition of hydrophilic copolymer which leads to an elevation in LCST. Similarly, addition of hydrophobic copolymer restricts the arrangement of water molecule near to polymeric system and facilitates the hydrophobic interactions within the polymer to cause aggregation of polymer above LCST [10]. On the other hand, some polymeric systems exhibit different types of thermoresponsive behavior than that of LCST-based polymers. Those polymers will exist as two phases (insoluble) below the critical solution temperature, whereas above the critical solution temperature they will exist as a single phase (soluble) in a solvent. Such polymeric systems are classified as upper critical solution temperature (UCST)-based polymers. In the case of polymeric systems with UCST behavior, the driving forces which bring about phase separation are positive entropy and enthalpy below the UCST and negative entropy and enthalpy above the UCST. As a result below the UCST, the polymer

is insoluble in water medium and above the UCST it is soluble [1]. In order to show UCST behavior in aqueous medium, the moieties within the polymeric system should have strong interactions (polymer–polymer interaction) than the interaction between water and polymer at lower temperature [11]. In addition to that, polymers can be made to show UCST behavior by increasing the interactions between polymer moieties; Plamper et al. reported that in the presence of trivalent counterion LCST-based polymer poly(*N,N*-dimethylaminoethyl methacrylate) showed UCST behavior in aqueous medium due to the increased polymer–polymer interactions [12]. Because of the unique phase separation behavior, responsive polymers are widely used in many fields of research as a catalyst, sensors, drug delivering systems, and diagnostics. The vital criteria for any system to be used as a drug or as a drug carrier are water solubility, nontoxicity, biocompatibility, and biodegradability. However, being nonbiodegradable/nonbiocompatible had restricted the wide range of usages of responsive polymers in biomedical applications. Attaining biocompatibility/biodegradability and tuning of LCST/UCST point is crucial for adapting thermoresponsive polymers as a tool in biomedical field. Thus, biocompatible thermoresponsive polymers are mainly prepared by various controlled radical polymerization techniques like atom transfer radical polymerization (ATRP), reversible addition–fragmentation chain transfer (RAFT) polymerization, and nitroxide-mediated polymerization (NMP) to get polymers with suitable end group for easy copolymerization, desired molecular weight, low polydispersity index (PDI). For example, Cheng we et al. reported PNIPAM-g-poly(amino ester)s which showed LCST behavior similar to that of PNIPAM. In this copolymer, PNIPAM provided suitable LCST behavior and poly(amino ester)s moiety provided biodegradability along with pH-responsive nature [13].

2 Selected Thermoresponsive Polymers and Their Behavior

2.1 Poly(*N*-Alkylacrylamide)

List of commonly available poly(*N*-alkylacrylamide)-based thermoresponsive polymers is given in Table 1. Out of several poly(*N*-alkylacrylamide)-based polymers, poly(*N*-Isopropylacrylamide) (PNIPAM) is extensively studied thermoresponsive polymer to display sharp LCST at 33 °C which closely resembles with biological body temperature and room temperature [4, 14] and hence can be used for applications like drug delivery [15, 16]. Secondary force which plays a vital role during phase separation of PNIPAM-based polymer is “hydrogen bonding.” Phase transition of PNIPAM at LCST occurs due to the intramolecular coil collapsing resulting from the breaking of hydrogen bond followed by intermolecular aggregation of a collapsed molecule to form globular form [17]. During the phase transition of PNIPAM from coil to globule, four thermodynamically stable states such as coil, crumbled coil, molten globule, and completely collapsed globule (with ~60% of water in its hydrodynamic volume) were reported by Wang et al. He also stated that LCST of PNIPAM was elevated by

Table 1 Common poly(*N*-alkylacrylamide)-based thermoresponsive polymers [1]

Poly(<i>N</i> -alkylacrylamide)-based thermoresponsive polymers		
S. no.	Polymer	LCST point (°C)
1.	Poly(alkylacrylamide)	–
2.	Poly(<i>N</i> -isopropylacrylamide)	33
3.	Poly(<i>N</i> -cyclopropylacrylamide)	47
4.	Poly(<i>N,N</i> -diethylacrylamide)	33
5.	Poly(<i>N</i> -ethylacrylamide)	82
6.	Poly(<i>N</i> -propylacrylamide)	22
7.	Poly(<i>N</i> -methylacrylamide)	–

1–2 K while replacing water by deuterated water [18]. The presence of alkyl group in poly(*N*-alkylacrylamide) has a high influence on the existence of LCST property. As the number of carbon or alkyl groups on *N*-substitution increases, the interaction between hydrophobic groups within the polymeric system increases which in turn results in decreasing LCST of poly(*N*-alkylacrylamide)-based polymers [19]. In the case of poly(*N*-acrylamides) where alkyl group is hydrogen, the thermoresponsive property itself is lost as a consequence of unbalancing between hydrophilic and hydrophobic groups in polymeric system, whereas for PNIPAM, the presence of isopropyl group provides phase separation property to this polymeric system by forming hydrogen bond with water molecule below the LCST and loss of hydrogen bond above the LCST [20]. Even though numerous poly(*N*-alkylacrylamide)-based responsive polymers are available, LCST behavior at high temperature (>50 °C) has limited the use of such responsive polymers. While in the case of poly(*N,N'*-diethylacrylamide), despite having LCST at ambient temperature, its dependence on the tacticity of the polymeric system has limited its usages [21], whereas PNIPAM has a sharp LCST at 33 °C which is nearly independent of molecular weight, chain length, concentration, and tacticity, and hence has extensive applications in many fields. PNIPAM-based cross-linked polymers exhibit type-II swelling behavior; i.e., it will undergo continuous swelling–deswelling with induced temperature [22]. However, LCST range of PNIPAM is easily tuneable to the desired temperature range by altering hydrophilic–hydrophobic balance by incorporating copolymers. LCST of PNIPAM can be dropped by tagging hydrophobic side chain and can be elevated by tagging hydrophilic side chain [4, 23]. Block copolymer PNIPAM-*b*-PLL was synthesized by ring-opening polymerization, and LCST behavior was studied by Zhao et al. He reported that incorporation of hydrophilic poly(L-lysine) as a comonomer at the end on PNIPAM has affected the LCST of PNIPAM moiety to higher temperature (33.5 °C) at low pH (pH = 5.0). At lower pH, the protonation of PLL moiety will raise LCST point, whereas at higher pH (pH = 11.0) the deprotonation of PLL provides hydrophobic nature to PLL unit which leads to dropping of LCST point [24]. Karir et al. reported that PNIPAM-co-poly(L-tyrosinamide)-based copolymers possessed LCST at higher temperature (35 °C) which was expected since poly(L-tyrosinamide) is moiety and is hydrophilic in nature [25]. Hong et al. reported Pd nanoparticles

immobilized on PNIPAM-co-4-VP copolymers with LCST causing an increase in LCST of PNIPAM [26]. However, Yifei fan et al. showed that in starch-g-(PAM-co-PNIPAM), the content of PNIPAM moiety also plays a vital role. He concluded that the block copolymer consisted of 10–25 mol% of NIPAM repeating unit causes lacking of LCST behavior due to the low concentration of PNIPAM moiety whereas the copolymer with 50 mol% of PNIPAM moiety exhibited LCST behavior at around 68 °C due to high PNIPAM content [27].

2.2 *Poly(N-Vinyl Caprolactam) (PVCa)*

Poly(*N*-vinyl caprolactam) (PVCa) is an example of thermoresponsive polymer which is categorized under the class of poly(*N*-vinylamide)-based polymer. The nonionic PVCa polymer is soluble in water, and its chemical structure contains the repeating unit which consists of a seven-membered lactam ring with a hydrophilic amide group directly bonded to the hydrophobic vinyl group. PVCa exhibits LCST around 32 °C with a conformational transition from expanded coil to compact globule in aqueous medium. The phase transition of PVCa is assisted by the hydrogen bond between hydrophilic amide group and water molecule below the LCST and the extrusion of water molecule above the LCST. Below the LCST, the lactam ring will exist in a chair conformation which allows high hydration and prevents the interaction between hydrophobic groups within the polymer to make it water-soluble. Above the LCST, the increased motion of bounded water molecule will cause dehydration of polymer to result in precipitation of polymer [28]. LCST of PVCa is similar to PNIPAM; however, unlike PNIPAM its LCST depends on its molecular weight and concentration [29]. Jones et al. reported that LCST of PVCa can be altered by altering the molecular weight of polymer macromolecule [30]. The elevation in molecular weight or concentration of polymeric system in solution causes dropping of LCST of thermoresponsive polymer [31]. By exhibiting Flory–Huggins type-I phase transition (i.e., swelling behavior of cross-linked polymer will be discontinuous with respect to the induced temperature), it is on contrary to PNIPAM which shows type-II transition [32] and the phase transition of PVCa consists of biphasic systems which have first transition point at 31.5°C (dehydration of polymeric system) and second transition point at 37.5 °C (removal of water molecule followed by increased hydrophobic interactions) resulting in polymer molecule separation [1]. Compared to PNIPAM, PVCa-based polymers are more biocompatible and relatively less toxic in nature. Biocompatibility and low toxicity arise from a fact that the amide bond which is present in lactam ring is stable to hydrolysis below the LCST [29, 33, 34]. Being more biocompatible than PNIPAM, PVCa-based thermoresponsive polymers possess many interesting applications in biomedical field [4].

2.3 *Poly(Methyl Vinyl Ether) (PMVE)*

Poly(methyl vinyl ether) (PMVE) falls under the category of poly(vinyl ether)-based thermoresponsive polymers which shows type-III phase transition behavior. PMVE exhibits thermoresponsive property at LCST of 35–37 °C which is in close resemblance with the biological temperature which makes them suitable for many biomedical applications. Even though it is having LCST close to biological environment temperature, its applications are limited because the difficulties arise during the synthesis of PMVE-based polymers [35, 36].

2.4 *Poly(N-Ethyl Oxazoline) (PEtOx)*

PEtOx is a nonionic thermoresponsive polymer which comes under the category of poly(2-alkyl-2-oxazoline). It displays thermoresponsive behavior at LCST of 62–65 °C [37]. The thermoresponsive property or LCST of poly(*N*-ethyl oxazoline) can be easily altered within the range of 35–80 °C since it strongly depends on the molecular weight, concentration as well as the composition of copolymer. PEtOx will exhibit thermoresponsive property in aqueous medium only if the molecular weight of the polymers falls under the range of 20–500 kDa [22]. Similar to the phase transition of PNIPAM, PEtOx involves hydrogen bonding to show LCST property [38]. The higher LCST (~65 °C) of PEtOx-based polymers along with their sensitivity to unprotected functional groups makes them unsuitable for biomedical applications. Despite having drawbacks, it can be used for drug delivery applications due to the fact that it can form micelles above the LCST point [39]. Furthermore, the poly(oxazoline)-based polymers resembling in structure with polypeptides are biocompatible due to the presence of tertiary amide group which is resistant to hydrolysis [40].

2.5 *Poly(Acrylic Acid-Co-Acrylamide)*

This is an example of thermoresponsive polymer which possesses UCST. Poly(acrylic acid-co-acrylamide) exhibits UCST around 25 °C, above which it may be changed from hydrophobic into hydrophilic in nature [41].

3 **Synthesis of Thermoresponsive Polymers in Solution Using Different Polymerization Techniques**

Recent developments on the wide range of applications of thermoresponsive polymeric systems are facilitated by certain phenomena like tunable LCST/UCST based

on the required applications and biocompatibility. Both LCST/UCST and biocompatibility can be achieved by the incorporation of suitable copolymer at the end of thermoresponsive polymer. Hence, the synthetic methods for thermoresponsive polymers may require synthesis of homopolymer with a suitable end group which can allow easy functionalization to form copolymer with required LCST/UCST point while retaining biocompatibility and biodegradability. Hence, radical polymerization is most frequently used for the synthesis of polymers [42]. Particularly, conventional-free radical polymerization can be used to synthesize such polymers because of several advantages like moderate reaction temperature, wide range of monomers utilized, formation of high molecular weight polymer, and tolerance against solvent impurities, oxygen, and moisture. The drawbacks associated with the conventional radical polymerization are: (a) their inability to control the molecular weight and PDI (due to fast chain growth which in turn leads to immediate termination to form chains with a different length/molecular weight), (b) difficulty to form block copolymer (due to the absence of suitable end group for further copolymerization), (c) difficulty on controlling the tacticity of a polymer [43]. In order to address the abovementioned drawbacks, controlled/living radical polymerization (CLRP) can be used for synthesizing thermoresponsive polymers as well as copolymers. The advantages of this technique include (a) control over molecular weight as well as PDI (fast initiation to form all the chains with equal length which in turn will control the termination step), (b) suitable end group for easy functionalization of a homopolymer to form copolymer, (c) controlled tacticity of a polymer, (d) formation of polymer with required molecular weight (required molecular weight of the polymer can be achieved by tuning the monomer/initiator ratio) [44]. The major advantage of CLRP is during the polymerization most of the chains exist in the form of dormant species, so there is an equilibrium maintained between active chain and dormant chain to reduce the termination step. The equilibrium between active chain and dormant species is responsible for the synthesis of polymers with very low PDI [45, 46].

Figure 3 represents the major types of CLRP based on free radical generation step

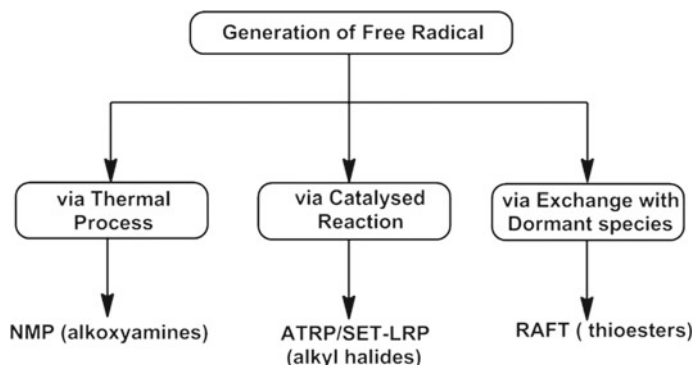


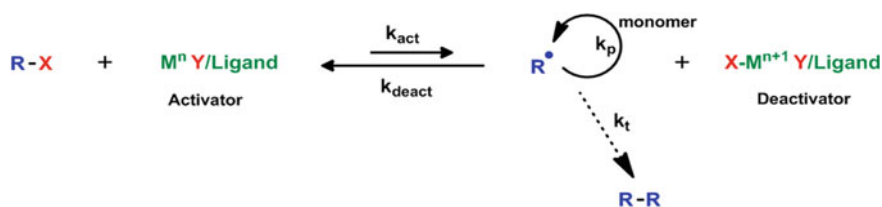
Fig. 3 Types of controlled living radical polymerization (types of dormant species are mentioned within bracket)

and dormant species formed during the polymerization [45]. As shown in Fig. 3, the well-established polymerization techniques used for the synthesis of thermoresponsive polymers are atom transfer radical polymerization (ATRP), reversible addition–fragmentation chain transfer (RAFT) polymerization, and nitroxide-mediated polymerization (NMP). As mentioned earlier, these CLRP polymerizations exhibit equilibrium between active species and dormant species. Furthermore, they are tolerable with many functional groups [47].

3.1 Atom Transfer Radical Polymerization (ATRP)

Ever since the first report of ATRP made by Matyjaszewski for styrene polymerization using 1-phenylethyl chloride (initiator) and CuCl/2,2'-bipyridine (catalytic system), ATRP has been used extensively as a versatile tool for polymerization of various monomers. [48] As shown in scheme 1, ATRP technique involves a crucial step, i.e., reversible addition of halogen atom to dormant species which reinforce its utility for carrying out polymerization techniques in various fields based on its applications [49, 50]. Other advantages associated with ATRP techniques are (a) possibility to achieve polymer with desired molecular weight by tuning the ratio between monomer and initiator, (b) ability to attain low PDI (<1.5) [51], (c) high rate of initiation step than that of propagation step leads to the uniform growth of all the chains to yield polymer chains with almost equal length, (d) the equilibrium between active species and dormant species continues to keep the concentration of active species low and dormant species high which in turn reduces the termination step from the initiation step (persistent radical effect) [52], (e) reversible addition of halogen atom to provide living nature to the polymer chains, (f) easy functionalization of polymer chain due to the presence of end-capped halogen atom to form copolymers/macromolecular architectures [46, 53].

Most of the thermoresponsive homopolymers and degradation products of them were nonbiocompatible and toxic in nature; therefore, copolymerization is often carried out by incorporating biocompatible or degradable blocks with it in order to achieve biocompatibility. In order to conduct the copolymerization extensively the polymer needs to have a living end group. Hence by providing polymer with living end, ATRP emerged as a versatile tool for homopolymer and block copolymer



Scheme 1 General mechanism for atom transfer radical polymerization (ATRP)

synthesis in both solution and surface-mediated reactions. Several reports have successfully highlighted the synthesis of biocompatible thermoresponsive polymers and their biocompatibility.

Jun loh et al. reported the synthesis of triblock copolymer using hydrophobic poly[(R)-3-hydroxybutyrate] (PHB) and hydrophilic PNIPAM to form thermoresponsive micelles. Their synthetic methodology also involved two steps, wherein they prepared Br-PHB-Br difunctional macroinitiator in the first step which was subsequently used as an ATRP macroinitiator for the synthesis of (PNIPAAm-PHB-PNIPAAm) triblock copolymers along with NIPAM and CuBr/HMTETA in dioxane (shown in Fig. 4). Using ATRP, they carried out polymerization in a well-controlled manner to obtain triblock copolymers with PDI in the range of 1.09–1.50 which varied with variation in chain length. Those synthesized triblock copolymers exhibited LCST property between 28 and 29 °C. They also carried out cytotoxicity studies using MTT assay in order to examine the biocompatibility of those copolymers and reported that (PNIPAAm-PHB-PNIPAAm) triblock copolymers were biocompatible

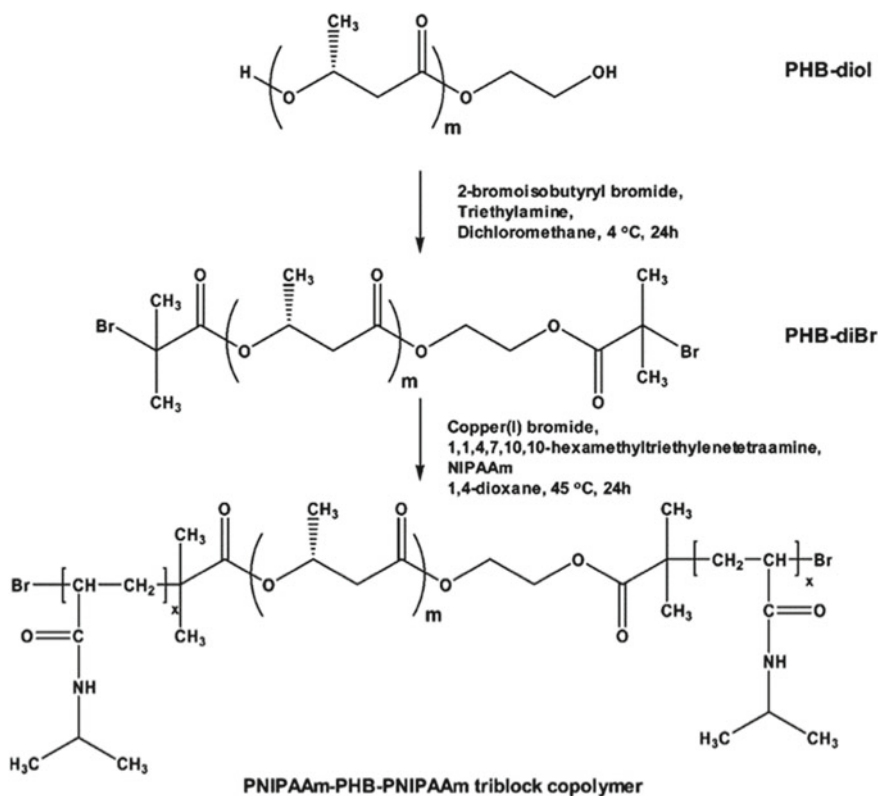


Fig. 4 Synthesis of triblock copolymers consisted of PNIPAAm-PHB-PNIPAAm using ATRP. Reprinted (adapted) with permission from [54]. Copyright (2019) American Chemical Society

and cell viability was found to be increased as PNIPAm content in the copolymer increased [54]. Vaishali et al. reported synthesis of thermoresponsive PS-*b*-PNIPAm diblock copolymer. They carried out ATRP for the synthesis of amphiphilic diblock copolymer in two steps using PS as a hydrophobic moiety and PNIPAM as a hydrophilic moiety. At first, PS-based macroinitiator (PS-Br) (PDI = 1.09) was synthesized using molar feed ratio of [styrene]0: [EBiB]0: [CuBr]0: [PMDETA]0 as 100:1:1:1 in anisole. Next step involved synthesis of diblock copolymer (PDI = 2.09) using molar feed of [NIPAm]0: [PS-Br]0: [CuBr]0: [HMTETA]0 as 100:1:1:1 in DCM where PS-Br played a role of macroinitiator. They have also studied the effect of solvent and temperature for the synthesis of PNIPAM-based diblock copolymer using PS-based macroinitiator and concluded that the polymerization did not occur in the presence of solvents like anisole, DMF, and ethyl acetate whereas effective polymerization took place in DCM medium. The synthesized diblock copolymer exhibited LCST at 33.5 °C which indicated that the conformational change during thermoresponsive behavior of PS-*b*-PNIPAm is in close resemblance with that of PNIPAM-based homopolymers [55]. Similarly, Zhilong et al. reported the application of ATRP for synthesis of thermosensitive triblock C18-PEGn-*b*-PNIPAAm copolymer with self-assembly behavior and tunable thermoresponsive nature. PEG moiety of block copolymer played an important role in regulating the nanostructure, stability, thermoresponsive nature as well as biocompatibility. PEG-*b*-PNIPAM-based copolymers with narrow PDI ranging from 1.1 to 1.2 were synthesized using ATRP of commercially available PEG-based surfactants and C18 precursors. Initially, C18-PEGn-Br macroinitiator was synthesized followed by ATRP which was carried out using [NIPAAm]/[C18-PEGn-MI]/[CuCl]/[Me₆TREN] (60/1/1/1) to yield C18-PEG-capped PNIPAM-based copolymers with narrow PDI. As expected, these copolymers exhibit LCST property at higher temperature (38–41 °C) than that of PNIPAM homopolymer due to the presence of hydrophilic PEG unit which allowed the formation of more stable micelles. The triblock copolymers formed stable micellar structure at low temperature which initially collapsed into smaller micellar form at moderate temperature followed by aggregation at higher temperature. They concluded that such thermoresponsive copolymers can be used in nanomedicines [56]. The authors conducted the ATRP to obtain thermoresponsive PNIPAM-based degradable hydrogel. Initially, Cl-PCL-Cl difunctional macroinitiator and PCLDMA were synthesized separately followed by ATRP of NIPAM, Cl-PCL-Cl, PCLDMA using CuCl/Me₆TREN in DMSO, which provided corresponding PNIPAM-based hydrogel. They carried out cytotoxicity studies using MTT test which confirmed that the synthesized PNIPAM-based hydrogels (concentration between 1 and 25 mg/ml) were biocompatible and non-toxic and may be considered as promising candidate for tissue engineering applications [57].

Recently, Li et al. reported the preparation of PPO-PMPC-PNIPAM-based novel doubly thermoresponsive triblock gelators. The synthetic strategy involved the synthesis of PPO-based macroinitiator at first which was used to form PPO43-PMPC160-Br macroinitiator using ATRP of MPC, CuBr/bpy in methanol. Further, ATRP was carried out using PPO43-PMPC160-Br, NIPAM, and CuBr/Me₄Cyclam in methanol to yield PPO43-MPC160-NIPAM81 triblock copolymers (shown in Fig. 5). The syn-

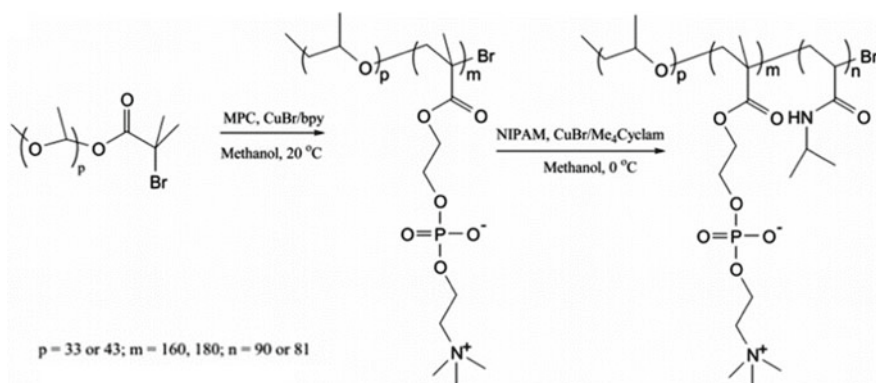


Fig. 5 Synthesis of PPO-PMPC-PNIPAM triblock copolymers using ATRP. Reprinted (adapted) with permission from [58]. Copyright (2019) American Chemical Society

thesized copolymer was soluble at ~ 5 °C, forming PPO core micelles between 10 and 20 °C (around the LCST of PPO chain), and micellar gel network was obtained above LCST of PNIPAM moiety, i.e., at above 33 °C. The cell viability studies indicated that these gels were biocompatible [58].

Qiao et al. reported the synthesis of thermoresponsive copolymers poly(DEA-co-OEGA)s and poly(DMDEA-co-OEGA)s with pendent OEG chains and cyclic orthoester. These polymers were easily hydrolyzable due to the presence of cyclic orthoester moiety, and the hydrolyzed products of these copolymers were found to be more biocompatible than that of poly(meth)acrylamides which is an essential factor for using these types of polymers for drug delivery applications. They stated that homopolymers of DEA or DMDEA were not water-soluble at ambient condition; therefore, these polymers were copolymerized using OEGA to give water-soluble copolymers. As shown in Fig. 6, ATRP was carried out in anisole using DEA or DMDEA, OEGA, EBiB, CuBr, and Me₆TREN to form the copolymers in a well-controlled manner. The synthesized poly(DEA-co-OEGA)-based copolymer (PDI = 1.11) showed LCST behavior at 27.2 °C (heating) and at 26.8 °C (cooling), and poly(DMDEA-co-OEGA) with PDI 1.13 showed LCST at 22.6 °C (heating) and at 19.2 °C (cooling). They also examined the influence of molecular weight of copolymer and content of OEGA on the cloud point of copolymer and reported that by altering the ratio between hydrophilic/hydrophobic moieties LCST of the thermoresponsive polymers can be altered. In order to extend the application of these copolymers for drug delivery systems, MTT assay was carried out for poly(DMDEA-co-OEGA), and the cell viability of these copolymers as well as their hydrolyzed products was found to be similar to that of PEG-based polymers. Hence due to their thermoresponsive property as well as pH-induced hydrolysis, these copolymers may be regarded as biocompatible drug delivery system [59].

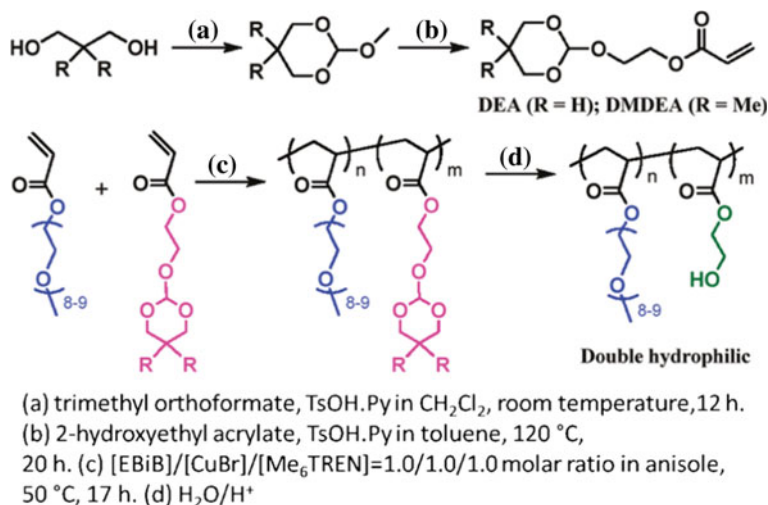


Fig. 6 Synthesis of poly(DEA-co-OEGA)s and poly(DMDEA-co-OEGA)s. Reprinted (adapted) with permission from [59]. Copyright (2019) American Chemical Society

Hongyun tai et al. had reported the ATRP of monofunctional (PEGMEMA and PPGMA) as well as multifunctional vinyl monomers (EGDMA) to obtain copolymer with biocompatibility, thermoresponsive property as well as photocrosslinkability. The deactivated ATRP method was carried out using PEGMEMA, PPGMA, EGDMA, CuCl, CuCl₂ (to provide deactivation), and bpy in butanone to obtain PEGMEMA-PPGMA-EGDMA copolymer (shown in Fig. 7). The synthesized copolymers exhibited LCST behavior at 32 °C which is similar to that of PNIPAM. They stated that these biocompatible polymers can be used in applications like wound healing and tissue engineering [60].

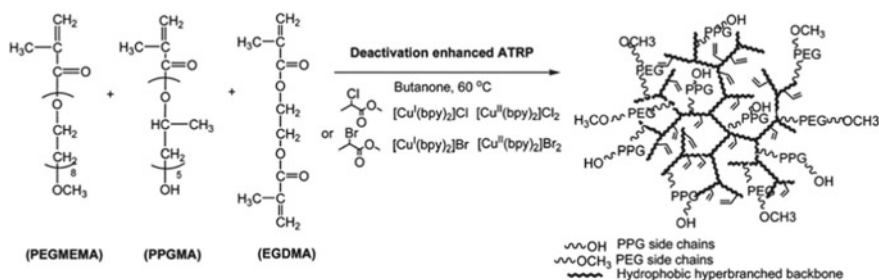
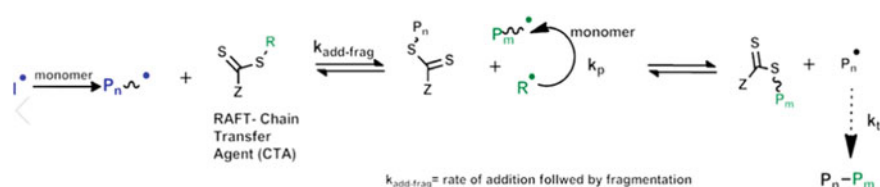


Fig. 7 Synthesis of PEGMEMA-PPGMA-EGDMA via deactivation enhanced ATRP (DE-ATRP). Reprinted (adapted) with permission from [60]. Copyright (2019) American Chemical Society

3.2 Reversible Addition–Fragmentation Chain Transfer (RAFT) Polymerization

Reversible addition–fragmentation chain transfer (RAFT) polymerization is a more versatile technique for the synthesis of polymers in a well-controlled manner with low PDI. Even though ATRP techniques provide well-controlled polymers with low PDI, their applications were limited for certain monomers like acrylamide-based monomers. On the other hand, RAFT technique arose as a successful tool for controlled polymerization due to their capability of polymerizing varieties of monomers. In RAFT, chain transfer agent plays important role in controlling the polydispersity index (PDI) of the polymer (Scheme 2). Similar to ATRP, RAFT also yields the polymer with living end group [46].

Several reports have been published exploring RAFT for the synthesis of thermoresponsive polymers with biocompatibility and low toxicity. Mori et al. reported L-proline-based thermoresponsive polymer, poly(*N*-acryloyl-L-proline methyl ester) abbreviated as poly(A-Pro-OMe) which was synthesized using RAFT polymerization technique. They carried out RAFT using A-Pro-OMe (monomer), benzyl dithiobenzoate (abbreviated as BDB (CTA)), AIBN (initiator) in chlorobenzene solvent at 60 °C (shown in Fig. 8). Fixing the molar feed ratio of [A-Pro-OMe]:[BDB]:[AIBN] as 100:2:1, they were able to conduct the polymerization in a well-controlled manner with PDI of 1.15. From the thermoresponsive study, they found that poly(A-Pro-OMe) exhibited LCST at 15–20 °C. They also reported the synthesis of poly(A-Pro-OMe)-co-DMA by copolymerizing poly(A-Pro-OMe) (homopolymer) with *N,N*-dimethylacrylamide (DMA), which showed linear increase in LCST with the content of DMA (composition of DMA up to 50%) [61]. The same strategy was reported by Cui et al. where thermoresponsive (PEG-*b*-PADMO) copolymer was synthesized using RAFT polymerization of PEG (hydrophilic block)



Scheme 2 General mechanism of reversible addition–fragmentation chain transfer polymerization (RAFT)

Fig. 8 Synthesis of poly(A-Pro-OMe) using RAFT. Redrawn from Mori et al. [61]



and poly(*N*-acryloyl-2,2-dimethyl-1,3-oxazolidine)-PADMO (hydrophobic block). They also synthesized PEG-based chain transfer agent at first which was further polymerized with *N*-acryloyl-2,2-dimethyl-1,3-oxazolidine (ADMO), AIBN to give PEG-*b*-PADMO block copolymer (PDI = 1.13–1.16). The synthesized PEG-*b*-PADMO block copolymers formed micellar structure (consisted of PADMO hydrophobic core and PEG hydrophilic water-soluble shells) at ambient temperature, and the presence of PEG provides biocompatibility to those copolymers. LCST of these block copolymers was found to be in the range of 40–72 °C (tunable with PADMO chain length) which was less than that of PEG homopolymer (LCST at around 100 °C) [62]. Zhu et al. reported poly(*N*-isopropylacrylamide)-*b*-[2-hydroxyethyl methacrylate-*b*-poly(*ε*-caprolactone)]_n (abbreviated as (PNIPAAm-*b*-(HEMA-PCL)_n) copolymer with thermosensitivity and biodegradability using RAFT polymerization technique. Initially, they carried out RAFT of NIPAAm (monomer) using AIBN (initiator) and benzylsulfanylthiocarbonylsulfanylpropionic acid (BSPA) as a CTA in THF to form PNIPAAm-BSPA as a macro-RAFT agent. Similarly, ring-opening polymerization was carried out using 2-hydroxyethyl methacrylate (HEMA) (initiator) and Sn(Oct)₂ (catalyst) to form HEMA-PCL block. Finally, PNIPAAm-*b*-(HEMA-PCL)_n copolymer was synthesized by RAFT of PNIPAAm-BSPA and HEMA-PCL. LCST behavior studies showed that such copolymers exhibit slightly higher LCST (36 °C) than PNIPAAm homopolymer due to the presence of carboxylic acid terminal group. Enzymatic degradation and cytotoxicity studies were carried out and confirmed that the copolymers are degradable and non-toxic due to the presence of PCL moiety [63].

As shown in Fig. 9, Zhang et al. reported the synthesis of thermoresponsive block copolymer poly(acryloyl glucosamine)-*b*-poly(*N*-isopropylacrylamide), which was abbreviated as PAGA180-*b*-PNIPAAm350, using RAFT polymerization to

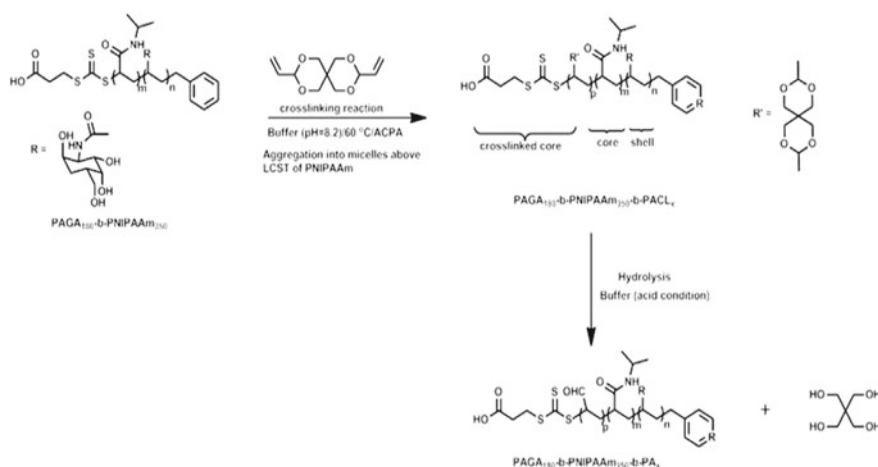


Fig. 9 Synthetic scheme of PAGA180-*b*-PNIPAAm350 via RAFT and its degradation. Redrawn from Zhang et al. [64]

obtain narrow dispersity (with PDI = 1.25). These polymers tend to undergo micellar formation above the LCST of PNIPAM; hence, PAGA180-b-PNIPAAm350 and 3,9-divinyl-2,4,8,10-tetraoxaspiro[5.5]undecane (cross-linking agent) were allowed to react at above the LCST point and it was observed that it formed the micellar systems through the formation of PAGA180-b-PNIPAAm350-b-PACL_x triblock copolymer. They mentioned that the presence of cross-linking agent in those synthesized block copolymers enables thermosensitivity as well as acid degradability in core-shell nanoparticles. LCST property of those block copolymers was studied and found out that both polymers with or without cross-linking agent showed LCST behavior at around 28 °C. They also confirmed that due to the presence of acid degradable groups, these polymers are easily degradable under acidic conditions [64]. Li et al. reported the synthesis of nanometer-sized micellar systems with water solubility, biocompatibility, and stimuli-responsive property (thermoresponsive and pH responsiveness). They synthesized amphiphilic polymers [P(NIPAAm-co-EIPPMMA)-b-PVPhol] and [P(NIPAAm-co-HEMA)-b-PVP] using RAFT polymerization which was further conjugated with fluorescein isothiocyanate (FITC), a fluorophore in order to use in bio-imaging applications. LCST studies showed that FITC-conjugated [P(NIPAAm-co-EIPPMMA)-b-PVPhol] copolymer had the transition behavior at around 32 °C whereas FITC-conjugated [P(NIPAAm-co-HEMA)-b-PVP] did not show transition property due to the high content of HEMA. So overall due to the thermoresponsive PNIPAAm moiety and FITC (acid-base indicator), the fluorescent nature of these polymers was tunable with respect to temperature as well as pH; hence, they can be used in bio-analysis [65].

Various responsive polymers have been used as nanoscopic drug carriers for encapsulating hydrophobic drug molecule. For example, Hyoungryu et al. reported thermoresponsive nanogel which was composed of random copolymer with hydrophilic oligoethyleneglycol (OEG) unit and hydrophobic pyridylsulfide (PDS) unit as side functionalities. This random copolymer precursor was synthesized using RAFT polymerization followed by reaction with dithiothreitol (DTT) causing the formation of nanogels (mentioned in Fig. 10). OEG unit in a polymer is responsible for biocompatibility, while PDS moiety is responsible for amphiphilic nano-assembly in water. Thermoresponsive property studies showed that these polymers exhibit LCST behavior which depends upon the composition of PDS unit; hence, random polymer which contains equal ratio of OEG:PDS exhibits LCST behavior at above 55 °C whereas the presence of excess of PDS content decreased LCST point to around 30 °C due to its hydrophobic nature. Biocompatibility was also confirmed by carrying out a Alamar blue assay test, and it was found out that these nanogels exhibit biocompatibility even with concentration of 1 mg/ml; hence, they can be used as a potential tool in biomedical field as a drug delivery system [66]. Similarly, another type of nanocapsules was reported by Aguirre et al. where they employed RAFT polymerization for the synthesis of random copolymers of *N*-vinylcaprolactam (VCL) and acrylic acid (AA) which was further absorbed onto cationic dimethyldioctadecylammonium bromide (DODAB) vesicle. RAFT of VCL and AA was carried out in dioxane using AIBN (initiator) and dibenzyltrithiocarbonate (DBTTC) (CTA) to

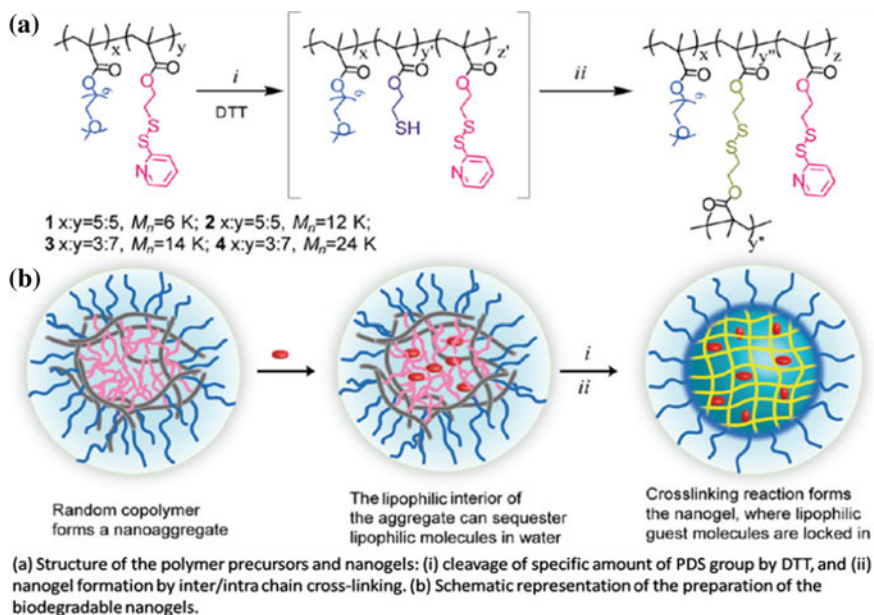


Fig. 10 Pictorial representation of nanogel precursors, polymer nanogels, and its synthetic approach using RAFT. Reprinted (adapted) with permission from [66]. Copyright (2019) American Chemical Society.

obtain RAFT copolymers with different lengths, i.e., VCL9-co-AA6 or VCL18-co-AA12. Then, semi-continuous emulsion polymerization was carried out both in the presence of cross-linkers (EGDMA or MBA) and in the absence of cross-linkers to form thermoresponsive nanocapsule. Those synthesized nanocapsules showed LCST behavior between the ranges of 33 and 35 °C which was independent of type of cross-linker used. The presence of VCL in these nanocapsules provided biocompatibility; hence, they can be used as drug carriers [67].

Shen et al. had specially studied the cytotoxic effect of water-soluble polymers (Fig. 11); hence, the author had synthesized three water-soluble polymers, poly(*N*-2-hydroxypropyl)-methacrylamide) (P(HPMA)), poly(oligoethylene glycol methyl ether acrylate) (P(OEG-A))-based polymers with two different end groups P(OEG-A)D (ω -dithiobenzoate end group) and P(OEG-A)T (ω -trithiobenzoate end group), and poly-(oligoethylene glycol methyl ether methacrylate) (P(OEG-MA)) using different RAFT agents like CDTB or BSPA or CDB. All those polymers were synthesized in a well-controlled manner with PDI in the range between 1.03 and 1.25. They studied the cytotoxicity studies based on the effect of CTA on cells. Cell viability of P(OEG-A)D, P(OEG-MA)D, P(OEG-MA)T, and P(HPMA)D was studied using cell titer blue assay test. Results obtained from assay test showed that RAFT polymers which were synthesized using BSPA RAFT agent do not have any significant toxicity on cells, whereas dithiobenzoate end group-based OEG polymer

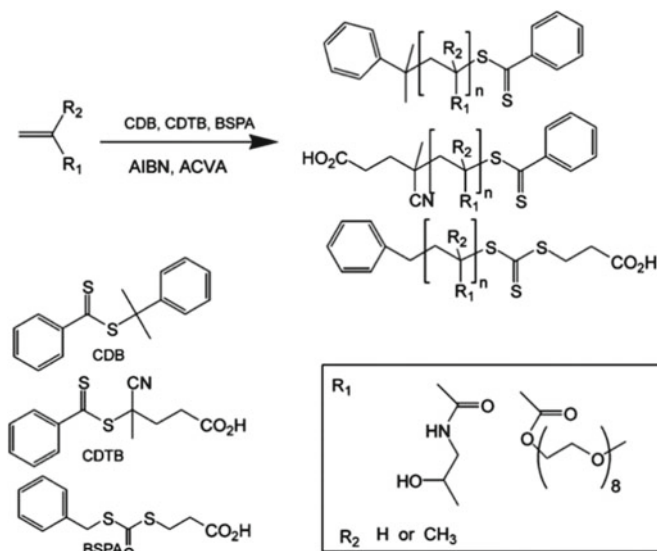


Fig. 11 Synthesis of RAFT polymers of different monomers. Reprinted (adapted) with permission from [68]. Copyright (2019) American Chemical Society.”

and P(HMPA) synthesized using CDTB RAFT agent showed high toxicity on cells. Dithiobenzoate-ended P(HPMA) samples (high concentration) were highly toxic on all the cells, whereas same sample with low concentration and trithiobenzoate end group showed less toxic effect [68].

The author had applied RAFT-mediated aqueous dispersion polymerization successfully for the synthesis of thermosensitive core–shell nanogel with biocompatibility and antifouling property. Initially, the macro-chain transfer agent (CTA) PEG5k-TTC or PPEGMAxTTC/DT was prepared which was used for the synthesis of MEO₂MA-based homopolymer and MEO₂MA/PEGMA-based copolymers (mentioned in Fig. 12). MEO₂MA homopolymer showed LCST behavior at 26 °C, whereas MEO₂MA/PEGMA-based copolymers showed at 26–90 °C. In those synthesized MEO₂MA/PEGMA-based nanogels, the presence of PEG moiety made them biocompatible [69]. Jeong et al. reported poly(*N*-vinylpiperidone) (PVPip)-based thermoresponsive block copolymer with biocompatibility. Initially, RAFT was carried out using VPip (monomer), AIBN (initiator), and xanthate-ethyl 2-(ethoxycarbonothioylthio)propanoate as a CTA in dioxane to obtain PVPip with PDI of 1.59 and the obtained polymer showed LCST behavior at 84 °C. In order to form biocompatible thermoresponsive block copolymer, they carried out chain extension of PVPip using RAFT where PVPip acted as a macro-CTA for polymerization of vinyl acetate to form the (PVPip-*b*-PVAc) block copolymer (PDI of 1.27). Due to the presence of hydrophilic PVAc moiety and hydrophobic PVPip moiety, those copolymers can form micellar system in water. LCST property studies also were carried out, and LCST was reported at lower temperature (55–62 °C) than that

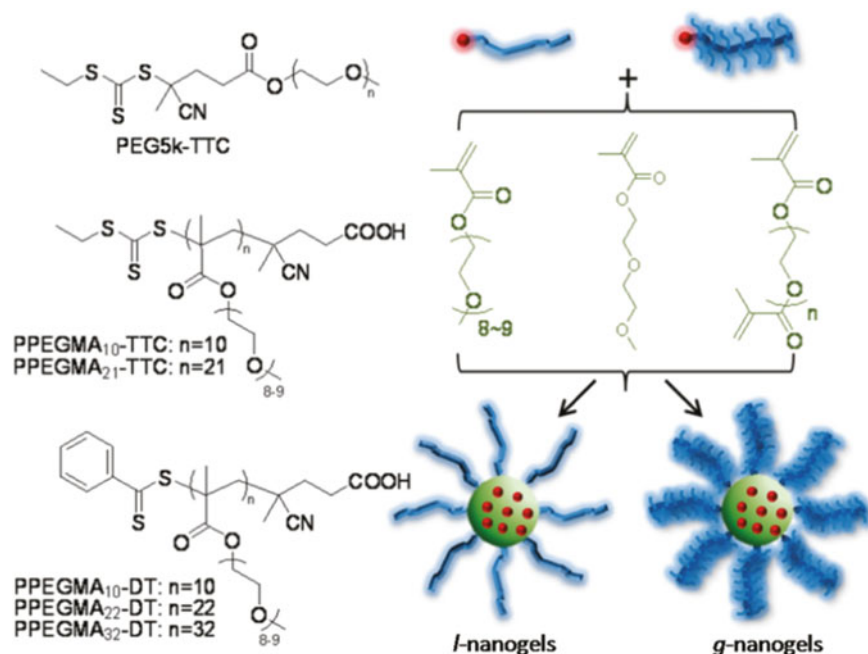


Fig. 12 Structure of macro-CTAs and synthesis of core-shell nanogels via RAFT dispersion polymerization. Reprinted (adapted) with permission from [69]. Copyright (2019) American Chemical Society

of homopolymer from which it was synthesized. This decrease in LCST was due to the incorporation of hydrophobic moiety PVAc into the polymer. Finally in order to find the biocompatibility of the copolymers, cytotoxicity was measured using LDH release study, and based on the results obtained, it was confirmed that the presence of even high dosage of polymer (1% w/v) did not affect the LDH release. These polymers are biocompatible and used in biofields [70]. Chen et al. reported synthesis of poly(*N*-acryloylsarcosine methyl ester) (PNASME) through RAFT polymerization and studied the effect of polymer molecular weight, polymer concentration, terminal group, and salt on LCST property. In order to carry out these studies, they had synthesized PNASME-based homopolymer as well as PNASME-*b*-PNIPAM diblock copolymer by two steps. Initially, they synthesized PNASME-based macro-RAFT agent (PNASME with PDI 1.09). Then, RAFT was carried out using the synthesized macro-RAFT agent to provide PNASME-*b*-PNIPAM block copolymer with PDI 1.32. PNASME₁₇₀-*b*-PNIPAM₆₃ showed two LCST points, i.e., one at 38 °C (corresponded to PNIPAM moiety) and another one at 43 °C (corresponded to PNASME moiety). They also found that above 38 °C (LCST of PNIPAM), micelles were formed which consisted of core of insoluble PNIPAM block surrounded by corona of PNASME block. Further heating to above the LCST of PNASME caused

depositing of PNASME on PNIPAM core. Based on the studies carried out on determining the factors affecting LCST, it was observed that the degree of polymerization increased from 41 to 124 and LCST was decreased from 50 to 45 °C (after 44 °C no change was observed). They have also studied the effect of salt on LCST using anion series as follows: $\text{CO}_3^{2-} > \text{SO}_4^{2-} > \text{S}_2\text{O}_3^{2-} > \text{H}_2\text{PO}_4^- > \text{F}^- > \text{Cl}^- > \text{Br}^- \sim \text{NO}_3^- > \text{I}^- > \text{ClO}_4^- > \text{SCN}^-$. Based on the anion series, it was observed that kosmotropes (anions left of chloride ion) caused polyacrylamides to precipitate by strong hydration; hence, LCST was decreased. On the contrary, chaotropes (anions to the right of chloride ion) which were less hydrated increased LCST of polyacrylamides. Besides that, they also studied the effect of addition of urea and phenol on LCST. In the case of PNIPAM, addition of both urea and phenol lowered the LCST whereas in the case of PNASME addition of urea had increased the solubility of PNASME; hence, LCST was found to be increased whereas the addition of phenol decreased the solubility of PNASME; hence, LCST also decreased. Based on these studies, the author claimed that by having tunable thermoresponsive property those polymers can be very useful for applications [71]. Recently, Huang et al. reported synthesis of well-defined thermoresponsive poly($\text{C}_2\text{NVP-co-NVP}$) amphiphilic block copolymers (PDI < 1.5) utilizing RAFT technique of 3-ethyl-1-vinyl-2-pyrrolidone (C_2NVP) and N-vinylpyrrolidone (NVP), AIBN, and S-(1-methyl-4-hydroxyethyl acetate) *O*-ethyl xanthate (MHEX) as a RAFT agent in ethanol. They have studied the effect of molecular weight (Mw) and composition on copolymer and reported that as the Mw increases cloud point decreased from 50.5 to 45 °C. Similarly, the cloud point was decreased from 48 to 29 °C as the composition of C_2NVP increased. They also synthesized thermosensitive nanocarriers [P($\text{C}_2\text{NVP-co-NVP}$)-*b*-PCL] using poly($\text{C}_2\text{NV-co-NVP}$) (hydrophobic unit) and polycaprolactone (PCL) (hydrophilic unit) for use in biomaterials, drug delivery systems [72].

Similarly, poly(oligo (ethylene glycol) vinyl acetate)s-based thermoresponsive polymers were reported by Hedir et al. in the same year where the authors employed RAFT for the synthesis of polymer (PDI range 1.13–1.53) using oligo (ethylene glycol) vinyl acetate as a monomer (MeO_2VAc), 1,1'-azobis-(cyclohexanecarbonitrile) (ABCN) as a initiator, and *O*-*p*-methoxyphenylxanthate as the chain transfer agent (CTA) (shown in Fig. 13). Thermoresponsive studies showed that the synthesized polymer poly(MeO_2VAc) exhibited LCST behavior at 83 °C; hence in order to tune LCST property poly(MeO_2VAc), homopolymer was again copolymerized with other less active monomers, i.e., vinyl acetates (VAc) to form poly($\text{MeO}_2\text{VAc-co-VAc}$)s which shows decrease in LCST point with high content of VAc and low content of MeO_2VAc in copolymer. As a further development in order to form degradable polymers, poly(MeO_2VAc) was copolymerized with 5,6-benzo-2-methylene-1,3-dioxepane (BMDO) moiety to give poly(MDO-co- MeO_2VAc)s which showed LCST behavior at 76 °C. Biocompatibility of these polymers was studied using cell viability studies [MC3T3 (murine pre-osteoblasts)] and found out that both polymer and copolymer are not affecting the cells which proves the biocompatibility of the reported polymers [73].

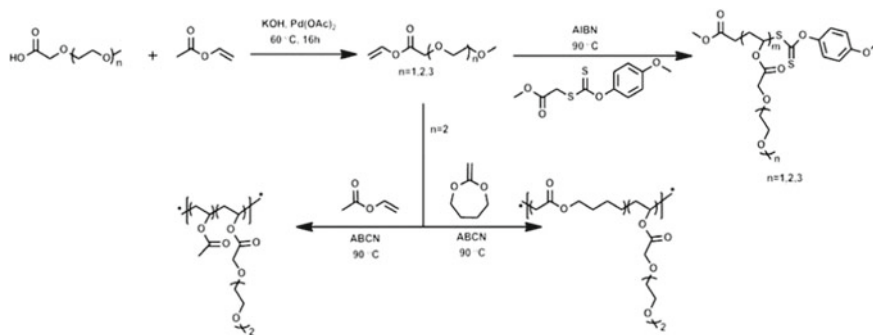
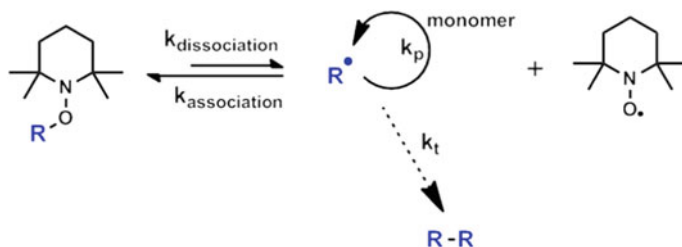


Fig. 13 Synthetic methodology of MeOnVAc-based copolymers using RAFT/MADIX polymerization. Redrawn from Hedir et al. [73]

3.3 Nitroxide-Mediated Polymerization (NMP)

Nitroxide-mediated polymerization (NMP) is developed as a controlled/living radical polymerization technique for the polymerization of different monomers. General mechanism of NMP is shown in Scheme 3. In NMP, the thermal process will result in the formation of nitroxide radical which plays a major role in controlling the polymerization by reversible capping and decapping of growing radical chain polymer. As a result of capping of growing chain radical with nitroxide radical (dormant alkoxyamine), the concentration of active propagating radicals will be decreased; hence, termination step will be controlled to result in the formation of narrow dispersed polymer [46].

Chenel et al. reported the synthesis of comb-shaped PEG-based copolymers which can be used in biomedical field due to the presence of biocompatible PEG moiety. They employed SG1 (*N*-tert-butyl-*N*-(1-diethylphosphono-2,2-dimethylpropyl) nitroxide-based initiator, MePEGMA, AN, and block builder to form well-defined P(MePEGMA-co-AN)-SG1-based comb-shaped copolymer (shown in Fig. 14). MTT assays were carried out in order to find the cytotoxicity, and based on the results obtained from MTT assay, they stated that those copolymers are non-cytotoxic



Scheme 3 General mechanism of nitroxide-mediated polymerization (NMP)

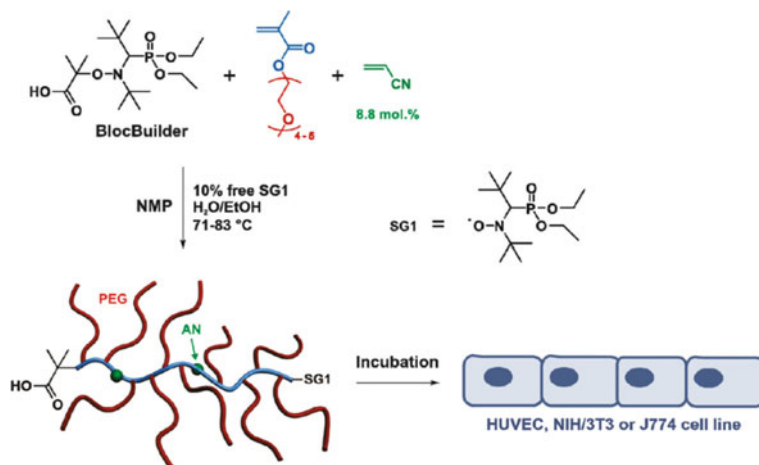


Fig. 14 Synthesis of comb-shaped P(MePEGMA-co-AN)-SG1 copolymer by NMP and cytotoxicity studies. Reprinted (adapted) with permission from [74]. Copyright (2019) American Chemical Society

even at higher dose [74]. Similarly, Popescu et al. had synthesized functional acrylate monomers using cascade of enzymatic transacylation which were then copolymerized with (2-hydroxyethyl acrylate) (HEA) (hydrophilic monomer) using free radical polymerization (FRP) or NMP. NMP of diethylene glycol ethyl ether acrylate (DEGEA) or dihydroxyhexyl acrylate (DHHA) was carried out using block builder, initiator, and SG1-free nitroxide to form homopolymer of poly(DEGEA) or P(DHHA). Similarly, PDEGEA was copolymerized with HEA (hydrophilic monomer) to form corresponding P(DEGEA-co-HEA) copolymer and PDHHA was copolymerized with methyl acrylate (MA) to form P[(DHHA)-co-(MA)]. LCST property studies showed that PDEGEA homopolymer (synthesized via NMP) exhibited LCST behavior at 13.2 °C whereas the same polymer (through FRP) showed LCST at 16.5 °C. Similarly, copolymers synthesized using FRP and NMP showed difference in LCST behavior. For example, P(DEGEA75-co-HEA25) (through FRP) showed LCST at 23.7 °C whereas P(DEGEA75-co-HEA25) (through NMP) showed LCST property at 21.3 °C which was attributed to the reason that NMP produced polymer with large SG1 hydrophobic end group; hence, hydrophobicity increased and LCST decreased. Similarly, the thermoresponsive properties of DHHA-based polymers were studied. PDHHA homopolymer does not exhibit LCST behavior for both methods of preparation, whereas in the case of copolymers with MA it showed similar difference in LCST between FRP and NMP method of preparation; i.e., P(DHHA63-co-MA37) showed LCST at 23 °C (for FRP method) and at 44.5 °C (for NMP method). In this case, the polymer synthesized by NMP method showed high LCST due to the reason that conversion of polymer to copolymer is less; hence, the copolymer will contain high content of hydrophilic block (PDHHA) which in turn will increase the LCST of copolymer [75].

It was recently reported that poly(OEGMA-co-MEO₂MA)-b-poly((3-[N-(3-methacrylamidopropyl)-N,N-dimethyl]ammoniopropane sulfonate)-co-N-(3-(dimethylamino) propyl)methacrylamide) copolymer showed both LCST and UCST properties. Initially, poly(OEGMA-co-MEO₂MA) macro-RAFT was synthesized at first which was then further used for copolymerization to give (poly(OEGMA-co-MEO₂MA)-b-poly(DMAPMA)) copolymer (PDI 1.04–1.09). Then, selective quaternization of poly(DMAPMA) block was performed to give copolymer which showed both LCST and UCST properties. From the LCST studies, it was reported that poly(OEGMA-co-MEO₂MA) block induced LCST property (60–61 °C) (tunable by altering OEGMA unit) whereas poly((3-[N-(3-methacrylamidopropyl)-N,N-dimethyl]ammoniopropanesulfonate)-co-N-(3-(dimethylamino) propyl) methacrylamide) block induced UCST property (10–21 °C which depends on degree of quaternization). By having tunable LCST and UCST property, these polymers can be used in nanomedicine field [76]. In the same year, another type of polymer with UCST was reported by Roth et al. Here, they carried out RAFT for the synthesis of poly[oligo(ethylene glycol) methyl ether methacrylate] (POEGMA)-based polymers with different end groups which tends to show UCST behavior in aliphatic alcohols. These polymers exhibit UCST property which depends on the molecular weight, and as the molecular weight of the polymer increased UCST also increased. In addition to that, the hydrophobic end groups lowered UCST whereas the presence of aromatic group raised the UCST point. They have also studied the effect of cosolvents on the UCST of POEGMA and found that in chloroform where POEGMA is highly soluble UCST decreased (below –10 °C) whereas in hexane (nonpolar solvent), the solubility of POEGMA is decreased and in turn UCST point also increased (above 59.3 °C with 60% of hexane). In the presence of water, UCST of POEGMA decreased sharply by forming strong H-bond to make POEGMA more soluble [77].

Later, Chua et al. reported the synthesis of series of acrylamide- and methacrylamide-based copolymers with ethyleneglycol (EG) as a side chain by RAFT polymerization technique. Initially, pentafluorophenyl acrylate/(meth)acrylate monomers were prepared which undergo RAFT homopolymerization in the presence of CTA to form homopolymers poly PFP (PDI 1.19) and poly PFP(M)A (PDI 1.21) (shown in Fig. 15). The synthesized homopolymers were then copolymerized with oligo(ethylene glycol) methyl ether amines (OEGMEAs) to form poly MEO_nAM (does not show LCST behavior) and poly MEO_nMAM (for $n = 2$, LCST at 55.8 °C). They observed that poly PFP homopolymer does not show any LCST property; hence, they again copolymerized it with hexylamine to form poly[(MEO₂)_{1-x}-co-Hexx]AM which showed LCST behavior at 77.7 °C which was further decreased by increasing the content of hexylamine moiety in a copolymer. In addition to the LCST property, (meth)acrylamido PEG-based polymers exhibit UCST behavior in alcohol. Both poly MEO₂AM and poly MEO₂MAM did not show any UCST property. On the other hand, poly MEO₃MAM and poly OEG350MAM showed transition at –3.0 and 4.4 °C, respectively, which increased as the content of OEG increased, whereas the same derivatives based on acrylamido did not exhibit any UCST property. Cytotoxicity of acrylamide-based PEG analogues (poly MEO₂AM

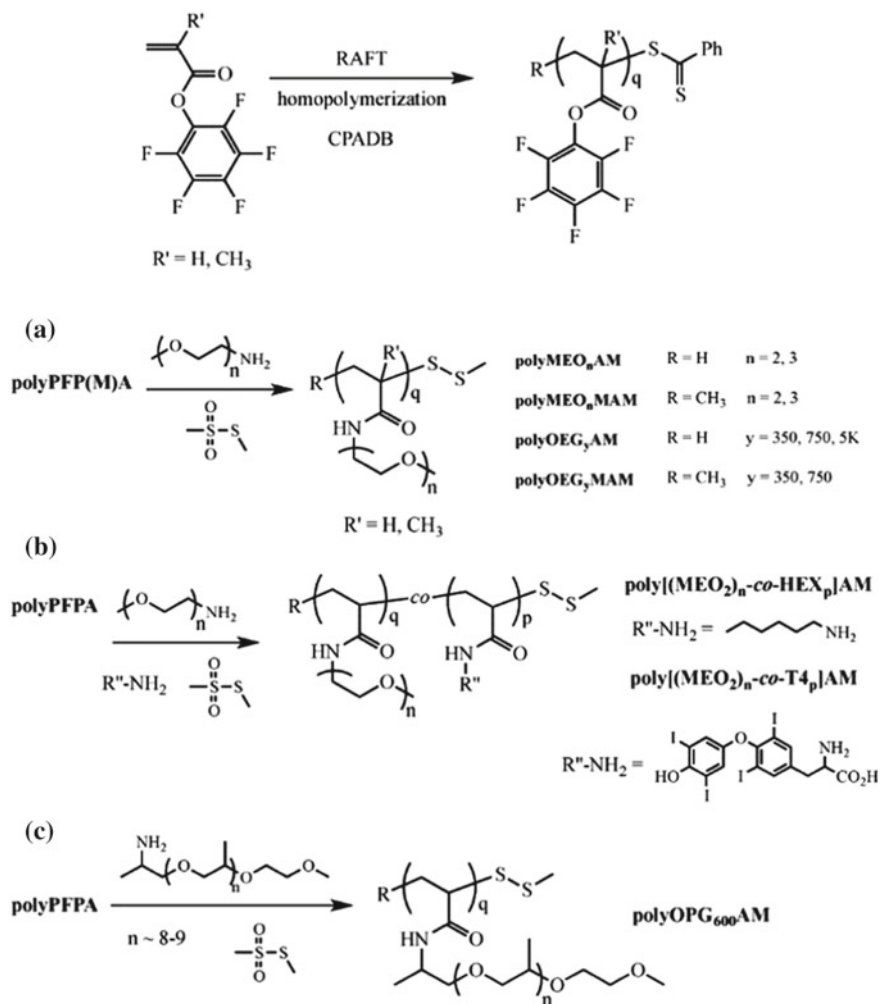


Fig. 15 Synthetic methodology of acrylamide and methacrylamide-based copolymers by RAFT. Reprinted (adapted) with permission from [78]. Copyright (2019) American Chemical Society

and poly MEO₃AM) was carried out, and it was concluded that these polymers provide >85% cell viability even after 3 days with high concentration. Hence, they were proven to be biocompatible thermoresponsive polymers [78]. Another polymer with UCST behavior is based on amphiphilic copolymer, methoxy-poly(ethylene glycol)-block-poly(acrylamide-co-acrylonitrile) (abbreviated as mPEG-b-P(AAm-co-AN)) which can be synthesized using RAFT and Michael-type addition reaction. Synthetic procedure involved in the synthesis of P(AAm-co-AN) using RAFT and synthesis of α -acryloyl- ω -methoxy-poly(ethyleneglycol) (APEG) separately followed by

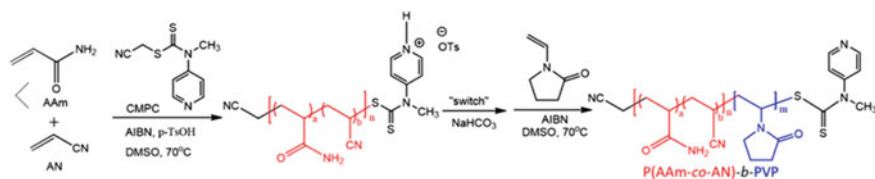


Fig. 16 Synthesis of P(AAm-co-AN)-b-PVP-based UCST block copolymer. Reprinted (adapted) with permission from [80]. Copyright (2019) American Chemical Society

Michael addition of P(AAm-co-AN) and APEG to form mPEG-b-P(AAm-co-AN)-based copolymer. Critical micelle concentration (CMC) was measured and observed that as the content of acrylamide increased hydrogen bond interaction within polymer increased; hence, CMC decreased. From the UCST behavior studies, it was shown that those copolymers were opaque at lower temperature and became transparent at higher temperature. In addition to that, UCST can be increased up to 65 °C by increasing the concentration up to 1.0 mg/ml. From the MTT assay, those polymers were proven to be compatible with normal cells and cancer cells. They also studied the drug release by loading the micelles with DOX drug and found out that cytotoxicity of free DOX was reduced after loaded within those synthesized micelles and drug-releasing capacity was increased as the temperature increases. They reported that this type of micelles can be a promising drug delivering system by being biocompatible and non-toxic [79].

In another study, poly(acrylamide-co-acrylonitrile)-b-polyvinylpyrrolidone (abbreviated as P(AAm-co-AN)-b-PVP)-based copolymer was synthesized using RAFT which is shown in Fig. 16. The synthesized block copolymer exhibited UCST behavior and micelle formation in aqueous medium. Since conventional RAFT agents were incompatible with more activated monomers (AAm and AN) and less activated monomer (VP), they have synthesized switchable RAFT agent cyanomethyl methyl(4-pyridyl)carbamodithioate (CMPC) which was used to synthesize macro-RAFT agent P(AAm-co-AN) with PDI 1.37 using AN, AIBN, and AAm in DMSO. Further, the copolymerization of macro-RAFT agent with vinylpyridine afforded (P(AAm-co-AN)-b-PVP) block copolymer with PDI of 1.25. Thermoresponsive studies were carried out for homopolymer and block copolymer, and it was observed that P(AAm-co-AN) showed UCST behavior at 20 °C whereas for the corresponding block copolymer (P(AAm-co-AN)-b-PVP) it was 30 °C. To extend the study, they deposited the block copolymer as layer-by-layer (LbL) film using TA as a partner molecule and synthesized thermoresponsive surface with reversible micelle–unimer transition within range of 40–50 °C films which can be potentially used for controlling responses of soft interfaces in biological environments [80]. In another report, RAFT was employed for the synthesis of ionic random copolymers P(OEtOxA)-ran-P[VBTP][Cl] and P(OEtOxA)-ran-P[VBUlM][Br] which showed both LCST (due to the presence of LCST-based segments P(OEtOxA)) and UCST (due to the UCST-based segments P[VBTP][Cl] and P[VBUlM][Br]) in the presence of halide ions in H₂O. This random polymers

exhibited only LCST property when the content of poly ionic liquid (PIL) was relatively low. Similarly, the copolymer with very high percentage of PIL (>90%) exhibited only UCST behavior. LCST and UCST behaviors were exhibited by a random copolymer which contained relatively high percentage of PIL in the presence of halide ion. Synthetic methodology consisted of the synthesis of macromonomer oligo(2-ethyl-2-oxazoline)acrylate (OEtOxA) using CROP followed by copolymerizing OEtOxA with [VBTP][Cl] (triphenyl-4-vinylbenzylphosphonium chloride) and P[VBuIm][Br] (3-n-butyl-1-vinylimidazolium bromide) to give corresponding random copolymers. As mentioned earlier, the thermoresponsive studies showed that P(OEtOxA) showed LCST at 56.9 °C and copolymer with very high content of P[VBTP][Cl] does not exhibit any LCST behavior. P[VBTP][Cl]-based copolymer showed increased LCST as the content of P[VBTP][Cl] increased. In the case of copolymer, which contains almost equal content of non ionic and ionic block; demonstrated both LCST and UCST behavior. By having tunable thermoresponsive property based on requirements, such polymers can be a pleasing tool as smart materials in biomedical fields [81].

4 Thermoresponsive Polymers on Surfaces Using Different Surface Polymerization Techniques

Often, thermoresponsive polymers are grafted on to various surfaces to make smart surfaces which respond to external stimuli like temperature or pH [82]. Such smart surfaces can be used as a versatile tool and bio-analytical and biomedical fields. Controlled/living radical polymerization (CLRP) techniques have been extensively employed as a synthetic tool to make smart surfaces.

SET-LRP and ATRP can be employed for the synthesis of doubly hydrophilic graft polymers which consisted of PNIPAM backbone and poly (2-vinylpyridine) (P2VP) side chain. As shown in Fig. 17, initially PNIPAM-b-PHEA diblock copolymer was synthesized using SET-LRP of NIPAM, benzyl chloride, CuCl/Me₆TREN, and 2-hydroxyethyl acrylate (HEA) in DMF. The reaction of PNIPAM-b-PHEA copolymer with 2-chloropropionyl chloride gave macroinitiator PNIPAM-b-PHEA-Cl which was used for ATRP of 2-vinylpyridine to form PNIPAM-b-(PEA-g-P2VP) (PDI in the range of 1.33–1.39). The synthesized PNIPAM-b-(PEA-g-P2VP) copolymer formed micelles at above 32 °C which consisted of insoluble PNIPAM core and PEA-g-P2VP-based corona. The author stated that those grafted copolymers can be used in applications like biological vectors and protective shells for sensitive enzymes [83].

As shown in Fig. 18, the author had synthesized poly(2-(2-methoxyethoxy)ethyl methacrylate co-oligo(ethylene glycol) methacrylate [P(MEO₂MA)-co-OEGMA]) copolymer abbreviated as P(MEO₂MA-co-OEGMA) using ATRP. These synthesized copolymers were further grafted on porous polymer monoliths to give copolymer-grafted monoliths with thermoresponsive property. From the thermoresponsive studies, LCST was found at 25.7 °C for 90/10 ratio of MEO₂MA/OEGMA and increased

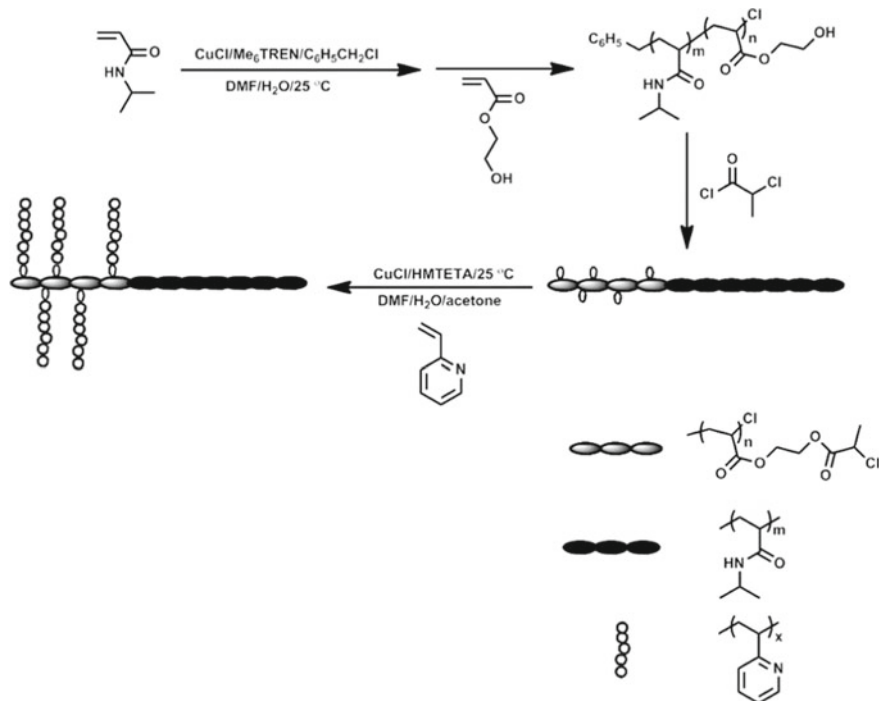


Fig. 17 ATRP of PNIPAM, PEA, and P2VP for the synthesis of PNIPAM-b-(PEA-g-P2VP)-based graft copolymer. Redrawn from Feng et al. [83]

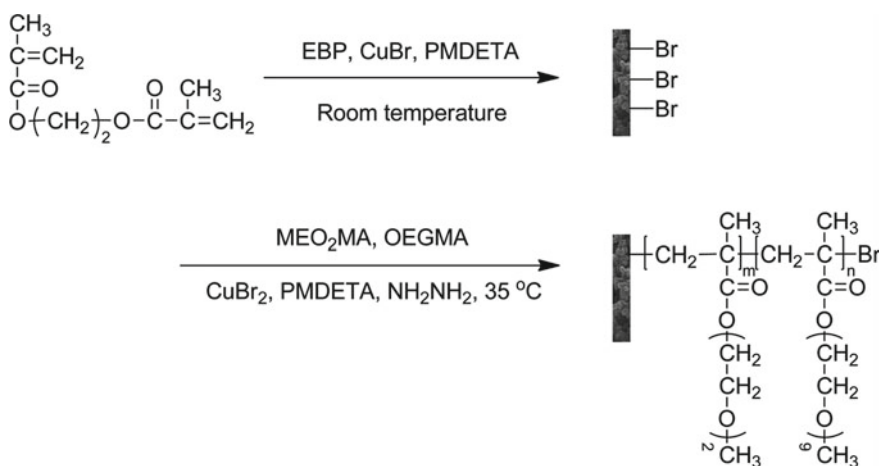


Fig. 18 Synthesis of grafted polymer consisted of P(MEO₂MA-co-OEGMA) using ATRP method. Reprinted (adapted) with permission from [84]. Copyright (2019) American Chemical Society

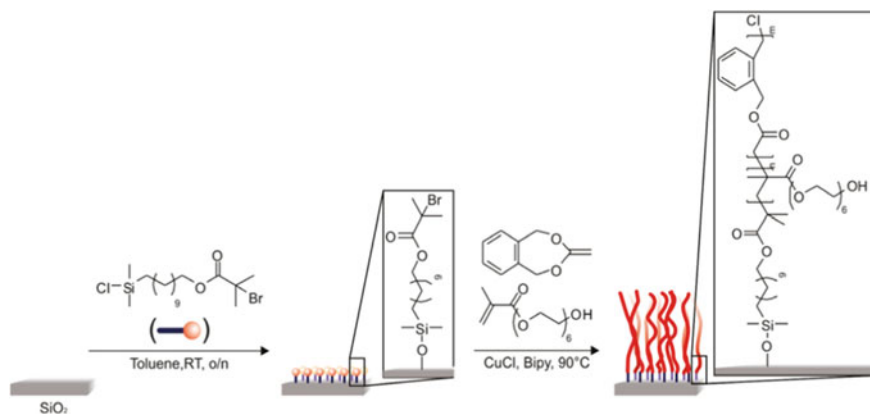


Fig. 19 Synthesis of P(PEGMA-co-BMDO) copolymer brushes using ATRP. Reprinted (adapted) with permission from [85]. Copyright (2019) American Chemical Society

as the content of OEGMA increased. For example, 80/20 ratio of MEO₂MA/OEGMA showed LCST at 44.1 °C. Those grafted copolymers were applied as a stationary phase in thermoresponsive chromatography for steroids [84].

Degradable polymer brushes were synthesized by using surface-initiated ATRP. ATRP of cyclic ketene acetal monomer- 5,6-benzo-2-methylene-1,3-dioxepane (BMDO) with PEGMA was carried out using synthesized surface immobilized initiator named (11-(2-bromo-2-methyl)propionyloxy)undecyldimethylchlorosilane (shown in Fig. 19). Based on the degradability results, it was concluded that these polymer brushes were stable under neutral or high pH while under acidic conditions they were degraded and degree of degradation can be extended by increasing the content of BMDO and decreasing pH. The author suggested that those brushes can be an interesting platform for degradable coatings which can be used in various applications (controlled drug release or tissue engineering) [85].

Biocompatible silicon oxide surfaces were prepared using surface-initiated NMP of oligo(ethylene glycol) (OEG)-based monomer. As mentioned in Fig. 20, the polymerization was initiated using TEMPO anchored on silicon oxide to give both homopolymer- and copolymer-based surfaces which can be used in fabrication of devices for the use as biological and chemical devices [86].

5 Conclusion

From the above discussion, it is clear that the thermoresponsive behavior and biocompatibility largely depend on the nature of repeating units even though fine-tuning is possible by changing the end group or controlling the molecular weights. Biocompatibility is an important issue for their applications, especially for drug delivery, which should be addressed on case-by-case basis rather than as a universal solution.

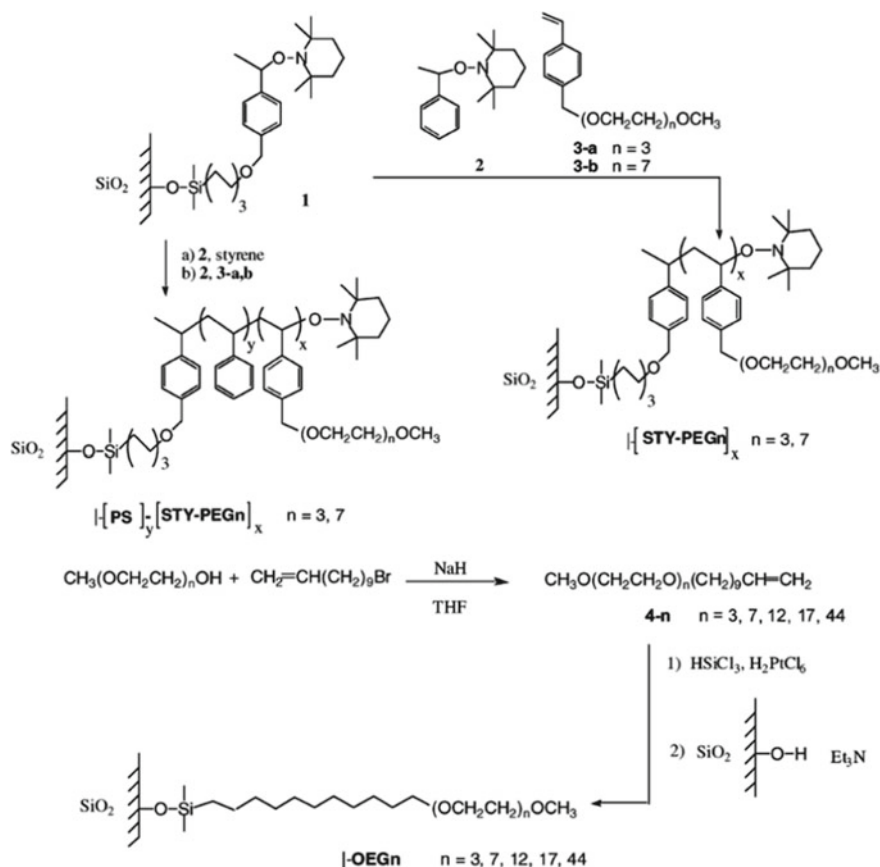


Fig. 20 Synthesis of OEGn-based polymer brushes on silicon oxide surfaces using NMP. Reprinted (adapted) with permission from [86]. Copyright (2019) American Chemical Society

A biodegradable connecting linker plays an important role in improving biocompatibility. The choice of polymerization technique is important since it can provide the control over dispersity and molecular weight in various degrees. Particularly, atom transfer radical polymerization (ATRP) has been widely used because of better control over molecular weight or choice of a particular end group. On the other hand, RAFT polymerization techniques have been used occasionally for their versatility. Finally, in some special cases, polymerizations have been performed on surfaces to make thin thermoresponsive brushes, which can find applications in controlled drug release or tissue engineering.

References

1. Teotia AK, Sami H, Kumar A (2015) Thermo-responsive polymers: structure and design of smart materials. In: Zhang Z (eds) Switchable and responsive surfaces and materials for biomedical applications. Woodhead Publishing, pp 3–43. <https://doi.org/10.1016/c2013-0-16356-8>
2. James HP, John R, Alex A, Anoop KR (2014) Smart polymers for the controlled delivery of drugs—a concise overview. *Acta Pharmacol Sin B* 4:120–127. <https://doi.org/10.1016/j.apsb.2014.02.005>
3. Ilmain F, Tanaka T, Kokufuta E (1991) Volume transition in a gel driven by hydrogen bonding. *Nature* 349:400–401. <https://doi.org/10.1038/349400a0>
4. Ward MA, Georgiou TK (2011) Thermoresponsive polymers for biomedical applications. *Polymers* 3:1215–1242. <https://doi.org/10.3390/polym3031215>
5. Zhu YC, Batchelor R, Lowe AB, Roth PJ (2016) Design of thermoresponsive polymers with aqueous LCST, UCST, or both: modification of a reactive poly(2-vinyl-4,4-dimethylazlactone) Scaffold. *Macromolecules* 49:672–680. <https://doi.org/10.1021/acs.macromol.5b02056>
6. Southall NT, Dill KA, Haymet ADJ (2002) A view of the hydrophobic effect. *J Phys Chem B* 106:521–533. <https://doi.org/10.1021/jp015514e>
7. Aguilar MR, San Roman J (2014) Introduction to smart polymers and their applications. In: Aguilar MR, San Roman J (eds) Smart polymers and their applications. Woodhead Publishing, pp 1–11. <https://doi.org/10.1533/9780857097026.1>
8. Hoffman AS, Stayton PS, Bulmus V, Chen G, Chen J, Cheung C, Chilkoti A, Ding Z, Dong L, Fong R (2000) Really smart bioconjugates of smart polymers and receptor proteins. *J Biomed Mater Res* 52:577–586. [https://doi.org/10.1002/1097-4636\(20001215\)52:4%3c577:aid-jbm1%3e3.0.co;2-5](https://doi.org/10.1002/1097-4636(20001215)52:4%3c577:aid-jbm1%3e3.0.co;2-5)
9. Liu RX, Fraylich M, Saunders BR (2009) Thermoresponsive copolymers: from fundamental studies to applications. *Colloid Polym Sci* 287:627–643. <https://doi.org/10.1007/s00396-009-2028-x>
10. Feil H, Bae YH, Feijen J, Kim SW (1993) Effect of comonomer hydrophilicity and ionization on the lower critical solution temperature of N-isopropylacrylamide copolymers. *Macromolecules* 26:2496–2500. <https://doi.org/10.1021/ma00062a016>
11. Shimada N, Ino H, Maie K, Nakayama M, Kano A, Maruyama A (2011) Ureido-derivatized polymers based on both poly(allylurea) and poly(L-citrulline) exhibit UCST-type phase transition behavior under physiologically relevant conditions. *Biomacromol* 12:3418–3422. <https://doi.org/10.1021/bm2010752>
12. Plamper FA, Schmalz A, Ballauff M, Muller AHE (2007) Tuning the thermoresponsiveness of weak polyelectrolytes by pH and light: lower and upper critical-solution temperature of poly(N, N-dimethylaminoethyl methacrylate). *J Am Chem Soc* 129:14538–14539. <https://doi.org/10.1021/ja074720i>
13. Wu DC, Liu Y, He CB (2008) Thermal- and pH-responsive degradable polymers. *Macromolecules* 41:18–20. <https://doi.org/10.1021/ma7024896>
14. Fujishige S, Kubota K, Ando I (1989) Phase-transition of aqueous-solutions of poly(N-Isopropylacrylamide) and poly(N-isopropylmethacrylamide). *J Phys Chem* 93:3311–3313. <https://doi.org/10.1021/j100345a085>
15. Pentela N, Ayyappan VG, Krishnamurthy M, Boopathi AA, Rainu S, Sampath S, Mandal AB, Samanta D (2017) A comparative study of pH-responsive microcapsules from different nanocomposites. *Green Mater* 5:53–62. <https://doi.org/10.1680/jgrma.16.00023>
16. Pentela N, Duraipandy N, Sainath N, Parandhaman T, Kiran MS, Das SK, Jaisankar SN, Samanta D (2018) Microcapsules from diverse polyfunctional materials: synergistic interactions for a sharp response to pH changes. *New J Chem* 42:8366–8373. <https://doi.org/10.1039/C7NJ03744A>
17. Winnik FM (1990) Phase transition of aqueous poly-(N-isopropylacrylamide) solutions: a study by non-radiative energy transfer. *Polymer* 31:2125–2134. [https://doi.org/10.1016/0032-3861\(90\)90085-D](https://doi.org/10.1016/0032-3861(90)90085-D)

18. Wang XH, Wu C (1999) Light-scattering study of coil-to-globule transition of a poly(N-isopropylacrylamide) chain in deuterated water. *Macromolecules* 32:4299–4301. <https://doi.org/10.1021/ma9902450>
19. Cao Y, Zhu XX, Luo JT, Liu HY (2007) Effects of substitution groups on the RAFT polymerization of N-Alkylacrylamides in the preparation of thermosensitive block copolymers. *Macromolecules* 40:6481–6488. <https://doi.org/10.1021/ma0628230>
20. Heskins M, Guillet JE (1968) Solution properties of poly(N-isopropylacrylamide). *J Macromol Sci A* 2:1441–1455. <https://doi.org/10.1080/10601326808051910>
21. Kobayashi M, Ishizone T, Nakahama S (2000) Synthesis of highly isotactic poly(N, N-diethylacrylamide) by anionic polymerization with grignard reagents and diethylzinc. *J Polym Sci A* 38:4677–4685. [https://doi.org/10.1002/1099-0518\(200012\)38:1+%3c4677:AID-POLA70%3e3.0.CO;2-%23](https://doi.org/10.1002/1099-0518(200012)38:1+%3c4677:AID-POLA70%3e3.0.CO;2-%23)
22. Christova D, Velichkova R, Loos W, Goethals EJ, Du Prez F (2003) New thermo-responsive polymer materials based on poly (2-ethyl-2-oxazoline) segments. *Polymer* 44:2255–2261. [https://doi.org/10.1016/s0032-3861\(03\)00139-3](https://doi.org/10.1016/s0032-3861(03)00139-3)
23. Jiang J, Tong X, Zhao Y (2005) A new design for light-breakable polymer micelles. *J Am Chem Soc* 127:8290–8291. <https://doi.org/10.1021/ja0521019>
24. Zhao C, Zhuang X, He C, Chen X, Jing X (2008) Synthesis of novel thermo- and pH-responsive poly(L-lysine)-based copolymer and its micellization in water. *Macromol Rapid Commun* 29:1810–1816. <https://doi.org/10.1002/marc.200800494>
25. Karir T, Sarma HD, Samuel G, Hassan PA, Padmanabhan D, Venkatesh M (2013) Preparation and evaluation of radioiodinated thermoresponsive polymer based on poly(N-isopropyl acrylamide) for radiotherapy. *J Appl Polym Sci* 130:860–868. <https://doi.org/10.1002/app.39235>
26. Hong MC, Choi MC, Chang YW, Lee Y, Kim J, Rhee H (2012) Palladium nanoparticles on thermoresponsive hydrogels and their application as recyclable Suzuki-Miyaura coupling reaction catalysts in water. *Adv Synth Catal* 354:1257–1263. <https://doi.org/10.1002/adsc.201100965>
27. Fan Y, Boulif N, Picchioni F (2018) Thermo-responsive starch-g-(PAM-co-PNIPAM): controlled synthesis and effect of molecular components on solution rheology. *Polymers* 10:92. <https://doi.org/10.3390/polym10010092>
28. Sun S, Wu P (2011) Infrared spectroscopic insight into hydration behavior of poly(n-vinylcaprolactam) in water. *J Phys Chem B* 115:11609–11618. <https://doi.org/10.1021/jp2071056>
29. Ramos J, Imaz A, Forcada J (2012) Temperature-sensitive nanogels: poly(N-vinylcaprolactam) versus poly(N-isopropylacrylamide). *Polym Chem* 3:852–856. <https://doi.org/10.1039/C2PY00485B>
30. Jones MW, Gibson MI, Mantovanib G, Haddletona DM (2011) Tunable thermo-responsive polymer-protein conjugates via a combination of nucleophilic thiol-ene “click” and SET-LRP. *Polym Chem* 2:572–574. <https://doi.org/10.1039/C0PY00329H>
31. Chilkoti A, Dreher MR, Meyer DE, Raucher D (2002) Targeted drug delivery by thermally responsive polymers. *Adv Drug Deliv Rev* 54:613–630. [https://doi.org/10.1016/s0169-409x\(02\)00041-8](https://doi.org/10.1016/s0169-409x(02)00041-8)
32. Enzenberg A, Laschewsky A, Boeffel C, Wischerhoff E (2016) Influence of the near molecular vicinity on the temperature regulated fluorescence response of poly(N-vinylcaprolactam). *Polymers* 8:109–129. <https://doi.org/10.3390/polym8040109>
33. Vihola H, Laukkanen A, Valtola L, Tenhu H, Hirvonen J (2005) Cytotoxicity of thermosensitive polymers poly(N-isopropylacrylamide), poly(N-vinylcaprolactam) and amphiphilically modified poly (N-vinylcaprolactam). *Biomaterials* 26:3055–3064. <https://doi.org/10.1016/j.biomaterials.2004.09.008>
34. Chee CK, Rimmer S, Soutar I, Swanson L (2006) Fluorescence investigations of the conformational behaviour of poly(N-vinylcaprolactam). *React Funct Polym* 66:1–11. <https://doi.org/10.1016/j.reactfunctpolym.2005.07.007>

35. Moerkerke R, Meeussen F, Koningsveld R, Berghmans H, Mondelaers W, Schacht E, Dušek K, Šolc K (1998) Phase transitions in swollen networks. 3. Swelling behavior of radiation cross-linked poly(vinyl methyl ether) in water. *Macromolecules* 31:2223–2229. <https://doi.org/10.1021/ma971512+>
36. Zhang WZ, Chen XD, Luo WA, Yang J, Zhang MQ, Zhu FM (2009) Study of phase separation of poly(vinyl methyl ether) aqueous solutions with rayleigh scattering technique. *Macromolecules* 42:1720–1725. <https://doi.org/10.1021/ma802671a>
37. Chiu TT (1986) Poly(2-ethy-2-oxazoline): a new water-and organic soluble adhesive. *Water Soluble Polym* 213:425–433. <https://doi.org/10.1021/ba-1986-0213.ch023>
38. Chen CH, Wilson J, Chen W, Davis RM, Riffle JS (1994) A light-scattering study of poly(2-alkyl-2-oxazoline)s: effect of temperature and solvent type. *Polymer* 35:3587–3591. [https://doi.org/10.1016/0032-3861\(94\)90532-0](https://doi.org/10.1016/0032-3861(94)90532-0)
39. Schmaljohann D (2006) Thermo-and pH-responsive polymers in drug delivery. *Adv Drug Deliv Rev* 58:1655–1670. <https://doi.org/10.1016/j.addr.2006.09.020>
40. Hoogenboom R, Schlaad H (2011) Bioinspired poly(2-oxazoline) s. *Polymers* 3:467–488. <https://doi.org/10.3390/polym3010467>
41. Aoki T, Kawashima M, Katono H, Sanui K, Ogata N, Okano T, Sakurai Y (1994) Temperature-responsive interpenetrating polymer networks constructed with poly(acrylic acid) and poly(N, N-dimethylacrylamide). *Macromolecules* 27:947–952. <https://doi.org/10.1021/ma00082a010>
42. York AW, Kirkland SE, McCormick CL (2008) Advances in the synthesis of amphiphilic block copolymers via RAFT polymerization: stimuli-responsive drug and gene delivery. *Adv Drug Deliv Rev* 60:1018–1036. <https://doi.org/10.1016/j.addr.2008.02.006>
43. Matyjaszewski K, Patten TE, Xia JH (1997) Controlled/“living” radical polymerization. Kinetics of the homogeneous atom transfer radical polymerization of styrene. *J Am Chem Soc* 119:674–680. <https://doi.org/10.1021/ja963361g>
44. Patten TE, Matyjaszewski K (1999) Copper(I)-catalyzed atom transfer radical polymerization. *Acc Chem Res* 32:895–903. <https://doi.org/10.1021/ar9501434>
45. Matyjaszewski K, Xia JH (2001) Atom transfer radical polymerization. *Chem Rev* 101:2921–2990. <https://doi.org/10.1021/cr940534g>
46. Mishra V, Kumar R (2012) Living radical polymerization: a review. *J Sci Res* 56:141–176
47. Arslan H (2012) Block and graft copolymerization by controlled/living radical polymerization methods. In: Gomes ADS (eds) *Polymerization*. InTechOpen., pp 279–320. <https://doi.org/10.5772/45970>
48. Haddleton DM, Crossman MC (1997) Synthesis of methacrylic multi-arm star copolymers by “arm-first” group transfer polymerisation. *Macromol Chem Phys* 198:871–881. <https://doi.org/10.1002/macp.1997.021980317>
49. Matyjaszewski K (2005) Macromolecular engineering: from rational design through precise macromolecular synthesis and processing to targeted macroscopic material properties. *Prog Polym Sci* 30:858–875. <https://doi.org/10.1016/j.progpolymsci.2005.06.004>
50. Braunecker WA, Matyjaszewski K (2007) Controlled/living radical polymerization: features, developments, and perspectives. *Prog Polym Sci* 32:93–146. <https://doi.org/10.1016/j.progpolymsci.2006.11.002>
51. Wever DAZ, Raffa P, Picchioni F, Broekhuis AA (2012) Acrylamide homopolymers and acrylamide-N-isopropylacrylamide block copolymers by atomic transfer radical polymerization in water. *Macromolecules* 45:4040–4045. <https://doi.org/10.1021/ma3006125>
52. Fischer H (1986) Unusual selectivities of radical reactions by internal suppression of fast modes. *J Am Chem Soc* 108:3925–3927. <https://doi.org/10.1021/ja00274a012>
53. Wang Y, Zhang MJ, Zhang YZ, Magenau AJD, Matyjaszewski K (2012) Halogen conservation in atom transfer radical polymerization. *Macromolecules* 45:8929–8932. <https://doi.org/10.1021/ma3018958>
54. Loh XJ, Zhang ZX, Wu YL, Lee TS, Li J (2009) Synthesis of novel biodegradable thermoresponsive triblock copolymers based on poly(R)-3-hydroxybutyrate and poly(N-isopropylacrylamide) and their formation of thermoresponsive micelles. *Macromolecules* 42:194–202. <https://doi.org/10.1021/ma8019865>

55. Shinde VS, Girme MR, Pawar VU (2011) Thermoresponsive polystyrene-*b*-poly (N-isopropylacrylamide) copolymers by atom transfer radical polymerization. *Indian J Chem* 50A:781–787
56. Quan ZL, Zhu KZ, Knudsen KD, Nystrom B, Lund R (2013) Tailoring the amphiphilicity and self-assembly of thermosensitive polymers: end-capped PEG-PNIPAAm block copolymers. *Soft Matter* 9:10768–10778. <https://doi.org/10.1039/C3SM51945G>
57. Galperin A, Long TJ, Garty S, Ratner BD (2013) Synthesis and fabrication of a degradable poly(N-isopropyl acrylamide) scaffold for tissue engineering applications. *J Biomed Mater Res A* 101:775–786. <https://doi.org/10.1002/jbm.a.34380>
58. Li CM, Buurma NJ, Haq I, Turner C, Armes SP, Castelletto V, Hamley IW, Lewis AL (2005) Synthesis and characterization of biocompatible, thermoresponsive ABC and ABA triblock copolymer gelators. *Langmuir* 21:11026–11033. <https://doi.org/10.1021/la0515672>
59. Qiao ZY, Du FS, Zhang R, Liang DH, Li ZC (2010) Biocompatible thermoresponsive polymers with pendent oligo(ethylene glycol) chains and cyclic ortho ester groups. *Macromolecules* 43:6485–6494. <https://doi.org/10.1021/ma101090g>
60. Tai HY, Wang WX, Vermonden T, Heath F, Hennink WE, Alexander C, Shakesheff KM, Howdle SM (2009) Thermoresponsive and photocrosslinkable PEGMEMA-PPGMA-EGDMA copolymers from a one-step ATRP synthesis. *Biomacromol* 10:822–828. <https://doi.org/10.1021/bm801308q>
61. Mori H, Iwaya H, Nagai A, Endo T (2005) Controlled synthesis of thermoresponsive polymers derived from L-proline via RAFT polymerization. *Chem Commun* 4872–4874. <https://doi.org/10.1039/b509212d>
62. Cui QL, Wu FP, Wang EJ (2011) Thermosensitive behavior of poly(ethylene glycol)-based block copolymer (PEG-*b*-PADMO) controlled via self-assembled microstructure. *J Phys Chem B* 115:5913–5922. <https://doi.org/10.1021/jp200659u>
63. Zhu JL, Zhang XZ, Cheng H, Li YY, Cheng SX, Zhuo RX (2007) Synthesis and characterization of well-defined, amphiphilic poly(N-isopropylacrylamide)-*b*-2-hydroxyethyl methacrylate-poly(epsilon-caprolactone) (n) graft copolymers by RAFT polymerization and macromonomer method. *J Polym Sci A* 45:5354–5364. <https://doi.org/10.1002/pola.22280>
64. Zhang L, Bernard J, Davis TP, Barner-Kowollik C, Stenzel MH (2008) Acid-degradable core-crosslinked micelles prepared from thermosensitive glycopolymers synthesized via RAFT polymerization. *Macromol Rapid Commun* 29:123–129. <https://doi.org/10.1002/marc.200700663>
65. Li YY, Cheng H, Zhu JL, Yuan L, Dai Y, Cheng SX, Zhang XZ, Zhuo RX (2009) Temperature- and pH-sensitive multicolored micellar complexes. *Adv Mater* 21:2402–2406. <https://doi.org/10.1002/adma.200803770>
66. Ryu JH, Chacko RT, Jiwanpanich S, Bickerton S, Babu RP, Thayumanavan S (2010) Self-cross-linked polymer nanogels: a versatile nanoscopic drug delivery platform. *J Am Chem Soc* 132:17227–17235. <https://doi.org/10.1021/ja1069932>
67. Aguirre G, Ramos J, Heuts JPA, Forcada J (2014) Biocompatible and thermo-responsive nanocapsule synthesis through vesicle templating. *Polym Chem* 5:4569–4579. <https://doi.org/10.1039/c4py00297k>
68. Pissuwan D, Boyer C, Gunasekaran K, Davis TP, Bulmus V (2010) In vitro cytotoxicity of RAFT polymers. *Biomacromol* 11:412–420. <https://doi.org/10.1021/bm901129x>
69. Shen WQ, Chang YL, Liu GY, Wang HF, Cao AN, An ZS (2011) Biocompatible, antifouling, and thermosensitive core-shell nanogels synthesized by RAFT aqueous dispersion polymerization. *Macromolecules* 44:2524–2530. <https://doi.org/10.1021/ma200074n>
70. Jeong NS, Redhead M, Bosquillon C, Alexander C, Kelland M, O'Reilly RK (2011) The missing lactam-thermosensitive and biocompatible poly(N-vinylpiperidone) polymers by xanthate-mediated RAFT polymerization. *Macromolecules* 44:886–893. <https://doi.org/10.1021/ma1026466>
71. Chen SL, Wang K, Zhang WQ (2017) A new thermoresponsive polymer of poly(N-acryloylsarcosine methyl ester) with a tunable LCST. *Polym Chem* 8:3090–3101. <https://doi.org/10.1039/c7py00274b>

72. Huang YS, Chen JK, Chen T, Huang CF (2017) Synthesis of PNVP-bzased copolymers with tunable thermosensitivity by sequential reversible addition-fragmentation chain transfer copolymerization and ring-opening polymerization. *Polymers* 9:231–244. <https://doi.org/10.3390/polym9060231>
73. Hedir GG, Arno MC, Langlais M, Husband JT, O'Reilly RK, Dove AP (2017) Poly(oligo(ethylene glycol) vinyl acetate): a versatile class of thermoresponsive and biocompatible polymers. *Angew Chem* 56:9178–9182. <https://doi.org/10.1002/ange.201703763>
74. Chenal M, Mura S, Marchal C, Gignes D, Charleux B, Fattal E, Couvreur P, Nicolas J (2010) Facile synthesis of innocuous comb-shaped polymethacrylates with peg side chains by nitroxide-mediated radical polymerization in hydroalcoholic solutions. *Macromolecules* 43:9291–9303. <https://doi.org/10.1021/ma101880m>
75. Popescu D, Hoogenboom R, Keul H, Moeller M (2010) Thermoresponsive polyacrylates obtained via a cascade of enzymatic transacylation and FRP or NMP. *Polym Chem* 1:878–890. <https://doi.org/10.1039/C0PY00051E>
76. Tian HY, Yan JJ, Wang D, Gu C, You YZ, Chen XS (2011) Synthesis of thermo-responsive polymers with both tunable UCST and LCST. *Macromol Rapid Commun* 32:660–664. <https://doi.org/10.1002/marc.201000713>
77. Roth PJ, Jochum FD, Theato P (2011) UCST-type behavior of poly oligo(ethylene glycol) methyl ether methacrylate (POEGMA) in aliphatic alcohols: solvent, co-solvent, molecular weight, and end group dependences. *Soft Matter* 7:2484–2492. <https://doi.org/10.1039/C0SM01324B>
78. Chua GBH, Roth PJ, Duong HTT, Davis TP, Lowe AB (2012) Synthesis and thermoresponsive solution properties of poly oligo(ethylene glycol) (meth)acrylamides: biocompatible peg analogues. *Macromolecules* 45:1362–1374. <https://doi.org/10.1021/ma202700y>
79. Huang G, Li H, Feng ST, Li XQ, Tong GQ, Liu J, Quan CY, Jiang Q, Zhang C, Li ZP (2015) Self-assembled UCST-type micelles as potential drug carriers for cancer therapeutics. *Macromol Chem Phys* 216:1014–1023. <https://doi.org/10.1002/macp.201400546>
80. Palanisami A, Sukhishvili SA (2018) Swelling transitions in layer-by-layer assemblies of UCST block copolymer micelles. *Macromolecules* 51:3467–3476. <https://doi.org/10.1021/acs.macromol.8b00519>
81. Jana S, Biswas Y, Anas M, Saha A, Mandal TK (2018) Poly oligo(2-ethyl-2-oxazoline)acrylate-based poly(ionic liquid) random copolymers with coexistent and tunable lower critical solution temperature- and upper critical solution temperature-type phase transitions. *Langmuir* 34:12653–12663. <https://doi.org/10.1021/acs.langmuir.8b03022>
82. Murugan P, Krishnamurthy M, Jaisankar SN, Samanta D, Mandal AB (2015) Controlled decoration of the surface with macromolecules: polymerization on a self-assembled monolayer (SAM). *Chem Soc Rev* 44:3212–3243. <https://doi.org/10.1039/C4CS00378K>
83. Feng C, Li YJ, Yang D, Li YG, Hu JH, Zhai SJ, Lu GL, Huang XY (2010) Synthesis of well-defined PNIPAM-b-(PEA-g-P2VP) double hydrophilic graft copolymer via sequential SET-LRP and ATRP and its “schizophrenic” micellization behavior in aqueous media. *J Polym Sci A* 48:15–23. <https://doi.org/10.1002/pola.23716>
84. Li N, Qi L, Shen Y, Li YP, Chen Y (2013) Thermoresponsive oligo(ethylene glycol)-based polymer brushes on polymer monoliths for all-aqueous chromatography. *ACS Appl Mater Interfaces* 5:12441–12448. <https://doi.org/10.1021/am403510g>
85. Riachi C, Schuwer N, Klok HA (2009) Degradable polymer brushes prepared via surface-initiated controlled radical polymerization. *Macromolecules* 42:8076–8081. <https://doi.org/10.1021/ma901537x>
86. Andruzzi L, Senaratne W, Hexemer A, Sheets ED, Ilic B, Kramer EJ, Baird B, Ober CK (2005) Oligo(ethylene glycol) containing polymer brushes as bioselective surfaces. *Langmuir* 21:2495–2504. <https://doi.org/10.1021/la047574s>

Chapter 8

Reversible Addition-Fragmentation Chain Transfer (RAFT) Polymerization in Ionic Liquids: A Sustainable Process



Arunjunai R. S. Santha Kumar and Nikhil K. Singha

Abstract Ionic liquid (IL) is an important class of materials which have asymmetric organic cation and inorganic anion. Most of the ILs remain as liquids at ambient temperature and are non-toxic in nature. They have low-to-zero vapor pressure and high thermal stability and have the potential to replace many volatile organic solvents. They have several advantages over conventional solvents and are considered as 'green' solvents. In polymer science, they are used as solvents for polymerization as well as an additive in polymer processing. In this case, IL was used as the solvent for the polymerization of different acrylates via a reversible addition-fragmentation chain transfer (RAFT) process, a method of controlled radical polymerization. RAFT polymerization in IL was observed to be remarkably fast. The IL used in the polymerization process was successfully recovered and reused without any loss in efficiency or efficacy. It was also observed that the presence of even a small amount of IL can increase the rate of polymerization.

Keywords Ionic liquids · RAFT polymerization · Green solvents · Sustainable solvents · Kinetics · Recycling · Furfuryl methacrylate · Butyl methacrylate

1 Introduction

Ionic liquids (ILs) are organic salts with asymmetric ions that remain as liquids below 100 °C. The common ILs are made of organic cations based on imidazolium, ammonium, and pyridinium organic compounds, and anions include halides, nitrates, hexafluorophosphates, tetrafluoro borates, fluorosulfonylamides, etc. The properties of ILs depend on these constituting ions. There are numerous combinations of the ions including binary and ternary mixtures which can be used to tailor-make ILs with task-specific properties. The polarity, melting temperature, miscibility, and solvation are a few examples of properties that can be easily manipulated by changing

A. R. S. Santha Kumar · N. K. Singha (✉)
Rubber Technology Centre, Indian Institute of Technology Kharagpur, Kharagpur, West Bengal
721302, India
e-mail: nks8888@yahoo.com; nks@rtc.iitkgp.ernet.in

© Springer Nature Singapore Pte Ltd. 2020
V. Katiyar et al. (eds.), *Advances in Sustainable Polymers*, Materials Horizons: From
Nature to Nanomaterials, https://doi.org/10.1007/978-981-15-1251-3_8

the constituting ions of the ILs, which earned ILs its rightful name ‘designer solvents.’ For example, increasing the alkyl chain length of the imidazolium cation, from methyl (T_m 125 °C) to butyl (T_m 65 °C) will reduce the melting point of the IL with the same counter anion significantly. As they are salts, they have no measurable vapor pressure, even at high temperature. Thus, they can be employed for high-temperature solvent applications up to 350 °C at relatively low pressure. They have thermal stability, no volatile organic content (VOC), no vapor pressure at higher temperature, combined with its ability to recycle increases the environmental safety of these solvents. Hence, they are referred to as ‘green’ solvents. ILs are generally non-corrosive, non-flammable, and viscous solvents compared to common organic solvents. Their polarity is similar to that of alcohols. ILs have been used as solvents for organic reactions for more than a decade. They interact with the solutes through weak van der Waals forces [1], dispersion forces, strong hydrogen bonding [2], dipole–dipole, and ionic interactions [3]. In 1990, Carlin et al. [4] first used IL as a solvent for polymerization with Ziegler–Natta catalysis. Later in 2000, Noda et al. [5] described free radical polymerization in IL. In 2002, the first RAFT polymerization in IL was studied by Perrier et al. [6]. IL has been used as a solvent for a variety of polymerization reactions like polycondensation [7], cationic polymerization [8] other controlled radical polymerizations [9], and so on. It should be noted that the imidazolium-based ILs deactivate the anionic initiators, and hence anionic polymerization reaction is very tedious in ILs [10]. The ILs are known to increase the rate of polymerization reactions and increase the yield of polymer. For example, Vygodskii et al. [11] reported that PMMA produced in IL had molecular weight up to 5.7×10^6 Da. Even though it has been established that ILs increase the rate of polymerization, the exact mechanism for this positive effect is still speculative. There have been many reviews [12–16] and books [17–21] written on this topic.

2 Polymerization of Methacrylates in ILs

The RAFT polymerization of methacrylates such as furfuryl methacrylate (FMA) and butyl methacrylate (BMA) has been studied in different commercially available ionic liquids like 3-butyl-1-methyl imidazolium hexafluorophosphate (BMIM[PF₆]), 3-butyl-1-methyl imidazolium tetrafluoroborate (BMIM[BF₄]), and 3-ethyl-1-methyl imidazolium ethyl sulfate (EMIM[EtOSO₃]). These are room temperature ionic liquids with different counterions and varying polarity. FMA, a functional monomer, is polymerized using 2-cyano-2-propyl dodecyl trithiocarbonate (CPDTC) as a RAFT agent, thermally initiated and studied in both organic and ionic solvents and also in bulk conditions. BMIM[PF₆] is used, and it is relatively non-polar and is immiscible with water. The FMA is partially miscible with BMIM[PF₆], where mechanical stirring helps in achieving a homogenous mixture. The summary of the polymerization reactions and the polymers obtained are listed in the following table.

Table 1 shows that the IL offers a higher monomer conversion rate, both in case of high-temperature AIBN-initiated polymerization. It can also be noted that the

Table 1 Summary of RAFT polymerization of FMA using BMIM[PF₆] as IL and toluene as solvent^a

S. no	RAFT agent	Solvent	Time (h)	Conversion (%)	M_n , GPC (g/mol)	M_n , theo (g/mol)	\bar{D}
1	CPDTC	IL	1	98	9800	10,200	1.38
2	CPDTC	Toluene	1	27	5100	3100	1.28
3 ^b	CPBDT	IL	5	40	3600	4400	1.05
6	CPDTC	Recycled IL	1.2	95	9100	9900	1.31
7 ^c	CPDTC	–	1	98	Gelled	–	–
8	Without RAFT	IL	1	98	Gelled		

^a[M]:[RAFT]:[Initiator] = 240:4:1, Temp^r = 70 °C, AIBN initiator, 2-cyano-2-propyl dodecyl trithiocarbonate as RAFT agent. ^bCPBDT, 2-cyano 2-propyl benzodithioate was used as RAFT reagent. ^cPolymerization is carried out in bulk at 70 °C

dispersity of the polymers obtained is narrow indicating a controlled polymerization reaction. In case of organic solvents, the monomer conversion is found to be low, and the molar mass distribution of the polymers is found to be broad in GPC. Also, it should be noted that the reactions in ILs are faster than the same in organic liquids. The polymerization is studied in bulk conditions with/without RAFT agents which resulted in gelation, rendering the product useless. The IL used is recycled using chloroform/toluene, which is discussed later in the chapter, and the polymerization of FMA is studied in recycled IL also. It can be seen that the polymerization in recycled IL produces similar results as that of pure ILs, showing that ILs can be reused and it could be an alternate ‘green’ solvent to replace the organic solvents.

The question of the miscibility of monomer and the IL is important as it would directly affect the rate of polymerization. The FMA is polymerized with CPDTC which has a long aliphatic non-polar chain which could stabilize the monomer droplets in BMIM[PF₆]. This would form stabilized nano-droplets of monomer in IL and control the particle size of the polymer formed [22]. The particle size is measured to be 26 d.nm with Dynamic Light Scattering (DLS), and the histogram is shown in Fig. 1. To investigate further, another RAFT agent without a long-chain hydrocarbon is used to compare the particle size of the polymer. 2-cyano-2-propyl benzodithioate (CPBDT) is used, and the results are given in Table 1 and Fig 1. The absence of long-chain hydrocarbon leads to poor stabilization and Ostwald ‘ripening,’ and the particle size of the resulting polymer is not homogeneous (20, 1300 and 5100 d.nm) and it is found to be higher than that of the polymer polymerized by CPDTC. To show the stabilization effect of CPDTC RAFT, TEM images are taken of the FMA/BMIM[PF₆] mixture with CPDTC and shown in Fig. 2. The CPDTC provided good stabilization effect and a stable suspension with uniform particle size is obtained.

BMA is a relatively non-polar monomer found to be immiscible with the non-polar BMIM[PF₆] IL. This gives an opportunity to study the effects of IL on a monomer/IL

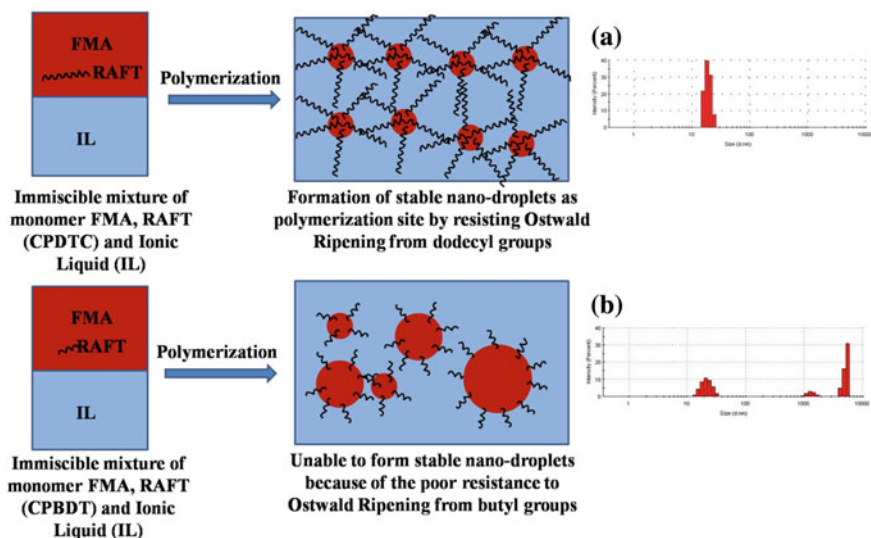


Fig. 1 Schematic representation of size variation of the particles in the presence of CPDTC (a) and CPBDT (b) RAFT reagent in FMA and IL mixture. Reproduced from Ref. [24] with permission from the Royal Society of Chemistry

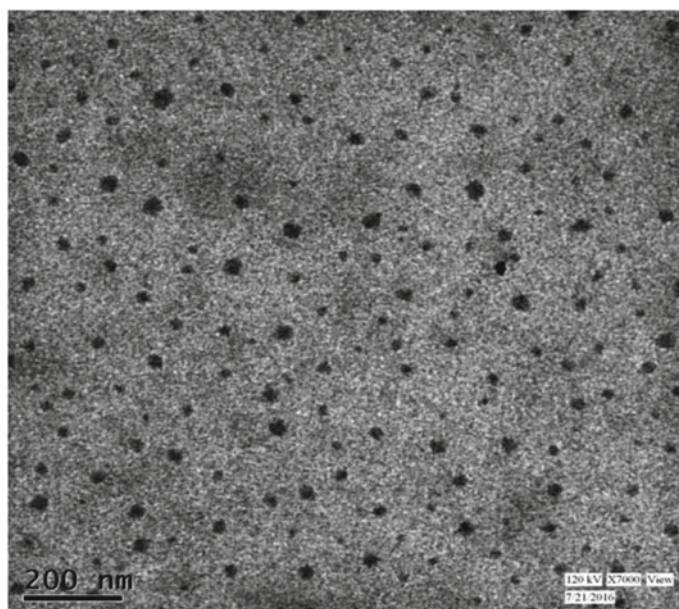


Fig. 2 TEM image of FMA in IL in the presence of CPDTC as the RAFT reagent. Reproduced from Ref. [25] with permission from the Royal Society of Chemistry

Table 2 Polymerization of BMA at different reaction conditions using AIBN as initiator^a

S. no	Solvent	Time (h)	[M]/[RAFT]	Conversion (%)	$M_{n, \text{Theo}}$ (g/mol)	$M_{n, \text{GPC}}$ (g/mol)	Dispersity (\mathcal{D})
1	Bulk	2	120	81.3	13,900	12,700	1.31
2	Toluene	12	120	68.2	11,800	10,100	1.36
3	DMF	12	120	58.8	10,300	9500	1.33
4	BMIM[PF ₆]	2	130	91.3	16,900	14,500	1.16

^a[RAFT]:[Initiator] = 4:1, reactions carried out at 70 °C under N₂ atmosphere, 2-cyano-2-propyl dodecyl trithiocarbonate as RAFT agent. $M_{n, \text{Theo}} = \left(\rho \times \frac{[\text{Monomer}]}{[\text{RAFT}]} \times M_{w, \text{Monomer}} \right) + M_{w, \text{RAFT}}$; where ρ is the monomer conversion. Reproduced from Ref. [24] with permission from Elsevier

immiscible system. The polymerization of BMA is studied using RAFT agents like CPDTC and CPBDT in BMIM[PF₆] IL, DMF, toluene, and in bulk conditions. The summary of the study with the molecular weight and dispersity index of the polymer obtained are given in Table 2.

It is observed that ILs increase the rate of polymerization even in the case of immiscible monomer. The monomer conversion is also found to be high and the dispersity obtained is low compared to the organic solvents, indicating a narrow molar mass distribution. The polymerization is found to be faster than the organic solvents. At high polymerization rate, ILs also help to diffuse the heat generated during the reaction [23]. BMA is also polymerized in different ILs like BMIM[PF₆], BMIM[BF₄], and EMIM[EtOSO₃] and found to have varying rates of polymerization. This shows that ILs with different counter ions or different alkyl chain lengths have varying influence on the rate of polymerization. The synthesized PBMA polymer has been successfully used as a macro-RAFT to polymerize MMA monomer in IL, demonstrating block copolymerization in IL [24].

The polymers obtained, PBMA and PFMA, were characterized by NMR, GPC, MALDI-ToF, and DSC analyses [24, 25]. The absence of the resonances at $\delta = 6.4$ ppm corresponding to vinyl protons in ¹H NMR proved that there is no unreacted monomer in the polymer. Also, the NMR spectra did not show any impurities related to ILs being entrapped in the polymer. The chemical shift corresponding to -SCH₂ proton of the RAFT, which resonates at 3.2 ppm was used to calculate the molecular weight of the polymer. GPC analyses were carried with THF eluent to determine the molecular weight and dispersity of the polymers. In the block copolymerization of BMA and MMA, unimodal GPC traces were obtained, which confirmed the formation of block copolymers.

2.1 Polymerization Kinetics of Methacrylates in ILs

The ILs increase the rate of polymerization in both miscible and immiscible monomer systems. To investigate the influence of ILs, we studied the polymerization kinetics

of both FMA and BMA in ILs with various reaction conditions. The kinetic plot of FMA polymerization is linear with the R^2 value approaching unity (0.99) showing the controlled nature of the RAFT polymerization in IL. The rate of polymerization is higher than that of organic solvents with k_{app} approximately 16 times higher in IL. Also, the dispersity of the polymer was below 1.4 throughout the molecular weight evolution which shows that ILs do not interfere with the RAFT process.

The polymerization kinetics of BMA has been studied in different ILs and also compared with different organic solvents. Figure 3 shows that the rate of polymerization is high in IL when compared to the same in organic solvents. The k_{app} in IL is approximately seven times higher than that of toluene, a common organic solvent used to polymerize BMA. When comparing the rate of polymerization in different ILs, the relatively non-polar BMIM[PF₆] accelerates the rate of polymerization more than the relatively polar BMIM[BF₄] [26]. When compared, the K_{app} of FMA ($6.4 \times 10^{-2} \text{ min}^{-1}$) and BMA ($1.4 \times 10^{-2} \text{ min}^{-1}$) in the same BMIM[PF₆], where the polarity of the FMA is closer to the IL, it is evident that the polarity of IL has a greater influence on the rate of polymerization of the monomer.

Taking BMIM[PF₆] as a model IL solvent, we studied the kinetics of BMA polymerization using different RAFT agents such as 2-(Dodecylthiocarbonothioylthio)-2-methylpropionic acid (CPCTP), 2-cyano-2-propyl dodecyl trithiocarbonate (CPDTC) with long-chain end groups and 4-cyano-4-(phenylcarbonothioylthio)pentanoic acid (DCTMP), 2-cyano-2-propyl benzodithioate (CPBDT) with phenyl group. As seen in Fig. 4, the RAFT agents with dodecyl functional groups offer a higher rate of polymerization. It was speculated that the long aliphatic chain (dodecyl) would stabilize the monomer in IL polymerization system to form nano-suspensions of monomer droplets. This explains the higher rate of propagation in long chain containing RAFT agents compared to those of phenyl active groups. Therefore, a careful selection of RAFT

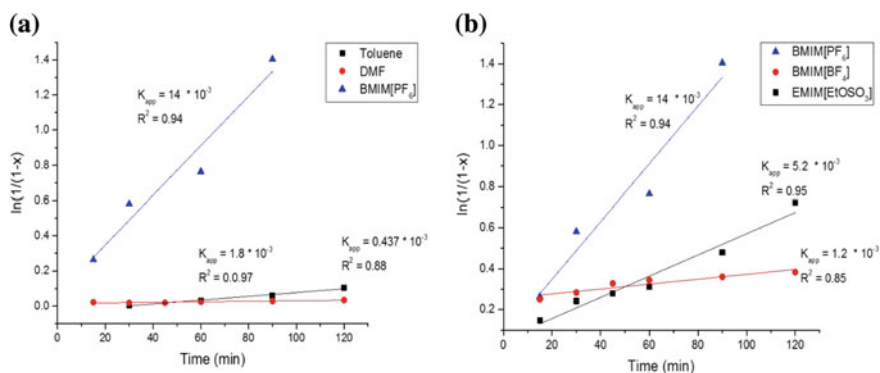
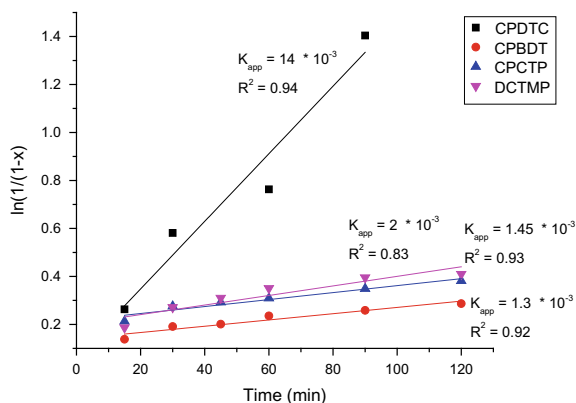


Fig. 3 Kinetic plots of BMA polymerization with CPDTC as RAFT agent in **a** different solvents such as toluene, DMF, and BMIM[PF₆] and **b** different ionic liquids such as BMIM[PF₆], BMIM[BF₄], and EMIM[EtOSO₃]. Reproduced from Ref. [24] with permission from Elsevier

Fig. 4 Kinetic plots of BMA polymerization in BMIM[PF₆] solvent with different RAFT agents



agent would facilitate synthesis of polymer nanoparticles by stabilizing monomers into a nano-suspension in IL solvents.

To investigate further, we formed two binary solvents of IL and organic solvents and studied the polymerization kinetics of BMA in them as shown in Fig. 4. The binary solvents are made by mixing BMIM[PF₆] IL with toluene and DMF in two proportions 50:50 and 25:75 with IL as minor portion. The DMF:IL system is miscible with BMA, and the toluene:IL system is immiscible. From the polymerization kinetics of these two systems, it is evident that IL would increase the rate of polymerization irrespective of the miscibility with the monomer. This can be explained with the previously existing hypotheses that the IL being a viscous liquid would show ‘solvent cage’ effect [27] or diffusion-controlled termination [28, 29] which would increase the rate of polymerization. This would justify the increase in the polymerization rate in the immiscible system. But in the miscible system like DMF(75%):IL(25%), both the ‘solvent cage’ effect and the diffusion-controlled termination are negligible. This phenomenon as explained before by Thurecht et al. [30] proves the existence of ionic interaction between the IL and the propagating radical which forms a radical-IL ‘complex’ [24] or a ‘protected’ radical [30, 31] which would decrease the rate of termination and thus accelerating the rate of polymerization. From Fig. 5, it can also be inferred that the presence of even a small amount of IL would increase the rate of polymerization.

2.2 Recovery and Reuse of ILs

After the polymerization of the methacrylates, FMA and BMA, a small amount of chloroform was added to the reaction mixture. The chloroform dissolves the polymer formed but is immiscible with ionic liquid as it is a non-polar solvent. This forms a bilayer as seen in Fig. 6. The chloroform with polymer solution forms the upper layer, and the ionic liquid forms the bottom layer which can be easily

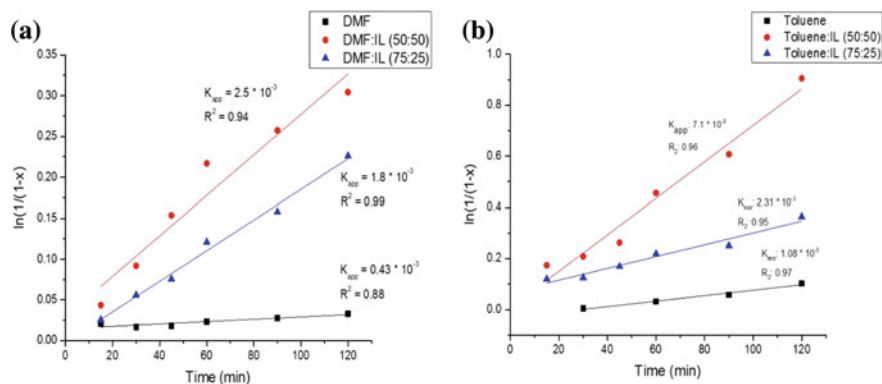


Fig. 5 Kinetic plots of BMA polymerization using CPDTC RAFT agent **a** DMF and BMIM[PF₆] binary solvent mixtures and **b** toluene and BMIM[PF₆] binary solvent mixtures. Reproduced from Ref. [24] with permission from Elsevier

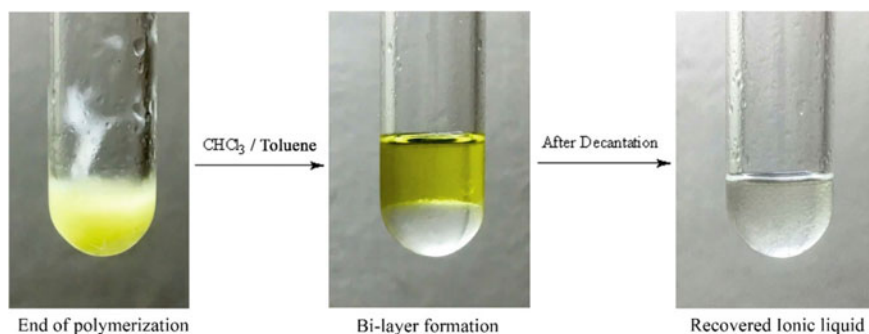


Fig. 6 Recovery of ionic liquid after BMA polymerization. Reproduced from Ref. [24] with permission from Elsevier

separated by decantation. We were able to recover more than 90% of the IL used in the polymerization. The purity of the recovered IL was checked with NMR [24]. The recovered IL was reused up to three times, and the results are tabulated in Table 3.

It can be seen that polymerization of BMA in pure IL and recycled IL produces similar results, and there is no change in the efficacy or efficiency of the IL after recycling. The ILs were recovered after every reaction, and the recovery% depends on the sophistication of the recovery technique. Also, we observed that toluene and hexane can also be employed to recover BMIM[PF₆] IL in methacrylate polymerization.

Table 3 RAFT polymerization of BMA in recycled IL^a

Solvent	Conversion (%)	$M_{n(\text{theo})}$ (g/mol)	$M_{n(\text{GPC})}$ (g/mol)	Dispersity (\bar{D})	Ionic liquid recovered (%)
BMIM[PF ₆]	96	15,300	14,600	1.20	94
BMIM[PF ₆]—1st recycle	92	14,200	13,300	1.22	95
BMIM[PF ₆]—2nd recycle	94	14,950	12,400	1.23	94
BMIM[PF ₆]—3rd recycle	93.5	14,800	14,400	1.22	92

^a[BMA]/[RAFT]/[AIBN] = 450:4:1. Reactions carried out at 70 °C under N₂ atmosphere for 2 h. Reproduced from Ref. [24] with permission from Elsevier

3 Conclusion

In summary, the methacrylates such as FMA and BMA were successfully polymerized in ILs using RAFT polymerization technique. The CPDTC RAFT agent was found to act as a stabilizer for the FMA monomer in BMIM[PF₆] IL which can be used to control the particle size of the polymer. The rate of polymerization in IL was found to be higher than the same in organic solvents. The study on the polymerization kinetics shows that the IL accelerates the rate of polymerization irrespective of its miscibility with the monomer. The polarity of the IL affects the rate of polymerization. The study with binary solvent systems shows that the presence of even a small amount of IL would increase the rate of polymerization. The demonstration of the recycling of ILs shows that ILs are viable alternative ‘green’ solvents, to replace volatile organic solvents, which would improve the sustainability of the polymer synthesis.

Acknowledgements We thankfully acknowledge the financial support from the Science and Engineering Research Board, Department of Science and Technology, New Delhi, India.

References

1. Parsegian, Gelbart WM (2006) Van der Waals forces: a handbook for biologists, chemists, engineers, and physicists. *Phys Today* 59:52–53
2. Hunt PA, Ashworth CA, Matthews RP (2015) Hydrogen bonding in ionic liquids. *Chem Soc Rev* 44:1257–1288
3. Hayes R, Warr GG, Atkin R (2015) Structure and nanostructure in ionic liquid. *Chem Rev* 115:6357–6426
4. Carlin RT, Osteryoung RA, Wilkes JS, Rovang J (1990) Studies of titanium(IV) chloride in a strongly Lewis acidic molten salt: electrochemistry and titanium NMR and electronic spectroscopy. *Inorg Chem* 29:3003–3009

5. Noda A, Watanabe M (2000) Highly conductive polymer electrolytes prepared by in situ polymerization of vinyl monomers in room temperature molten salts. *Electrochim Acta* 45:1265–1270
6. Perrier S, Davis TP, Carmichael AJ, Haddleton DM (2002) First report of reversible addition–fragmentation chain transfer (RAFT) polymerisation in room temperature ionic liquids. *Chem Commun* 19:2226–2227
7. Lozinskaya EI, Shaplov AS, Vygodskii (2004) Direct polycondensation in ionic liquids. *Eur. Polym. J.* 40:2065–2075
8. Vijayaraghavan R, Macfarlane DR (2007) Organoborate acids as initiators for cationic polymerization of styrene in an ionic liquid medium. *Macromolecules* 40(18):6515–6520
9. Carmichael AJ, Haddleton DM, Bon SAF, Seddon KR (2000) Copper(i) mediated living radical polymerisation in an ionic liquid. *Chem Commun* 14:1237–1238
10. Kokubo H, Watanabe M (2008) Anionic polymerization of methyl methacrylate in an ionic liquid. *Polym Adv Technol* 19:1441–1444
11. Vygodskii YS, Mel'nik OA, Lozinskaya EI, Shaplov AS, Malyshkina IA, Gavrilova ND, Lyssenko KA, Antipin MY, Golovanov DG, Korlyukov AA, Ignat'ev N, Welz-Bierman U (2007) The influence of ionic liquid's nature on free radical polymerization of vinyl monomers and ionic conductivity of the obtained polymeric materials. *Polym Adv Technol* 18:50–63
12. Kubisa P (2009) Ionic liquids as solvents for polymerization processes—Progress and challenges. *Prog Polym Sci* 34:1333–1347
13. Plechkova NV, Seddon KR (2008) Applications of ionic liquids in the chemical industry. *Chem Soc Rev* 37:123–150
14. Sheldon R (2001) Catalytic reactions in ionic liquids. *Chem Commun* 23:2399–2407
15. Mathews CJ, Smith PJ, Welton T (2000) Palladium catalysed Suzuki cross-coupling reactions in ambient temperature ionic liquids. *Chem Commun* 14:1249–1250
16. Hallett JP, Welton T (2011) Room-temperature ionic liquids: solvents for synthesis and catalysis. *Chem Rev* 111:3508–3576
17. Plechkova NV, Seddon KR (eds) (2015) *Ionic liquids completely UnCOILed*. Wiley & Sons Inc, Hoboken, NJ
18. Zhang H, Behera PK, Singha NK, Hong K, Mays JW (2015) *Polymerization in Ionic Liquids*. Encyclopedia of polymer science and technology. Wiley & Sons Inc, Hoboken, NJ, USA, pp 1–19
19. Behera PK, Usha KM, Guchhait PK, Jehnichen D, Das A, Voit B, Singha NK (2016) A novel ionomeric polyurethane elastomer based on ionic liquid as crosslinker. *RSC Adv* 6:99404–99413
20. Wasserscheid P, Welton T (2008) *Ionic Liquids in synthesis*, vol 1, 2nd edn. Wiley-VCH Verlag GmbH & Co. KGaA, Weinheim, Germany
21. Singha NK, Hong K, Mays JW (2017) Polymerization in ionic liquids. In: Eftekhari A (eds) *Royal Society of Chemistry Publishing*, pp 1–22
22. Chakrabarty A, Singha NK (2015) Tunable morphology and hydrophobicity of polyfluoroacrylate/clay nanocomposite prepared by in situ RAFT polymerization in miniemulsion. *Macromol Chem Phys* 216:650–661
23. Zhao Y, Zhen Y, Jelle BP, Boström T (2017) Measurements of ionic liquids thermal conductivity and thermal diffusivity. *J Therm Anal Calorim* 128:279–288
24. Santha Kumar ARS, Roy M, Singha NK (2018) Effect of ionic liquids on the RAFT polymerization of butyl methacrylate. *Eur Polym J* 107:294–302
25. Singha NK, Pramanik NB, Behera PK, Chakrabarty A, Mays JW (2016) Tailor-made thermoreversible functional polymer via RAFT polymerization in an ionic liquid: a remarkably fast polymerization process. *Green Chem* 18:6115–6122
26. Ab Rani MA, Brant A, Crowhurst L, Dolan A, Lui M, Hassan NH, Hallett JP, Hunt PA, Niedermeyer H, Perez-Arlandis JM, Schrems M (2011) Understanding the polarity of ionic liquids. *Phys Chem Chem Phys* 13:16831
27. Strehmel V, Laschewsky A, Wetzell H, Görnitz E (2006) Free radical polymerization of n -Butyl Methacrylate in ionic liquids. *Macromolecules* 39:923–930

28. Hong K, Zhang H, Mays JW, Visser AE, Brazel CS, Holbrey JD, Reichert WM, Rogers RD (2002) Conventional free radical polymerization in room temperature ionic liquids: a green approach to commodity polymers with practical advantages. *Chem Commun* 13:1368–1369
29. Zhang H, Hong K, Mays JW (2002) Synthesis of block copolymers of styrene and Methyl Methacrylate by conventional free radical polymerization in room temperature ionic liquids. *Macromolecules* 35:5738–5741
30. Thurecht KJ, Gooden PN, Goel S, Tuck C, Licence P, Irvine DJ (2008) Free-radical polymerization in ionic liquids: the case for a protected radical. *Macromolecules* 41:2814–2820
31. Harrisson S, Mackenzie SR, Haddleton DM (2002) Unprecedented solvent-induced acceleration of free-radical propagation of methyl methacrylate in ionic liquids. *Chem Commun* 23:2850–2851

Chapter 9

Creation of Electrically and Optically Functional Materials from Cellulose Derivatives via Simple Modification and Orientation Control



Yoshikuni Teramoto and Kazuma Miyagi

Abstract The authors demonstrate a series of investigations that led to the creation of functional materials from cellulose derivatives (cellulose acetate (CA), cyanoethyl cellulose (CyEC), and ethyl cellulose (EC)), which have relatively simple structures and are supposed to be practical for industrial use. For these derivatives, we performed molecular modification with introducing simple substituent or combining with different polymers, applied processing with deformation, and controlled the orientation behavior of molecular chains and segments, in order to create electrical and optical functional materials. As an optical function, we established the design guidelines for CA-based materials that can precisely control the optical anisotropy including zero birefringence. As an electrical function, we obtained a CyEC-based material showing the largest dielectric constant among thermally stable organic polymers. Very recently, we have proposed a dual mechanochromism in which by mechanical stimulus, not only the cholesteric color changes, but also the polarity of the selectively reflected circularly polarized light is reversed, utilizing the inherent cholesteric liquid crystallinity of EC.

Keywords Cyanoethyl cellulose · Cellulose acetate · Ethyl cellulose · Dielectric constant · Birefringence · Cholesteric liquid crystal · Selective reflection · Coloration · Circular dichroism

1 Introduction

Cellulose derivatives, which are the main chemical products in the wood science and technology field, are the first man-made plastics and have still maintained their industrial importance while making excellent use of their physical properties including

Y. Teramoto (✉)

Division of Forest and Biomaterials Science, Graduate School of Agriculture, Kyoto University, Kyoto 606 8502, Japan

e-mail: teramoto.yoshikuni.3e@kyoto-u.ac.jp

K. Miyagi

Department of Applied Life Science, Faculty of Applied Biological Sciences, Gifu University, Gifu, Japan

© Springer Nature Singapore Pte Ltd. 2020

V. Katiyar et al. (eds.), *Advances in Sustainable Polymers*, Materials Horizons: From Nature to Nanomaterials, https://doi.org/10.1007/978-981-15-1251-3_9

spinnability, film formability, mechanical strength, and sorption performance. On the other hand, the authors are aiming for higher performance or functionality of biomass as a material. In addition to appealing factors as eco-materials such as “bio-based” and “abundance of potential resources,” we believe that the further development of cellulose derivatives can be achieved if unknown functionality can be derived based on precise findings at molecular or molecular assembly scale.

Since the beginning of this century, we have systematically understood the thermodynamic and physical properties of ester derivatives and graft copolymers of cellulosic polysaccharides. Our achievements in the 2000s [1, 2] were mainly as follows:

- Establishment of their synthesis, purification, and structure evaluation methods
- Systematization of the thermal transition and mechanical behavior based on a clear understanding of the molecular structure
- Detailed analysis of higher-order structural development processes such as amorphous relaxation (physical aging) and crystallization

In this chapter, we present our recent research aspiring to the integration and utilization of knowledge obtained by subdividing for each segment in order to derive latent functionalities of cellulose derivatives. As functionalities to be expressed, we targeted the optical and electrical ones of their bulk materials. For that purpose, we decided to make use of necessary and sufficient chemical modifications and appropriate processing techniques such as stretching and compressing for orientation control. The main points of the research are as follows:

- The optical and electrical properties of the cellulose derivatives (such as cellulose acetate (CA) and cyanoethyl cellulose (CyEC)) industrially produced at present or in the past have been applied to products such as a protective film for liquid crystal displays and a binder for organic light-emitting displays, respectively. However, the function and performance leave room for further broad control by mild chemical modification.
- The specific targets were to obtain a material with the highest dielectric constant in organic polymers on the electrical side, and to control precisely the birefringence in the optical aspect.
- We also noticed that the contribution to the physical properties exerted by the trunk chain and the side chain (and its segments) of cellulose derivatives is not merely a summation. This has the potential to develop into a basic concept for obtaining derivatives with desirable physical properties.
- Our recent research achievement includes the application of liquid crystallinity of cellulose derivatives. Cellulose derivatives are often capable of expressing cholesteric liquid crystal (ChLC) in concentrated solutions and show the selective reflection of circular polarized light [3]. We prepared cellulosic/synthetic polymer composites in the usual manner. The composite films exhibited a wide-ranging color change over the visible region by compressing. Moreover, we found that the circular dichroism of the films was inverted by the compression. Such a stress-induced circular dichroic inversion of ChLC-based materials has not been recognized in a definite form so far.

It is an unexpected delight of the authors if the functional extension of cellulose derivatives by the combination of simple chemical modifications or composing and processing, demonstrated in this document, leads to the development of biomass-based advanced materials.

2 Improvement of Dielectric Constant

2.1 Background

Dielectric constant is one of the physical properties representing the response of dielectric materials under an electromagnetic field. When a dielectric material (normally insulator) is placed in an external electric field, the average position of the nuclei and electrons constituting the dielectric material moves slightly from the original position and the dipole moments thus are oriented. For conductors, the influence of the electric field is easy to be relaxed due to the mobility of free electrons; whereas, the time scale of structural relaxation in dielectric materials is generally long. In other words, the dielectric materials can accumulate charge bias (electric energy).

When developing electronic devices, it is useful to use high dielectric inorganic substances. However, it is worth challenging to increase the dielectric constant of organic plastics that are thermally moldable, flexible, and capable of undergoing processing.

Many researchers have reported on poly(vinylidene fluoride) (PVDF), a commercial material used in the conversion of stored to active electrical energy. In particular, some of them have recently investigated the effects of processing conditions such as the stretching ratio and temperature on the microstructures including crystallites and orientation along with dielectric properties of PVDF [4–6].

On the other hand, we applied the concept of “chemical modification of cellulose derivatives and subsequent orientation control” to improve the dielectric constant. That is, attempts have been made to improve the dielectric properties of cyanoethyl cellulose (CyEC) by a combination of esterification and uniaxial thermal drawing.

Cyanoethylation of cellulose endows favorable mechanical and dielectric properties [7, 8]. However, the product cyanoethyl cellulose (CyEC) exhibits a high T_g and melting temperature (T_m), which can be attributed to the strong attractive interactions between the highly polar cyano ($C\equiv N$) groups. Such properties limit the processability of this material. Therefore, in this study, we have made an attempt to improve the thermal moldability of CyEC by esterifying the residual hydroxyl groups of CyEC ($DS = 2.54$) [9]. On the other hand, we also expected that the esterification would improve the stretchability of CyEC by conferring high moldability. We presumed that the esterification would transform the originally high-crystalline CyEC into a less crystalline material and that the increased mobility of the molecular chain segments (with polarized cyano groups) would increase the dielectric constant. In addition, we

assumed that a uniaxial stretching would cause orientations of overall molecules and local segments, thereby increasing the sum of the active dipole moments.

2.2 Sample Preparation

For esterification of CyEC (cyanoethyl $DS = 2.54$), *n*-alkanoic acid (m is the carbon number of the side chain; $m = 3, 4, 5, 8, 12, \text{ and } 18$) was used as an attack reagent precursor, pyridine as an acid scavenger, and *p*-toluenesulfonic acid as an activator. The reaction was carried out in a homogeneous system using *N,N*-dimethylacetamide as a solvent. CyEC ester derivatives are denoted as *Cm*-CyEC, and solution cast film ($\sim 100 \mu\text{m}$ thick) was uniaxially stretched at a stretching speed of 2 mm/min using a hand-cranked drawing device at the vicinity of the onset glass transition temperature (T_g) under a nitrogen atmosphere. Thereafter, it was rapidly cooled to obtain a stretched film having a thickness of 60–100 μm .

2.3 Fundamental Characterization of *Cm*-CyEC

In general, for fully substituted type ($DS = 3$) normal alkanolic ethers and esters of cellulose, as the side chain becomes longer, the T_g of these derivatives sharply decreases, and the materials are plasticized. The original cellulose tends to form crystals due to the strong hydrogen bonds between the molecules and hydrogen bonds are also strong in the amorphous part, leading to the thermal decomposition before glass transition on heating. The amorphous part of the methyl and acetylated derivative has a T_g of $\sim 200^\circ\text{C}$. It rapidly decreases as the side chain becomes longer to saturate at $\sim 60^\circ\text{C}$ at the side chain carbon number of ~ 5 . When the side chain becomes longer (roughly 10 or more carbon atoms), the side chain can form a crystal-like ordered structure, and a thermotropic liquid crystallinity is expressed as the whole molecule [1, 10]. The liquid crystal structure to be exhibited is a cholesteric phase in the case of ethers and a columnar phase for the esters. Thus, the thermal transition behavior of cellulose derivatives usually depends greatly on the structure of the binding site of the cellulose main chain and the side chain.

On the other hand, the ester of CyEC (cyanoethyl $DS = 2.54$), *Cm*-CyEC, prepared here manifests different thermal transition behaviors because an attractive interaction between the cyano groups on the cyanoethyl moiety introduced into the cellulose main chains is remarkable, as shown in Fig. 1. That is, even if the longer side chains are incorporated, the T_g is detected at 150–160 $^\circ\text{C}$, which is not much different from that of the original CyEC (166 $^\circ\text{C}$). In the medium ester side chain length ($m = 3$ –

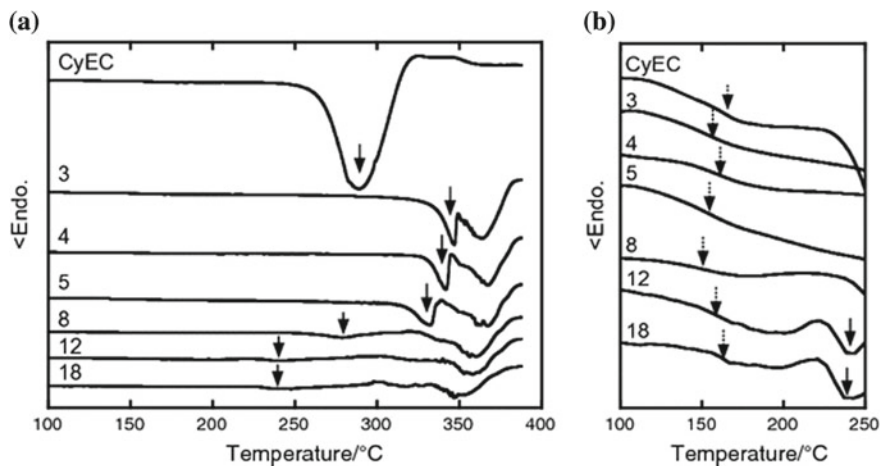
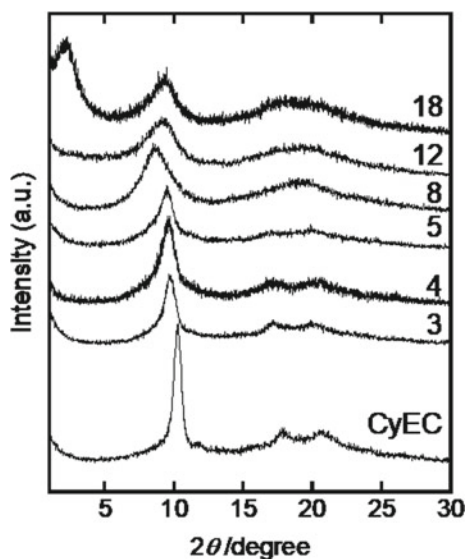


Fig. 1 DSC thermograms of CyEC and its ester derivatives in the first heating. Numerals denote the carbon number m of ester side chains. Melting points of samples are indicated by solid arrows in (a). Panel (b) presents enlarged thermograms around T_g (indicated by broken arrows). Reprinted with permission from Ref. [9]. Copyright© 2015, Springer Science Business Media Dordrecht

5), a three-dimensional crystalline-like ordered structure is observed by wide-angle X-ray diffractometry (WAXD) (Fig. 2) at 210 °C ($\geq T_g$), where the measurement at this temperature substantially corresponds to the annealing operation. When $m \geq 8$, the spacing between the main chains is found to expand remarkably, the three-dimensional regular structure disappears, and the ordered structure like columnar

Fig. 2 WAXD profiles of CyEC and its ester derivatives (numerals denote m), measured at 210 °C



liquid crystal is observed as the whole Cm -CyEC. In the case of $m = 18$, in addition, another large periodic ordered structure is observed. In this way, the attractive interaction between the cyano groups of the original CyEC of $DS = 2.54$ has a large influence on the higher-order structure even if bulky normal alkanolic side chain is introduced to the residual hydroxyl group.

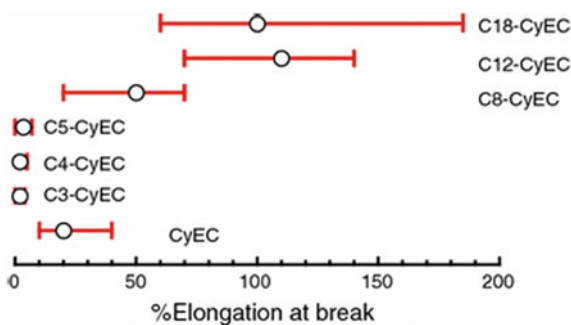
2.4 Stretching and Segmental Orientation

The objective of preparing a series of Cm -CyEC is originally to increase both the orientation and motility of the dipole moments. Because the reproducibility of uniaxially thermal drawing at around onset T_g is supposed to be high as an orientation process, the thermal stretchability of as-cast films of CyEC and Cm -CyEC is investigated first. Figure 3 shows m dependency of % elongation (γ) at the break by thermal drawing. For the specimens of Cm -CyEC with large side chains ($m = 8, 12, \text{ and } 18$), the thermal stretchability is great because of the internal plasticizing effect by introducing ester side chains. However, the samples with $m = 3\text{--}5$ display rather less stretchability than CyEC, probably due to the attractive interaction between cyano groups and promotion of orientation crystallization of these samples.

For the most thermoplasticized C18-CyEC, the heat stretching behaviors are further compared with those of the original CyEC. As shown in their WAXD profiles (Fig. 4), annealing orientation crystallization is noticeable for CyEC, but C18-CyEC provides the profiles similar to that of the as-cast sample even after drawing and does not appear to form a three-dimensional crystal lattice. From the X-ray fiber pattern of C18-CyEC, it is observed that the long alkyl side chains in a state of hexagonal packing oriented preferentially along the main chain direction.

In order to investigate the orientation of the more local segment of C18-CyEC, the infrared dichroism has been evaluated. Focusing on $C\equiv N$ stretching band (2250 cm^{-1}) of cyanoethyl groups and $C=O$ stretching band (1750 cm^{-1}) of ester groups, Fig. 5 shows the change in the orientation function f_ϕ of those by the thermal drawing. The order parameter f_ϕ varies from $-1/2$ (draw direction and dipole

Fig. 3 Percent elongation at break of cast films of CyEC and its ester derivatives. Films were processed at onset T_g . Reprinted with permission from Ref. [9]. Copyright© 2015, Springer Science Business Media Dordrecht



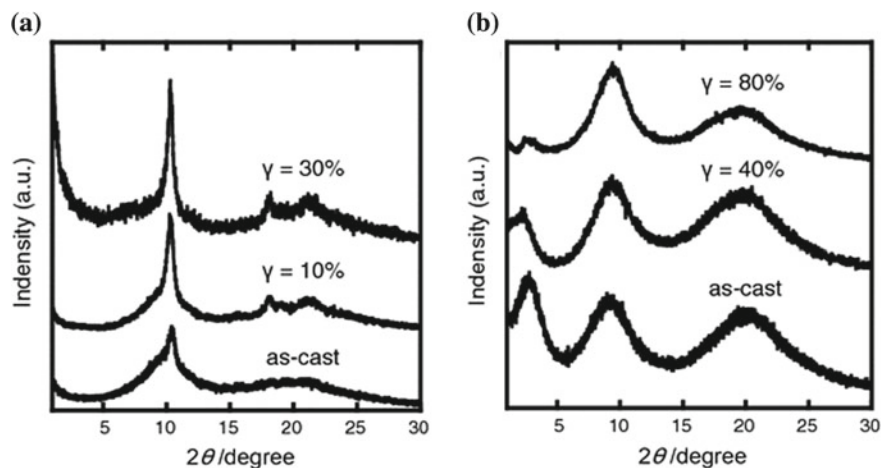
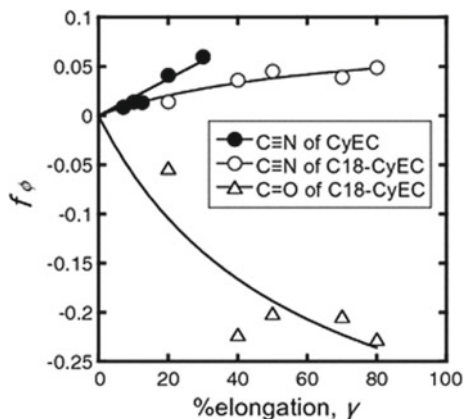


Fig. 4 WAXD intensity profiles of drawn films: **a** CyEC; **b** C18-CyEC. Notation γ denotes % elongation. Reprinted with permission from Ref. [9]. Copyright© 2015, Springer Science Business Media Dordrecht

Fig. 5 f_ϕ values for the cyano group of CyEC and for the cyano and ester groups of C18-CyEC, plotted against γ . Reprinted with permission from Ref. [9]. Copyright© 2015, Springer Science Business Media Dordrecht



moment are perfectly perpendicular) to 1 (draw direction and dipole moment are perfectly parallel). f_ϕ of zero indicates no preferential orientation. Since the f_ϕ of $\text{C}\equiv\text{N}$ took positive values and increased with γ , it is confirmed that the cyano moiety is preferentially oriented in the drawing direction. On the other hand, it is found that the $\text{C}=\text{O}$ groups are preferentially oriented perpendicular to the stretching axis because the f_ϕ of $\text{C}=\text{O}$ at the junction part of the ester side chains has a negative value. These data support the findings of the X-ray fiber pattern that the alkane portion of the ester side chain of C18-CyEC and the cellulose main chain are oriented in parallel.

2.5 Dielectric Properties

In general, the dielectric constant of a material increases as the sum of the dipole moments in the material increases and as the dipoles move more easily. For the as-cast films of CyEC ($m = 0$) and C_m -CyEC, the change of dielectric constant with respect to m measured at 1 kHz and 25 °C is plotted in Fig. 6. The dielectric constant decreases with increasing m . The esterification of CyEC here introduces new C=O dipole, but at the same time essentially nonpolar alkane chains are also incorporated. Therefore, the esterification does not simply lead to an increase in the dipole concentration in the series of C_m -CyEC.

On the other hand, when the film sample is stretched and the dielectric constant is evaluated, it shows the opposite behavior between CyEC and C18-CyEC. Initially, the dielectric constants of the as-cast films of CyEC and C18-CyEC were about 16 and 9, respectively. When stretched, that of CyEC moderately decreased to ~ 11 with $\gamma = 50\%$, while C18-CyEC showed an increase in the dielectric constant 2.5 times (up to ~ 23) for $\gamma = 150\%$. A schematic for explaining this contrasting behavior is shown in Fig. 7. As modeled in (a), CyEC develops annealing and orientation crystallization during the thermal drawing of the film; at that time, it seems that the C \equiv N moieties of the adjacent molecular chains are placed in anti-parallel, the dipole moment is canceled out, and their mobility also decreases. On the other hand, as shown in the schematic of the higher-order structure of C18-CyEC in (b), the bulky alkane chains are oriented along the cellulose main chain in this thermally stretched film. As a result, the free volume of both C \equiv N and C=O dipoles increases. Moreover, since this sample has no crystal development such as forming a three-dimensional lattice, the mobility of dipoles is not hindered.

In this manner, by controlling the orientation and mobility of the local segment of the cellulose derivative, it is possible to obtain a material having the highest dielectric constant (~ 23) as organic polymers.

Fig. 6 Plots of ϵ' versus carbon number in ester side chain, m . Arrows indicate a change of dielectric constant with increasing % elongation, γ , for drawn films

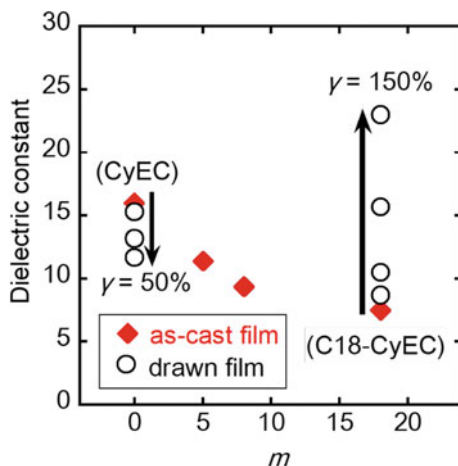
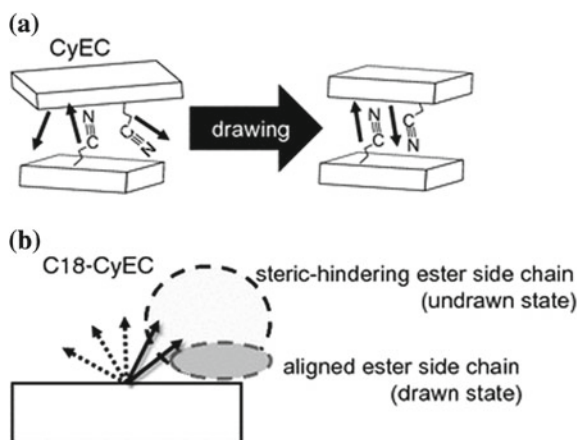


Fig. 7 Schematics of dipole moment movements: **a** CyEC *per se*; **b** C18-CyEC. Arrows indicate dipole moments. Flat plates indicate cellulosic main chains. Reprinted with permission from Ref. [9]. Copyright© 2015, Springer Science Business Media Dordrecht



2.6 Summary and Future Prospects

Many synthetic methods of cellulose derivatives have been proposed so far, and interpretation of the influence of molecular composition such as *DS* has traditionally been made with respect to the physical properties of the resulting bulk materials. Recently, the effect of the introduction of plural substituents on the thermal or mechanical properties is gaining attention from the industry [11–13]. If we can effectively exploit the local structure provided by heterogeneous side chain moieties, as shown in this section, meanwhile, we can still develop new special properties and functionalities that are not only mechanical properties, from cellulose derivatives.

3 Birefringence Control

3.1 Background

Graft copolymerization of cellulosic polymers is one of the possible ways to incorporate different polymer components at the ultrafine structure level. This not only improves the original properties of the polysaccharide, but also leads to the introduction of new functions derived from the polymers combined as grafts. In the beginning of this century, we focused on graft copolymers mainly composed of cellulose ester derivatives and aliphatic polyesters and studied the thermal transition, mechanical properties, and evolution of molecular aggregate structure such as crystal and amorphous structure relaxation, enzymatic degradability, and so on, in detail and systematically [1, 2]. The points of the series of research were to prepare pure graft copolymers (not containing oligomer impurities of ingredients to be grafted) and to

develop discussion based on the molecular structure by eliminating speculation as much as possible.

In the subsequent decade, we have reported the orientation control by thermal drawing process and the expression of the optical functionalities by it [14, 15]. This section explains its outline. Specifically, it deals with the orientation behavior and optical anisotropy of cellulosic graft copolymers.

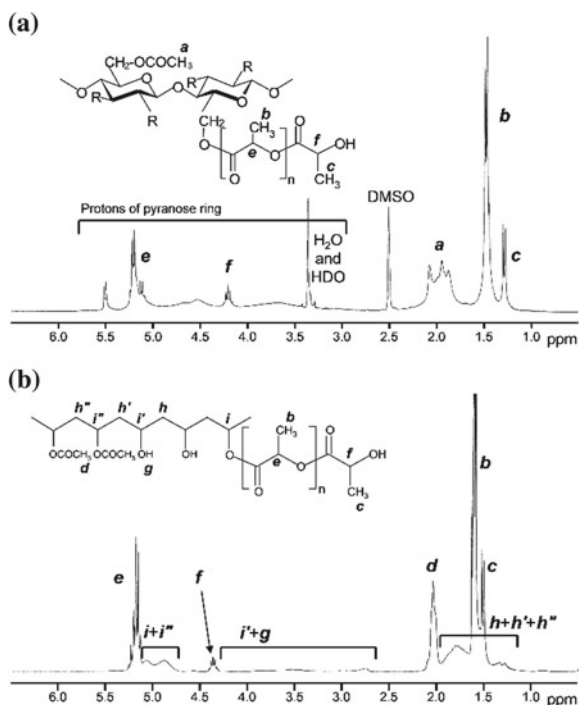
So far, the remarkable results have been reported on the stretching orientation behavior and optical properties of bulk materials of the closely mixed multi-component polymers such as random copolymers [16] and miscible polymer blends [17–19]. That is, birefringence induced by deformation (strain) of the bulk materials can be designed in advance by appropriately combining two components whose polarity of birefringence is opposite to each other. In certain cases, the original optical isotropy is maintained regardless of the degree of deformation (zero birefringent material). There is no similar study on graft copolymers but adopting them would have the merit that the degree of freedom of composite design is high because compatibility between components is not a problem by graft copolymerization. In addition, we are also interested in the fundamental aspect of whether the applied stress is transferred to the trunk or graft to lead an orientation when stretching the bulk film materials of graft copolymers.

This section covers two graft copolymer series of cellulose acetate (CA) with poly(L-lactide) (PLLA) or polymethylmethacrylate (PMMA). A fluorescence polarization technique has been employed to obtain the information about the overall degree and the type of molecular orientation developed in the drawing of graft copolymer films, while birefringence is used as a measure for the estimation of the state of optical anisotropy of the drawn films.

3.2 CA-Graft-PLLA: Discontinuous Birefringence Change Accompanying Branch Chain Length

The graft copolymers are synthesized by ring-opening copolymerization of L-lactide initiated at the residual hydroxyl groups of CA ($DS = 2.15$) in the presence of tin(II) 2-ethylhexanoate, which is known to be a highly selective catalyst [20]. Further, the graft copolymers (PVAVAc-*graft*-PLLA) having a poly(vinyl alcohol-*co*-vinyl acetate) (PVAVAc, $OCOCH_3/OH = 64/32$) as a main chain are prepared in the same manner, and the products are used as comparative samples of the effect of rigidity of the trunk polymer. As shown in Fig. 8, the molar substitution degree (MS, the number of lactyl groups introduced per repeating unit of the trunk polymer) is quantified by 1H NMR. The graft copolymers of both series generally have a high graft density (one graft per two repeating units of the trunk chain), and the degree of polymerization of grafts is $\leq \sim 5$. All the products of both graft copolymer series are non-crystallizable, and their solution cast films show no domain segregation of the two components that constitute the trunk and side chains.

Fig. 8 Typical ^1H NMR spectra of **a** CA-*graft*-PLLA and **b** PVAVAc-*graft*-PLLA. Reprinted with permission from Ref. [14]. Copyright© 2011, Springer Science Business Media B.V



Rectangular films charged with a 2.5-nm-long fluorescent probe molecule at low concentration are uniaxially stretched at a temperature in the vicinity of T_g . The overall behavior of the orientation is estimated from the statistical second ($\langle \cos^2 \omega \rangle$) and fourth ($\langle \cos^4 \omega \rangle$) moments obtained by a fluorescence polarization method. Upon stretching, any film of both series impart a positive orientation function, i.e., $f = (3 \langle \cos^2 \omega \rangle - 1)/2 > 0$, which increases with the extent of deformation. When compared between both the graft copolymers, the CA system had high molecular orientation even at low draw ratio, while the PVAVAc series generally exhibited lower degree of molecular orientation. Therefore, the semirigidity of CA and the flexibility of the vinyl chain greatly influenced the molecular orientation of each graft copolymer, and at the same time the molecular arrangement of the entire graft copolymers was disturbed by the introduction of the graft chains.

Birefringent phenomenon occurs based on the orientation distribution of the anisotropic units (several Å long) of polarizability in polymer molecules in general. Plots of birefringence vs. % elongation for film samples of the two series of graft copolymers are shown in Fig. 9. Both CA and PLLA of acetyl $DS \lesssim 2.75$ have positive birefringence. As schematically illustrated in Fig. 10, in the CA system, (i) the polarizability at the junction part of the graft chains contributes negatively to the stretching axis with $MS \leq 0.75$ and thus the birefringence (Δn) decreases, (ii) with increasing MS to ~ 1.5 , Δn increases monotonically, and (iii) when $MS = 3$, the graft chains disturbed the arrangement of the entire molecules and Δn decreases

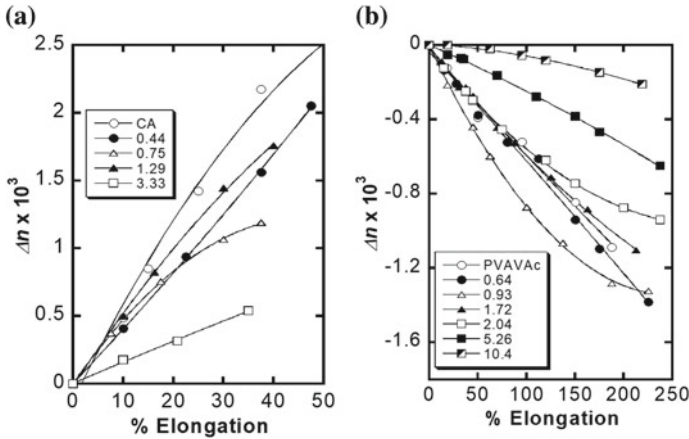
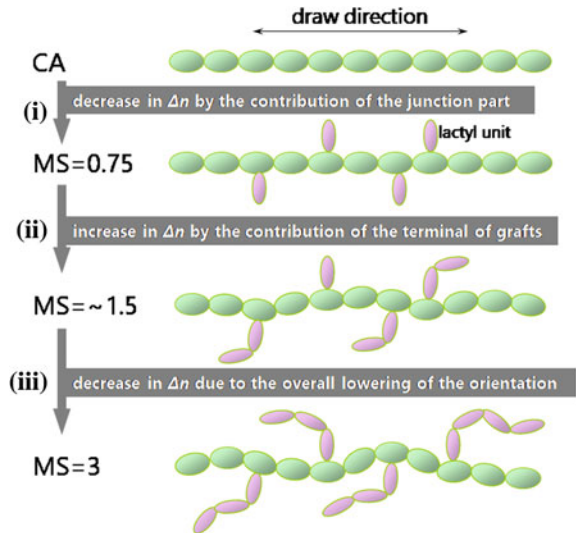


Fig. 9 Plots of birefringence versus % elongation for film samples of the two series of graft copolymers, CA-graft-PLLA (a) and PVAVAc-graft-PLLA (b). Numerals inserted in the legend denote MS values for the graft copolymers. Reprinted by partially modifying the items with permission from Ref. [14]. Copyright© 2011, Springer Science Business Media B.V

Fig. 10 Schematic of the orientation behavior of polarization anisotropic unit of CA-graft-PLLA



accordingly. That is, the change in Δn with increasing MS is not monotonous. On the other hand, the change in Δn associated with increasing MS is not monotonic as well even for the PVAVAc-graft-PLLA samples with negative birefringence as a graft copolymer due to the original negative Δn of PVAVAc in the trunk. We thus found a subtle variation in the orientation mode (polarity and extent) of each polarizability unit of the trunk chain CA or PVAVAc and the grafted oligo(L-lactide) by stretching their bulk films, using Δn as a probe.

3.3 CA-Graft-PMMA: Reversal of Polarity of Birefringence Due to Increase in Graft Chain Length

We examined the molecular orientation and optical anisotropy that are induced by the stretching of cellulose acetate (CA)-*graft*-poly(methyl methacrylate) (PMMA) films. This is a combination of trunk with positive birefringence and PMMA graft chains with negative birefringence. The copolymers are prepared by atom transfer radical polymerization (ATRP).

2-Bromoisobutyryl group is introduced into the residual hydroxyl group of CA ($DS = 2.15$) to synthesize a macroinitiator (CAMBBR). Then, ATRP of methyl methacrylate to CAMBBR is performed. The degree of 2-bromoisobutyryl substitution (DS_{BBr}) of CAMBBR is determined from quantitative ^{13}C NMR. CAMBBR samples with $DS_{BBr} = 0.40\text{--}0.73$ are obtained. From the ^1H - ^{13}C gHSQC NMR spectrum (Fig. 11) of the graft copolymers, the signals of ^1H and ^{13}C are assigned, and MS of the PMMA graft chain is calculated by the quantitative ^{13}C NMR. The average degree of polymerization (DPs) of PMMA grafts is determined from ^1H NMR, and the MS is divided by the corresponding DPs to calculate DS (DS_{grafted}) of PMMA grafts of 2-bromoisobutyryl group contributing to ATRP. The molecular composition of the products is exemplified in Table 1. The polydispersity (M_w/M_n) of PMMA grafts is 1.01–1.16, indicating that polymerization proceeds with ATRP.

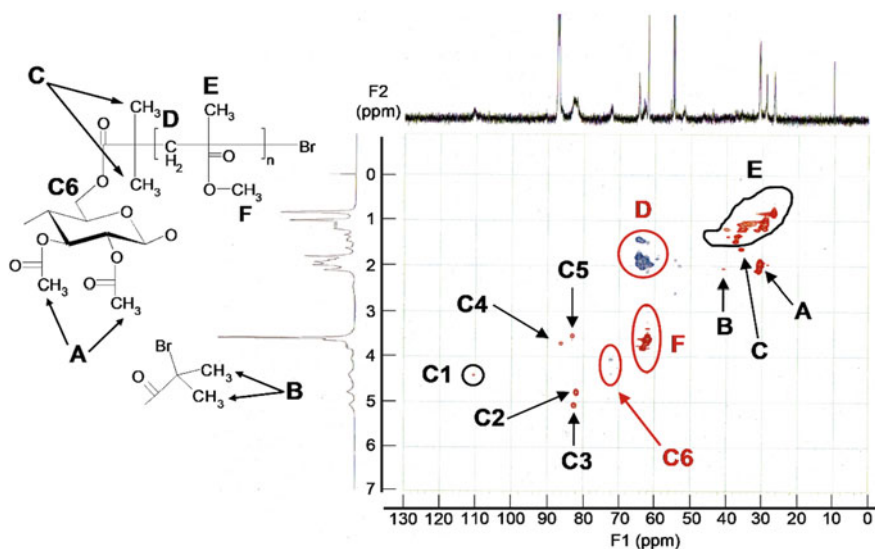


Fig. 11 ^1H - ^{13}C gHSQC NMR spectrum of the graft copolymer obtained by ATRP. Reprinted with permission from Ref. [15]. Copyright© 2013, American Chemical Society

Table 1 Quantitative results of the molecular composition of the product

Entry	MS	DP _S	DS _{grafted}	DS _{BBr}
1	1.62	66.5	0.02	0.60
2	4.60	46.9	0.10	0.60
3	5.26	46.4	0.11	0.60
4	6.84	45.6	0.15	0.60

Reprinted with permission from Ref. [15]. Copyright© 2013, American Chemical Society

As a result of DSC thermal analysis, it is found that the incompatible CA and PMMA are closely composited, since T_g is single in each of the graft copolymers. In addition, their T_g decreases with increasing MS, and CA originally poor in processability could be thermoplasticized by the grafting.

As a result of the fluorescence polarization measurement, it is shown that the molecular orientation of the stretched films is in accordance with the distribution form of the elliptic spheroid shape, and in the graft copolymers, the molecular orientation decreases with the increase of the MS. This is because the contribution of the flexibility of the PMMA graft chains becomes larger than that of the semirigidity of the CA trunk with the increase in the amount of graft chain introduction. This suggests that the PMMA graft chains are fixed onto the cellulosic trunk chain, the anchoring effect is difficult to act on the graft chain terminal part, and the orientation is easy (Fig. 12).

As can be seen in Fig. 13, Δn of CA and CAmbBr is positive, but that of graft copolymer decreased with increasing MS and DS_{grafted} . Furthermore, the graft copolymer with the largest DS_{grafted} and MS among the investigated shows negative Δn . This is because the terminal side of the PMMA graft chain ($\Delta n < 0$) contributes more negative than the positive polarizability anisotropy of the trunk chain.

From the above, it was possible to establish a method to adjust not only the magnitude of the birefringence of the graft copolymer but also the polarity. By this research, we have proposed a new design guideline for optical functional materials including zero birefringent material.

Fig. 12 Schematic of the concept of the orientation and birefringence including polarity inversion for CA-graft-PMMA. Reprinted with permission from Ref. [15]. Copyright© 2013, American Chemical Society

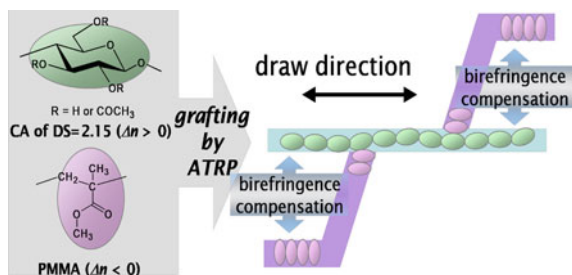
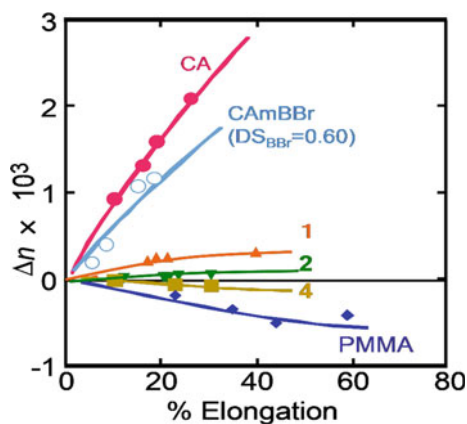


Fig. 13 Plots of birefringence versus % strain. Numerical values 1, 2, and 4 indicate entry numbers in Table 1. Reprinted with permission from Ref. [15]. Copyright© 2013, American Chemical Society



3.4 Summary

We have established a methodology to precisely control birefringence of cellulosic graft copolymers by molecular design and characterization of accurate molecular composition. In order to practically make use of this concept, it is necessary to obtain the desired derivative by a simpler synthesis method.

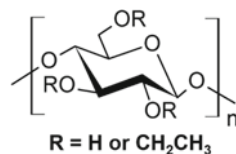
4 Dual Mechanochromism

4.1 Background

Mechanochromic materials whose color tone changes in response to mechanical stimuli are expected to be applied in various ways such as the visualization of mechanical damage and energy-saving-type display devices. The mode of introduction of mechanochromism proposed so far includes the incorporation of a mechanophore (a molecule to be colored by dynamic stimulus) into the material constituent molecules [21] and embedding of microcapsules containing a mechanophore [22]. On the other hand, mechanochromic materials using structural colors have also been reported [23, 24]. This is the concept of constructing a laminated structure in the order of visible light wavelength within the materials. Because of the selective reflection of light with wavelengths equivalent to the layer spacing, the color tone of these materials varies with the change in interlayer spacing due to bulk deformation.

Very recently, we focused on cholesteric liquid crystals (ChLC) having a helicity in addition to the laminated structure. ChLC selectively reflects circularly polarized light having the same wavelength as the helical pitch and the same handedness as the helix, so it shows not only coloration but also circular dichroism (CD). Therefore, by using cellulosic ChLC as the basic structure of mechanochromic material [25,

Fig. 14 Chemical structure of EC



26], we expect that a novel mechanochromic material which changes CD could be realized in addition to the color tone control known for the above ones.

4.2 Preparation of ChLC Film by Combining Cellulose Derivative and Synthetic Polymer

Based on the method established by Nishio [27], ChLC films have been prepared by the following procedure: ChLC is expressed by dissolving ethylcellulose (EC, Fig. 14) in acrylic acid (AA) at high concentration; after adding a photopolymerization initiator, the ChLC solution is molded into a film, and photopolymerization of AA is performed by UV irradiation to obtain EC/poly(acrylic acid) (PAA) composite films in which the ChLC structure is immobilized.

4.3 Color Tone Change by Compressing EC/PAA Films

For the prepared EC/PAA films, we accomplished color change by mechanical stimulus and color tone recovery by heat treatment (Fig. 15).

By photopolymerization of a 47 wt% EC/AA solution, we obtained an EC/PAA film exhibiting red color due to selective reflection of its ChLC nature. Compression of the film at 30 °C results in a blue shift in coloration of the film as the compressive strain increases. However, when the compressive strain exceeds a certain level, the film tends to break; the range of change in color tone is thus limited. In this regard,

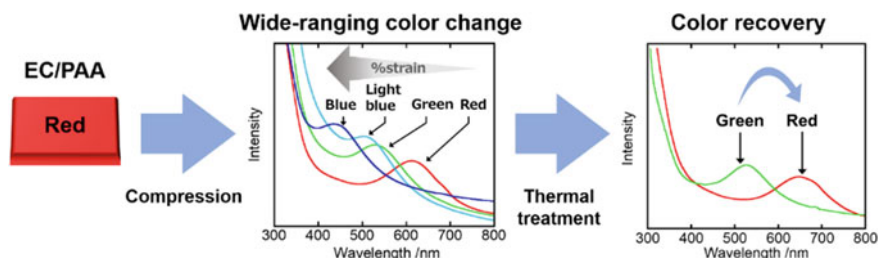


Fig. 15 Wide-ranging color change by applying compression stimuli and color recovery through the thermal treatment of EC/PAA films

since the T_g is detected at $\sim 120^\circ\text{C}$ by DSC for the EC/PAA film, it is natural that the film is in a glass state at 30°C and brittle fracture is likely to occur. When the film is compressed at 130°C , meanwhile, no brittle fracture occurs even at a compressive strain of 30% and a color tone change can be achieved over the whole visible light region. From the results of WAXD measurement of the film before and after compression, it is found that this color tone change is mainly caused by the increase in the helical angle of the cholesteric helix by compression.

When the EC/PAA film is air-cooled immediately after being compressed at 130°C , the shape and color tone can be fixed by the vitrification of the film, and even if the film is left standing at room temperature for a long time, it remains in the fixed state. Furthermore, it is revealed that when the vitrified film is subjected to a heat treatment at 130°C , the shape and color tone before compression could be recovered. This is due to rubber elasticity by heating at a temperature higher than the T_g of the film.

4.4 Circular Dichroism Inversion by Compression of EC/PAA Film

We also found that EC/PAA film shows circular dichroism reversal by mechanical stimulus (Fig. 16). To our knowledge, there is no example reporting such phenomena systematically not only in cellulose but also in the whole liquid crystal field.

For circularly polarized glasses used in general 3D televisions, the left (right) lens transmits only left (right) circularly polarized light. By using this, we can visually confirm CD. When the 47 wt% EC/PAA film before and after compression at 130°C are observed with the 3D glasses, the reflected light mainly passes through the left lens before compression; whereas, after compression the right lens transmits

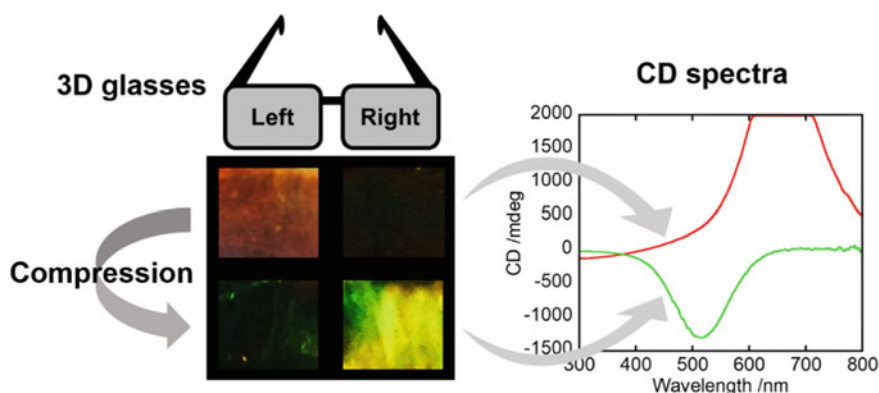


Fig. 16 Stress-induced circular dichroic inversion of EC/PAA films

it markedly. This result shows that the CD of the EC/PAA film is reversed from left-handed to right-handed by compression. This phenomenon can also be confirmed spectroscopically. That is, a positive CD signal meaning reflection of left-handed circularly polarized light is detected before compression; whereas, a negative CD signal meaning reflection of right-handed one is observed after compression.

4.5 Mechanism of CD Inversion

Should this inversion of CD be due to the inversion of the helix in the ChLC structure? In this regard, Gray et al. reported a reversal phenomenon of CD in ChLC of a concentrated aqueous solution of hydroxypropylcellulose (HPC) [28]. That is, the polarity of the CD was reversed between the ChLC film obtained by casting after a shear orientation and the ChLC film prepared by casting from the non-oriented state. This is because shear-aligned HPC acts like a retardation plate in the shear-oriented film. Therefore, the inversion of CD can occur even if the cholesteric helix itself does not reverse.

With reference to this report, we thought that the CD would be reversed as a result of increasing the orientation of the film by compression in our system as well. In order to confirm this hypothesis, the following preliminary experiment was conducted: an observation was made via 3D glasses with 60 wt% EC/PAA film (colorless) superposed on a 47 wt% EC/PAA film (red). As a result, the reflected light was mainly transmitted through the left lens, and a selective reflection of left-handed circularly polarized light was seen. On the other hand, when compressing the 60 wt% film and stacking it on the 47 wt% film, the reflected light came to pass through the right lens despite the fact that no mechanical stimulus was added to the latter ChLC film. This result can be interpreted as follows: when a left-handed circularly polarized light reflected by the 47 wt% film passes through the 60 wt% film, the 60 wt% film oriented by compression acts like a retardation plate, and the reflected light is reversed to right circularly polarized light (Fig. 17).

As described above, the reversal of the circular dichroism due to the compression of the EC/PAA film is likely due to the birefringence of the circularly polarized light accompanying the orientation within the film. We would like to clarify the mechanism of this phenomenon in more detail from further experiments in the future.

4.6 Future Prospects

We found that ChLC film obtained by combining cellulose derivative and synthetic polymer manifests a unique optical property “dual mechanochromism” which has not been clearly recognized so far. A series of film features not only visualization of dynamic stimulus by color change but also that of its history. As a starting point, we

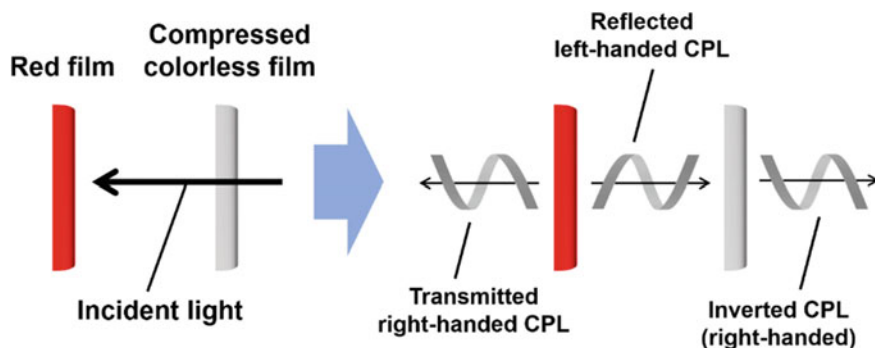


Fig. 17 Schematic image of the inversion of circular polarized light (CPL) originating from a retardation film-like effect of the compressed EC/PAA films

would like to continue to make efforts to design useful materials that make use of the unique features of cellulosic ChLC.

Acknowledgements The works shown in Sects. 2 and 3 were carried out at the laboratory of Professor Yoshiyuki Nishio of Kyoto University. Y. T. is sincerely grateful to Professor Nishio for his profound and valuable suggestion. Y. T. would also like to express his heartfelt thanks to Takeshi Unohara, Hirofumi Yamanaka, and Shingo Takechi who took charge of those studies as master's students.

References

1. Teramoto Y (2015) Functional thermoplastic materials from derivatives of cellulose and related structural polysaccharides. *Molecules* 20:5487–5527. <https://doi.org/10.3390/molecules20045487>
2. Nishio Y, Teramoto Y, Kusumi R, Sugimura K, Aranishi Y (2017) Blends and graft copolymers of cellulosics: toward the design and development of advanced films and fibers. Springer
3. Nishio Y, Sato J, Sugimura K (2016) Liquid crystal of cellulosics: fascinating ordered structures for the design of functional material systems. In: Rojas OJ (ed) *Cellulose chemistry and properties: fibers, nanocelluloses and advanced materials*. Springer International Publishing, pp 241–286
4. Tan S, Hu X, Ding S, Zhang Z, Li H, Yang L (2013) Significantly improving dielectric and energy storage properties via uniaxially stretching crosslinked P(VDF-*co*-TrFE) films. *J Mater Chem A* 1:10353–10361. <https://doi.org/10.1039/c3ta11484h>
5. Ye HJ, Yang L, Shao WZ, Sun SB, Zhen L (2013) Effect of electroactive phase transformation on electron structure and dielectric properties of uniaxial stretching poly(vinylidene fluoride) films. *RSC Adv* 3:23730–23736. <https://doi.org/10.1039/C3RA43966F>
6. Sharma M, Madras G, Bose S (2014) Process induced electroactive β -polymorph in PVDF: effect on dielectric and ferroelectric properties. *Phys Chem Chem Phys* 16:14792–14799. <https://doi.org/10.1039/C4CP01004C>
7. Yamawaki Y, Morita M, Sakata I (1990) Mechanical and dielectric properties of cyanoethylated wood. *J Appl Polym Sci* 40:1757–1769. <https://doi.org/10.1002/app.1990.070400929>

8. Hirai N, Morita M, Suzuki Y (1993) Electrical properties of cyanoethylated wood meal and cyanoethylated cellulose. *Mokuzai Gakkaishi* 39:603–609. <https://doi.org/10.1002/app.1990.070400929>
9. Takechi S, Teramoto Y, Nishio Y (2016) Improvement of dielectric properties of cyanoethyl cellulose via esterification and film stretching. *Cellulose* 23:765–777. <https://doi.org/10.1007/s10570-015-0852-3>
10. Fukuda T, Sugiura M, Takada A, Sato T, Miyamoto T (1991) Characteristics of cellulosic thermotropics. *Bull Inst Chem Res, Kyoto Univ* 69:211–218
11. Sawai D, Nozoe Y, Yoshitani T, Tsukada Y (2012) Development of new cellulose-based polymers with excellent melt-processability. *FUJIFILM Res Dev*, pp 55–58
12. Yao K, Okoshi M, Kawashima M, Yamai K (2013) The development of flame-resistant bio-based plastic from inedible wood material. *Fuji Xerox Tech Rep* 22:96–103
13. Soyama M, Kiuchi Y, Iji M, Tanaka S, Toyama K (2014) Improvement in impact strength of modified cardanol-bonded cellulose thermoplastic resin by adding modified silicones. *J Appl Polym Sci* 131:1–7. <https://doi.org/10.1002/app.40366>
14. Unohara T, Teramoto Y, Nishio Y (2011) Molecular orientation and optical anisotropy in drawn films of cellulose diacetate-*graft*-PLLA: Comparative investigation with poly(vinyl acetate-*co*-vinyl alcohol)-*graft*-PLLA. *Cellulose* 18:539–553. <https://doi.org/10.1007/s10570-011-9508-0>
15. Yamanaka H, Teramoto Y, Nishio Y (2013) Orientation and birefringence compensation of trunk and graft chains in drawn films of cellulose acetate-*graft*-PMMA synthesized by ATRP. *Macromolecules* 46:3074–3083. <https://doi.org/10.1021/ma400155f>
16. Iwata S, Tsukahara H, Nihei E, Koike Y (1996) Compensation for birefringence of oriented polymers by random copolymerization method. *Jpn J Appl Phys* 35:3896–3901. <https://doi.org/10.1143/JJAP.35.3896>
17. Hahn BR, Wendorff JH (1985) Compensation method for zero birefringence in oriented polymers. *Polymer* 26:1619–1622. [https://doi.org/10.1016/0032-3861\(85\)90273-3](https://doi.org/10.1016/0032-3861(85)90273-3)
18. Ohno T, Nishio Y (2007) Molecular orientation and optical anisotropy in drawn films of miscible blends composed of cellulose acetate and poly(*N*-vinylpyrrolidone-*co*-methyl methacrylate). *Macromolecules* 40:3468–3476. <https://doi.org/10.1021/ma062920t>
19. Yamaguchi M, Masuzawa K (2007) Birefringence control for binary blends of cellulose acetate propionate and poly(vinyl acetate). *Eur Polym J* 43:3277–3282. <https://doi.org/10.1016/j.eurpolymj.2007.06.007>
20. Kowalski A, Duda A, Penczek S (1998) Kinetics and mechanism of cyclic esters polymerization initiated with tin(II) octoate, 1. Polymerization of ϵ -caprolactone. *Macromol Rapid Commun* 19:567–572. <https://doi.org/10.1002/marc.1998.030191106>
21. Davis DA, Hamilton A, Yang J, Cremar LD, Van Gough D, Potisek SL, Ong MT, Braun PV, Martínez TJ, White SR, Moore JS, Sottos NR (2009) Force-induced activation of covalent bonds in mechanoresponsive polymeric materials. *Nature* 459:68–72
22. Rifaie-Graham O, Apebende EA, Bast LK, Bruns N (2018) Self-reporting fiber-reinforced composites that mimic the ability of biological materials to sense and report damage. *Adv Mater* 1705483:1–16. <https://doi.org/10.1002/adma.201705483>
23. Ito T, Katsura C, Sugimoto H, Nakanishi EKI (2013) Strain-responsive structural colored elastomers by fixing colloidal crystal assembly. *Langmuir* 29:13951–13957
24. Yue Y, Kurokawa T, Haque MA, Nakajima T, Nonoyama T, Li X, Kajiwaru I, Gong JP (2014) Mechano-actuated ultrafast full-colour switching in layered photonic hydrogels. *Nat Commun*, p 4659
25. Miyagi K, Teramoto Y (2018) Dual mechanochromism of cellulosic cholesteric liquid crystalline films: wide-ranging colour control and circular dichroism inversion by mechanical stimulus. *J Mater Chem C* 6:1370–1376. <https://doi.org/10.1039/C7TC05092E>
26. Miyagi K, Teramoto Y (2018) Exploration of immobilization conditions of cellulosic lyotropic liquid crystals in monomeric solvents by in situ polymerization and achievement of dual mechanochromism at room temperature. *RSC Adv* 8:24724–24730. <https://doi.org/10.1039/C8RA04878A>

27. Nishio Y, Suzuki S, Takahashi T (1985) Structural investigations of liquid-crystalline ethylcellulose. *Polym J* 17:753–760. <https://doi.org/10.1295/polymj.17.753>
28. Ritcey AM, Charlet G, Gray DG (1988) Effect of residual linear orientation on the optical properties of cholesteric films. *Can J Chem* 66:2229–2233

Chapter 10

Biocompatible Anisotropic Designer Particles



T. T. Aiswarya and Sampa Saha

Abstract In recent years, particle technologies have been broadly focused on the manipulation of size, shape and surface chemistry. The electrohydrodynamic co-jetting of different polymer solutions lead to a unique design of particles with multiple and distinct surface patterns of micro- or nano-compartments. Moreover, the ability to selectively modify individual areas on the surface of a particle, cylinder or a fiber is another important physico-chemical property, which necessitates the anisotropic distribution of interfacial binding sites. The current chapter will focus on the spatiospecific surface modification of individual compartments that can yield a novel type of shape-shifted microcylinders via surface-selective click chemistry in conjunction with surface-initiated atom transfer radical polymerization (ATRP). Additional examples will also be discussed toward microparticles with fully orthogonal surface patches that take advantage of a combination of chemically orthogonal polylactide-based polymers and their fabrication via electrohydrodynamic co-jetting to yield rarely reported multifunctional microparticles. Finally, these microparticles will be applied as drug delivery vehicles to carry multiple drugs and to release them at desirable rates. Several microstructured particles are highly sought after for their potential to present multiple distinct ligands in a directional manner for targeted drug delivery applications.

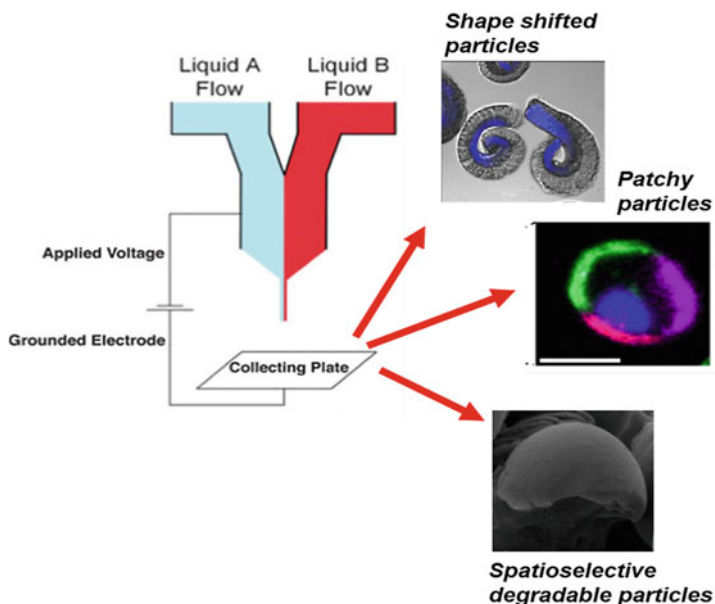
T. T. Aiswarya · S. Saha (✉)

Department of Materials Science and Engineering, Indian Institute of Technology Delhi, Hauz Khas, New Delhi 110 016, India
e-mail: ssaha@polymers.iitd.ac.in

© Springer Nature Singapore Pte Ltd. 2020

V. Katiyar et al. (eds.), *Advances in Sustainable Polymers*, Materials Horizons: From Nature to Nanomaterials, https://doi.org/10.1007/978-981-15-1251-3_10

217

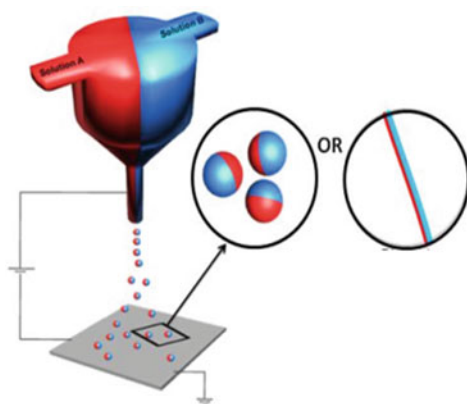


Keywords Electrohydrodynamic co-jetting (EHDC) · Anisotropy · Orthogonal chemistry · Surface functionalization · Biodegradable microparticles · Drug delivery

1 Introduction

Particle engineering has undergone a breakthrough with a continuous increase in adaptability, tunability and flexibility of particles. The broad focus on the manipulation of size, shape and surface chemistry has helped in the development of microparticles with controlled internal and external architectures, with assuring properties for triggered drug delivery and self-assembly applications. There are many techniques that are used in preparation of these materials such as controlled deformation technique to produce monodisperse elliptical polymeric particles, swelling and phase separation method and self-assembly of block copolymers [1–4]. Among these methods, electrohydrodynamic co-jetting (EHDC) is one of the most attractive techniques because of its ease and simplicity (Fig. 1). In this process, different polymeric solutions are injected through two or more needles arranged in side by side fashion and flown under a laminar regime. This prevents any lateral mixing of the polymers and provides a stable interface between the fluids leading to the formation of a droplet at the tip of the cojoined multiple needles. The droplet formed gets converted into a Taylor cone upon applying electric field, and electrified polymeric jet is ejected from the tip that results in formation of millions of individual droplets [5]. The immediate reduction in diameter of droplets takes place causing an increase in the total surface

Fig. 1 Schematic and digital micrograph representation of the electrohydrodynamic co-jetting process. Reprinted with permission from ref. [16]; Copyright 2014 Wiley



area of the particle due to rapid evaporation of the solvent leaving behind solidified nano or microparticles in the collecting electrode [6]. Depending on the various process parameters like polymer concentrations, flow rate, viscosity, voltage, etc., shape and size of particles can be tailored. This technique also allows the formation of multicompartmental fibers obtained from different polymeric solutions to align into a single fiber that can be collected as a mat on the collector or a bundle of fibers on a rotating drum collector. The ability to control the property of individual compartments on the same particle allows incorporation of multiple materials and material combinations with different sets of functionalization that can give rise to orthogonal properties [7]. These microparticles can be applied as drug delivery vehicle to carry multiple drugs and then releases them at the desirable rates [8, 9]. Theoretical studies about controlling self-assembly and molecular recognition show that materials that are anisotropic in nature can be effectively used for multiple applications [10, 11]. Synthesis of non-spherical particles is currently the topic of study that has been investigated extensively along with multiple functionalization of hemispherical part of a sphere. These particles can be designed and recognized from each side such as top to bottom or left to right to yield particles of pre-programmed functionality. This approach provides a new science based on nano or microparticles and fibers that bring wide opportunities to design different materials with various shape and size combinations. Different multicompartmental particle shapes like snow-man, dumbbell like, acorn like, disk shape, rods, etc. like structures can be prepared in one step [12, 13]. These anisotropic particles also belong to a family of particles where asymmetry originates from the particles shape and chemical composition. The anisotropic particles can also be a combination of hydrophobic and hydrophilic hemisphere that may act as colloidal surfactants of intermediate hydrophobicity and can be active in stabilizing emulsions [14, 15]. An important property that distinguishes these microparticles is their competence to selectively modify individual surface of a particle. The current chapter will focus on the spatioselective surface modification of a particular compartments can yield a novel type shape-shifted microcylinders via surface-selective click chemistry in conjunction with surface-initiated atom transfer radical polymerization

(ATRP), patchy particles, degradable particles and applications of these material systems and their purpose of study has been elaborately defined.

2 Fabrication of Polylactide-Based Multicompartmental Microparticles/Cylinders/Fibers Using Electrohydrodynamic Co-jetting Technique

As discussed above, the electrohydrodynamic co-jetting technique is one-step method for fabricating multicompartmental particles with various shape and size as shown in Fig. 2. Since each of the compartments can be tailored and modified independently it can be utilized in various cases where two incompatible materials are engineered in close proximity to one another [7, 8, 16, 17]. Selective surface modifications of individual compartments of these microparticles are completely probable. In order to selectively modify a particular surface, it is necessary to apply orthogonal immobilization chemistries [18]. In addition to this, drugs and other functional biomolecules can directly be incorporated into particles by dissolving them along with the polymers in the jetting solution. This gives 100% encapsulation efficiency, unlike other encapsulation techniques such as double emulsion particle preparation method.

Electrohydrodynamic co-jetting (EHDC) method consists of a stainless steel needle system that is connected to a high voltage power supply. A high precision syringe controls the flow rate of individual polymeric solutions coming from the needle and

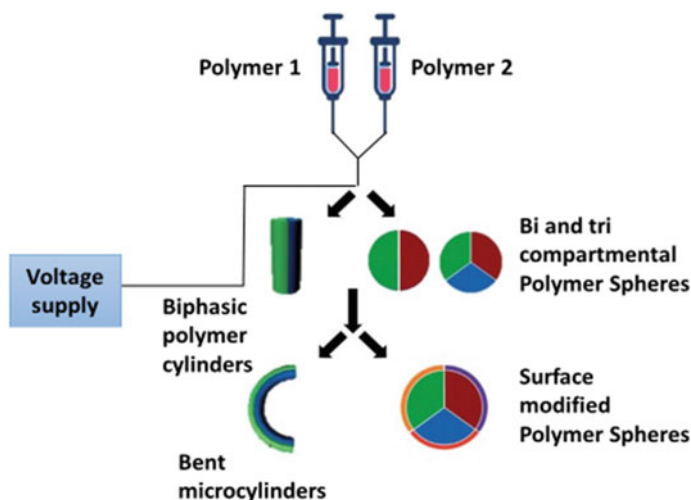


Fig. 2 Setup of electrohydrodynamic co-jetting technique used for fabrication of microparticles of various shape and size

high voltage controls the strength of electric field applied to the flowing polymeric solution. Liquid droplets containing two or more polymer solutions produced by the laminar flow are result of arrangement of capillary needles in side by side fashion. These droplets when subjected to an electric field are seen to experience two major forces: coulombic forces due to the external field and repulsive forces between the surface charges on the droplet. The coulombic force exceeds the surface tension at certain critical field strength resulting in the distortion of the droplet into a conical shape and an electrified jet forming millions of secondary droplets ensues from the tip of this cone. This cone jet produces a narrow size distribution of particles. Polymeric solutions once introduced into the needles are subjected into a required flow rate and electric field for the formation of desired shape of the particles. It was observed that for all polymeric solutions cone jet mode is obtained but at different applied voltages and flow rate In response to the electric field, the compound droplet that is generated at the tip of the capillary needle assembly distorts into a Taylor cone as a result of applied voltage as shown in Fig. 1 [18]. Multicompartmental particles are formed on the collector electrode as a result of solvent evaporation and particle solidification. The mixing of polymeric solutions coming from different needle is prevented by the rapid evaporation and laminar flow and the number of compartments formed depends on the number of needles. This makes electrohydrodynamic co-jetting an effective method to form particles having high drug loading capacity with uniform dispersion of different drugs in their individual compartments to prevent drug–drug interactions. By altering the flow rate, applied voltages, polymer concentration, etc. microparticles or microfibers having multiple compartments can be produced. Spatioselective surface modification can be done once the biphasic particles and fibers are fabricated containing polymers with functionality in one compartment. The functionalized compartment can be modified later to attach biomolecules as well as polymers on the surface of fabricated particles. For example, the polymer architectures elaborated by click chemistry reactions, having a higher selectivity and tolerance to a wide range of functional groups, which can be utilized in functionalizing these particles surfaces [19–21]. In one of the studies, copper(I)-mediated 1,3-dipolar cycloaddition of azides and alkynes was used for this purpose [18]. Modification of poly [lactide-*co*-(propargyl glycolide)] particles is done by reacting the particles with azido-PEG-amine in the presence of Cu^+ ions, generated by the reaction of Cu^{2+} in presence of sodium ascorbate. The surface modification was confirmed by confocal micrograph image where green fluorescence of FITC used on one side of the compartment as seen (Fig. 3).

As discussed earlier, the multifunctional microcylinders can also be fabricated using this technique which involves fabrication of bundles of multicompartmental fibers which are later converted to multifunctional microcylinders of desired length [22, 23]. Fibers are formed using electrohydrodynamic co-spinning method in which fibers are collected from the tip of the needle assembly. The multiple polymer solutions are passed through the multiple needles and the single compartmental fiber is formed which can be collected onto the rotating drum substrate without any breakage to achieve an ordered alignment of fiber bundle, crucial for microcylinder fabrication. Generally, a low flow rate and low concentration of polymer, for example, poly

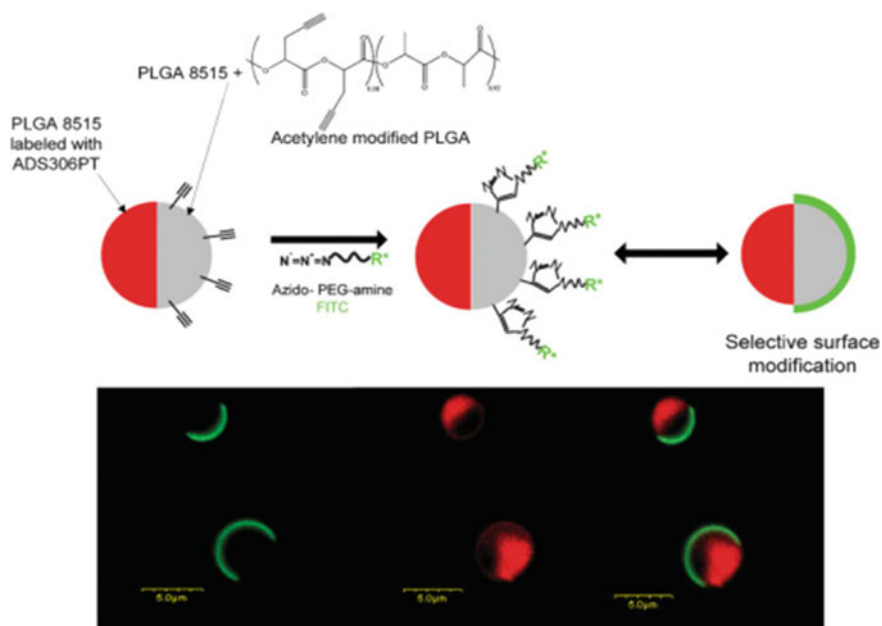


Fig. 3 Biphasic microfibers with one phase labeled with ADS306PT and other phase containing poly [lactide-co-(propargyl glycolide)]. Azido-PEG-amines were reacted with acetylene groups and FITC were reacted with free amine groups. Uniform surface modification on phase that contains acetylene groups were confirmed from green fluorescence on a single side. Reprinted with permission from ref. [18]; Copyright 2008 Wiley

(lactic-co-glycolic acid) favors the formation of fiber in order to achieve multicompartmental fibers. The rotation of wheel assembly at an optimized RPM favors the deposition of fiber in an ordered bundle for long interval of time.

As mentioned above, it is possible to achieve tri or tetra phasic fibers by simultaneous use of three or more solutions in jetting process. Once the fibers are collected, it can be converted to the microcylinders by an automated or semi-automated cryosectioning method. In this process, fiber bundle of 1 cm is cryosectioned after embedding it in a gel here by controlling the speed of cytochrome and the slice thickness, the length of microcylinders can be controlled. A well-dispersed rod-shaped colloid is obtained by ultra-sonication of suspended fibers bundle in phosphate saline solution as shown in Fig. 4. The microcylinders formed can be spatioselectively surface modified by using Huisgen 1,3-dipolar cycloaddition reaction [22]. In this particular study, the process is utilized for the fabrication of microcylinders having large and small compartments that can be achieved by manipulation of the number of the needles. A small amount of acetylene functionalized PLGA, poly (lactide-co-propargyl glycolide) was mixed with the jetting solution in one of the compartment in order to introduce free acetylene groups in the bulk of compartment. The process was used on four-compartment cylinder configuration. Reaction of microcylinders was

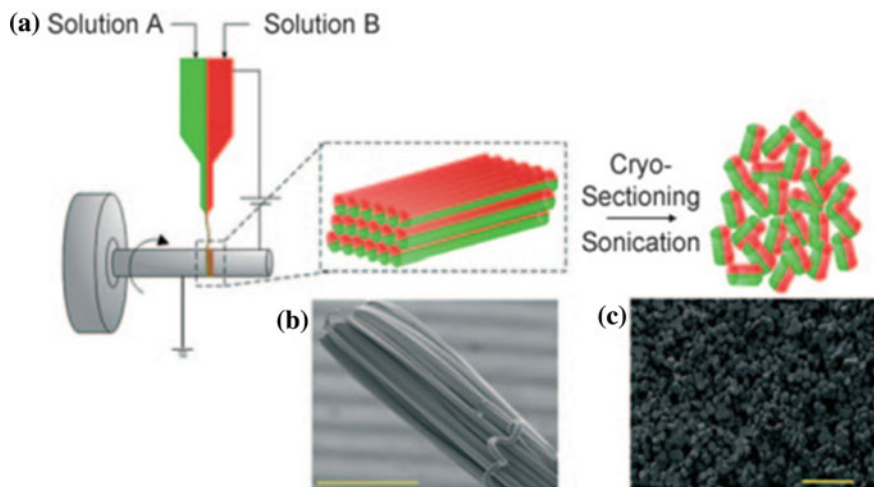


Fig. 4 (a) Electrohydrodynamic co-spinning and cryosectioning results in fiber bundles that later yield uniform microcylinders. (b) SEM micrograph of bicompartmental fiber bundles. Reprinted with permission from ref. [22]; Copyright 2009 Wiley

done with biotin-(ethylene oxide) azide in the presence of copper sulfate and sodium ascorbate resulting in the biotin immobilization in one of the compartments of the microcylinders. Incubation of these cylinders with streptavidin favored the selective binding of streptavidin with biotin which was confirmed using CLSM microscopy. The red fluorescence dye tagged with streptavidin can be seen on the surface of one of the compartments' cylinders, shown in Fig. 5.

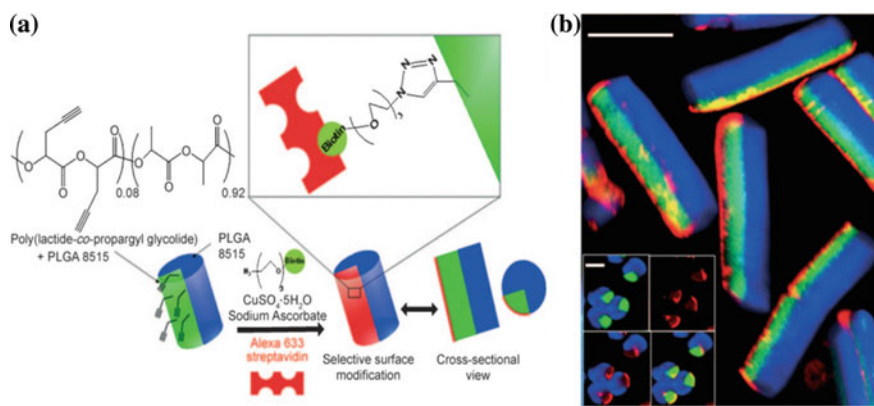


Fig. 5 (a) Selective surface modification of multicompartmental microcylinders. (b) Confirmation of spatioselective surface modification from axial and cross-sectional CLSM micrographs. Reprinted with permission from ref. [22]; Copyright 2009 Wiley

3 Controlled Bending Transitions of Compositionally Anisotropic Microcylinders

Anisotropic materials are a single material system possessing multiple properties in different directions. Multicompartmental particles are a good example of anisotropic particles as different compartments can be designed distinctively. In addition, Janus particles showing two different property at two different phases is another good system for studying anisotropic behavior [24, 25]. Interestingly, anisotropic behavior of polymer particles can be further elaborated in controllable transitions in shape and size of a material by changing polymer material property in directional manner. Particles of various shape and size that further show transitions in shape or size as a result of different conditions have vast applications such as sensors, actuators and surface patterning. These particles which further show transition behavior can be fabricated using EHDC technique followed by spatiospecific chemistry. Various shape changes take place as a result of changing temperature or other conditions. Figure 6 shows how microcylinders are prepared using EHDC technique, further brushes are grown on the cylinders to modify its properties by using click chemistry followed by ATRP [7], and brushes in the cylinder make them responsive toward hydrophilic environment that shows how the shape is change when subjected to water. Different dyes are used to show different compartment which shows how the

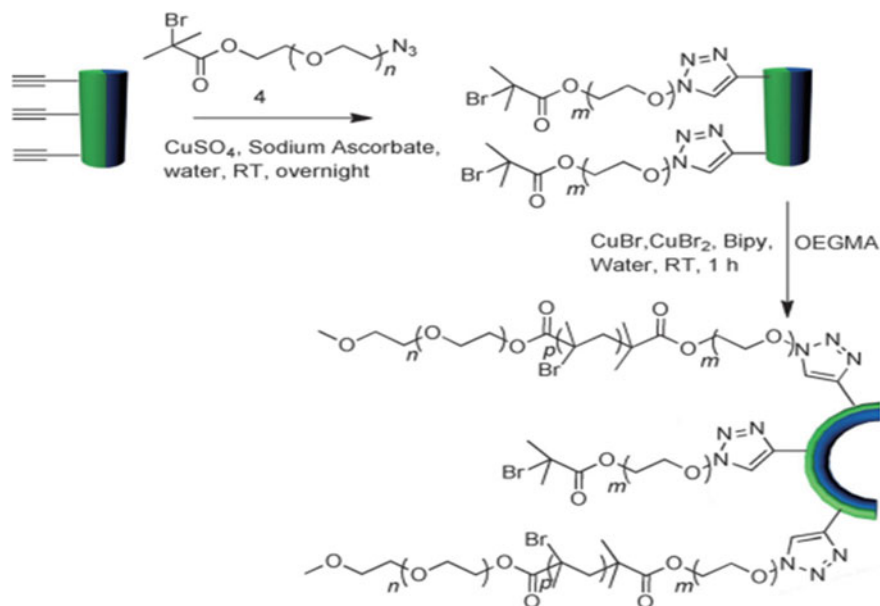


Fig. 6 Selective surface modification of bicompartmental microcylinders with a PEGMA surface layer. Reprinted with permission from ref. [26]; Copyright 2012 Wiley

compartments are formed without getting mixed or influencing the shape of the final particle.

Spatioselective growth of polymer brush (hydrophilic brush) from one of the compartments make the cylinder change their shape because growing polymer chains on the soft surface face repulsive force from each other which make the cylinders to bend in a particular direction.

Fabrication of microcylinders showing transitions in particle morphology as a result of increasing one of the dimensions of the microcylinders (length) have been studied by Saha et al. it shows how material shape changes by changing the length of microparticles (Fig. 7). The study clearly demonstrates the change of shape of material as a result of site -selective growth of polymer brushes of surface layer leading to asymmetric expansion of one compartment. Also blending or chemical modifications of these polymers with hydrophilic brushes result in formation of semiporous bent architecture upon drying which can be used for active and controlled drug release applications.

Moreover, aspect ratio of the cylinder can be adjusted in order to achieve a fine tuning from simple bent to coiled structures. Short and long cylinders show different bending behaviors, as short cylinders having high bending stiffness than the long ones, curl around the cylinder ends forming a circular structure, whereas long

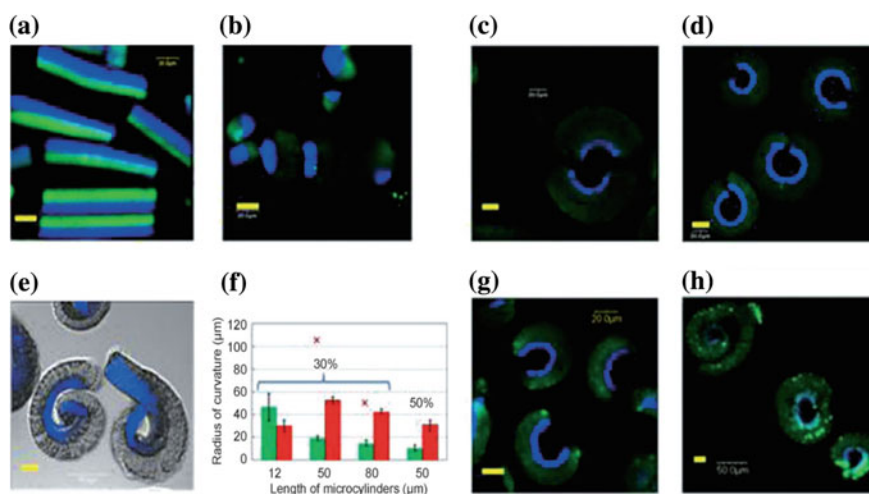


Fig. 7 Representative images of (a) brush free bicompartmental microcylinders of 120 μm length (before polymerization) and after spatioselective surface-initiated polymerization of OEGMA on microcylinders of different lengths: (b) 12 μm, (c) 50 μm, (d) 80 μm and (e) 120 μm. All multiphasic cylinders contain around 30% of acetylene-PLGA in one compartment. (f) Measured inner (green) and red (outer) radii of curvature versus length of biphasic microcylinders, for brush bilayers at two different acetylene concentrations. Effect of grafting density on bending for (g) 50 μm and (h) 80 μm biphasic cylinders (after polymerization) which contains 50% of acetylene-PLGA in one compartment. Yellow scale bars are 20 μm. Reprinted with permission from ref. [26]; Copyright 2012 Wiley

cylinders form spiral structures as a result of lower bending stiffness [26]. Here, the curvature can be tuned depending upon the length of cylinders used and amount of functionalized polymer used while jetting. Tetra compartmental microcylinders can also be prepared in which one compartment can be modified to change the shape of the particles in order to avail wide range of architectures by using same methodology.

4 Chemically Orthogonal Three-Patch Particles

Multiple patches in a single particle provide distinct and multiple properties. These particles are highly desirable as it can present distinct and multiple ligands in a directional manner. Preparation of these patchy particles involves different methods such as photolithography, microfluidic, microcontact printing, dip-pen nanolithography which suffer from multiple steps, rigorous procedures. EHDC provided a unique solution to it in which a particle with multiple independent compartments can be fabricated and further surface modifications on each compartment are possible depending on the surface chemistry which must be orthogonal [10]. EHDC is a single step technique by which functionalized polymers can be used while fabricating the particles and further modification of those functionalized polymers can be done. The design of spatially controlled three-dimensional objects like microparticles can be established by linking electrohydrodynamic co-jetting and synthetic polymer chemistry. The spatially controlled immobilization can be effectively used for attaching chemically orthogonal anchor groups on the distinct surface patches of the same particle [7]. A new method was developed by Rahmani et al. [7] combining synthetic polymer chemistry with electrohydrodynamic co-jetting to create two or three patches in microparticles that display orthogonal functionalities. Spatially controlled orthogonal immobilization methods are used for the distribution of ligands that are chemically distinct in a directional manner on the same microparticle. Bicompartamental microparticles can be synthesized with one hemispherical patch that selectively displays one functional anchor group and the second compartment comprising of nonfunctional PLGA polymer that acts as an internal reference material for the surface reactions. Chemical orthogonality is imparted in poly (lactide-*co*-glycolide) (PLGA)-based polymer when functionalized PLGA is added to different compartments of the microparticles as they can guide to orthogonal surface modifications without showing any cross reactivity (Fig. 8).

Bicompartamental particles having surface functionality in one compartment that contains triphenylphosphine functionalized PLA (with green dye) were reacted with azide-PEG-Biotin (PEG: polyethylene glycol) via Staudinger ligation. For imaging purpose, biotin was labeled with TRITC-Streptavidin (red dye). Coexistence of green and red fluorescence in the CLSM images confirmed the spatially controlled surface modification (Fig. 9a). These microparticles were incubated with bovine serum albumin (BSA) protein and tetramethylrhodamine (red dye). Incubated particles were exposed to UV light (365 nm) to initiate photo-immobilization of the BSA to the reactive surface patch (Fig. 9b) containing PLA modified with benzophenone.

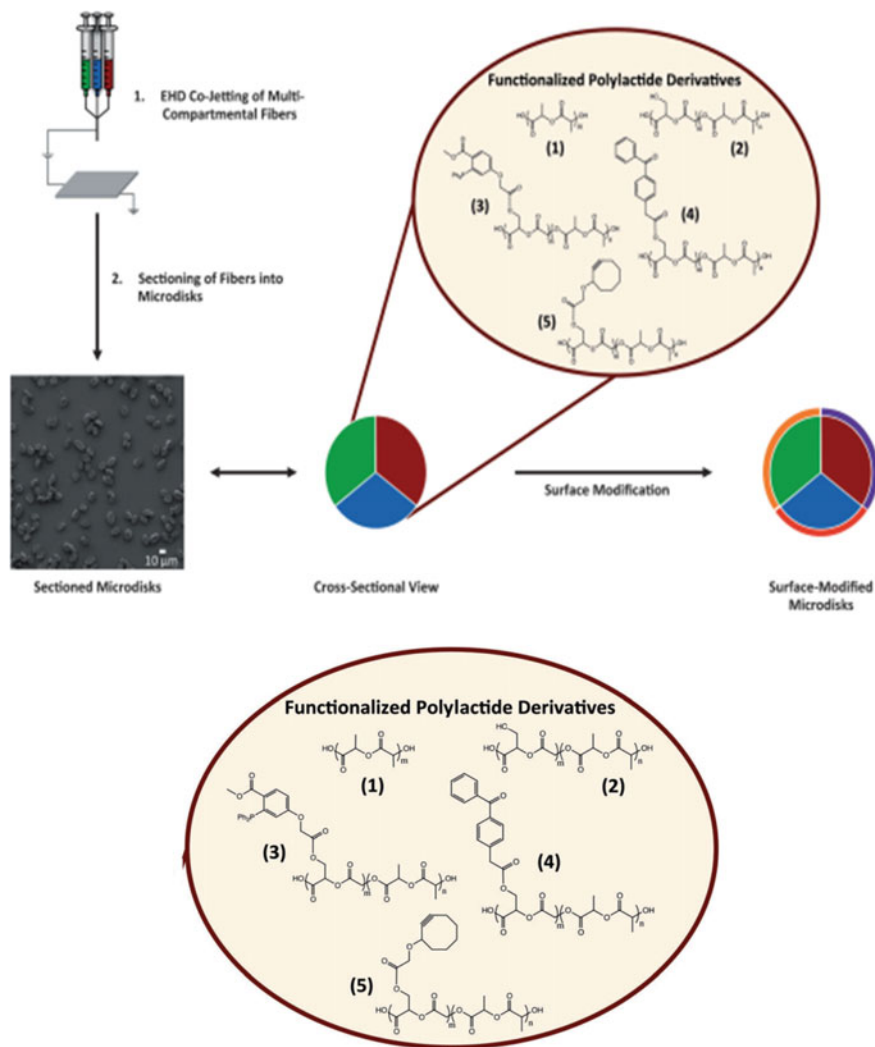


Fig. 8 Microparticles with orthogonal functionality fabricated through EHD co-jetting technique. Incorporation of functionalized poly lactide derivatives (1–5) into different jetting solutions resulted in compartmentalization of fibers. Reprinted with permission from ref. [7]; Copyright 2014 Wiley

Bicompartmental microparticles composed of cyclooctyne functionalized undergo copper-free click reactions, which was verified by CLSM analysis. Selective surface binding confirms spatially controlled surface modification of microparticles with azide-PEG-biotin followed by the attachment of Alexa Fluor 647 Streptavidin

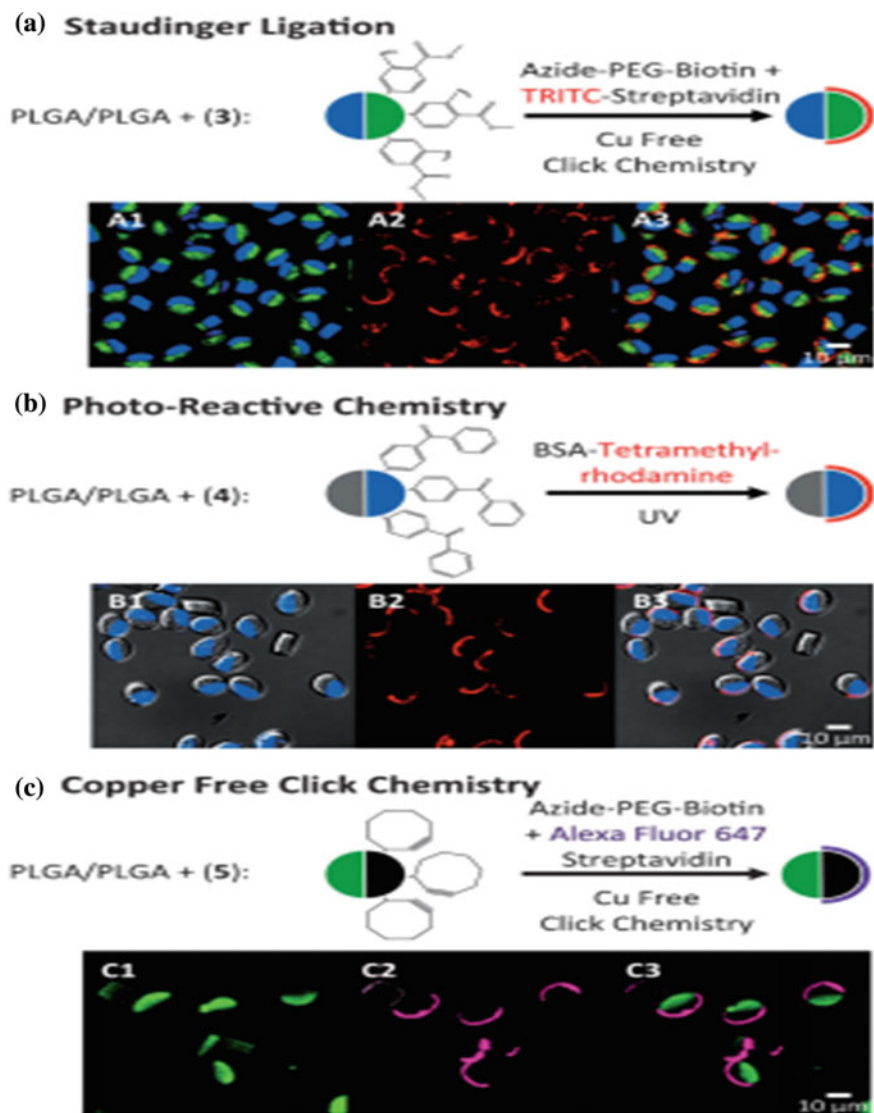


Fig. 9 Microparticles containing three types of orthogonally functionalized PLA derivatives in one hemisphere were surface modified. In (a)–(c), microparticles display polymers 3–5 in single hemisphere are selectively surface functionalized via Staudinger ligation (a), photo-immobilization (b), alkyne/azide click chemistry (c) Spatioselective nature of the surface modifications confirmed through CLSM imaging. Reprinted with permission from ref. [7]; Copyright 2014 Wiley

(magenta dye). Further experiments were conducted by immobilization of two different functionalized PLA derivatives in different hemispheres within same microparticle. Bicompartamental particles containing hydroxyl functionalized PLA and photoreactive PLA derivative (Polymer 4) in separate compartments. Localization of various moieties in different hemispheres can be observed from Raman confocal microscopy Fig. 10a). Presence of base polymer PLGA was confirmed in both hemispheres (red), but the PLA derivative 4 is constrained in single side (yellow). In the first step, the particles were reacted with BSA tetramethylrhodamine (red dye) in the presence of UV light followed by reaction with amine-PEG-FITC (green dye) via EDC/sulfo-NHS (Fig. 10b) chemistry.

In addition to these, Rahmani et al. have shown the fabrication of three patched particles fabricated using PLA polymer with three different functionalities which are orthogonal to each other as discussed before. This work clearly shows the ease of formation of these particles as well as proper formation of the particles without

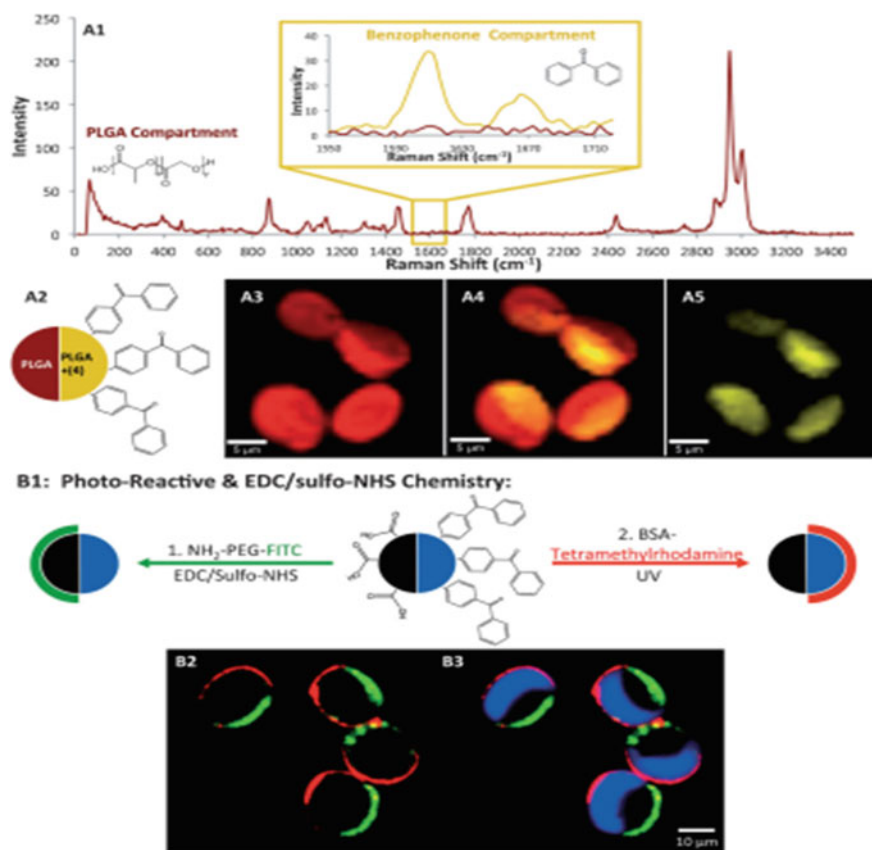


Fig. 10 Chemically orthogonal microparticles characterized through Raman microscopy (Fig. 3a), CLSM imaging (Fig. 3b). Reprinted with permission from ref. [7]; Copyright 2014 Wiley

disturbing any of the properties of the adjacent polymer present. These particles can be used in drug delivery applications as size of the particles fabricated in EHDC technique can be regulated by varying the concentration of polymeric solutions or voltage. Use of multi-patched particles widens the area of research by providing multidisciplinary applications in biomedical field starting from targeted drug delivery to micro-machines/actuators. Multi patches systems have potential to show even wider application areas and EHDC technique can be utilized for fabricating vast range of materials of various size and shape that can be tuned while preparing those particles.

5 Selective In Vitro Hydrolytic Degradation of Compositionally Anisotropic Microparticles

In controlled drug delivery systems, biodegradable polymers are of great interest as they provide a promising way for continuous release of drug by diffusion or erosion mechanisms. Biodegradation process in polymers contributes toward drug elution from the matrix which is further tuned depending upon the rate of degradation required. Number of parameters has been identified that effects polymer degradation, such as morphology, autocatalysis, amorphous or crystalline. [27]. In addition to these, chemical composition structure and molecular weights also greatly influence the rate of degradation of these polymeric materials. Amorphous polymers enhance the rate of degradation as incorporation of water molecules into the bulk of these polymeric chains becomes easier as compared to crystalline polymers. Molecular weight is another factor affecting the rate of degradation as low molecular weight material tends to degrade faster due to presence of shorter chains inside the polymer matrixes. In addition, incorporation of hydrophilic groups in the polymer backbone may also facilitate its hydrolytic degradations.

In case of multicompartamental system, degradation of either compartment can be tuned based on the nature of polymers used to make the compartment. Based on this hypothesis, hydroxyl functionalized PLGA was synthesized to be used as one of the compartments in bicompartamental particles fabricated using EHDC as mentioned above [28]. The process include ring-opening co-polymerizations of monomer A and L-lactide in melt using benzyl alcohol (BnOH) as the initiator and Sn(Oct)₂ as the catalyst, to yield polymer A. Polymer A further undergoes reactions to yield the final product polymer 2 which contains reactive hydroxyl groups on their main chain as shown in Fig. 11. The compartment which comprises of hydroxyl functionalized PLGA having hydroxyl group as pendent group in one of the copolymers may definitely facilitate water ingresson resulting faster degradation of that specific compartment.

Controlled drug release study of this rapidly degrading polymer containing particles was done by Rahmani [29]. Microparticles were fabricated with varying percentage of polymer 2 in one compartment (0, 10, 50 and 100% w/w). It was observed

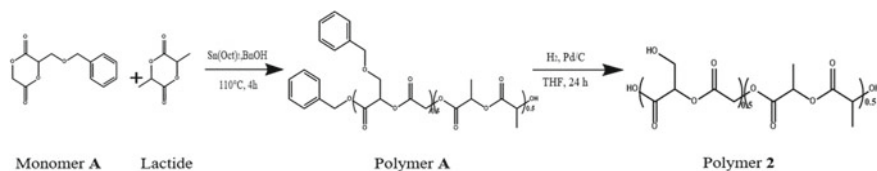


Fig. 11 Synthesis of hydroxyl functionalized poly(lactide)

that the particles containing 100% polymer 2 in one compartment degraded rapidly resulting in the loss of that whole compartment within 24 h, while hemisphere containing PLGA remained unchanged [30]. Further degradation starting at the interface of the two compartments and through the bulk of the second compartment yielded hollow half spheres by the second day. This rapid degradation of the PLGA compartment is most likely due to the lower pH environment induced by the degradation of polymer 2. The particles with 50% of this polymer degraded at a slower rate, with pores seen selectively in one compartment by day 2, followed by the degradation of that compartment by day 4. The particles containing only 10% of polymer 2 in one compartment degraded at a much slower rate with pores seen only after 11 days [29].

Drug release study was done using same particles and irinotecan (2% w/w), a cancer therapeutic was used as model drug which was selectively encapsulated in rapidly degrading compartment. The reference used was PLGA on both sides which were also loaded with irinotecan. It was noticed that higher the polymer 2, the faster is the degradation of the particles leading to the faster release of drug. Within 15 days, the particles containing PLGA had a constant release of irinotecan to ~75%. When polymer 2 loaded at 10% w/w, it was increased to 95% within the same time frame. While, the incorporation of polymer 2 at 50% and 100% w/w, resulted in a rapid release of irinotecan (approximately 100% of the encapsulated therapeutic was released by 10 days) [29].

Controlled drug delivery is a vast field where biomedical studies deal with simultaneous release of different types of drug for treatment of diseases like diabetic, cancer, Parkinson's, etc. When two or more different types of drugs are needed to be released at same time with different release profiles, these kinds of compositionally anisotropic particles devised by EHDC will be particularly useful.

6 Compositionally Anisotropic Bicompartamental Particles for Dual-Drug Delivery

Various studies showed wide applications of this bicompartamental and compositionally anisotropic particles in multiple drug delivery applications. For example, one could envision sequential release of anti-angiogenic and chemotherapeutic drugs from multicompartamental particles made of biodegradable polymers with independent release kinetics. Coupled with incorporation of imaging agents in a slowly

degrading compartment, multicompartmental particles may offer possibilities of real-time monitoring of circulation and degradation behavior, combining therapeutics with diagnostics. Bicompartamental particles showing dual behavior are extensively used in drug delivery applications because its design which makes it used for releasing more than one type of drug from a single system. Controlled release is needed in some of the special treatment processes where drug needs to be released at a particular rate. Dual-drug delivery systems also reduce the complications of inhaling drugs by the patients as in multiple drug carrier system, single phasic matrix system can show some reactivity with the second drug which leads to delay in inhaling the second drug as it needs the first matrix to degrade fully. However, in dual-drug delivery system can be designed in such a manner that one side of the particle degrades first and the second material has the property of initiating the degradation after a specific amount of time or release at a very slow rate compared to the first one. In other words, many combinations can be prepared and the drug release can be tuned as per the required application. Dual-drug delivery systems provide a vast area of application in biomedical fields.

Ekaterina et al. have used EHDC for fabrication of dual-responsive multicompartmental smart materials particles [31]. Here, Ekaterina et al. have fabricated dual stimuli-responsive PEG-based polymer was synthesized by post-polymerization modification of PAGE through click reaction. The particles were fabricated using photosensitive materials that can accelerate the degradation in water because of UV and oxidative treatment. In order to confirm the formation of bicompartamental particles, SEM and CLSM images were studied. A similar study using EHDC techniques was done by Sangyuel et al. in which polymer particles were fabricated using poly (ethylene oxide) and poly (acrylamide-co-acrylic acid) on one side and poly (acrylamidedeco acrylic acid) and dextran on other side of the compartment. Differential hydrolytic susceptibility was caused by compositional anisotropic material which provided selective degradation of one compartment containing PEO. Furthermore, fabrication of anisotropic particles using other techniques are also reported such as Olga et al. in their study have observed the behavior of Janus particles used for lung cancer treatment [32]. In their work, self-assembled dual-responsive particles were synthesized using biodegradable and biocompatible mixtures of polymers. Doxorubicin and curcumin drugs were loaded into polymeric carriers using PLGA and PVA polymers by emulsion technique which successfully fabricated nanoparticles accommodating two different types of drug both having different solubility and biological behavior. The prepared drug carriers were observed to be accumulated into cytoplasm and nuclei that was first initiated by cancer cells. The application part of these particles was studied by inflation delivery of nanoparticles into lungs of mice. The study showed that these drugs were incorporated into polymer matrix without affecting the chemical natures of the drugs or their activity in treatment of cancer cells. In another interesting example, Prathipan et al. in their study have shown fabrication of disk-shaped drug delivery particle system for the treatment of Parkinson's disease which can be administered orally. The disk-shaped particles were used due to their slow release characteristics and improved adhesions as well as particle movement in the gastrointestinal tract. Two hydrophilic drugs (levodopa (LD) and carbidopa

(CD)) were loaded into these particles and their releases were studied. Due to the decarboxylation and wide distribution throughout body only 1% of levodopa (LD) is reached in the after each oral dose so another drug carbidopa (CD) can be used along with LD to prevent decarboxylation of LD. Achieving a continuous delivery of both the drugs is a challenge as both the drugs have lower half-life ($t_{1/2}$ –LD = 50–90 min and $t_{1/2}$ –CD = 1–2 h). This study showed a right balance in tuning the release rate of both drugs from bicompartamental particle. This study was related to release of drug to the degradation rate of both the polymers into gastric system. The degradation mechanism and release behavior of the drugs were seemed to be based on swelling, diffusion and erosion mechanism of polymer particles. Author has shown how levodopa releases from amorphous PLGA in higher rate as compared to carbidopa from PLA phase (semi-crystalline polymer) that shows slower degradation rate. Selecting a drug carrier system can be manipulated according to the desired rate of multiple release drugs. This study shows that both the polymers displayed simultaneous release of the drugs from each compartment without any drug–drug interactions. Drug release is governed by the degradation behavior of polymer used. PLGA being amorphous in nature showed higher release rate compared to PLA having semi-crystalline nature. Furthermore, it was observed that PLA compartment displayed an increased surface roughness than PLGA surface. Rapid evaporation during solidification stage results in anisotropic solvent evaporation from various compartments as a combined effect of higher viscosity, chain entanglement and higher crystallinity that originates from the PLA domain of the microparticles. It was observed that particles undergo considerable shrinkage during the solvent evaporation. This results in the shrinkage between both the compartments. The compartment containing semi-crystalline polymer undergoes more shrinkage than compartment containing amorphous polymer, this results in difference in surface roughness between both the compartments. In vitro drug release study was executed to observe the release profile for both the drugs in simulated gastric as well as in intestinal fluid (SGF and SIF) for up to 24 h. The result indicated that from PLGA compartment, LD and CD were released faster than that from PLA compartment. It was observed that compartment made of PLA degraded at a slower rate due to its hydrophobic nature and semi-crystalline structure. Hydrophilic nature of PLGA accelerates drug release from PLGA compartment. Comparative release study of microparticle loaded with both the drugs at a ratio of LD/CD = 4:1 with commercial tablet Syndopa was also conducted. Two set of particles were fabricated that have LD or CD in PLA or PLGA compartments (samples A and B) with drug ratio of 4:1. The release profile was investigated in SGF for 5 h followed by in SIF for 24 h. In case of system A, it was observed that release rate of CD was higher than that of LD from PLGA compartment even though LD is having 4 times higher concentration than CD. For further study, two more set of particles were fabricated with a higher drug dose (samples C and D) while keeping drug ratio same as earlier (LD/CD = 4:1). It was seen that there occurs a sustained release following initial outburst as in case of sample B. The release rate of CD was observed to be increased with the decrease in the CD concentration ($B > C > D$) which may be due to the greater compatibility since their difference in solubility parameter is ~ 3 . This resulted in the greater interaction between CD and

semi-crystalline PLA matrix. The polymer matrix will entrap the drug so the release percentage is lowered. Release percentage of LD from PLGA matrix has observed to be remain stable in all the formulations which may be as a result of less compatibility between the matrix and drug (difference in solubility parameter ~ 5). Release profile of both the drug was compared with Syndopa tablet under same conditions. It was observed that a complete release of both drugs within a span of 2 h lacking to provide controlled and sustained release of dual drugs, so multiple dosing of drugs would be needed daily in order to maintain a certain plasma concentrations. Both the drugs LD and CD were observed to get released in time period of 2 h lacking in controlled and sustained release of the drugs, resulting in the need of multiple dosing of both the drugs into a single system maintaining its plasma concentrations. These studies showed how compositionally anisotropic and compartmental particles can be useful in delivering multiple drugs at desired fashions without losing their activity via drug–drug interactions.

These studies showed how compositionally anisotropic and compartmental particles can be useful in delivering multiple drugs at desired fashions without losing their activity via drug–drug interactions.

7 Conclusion

Recent developments in particle science have brought vast improvements in various fields but most astonishing and fascinating works are reported in biomedical fields which include diagnostics and drug delivery technologies for sustained, controlled and targeted delivery. For safe and efficient delivery of drugs at the targeted site, the anisotropic bicompartmental particles are a potent candidate that assures better results compared to conventional medicine. In addition the surface modification of bicompartmental particles has opened door for the further development and research in this field such as triggered delivery of active, microactuators, sensors, etc. In the upcoming era, multicompartmental patchy particles will be in high demand especially, when targeted or triggered delivery of multiple drugs with imaging facility will be desired in addition to high cell uptake.

Acknowledgements Department of Material Science and Engineering, Institute of Technology, Delhi, India is appreciated for providing research and teaching funds.

References

1. Indalkar YR, Gaikwad SS, Ubale AT (2013) Janus particles recent and novel approach in drug delivery: an overview. *J Curr Pharma Res* 3:1031–1037. <https://doi.org/10.33786/jcpr.2013.v03i04.010>

2. Tréguer-Delapierre M, Madeira A, Hubert C, Ravaine S (2018) Recent advances in the synthesis of anisotropic particles. In: Anisotropic particle assemblies, 1–35. <https://doi.org/10.1016/b978-0-12-804069-0.00001-0>
3. Tran L, Lesieur S, Faivre V (2014) Janusnanoparticles: materials, preparation and recent advances in drug delivery. *Expert Opin Drug Deliv* 11:1061–1074. <https://doi.org/10.1517/17425247.2014.915806>
4. Lee G, Cho Y, Park S, Yi G (2011) Synthesis and assembly of anisotropic nanoparticles. *Korean J Chem Eng* 28:1641–1650. <https://doi.org/10.1007/s11814-011-0183-5>
5. Roh K, Martin D, Lahann J (2005) Biphasic janus particles with nanoscale anisotropy. *Nat Mater* 4:759–763. <https://doi.org/10.1038/nmat1486>
6. Lahann J (2011) Recent progress in Nano-biotechnology: compartmentalized micro and nanoparticles via electrohydrodynamic co-jetting. *Small* 7:1149–1156. <https://doi.org/10.1002/sml.201002002>
7. Rahmani S, Saha S, Durmaz H, Donini A, Misra A, Yoon J, Lahann J (2014) Chemically orthogonal three-patch microparticles. *Angew Chem Int Ed* 53:2332–2338. <https://doi.org/10.1002/anie.201310727>
8. Hwang S, Lahann J (2012) Differentially degradable janus particles for controlled release applications. *Macromol Rapid Commun* 33:1178–1183. <https://doi.org/10.1002/marc.201200054>
9. 2019 In: Researchportal.port.ac.uk. https://researchportal.port.ac.uk/portal/files/5753099/Ashleigh_Smith_PhD_2015.pdf
10. Lallana E, Sousa-Herves A, Fernandez-Trillo F, Riguera R, Fernandez-Megia E (2011) Click chemistry for drug delivery nanosystems. *Pharm Res* 29:1–34. <https://doi.org/10.1007/s11095-011-0568-5>
11. Glotzer S, Solomon M (2007) Anisotropy of building blocks and their assembly into complex structures. *Nat Mater* 6:557–562. <https://doi.org/10.1038/nmat1949>
12. Hwang S, Roh K, Lim D, Wang G, Uher C, Lahann J (2010) Anisotropic hybrid particles based on electrohydrodynamic co-jetting of nanoparticle suspensions. *Phys Chem Phys* 12:11894. <https://doi.org/10.1039/c0cp00264j>
13. Khoee S, Nouri A (2018) Preparation of janus nanoparticles and its application in drug delivery. Design and development of new nanocarriers, pp 145–180. <https://doi.org/10.1016/b978-0-12-813627-0.00004-1>
14. Lee K, Yoon J, Lahann J (2011) Recent advances with anisotropic particles. *Curr Opin Colloid Interface Sci* 16:195–202. <https://doi.org/10.1016/j.cocis.2010.11.004>
15. Li F, Josephson D, Stein A (2010) Colloidal assembly: the road from particles to colloidal molecules and crystals. *Angew Chem Int Ed* 50:360–388. <https://doi.org/10.1002/anie.201001451>
16. Bhaskar S, Pollock K, Yoshida M, Lahann J (2010) Towards designer microparticles: simultaneous control of anisotropy, shape, and size. *Small* 6:404–411. <https://doi.org/10.1002/sml.200901306>
17. Bhaskar S, Pollock KM, Hitt J, Nandivada H, Deng X, Lahann J (2010) Multicompartmental microstructured materials via electrohydrodynamic co-jetting: a diagnostic and biosensing platform. In: ILASS-Americas 22nd Annual Conference on Liquid Atomization and Spray Systems, Cincinnati, OH, May 2010
18. Bhaskar S, Roh K, Jiang X, Baker G, Lahann J (2008) Spatioselective modification of bicompartamental polymer particles and fibers via Huisgen 1,3-Dipolar cycloaddition. *Macromol Rapid Commun* 29:1655–1660. <https://doi.org/10.1002/marc.200800459>
19. Avti P, Maysinger D, Kakkar A (2013) Alkyne-Azide “click” chemistry in designing nanocarriers for applications in biology. *Molecules* 18:9531–9549. <https://doi.org/10.3390/molecules18089531>
20. Fleischmann S, Hinrichs K, Oertel U, Reichelt S, Eichhorn K, Voit B (2008) Modification of polymer surfaces by click chemistry. *Macromol Rapid Commun* 29:1177–1185. <https://doi.org/10.1002/marc.200800095>
21. Zhang X, Zhang Y (2013) Applications of Azide-based bioorthogonal click chemistry in glycobiology. *Molecules* 18:7145–7159. <https://doi.org/10.3390/molecules18067145>

22. Bhaskar S, Hitt J, Chang S, Lahann J (2009) Multicompartmental microcylinders. *Angew Chem* 121:4659–4663. <https://doi.org/10.1002/ange.200806241>
23. Lee K, Yoon J, Rahmani S, Hwang S, Bhaskar S, Mitragotri S, Lahann J (2012) Spontaneous shape reconfigurations in multicompartmental microcylinders. *Proc Natl Acad Sci* 109:16057–16062. <https://doi.org/10.1073/pnas.1213669109>
24. Nie Z, Li W, Seo M, Xu S, Kumacheva E (2006) Janus and ternary particles generated by microfluidic synthesis: design, synthesis, and self-assembly. *J Am Chem Soc* 128:9408–9412. <https://doi.org/10.1021/ja060882n>
25. Perro A, Reculosa S, Ravaine S, Bourgeat-Lami E, Duguet E (2005) Design and synthesis of Janus micro and nanoparticles. *J Mater Chem* 15:3745. <https://doi.org/10.1039/b505099e>
26. Saha S, Copic D, Bhaskar S, Clay N, Donini A, Hart A, Lahann J (2011) Chemically controlled bending of compositionally anisotropic microcylinders. *Angew Chem Int Ed* 51:660–665. <https://doi.org/10.1002/anie.201105387>
27. Li S (1999) Hydrolytic degradation characteristics of aliphatic polyesters derived from lactic and glycolic acids. *J Biomed Mater Res* 48:342–353. [https://doi.org/10.1002/\(sici\)1097-4636\(1999\)48:3%3c342:aid-jbm20%3e3.0.co;2-7](https://doi.org/10.1002/(sici)1097-4636(1999)48:3%3c342:aid-jbm20%3e3.0.co;2-7)
28. Parthipan A, Gupta N, Pandey K, Sharma B, Jacob J, Saha S (2018) One-step fabrication of bicompartamental microparticles as a dual drug delivery system for Parkinson's disease management. *J Mater Sci* 54:730–744. <https://doi.org/10.1007/s10853-018-2819-x>
29. Rahmani S (2019) Multifunctional drug carriers with programmable properties. In: Deepblue.lib.umich.edu. <https://deepblue.lib.umich.edu/handle/2027.42/111636>
30. Esfahani R, Jun H, Rahmani S, Miller A, Lahann J (2017) Microencapsulation of live cells in synthetic polymer capsules. *ACS Omega* 2:2839–2847. <https://doi.org/10.1021/acsomega.7b00570>
31. Nair M, Jayant R, Kaushik A, Sagar V (2016) Getting into the brain: potential of nanotechnology in the management of NeuroAIDS. *Adv Drug Deliv Rev* 103:202–217. <https://doi.org/10.1016/j.addr.2016.02.008>
32. Swider E, Koshkina O, Tel J, Cruz L, de Vries I, Srinivas M (2018) Customizing poly (lactic-co-glycolic acid) particles for biomedical applications. *Acta Biomater* 73:38–51. <https://doi.org/10.1016/j.actbio.2018.04.006>

Chapter 11

Development of Biomass-Derived Cellulose Nanocrystals and its Composites



Kona Mondal, Neha Mulchandani, Somashree Mondal and Vimal Katiyar

Abstract Cellulose nanocrystals are the most fascinating smart bio-based nanomaterials derived from the most abundant and inexhaustible, naturally occurring biopolymer “cellulose.” These nanomaterials have received a tremendous amount of interest in both industry and scientific research due to their unique structural and physicochemical properties including mechanical, optical, chemical, and rheological along with bio-compatibility, biodegradability, renewability, low density, and adaptable surface chemistry. However, few challenges are addressed due to the hydrophilic nature of these nanocrystals while acting as reinforcing agent for developing composite films. The surface modification or functionalization of these nanomaterials is one such strategy to meet the various challenging demands such as the development of high-performance nanocomposites, using hydrophobic polymer matrices. Considering the increasing potential of this sustainable bio-nanomaterial, the current chapter aims to collate the knowledge about the various biomass-based sources, the details of synthesis techniques, and wide applications along with the compatibility of sustainable polymers of cellulose nanocrystals. Further, the details about the various characteristic properties of these bio-nanomaterials and its composites are discussed along with their potential in wide range of applications.

Keywords Bio-nanomaterials · Sustainable · Biodegradability · Composites

1 Introduction

The growing and emerging trends of developing and utilizing nanoscaled material in several aspects of life offers a new approach toward research, innovation, and governance. Further, the bio-based, novel, and renewable nanomaterials have gained much interest with the aim of reducing environmental hazards. Meanwhile, the synthesis

K. Mondal · N. Mulchandani · S. Mondal · V. Katiyar (✉)
Department of Chemical Engineering, Indian Institute of Technology Guwahati,
Kamrup, Assam 781039, India
e-mail: vkatiyar@iitg.ac.in

and functionalization of nanomaterials with their well-defined structure and modifications have attracted an increasing attention due to their various potential applications in the field of nanoscience and nanotechnology. The advancement of these nanomaterials has led to the development of functionalized nanoparticles that have broadened their area of application in research as well as in industrial sectors, such as in medicine, electronics, packaging, composites, biomaterials, and energy production [1]. However, due to the growing concerns of global warming and sustainable development, the need of substituting conventional or petroleum-based resources as raw material with renewable bio-based is essential [2]. Furthermore, the ability to transform cheap and abundant material to yield high value-added products will aid significant benefit. Recently, these nanomaterials have largely used in the context of developing new composite materials with enhanced properties and functionalities derived from the nanomaterials and the structures they form. Cellulose nanocrystals (CNC) are the recently developed, biodegradable, environment-friendly, and nontoxic green bio-nanomaterials.

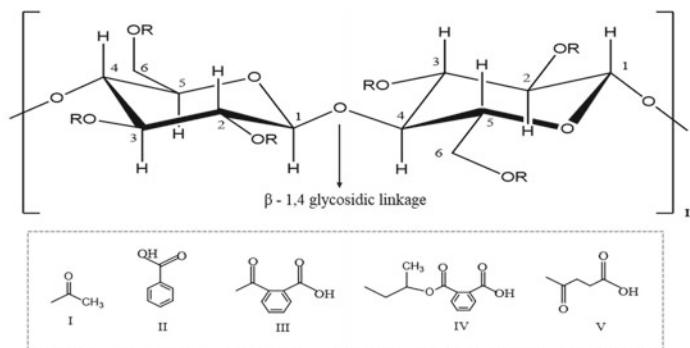
Cellulose is a standout amongst the richest crude materials found on the surface of earth. It is a boundless biopolymer which has its broad use because of its reasonable properties. Cellulose can be derived from various sources like plant sources, microbial sources, and also from aquatic animals. Cellulose is a fibrous and water-insoluble polymer that has various advantages like biodegradability, renewability, and bio-compatibility. Previously, cellulose had its use limited to the clothes, paper and pulp, and construction industry, but now, owing to its abundancy and unique properties, it is being processed at nanoscale in the form of CNCs. Using various isolation processes, different types of nanomaterials can be derived from cellulose. Recent advances are focused on deriving nanomaterials and nanofibers (which have dimensions of nanometers) and using them based on their distinct properties. CNCs are a subtype of such nanomaterials which are highly crystalline in nature and are usually rod or needle shaped. The nanocrystals have certain biophysicochemical properties which owes to its huge range of applications, such as low thermal expansion, gas impermeability, and surface chemistry that is adaptable to various environmental changes, optical transparency, and better mechanical properties [3, 4]. Depending on the source from which the crystals are derived, the CNCs vary in properties. Also the properties of CNCs depend on the isolation process. Acid hydrolysis is the most common technique for deriving crystals from cellulose where strong acids like sulfuric and hydrochloric acid are usually used. However, there are various other methods available such as oxidation, water hydrolysis, mechanical refining, enzymatic hydrolysis, etc. Nanocomposites, where CNCs act as reinforcement, have higher elastic modulus and a good amount of shift in glass transition. CNCs have high length-to-diameter ratio and also large surface area because of its size that ranges in nanometers. Due to these reasons, CNCs are suitable for nanocomposites. Also the mechanical properties of the nanocomposites are improved by greater interfacial area and better interactions between the matrix and the reinforcement. This chapter is mainly focused on the structure and dimensions of the CNCs, its various sources, various methods of isolation, and the different properties of CNCs depending the sources of extraction and the isolation technique and the applications thereof.

2 Cellulose Nanocrystals

Cellulose consists of fiber like structures which are usually crystalline in nature. These microfibrils have different properties depending on the source from which it is derived. On undergoing various chemical, physical, and enzymatic treatments, these highly crystalline structures can form CNC. Also, it has various shapes including rod, needle, and spherical depending on the source material. They can too differ in properties based on the process of isolation. They have high crystalline structures and high modulus as compared to that of bulk cellulose.

2.1 Structural Arrangement of Cellulose

Cellulose is comprised of $\beta(1-4)$ connected glucose deposits and the uridine diphosphate-glucose atom which functions as a substrate for the cellulose biosynthesis. Cellulose is a linear homopolymer usually derived from anhydroglucose which is one of the glucose residues. All the other alternate glucose residues in the same cellulose chain are $\beta(1-4)$ linked by synthase protein isoform (CESA isoform) and are rotated by 180° . The auxiliary redundant unit of cellulose chain is the dimer, (two glucose residues $\beta(1-4)$ -linked) known as cellobiose. In each cellulose chain, two different terminal groups are found as shown in Fig. 1. One end of the each chain is attached to a reducing group with a structure that is aliphatic in nature and a carbonyl group. A closed ring structure along with a non-reducing group is attached to the other end of chain. At the non-reducing ends, glucose residues are added by CESA isoforms, which allow chain elongation. Cellulose is a rigid linear structure



- Cellulose ethers 'R' groups are as follows: Methylcellulose [H, CH₃]; Ethylcellulose [H, CH₂CH₃]; Hydroxyethylmethylcellulose [H, CH₃, [CH₂CH₂O]_n H]; Hydroxypropylcellulose [H, [CH₂CH(CH₃)O]_n H]; Carboxymethylcellulose [H, CH₂COONa]
- Cellulose esters 'R' groups are as follows: Acetate [H, I]; Acetate trimellitate [H, I, II]; Acetate phthalate [I, III]; Hydroxypropylmethylphthalate [H, CH₃, CH₂CH(OH)CH₃, III, IV]; Hydroxypropylmethylphthalate acetate succinate [H, CH₃, CH₂CH(OH)CH₃, I, V]

Fig. 1 Chemical structure of cellulose

and is water insoluble having a unique structure because of $\beta(1-4)$ -linkages. Further, many thousands of glucose repeat units are linked together covalently through ether groups by $\beta(1-4)$ linkage, called as a glycosidic bond (Fig. 1).

There are six different polymorphs of cellulose, namely—cellulose I, II, III_I, III_{II}, IV_I, and IV_{II}. These polymorphs are crystalline in nature. Cellulose I and cellulose II exist in nature while the others are produced by chemical and heat treatments. Cellulose I is subdivided into allomorphs, I α and I β . Cellulose I α -like chain has similarity with crystalline algal cellulose I α [5]. Cellulose is often found in amorphous form as cellulose I [6]. In both the cellulose forms, the inter-chain hydrogen bonding has two different patterns. The bonding O₆—H—O₃ in cellulose I is dominant whereas, in cellulose II, the inter-chain hydrogen bonding O₆—H—O₂ is dominant. The inelastic and straight shape of each cellulose chain is imparted by the O₃—H—O₅ bonding. The intra-hydrogen bonding plays the prior role for imparting these characteristics. This bonding is found in both polymorphs (I and II) [7–9]. The higher visualization of the structure of cellulose demonstrates that there are two distinctive chains in a unit cell in I β , wherein, all the glucosyl residues are similar but they face in opposite direction alternately whereas in I α , there is a single chain structure in a triclinic unit cell. In this structure of cellulose, alternate glucosyl residues differ slightly in configuration and hydrogen bonding. The O₂ and O₆ have various possibilities of hydrogen bonding. The O₂—H—O₆ bonding (intra chain) is present in both I α and I β . But the chain bonding is shorter in that of I α [8]. The O₂ and O₆ are very reactive hydroxyl groups, but the less reactivity of O₃ atoms is due to the O₃—H—O₅ bonding which is strong [10].

2.2 Cellulosic Nanomaterials

Cellulosic nanomaterials are made from a very common material found on earth, cellulose. They can be made from materials such as plants, wood, algae, and bacteria. Cellulosic nanomaterials from different sources are of different types and shapes having various different properties. These are whisker like materials and crystalline in nature with a range of mechanical properties. Some cellulosic nanomaterials have unique properties that are important for the applications in optics, nanotechnology, and in fields of material science. As the name suggests, these materials are nano-sized and have highly ordered cellulose chain bundles. These bundles of cellulose chain are aligned along the axis of the bundle. To this, they impart new properties in contrast to the properties of their sources. Cellulose nanomaterials have low thermal expansion, high mechanical properties, and high aspect ratio. They have hydroxyl groups attached to the surface which when chemically modified impart additional functionalities. The nanomaterials have higher surface area, modulus, amorphous fractions, and specific strength in comparison to normal cellulose. The huge industrial applications of cellulosic nanomaterials may be accounted for their minimum environmental risks, low safety risks, sustainability and biodegradability, and also lower processing costs.

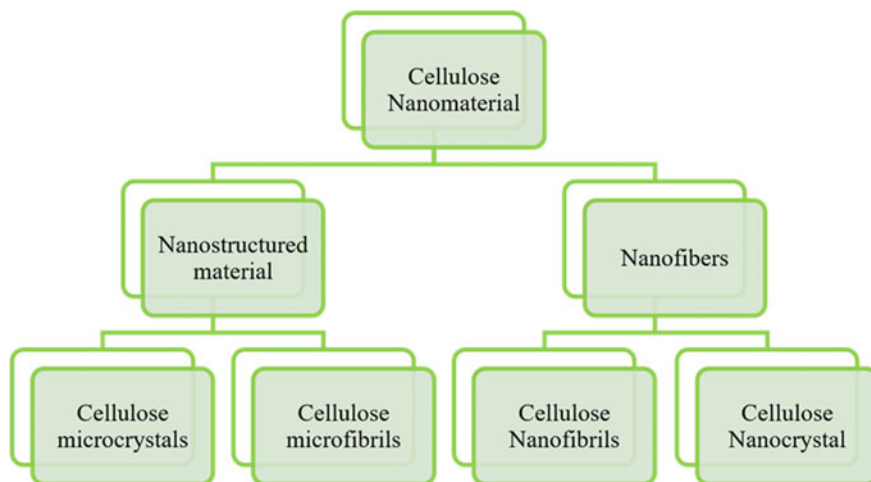


Fig. 2 Different forms of nanocellulose

Cellulose nanomaterials can be broadly classified into two types viz. nanostructured materials and nanofibers (Fig. 2). These two can be further subdivided depending on the size of the particles. Nanostructured materials can be classified as microcrystals and microfibrils whereas the nanofibers can be categorized into nanofibrils and nanocrystals.

2.3 Various Crystalline forms of Cellulose Nanocrystals

CNCs are highly crystalline because of the linear and homogeneous nature of the cellulose polymer and also the intermolecular hydrogen bonding between the cellulose chains that are adjacent to each other. The source of the cellulose and the isolation process determines the size of the crystal and the degree of crystallinity. For example, the degree of crystallinity in bacterial cellulose is 50–60%, 80% in tunicates, and 90% in some algae. Acid hydrolysis is generally employed to isolate the crystalline cellulosic structures in the form of CNCs. This idea of acid hydrolysis to isolate cellulose nanocrystal from disarranged inter-crystalline areas of cellulose chain networks was developed by Nickerson and Habrle [11]. It was later confirmed by Rånby [12] when he produced colloidal suspensions of cellulose crystals.

The different polymorphs of cellulose may have different properties such as nanocrystal I, cellulose nanocrystal II, cellulose nanocrystal: I \rightarrow II (i.e. cellulose nanocrystal II derived from cellulose I), and cellulose nanocrystal III. All these polymorphs are produced using different methods like acid hydrolysis, sulfuric acid hydrolysis specifically. Depending on the polymorphs, the CNCs contrast in their properties and their effect on the properties of the network of the polymer. All these

polymorphs of cellulose nanocrystal differ in their reinforcing ability and network formation ability along with precisely percolated network formability.

The cellulose nanocrystal can be of fibrous structure, in the form of microfibrils and macrofibrils. The microfibrils are fundamental structures that build the microfibrillar part of every single layer of cell wall. The rudimentary fibrils are made of just $\beta(1-4)$ -connected glucose residues that are CESA complex synthesized [13]. Microfibril mainly comprises of elementary fibrils and these fibrils are mainly associated with polymers, non-cellulosic in nature. Every microfibril has 36 glucose chains in approximation. Inter-hydrogen bonding and intra-hydrogen bonding stabilizes the glucose chains and provides higher stability to microfibrils [7, 8]. The degree of polymerization of cellulose chains is in the range of 2000–25,000 glucose residues [14]. In case of primary cell wall of aspen wood, the degree of polymerization is 4200, whereas in case of secondary cell wall, it is 9200 [15].

Recently, microbial auxiliary model dependent on direct visualization of the maize parenchyma cell walls, primary cell walls to be specific, was proposed with the use of atomic force microscopy [13]. As per the model, there are thirty-six glucose chains which are re-distributed based on their respective location into three groups. The first group that comprises the center actual-crystal core is made of six glucose chains which form a hexagonal shape cross-section. The first group is seen to be completely crystalline in structure. The next group is made of twelve sub-crystalline chains and is directly connected with the crystal core. The last group consists of eighteen sub-crystalline or noncrystalline chains situated at the outside of crystal. The second and third groups add to the protection and transitional stages between the crystal centers and later keep noncrystalline polymers.

2.4 Dimensions of Cellulose Nanocrystals

The measurements, length and width of the CNCs may vary depending on the nature of the cellulose microfibrils and the states of corrosive hydrolysis such as time, temperature, etc. The dimensions of the CNCs are shown in Table 1 based on the various sources and extraction methods. Since the hydrolysis process is diffusion-controlled, cellulose nanocrystal has a huge range of length and width. There is a variation in average length of the rod-shaped particles from tens to nanometers. The width ranges from 3 to 50 nm. The aspect ratio of CNCs play a major role in determining its reinforcing capability. The aspect ratio is nothing but the ratio of its geometrical length-to-diameter and higher the aspect ratio, higher the reinforcing ability. The mechanical performance of CNCs is improved by the networks. Aspect ratio or angle proportion assumes a vital job in the development of these systems.

Table 1 Dimensions of cellulose nanocrystal based on various sources

Source	Preparation method	Length (nm)	Width (nm)	Aspect ratio	Reference
Wood	H ₂ SO ₄ hydrolysis	100–150	3–5	20–100	[16]
Sisal	H ₂ SO ₄ hydrolysis	100–300	3–5	–60	[17]
<i>Tunicates</i>	H ₂ SO ₄ hydrolysis	>1000	10–20	–100	[18]
Valonia	H ₂ SO ₄ hydrolysis	1000–2000	10–20	50–200	[19]
Bacteria	H ₂ SO ₄ hydrolysis	100–1000	10–50	2–100	[20]
Ramie	H ₂ SO ₄ hydrolysis	70–200	5–15	12	[21]
Cotton	HCl hydrolysis	100–300	5–10	10–30	[22]
Bacteria	HCl hydrolysis	160–420	15–25	7–23	[23]

3 Biomass-Based Sustainable Sources of Cellulose Nanocrystals

CNCs are derived from various sources such as plant cell walls, algae, bacteria, cotton, rice husk, and microcrystalline cellulose. Depending on the source, maturity, extraction method and reaction parameters; various structures, properties, and application of CNCs can be obtained.

3.1 Lignocellulosic Sources

Woody and non-woody plants are a source of lignocellulosic fibers which is a good feedstock for the production of various nanocrystals. Lignocellulosic fibers can be broadly classified on the basis of part of the plant as leaf, stem, grass, seed or fruit, and straw.

Woody and non-woody plants can be termed as cellular hierarchical biocomposites that have been created by nature. In these, the semi-crystalline cellulose microfibril acts as reinforcement while the matrix material in such biocomposites is lignin or hemicellulose, waxes, and trace elements [24, 25]. There are a number of factors that prominently affects the properties of natural fibers. They are chemical composition, internal structure of fiber along with variation between different parts of the plant. On removing hemicellulose, lignin, and all other impurities, pure cellulose is obtained. Wood is the primary source of cellulosic fibers and an important raw material in production of cellulose nanocrystal.

Various sources such as aquatic plants, crops, herbs, and their by-products too are used as cellulosic sources. Fibers from these sources have cellulosic microfibrils less tightly wound around the primary cell wall in contrast to the secondary wall in case of wood. Bleaching methods in case of non-woody plant are less chemical and more energy demanding since due to the lower content of lignin as compared to woody plants. Other lignocellulosic sources can be sesame husk [26], sugarcane bagasse

[27, 28], groundnut shells [29], straws [30], jute [31], bamboo [32], and coconut [33]. Based on the sources and different isolation processes, cellulose crystals may vary in their morphology, degree of crystallization, surface charge, porosity, mechanical properties, stability, etc.

3.2 Algal Sources and Bacterial Sources

Algae is also a source of microfibrils other than lignocellulosic materials. Due to the high carbohydrate content of red algae, which is composed of agar and cellulose, it has numerous applications [34]. One such red algae is *Gelidium*. For preparation of cellulose nanomaterials, *Gelidium elegans* is used [35]. Since this red algae is readily available and abundant, it is widely used in production of cellulose nanomaterials. Cellulose producing algae usually belong to the orders *Siphonocladales* (*Dictyosphaeria*, *Valonia*, *Boergesenia* and *Siphonocladus*) and *Cladophorales* (*Microdyction*, *Rhizoclonium*, *Cladophora* and *Chaetomorpha*) [36]. Cellulose microfibril structures are different for varying algae species because of the biosynthesis process. For example, cellulose obtained from *Cladophora* or *Valonia* has a high degree of crystallinity that may reach up to 95% [37].

Cellulose that is derived from bacteria has high chemical purity, less weight, large water holding capacity, good mechanical properties, and high chemical stability. It is nontoxic, biodegradable, renewable, and has a highly crystalline network structure. There are certain species of bacteria that use a large variety of nitrogen and carbon sources for the production of cellulose. An example of such a bacteria is *Komagataeibacter xylinus*. There are various advantages of cellulose that are derived from microbes over the plant derived cellulose. They have higher purity, greater mechanical properties, higher water holding capacity, distinct nanostructure, and greater stability [38]. The cellulose microfibrils, that are formed, are in the shape of flat and thick pellicles on the surface of the growth medium [39]. Cellulose from bacterial sources has a high degree of polymerization and also has better chemical and mechanical properties.

3.3 Other Sources

Other sources of cellulose may be animals, precisely aquatic animals. Tunicates are proven to be a good source of cellulose. Tunicates are aquatic animals and fall in the category of invertebrates. Cellulose is present in the tunic tissues of the tunicates and it acts as a skeletal support to the tissues which covers their entire epidermis. Tunicates have a leathery structure that provides a good source for cellulose microfibrils. The structure and properties of the cellulose microfibrils depend on the various species of tunicates from where they are obtained. Table 2 showing CNCs derived from various

Table 2 Various cellulose nanocrystals derived from various sources

	Source	Dimension	Application and advantages	References
Lignocellulosic source	Seesame husk	30–120 nm	As reinforcement in polymer matrix	[26]
	Cotton	8 ± 3.4 nm (diameter)	Used in polymer composites since it has high crystallinity, low cost, etc.	[40]
	Palm oil	12.15 nm	Used in nanocomposites as it has high thermal stability	[41]
	Jute	550 ± 100 nm (length)	Used as reinforcing element in nanocomposites	[31]
	Rice husk	–	Used in drug delivery system	[42]
Algal source	Red algae (<i>Gelidium</i>)	21.8 ± 11.1 nm (diameter)	It has good thermal stability and is used in nanocomposite	[35]
Bacterial source	Bacteria (<i>Acetobactor xylinum</i>)	–	Used in biopackaging material	[43]

sources, its dimensions and its advantages and applications. This table has the recent advances made by CNCs.

4 Various Extraction Techniques of Cellulose Nanocrystals

The morphology, physiochemical properties, and mechanical characteristics of CNCs exhibit variations depending on their source of raw material and the extraction process. The latter step is crucial for further processing and developing CNCs into functional, high-value added products, and, as such, efforts to face the shortcomings in the conventional methodology, to increase the production with a reduced cost are continuously reported in the literature. As stated above, CNCs can be extracted from various raw materials on the earth that firstly need to follow a pre-treatment procedure for the removal of the matrix materials (e.g. lignin, hemicelluloses, fats, waxes, proteins, etc.) resulting in the extraction of the individual cellulose fibers. Depending on the source of the cellulose, the naturally occurring bulk cellulose primarily consists of highly ordered crystalline domains and some disordered amorphous regions

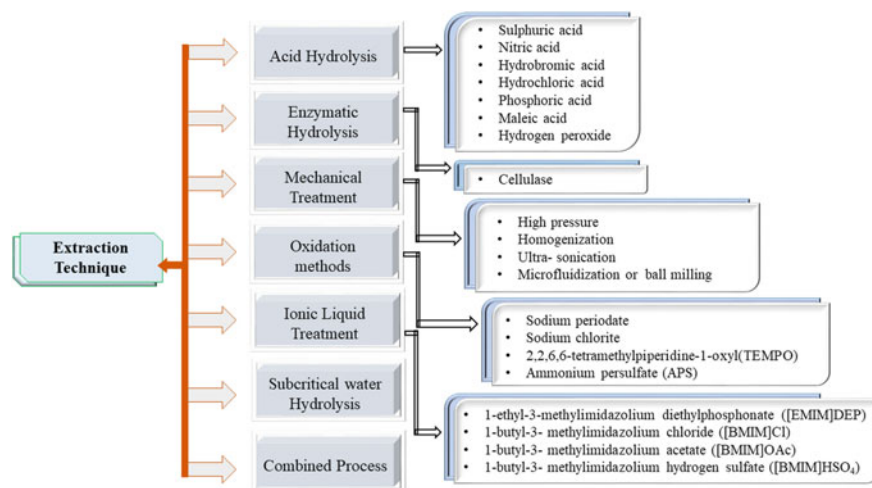


Fig. 3 Various extraction techniques of CNCs

in varying proportions. When these microfibrils are subjected to a proper combination of chemical, mechanical, oxidation and/or enzymatic treatments, the crystalline domains of the cellulose microfibrils can be isolated, giving rise to the formation of CNCs. The production of CNCs in an economic and sustainable way and further exploration of its functional products are currently the major tasks for the researchers both from the academia and industrial point of view. Several processes have been reported in literature for the extraction of CNCs, namely chemical acid hydrolysis, enzymatic hydrolysis, mechanical refining, ionic liquid treatment, subcritical water hydrolysis, oxidation method, and combined processes (Fig. 3).

4.1 Acid Hydrolysis

The most commonly used technique for the fabrication of CNC is acid hydrolysis. During the process, acid molecules are diffused through the cellulose microfibrils, resulting in cleavage of glycosidic bonds within cellulose molecular chains in the amorphous regions along the cellulose fibrils, thus leading to the breaking of the hierarchical structure of the fibril bundles into crystals form. The function of using acid in hydrolysis is to release hydronium ions that tend to penetrate the cellulosic material in the amorphous domains and also react with the oxygen molecules on the glycosidic linkages between two anhydroglucose moieties for the initiation of protonation of oxygen molecules and thus, hydrolytic cleavage of glycosidic linkages of amorphous regions occur. Moreover, the selective cleavage of cellulosic chains is done because of the difference in the kinetics of hydrolysis between paracrystalline and crystalline regions. Also, breaking down the polysaccharides into simple sugars

during acidic treatment could help to hydrolyze the residual pectin and hemicellulose. The size of the crystallites depends on the freedom of motion after hydrolytic cleavage and accordingly, they can grow and the dimension of crystallites will be larger than the original microfibrils.

In this hydrolysis technique, a specific concentration of desired acid is mixed with deionized water to form an acid solution which will be added to the pure cellulose. The final mixture at the end of the acid hydrolysis process is subjected to a number of separation and washing steps which is followed by the dialysis against deionized water for the removal of excess acid and neutralized salts. The hydrolyzed acid suspension is subjected to ultrasonication, homogenization, and centrifugation during separation and washing steps to get homogeneous dispersion of CNCs in aqueous media. Further, hydrolysis coupled with ultrasonication and homogenization is used to increase the activity of acids to degrade amorphous regions of cellulose. At the last, after dialysis, the neutralized suspension is subjected to centrifugation for the removal of deionized water followed by lyophilization/freeze-drying to obtain powdered CNC. A schematic representation of the acid hydrolysis process is shown in Fig. 4.

Several types of acids have been used by researchers to date, ranging from strong acid to weak bio-based acids such as sulfuric acid, hydrobromic acid, hydrochloric acid, phosphoric acid, maleic acid, and hydrogen peroxide to extract CNCs from different resources. However, sulfuric and hydrochloric acids are frequently used for the acid hydrolysis of cellulose from various sources. The effect of processing conditions on the physicochemical, thermal, and mechanical properties of CNC has been mentioned in literature by numerous researchers. Also, the particle size, crystallinity, morphology, thermal stability, and mechanical properties of CNC depend on the temperature and time of the hydrolysis along with the nature, concentration of

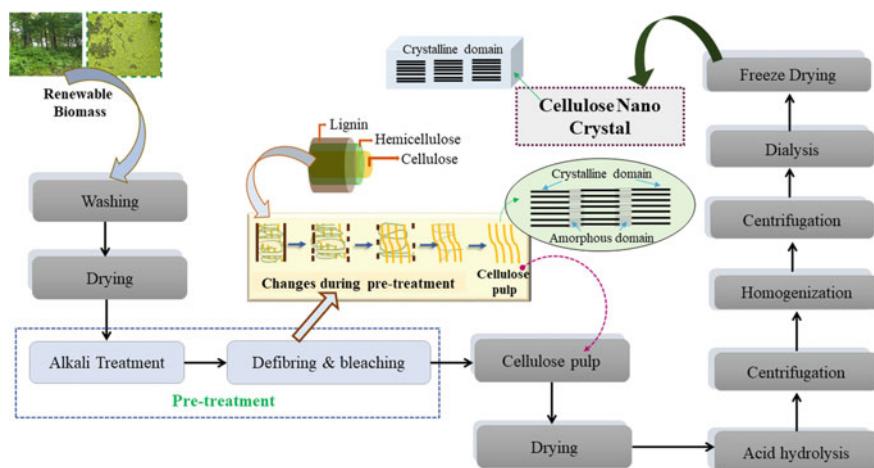


Fig. 4 A schematic representation of the acid hydrolysis process

acid, and fiber to acid ratio. It has been observed by the researchers that an increase in hydrolysis time showed reduction in the length of the CNCs and an increase in acid/fiber ratio reduced the crystals dimensions [44]. Moreover, the selection of acid affects the properties of the fabricated CNCs.

Sulfuric acid, the most commonly used acid for the CNC extraction, provides highly stable aqueous suspensions, due to the esterification of surface hydroxyl groups to give charged sulfate groups, whereas hydrochloric acid leads to an unstable CNC suspension, with minimal surface charge. Further, hydrochloric acid provides low-density surface charges along with limited dispersibility and also promotes flocculation in aqueous suspensions [45, 46]. Although the mentioned drawback can be arrested by surface modification or functionalization method. On the other hand, in the case of using sulfuric acid, a stable colloidal suspension is produced due to the high negative surface charge promoted by sulfonation of CNCs surface. In this context, these sulfate groups catalyze and initiate the degradation of cellulose at higher temperature. Thus, produced CNCs have limited thermal stability, which may restrict the use of CNCs in processing of CNC-based nanocomposites at high temperature [47]. Though several ways have been adopted to address the drawback related to their thermal stability, one of the ways is mixing the above-mentioned acids to generate CNCs with high thermal stability along with low dispersibility.

Other acids such as phosphoric acid surprisingly have achieved little attention in increasing the thermal stability and bio-compatibility by using functionalization of phosphate groups. This acid has also been used for the fabrication of CNCs by hydrolysis from cotton and cedar kraft pulp [48]. The acid has been added drop by drop to the cellulose slurry up to a predetermined concentration and further heated. Although, the yield of CNC completely depends on the reaction temperature and acid concentration. Generally around 80% yield has been achieved by the researchers. Espinosa et al. [47] reported the dimension and surface-charged density of phosphoric acid hydrolyzed fabricated CNCs. The fabricated CNCs had a width of ~31 nm, length of ~316 nm, and charge density of ~11 mmol/kg cellulose and obtained at the optimized conditions of 10.7 M phosphoric acid and 90 min reaction time at 100 °C. Application of phosphorylated microcrystalline cellulose and phosphorylated regenerated cellulose hydrogels have been investigated in bone regeneration [49]. Literature also states that phosphorylated CNCs have shown much higher thermal stability than partially sulphated CNCs.

A mineral acid, other than sulfuric acid, reported for fabrication of CNCs is hydrobromic acid (HBr). Further, to increase the yield of CNCs, ultrasonication had also been applied during hydrolysis reaction and the optimized condition 2.5 M HBr, 100 °C and 3 h, which resulted in a yield of around 80%. Cotton fiber had been chosen as source material for the production of CNCs. Moreover, HBr-modified CNCs can be used for site-specific grafting reactions.

In the context of reducing waste, coming from strong acids during the production of CNCs, ammonium persulfate (APS) can be used as substitute to sulfuric acid due to its inexpensive oxidizing nature with high water solubility and low stability. It has been reported that APS-based CNC production is a sustainable way which generates lesser hazard. This process is very advantageous for scaling up as APS

has the capability to remove lignin, hemicellulose, pectin, and other plant contents in a single step process. In contrast, the yield of CNCs is less compared to the strong acid hydrolysis process. Additionally, the fabrication of CNCs by APS was done by Leung et al. and the achieved yield was 28–36% from the complex flax and hemp fibers compared to the 81% yield from pure cellulose source from Whatman filter paper [50].

Although all the acid hydrolysis procedures are simple, yet a few limitations are essential to be addressed. Due to the use of strong acids, the drawbacks mainly include large water usage, corrosion of equipment, and the generation of waste acid solution. Furthermore, the cost of CNC production is increased due to the requirement of corrosion-resistant equipment. Further, during fabrication of CNCs, crystalline regions are subjected to hydrolysis and structural changes occur in this step, though, in harsh conditions the crystallinity got decreased [51]. Although researchers have started to find out the way of replacing strong liquid acids by solid acids for environmental and sustainable reasons [52]. In this context, cation-exchange resin hydrolysis technique has been used to fabricate CNCs with 84% crystallinity and with a 50% yield and they have reported that this method causes less waste and corrosion. Phosphotungstic acid is also another substitute for CNC production reported by Liu et al. [53] and the produced CNCs showed relatively good dispersibility in aqueous phase and high thermal stability. Another work by Du et al. [54] reported CNC production by ferric chloride catalyzed formic acid hydrolysis with a high crystallinity and excellent thermal stability of 70–80% yield.

Moreover, bio-based acids are now getting attention as substitutes to strong acids for the production of sustainable CNCs. In contrast, these bio-based acids have weak penetration power, and due to this reason, ultrasonication is required for breaking down of glycosidic linkages of cellulose chains. Yu et al. [55] reported the preparation of carboxylated CNCs from microcrystalline cellulose with citric/hydrochloric acid hydrolysis. The fabricated CNCs from this method had shown better crystallinity, best suspension stability, and better thermal stability with the hydrolysis time of 4 h. Another work reported by Tang et al. [56] reports the usage of ultrasonication for disintegration of esterified cellulosic slurry with acetic/sulfuric acid hydrolysis. Further, the ultrasonication aids in breaking the amorphous region of the cellulosic material. Kontturi et al. [57] mentioned about the preparation of the CNCs using hydrogen chloride (HCl) vapor with less water consumption along with a higher yield. Use of vapor of HCl helps in raising rapid hydrolysis of cotton-based cellulose fibers. The CNCs produced from this method showed improved crystallinity without any mass loss in the cellulose substrate during hydrolysis with a minimal impact on the morphology. With this system, the yield obtained was 97.4% which is better than employing only liquid HCl with 11% yield. Further, Chen et al. [58] have reported the high thermal stability of functional CNCs using organic acids such as oxalic, maleic, and *p*-toluene sulfonic acids. They also mentioned about the easy recovery of solid organic acids after hydrolysis reactions through crystallization at a lower or ambient temperature using their low water solubility.

4.2 Enzymatic Hydrolysis

Moreover, hydrolysis using concentrated acid poses serious environmental risk in terms of both disposal and energy consumption. Further, the increasing demand of green and sustainable technology aided to search an alternative of acid hydrolysis which must be economically and environmentally feasible. In addition, the corrosive nature of the acids also adds high cost to the production for using highly corrosion-resistant reactor. However, acid-treated CNCs are poor in thermal and mechanical properties which may affect the performance of composites. Therefore, an alternative way of CNC production needs to be found which would be eco-friendly without affecting the property of native cellulose. In addition, the enzymatic hydrolysis has shown its potential effects in the conversion of cellulosic biomass into fuels and chemical with higher yields, selectivity, lower energy costs, and milder operating conditions than others [59]. Further, the global focus on refining of lignocellulosic biomass has been enlarged so as to include the intermediate products like nanocellulose [60]. Thus, enzymatic hydrolysis could be employed as an approach with low environmental impact in the downstream process of cellulose to CNCs. Aiming to make this process economically viable, effort needs to be made to increase the efficiency of cellulolytic enzymes by enhancing the resistance to operational conditions such as pH and temperature or by increasing the speed and importantly, by reducing their price. In this context, a mixture of various enzymes collectively known as cellulose enzymes is available in market under different trade names. Generally, the mixture includes endo-1,4- β -glucanases (EGs) which breaks cellulose chains in random locations away from the main chain ends, exoglucanases or cellobiohydrolases (CBHs) which breaks cellulose by splitting off molecules from both ends of the chain and produce dimmers, and β -glucosidases, which hydrolyze the cellobiose units that are produced during the EG and CBH attacks, turning them into glucose [61]. Furthermore, EGs help to degrade the amorphous regions of the cellulose chains to produce smaller cellulosic fragments and CBHs targets the short crystalline regions of the cellulose. This favorable effect presents an advantage for the controlled production of CNCs [62]. Thus, cellulase can be used as an alternative to acid hydrolysis to obtain nanocrystals. Although, few reports exist on the fabrication of CNCs through enzymatic hydrolysis, George et al. [63] have compared morphological and thermal properties of bacterial CNCs with acid hydrolyzed CNCs where CNCs was used as filler in poly(vinyl alcohol) nanocomposites. Satyamurthy et al. [64] have produced CNCs using a controlled microbial hydrolysis of MCC using cellulolytic fungus *Trichoderma reesei* with a yield of 22% and the author reported that the crystallinity obtained by microbial hydrolysis was lesser compared to acid hydrolyzed [65]. Thus, to overcome the problems that occur during enzymatic hydrolysis, few pre-treatment methods have been reported before processing to enzymolysis for CNC fabrication. In this context, Chen et al. [66] has reported the pre-treatment of natural cotton with DMSO (dimethyl sulfoxide), NaOH (sodium hydroxide) or ultrasonic waves before proceeding toward enzymatic hydrolysis and obtained the yield of 32.4%. In a similar study, Xu et al. [67] demonstrated the

endoglucanase derived from *Aspergillus oryzae* to hydrolyze pre-treated hemp and flax fibers. In this work, sonication-microwave was used to pre-treat the sample in 2% NaOH solution for better quality and higher yield. Though they have effectively eliminated the need of acid for hydrolysis, but pre-treatment is still costlier for enzymatic hydrolysis before processing. However, cellulose from *Aspergillus niger* has shown the capability of fabricating CNCs with minimal processing from feedstock of kraft pulp with 10% yield. In addition, recently, Hu et al. [68] developed a bio-absorbable bacterial cellulose for wound dressing applications and their biodegradability was investigated by using different enzymes. Wang et al. [69] has also done similar in vitro study of biodegradability of bacterial cellulose by cellulose in simulated body fluid. In contrast, Domingues et al. [70] compared CNCs obtained by acid hydrolysis of eucalyptus fibers with CNCs from bacterial cellulose using enzymatic hydrolysis.

Fabrication of CNCs by enzymatic hydrolysis has been observed to be potential with acceptable yields, advanced selectivity, and milder operating conditions in comparison to the chemical process. However, economical and technical constraints are responsible for hindering this technique from commercialization. Mainly, the high cost of enzyme and rate-limiting step of cellulose degradation with a long processing period are considered as drawbacks. The slow rate of enzymatic hydrolysis has been found to be affected by various factors that encompasses structural features resulting from pre-treatment and enzyme mechanism.

4.3 Mechanical Methods

Mechanical approaches for the fabrication of CNCs have also been investigated as a part of the process indicating combinations of acid hydrolytic, enzymatic treatment and oxidative methods, or directly [71–73]. Most commonly used methods are microfluidization, ultrasonication, high-pressure homogenization or ball milling. These procedures are commonly employed for the fabrication of cellulose nanofibers (CNFs). In addition, CNFs are characterized as nanocellulosic materials with a diameter in nanometers or tens of nanometers with a length up to several microns [74]. Relating to this method, recently, people have studied high energy bead milling (HEBM) process for the fabrication of CNCs from aqueous or dilute acid (phosphoric acid) dispersion of commercially available microcrystalline cellulose (MCC). The dispersed sample got micronized through a HEBM process. They have reported about the similar characteristic morphology and aspect ratio of produced CNCs with that of acid hydrolyzed CNCs. The resulted CNCs were rod-like and presented a crystallinity index of 85–95% with yield of 57–76%. Furthermore, they have found that the fabricated CNCs are thermally stable to withstand the melt processing temperature of most common thermoplastics. Generally, in ball milling technique, cellulose suspension can be disintegrated by the high the energy collision between the balls made by ceramic, metal, or zirconia in a hollow cylindrical container while the container rotates. However, chemical pre-treatment is helpful for weakening hydrogen bonds

and eliminating the small particles. But the fibrous morphology is easily damaged by the ball mill. In this context, high-intensity ultrasonication has been employed as one of the mechanical method for the isolation of CNCs [72, 75]. The fabricated CNCs were rod-shaped and produced from an aqueous dispersion of MCC using physical method of ultrasonication. The obtained diameter of fabricated CNCs was between 10 and 20 nm with a length of 50–250 nm in range with a production yield of 10%. Another study has reported the better yield of 85.38% of esterified-CNCs fabricated from pure wood pulp filter paper through ultrasonic extraction. They revealed that E-CNCs were prepared with cellulose pulp using a mixture of acetic and sulfuric acid with the aid of ultrasonication. The yield obtained was better in this method as compared to that without the method used ultrasonication. In this particular study, ultrasonication showed an important role in the degradation of cellulose and esterification. The effect of this method may be explained by the formation, growth, and collapse of cavities in aqueous solution [76]. Cavitation occurred during ultrasonication, showed energy of approximately 10–100 kJ/mol and which falls under the hydrogen bond energy scale [77]. The impact of ultrasonication can effectively disintegrate the amorphous region of cellulose due to the energy and also beneficially effective for the reagent to enter the interior of cellulose fibers.

4.4 Oxidation Methods

The presence of hydroxyl groups on cellulose is highly reactive and can be easily oxidized by strong oxidants to aldehydes, ketones, and carboxyl groups. Thus, the structure of cellulose is destructed and the degree of polymerization is also decreased. Therefore, taking the advantages of the presence of reactive group of cellulose, the researchers have successfully fabricated CNCs by the use of oxidation method. Saito and Isogai [78] had reported a new method to introduce charged carboxylated groups into cellulosic materials which helped disintegration into nanofibrils with smaller widths, by utilizing a much lower energy input in comparison to that of the traditional pure mechanical treatments. The two-step oxidation method was employed to prepare CNCs and microfibrils using sodium periodate followed by sodium chlorite as oxidant [50] and finally, two-step centrifugation. Generally, periodate is firstly utilized to oxidize the C₂ and C₃ hydroxyl groups using chlorite. They have reported the diameter and length of fabricated CNCs and microfibrils accordingly 13 nm, 120–200 nm and 120 nm, 0.6–1.8 μm. In this case, the produced CNCs with carboxyl groups on the surface had shown a high crystallinity ~91% and high charge density which could form a stable suspension in aqueous phase. Further, the resultant microfibrils could be translated to cellulose nanofibers (CNFs) by mechanical agitation. However, this two-step oxidation method requires the expensive and toxic periodate along with the disintegration process with very high energy consumption.

TEMPO (2,2,6,6-tetramethylpiperidine-1-oxyl)-mediated oxidation has also been employed to prepare carboxyl CNCs which is one of the region-selective chemical

modifications of the primary hydroxyl groups of CNCs. The reaction occurs on the surface of cellulose fibers and in amorphous domains. As the carboxyl content is increased to a certain amount, cellulose starts to disperse in aqueous solution but the crystalline regions remain intact and can, therefore, be released. Another literature stated about the direct use of ultrasonic-assisted TEMPO–NaBr–NaClO system for the production of carboxylic CNCs from cotton linter pulp. A stable well-dispersed aqueous suspension was obtained after the oxidation process where some of the amorphous regions of the cellulose were found to be gradually hydrolyzed. They have reported the microscopic observations of the CNCs 5–10 nm in width and 200–400 nm in length. Furthermore, TEMPO–NaBr–NaClO system was used by Cao et al., who reported the stable transparent dispersion of CNCs with a yield of 80% and high crystallinity and surface area. Moreover, TEMPO-mediated CNCs are able to be completely disperse at the individual nanofibril level in water by electrostatic repulsion and/or osmotic effects. This behavior is responsible for the presence of anionically charged sodium carboxylate groups at the fiber surface. In contrast, this method also exhibits some serious constraints, such as toxic TEMPO reagents leading to cause environmental issues, oxidation time, and limited oxidation at C6 primary hydroxyl groups in CNCs. Furthermore, the oxidation reaction helps to reduce the rigidity/lengths of the CNCs due to breakage of the glycosidic linkages. Another oxidant APS could be used to fabricate carboxylated CNCs by one-step procedure from various cellulosic sources with yields in the range of 14–81%. However, this method also consumed the time for alkaline pre-treatments and long reaction times of 16–24 h. The overall yield of CNCs was higher by the oxidation degradation method after comparing with mineral acid hydrolysis and enzymatic hydrolysis. However, in this process of reaction, a large number of oxidants were consumed, and the reaction time was longer. Also, a large amount of water and energy needs to be consumed which leads to the fact that the cost of CNCs production would be very high.

4.5 Ionic Liquid Treatment

Ionic liquids (ILs) is a kind of organic salt solution with low melting point, generally, less than 100 °C, which is composed of organic cations and other anions. This treatment has received growing attention by the researchers due to its recyclability, high stability, non-flammability, low melting point, and low vapor pressure reagents, which leads to innovative and sustainable solutions. Further, their unique solvating properties and environment-friendly nature helped them to use as solvent for dissolving and separating medium from lignocellulosic materials for fabrication of CNCs. Additionally, it is considered as green solvent. In spite of their unique advantages,

their embodied energy and cost, the recyclability, and the reuse of ILs, undoubtedly, appear to be indispensable for the conception of any environmentally and economically viable CNCs isolation process. Commonly used ILs are imidazolium-based acidic solutions, such as 1-ethyl-3-methylimidazolium diethylphosphonate ([EMIM]DEP), 1-butyl-3-methylimidazolium chloride ([BMIM]Cl), 1-butyl-3-methylimidazolium acetate ([BMIM]OAc), and 1-butyl-3-methylimidazolium hydrogen sulfate ([BMIM]HSO₄). These solvents are found to be most interesting and mostly investigated solvents for fabrication of CNCs from cellulose. The recovery rate of these ILs can be reached at 99.5% by evaporating the anti-solvents, has estimated by some researchers.

Various current works have stated about the effectiveness of ILs for selective and controlled cellulose hydrolysis leading to nanoscale particles isolation as an alternative to conventional methods. In the recent works, ([BMIM]HSO₄) has been utilized to fabricate CNCs from MCC [79]. The author clearly demonstrated about the potential effect of [BMIM]HSO₄ for the isolation of rod-like morphology of CNCs with yield of 48% and with the diameter of 14–22 nm and the length of 50–300 nm. Also it has been reported that mechanism of ILs hydrolysis was similar to the acid hydrolysis. During this treatment, the amorphous domain got dissolved and thereby increase of crystallinity occurred. Further, the native conformation of cellulose type I remained in this treatment compared to MCC. A two-step hydrolysis process was explored by Mao et al. employing ([BMIM]HSO₄) [80]. In this work, they first allowed 24 h for swelling at room temperature followed by 12 h hydrolysis at 100 °C and the developed CNCs was conferred with good surface properties and high production yield. Later, they hydrolyzed softwood, hardwood, and MCC by optimizing two-stage method with ([BMIM]HSO₄) aqueous, and the yield of CNCs was 57.7, 57, and 75.6%, respectively. Further, similar work by Tan et al. where ([BMIM]HSO₄) was utilized as both solvent and acid catalyst [81]. In this case, hydrolysis of MCC was done at 70–100 °C for 1 h 30 min in ([BMIM]HSO₄) solvent. The author has reported the rod-like morphology of CNCs obtained with conserved cellulose type I structure during the catalytic conversion process with crystallinity of 95.8% compared to the original MCC. Currently, for the first time, Abushammala et al. [82] have stated the use of [BMIM]OAc for the direct extraction of CNCs from wood. They demonstrated the capability of [BMIM]OAc to dissolve lignin in situ and at the same time, resulting in the swelling of cellulose only during treatment. The developed CNCs showed crystallinity of 75% and a high aspect ratio of 65 with a yield of 44%. This study explained that [EMIM]OAc had three main functions in the process, respectively, (a) dissolving cellulose in situ when cotton fibers were infiltrated, (b) reducing intermolecular cohesion in wood by acetylation, and (c) catalyzing the hydrolysis reaction of cellulose. Lazko et al. reported the use of [BMIM]Cl for infiltration at 80 °C and subsequently sulfuric acid was added with a concentration of 1–4 wt% [83]. Further, allowing the time of 2–16 h for reaction to complete production of CNC showed diameter of 20 nm and length of 150–350 nm. It has been found that obtained CNCs prepared by [BMIM]Cl had less sulfonic group content on the surface compared to [BMIM]HSO₄ with increased thermal stability. Furthermore, Iskak et al.

had used [BMIM]Cl for preparation of CNCs and they varied reaction time and temperature to check the yield, particle size, and crystallinity index of CNCs [83]. The obtained CNCs showed particle size of 9 nm with crystallinity index of 73% with 30 min reaction time, while increasing the temperature of reaction at 100 °C, obtained CNCs showed 76% crystallinity index with 90% yield. Moreover, researchers have updated a new one-pot preparation of hydrophobic CNCs from wood pulp using solvent system tetrabutylammonium acetate/dimethylacetamide in conjunction with acetic acid, where both the dissolution of amorphous cellulose and acetylation of hydroxyl group takes place [84]. The developed CNCs were found to be hydrophobic with rod-shaped morphology, good thermal stability, and high crystallinity index, but the yield was unknown.

4.6 Subcritical Water Hydrolysis

The natural ability of water to hydrolyze polysaccharides is well known in hydrothermal process of elimination of hemicelluloses [85]. Very few investigations have been reported on subcritical water hydrolysis for the fabrication of CNCs. However, the subcritical water possessed higher diffusion, activity, and ionization than common water as sub and supercritical water has lower ionization value (K_w). Additionally, the rate of hydrolysis mainly depends on few characteristics such as presence of water molecules and the availability of H_3O^+ and water. Therefore, the utilization of subcritical water could be efficient for the hydrolysis reactions. It has been previously demonstrated that water at high temperature and pressure is able to hydrolyze lignocellulosic materials. Moreover, utilization of water as a reagent is a promising technique for not only its environment-friendly characteristics but for its low and cleaner effluents, low corrosion, and cost effectiveness [86]. Utilization of subcritical water hydrolysis has been reported by Novo et al. [86] for the production of CNCs from commercial microcrystalline cellulose. Optimization of the reaction conditions had been done to obtain good quality of CNCs with higher yield. The optimized condition was 120 °C and 20.3 MPa for 60 min for subcritical water to hydrolyze cellulose. The resulted rod-shaped CNCs showed high crystallinity index of 79% with a yield of 21.9% and high thermal stability along with similar aspect ratio in comparison to conventional CNCs. Further, the reactor is needed for this eco-friendly technique. During experiment, the pressure inside the reactor could be decreased by opening the restrictor valve or increased by injecting water with precision pump. The author has compared the production cost of CNCs using subcritical and conventional methods and they found lesser cost of 0.02 \$/kg for subcritical treatment than conventional which is around 1.54 \$/kg. Also, they have mentioned about the influence of pressure and temperature on the yield of CNCs. It has observed, while increasing the temperature, the stability of CNCs aqueous suspensions was enhanced gradually though it was lesser than the stability of acid hydrolyzed CNCs. This method would be a promising approach for industry.

4.7 Combined Processes

The characteristic properties and yield of CNCs play a vital role in all aspects of applications. Therefore, a prevalent technique must be developed to improve the properties and yield for the fabrication of CNCs. Though, a sufficient number of methods have been reported for the fabrication of CNCs but all these methods have their own limitations. Further, various sources of cellulosic materials also have the influence which affects the characteristic property and yield. In this regard, the improvement of extraction technologies and development of combined processes using a combination of two or several aforementioned methods could be one of the most effective ways to improve the properties of CNCs and simultaneously would be able to arrest the limitations of single process technique. Some of the new combined approaches have been made in recent days for isolation of CNCs from cellulose. However, various limitations need to be considered such as environmental pollution due to the generated effluents, corrosion of the equipment, and the hurdle to control the degree of hydrolysis [87]. In this context of combined process, Tang et al. have employed the low-intensity sonication concept to improve the yield of CNCs based on sulfuric acid hydrolysis extracted from commercial MCC [88]. The developed CNCs showed a good amount of increment over the yield from 33 to 40% as a result of the supplement of sonication at 100 W for 30 min compared to the traditional sulfuric acid hydrolysis. Further, they have reported a different combined approach including enzymatic hydrolysis, phosphoric acid hydrolysis, and sonication for isolation of CNCs from old corrugated contained fibers. Consequently, the result showed high crystallinity, good thermal stability, and improved dispersion with a higher yield of 28.98% in comparison to single acid hydrolysis process [56]. Another investigation by Rohaizu and Wanrosli studied the use of sono-assisted treatment TEMPO oxidation of lignocellulosic biomass of palm oil for production of CNCs [89]. They revealed that the sono-assisted treatment has a remarkable effect on the yield of around 39% and more than 100% increment of carboxylate content in comparison to non-assisted process. The resulted CNCs are comprised of good thermal stability, high crystallinity index of 72%, and a production yield of 93%. Further, Beltramino et al. employed the combined process using acid hydrolysis assisted with enzymatic treatment [90]. The optimized condition revealed the reduction in hydrolysis time by 44% and increased yield of around 80%. In addition, the optimal conditions helped to generate particle size of around ~200 nm with decreased surface charge and sulfur content.

Another combined technique of microwave-assisted ultrasonic treatments of plant fiber materials to attain high efficiency was established by Lu et al. [91]. The author fabricated CNCs from filter paper using sulfuric acid hydrolysis under microwave-assisted ultrasonic treatment. The optimized condition showed the yield and crystallinity of CNCs with the crystal form of cellulose I α , respectively, 85.75 and 80%. In this context, Chowdhury and Abd Hamid have reported the combined use of ultrasonication and microwave for the preparation of CNCs from the stalk of *Corchorus olitorius* [92]. They mentioned the pre-treatment of jute stalk powder using sodium

hydroxide under microwave irradiation followed by bleaching with hydrogen peroxide for extracting crude cellulose. The obtained crude cellulose was hydrolyzed by ultrasonication in the presence of various hydrolyzing mediums. The fabricated CNCs showed high crystallinity index of 83% with yield of 48% using ILs and a yield of 43% using sulfuric acid. Therefore, combined methods could be an effective way for obtaining better yield of CNCs from various sources.

4.8 Purification and Fractionation

Fabrication of CNCs has been done predominantly either using pure acid hydrolysis or combined with other process. After hydrolysis, the obtained aqueous suspension of CNCs is quenched by filtering the substances over small-pore fritted glass filter or by diluting with distilled or Millipore water at room temperature. However, some constraints came after hydrolysis during removal of free acid, as these post treatments are time and cost consuming and it could be a limitation for industrial scale. Centrifugation has been employed to remove the part of excess acid and water-soluble fragments. In contrast, the remaining free acid molecules from the dispersion can be eliminated by using dialysis against water till the neutral pH is obtained, but this step is costly and time consuming which usually takes more than two or three days. The possible ways to overcome this issues could be the addition of sodium hydroxide solution to the hydrolyzed suspension to attain pH ~9 and afterward washed with distilled water until neutrality attained. This neutralization procedure is simple with minimum processing steps to produce CNCs but it is a time-consuming step. Moreover, chemical neutralization method using NaOH was considered as simple, economic, and efficient in comparison to dialysis [93]. Sonication can be used to disintegrate the aggregates to obtain a complete dispersion of nanocrystal which could serve the purpose of neutralization. The final aqueous suspension of nanocrystals can be stored in a refrigerator after possible filtration for removal of residual aggregates. Further, the addition of few drops of chloroform can be helpful to avoid bacterial contamination. However, CNCs produced by enzymatic, ionic liquids, subcritical water, oxidation, and mechanical methods do not require dialysis. In this case, the important steps are washing, neutralization, centrifugation, and sonication. The aqueous suspensions of CNCs could be separated into isotropic and anisotropic phases by increasing the concentration through water evaporation. Literature also stated that smaller particles present in the isotropic phase, whereas the longer one remains in the anisotropic phase [94]. Moreover, CNCs is stated as aqueous suspension due to its hydrophilic nature and tendency to agglomerate during drying. Therefore, drying is a vital step for fabrication of CNCs. The recommended procedures are supercritical, freeze, and spray drying. However, freeze and supercritical drying approaches generate highly networked structures of agglomerates having multi-scalar dimensions. During freeze-drying, the self-assembled behavior of CNCs was observed by Han et al. [95]. Moreover, spray drying has been recommended for a technically suitable production for dry or powdered CNCs.

5 Typical Properties of Cellulose Nanocrystals and Its Composites

5.1 Mechanical Properties

The quantitative evaluation of tensile modulus and strength of CNC is immensely challenging due to the limitations in measuring the mechanical properties of nanomaterials along multiple axes. In this context, other factors such as crystallinity index, dimensions of the samples, anisotropy, and defects in nanocrystals also affect the results of mechanical properties. The mechanical properties of CNCs are largely controlled by their dimensions and morphology as determined from the percolation theory. According to this theory, the higher aspect ratio of CNCs will result in the better mechanical properties as the lower amount of nanofillers are required for the percolation [96]. The elastic property of CNCs have been measured indirectly and theoretically by using atomic force microscopy (AFM), X-ray diffraction (XRD) analysis, inelastic X-ray scattering, Raman scattering, etc. Furthermore, the theoretical tensile strength of CNCs has found to be in the range of 7.5–7.7 GPa which is better than the steel wire [97]. In another study, the elastic modulus of CNCs extracted from tunicates was determined by AFM. In this study, the AFM tip was used to perform a three-point bending test and elastic moduli of around ~150 GPa was found in this study. Moreover, the transverse elastic modulus of CNCs was determined using AFM by comparing the experimental force–distance curves with three-dimensional finite elemental calculations. The result has shown that the transverse modulus of an individual CNC lies in the range of 18–50 GPa. In addition, Raman spectroscopy also determined the deformation micromechanics analysis of tunicate cellulose whiskers and evaluated the value of ~143 GPa [98].

The composites-based CNC and biodegradable copolymers have been reported by Muiruri et al. wherein they grafted the CNC on the copolymer based on (PCL) and poly(D-lactic acid) (PDLA), and blended with poly(L-lactic acid) (PLLA). The authors reported that the stereocomplexation led to the enhancement in the thermal properties of the resulting nanocomposites with 20% enhancement in the elongation at break. The reason behind the improved toughness was attributed to the crazing and fibrillation during deformation. These improved properties may widen the industrial acceptance of such nanocomposites [99]. Furthermore, the same group reported the dual CNC-based fillers in order to control the morphology and the interfacial tension of the biodegradable nanocomposites. In one case, the composite consisted of CNC as a core and PCL–PDLA copolymer as the outer layer (rubbery). In the other case, the outer layer consisted of the rubber layer grafted with PDLA blocks and CNC as a core. The resulting materials were mixed with PLLA followed-by solution casting, pulverization, and injection molding to form the specimens for impact test. It was found that both the fillers led to the increase in tensile toughness (100 fold) as well as impact strength (3 fold) when added to the PLLA matrix. The reason for the improved mechanical properties is attributed to the synergistic matrix crazing and cavitation effect of the fillers leading to extensive plastic deformation and these

improved properties makes the resulting composites as promising candidates for orthopedic and packaging applications [100].

Owing to the applicability of CNCs in widespread applications and comparable properties with carbon fibers, Kevlar, stainless steel, etc., Jahan et al. used CNCs as the reinforcing agent into the matrix of poly(vinyl alcohol) (PVA) in order to fabricate the composite membranes for biogas separation. The elastic modulus and mechanical strength of the membranes were found to increase at higher humidity in presence of CNC and no significant change was observed in % elongation at break. The lower content of CNC in the composite membranes resulted in better swelling and improved elastic modulus and thus, it may be considered as a candidate for gas separation applications [101].

The effective utilization of CNCs in fabrication of composites in order to enhance the properties of the composites is often restricted by their aggregation and on several occasions, the mechanical properties of CNCs are different from that of the theoretical values. In order to overcome this drawback, Meesorn et al. added PVA with the speculation that it would act as a dispersant and disrupt the interactions between CNC–CNC and enhance the stress transfer. The composites based on poly(ethylene oxide-co-epichlorohydrin) (EO-EPI) and CNC (10% w/w) were prepared with varying amount of PVA (1–5% w/w) by solution casting. In a similar fashion, the composites were prepared by loading CNC into the matrices of polyurethane (PU) and poly(methyl acrylate) (PMA). A significant enhancement in the mechanical properties was achieved with a quadruple enhancement in stiffness and tensile strength upon addition of 5% PVA in all the composites. The authors suggested the application of CNCs as reinforcing agents in a wide range of matrices. Additionally, an improved distribution of CNCs was obtained in the polymer matrices in presence of PVA which supported the hypothesis that the dispersant leads to the increased stress transfer by improved dispersion of CNC [102].

5.2 *Rheological Properties*

The properties of rheological behavior of CNCs are influenced by several factors such as liquid crystallinity, ordering, and gelation. Moreover, rheological parameters showed different characteristics based on the concentration of CNC suspension. The dilute CNC suspensions exhibit shear thinning behavior which shows dependency on concentration at low rates, whereas at higher concentration, it exhibits anomalous behavior and the suspension is lyotropic. The reason behind this type of behavior is due to the rod-shaped morphology of nanocrystals which tends to align at a critical shear rate. The chirality of the CNC suspension breaks down to a simple nematic structure when shear rate reaches to a critical point [103]. Further, the relaxation time constant depends on the aspect ratio and in case of CNCs with higher aspect ratio shows alignment for longer time even after shear. The aspect ratio of rod-like particles is found to be higher than spherical particles which is essential in improving the rheological properties at lower particle loadings [104]. Additionally, the rheological

properties of CNCs also influenced by the acid used for hydrolysis. In this regards, sulfuric acid-treated CNCs show shear thinning behavior that is independent of time, whereas hydrochloric acid-treated CNC has shown higher shear thinning behavior, anti-thixotropy at lower concentrations and thixotropy at higher concentrations [105]. In order to develop the formulations of the products, the knowledge of rheological properties and microstructures of the polymers incorporated with CNC is important. In this regard, Peng et al. studied about the rheological properties of the polymers loaded with rod-like CNC and spherical CNC [106]. These fillers were loaded into different polymeric systems (anionic, cationic, non-ionic) such as PVA, (PEG), gum arabic, chitosan, sodium carboxymethyl cellulose (SCMC), monomethyl ether (ME), sodium alginate (SA), and hydroxypropyl methylcellulose (HPMC) so as to determine the interaction between CNCs and particles and its effect on the rheological properties. The rod-like CNCs resulted in the enhanced viscosity as compared to the spherical CNCs. Upon investigating the gelation behavior of CNC dispersion into the different polymeric systems, it was found that the thickening effect was higher in case of cationic systems as compared to anionic systems which in turn was higher than non-ionic polymeric system which may be accounted for the different interactions between the polymer and CNC along with the properties of the polymeric chains. The flexible chains (in case of non-ionic polymers) resulted in negligible viscosity enhancement. At a particular concentration, the strongest thickening effect was observed in case of HPMC.

The role of CNCs as a filler in the matrices of biodegradable polymers such as PLA is well-known and widely explored by various researchers to improve the mechanical and barrier properties of the composites [107]. In order to improve the processability of the composites involving high shear rates, the rheological properties are of prime importance. CNCs when used as fillers into the polymer matrix provide high stability to the polymer network by incorporating themselves between the polymer chains. In a study reported by Shojaeiarani et al., CNCs were incorporated into the PLA matrix and the composites were prepared by diluting the master batches using spin coating and film casting [106]. An improvement in the storage modulus was observed upon incorporation of CNCs. The storage modulus of the spin-coated nanocomposites was higher than that of the film casted sample. The spin-coating method was considered to be a promising approach for fabricating PLA-CNC nanocomposites with improved properties.

Furthermore, as reported by Khandal et al., the rheological behavior of CNC was tailored by functionalization with polyethyleneimine (PEI) [108]. They prepared a stable suspension of CNC-PEI that exhibited interesting rheological properties. The Newtonian suspension turned into a non-Newtonian gel upon modification with PEI wherein a dramatic increase in complex viscosity was observed. Also, the increasing shear rate resulted in the loss of linear viscoelastic properties which could be attributed to the breaking of inter-particle network. In another study reported by Gupta et al., the CNCs coated with lignin were used as biofillers to modify the rheological properties of the composites based on PLA [109]. The increased dispersion of the biofiller (percolation threshold constant: 0.66 wt%) and the improved interfacial interaction with the matrix of PLA led to the improved rheological and

thermo-mechanical properties. The lignin-coated CNCs were considered to be as promising candidates for improving the properties of the PLA matrix and in turn lead to the development of completely bio-based composites.

The dispersion of CNCs in the aqueous solution of polyoxoethylene (POE) and its rheological properties have been investigated by Azouz et al. [110]. They observed that incorporation of CNC, the viscosity of the suspension was found to decrease at first followed by an increase in viscosity. The POE adsorbed CNC was freeze-dried followed by its extrusion with low-density polyethylene (LDPE). This melt processing of CNC-based composites with hydrophobic polymer was considered to be a promising approach for the industrial-scale production.

5.3 Surface Modification/Functionalization

The presence of plenty of hydroxyl groups makes CNC more suitable for many type of surface functionalization for several applications. However, the hydrophilic nature of this nanocrystals hinder its application for fabrication of composite films as effective dispersion of this nanoparticle into the polymer hydrophobic matrix is a big issue due the strong intermolecular hydrogen bonding between cellulosic chains. Thus, for arresting the incompatibilization limitation between polymer matrix and CNC, surface modification has been carried out. Most commonly used procedure for surface modifications/functionalization of CNCs are esterification, etherification, oxidation, amidation, carbamation, nucleophilic substitution, silylation, polymer grafting, etc. Furthermore surface modification can be done with different mechanisms like by grafting with the organic and inorganic molecule aiming to increase the hydrophobicity. In addition, the abundant surface hydroxyl groups not only provide opportunities for diverse chemical modification but also render the hydrophilicity to CNCs. Though the hydrophilic nature of CNCs is attractive for water-based applications and this presents a challenge for their homogeneous dispersion in common nonpolar solvents and hydrophobic polymer matrixes [97]. In addition, the chemical functionalization introduces either negative or positive electrostatic charges on the CNC surface which provides better dispersion in any solvent or polymer. It also helps to tune the surface energy characteristics to improve compatibility. Moreover, all these functional groups act as nucleating sites for polymer grafting on CNC surface. On the other hand, polymer grafting is usually carried out by two approaches, namely “grafting from” and “grafting onto” methods.

In literature, various methods have been reported for the hydrophobic modification of CNCs. One of the ways is adsorption of surfactants or polymers or covalent modification of the particle surfaces [111, 112]. For example, the quaternary ammonium salts bearing long alkyl tails have been used to modify CNCs based on ionic interactions between the sulfate half ester groups on the CNC and the ammonium group of the surfactant; these modified CNCs require extensive purification to remove excess surfactant, and such ionic bonds are not robust enough to withstand some processing techniques and media [113–115]. Covalent modifications of CNCs generally include

esterification (mostly acetylation, butyration, and palmitoylation), urethanization (also known as carbonylation), amidation, and silylation with moderate increased contact angles [116, 117]. Additionally, the esterification involves the conversion of the surface hydroxyls of cellulose to esters and sulfation and phosphorylation are some commonly used methods for the cellulose esterification. In etherification, most commonly used chemical is glycidyltrimethylammonium chloride or its derivatives to cationize the surface. The crystalline morphology and dimensions of CNCs can be preserved by mild alkaline cationization condition. In addition, TEMPO-mediated oxidation enables to produce surface-carboxylated CNCs [118]. Furthermore, the oxidized CNCs have been used as the starting material where carboxylic moieties are directly converted to amides by reacting with primary amines. The surface modification of CNCs using isocyanates was reported by Siqueira et al., who modified sisal-based CNCs with n-octadecyl isocyanate without any catalyst [119]. Silanes can also be grafted onto CNCs, which is one technique used to enhance the interactions with polymer matrices.

Furthermore, the most of these modifications are carried out in organic solvents. For larger modifications such as attaching polymer chains (polypropylene, polytetrahydrofuran, poly(ϵ -caprolactone) (PCL), polyethylene glycol (PEG), etc.) via grafting onto CNC is another process though steric hindrance limits the graft densities achievable. The catalytic ring-opening polymerization from CNCs, using the surface hydroxyl groups as initiating sites, is the most common route for the synthesis of CNCs with grafted polyesters such as the bio-based PLA. In addition, atom transfer radical polymerization has been extensively explored to synthesize well-defined polymers on CNC surfaces. These grafting from approaches have yielded highly compatible CNCs with higher contact angle; however, the pre-attachment of initiator, polymerization reactions themselves, and the separation are lengthy. However, the abundant hydroxyl groups on the surface of negatively charged CNCs act as both nucleating sites and a reducing agent for the growth of the metal nanoparticles. To date, several reports of CNC-supported metal nanoparticles such as Au, Pt, Ag, Pd, Fe, etc., have been reported in literature through the green chemistry route, having potential applications as high-performance conductive polymer nanocomposites, biocatalysts for pollutant remediation and electrocatalytic activity. Moreover, the fabrication of such CNC-supported metal nanoparticles has been shown to improve the dispersion quality and chemical stability and solve the problems related to coagulation and agglomeration of the nascent metal nanoparticles. Dhar et al. have also reported the good dispersion ability and improved crystallinity of magnetic CNCs into the hydrophobic (PLA) matrix by modification of the surface of CNCs using iron nanoparticles [120]. Hu et al. have used plant polyphenols (tannic acid) for surface modification of CNCs with improved hydrophobicity [121]. However, the main challenge in this process lies in preserving the original morphology and maintaining the integrity of the CNCs.

6 Conclusion

In this chapter, the synthesis of biomass-derived CNC and the fabrication of the composites based on CNC have been detailed. Various biomass-based sources for the synthesis of CNCs have been highlighted followed the extraction techniques thereof. The applications of CNCs have further been marked by using it as filler in the development of composites. The modification of CNC has been carried out by the surface functionalization in order to improve the properties of the composites for industrial applications. The rheological and mechanical properties of CNC-based composites have been reported based on several case studies. The potential of CNCs and its composites in the various applications have, thus, been underlined along with a focus on improved processability.

References

1. Mishra RK, Ha SK, Verma K, Tiwari SK (2018) Recent progress in selected bio-nanomaterials and their engineering applications: an overview. *J Sci Adv Mater Devices* 3:263–288. <https://doi.org/10.1016/j.jsamd.2018.05.003>
2. Owusu PA, Asumadu-Sarkodie S (2016) A review of renewable energy sources, sustainability issues and climate change mitigation. *Cogent Eng* 3:1167990. <https://doi.org/10.1080/23311916.2016.1167990>
3. Lagerwall JPF, Schütz C, Salajkova M, Noh J, Hyun Park J, Scalia G, Bergström L (2014) Cellulose nanocrystal-based materials: from liquid crystal self-assembly and glass formation to multifunctional thin films. *NPG Asia Mater* 6:e80. <https://doi.org/10.1038/am.2013.69>
4. Lin N, Huang J, Dufresne A (2012) Preparation, properties and applications of polysaccharide nanocrystals in advanced functional nanomaterials: a review. *Nanoscale* 4:3274–3294. <https://doi.org/10.1039/c2nr30260h>
5. Sturcová A, His I, Apperley DC, Sugiyama J, Jarvis MC (2004) Structural details of crystalline cellulose from higher plants. *Biomacromolecules* 5:1333–1339. <https://doi.org/10.1021/bm034517p>
6. O'Sullivan AC (1997) Cellulose: the structure slowly unravels. *Cellulose* 4:173–207. <https://doi.org/10.1023/a:1018431705579>
7. Nishiyama Y, Sugiyama J, Chanzy H, Langan P (2003) Crystal structure and hydrogen bonding system in cellulose I α from synchrotron X-ray and neutron fiber diffraction. *J Am Chem Soc* 125:14300–14306. <https://doi.org/10.1021/ja037055w>
8. Nishiyama Y, Langan P, Chanzy H (2002) Crystal structure and hydrogen-bonding system in cellulose I β from synchrotron X-ray and neutron fiber diffraction. *J Am Chem Soc* 124:9074–9082
9. Langan P, Nishiyama Y, Chanzy H (2001) X-ray structure of mercerized cellulose II at 1 Å resolution. *Biomacromolecules* 2:410–416
10. Rowland SP, Howley PS (1988) Hydrogen bonding on accessible surfaces of cellulose from various sources and relationship to order within crystalline regions. *J Polym Sci Part Polym Chem* 26:1769–1778. <https://doi.org/10.1002/pola.1988.080260708>
11. Nickerson RF, Habrie JA (2002) Cellulose intercrystalline structure. <https://pubs.acs.org/doi/abs/10.1021/ie50455a024>. Accessed 6 Apr 2019
12. Rånby BG (1951) Fibrous macromolecular systems. Cellulose and muscle. The colloidal properties of cellulose micelles. *Discuss Faraday Soc* 11:158–164. <https://doi.org/10.1039/d19511100158>

13. Ding S-Y, Himmel ME (2006) The maize primary cell wall microfibril: a new model derived from direct visualization. *J Agric Food Chem* 54:597–606. <https://doi.org/10.1021/jf051851z>
14. Malcolm Brown R, Saxena IM, Kudlicka K (1996) Cellulose biosynthesis in higher plants. *Trends Plant Sci* 1:149–156. [https://doi.org/10.1016/s1360-1385\(96\)80050-1](https://doi.org/10.1016/s1360-1385(96)80050-1)
15. Mellerowicz EJ, Baucher M, Sundberg B, Boerjan W (2001) Unravelling cell wall formation in the woody dicot stem. *Plant Mol Biol* 47:239–274
16. Beck-Candanedo S, Roman M, Gray DG (2005) Effect of reaction conditions on the properties and behavior of wood cellulose nanocrystal suspensions. *Biomacromolecules* 6:1048–1054. <https://doi.org/10.1021/bm049300p>
17. de Rodriguez NLG, Thielemans W, Dufresne A (2006) Sisal cellulose whiskers reinforced polyvinyl acetate nanocomposites. *Cellulose* 13(3):261–270 <https://doi.org/10.1007/s10570-005-9039-7>
18. Kimura F, Kimura T, Tamura M, Hirai A, Ikuno M, Horii F (2005) Magnetic alignment of the chiral nematic phase of a cellulose microfibril suspension. *Langmuir ACS J Surf Colloids* 21:2034–2037. <https://doi.org/10.1021/la0475728>
19. Revol J-F (1982) On the cross-sectional shape of cellulose crystallites in *Valonia ventricosa*. *Carbohydr Polym* 2:123–134. [https://doi.org/10.1016/0144-8617\(82\)90058-3](https://doi.org/10.1016/0144-8617(82)90058-3)
20. George J, Bawa A, Hatna S (2010) Synthesis and characterization of bacterial cellulose nanocrystals and their PVA nanocomposites. *Adv Mater Res* 123:383–386. <https://doi.org/10.4028/www.scientific.net/AMR.123-125.383>
21. Junior de Menezes A, Siqueira G, Curvelo AAS, Dufresne A (2009) Extrusion and characterization of functionalized cellulose whiskers reinforced polyethylene nanocomposites. *Polymer* 50:4552–4563. <https://doi.org/10.1016/j.polymer.2009.07.038>
22. Araki J, Wada M, Kuga S (2000) Steric stabilization of a cellulose microcrystal suspension by poly(ethylene glycol) grafting. *Langmuir* 17:21–27. <https://doi.org/10.1021/la001070m>
23. George J, Siddaramaiah (2012) High performance edible nanocomposite films containing bacterial cellulose nanocrystals. *Carbohydr Polym*
24. Jawaid M, Mohammad F (2017) Nanocellulose and nanohydrogel matrices: biotechnological and biomedical applications. Wiley
25. Dufresne A (2013) Nanocellulose: a new ageless bionanomaterial. *Mater Today* 16:220–227. <https://doi.org/10.1016/j.mattod.2013.06.004>
26. Sekhar Purkait B, Ray D, Sengupta S, Kar T, Mohanty A, Misra M (2010) Isolation of cellulose nanoparticles from sesame husk. *Ind Eng Chem Res* 50. <https://doi.org/10.1021/ie101797d>
27. de Oliveira FB, Bras J, Pimenta MTB, Curvelo AA da S, Belgacem MN (2016) Production of cellulose nanocrystals from sugarcane bagasse fibers and pith. *Ind Crops Prod* 93:48–57. <https://doi.org/10.1016/j.indcrop.2016.04.064>
28. Kumar A, Negi YS, Choudhary V, Bhardwaj NK (2014) Characterization of cellulose nanocrystals produced by acid-hydrolysis from sugarcane bagasse as agro-waste. *J Mater Phys Chem* 2:1–8. <https://doi.org/10.12691/jmpc-2-1-1>
29. Bano S, Negi YS (2017) Studies on cellulose nanocrystals isolated from groundnut shells. *Carbohydr Polym* 157:1041–1049. <https://doi.org/10.1016/j.carbpol.2016.10.069>
30. Oun AA, Rhim J-W (2016) Isolation of cellulose nanocrystals from grain straws and their use for the preparation of carboxymethyl cellulose-based nanocomposite films. *Carbohydr Polym* 150:187–200. <https://doi.org/10.1016/j.carbpol.2016.05.020>
31. Kasyapi N, Chaudhary V, Bhowmick A (2013) Bionanowhiskers from jute: preparation and characterization. *Carbohydr Polym* 92:1116–1123. <https://doi.org/10.1016/j.carbpol.2012.10.021>
32. Chen W, Yu H, Liu Y (2011) Preparation of millimeter-long cellulose I nanofibers with diameters of 30–80 nm from bamboo fibers. *Carbohydr Polym* 86:453–461. <https://doi.org/10.1016/j.carbpol.2011.04.061>
33. do Nascimento DM, Dias AF, de Araújo Junior CP, de Freitas Rosa M, Morais JPS, de Figueirêdo MCB (2016) A comprehensive approach for obtaining cellulose nanocrystal from coconut fiber. Part II: environmental assessment of technological pathways. *Ind Crops Prod* 93:58–65. <https://doi.org/10.1016/j.indcrop.2016.02.063>

34. Kim HM, Wi SG, Jung S, Song Y, Bae H-J (2015) Efficient approach for bioethanol production from red seaweed *Gelidium amansii*. *Bioresour Technol* 175:128–134. <https://doi.org/10.1016/j.biortech.2014.10.050>
35. Chen YW, Lee HV, Juan JC, Phang S-M (2016) Production of new cellulose nanomaterial from red algae marine biomass *Gelidium elegans*. *Carbohydr Polym* 151:1210–1219. <https://doi.org/10.1016/j.carbpol.2016.06.083>
36. Mihranyan A (2011) Cellulose from cladophorales green algae: from environmental problem to high-tech composite materials. *J Appl Polym Sci* 119:2449–2460. <https://doi.org/10.1002/app.32959>
37. George J, Sabapathi S (2015) Cellulose nanocrystals: synthesis, functional properties, and applications. *Nanotechnol Sci Appl* 8:45–54. <https://doi.org/10.2147/nsa.s64386>
38. Gowen RJ, Bradbury NB, Brown JR (1989) The use of simple models in assessing two of the interactions between fish farming and the marine environment
39. George J, Ramana KV, Sabapathy SN, Bawa AS (2005) Physico-mechanical properties of chemically treated bacterial (*Acetobacter xylinum*) cellulose membrane. *World J Microbiol Biotechnol* 21:1323–1327. <https://doi.org/10.1007/s11274-005-3574-0>
40. do Nascimento JHO, Luz RF, Galvão FMF, Melo JDD, Oliveira FR, Ladchumananandasivam R, Zille A (2015) Extraction and characterization of cellulosic nanowhisker obtained from discarded cotton fibers. *Mater Today Proc* 2:1–7. <https://doi.org/10.1016/j.matpr.2015.04.001>
41. Lamaming J, Hashim R, Sulaiman O, Peng LC, Sugimoto T, Nordin N (2015) Cellulose nanocrystals isolated from oil palm trunk. *Carbohydr Polym* 127. <https://doi.org/10.1016/j.carbpol.2015.03.043>
42. Ooi SY, Ahmad I, Amin MCIM (2016) Cellulose nanocrystals extracted from rice husks as a reinforcing material in gelatin hydrogels for use in controlled drug delivery systems. *Ind Crops Prod* 93:227–234. <https://doi.org/10.1016/j.indcrop.2015.11.082>
43. George J, Ramana KV, Sabapathy SN, Jagannath JH, Bawa AS (2005) Characterization of chemically treated bacterial (*Acetobacter xylinum*) biopolymer: some thermo-mechanical properties. *Int J Biol Macromol* 37:189–194. <https://doi.org/10.1016/j.ijbiomac.2005.10.007>
44. Jonoobi M, Oladi R, Davoudpour Y, Oksman K, Dufresne A, Hamzeh Y, Davoodi R (2015) Different preparation methods and properties of nanostructured cellulose from various natural resources and residues: a review. *Cellulose* 22:935–969. <https://doi.org/10.1007/s10570-015-0551-0>
45. Klemm D, Kramer F, Moritz S, Lindström T, Ankerfors M, Gray D, Dorris A (2011) Nanocelluloses: a new family of nature-based materials. *Angew Chem Int Ed* 50:5438–5466. <https://doi.org/10.1002/anie.201001273>
46. Vasconcelos NF, Feitosa JPA, da Gama FMP, Morais JPS, Andrade FK, de Souza Filho MDSM, de Freitas Rosa M (2017) Bacterial cellulose nanocrystals produced under different hydrolysis conditions: properties and morphological features. *Carbohydr Polym* 155:425–431. <https://doi.org/10.1016/j.carbpol.2016.08.090>
47. Camarero Espinosa S, Kuhnt T, Foster EJ, Weder C (2013) Isolation of thermally stable cellulose nanocrystals by phosphoric acid hydrolysis. *Biomacromolecules* 14:1223–1230. <https://doi.org/10.1021/bm400219u>
48. Lemke CH, Dong RY, Michal CA, Hamad WY (2012) New insights into nano-crystalline cellulose structure and morphology based on solid-state NMR. *Cellulose* 19:1619–1629. <https://doi.org/10.1007/s10570-012-9759-4>
49. Granja PL, Pouységu L, Deffieux D, Daudé G, Jéso BD, Labrugère C, Baquey C, Barbosa MA (2001) Cellulose phosphates as biomaterials. II. Surface chemical modification of regenerated cellulose hydrogels. *J Appl Polym Sci* 82:3354–3365. <https://doi.org/10.1002/app.2194>
50. Leung ACW, Hrapovic S, Lam E, Liu Y, Male KB, Mahmoud KA, Luong JHT (2011) Characteristics and properties of carboxylated cellulose nanocrystals prepared from a novel one-step procedure. *Small* 7:302–305. <https://doi.org/10.1002/smll.201001715>
51. Geboers J, de Vyver SV, Carpentier K, Jacobs P, Sels B (2011) Efficient hydrolytic hydrogenation of cellulose in the presence of Ru-loaded zeolites and trace amounts of mineral acid. *Chem Commun* 47:5590–5592. <https://doi.org/10.1039/C1CC10422E>

52. Tang L, Huang B, Ou W, Chen X, Chen Y (2011) Manufacture of cellulose nanocrystals by cation exchange resin-catalyzed hydrolysis of cellulose. *Bioresour Technol* 102:10973–10977. <https://doi.org/10.1016/j.biortech.2011.09.070>
53. Liu Y, Wang H, Yu G, Yu Q, Li B, Mu X (2014) A novel approach for the preparation of nanocrystalline cellulose by using phosphotungstic acid. *Carbohydr Polym* 110:415–422. <https://doi.org/10.1016/j.carbpol.2014.04.040>
54. Du H, Liu C, Mu X, Gong W, Lv D, Hong Y, Si C, Li B (2016) Preparation and characterization of thermally stable cellulose nanocrystals via a sustainable approach of FeCl₃-catalyzed formic acid hydrolysis. *Cellulose* 23:2389–2407. <https://doi.org/10.1007/s10570-016-0963-5>
55. Yu H-Y, Zhang D-Z, Lu F-F, Yao J (2016) New approach for single-step extraction of carboxylated cellulose nanocrystals for their use as adsorbents and flocculants. *ACS Sustain Chem Eng* 4:2632–2643. <https://doi.org/10.1021/acssuschemeng.6b00126>
56. Tang Y, Shen X, Zhang J, Guo D, Kong F, Zhang N (2015) Extraction of cellulose nanocrystals from old corrugated container fiber using phosphoric acid and enzymatic hydrolysis followed by sonication. *Carbohydr Polym* 125:360–366. <https://doi.org/10.1016/j.carbpol.2015.02.063>
57. Kontturi E, Meriluoto A, Penttilä PA, Baccile N, Malho J-M, Potthast A, Rosenau T, Ruokolainen J, Serimaa R, Laine J, Sixta H (2016) Degradation and crystallization of cellulose in hydrogen chloride vapor for high-yield isolation of cellulose nanocrystals. *Angew Chem Int Ed* 55:14455–14458. <https://doi.org/10.1002/anie.201606626>
58. Chen L, Zhu JY, Baez C, Kitin P, Elder T (2016) Highly thermal-stable and functional cellulose nanocrystals and nanofibrils produced using fully recyclable organic acids. *Green Chem* 18:3835–3843. <https://doi.org/10.1039/c6gc00687f>
59. Yang B, Dai Z, Ding S-Y, Wyman CE (2011) Enzymatic hydrolysis of cellulosic biomass. *Biofuels* 2:421–449. <https://doi.org/10.4155/bfs.11.116>
60. Li Y, Liu Y, Chen W, Wang Q, Liu Y, Li J, Yu H (2016) Facile extraction of cellulose nanocrystals from wood using ethanol and peroxide solvothermal pretreatment followed by ultrasonic nanofibrillation. *Green Chem* 18:1010–1018. <https://doi.org/10.1039/C5GC02576A>
61. Rabinovich ML, Melnick MS, Bolobova AV (2002) The structure and mechanism of action of cellulolytic enzymes. *Biochem Mosc* 67:850–871. <https://doi.org/10.1023/A:1019958419032>
62. Grimm FA, Iwata Y, Sirenko O, Chappell GA, Reif DM, Braisted J, Gerhold DL, Yeakley JM, Shepard P, Seligmann B, Roy T, Boogaard PJ, Ketelslegers HB, Rohde AM, Rusyn I (2016) A chemical–biological similarity-based grouping of complex substances as a prototype approach for evaluating chemical alternatives. *Green Chem* 18:4407–4419. <https://doi.org/10.1039/c6gc01147k>
63. George J, Ramana KV, Bawa AS, Siddaramaiah (2011) Bacterial cellulose nanocrystals exhibiting high thermal stability and their polymer nanocomposites. *Int J Biol Macromol* 48:50–57. <https://doi.org/10.1016/j.ijbiomac.2010.09.013>
64. Satyamurthy P, Jain P, Balasubramanya RH, Vigneshwaran N (2011) Preparation and characterization of cellulose nanowhiskers from cotton fibres by controlled microbial hydrolysis. *Carbohydr Polym* 83:122–129. <https://doi.org/10.1016/j.carbpol.2010.07.029>
65. Neumann J, Cho C-W, Steudte S, Köser J, Uerdingen M, Thöming J, Stolte S (2012) Biodegradability of fluoroorganic and cyano-based ionic liquid anions under aerobic and anaerobic conditions. *Green Chem* 14:410–418. <https://doi.org/10.1039/C1GC16170A>
66. Chen X, Deng X, Shen W, Jiang L (2012) Controlled enzymolysis preparation of nanocrystalline cellulose from pretreated cotton fibers. *BioResources* 7:4237–4248. <https://doi.org/10.15376/biores.7.3.4237-4248>
67. Xu Y, Salmi J, Kloser E, Perrin F, Grosse S, Denault J, Lau PCK (2013) Feasibility of nanocrystalline cellulose production by endoglucanase treatment of natural bast fibers. *Ind Crops Prod* 51:381–384. <https://doi.org/10.1016/j.indcrop.2013.09.029>
68. Hu Y, Catchmark JM (2011) Integration of cellulases into bacterial cellulose: toward bioabsorbable cellulose composites. *J Biomed Mater Res B Appl Biomater* 97B:114–123. <https://doi.org/10.1002/jbm.b.31792>

69. Wang B, Lv X, Chen S, Li Z, Sun X, Feng C, Wang H, Xu Y (2016) In vitro biodegradability of bacterial cellulose by cellulase in simulated body fluid and compatibility in vivo. *Cellulose* 23:3187–3198. <https://doi.org/10.1007/s10570-016-0993-z>
70. Domingues AA, Pereira FV, Sierakowski MR, Rojas OJ, Petri DFS (2016) Interfacial properties of cellulose nanoparticles obtained from acid and enzymatic hydrolysis of cellulose. *Cellulose* 23:2421–2437. <https://doi.org/10.1007/s10570-016-0965-3>
71. Pandey JK, Takagi H, Nakagaito AN, Kim H-J (2014) Handbook of polymer nanocomposites. Processing, performance and application: volume C: polymer nanocomposites of cellulose nanoparticles. Springer
72. Amin KNM, Annamalai PK, Morrow IC, Martin D (2015) Production of cellulose nanocrystals via a scalable mechanical method. *RSC Adv* 5:57133–57140. <https://doi.org/10.1039/C5RA06862B>
73. Abdul Khalil HPS, Bhat AH, Ireana Yusra AF (2012) Green composites from sustainable cellulose nanofibrils: a review. *Carbohydr Polym* 87:963–979. <https://doi.org/10.1016/j.carbpol.2011.08.078>
74. Allen TC, Cuculo JA (1973) Cellulose derivatives containing carboxylic acid groups. *J Polym Sci Macromol Rev* 7:189–262. <https://doi.org/10.1002/pol.1973.230070103>
75. Li W, Yue J, Liu S (2012) Preparation of nanocrystalline cellulose via ultrasound and its reinforcement capability for poly(vinyl alcohol) composites. *Ultrason Sonochem* 19:479–485. <https://doi.org/10.1016/j.ultrsonch.2011.11.007>
76. Zhao H, Feng X, Gao H (2007) Ultrasonic technique for extracting nanofibers from nature materials. *Appl Phys Lett* 90:073112. <https://doi.org/10.1063/1.2450666>
77. Tischer PCS, Sierakowski MR, Westfahl Jr H, Tischer CA (2010) Nanostructural reorganization of bacterial cellulose by ultrasonic treatment. *Biomacromolecules* 11:1217–1224. <https://doi.org/10.1021/bm901383a>
78. Saito T, Isogai A (2006) Introduction of aldehyde groups on surfaces of native cellulose fibers by TEMPO-mediated oxidation. *Colloids Surf Physicochem Eng Asp* 289:219–225. <https://doi.org/10.1016/j.colsurfa.2006.04.038>
79. Man Z, Muhammad N, Sarwono A, Bustam MA, Vignesh Kumar M, Rafiq S (2011) Preparation of cellulose nanocrystals using an ionic liquid. *J Polym Environ* 19:726–731. <https://doi.org/10.1007/s10924-011-0323-3>
80. Mao J, Osorio-Madrado A, Laborie M-P (2013) Preparation of cellulose I nanowhiskers with a mildly acidic aqueous ionic liquid: reaction efficiency and whiskers attributes. *Cellulose* 20:1829–1840. <https://doi.org/10.1007/s10570-013-9942-2>
81. Tan XY, Abd Hamid SB, Lai CW (2015) Preparation of high crystallinity cellulose nanocrystals (CNCs) by ionic liquid solvolysis. *Biomass Bioenergy* 81:584–591. <https://doi.org/10.1016/j.biombioe.2015.08.016>
82. Abushammala H, Krossing I, Laborie M-P (2015) Ionic liquid-mediated technology to produce cellulose nanocrystals directly from wood. *Carbohydr Polym* 134:609–616. <https://doi.org/10.1016/j.carbpol.2015.07.079>
83. Iskak NAM, Julkapli NM, Hamid SBA (2017) Understanding the effect of synthesis parameters on the catalytic ionic liquid hydrolysis process of cellulose nanocrystals. *Cellulose* 24:2469–2481. <https://doi.org/10.1007/s10570-017-1273-2>
84. Miao J, Yu Y, Jiang Z, Zhang L (2016) One-pot preparation of hydrophobic cellulose nanocrystals in an ionic liquid. *Cellulose* 23:1209–1219. <https://doi.org/10.1007/s10570-016-0864-7>
85. Evangelina Vallejos M, Dib Zambon M, Cristina Area M, da Silva Curvelo AA (2012) Low liquid–solid ratio (LSR) hot water pretreatment of sugarcane bagasse. *Green Chem* 14:1982–1989. <https://doi.org/10.1039/C2GC35397K>
86. Novo LP, Bras J, García A, Belgacem N, Curvelo AAS (2015) Subcritical water: a method for green production of cellulose nanocrystals. *ACS Sustain Chem Eng* 3:2839–2846. <https://doi.org/10.1021/acssuschemeng.5b00762>
87. Brinchi L, Cotana F, Fortunati E, Kenny JM (2013) Production of nanocrystalline cellulose from lignocellulosic biomass: technology and applications. *Carbohydr Polym* 94:154–169. <https://doi.org/10.1016/j.carbpol.2013.01.033>

88. Tang Y, Yang S, Zhang N, Zhang J (2014) Preparation and characterization of nanocrystalline cellulose via low-intensity ultrasonic-assisted sulfuric acid hydrolysis. *Cellulose* 21:335–346. <https://doi.org/10.1007/s10570-013-0158-2>
89. Rohaizu R, Wanrosli WD (2017) Sono-assisted TEMPO oxidation of oil palm lignocellulosic biomass for isolation of nanocrystalline cellulose. *Ultrason Sonochem* 34:631–639. <https://doi.org/10.1016/j.ultsonch.2016.06.040>
90. Beltramo F, Roncero MB, Torres AL, Vidal T, Valls C (2016) Optimization of sulfuric acid hydrolysis conditions for preparation of nanocrystalline cellulose from enzymatically pretreated fibers. *Cellulose* 23:1777–1789. <https://doi.org/10.1007/s10570-016-0897-y>
91. Lu Z, Fan L, Zheng H, Lu Q, Liao Y, Huang B (2013) Preparation, characterization and optimization of nanocellulose whiskers by simultaneously ultrasonic wave and microwave assisted. *Bioresour Technol* 146:82–88. <https://doi.org/10.1016/j.biortech.2013.07.047>
92. Chowdhury ZZ, Hamid SBA (2016) Preparation and characterization of nanocrystalline cellulose using ultrasonication combined with a microwave-assisted pretreatment process. *BioResources* 11:3397–3415. <https://doi.org/10.15376/biores.11.2.3397-3415>
93. Oun AA, Rhim J-W (2015) Effect of post-treatments and concentration of cotton linter cellulose nanocrystals on the properties of agar-based nanocomposite films. *Carbohydr Polym* 134:20–29. <https://doi.org/10.1016/j.carbpol.2015.07.053>
94. Hirai A, Inui O, Horii F, Tsuji M (2009) Phase separation behavior in aqueous suspensions of bacterial cellulose nanocrystals prepared by sulfuric acid treatment. *Langmuir* 25:497–502. <https://doi.org/10.1021/la802947m>
95. Han J, Zhou C, Wu Y, Liu F, Wu Q (2013) Self-assembling behavior of cellulose nanoparticles during freeze-drying: effect of suspension concentration, particle size, crystal structure, and surface charge. *Biomacromolecules* 14:1529–1540. <https://doi.org/10.1021/bm4001734>
96. Favier V, Dendievel R, Canova G, Cavaille JY, Gilormini P (1997) Simulation and modeling of three-dimensional percolating structures: case of a latex matrix reinforced by a network of cellulose fibers. *Acta Mater* 45:1557–1565. [https://doi.org/10.1016/S1359-6454\(96\)00264-9](https://doi.org/10.1016/S1359-6454(96)00264-9)
97. Moon RJ, Martini A, Nairn J, Simonsen J, Youngblood J (2011) Cellulose nanomaterials review: structure, properties and nanocomposites. *Chem Soc Rev* 40:3941–3994. <https://doi.org/10.1039/C0CS00108B>
98. Šturcová A, Davies GR, Eichhorn SJ (2005) Elastic modulus and stress-transfer properties of tunicate cellulose whiskers. *Biomacromolecules* 6:1055–1061. <https://doi.org/10.1021/bm049291k>
99. Muiruri JK, Liu S, Teo WS, Kong J, He C (2017) Highly biodegradable and tough polylactic acid-cellulose nanocrystal composite. *ACS Sustain Chem Eng* 5:3929–3937. <https://doi.org/10.1021/acssuschemeng.6b03123>
100. Muiruri JK, Liu S, Yeo JCC, Koh JJ, Kong J, Thitsartarn W, Teo WS, He C (2019) Synergistic toughening of poly(lactic acid)-cellulose nanocrystal composites through cooperative effect of cavitation and crazing deformation mechanisms. *ACS Appl Polym Mater* 1:509–518. <https://doi.org/10.1021/acscpm.8b00201>
101. Jahan Z, Niazi MBK, Gregersen ØW (2018) Mechanical, thermal and swelling properties of cellulose nanocrystals/PVA nanocomposites membranes. *J Ind Eng Chem* 57:113–124. <https://doi.org/10.1016/j.jiec.2017.08.014>
102. Meesorn W, Shirole A, Vanhecke D, de Espinosa LM, Weder C (2017) A simple and versatile strategy to improve the mechanical properties of polymer nanocomposites with cellulose nanocrystals. *Macromolecules* 50:2364–2374. <https://doi.org/10.1021/acs.macromol.6b02629>
103. Azizi Samir MAS, Alloin F, Sanchez J-Y, El Kissi N, Dufresne A (2004) Preparation of cellulose whiskers reinforced nanocomposites from an organic medium suspension. *Macromolecules* 37:1386–1393. <https://doi.org/10.1021/ma030532a>
104. Cassagnau P (2013) Linear viscoelasticity and dynamics of suspensions and molten polymers filled with nanoparticles of different aspect ratios. *Polymer* 54:4762–4775. <https://doi.org/10.1016/j.polymer.2013.06.012>

105. Araki J, Wada M, Kuga S, Okano T (1999) Influence of surface charge on viscosity behavior of cellulose microcrystal suspension. *J Wood Sci* 45:258–261. <https://doi.org/10.1007/BF01177736>
106. Peng B, Tang J, Wang P, Luo J, Xiao P, Lin Y, Tam KC (2018) Rheological properties of cellulose nanocrystal-polymeric systems. *Cellulose* 25:3229–3240. <https://doi.org/10.1007/s10570-018-1775-6>
107. Kamal MR, Khoshkava V (2015) Effect of cellulose nanocrystals (CNC) on rheological and mechanical properties and crystallization behavior of PLA/CNC nanocomposites. *Carbohydr Polym* 123:105–114. <https://doi.org/10.1016/j.carbpol.2015.01.012>
108. Khandal D, Riedl B, Tavares JR, Carreau PJ, Heuzey M-C (2019) Tailoring cellulose nanocrystals rheological behavior in aqueous suspensions through surface functionalization with polyethyleneimine. *Phys Fluids* 31:021207. <https://doi.org/10.1063/1.5046669>
109. Gupta A, Simmons W, Schueneman GT, Hylton D, Mintz EA (2017) Rheological and thermo-mechanical properties of poly(lactic acid)/lignin-coated cellulose nanocrystal composites. *ACS Sustain Chem Eng* 5:1711–1720. <https://doi.org/10.1021/acssuschemeng.6b02458>
110. Ben Azouz K, Ramires EC, Van den Fonteyne W, El Kissi N, Dufresne A (2012) Simple method for the melt extrusion of a cellulose nanocrystal reinforced hydrophobic polymer. *ACS Macro Lett* 1:236–240. <https://doi.org/10.1021/mz2001737>
111. Eyley S, Thielemans W (2014) Surface modification of cellulose nanocrystals. *Nanoscale* 6:7764–7779. <https://doi.org/10.1039/C4NR01756K>
112. Habibi Y, Lucia LA, Rojas OJ (2010) Cellulose nanocrystals: chemistry, self-assembly, and applications. *Chem Rev* 110:3479–3500. <https://doi.org/10.1021/cr900339w>
113. Salajková M, Berglund LA, Zhou Q (2012) Hydrophobic cellulose nanocrystals modified with quaternary ammonium salts. *J Mater Chem* 22:19798–19805. <https://doi.org/10.1039/C2JM34355J>
114. Abitbol T, Marway H, Cranston ED (2014) Surface modification of cellulose nanocrystals with cetyltrimethylammonium bromide. *Nord Pulp Pap Res J* 29:46–57. <https://doi.org/10.3183/npprj-2014-29-01-p046-057>
115. Ansari F, Salajková M, Zhou Q, Berglund LA (2015) Strong surface treatment effects on reinforcement efficiency in biocomposites based on cellulose nanocrystals in poly(vinyl acetate) matrix. *Biomacromolecules* 16:3916–3924. <https://doi.org/10.1021/acs.biomac.5b01245>
116. Abraham E, Nevo Y, Slattegard R, Attias N, Sharon S, Lapidot S, Shoseyov O (2016) Highly hydrophobic thermally stable liquid crystalline cellulosic nanomaterials. *ACS Sustain Chem Eng* 4:1338–1346. <https://doi.org/10.1021/acssuschemeng.5b01363>
117. Girouard NM, Xu S, Schueneman GT, Shofner ML, Meredith JC (2016) Site-selective modification of cellulose nanocrystals with isophorone diisocyanate and formation of polyurethane-CNC composites. *ACS Appl Mater Interfaces* 8:1458–1467. <https://doi.org/10.1021/acsami.5b10723>
118. Fujisawa S, Togawa E, Kuroda K (2017) Nanocellulose-stabilized Pickering emulsions and their applications. *Sci Technol Adv Mater* 18:959–971. <https://doi.org/10.1080/14686996.2017.1401423>
119. Siqueira G, Bras J, Dufresne A (2010) New process of chemical grafting of cellulose nanoparticles with a long chain isocyanate. *Langmuir* 26:402–411. <https://doi.org/10.1021/la9028595>
120. Dhar P, Kumar A, Katiyar V (2016) Magnetic cellulose nanocrystal based anisotropic polylactic acid nanocomposite films: influence on electrical, magnetic, thermal, and mechanical properties. *ACS Appl Mater Interfaces* 8:18393–18409. <https://doi.org/10.1021/acsami.6b02828>
121. Hu Z, Berry RM, Pelton R, Cranston ED (2017) One-pot water-based hydrophobic surface modification of cellulose nanocrystals using plant polyphenols. *ACS Sustain Chem Eng* 5:5018–5026. <https://doi.org/10.1021/acssuschemeng.7b00415>

Chapter 12

Biodegradable Nanocomposite Foams: Processing, Structure, and Properties



Shasanka Sekhar Borkotoky, Tabli Ghosh and Vimal Katiyar

Abstract The biodegradable nanocomposite foams can be developed using different fabrication techniques where the use of various kinds of bio-based nanofillers helps in tailoring the foam properties. A brief discussion on different techniques of fabrication, their economic viability, and industrial feasibility in regards to the polymeric foams is made in this chapter. Moreover, the available different biodegradable polymeric foams and their processing in the recent past years is detailed. However, the chapter mainly focuses on the biodegradable poly (lactic acid) (PLA)-based nanocomposite foams and their recent developments and breakthroughs. The addition of nanofillers for fabricating the foam greatly affects various foam properties such as cell size, cell density, and porosity. Other important properties such as thermal properties, mechanical properties, and wettability are also affected by the nanofiller materials. The degradation of PLA-based nanocomposite foams is greatly influenced due to the addition of various bio-based nanofiller materials. In this regard, the tailor-made properties of various biodegradable foams make them promising candidate in different areas of research.

Keywords Poly (lactic acid) · Biodegradable · Foams · Fabrication · Characterization

1 Introduction

Foam is an entity consisting of gaseous voids (75–95%) in liquid or solids. Synthetic foams can be developed from various materials including glass, metals, ceramic, polymer, and rubber. Among various available foams, the polymeric foams have some unique properties and some added advantages such as low weight, low density, and less usage of materials compared to non-foam materials. Further, the cost of production can also be reduced by the specified factors. The elastomeric foams have been widely utilized in different fields of applications such as insulation materials,

S. S. Borkotoky · T. Ghosh · V. Katiyar (✉)

Department of Chemical Engineering, Indian Institute of Technology Guwahati, Guwahati, Assam 781039, India

e-mail: vkatiyar@iitg.ac.in

© Springer Nature Singapore Pte Ltd. 2020

V. Katiyar et al. (eds.), *Advances in Sustainable Polymers*, Materials Horizons: From Nature to Nanomaterials, https://doi.org/10.1007/978-981-15-1251-3_12

271

sound-absorbing materials, and cushioning. Thus, the polymeric foaming technology is growing day by day and has established as one of the major areas of research. Further, the development of porous material is gaining importance day by day with the discovery of new areas of applications [1].

The polymeric foam industry was initially developed during 1930s to 1950s, where polystyrene (PS) foam was firstly developed in 1931. The development and use of foam took an established shape in 1980s. The recent area of research is focused on improving the properties of the foam, which is the driving force for developing new foam-based materials. The polymeric foams are generally classified according to different parameters such as material use, structure, nature, mechanism, cell size, and others as shown in Fig. 1. However, the polymeric foams can also be broadly classified into two major parts: non-degradable foams and biodegradable foams [2]. Non-degradable polymeric foams mainly dominate the current market share of the total polymeric foams. However, a continuous effort has been made to replace the available non-degradable foams by biodegradable foams due to the increasing market share of polymer foams. The recent shares by volume in various applications of polymeric foams are shown in Fig. 2 (based on a market report of Smithers Rapra, 2015). According to this, the polymer foams have major application in construction materials and find applications in furniture, automobiles, packaging, refrigeration, and others. A recent market survey suggests that the use of high-performance polymeric foams will increase ~4.8% annually due to the growth in emerging technologies (based on the market survey of Smithers Rapra, 2018). However, the above foam market is mainly dominated by the non-degradable conventional foams.

Moreover, the demand for the biodegradable polymeric foams in different new areas is rapidly increasing day by day. Researchers are also trying to find new areas of replacement to the conventional non-foamed polymers by developing composites, blends of biodegradable foams. As the ultimate disposal of non-degradable

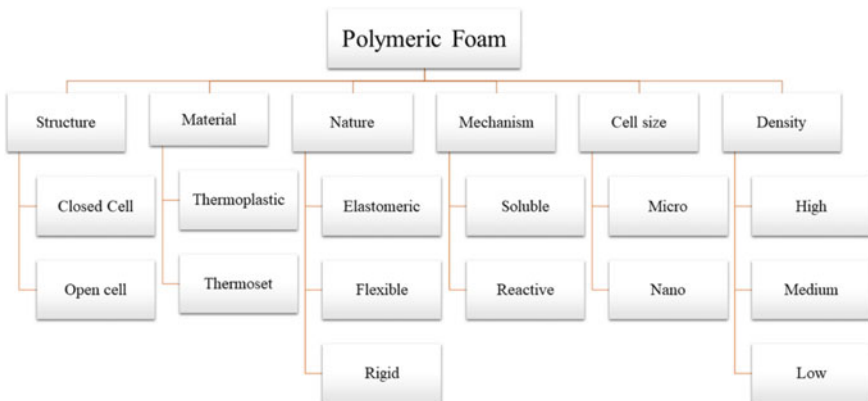


Fig. 1 Classifications of polymeric foams based on different parameters

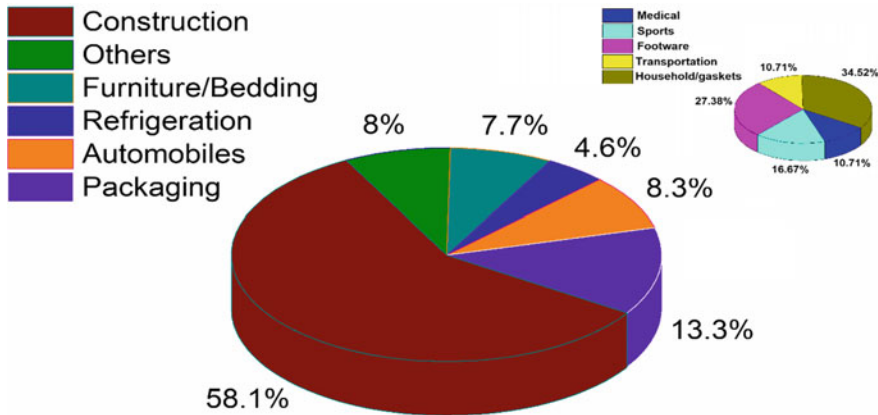


Fig. 2 Global market shares of polymeric foams in different segments

polymer foams is a major concern in the environmental point of view, the environmentally friendly technologies are now a primary requisite in this regard followed by the international agreements like the Kyoto protocol, Montreal protocol, and so on. Hence, the need for bio-based and biodegradable foams is gaining attention in recent years. Bio-based and biodegradable foams show a tremendous and promising impact in different fields like biomedical, food packaging, industrial, engineering, and advance applications. Some of the recently used biodegradable polymeric foams include starch, poly(hydroxyalkanoates) (PHAs), poly(3-hydroxybutyrate) (PHB), poly(lactic acid) (PLA), poly(ϵ -caprolactone) (PCL), and poly(3-hydroxybutyrate-co-hydroxyvalerate) (PHBV). The first developed biodegradable polymeric foam is starch, which is further improved for various properties. Biodegradable polymer foams have some inferior properties, which need to be modified to compete with the non-degradable polymeric foam materials for targeted applications. In this regard, the major differences between the biodegradable and non-degradable foams are illustrated in Fig. 3, where biodegradable foam-based materials provide non-toxicity, biocompatibility, and eco-friendly nature causing no harmful effect to the environment.

In recent years, a variety of biodegradable polymer materials are gaining importance for the fabrication of tailor-made foam materials for multifaceted advanced applications. However, one of the promising biodegradable polymers, which are gaining attention among the scientific community for the replacement of conventional polymeric foam, is PLA. Recent researches on bio-based foams are mainly focused on the development of PLA-based foams. Besides, PLA, the other biodegradable polymeric foams include PCL, polybutylene succinate (PBS), PHBV, cellulose, their blends, composites, etc., which are being used for wide application.

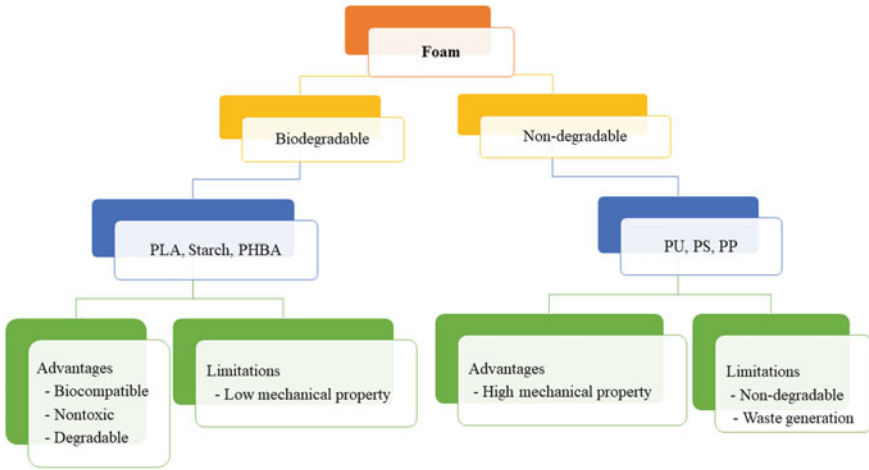


Fig. 3 Degradable and non-degradable foams

1.1 Poly (Lactic Acid) (PLA)

PLA is a bio-based and biodegradable polymer synthesized from natural resources including corn and carbohydrate-based feedstock. PLA has the properties comparable to some non-degradable petroleum-based polymers. The schematic illustration of the life cycle of biodegradable PLA can be observed in Fig. 4, where the composting and

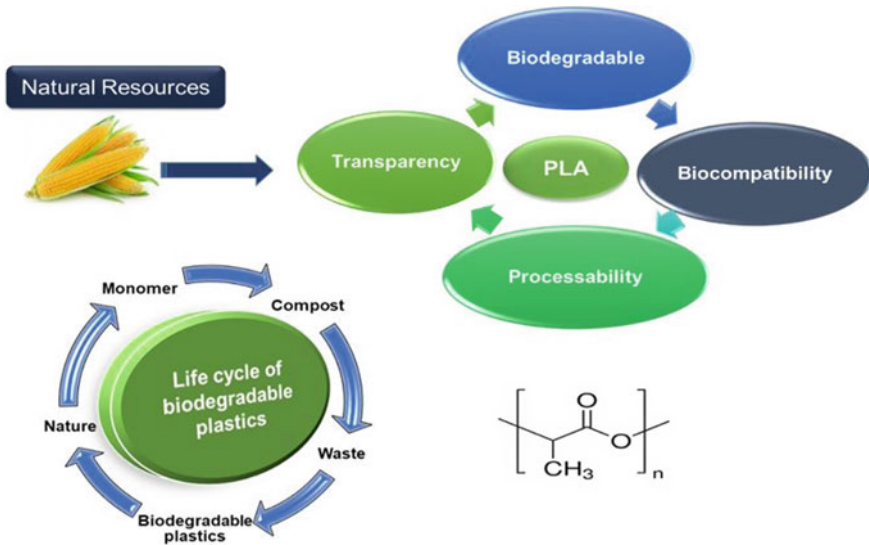


Fig. 4 Life cycle of poly (lactic acid)

biodegradation processes reduce environmental waste. Additionally, PLA has good processability which increases the market value of PLA-based foam materials. PLA is mainly synthesized by ring opening polymerization (ROP) of lactide monomer [3]. PLA is a thermoplastic which is glossy, transparent, and semi-crystalline in nature. The production of PLA requires less energy (up to 25–55%) compared to the energy consumed in the production of petroleum-based non-degradable foams. The content of D-isomer present in PLA influences its ultimate properties. The thermal degradation of PLA leads to the release of non-toxic materials such as CO₂, H₂O, and lactic acid due to hydrolysis of ester linkages. The mechanical and other properties of PLA are comparable with most of the petroleum-based conventional polymers. The properties of PLA can be improved by tuning it with the addition of different nanofillers, plasticizers, chain extenders, etc. [4].

However, one of the limitations of PLA is its low melt strength. The short degradation time of PLA makes it unsuitable for engineering applications. Another limitation of PLA is low thermal properties. The current researches on PLA are mainly focused in the directions to tune these limitations. PLA-based foams are mainly utilized in sophisticated bio-based medical applications like cell culture, tissue engineering, and so on due to its biodegradability. Simultaneously, it can be useful in other advanced applications by tailoring its properties for specific applications. The other applications include packaging, housewares, automobile parts, cushioning applications, insulation, furniture, high-grade decorative items, and electrical appliances. A focused study has to be performed to make it suitable for different applications [5].

2 Fabrication of Polymeric Foams

Polymer foaming can broadly be carried out in different established processes classified as batch foaming process and continuous foaming process. The batch process is mainly limited to the research in development fields to investigate the newly developed materials and their foaming behavior. On the other hand, the continuous process is an economically and industrially viable scale-up process in larger magnitude. A continuous process is achieved by an extrusion technique, consisting of steps like mixing with additives and pressurization of inert gases [6].

2.1 *Batch Foaming Process*

Fabrication of polymeric foams can be performed by using batch process. In this process of fabrication, foamed samples are prepared batch-wise. It is a discontinuous foaming process, and the reproducibility of this process is very good by maintaining exact process parameters. This process is mainly utilized to investigate the initial foaming behavior of polymers and composite systems. The process is also industrially viable with some limitations. In this process, carbon dioxide or nitrogen is mainly

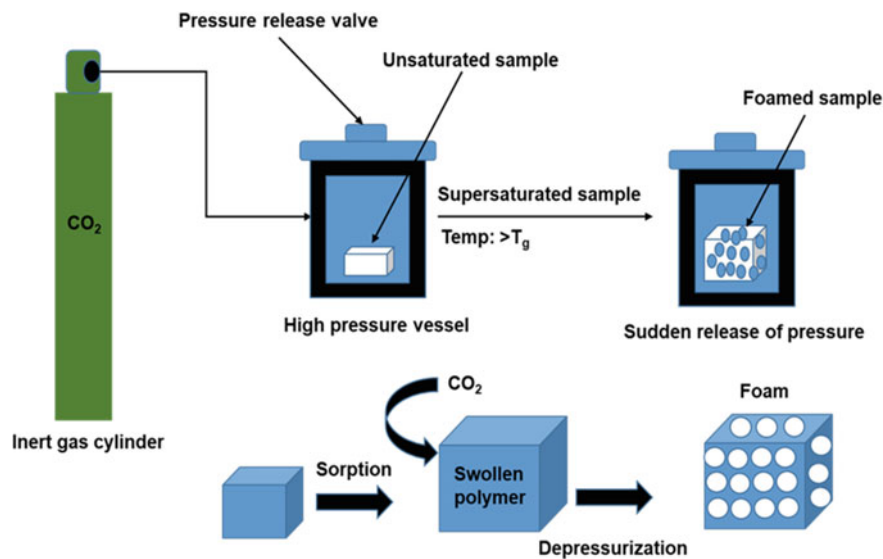


Fig. 5 A schematic representation of batch foaming process

used as physical blowing agent (PhyBA). A schematic diagram of the process is represented in Fig. 5. Since earlier days, two different methods have been generally utilized in the batch foaming process. In the first process, the pressure drop initiates the foaming in the polymer sample resulting in thermodynamic disequilibrium. The method is very useful to understand the different foaming parameters as well as the influence of additives or blending on cell nucleation. In the second technique, the thermodynamic disequilibrium is reached due to the increasing temperature. From this method, the foaming temperature and processing window of the foam can be evaluated for foam extrusion process.

2.2 Continuous Foaming Process

This process of fabrication of polymeric foam generally consists of extrusion (Fig. 6) and injection techniques. Different zones of the extruder can be operated at different temperatures, which make it possible to use temperature sensitive additives along with the polymer. This is one of the most beneficial CO₂-based foaming process techniques for the addition of different additives to the bio-based polymeric foams. In the die section of the extruder, the pressure is released and ultimately the polymer foam is generated. In this continuous process, the process parameters such as screw speed, saturation pressure, type and amount of additives (clay, plasticizer etc.), etc., can be optimized for obtaining tuned foam properties. The influence of the die geometry and temperature on the nucleation rate or the expansion ratio of the fabricated

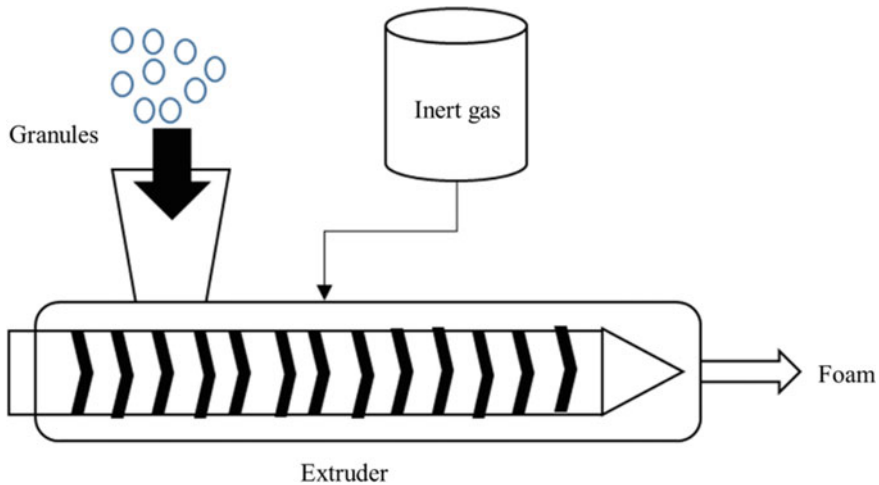


Fig. 6 A schematic representation of continuous foaming process

foams can be investigated by this process. In this process, the main advantage is the continuous high-speed production and scale-up of the technology. Different parameters like melt strength, viscosity, solubility, end groups, glass transition temperature, etc., affect the properties of the polymeric foams.

3 Polymer Foaming Technology

Polymer foaming is mainly achieved by two different techniques: physical foaming and reactive foaming.

3.1 Physical Foaming

In physical foaming, PBAs are used in the polymer melt. It also permits high-speed continuous foaming of the polymer by using extrusion and injection molding.

Physical foaming can be performed by using the following methods:

- (a) Casting and leaching (C/L)
- (b) Gas foaming
- (c) Thermally induced phase separation (TIPS).

C/L Methods In C/L technique, the polymer is dissolved in a highly volatile solvent and cast in a bed of porogen. After evaporation of the solvent, the sample is placed in water for leaching out the porogens followed by drying. The leaching of porogens

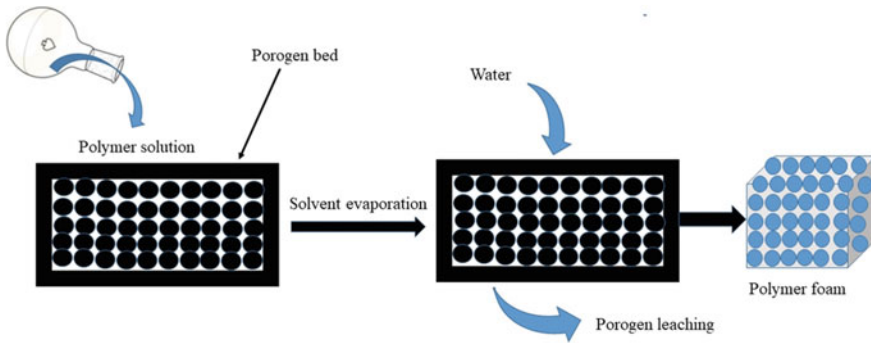


Fig. 7 Casting and leaching (C/L) technique of foam fabrication

ultimately leaves a porous structure. The selection of porogen is very important as it must be easily available and non-toxic in nature. Additionally, the porogen must be easily leached out after the solvent is evaporated. Mostly used porogens include salts like NaCl, KCl, etc. The size and amount of the porogen have the ultimate effect on cell size and cell density of the foams [7]. This technique is one of the cost-effective and easy methods to fabricate foams. The C/L method is represented in Fig. 7.

Gas Foaming Method In the gas foaming technique, different gases like nitrogen, carbon dioxide, etc., are used as PBA in the polymer melt. One of the greener approaches for gas foaming is using it in a supercritical state. Many investigations on polymer foam fabrication are reported using this technique. There are some criteria regarding the selection of PBA which includes safety, non-toxicity, transportation, reactivity, volatility, and economic viability.

TIPS Method Generally, two steps are followed for TIPS method of fabrication of foams. In the TIPS process of fabrication of foams, polymer pellets are partially foamed in the first step using PBA. These partially foamed pellets are transferred to a mold and again foaming has been performed using steam and low boiling liquid for extra foaming in the second step. Finally, a foamed structure is obtained taking the shape of the mold, and foamed beads are stuck to one another [8].

3.2 Reactive Foaming

In the reactive foaming technique, chemical reactions are carried out for the foaming of polymers. The production of gases in the chemical reactions fabricates the foamed structure. In this method of fabrication, the chemical blowing agents (CBA) are utilized for foaming of polymers. The selection of CBA has some minimum criteria including by-products, nucleating effects, processability with the base polymer, and color left-over in the polymer matrix.

4 Recent Advances in Biodegradable PLA-Based Foams

Generally, biodegradable polymeric foams like starch, PHBV, etc., are mainly used in food packaging applications. However, biodegradable PLA-based foams have the potential to replace the major market players (polypropylene, PS, etc.) in different commodity applications due to its unique properties. Recently, researchers are focusing toward the development of PLA-based sustainable foams due to its greener routes and comparable properties with some non-degradable foams. However, some improvements in the properties of PLA-based foams are still lacking compared to non-degradable foams. The improvement in the properties of PLA-based foams can be achieved by the incorporation of additives, flame retardants, plasticizers, and so on according to the ultimate application. Some investigations on PLA-based foams are found to be path-breaking towards the development of greener environment. Mainly, it is observed that PLA-based foams are developed using continuous extrusion foaming technique in the scale-up process. However, the investigations are also carried out in batch foaming to understand the parameters for improvements. PLA-based foams are used in various fields of biomedical applications including tissue engineering and cell culture. It is observed in the literature that most of the PLA-based foams used in bio-based sophisticated applications are fabricated by *C/L* technique due to its cost-effectiveness and less usage of machinery. Some of the recent developments observed in PLA-based foams are discussed in this section. The improvement in the thermal stability and crystallinity in PLA-based foams can be achieved by using additives like nanofillers, nanoclays, etc. The mechanical properties of PLA-based foams are very much dependent on the amount of closed and open cells present in the PLA foam matrix. Therefore, the increase in the closed cell percentage can easily achieve mechanical strength. The plasticizers in PLA-based foams improve the flexibility, which is a requirement in some sophisticated bio-based applications [9]. Recent studies reveal that for some applications related to cell proliferation, the large surface area is favorable along with wettability requirements, and PLA-based foams can be tuned to the desired properties by utilizing nanobiofillers [10].

A representative field emission scanning electron microscopy (FESEM) image of PLA-based foam is shown in Fig. 8, where the interconnected pores with cell walls are clearly visible in the micrograph. Generally, for the improvement in mechanical properties, foams are fabricated using extrusion or injection molding process using supercritical carbon dioxide as PBA. Some investigations on the improvements in mechanical properties of PLA-based foams suggest that using nanoclay (montmorillonite (MMT)) at lower concentrations in the PLA matrix improves the tensile strength of PLA foam. The nanoclay also helps in the generation of more nucleating sites which are also responsible for smaller pores in the matrix [11]. Similarly, an increase of specific tensile strength of PLA-based foams is also observed under foaming with compressed CO₂. The elongation at break increases up to ~15 times on foaming compared to unfoamed counterpart [12]. The reduction in cell size and increase in the cell density can also be achieved in PLA-based foams using a mixture of compressed CO₂ and N₂ (20:80 ratio) as PBA. Sequential addition of chain

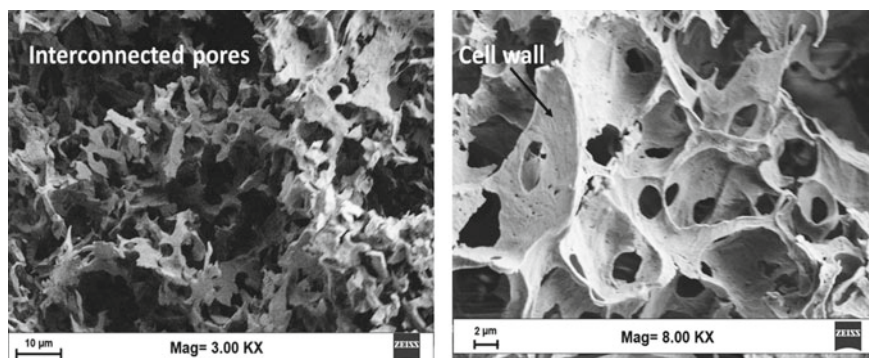


Fig. 8 FESEM micrographs of PLA-based foams fabricated at the Centre of Excellence for Sustainable Polymers (CoE-SusPol), IIT Guwahati

extenders such as 1, 4-butanediol and 1,4-butane di isocyanate in PLA gives high melt viscosity and elasticity to the PLA foam. Addition of crosslinkers in the PLA matrix improves the glass transition temperature (T_g) and thus affects the thermal properties [13]. Foaming of PLA in the presence of chain extender such as Joncryl 4368, which influences the polymer viscosity and crystallinity. Chain extender helps in the generation of smaller pores and improvement in cold crystallization temperature [14]. PS/poly(glycidyl methacrylate) random copolymer has also been used as chain extender in PLA matrix, which improves the viscous and elastic properties along with smaller cell generation in PLA foam using supercritical CO_2 as PBA [15].

Investigations are also observed for the fabrication of PLA-based foams for tissue engineering applications with very high interconnectivity of the pores. This is achieved by using foaming of PLA/PS blend and then extracting the PS phase, which leads to a highly interconnected porous PLA-foamed structure. The high interconnectivity of pores is suitable for the growing of human cells in the PLA foam matrix [16]. Similar types of PLA-based tissue engineering scaffolds can also be fabricated by using a solvent-free method. PLA and sucrose immiscible blends are first obtained from the extruder followed by solid-state foaming. The leaching of sucrose particles ultimately leaves a foamed PLA structure. A highly porous (porosity: 90%) structure with pore size ranging from 25 to 200 μm can be achieved by this process [17]. Some researchers utilize injection molding technique for the fabrication of high void fraction polylactide foams. Incorporation of talc in the PLA foaming process is under N_2 as PBA. They observed that talc/clay provides a more uniform cell structure with cell size $<50 \mu\text{m}$. The crystallization kinetics of PLA is also affected by different parameters like the pressure of the gas, the presence of nanoclay/talc, mold opening, and so on [18]. The continuous process of fabrication of low-density, microcellular PLA foams with crystallinity and well-controlled cell morphology has demonstrated by Wang et al. [19]. They have developed a tandem system utilizing CO_2 as PBA. They systematically investigated the extrusion foaming behaviors of linear and branched PLAs. They have concluded that molecular branching in PLA is responsible for

melt strength and elasticity. The integrity of the cells and cell density increases with branching. The extrusion foaming of PLA with endothermic chemical foaming agent (CFA) has demonstrated by Matuana et al. [20]. They observed that void fraction is closely related to the melt flow index of PLA. Various other parameters like processing speed, CFA concentration, and melt flow index affected the cellular morphology of PLA foam. Hence, by maintaining these parameters we can tune the PLA-based foam morphology according to the desired applications. Improvements in cell density, reduction in cell size and increase in bulk compressibility of PLA-based foams can also be achieved by using tapioca starch and cloisite Na⁺ in the PLA matrix by melt intercalation techniques. The PLA-based nanocomposite foams have superior and excellent properties compared to neat PLA foam due to the possible intercalation of nanoclays in the PLA matrix [21]. The average pore size of PLA-based foams can be achieved up to ~5 μm utilizing PLA/starch composite foaming by supercritical CO₂ in batch foaming process. The increase in crystallinity is observed in PLA/starch foams compared to neat PLA foam, which influences the mechanical properties along with the expansion ratio [22]. Similar kind of improvements in flexural and tensile strength in PLA/starch foams are noticed with the addition of plasticizers like glycerol, urea, and so on [23]. The maximum expansion ratio of ~50 for PLA-based foam can be achieved by using extrusion foaming of semi-crystalline PLA and thermoplastic starch blends. This system gives the minimum average pore size as ~25 μm [24].

Some improvements in PLA-based foams can also be accomplished by blending it with different other materials and subsequent foaming of the system. Blending of PLA with polymers like poly(butylene adipate-co-butylene terephthalate), poly(butylene adipate-co-terephthalate), PHBV, and so on has been demonstrated in recent past [25–27]. Extrusion foaming of the above PLA-based polymeric blends improves the mechanical and other properties of PLA foam. The decrease in the cell size (up to ~10 μm) and increase in the cell density is observed. The degree of crystallinity in PLA-based foams can also be improved by using flex-fiber composites and coupling agent [28]. Introduction of stereocomplex crystallites in the PLA matrix helps to improve the heat resistance property of microcellular PLA-based foam. A significant increase in cell density and decrement in cell size is also reported on the incorporation of stereocomplex crystallites [29]. Flame retardant property of PLA-based foams can be improved by using starch as a natural charring agent [30].

Introduction of hyperbranched polyester (HBP)/nanoclay in the PLA matrix by an injection molding process using N₂ as PBA has been reported by Pilla et al. [31]. They have achieved a maximum expansion ratio as 1.2 and minimum average cell size as ~10 μm. The addition of HBPs and nanoclay decreased the average cell size and increased the cell density of PLA-based foam. The development of first nanocellular PLA-based foams has been demonstrated by Fujimoto et al. [32]. They have fabricated PLA/layered silicate nanocomposite foam utilizing supercritical CO₂ as PBA in batch foaming technology. The expansion ratio of ~2.7 and average cell size of 360 nm can be achieved by this technique. The fabricated foam mainly consists of

a closed cellular structure which enhances the mechanical properties of PLA-based foams.

Some improvements in the nanocellular PLA-based foam technology has been carried out by Ema et al. [33], where foam processing and cellular structure of polylactide-based nanocomposites has been studied. They used an autoclave for foaming and utilized the batch foaming technique using supercritical carbon dioxide (CO₂) as a foaming agent. They investigated the foam processing of neat polylactide (PLA) and two different types of PLA-based nanocomposites (PLACNs). The maximum expansion ratio of ~5 and minimum average cell size as ~200 nm is achieved by this technique. The dispersed nanoclay particles acted as nucleating sites for cell formation and the cell growth occurs on the surfaces of the clays. The PLACNs provided excellent nanocomposite foams having high cell density.

The degradation of PLA-based foams is a very important phenomenon. Some investigations on the degradation behavior of PLA-based foams can be observed in the literature. The enzymatic degradation of PLA-based foams can be enhanced by changing the pore size. It is observed that the degradation rate of nanocellular PLA-based foam is ~2 times higher than the microcellular foam with the same crystallinity. This phenomenon is due to the large surface area of the nanocellular foam which can accommodate a large amount of water facilitating the enzymatic degradation faster than microcellular foam [34].

5 Nanostructured Materials in PLA-Based Foams

The addition of nanobiofillers in the polymer matrix for tuning of various properties is also a growing field of PLA-based foams. Some investigations have been reported in literature about the usage of nanobiofillers like silk, cellulose, chitosan, gum Arabic (GA), nanoclay, etc., in the PLA-based foams. These nanofillers are derived from bio-sources and are abundantly available in nature. Therefore, the utilization of these fillers in the PLA foam matrix has economic and environmental aspects.

5.1 *PLA- and Silk Fibroin-Based Nanocomposite Foams*

Silk is a widely used material for improving the properties of PLA-based foam materials. The fabrication of microcellular biodegradable PLA/silk composite foams using supercritical CO₂ has been reported by Kang et al. The reduction in cell size and increase in cell density is observed with the increase in silk fibroins in the PLA matrix. By utilizing this technique, average cell size up to ~15 μm can be achieved [35].

5.2 *PLA and Nanocellulose-Based Nanocomposite Foams*

Cyclic tensile properties of PLA-based foams can be tuned by using cellulose nanocrystals (CNC) as demonstrated by Qiu et al. [36] using high-pressure batch foaming process. Improvement in the cell density and decrement in wall thickness is observed for PLA/CNC-based foams. Incorporation of cellulose nanofibers (CNF) in the PLA foam matrix has been reported in some of the investigations. Improvements in strain at break and high tensile toughness in PLA/CNF-based microcellular foams have been demonstrated in past years [37]. Viscosity of the fabricated PLA/CNF-based foams is also influenced by CNF content as reported by Youn Cho et al. [38]. They used supercritical carbon dioxide as a PBA. They also found that compared to neat PLA foam, the PLA/CNF nanocomposite foams exhibited decreased cell size as well as increased cell density and foam density due to the improved viscous properties. CNF mainly acts as a nucleating agent in the PLA matrix at low concentrations; however, at higher concentration, it hinders the chain movement of PLA. The introduction of CNFs significantly improves the morphology of PLA foams. Both the amount of CNFs and surface acetylation contribute to the reduction in cell size and an increase in cell density of PLA-based foam [39]. Improvements in mechanical, thermal, and wettability properties of PLA/CNC-based microcellular foams fabricated by C/L technique utilizing sucrose as porogen medium has been reported. The bionanofiller mainly acts as a nucleating agent in the PLA matrix in lower loadings and acts as a physical barrier for chain folding in higher loading. CNC nanobiofillers also help in crystallization of PLA-based foams. CNC also influences the thermal stability of the fabricated PLA-based foams. The cell density increases, and cell size decreases with increasing CNC content. The hydrophobicity of PLA-based foams improves with increase in CNC due to the change in morphology and the effect of nanofiller. CNC also helps in increasing the surface area of PLA-based foams. The energy of crystallization also increases with CNC loading. The thermal degradation investigation of PLA/CNC-based foams reveals the increase in activation energy with CNC at lower loadings indicating an increase in thermostability by uniform dispersion of CNC nanobiofillers in PLA foam matrix. A change of ~40–50 kJ/mol in activation energy has been reported for PLA/CNC foam system compared to PLA/CNC film system due to the generation of more surface area and more sites of degradation in PLA/CNC-based foams. However, CNC has no significant effect on the mechanism of degradation of PLA-based foams [40, 41].

5.3 *PLA- and Nanochitosan-Based Nanocomposite Foams*

Nanobiofillers like chitosan and GA act as plasticizing agents in the PLA matrix. Chitosan is abundantly available in nature. It comes from natural resources. Chitosan is a very useful bionanofiller. It has the approval of the Food and Drug Administration (FDA) as a non-toxic material and can be utilized in foods and other biomedical

applications. However, due to its hydrophilic nature, some modifications in the surface have to be conducted to make it compatible with hydrophobic biopolymers. Chitosan microspheres have been utilized in PLA foam matrix for application of peptide carrier in biomedical fields [42]. Some investigations demonstrated the fabrication of PLA-based foams with chitosan for breast cancer cells [43]. Chitosan nanofiller has been widely utilized in poly (L-lactic acid) foam matrix for cell proliferation investigations [44]. On the other hand, poly (chitosan-grafted-lactic acid) scaffolds have been utilized for biocompatibility investigations [45]. PLA/modified chitosan (MC)-based microcellular foams have been fabricated by C/L technique. The ~2.3-fold increase in cell density and ~1.3-fold decrease in cell size have been demonstrated compared to neat PLA foams. The MC (oligomer-grafted-chitosan) improves the hydrophobicity of the fabricated PLA-based foams. The increase in the surface area has been reported with an increase in MC concentration due to the generation of smaller pores. MC acts as a nucleating agent in the PLA matrix. However, due to the presence of low-molecular-weight oligomers in MC, the thermal properties slightly decrease. The activation energy decreases with an increase in MC loading due to its plasticizing effect in PLA foam matrix [46].

5.4 PLA- and Nanogum-Based Nanocomposite Foams

GA is a polysaccharide obtained from trees like *Acacia senegal* and *Acacia seyal*. It has some added advantages like non-toxicity, biodegradability, and easy availability as it comes from natural resources. GA has Generally Recognized as Safe (GRAS) certification by United States Food and Drug Administration (USFDA). A recent investigation on PLA/modified GA (MG)-based microcellular foam demonstrated that MG acts as a plasticizer in the PLA foam matrix due to the presence of oligomer. MG helps in the generation of smaller pores in the matrix. From the porosimetric investigation, an increase in cell density and a decrease in cell size in PLA foam have been reported. The hydrophobicity of PLA-based foam increases with the increase in MG due to the change in surface morphology of PLA foam. However, a decrease in thermostability and thermo-mechanical properties has been reported [47].

From the above discussion, it can be concluded that the bio-based nanofillers can be effectively used in the PLA foam matrix to improve various properties. The use of bionanofillers in PLA foam matrix leads to the opening of a wider window of applications in the field of tissue engineering and cell proliferation for PLA-based foam.

6 Other Bio-based Sustainable Foams

Apart from PLA-based foams, some important and useful bio-based sustainable foam includes starch foam, cellulose foam, polyvinyl alcohol (PVOH), PCL, and

ethylene vinyl alcohol (EVOH). Starch is the first developed biodegradable foam in the history of biopolymer foams. The starch foam was first developed in 1964 (US patent 3137592) and further modified as a hydrophobic porous starch foam in 1975 (US patent 3891624). Water-soluble PVOH foams were developed in 1992 (US Patent 5089535). The applications of these biodegradable sustainable foams are limited. The starch foam is mainly utilized in the food packaging industry. PVOH and EVOH are the two water-soluble foams mainly utilized in packaging, oxygen barrier, and multilayer packaging applications. The water solubility of these two foams makes it environmentally friendly in nature, and disposal after end life is very easy. PCL is also used in packaging applications, tissue engineering, high engineering advance application with the aid of various bio-based materials such as chitosan, cellulose, and others. The bio-based sustainable foams have some limitations in properties like low mechanical and thermal properties [48].

The improvement in the properties of these biopolymers is the current need. A wide range of applications needs to be investigated for these biopolymers. Among these biopolymer foams, starch attracts the scientific community due to its agricultural routes. As discussed in the earlier section, improvements in PLA-based foams can be carried out using starch as an additive. Starch foam has the capability to compete with PS foam in the loose-fill market. Biodegradable Green Cell[®] foam (GCF) can be fabricated from the proprietary corn–starch blend [49]. It is mainly targeted for protective packaging applications. Starch foam is already an established player in the loose-fill global market. Starch-based packaging peanuts are made from crop-based sources and are non-toxic in nature. The biodegradable peanut for packaging brand, Biofoam, can be fabricated from grain sorghum. Starch-based loose-fill biodegradable peanuts are soluble in water, whereas PS-based loose-fill packaging is not soluble in water. Therefore, a significant research is required to improve the starch-based foam to make it comparable with PS-based foams. The improvements in the technology are required to overcome the drawbacks like higher weight, dust creation, high cost, and lower resilience of starch-based foams for different packaging applications. On the other hand, some important factors like life cycle analysis, testing, new processing technique, and proper disposal methodology need to be properly addressed for these bio-based polymer foams to make it more applicable and cost-effective in the near future.

References

1. Klempner D, Sendjarevic V, Aseeva RM (eds) (2004) Handbook of polymeric foams and foam technology. Hanser Verlag
2. Lee ST (2004) Introduction: polymeric foams, mechanisms, and materials. In: Polymeric foams. CRC Press, pp 15–29
3. Auras RA, Lim LT, Selke SE, Tsuji H (eds) (2011) Poly (lactic acid): synthesis, structures, properties, processing, and applications, vol 10. Wiley
4. Nofar M, Park CB (2014) Poly (lactic acid) foaming. *Prog Polym Sci* 39:1721–1741. <https://doi.org/10.1016/j.progpolymsci.2014.04.001>
5. Auras R, Harte B, Selke S (2004) An overview of polylactides as packaging materials. *Macromol Biosci* 4:835–864. <https://doi.org/10.1002/mabi.200400043>
6. Saucéau M, Fages J, Common A, Nikitine C, Rodier E (2011) New challenges in polymer foaming: a review of extrusion processes assisted by supercritical carbon dioxide. *Prog Polym Sci* 36:749–766. <https://doi.org/10.1016/j.progpolymsci.2010.12.004>
7. Mane S (2016) Effect of porogens (type and amount) on polymer porosity: a review. *Can Chem Trans* 4:210–225
8. Li S, Chen X, Li M (2010) Effect of some factors on fabrication of poly (L-lactic acid) microporous foams by thermally induced phase separation using N, N-dimethylacetamide as solvent. *Prep Biochem Biotechnol* 41:53–72. <https://doi.org/10.1080/10826068.2010.534222>
9. Tripathi N, Katiyar V (2016) PLA/functionalized-gum arabic based bionanocomposite films for high gas barrier applications. *J Appl Polym Sci* 133. <https://doi.org/10.1002/app.43458>
10. Dhar P, Tarafder D, Kumar A, Katiyar V (2015) Effect of cellulose nanocrystal polymorphs on mechanical, barrier and thermal properties of poly (lactic acid) based bionanocomposites. *RSC Adv* 5:60426–60440. <https://doi.org/10.1039/C5RA06840A>
11. Hwang SS, Hsu PP, Yeh JM, Chang KC, Lai YZ (2009) The mechanical/thermal properties of microcellular injection-molded poly-lactic-acid nanocomposites. *Polym Compos* 30:1625–1630. <https://doi.org/10.1002/pc.20736>
12. Ji G, Wang J, Zhai W, Lin D, Zheng W (2013) Tensile properties of microcellular poly (lactic acid) foams blown by compressed CO₂. *J Cell Plast* 49:101–117. <https://doi.org/10.1177/0021955X13477437>
13. Di Y, Iannace S, Di Maio E, Nicolais L (2005) Reactively modified poly (lactic acid): properties and foam processing. *Macromol Mater Eng* 290:1083–1090. <https://doi.org/10.1002/mame.200500115>
14. Ludwiczak J, Kozłowski M (2015) Foaming of polylactide in the presence of chain extender. *J Polym Environ* 23:137–142. <https://doi.org/10.1007/s10924-014-0658-7>
15. Zhou M, Zhou P, Xiong P, Qian X, Zheng H (2015) Crystallization, rheology and foam morphology of branched PLA prepared by novel type of chain extender. *Macromol Res* 23:231–236. <https://doi.org/10.1007/s13233-015-3018-0>
16. Zhou C, Ma L, Li W, Yao D (2011) Fabrication of tissue engineering scaffolds through solid-state foaming of immiscible polymer blends. *Biofabrication* 3:045003
17. Ma L, Jiang W, Li W (2014) Solvent-free fabrication of tissue engineering scaffolds with immiscible polymer blends. *Int J Polym Mater Polym Biomater* 63:510–517. <https://doi.org/10.1080/00914037.2013.854222>
18. Ameli A, Nofar M, Jahani D, Rizvi G, Park CB (2015) Development of high void fraction polylactide composite foams using injection molding: crystallization and foaming behaviors. *Chem Eng J* 262:78–87. <https://doi.org/10.1016/j.cej.2014.09.087>
19. Wang J, Zhu W, Zhang H, Park CB (2012) Continuous processing of low-density, microcellular poly (lactic acid) foams with controlled cell morphology and crystallinity. *Chem Eng Sci* 75:390–399. <https://doi.org/10.1016/j.ces.2012.02.051>
20. Matuana LM, Faruk O, Diaz CA (2009) Cell morphology of extrusion foamed poly (lactic acid) using endothermic chemical foaming agent. *Bioresour Technol* 100:5947–5954. <https://doi.org/10.1016/j.biortech.2009.06.063>

21. Lee SY, Hanna MA (2008) Preparation and characterization of tapioca starch-poly (lactic acid)-Cloisite NA⁺ nanocomposite foams. *J Appl Polym Sci* 110(4):2337–2344. <https://doi.org/10.1002/app.27730>
22. Hao A, Geng Y, Xu Q, Lu Z, Yu L (2008) Study of different effects on foaming process of biodegradable PLA/starch composites in supercritical/compressed carbon dioxide. *J Appl Polym Sci* 109:2679–2686. <https://doi.org/10.1002/app.27861>
23. Preechawong D, Peesan M, Supaphol P, Rujiravanit R (2005) Preparation and characterization of starch/poly (L-lactic acid) hybrid foams. *Carbohydr Polym* 59:329–337. <https://doi.org/10.1016/j.carbpol.2004.10.003>
24. Mihai M, Huneault MA, Favis BD, Li H (2007) Extrusion foaming of semi-crystalline PLA and PLA/thermoplastic starch blends. *Macromol Biosci* 7:907–920. <https://doi.org/10.1002/mabi.200700080>
25. Yuan H, Liu Z, Ren J (2009) Preparation, characterization, and foaming behavior of poly (lactic acid)/poly (butylene adipate-co-butylene terephthalate) blend. *Polym Eng Sci* 49:1004–1012. <https://doi.org/10.1002/pen.21287>
26. Pilla S, Kim SG, Auer GK, Gong S, Park CB (2010) Microcellular extrusion foaming of poly (lactide)/poly (butylene adipate-co-terephthalate) blends. *Mater Sci Eng C* 30:255–262. <https://doi.org/10.1016/j.msec.2009.10.010>
27. Zhao H, Cui Z, Sun X, Turng LS, Peng X (2013) Morphology and properties of injection molded solid and microcellular polylactic acid/polyhydroxybutyrate-valerate (PLA/PHBV) blends. *Ind Eng Chem Res* 52:2569–2581. <https://doi.org/10.1021/ie301573y>
28. Pilla S, Kramschuster A, Lee J, Auer GK, Gong S, Turng LS (2009) Microcellular and solid polylactide–flax fiber composites. *Compos Interfaces* 16:869–890. <https://doi.org/10.1163/092764409X12477467990283>
29. Jia P, Hu J, Zhai W, Duan Y, Zhang J, Han C (2015) Cell morphology and improved heat resistance of microcellular poly (L-lactide) foam via introducing stereocomplex crystallites of PLA. *Ind Eng Chem Res* 54:2476–2488. <https://doi.org/10.1021/ie504345y>
30. Wang J, Ren Q, Zheng W, Zhai W (2014) Improved flame-retardant properties of poly (lactic acid) foams using starch as a natural charring agent. *Ind Eng Chem Res* 53:1422–1430. <https://doi.org/10.1021/ie403041h>
31. Pilla S, Kramschuster A, Lee J, Clemons C, Gong S, Turng LS (2010) Microcellular processing of polylactide–hyperbranched polyester–nanoclay composites. *J Mater Sci* 45:2732–2746. <https://doi.org/10.1007/s10853-010-4261-6>
32. Fujimoto Y, Ray SS, Okamoto M, Ogami A, Yamada K, Ueda K (2003) Well-controlled biodegradable nanocomposite foams: from microcellular to nanocellular. *Macromol Rapid Commun* 24:457–461. <https://doi.org/10.1002/marc.200390068>
33. Ema Y, Ikeya M, Okamoto M (2006) Foam processing and cellular structure of polylactide-based nanocomposites. *Polymer* 47:5350–5359. <https://doi.org/10.1016/j.polymer.2006.05.050>
34. Bitou M, Okamoto M (2008) Fabrication of porous 3-D structure from poly (L-lactide)-based nano-composite foams. Effect of foam structure on enzymatic degradation. *Polym Degrad Stab* 93:1081–1087. <https://doi.org/10.1016/j.polymdegradstab.2008.03.014>
35. Kang DJ, Xu D, Zhang ZX, Pal K, Bang DS, Kim JK (2009) Well-controlled microcellular biodegradable PLA/silk composite foams using supercritical CO₂. *Macromol Mater Eng* 294:620–624. <https://doi.org/10.1002/mame.200900103>
36. Qiu Y, Lv Q, Wu D, Xie W, Peng S, Lan R, Xie H (2018) Cyclic tensile properties of the polylactide nanocomposite foams containing cellulose nanocrystals. *Cellulose* 25:1795–1807. <https://doi.org/10.1007/s10570-018-1703-9>
37. Dlouhá J, Suryanegara L, Yano H (2014) Cellulose nanofibre–poly (lactic acid) microcellular foams exhibiting high tensile toughness. *React Funct Polym* 85:201–207. <https://doi.org/10.1016/j.reactfunctpolym.2014.07.016>
38. Cho SY, Park HH, Yun YS, Jin HJ (2013) Influence of cellulose nanofibers on the morphology and physical properties of poly (lactic acid) foaming by supercritical carbon dioxide. *Macromol Res* 21:529–533. <https://doi.org/10.1007/s13233-013-1057-y>

39. Dlouhá J, Suryanegara L, Yano H (2012) The role of cellulose nanofibres in supercritical foaming of polylactic acid and their effect on the foam morphology. *Soft Matter* 8:8704–8713. <https://doi.org/10.1039/C2SM25909E>
40. Borkotoky SS, Dhar P, Katiyar V (2018) Biodegradable poly (lactic acid)/cellulose nanocrystals (CNCs) composite microcellular foam: effect of nanofillers on foam cellular morphology, thermal and wettability behavior. *Int J Biol Macromol* 106:433–446. <https://doi.org/10.1016/j.ijbiomac.2017.08.036>
41. Borkotoky SS, Chakraborty G, Katiyar V (2018) Thermal degradation behaviour and crystallization kinetics of poly (lactic acid) and cellulose nanocrystals (CNC) based microcellular composite foams. *Int J Biol Macromol* 118:1518–1531. <https://doi.org/10.1016/j.ijbiomac.2018.06.202>
42. Niu X, Feng Q, Wang M, Guo X, Zheng Q (2009) In vitro degradation and release behavior of porous poly (lactic acid) scaffolds containing chitosan microspheres as a carrier for BMP-2-derived synthetic peptide. *Polym Degrad Stab* 94:176–182. <https://doi.org/10.1016/j.polymdegradstab.2008.11.008>
43. Sahoo SK, Panda AK, Labhassetwar V (2005) Characterization of porous PLGA/PLA microparticles as a scaffold for three dimensional growth of breast cancer cells. *Biomacromolecules* 6:1132–1139. <https://doi.org/10.1021/bm0492632>
44. Jiao Y, Liu Z, Zhou C (2007) Fabrication and characterization of PLLA–chitosan hybrid scaffolds with improved cell compatibility. *J Biomed Mater Res A* 80:820–825. <https://doi.org/10.1002/jbm.a.31061>
45. Zhang Z, Cui H (2012) Biodegradability and biocompatibility study of poly (chitosan-g-lactic acid) scaffolds. *Molecules* 17:3243–3258. <https://doi.org/10.3390/molecules17033243>
46. Borkotoky SS, Pal AK, Katiyar V (2019) Poly (lactic acid)/modified chitosan-based microcellular foams: thermal and crystallization behavior with wettability and porosimetric investigations. *J Appl Polym Sci* 136:47236. <https://doi.org/10.1002/app.47236>
47. Borkotoky SS, Ghosh T, Bhagabati P, Katiyar V (2019) Poly (lactic acid)/modified gum arabic (MG) based microcellular composite foam: effect of MG on foam properties, thermal and crystallization behavior. *Int J Biol Macromol* 125:159–170. <https://doi.org/10.1016/j.ijbiomac.2018.11.257>
48. Ramesh NS, Lee S, Park CB (2007) Polymeric foams: science and technology
49. Arif S, Burgess G, Narayan R, Harte B (2007) Evaluation of a biodegradable foam for protective packaging applications. *Packag Technol Sci* 20:413–419. <https://doi.org/10.1002/pts.770>

Chapter 13

Biodegradable Copolyester-Based Natural Fibers–Polymer Composites: Morphological, Mechanical, and Degradation Behavior



Jyoti Giri and Rameshwar Adhikari

Abstract Random disposal and accumulation of commodity plastics in the open environment after their end use is an issue that has triggered a lot of concerns both in public and academic debates owing to their seemingly high contribution toward the environmental pollution and potential impacts on biota and human health. Thus, finding the greener solution to this problem has got immense socio-economic and ecological significance. As a result, there is an increasing trend of using biodegradable or compostable polymeric materials. It has been demonstrated that the incorporation of plants-based reinforcing fillers into biodegradable polymers to construct composite materials have proved benefits in various applications. A great deal of research has been performed in order to develop novel sustainable polymeric materials having tailored physical properties over a wide range. As a consequence, by using bio-based fillers, new composite materials have been developed and commercialized. In this chapter, initially, the attention will be made on the review of different methods of extracting microcrystalline (MCC) and nanocrystalline (NCC) celluloses from different agro-based wastes using a series of thermo-mechanical and chemical processing routes. After a quick review on the structure-properties correlation of the micro- and nanocomposites of copolyesters, we shed light on biodegradable *green* composites with special emphasis on their morphological studies and correlations to deformation and degradation behavior. On the ground of the results obtained from our laboratory complemented by literature works, the structure-property correlations of copolyester-based composites have been discussed. Finally, the chapter concludes highlighting the new trends, major challenges, and opportunities relevant to the related research field.

J. Giri · R. Adhikari (✉)

Central Department of Chemistry, Tribhuvan University, Kathmandu, Nepal
e-mail: nepalpolymer@yahoo.com

J. Giri

Department of Chemistry, Tri-Chandra Multiple Campus, Tribhuvan University, Kathmandu, Nepal

R. Adhikari

Research Centre for Applied Science and Technology, Tribhuvan University, Kathmandu, Nepal

Keywords Biodegradable polymer · Copolyester · Microcrystalline cellulose (MCC) · Nanocrystalline cellulose (NCC) · Gel permeation chromatography (GPC)

1 Introduction

One of the recent trends in materials science and engineering is to use polymers in different high-tech applications taking into account for their safe disposal after use. Polymers are being used extensively from the very early days of twentieth century, and nowadays, we can hardly imagine any fields in everyday life where the polymers are completely absent [1–6].

As most of the synthetic polymers we use today originate from raw materials based on fossil fuels, which is going to be used up quite quickly that, in the near future, we would not have alternative sources. Therefore, we need to think about the alternatives of synthetic polymers and at the same time, think for the lesser use of the polymers introducing enhanced functionality and recyclability into the conventional polymers [1, 6]. Nowadays, scientists are trying to develop renewable resources-based fillers such as microcrystalline cellulose (MCC), nanocrystalline cellulose (NCC), hemicelluloses, lignin, chitosan, proteins as well as the inorganic fillers, namely layered silicates, silica, calcium carbonate, carbon black, graphene, multiwalled carbon nanotube (MWCNT), etc. [2–13]. Depending upon the nature and compatibility of the fillers with polymers, the property of the composite materials can be modulated. Such composites find applications in aerospace engineering, medical devices, tissue engineering, and in designing the smart drug delivery systems [10, 14–21].

Moreover, inorganic fillers used in polymer composites on disposal after their utility into the open environment usually may give hazardous impacts to life. Many of them are toxic for living beings human health as the chemicals used for compatibilization as well as for fire retardancy (such as brominated polystyrene, tetrabromophthalic anhydride, and decabromophenyl oxide) are proved to pose threat to the natural environment [22, 23].

As an alternative, the greener methods have been introduced by using regenerated natural resources (such as cellulosic fibers) which give similar or even more advanced properties than the reinforcement effects in the conventional composites with inorganic fillers [3, 10]. It has been known that the cellulose fibers are stronger than several mineral-based fibers, have a high volume-to-weight ratio, and can be easily dispersed homogeneously into polymer matrices via common processing techniques [4, 7]. On the other hand, the renewable resources have the advantages of being inexpensive, regenerative, and local availability [2, 4, 8]. These may reduce significantly the use of fossil fuel by-products and promote green economy and smart materials development [17, 24–26].

Thus, the bio-based and biodegradable plastics are emerging as reliable alternatives to conventional commodity plastics [27, 28]. Several of them, however, have generally the problem of poor mechanical properties, difficulty in tuning crystallization behavior, high manufacturing costs, and reduced ease of processing. Currently,

biodegradable polyesters such as polybutylene adipate-*co*-terephthalate (PBAT), polyethylene terephthalate (PET), polylactic acid (PLA), polybutylene succinate (PBS), polycaprolactone (PCL), and polyglycolic acid (PGA) are being investigated [8–11, 25]. Among them, completely biodegradable blends and composites based on PBAT, PCL, PLA, and PHB are becoming quite popular [27–29]. Irrespective of the materials chosen for technical applications, it is a key issue to control the morphological details of the material at different length scales to design the tailored properties profile [10, 13, 25, 27]. As a consequence, a comprehensive understanding of the correlation between morphology, mechanical properties, and degradation behavior of such systems is required.

This chapter aims at discussing the structure and properties of a biodegradable copolyester-based composite materials with special attention to their mechanical, morphological, and biodegradation behavior. A brief introduction about the filler preparation and corresponding characterization techniques will be followed by an overview of natural fibers-based polymer composites. Then, the detailed discussion on the structure-properties correlation of the copolyester–natural fibers composites will be presented. The degradation behavior of the composites under soil burial condition will be discussed with an emphasis on molecular weight reduction and degradation mechanism. Finally, the chapter will be concluded highlighting some new trends and challenges in developing completely biodegradable and compostable composite materials.

2 Preparation and Characterization Techniques

The preparation of fillers for composites fabrication and the characterization of polymer interface as well as the morphology of the composite are some important aspects of tailoring the properties profile of the materials.

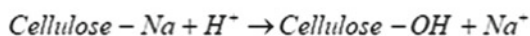
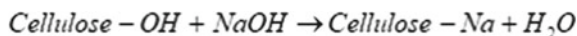
2.1 Preparation of Micro-and Nanocrystalline Cellulose

The common sources of MCC and NCC are the plant-based natural fibers such as sisal [30, 31], kenaf [32, 33], castor oil plant [34], bamboo [35–37], jute [2], pineapple leaf [38], cotton [39, 40], and ramie [41]. There are many processes to extract MCC and NCC from the bioresources which can broadly be classified as chemical, mechanical, and bacterial ones [5, 42–45].

2.1.1 Chemical Method

After preliminary treatments such as washing, drying, chopping, pulverizing, and sieving, the raw plant fibers are subjected to strong alkali treatment. The process is

Scheme 1 Mercerization of cellulose fiber with NaOH followed by acid treatments to microfibrillate the cellulose macrofibers [35]



Scheme 2 Oxidative bleaching of cellulose microfibers by sodium hypochlorite (NaClO) solution for synthesis of white crystalline MCC [6]



called as *mercerization* and causes the fibers to undergo fibrillation and delignification [35, 38]. Usually, alkali solutions used for this process are from caustic soda or caustic potash [38, 46] whereby the optimization of alkali concentration and processing temperature are important issues to consider [47]. The *mercerization* further involves the addition of Na⁺ groups into the cellulosic molecular segments which can later be removed by treating with acids (Scheme 1) [35]. The treatment with acids such as (COOH)₂, HCOOH, CH₃COOH, dilute H₂SO₄, and HCl also acts to dissolve the amorphous regions in the cellulose [48].

The raw fibers are converted to white shining crystals on bleaching with chemicals such as NaClO, NaCl, NaClO₃, NaClO₂, and H₂O₂. These usually produce nascent chlorine or oxygen to bleach the fibers and at the same time also dissolve hemicelluloses and amorphous regions exposing neat cellulose crystallites [6, 38, 46, 49–52]. Scheme 2, for instance, shows the bleaching action of the NaClO.

Cellulose fibers then easily give rise to the production of MCC. Further disintegration into the nanosized crystals can be achieved by controlled hydrolysis with strong acids under constant and vigorous stirring and sonication. The chemical disintegration is quite challenging in term of purification of the cellulosic fiber as a lot of mass loss may occur. Acid treatments leading to the formation of the NCC have been reported by several authors [53–55] by variation of acid concentration, time of treatment, temperature, and freeze-drying procedures. As a result, the NCC crystalline aggregates having several tens of nanometers width and up to several hundred nanometer lengths can be obtained.

2.1.2 Mechanical Method

(a) Compression and roller mechanical technique

In compression mechanical method, cellulosic fibers are placed between beds of two metal plates at high force of 10 ton for 10 s, whereas in roller mechanical technique, fibers are passed between two rollers in which one is mobile while the other is fixed. These techniques were used to fibrillate wood dust and corn stover into cellulose nanofibers [54, 55].

(b) Homogenization

In this technique, cellulose fibers are passed through a narrow valve at very high pressure and released suddenly to normal pressure which acts as the shear force to

explode the inner fibers. The basic concept of this technique is to release all binding forces initially applied to the nanofibers while forming macroscopic fibers. Usually raw and mercerized fibers are employed for homogenization. This technique was used for nanofibrillation of hard and softwood pulps, banana peels, and sugar cane baggage [45, 46, 56, 57].

(c) *Ultrasonication*

Ultrasonication is an electro-mechanical process of disintegrating macrocellulose into the NCC. Sound energy of more than 20 kHz is used to agitate particles present in the aqueous cellulose suspension which leads to the microscopic disintegration followed by breakage of intermolecular bonds [49, 58]. Besides the energy of the ultrasonic waves, the treatment time, temperature, and presence of impurities can significantly alter the yield, morphology, and hence the properties of the NCC.

2.1.3 Bacterial Synthesis

One of the most important features of the bacterial cellulose is its chemical purity, which distinguishes it from the cellulose extracted from higher plants, usually associated with hemicelluloses and lignin, removal of which involves several steps. Due to their unique ultra-fine and uniformly reticulated structure, the bacterial nanocellulose find wide applications in paper, textile, food, and cosmetics industries as well as in tissue engineering and medicine [59].

Bacteria such as *Acetobacter xylinus*, *Rhizobium*, *Agrobacterium*, *Escherichia coli*, and *Sarcina* have been found to biosynthesize cellulose nanofibers with highly crystalline texture [60, 61]. Further, NCC and MCC fibrils can be synthesized by bacteria in the presence of glucose, oxygen, nitrogen, and micronutrients. In this process, various carbon compounds in the nutrition media are utilized by the microorganisms to polymerize their molecules into a single, linear β -1, 4-glucan chains and secrete outside the bacterial cell. First, nascent β -1,4-glucan chains are produced. Then, a number of such chains combine to form interwoven microfibrils to give a thick gelatinized network of the fibers [59]. The amount and nature of bacterial cellulose production vary, besides the nature of the microorganisms with the type of carbon sources (such as glucose, mannitol, glycerol, fructose, sucrose, and galactose) [62].

2.2 Preparation of Polymer Composites

There is a vast number of references available for fabrication of polymer composites involving biodegradable polymers and natural fibers. In brief, the common processing route involves the physical mixing of the components in a drum, followed by agitation inside an internal mixture under inert atmosphere and palletization. The samples fabricated during melt compounding of the pellets are then subjected to molding

by various means such as compression, blowing, casting, injection and spinning, calendaring, blowing, and printing [4, 6–9, 11, 13, 14, 25, 35, 36, 41].

2.3 Characterization Techniques

There are wide varieties of techniques that characterize the specific properties of the polymeric materials. The choice of the techniques depends primarily on the nature of the properties that are relevant for the particular application. For the degradable materials intended for packaging, insulation and other low load-bearing fabrications, the stability against thermal and mechanical stress as well as the structural details linked to those properties are of particular interest. In this section, we briefly highlight the techniques used for such characterizations. For the detailed information on those issues, the readers are referred to specific monographs and reviews [63–68].

2.3.1 Structural Characterization by Microscopy

Morphological characterization of materials is generally performed by microscopic (optical as well as electron microscopy) and X-ray diffraction techniques. These methods provide a wide range of information on different length scales. The structural details of fibers and polymer composites ranging from a few Angstroms up to over 100 mm can be evaluated by these tools [7] (Fig. 1).

The optical microscopy (OM) offers the overview imaging of the microscopic structures which are a few microns up to a few millimeters in dimension. Polarizing

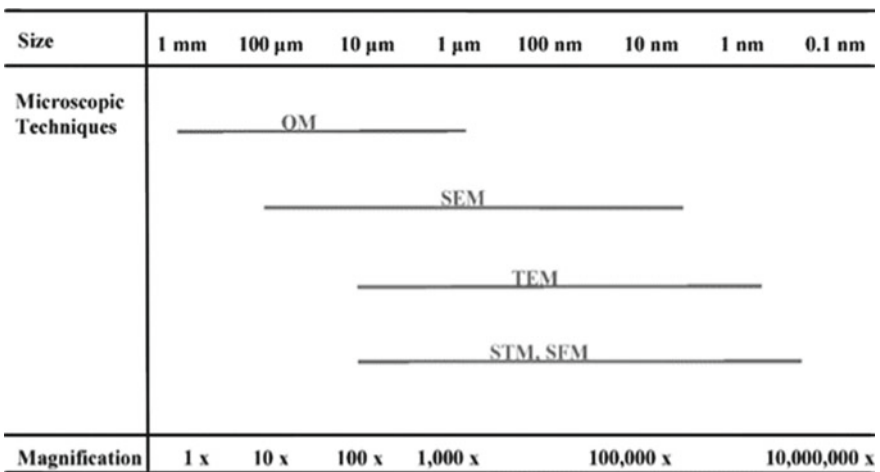


Fig. 1 Resolution ability of different microscopic tools [69]

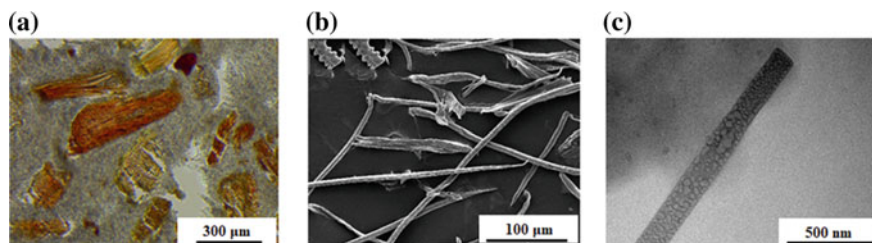


Fig. 2 Micrographs showing morphology of natural fibers at different length scales: **a** optical photograph of the fibers embedded in a polymer matrix, **b** microcrystalline cellulose (MCC), and **c** nanocrystalline cellulose obtained from the MCC [71]

optical microscopy (POM) gives, in most cases, the clear idea about the microscopic dimension as well as information about the structural heterogeneity of the materials including macroscopic crystalline textures [66, 70].

Scanning electron microscopy (SEM) [6, 71–74] and transmission electron microscopy (TEM) [56, 71, 74–76] offer the resolution of up to individual nanofibers illuminating the insight into the polymer–fiber interface. The SPM including scanning tunneling microscopy (STM) and scanning force microscopy (SFM) can easily go into atomic resolution domain of materials characterizations [62–68]. Thus, it can be easily followed that the scanning probe techniques and electron microscopy (EM) possess the central position among the modern nanoscale characterization tools for detailed characterization of the polymeric materials.

As illustration, Fig. 2 shows the morphology of cellulosic fibers on different length scales as observed by POM, SEM, and TEM. The overview of the natural fibers along the longitudinal axes is presented in Fig. 2a in which the grayscale of birefringence in the fiber surface represents the crystalline texture of the fibers. The field emission SEM imaging of the chemically processed MCC fibers illustrated in Fig. 2b depicts quite uniformly distributed cellulosic fibers while the micrograph in Fig. 2c shows the structure of individual nanofiber obtained from the same stuff as presented in Fig. 2b via strong acid treatment [71]. It should be, nevertheless, admitted that the information obtained by microscopic tools is limited to very local structural details. For more integral structural details of the materials, diffraction and spectroscopic techniques are required.

2.3.2 X-Ray Diffraction and Spectroscopic Characterization

Many polymeric materials, including natural polymers and fibers, are semicrystalline in nature and their crystalline behavior can be well revealed by X-ray diffraction (XRD). In this method, the intensity of the peaks along with the 2θ values precisely signifies the crystalline behavior. The diffractogram can be used to calculate the crystallinity index, determine the nature of crystals as well as quantify the d-spacing (practically the distance between two crystalline layers) [66, 77, 78]. The crystallinity

index can be calculated as [77]:

$$\text{Crystallinity index (\%)} = \frac{I_{200} - I_{\text{am}}}{I_{200}} \times 100\%$$

where

I_{200} Intensity value for crystalline cellulose, and
 I_{am} intensity value for amorphous cellulose.

It can be concluded that the cellulosic fibers depict the crystalline peaks at the 2θ values between 12° and 25° of the diffractogram [38, 46, 71, 79, 80]. For instance, the XRD patterns of banana peel MCC fibers obtained by a series of mechano-chemical processing steps are presented in Fig. 3. The size of the nanocrystals was manipulated by allowing the cellulosic nanomaterial through the homogenizer for 3, 5 and 7 times which resulted in the decrease of the particle size in the same order (which have been designated as N3, N5, N7, respectively in Fig. 2 [46]. The figure shows an increasing trend of the crystallinity on decreasing the particle size of NCC.

In the similar manner, the crystallization behavior of polymers and composites with natural fibers can be determined by XRD [81, 82]. The method allows the observation of influence of filler incorporation in nucleation of crystalline phases, of the polymer matrix.

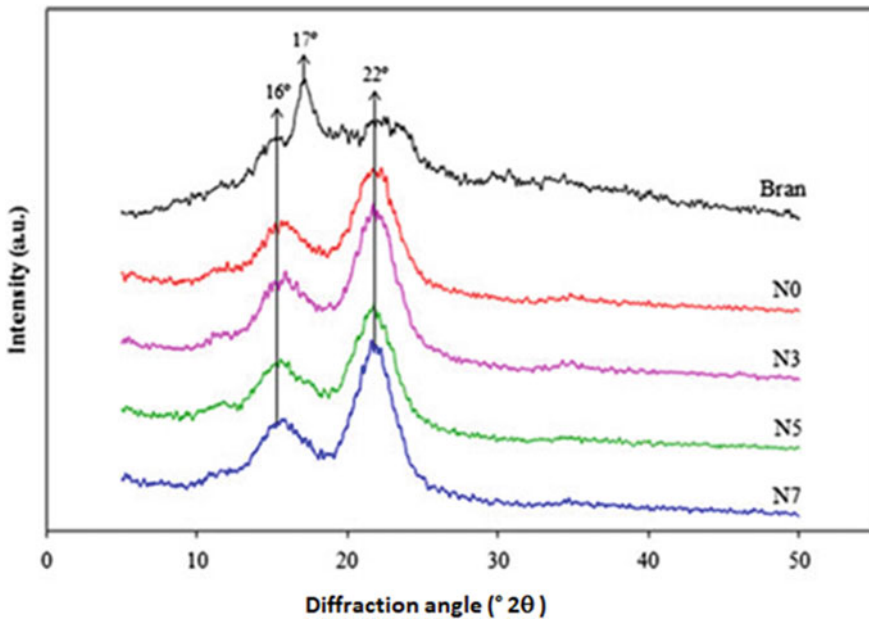


Fig. 3 XRD patterns for banana peel (Bran), NCC (N0) and the NCC passing through homogenizer for 3 (N3), 5 (N5) 7 (N7) times [46]

Spectroscopic techniques such as Fourier transform infrared (FTIR), Raman, and X-ray photoelectron spectroscopy (XPS) can be utilized in order to access molecular-level information on the interaction between different phases, nature of the interface, etc. In particular, in FTIR spectra, the spectral positions on wavenumber scale are directly linked to different functional groups and thus may signify the interaction at the interfacial region. The information can be later linked with the resulting physico-chemical properties of the materials [36, 83–85].

We illustrate the application of spectroscopy in characterization of polymer composites comprising biodegradable copolyester, the PBAT, and 5 wt% each of micro-(M5) and nanocrystalline (N5) celluloses, see Fig. 4. Let us first examine the peaks corresponding to the copolyester. The small peaks located at $1460\text{--}1354\text{ cm}^{-1}$ [86] give IR absorption for vibrational stretching of C–H bond in the CH_3 group of PBAT. Moreover, the peak at 1099 cm^{-1} indicates the presence of C–O–C stretching vibration of the ester bond of the PBAT. Similarly, the peak centered at 723 cm^{-1} represents the aromatic ring present in the polymer [87].

Figure 4 further shows the absorption spectra of the M-5 composites which are exactly similar in pattern as of the PBAT [85]. The PBAT, M-5, and N-5 all show absorption peaks at $2959\text{--}2845\text{ cm}^{-1}$ (corresponding to C–H stretching) [32, 88], the

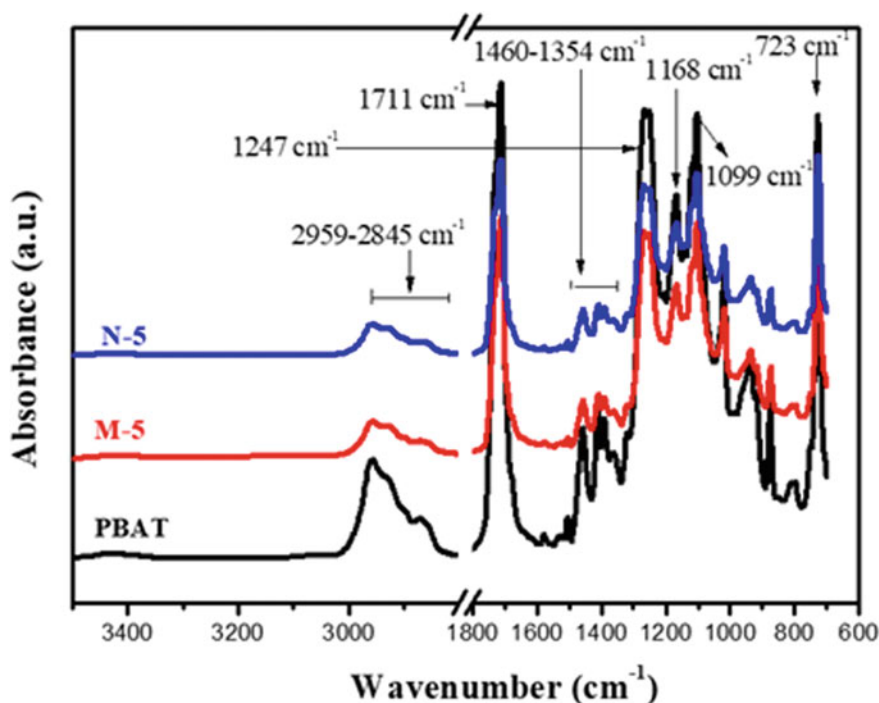


Fig. 4 FTIR absorption spectra of the PBAT compared to that of M-5 and N-5 composites [85]

intense peak at 1711 cm^{-1} (representing C=O stretching), and another intense peak at 1247 cm^{-1} (corresponding to C–O stretching of carbonyl group) [47, 85, 89].

In the spectra of the composites surfaces, there are no peaks corresponding to the MCC and the NCC. The presence of the only peaks corresponding to the PBAT in both the composites indicates the dominance of PBAT toward the surface of the composite films. The FTIR spectra further illustrate that, in spite of good compatibility between MCC as well as NCC with the PBAT, there is no significant bonding of chemical nature, also supporting the notion of microscopic results [85]. In brief, the spectroscopic data act as signature for chemical identity of the materials also illustrating the presence of any chemical interaction in the interfacial region and preference of any components toward the surface.

2.3.3 Mechanical, Thermal, and Degradation Behavior

Mechanical properties of polymeric materials and fibers can be determined by different methods such as tensile as well as compression, impact, and dynamic mechanical testing [68]. On the other hand, thermal and degradation behavior can be measured by various techniques as well [67]. These measurements not only provide the materials specific properties profile of the substances but also record the signature of various chemical treatments and interfacial modifications. Here, we present as an example of the effect of micro- and nanofibrillation of the cellulosic fibers on their thermostability [85].

The plot in Fig. 5 illustrates of thermogravimetric analysis of MCC and NCC [85]. Both show two-step degradation processes. The MCC shows an initial weight loss of up to 7% at around $120\text{ }^{\circ}\text{C}$ which corresponds to the removal of water and other volatile substances. The MCC itself starts to degrade at $225\text{ }^{\circ}\text{C}$, the major degradation occurring at T_{max} of $373\text{ }^{\circ}\text{C}$. The complete thermal degradation of the MCC takes place at around $400\text{ }^{\circ}\text{C}$ [85].

Similarly, NCC losses its weight by 10% due to the removal of water and other volatile substances at around $120\text{ }^{\circ}\text{C}$ while its degradation starts at $231\text{ }^{\circ}\text{C}$ followed by the major degradation occurring at T_{max} of $300\text{ }^{\circ}\text{C}$. The complete degradation of the NCC occurs at $408\text{ }^{\circ}\text{C}$ leaving the residual mass of 22.16% in the form of char after combustion at $600\text{ }^{\circ}\text{C}$. Thus, on comparing thermal behavior, one can observe that the MCC is found to be more thermally stable than the NCC [85].

Thus, the thermogravimetric measurements allow the comparison of the thermostability of the materials at hand, irrespective of whether the materials are the natural fibers or their blends or the composites with polymers.

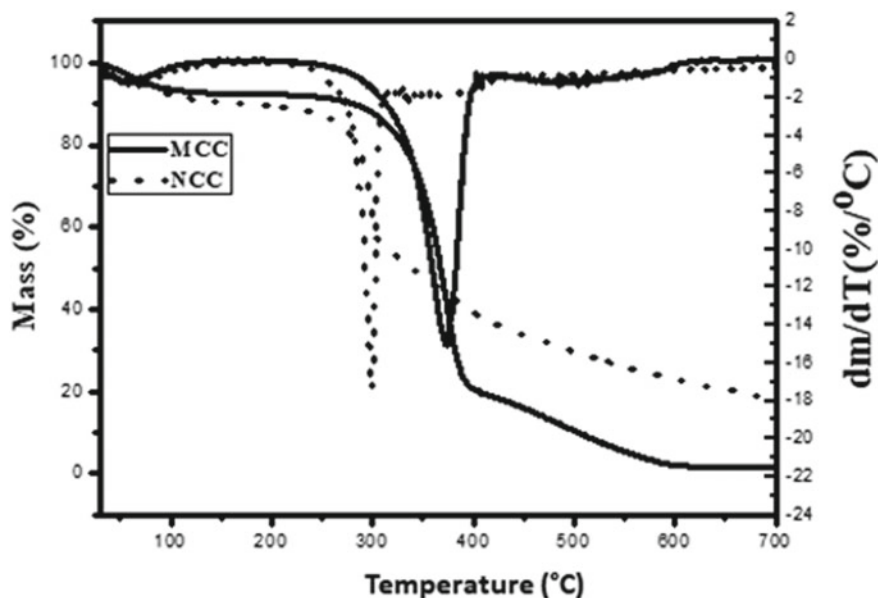


Fig. 5 TGA thermograms of MCC and NCC extracted from WS [85]

3 Natural Fibers and Degradable *Green* Composites

3.1 Natural Fiber Composites

It has been pointed out that the common fillers of both scientific and economic interests have been derived from wood flour [90–96], rice husks [96, 97], and other natural resources such as flax, sisal, kenaf, kraft, and jute. [98–101]. Particular attention has been paid in many previous studies on the use of agricultural and carpentry wastes (such as rice husks, cotton rests, and saw dusts. [90–92, 102]) as reinforcing filler to prepare the novel composite materials. A large volume of scientific data concerning the processing, properties, and morphological aspects of natural fillers in polyolefins [91, 102], polyesters [103], and thermosetting resins [104] can be found in the literature. Aiming at the study of the thermal, mechanical, and morphological properties of the composites of commodity plastics such as polypropylene (PP) and polyethylene (PE), the former was blended with carpentry waste of the wood *Shorea robusta* and investigated for morphological, mechanical, and thermal properties of the composites [105]. The morphological results are presented in Fig. 6.

Figure 6a is the SEM image of fracture surface of neat PP/60 wt% wood flour composite. There are sharp ridges at the interfacial region, formed by incompatibility between the components [105]. Figure 6b presents the SEM micrographs of the corresponding sample as presented in Fig. 6a but containing 5 wt% maleic anhydrides grafted PP (PP-g-MA) as a compatibilizer in the polypropylene matrix. The fracture

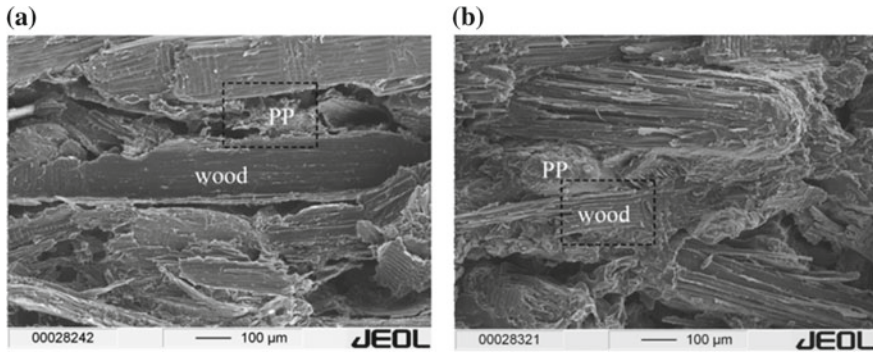


Fig. 6 SEM images of composites containing 60 wt% wood flour in PP matrix; **a** no compatibilizer and **b** with compatibilizer [105]

surface morphology of the composite presented is quite similar to that presented in Fig. 6a with typical structures of the wood fibers and the surrounding polypropylene matrix. However, the wood structures in Fig. 6b appear rougher and have no cracks at the boundaries with the matrix. The filler particles further keep their basic morphology, but exhibit coarser surface textures implying the presence of good bonding between the particles and matrix [105].

Such morphological behavior is typical of hydrophobic polymers with hydrophilic natural fibers. There is generally a clear indication of role of compatibilizers in the morphological properties of the composites [10].

The results so far outlined in this section help to illustrate the basic morphology of natural fibers composites and the effect of compatibilizer on morphology and thus on resulting properties of the materials [105]. The presence of natural fibers in contact with commodity plastics may facilitate the weathering process of the polymer. However, it should be kept in mind that these composites are unable to spontaneously biodegrade. In the next section, the structure and properties of some completely degradable composite materials will be illuminated.

3.2 Degradable Polymer Composites

Biodegradable polyesters and copolyesters [30, 106–108] have been recently used as a matrix to prepare new materials. Among the biodegradable polymers, PLA and polybutylene succinate (PBS), aliphatic–aromatic copolyesters, etc., have got particular commercial attention due mainly to their biodegradability and sustainability [28, 29, 36, 52].

Thus, aiming at the development of completely biodegradable composite materials based on locally available low-cost bamboo flour (BF) as filler, structure-properties correlations in the composites of the aliphatic–aromatic copolyester (a commercial

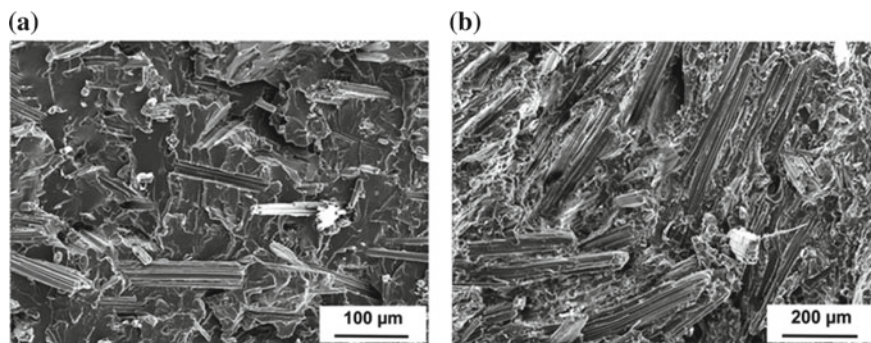


Fig. 7 Scanning electron micrographs of the Ecoflex/BF composites: **a** 20 wt% BF and **b** 60 wt% BF; cryo-fractured surface of the specimens [36]

product, the PBAT, called as Ecoflex) and BF were studied. For instance, the SEM micrographs of the fracture surfaces of two different composites (having 20 and 60 wt% of alkali-treated bamboo flour) are presented in Fig. 7 [36].

In the composites with 20 wt% BF (Fig. 7a), both the matrix and filler can be easily recognized. At several locations, BF which have been pulled-out from the matrix can be observed. Also, the holes formed by the pulled-out fibers are visible on the micrographs [36].

At high BF content, the matrix fraction practically disappears on the micrographs as it functions only as binding materials for the BF. In the composite with 60 wt% BF (Fig. 7b), the fibers are as randomly and uniformly distributed as in the case of low filler content composite. The fibers have no preferential orientation. It is indeed very interesting to note that a very large amount of BFs can be dispersed into the polymer matrix without using any compatibilizer [36].

For gaining closer insight into the morphology of the Ecoflex/BF composites, the compression-molded samples were studied by wide-angle X-ray scattering (WAXS) using reflection modes which provided the information on the structure of materials on the surface as well as bulk of the specimens. The results are presented in Fig. 8 [36]. In the pure Ecoflex, several peaks corresponding to the semicrystalline framework of the matrix could be ascertained. The Ecoflex crystalline reflections of the composites observed at values of 2θ 17.3°, 20.2°, and 23° progressively disappeared, implying that the structure of the matrix was gradually destroyed by the presence of BFs. As a result, in the composites with 40% BF or more, the structure of the BFs predominated, and the diffractogram of cellulose appeared [36].

It was demonstrated that quite high amount of BF could be easily incorporated quite homogeneously into the biodegradable polymeric matrix. The filler weakly adhered to the matrix as demonstrated by the pulling-out of BFs on the electron micrographs, which was further attested by thermogravimetric analysis [36].

The tensile mechanical properties of Ecoflex/BF composites are presented in Fig. 9 [36]. The results illustrate that the pristine polymer exhibits large plastic deformation, accompanied by yielding, cold drawing, and strong strain-hardening

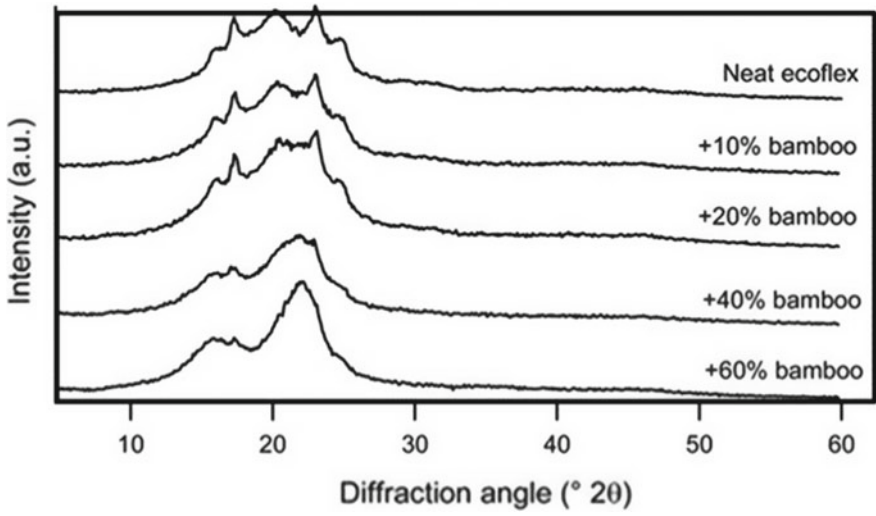


Fig. 8 WAXS patterns of Ecoflex/BF composites containing various amount of BFs recorded in reflection mode [36]

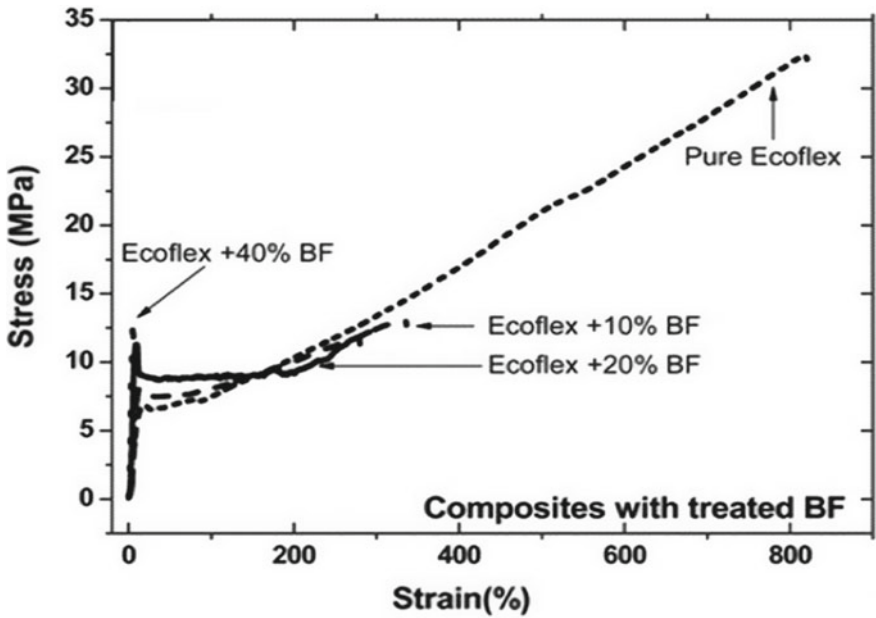


Fig. 9 Tensile stress–strain curves of Ecoflex/BF composites having various BF concentrations [36]

phenomena showing elongation at break of 800% and tensile strength of over 30 MPa. The addition of 20 wt% of the filler BF results in a drastic reduction in both strain at break and tensile strength. Nevertheless, the yield strength of the composites increases with filler content. The composites were thus reported for being suitable for low load-bearing applications [36].

In spite of the matrix being degradable, such materials (as the composites based on PLA, PHB, Ecoflex, etc.) may not be termed as completely degradable as the filler and matrix remain intact due to the presence of compatibilizers at the filler/matrix interface [30, 36, 103]. In the next section, we will deal with the composite materials using micro- and nanocrystalline celluloses derived from agricultural wastes and also shed light on the degradation behavior of such materials.

3.3 Completely Degradable Green Polymer Composites

The completely degradable *green* composites are those in which the polymers are derived from green sources. Besides, all the constituents of the composites must undergo degradation under soil composting conditions. Such composites are indeed the need of the present situation. Degradable polymers with aromatic ring usually do not go biodegradation or composting process as breakage of such ring needs high energy, and in the soil, there are no microbes which can enzymatically deteriorate the aromatic rings to convert the polymers into simpler forms [14]. Polymers containing simple hydrolysable chemical bonds (such as ester, ether bonds) get easily decomposed under soil burial conditions and attacked by microorganisms and minerals [30, 109]. Thus, PLA, PHA, PHBV, and their composites with bio-fillers such as MCC, NCC, starch, hydroxyapatite, lignin, chitin, and chitosan are used to prepare completely green composites [36, 83, 85]. These composites even due to the presence of the biogenic fillers undergo early degradation. There are many research reports on evaluating the effect of filler nature and duration of soil burial on the biodegradation of polymeric materials [2, 83, 85, 110–112].

3.3.1 Introduction to Biodegradation

Polymers comprise giant molecules which may undergo degradation when their bonds break. The later process can be induced by exposure of the materials to light (such as UV radiation), environmental weathering, and soil composting or microbial incubation [29, 42, 112–114].

Incubating the polymeric materials with specific microorganisms may break the macromolecules during their metabolic activity. The bacteria produce primary and secondary metabolites or some specific enzymes which have the capacity to break the stereospecific and stereoselective bonds. *Bacillus subtilis*, *Aspergillus niger*, *Streptococcus aureus*, *Candida*, and *E. Coli* are some of the organisms which are been proved as potential agents for degradation of polymeric materials [16, 78, 109,

113–115]. Besides the nature of microbes, the types, and dimension of biogenic filler and the surrounding environment in terms of pH, temperature, and presence of different ions affect the degradation process [62, 70, 87, 90, 94, 109, 110, 116, 117].

Soil offers a natural environment in the upper layer of earth crust the habitat for different organisms such as bacteria, virus, fungi, insect, small rodents, reptile, and mammals. Usually, we expect the good degradation process when the soil contains a large population of microorganisms, acidity and the corrosive minerals contents [27–29].

Turning toward the renewable flora-based resource of the nature, either from agriculture or from the forest products, it can be observed that major part of the plant bodies is made up of macromolecular cellulosic materials [6, 33, 38, 41, 43, 44, 46–48]. After end use of the products, a large part of agricultural and forest residues become wastes. Thus, it is wise to utilize such wastes as renewable resources to prepare MCC and NCC, which is in line with principles of green chemistry signifying the conversion of waste to value-added products [28, 117–121].

3.3.2 Morphological Characterization

In this section, among different kinds of biodegradable polymer composites, we focus on the structural characterization of some PBAT-based composite materials. An agricultural waste, the wheat stalk, was used for the extraction of MCC and NCC by thermo-chemical and mechanical treatments. The MCC and NCC were then compounded with the PBAT via melt mixing. For example, the lower (top) and higher (bottom) magnification SEM micrographs depicting the internal morphology of the composite comprising 40 wt% MCC (i.e., the sample M-40) are shown in Fig. 10 [85].

The micrograph with lower magnification (Fig. 10a) shows that there are regions with relatively smoother as well as rougher textures. The smoother areas represent the less deformed parts, whereas the rough areas stand for not deformed ones during fracture surface preparation. Nevertheless, at the first glance, it can be observed that

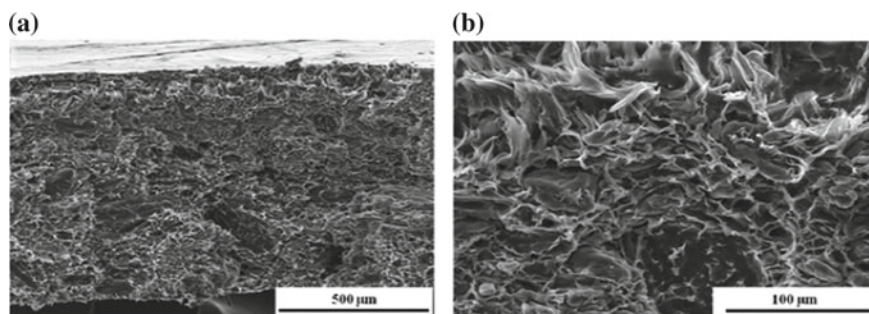


Fig. 10 Lower (top) and higher (bottom) magnifications of SEM micrograph of cryo-fractured surface of PBAT composite 40 wt% of MCC [85]

the composite is a quite homogeneous mixture of the polymer and the MCC. The average thickness of the MCC fibers is $5\ \mu\text{m}$ while the average length is about $100\ \mu\text{m}$ [85].

A closer look in Fig. 10b reveals further that there is a quite strong physical interaction between the polymer matrix and filler although there is no specific chemical bonding [85].

The properties of the composites were evaluated via soil composting tests, contact angle as well as water absorption measurements, scanning electron microscopy (SEM), and gel permeation chromatography (GPC) [85]. The cellulosic filler was found, as per SEM results, to uniformly disperse in the polymer matrix forming a quite homogeneous composite which visibly degraded completely within a few months under soil composting and showed high water absorption, these properties being enhanced with the filler content [85]. Compared to the neat PBAT, the composites showed enhanced surface hydrophilicity thereby increasing the vulnerability of degradation. In spite of the seemingly remarkable decrease in mechanical stability of the polymers under soil burial for several months, no substantial lowering of the molecular weight was observed [85].

These results are in consistence with the conclusions drawn in similar works reported in the literature including blends and composites with chitosan [122], starch [123], clay [124], and other systems comprising polylactides and other degradable systems [45, 53, 125].

For the sake of comparison, in Fig. 11, we present the morphology of a nanocomposite of the PBAT comprising 5 wt% of the NCC [85]. Indeed, the nanofiller content that brings the significant effect of large surface areas on the properties of the nanocomposites lies in the range of 1–5 wt% [126–128]. Thus, it makes sense to present the results comprising a lower amount of the nanofiller.

The dispersion of the NCC in the polymer matrix is uniform, with no noticeable tendency of agglomeration of the filler into the polymer matrix. The agglomeration tendency of the nanofiller into the polymer is a sign of the incompatibility of the filler with the adhering matrix [129]. The micrographs presented in Fig. 11 depict

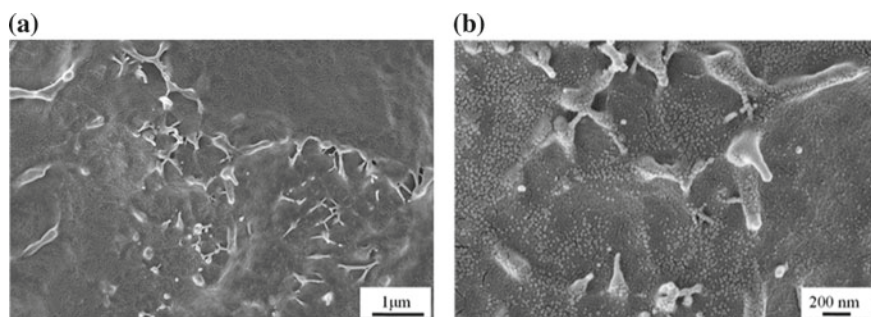


Fig. 11 Lower (top) and higher (bottom) magnifications SEM micrographs of PBAT composite comprising 5 wt% of NCC [85]

a reasonable PBAT/NCC compatibility, which is also supported by the presence of cylinder shaped fillers with the thickness in the range of 40–80 nm [85].

Looking at the thickness of individual nanocrystals and corresponding microcrystals, the average number of the nanocrystals per microcrystal bundle can be estimated to be approximately 100. Thus, it can be concluded that the nanofibrillation could bring, in case of cellulosic materials, an increase in the surface area by about 100 times. Hence, the nanocomposites can be considered to be much more effective than the conventional ones [85].

3.3.3 Surface Properties

The surface property of the composites, particularly the hydrophilicity, also correlates with their susceptibility toward biodegradation. The nature of the surface determines how the material responds with highly polar substances such as water. During contact angle measurements, generally, the water droplets form the angles with interacting surfaces whose dimension depends upon hydrophilicity or hydrophobicity of the substrate. Higher contact angle represents hydrophobicity, whereas the lower contact angle stands for hydrophilicity [85, 130, 131].

Figure 12 shows spontaneous contact angles formed by water droplets on the surfaces of pure PBAT and two different composites [85]. At first glance, the contact angle on the PBAT surface looks slightly larger (implying slightly higher hydrophobicity) than on that of the composites. Indeed, the contact angles measured for the surfaces of PBAT, M-5 and N-5 composites are 83.3°, 77.1°, and 70.1°. The decreased hydrophobicity of the composites surfaces compared to the pure PBAT can be attributed to the presence of the hydrophilic cellulosic fractions [132]. The fact, that the spontaneous contact angles of both M-5 and N-5 composites are similar, further illustrates that the hydrophobicity of the specimens primarily depends not only on the chemical nature but also on the dimensional nature (micro- or nanoscale) of the bio-. The results imply that the lower the particle size of the hydrophilic fillers, the higher would be the ease of filler dispersion in composites and thus higher would be the interaction with water. The result is consistent with literature work [131].

The results from surface contact angle measurement, however, suggest that there is some segregation of the cellulose toward the sample surface that attracts water onto it although there was no clear evidence of surface segregation of the filler as per spectroscopic and microscopic data [133].

In summary, the wetting behavior can be correlated with the degradation susceptibility of the composites at hand, the nanocomposites being more susceptible to water absorption and thereby providing higher ease of degradation under soil burial conditions (to be discussed in the next section) [85, 134, 135].

The composites dealt with in Figs. 10, 11, and 12 have been found to possess excellent water absorption tendencies, thereby increasing the ease of hydrolysis and bond cleavage under microbial attack.

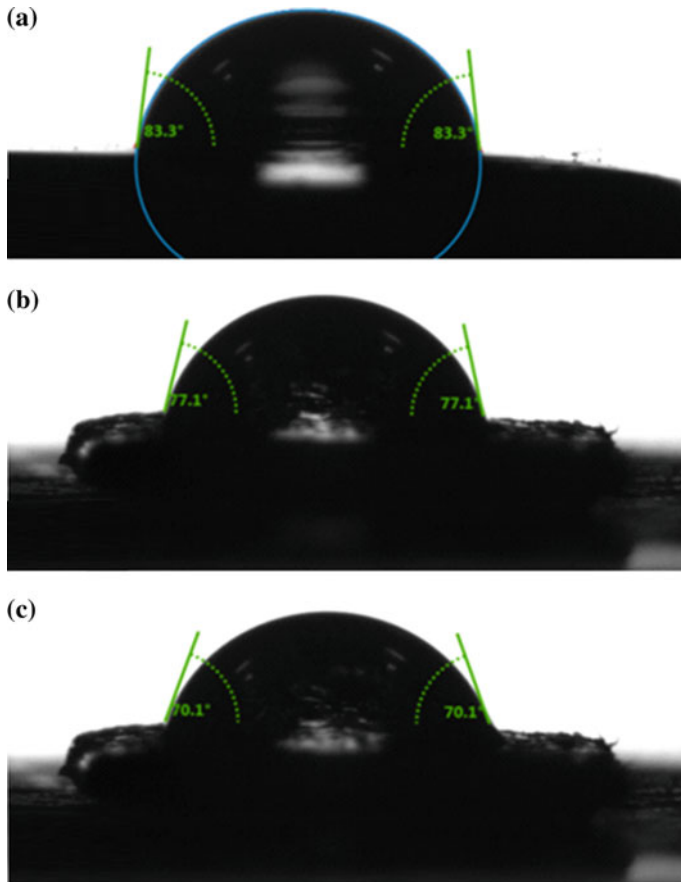


Fig. 12 Photographs showing spontaneous contact angles of water droplets on the PBAT surfaces of **a** pure PBAT, **b** composite comprising 5 wt% of MCC, and **c** composite comprising 5 wt% of NCC [85]

3.3.4 Degradation Under Soil Burial Conditions

Morphological investigations of the materials subjected to degradation under soil burial conditions were carried out. Thus, the information on the physical states upon various stress conditions was obtained. The structural features of the samples after the experiments are presented in Fig. 13 [85].

The photographs in Fig. 13 show that compared to the highly ductile nature of the PBAT, on soil composting, both the PBAT as well as its composites became quite brittle [85]. The surface of the composites was found to be attacked by the microbes. After 4 months of composting, the samples turned very brittle, the fragility of the specimen is more pronounced for the composites having a higher amount of the MCC [85].

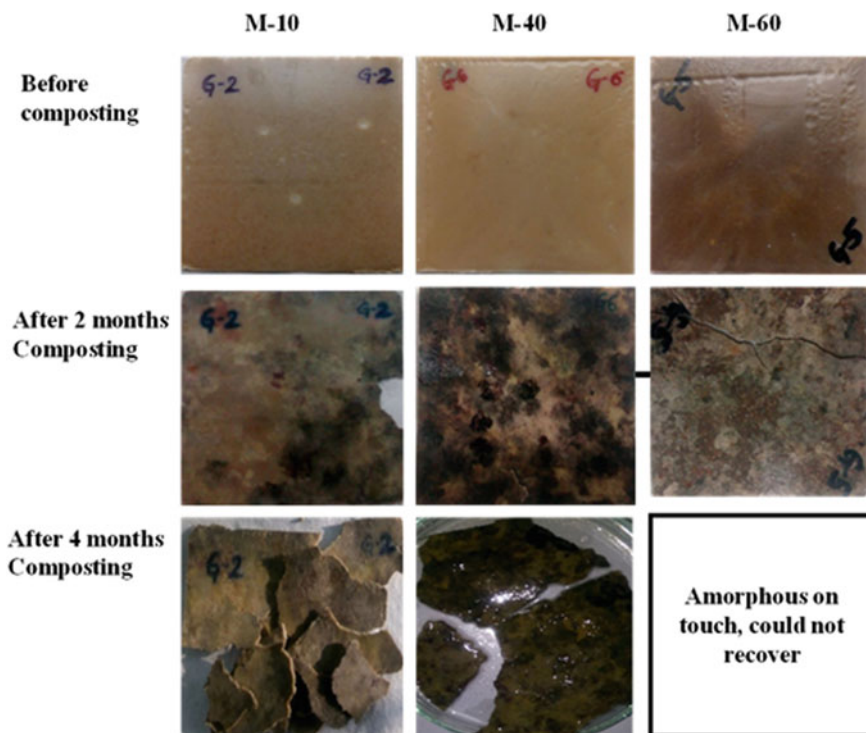


Fig. 13 Photographs of different PBAT/MCC composites subjected to soil burial for different periods of time as indicated [85]

Among the results presented in Fig. 13, morphological features of the composite M-20 were further studied in detail by scanning electron microscopy. In the beginning of the degradation, the voids of various diameters appeared on the samples surfaces, as a result of consumption of the filler particles as nutrients, by the microbes. With increasing soil burial period, the fillers content decreased which completely vanish after 4 months.

It can be expected that the degradation process of the composites materials under soil burial condition is accompanied by a drastic reduction in the molecular weight (M_w) of the polymers which finally would lead to embrittlement of the polymeric materials. Thus, the molecular weight of the polymers after the various interval of soil burial was analyzed [136–138].

The variation of the molecular properties of the PBAT in neat form and in the form of composites was investigated by gel permeation chromatography (GPC) using PS standard [85].

It was found that, under soil burial conditions, the M_w values of the pure PBAT decreased from 48.62–21.60 kg/mol in 4 months. In the case of the composite comprising 40 wt% of MCC, the M_w values decreased in same way [85]. Molecular

weight lowering was also observed on soil composting of poly(butylene sebacate) [110].

The PBAT showed significant ease of degradation in molecular weights under soil burial conditions which was further enhanced by the presence of the cellulosic filler. However, it was stressed that the polymer chains did not completely degrade but rather turned into smaller fragments that might be present for longer times as microscopic particles in the soil forming a sort of microplastics aggregates [85].

4 Biodegradation Mechanisms

Usually, any kind of degradation starts from the points of weak bonding in the heterogeneous materials. It is known that the chemical linkages, such as with ester, ether, amide, and hydrogen bonds are susceptible to hydrolysis that are easily attacked by chemicals and microbes [139–141].

The degradation process may proceed with the action of some kinds of acids or enzymes on those weak active sites thereby fragmenting the giant molecules into smaller entities including the liberation of some gases. The polymeric materials can even undergo photolytic degradation on long exposure to sunlight, microwaves, or UV-radiations and generate free radicals [42].

The biodegradation is a complex process which has been considered to take places in three basic stages [139]: biodeterioration, biofragmentation, and assimilation, in which also the influence of the abiotic factors cannot be undermined. The biodiversity of the microorganisms and their efficacy toward the formation of complex biofilm and their catalytic abilities transform the degraded substances to the nutrients represent highly sophisticated natural phenomena [62, 115].

The biodeterioration stage can be pretty well assessed by thermal and microscopic methods while the fragmentation stage can be monitored by evaluating the changes in the molecular characteristics. The production of carbon dioxide gas is a simple signature of the bioassimilation process which, of course, involves the formation of various kinds of metabolites and microbial biomass [59–62, 115, 116]. The terminal groups and gaseous substances, as well as the biofilms produced during the degradation processes, can be analyzed by different spectroscopic techniques [30, 109, 114, 139].

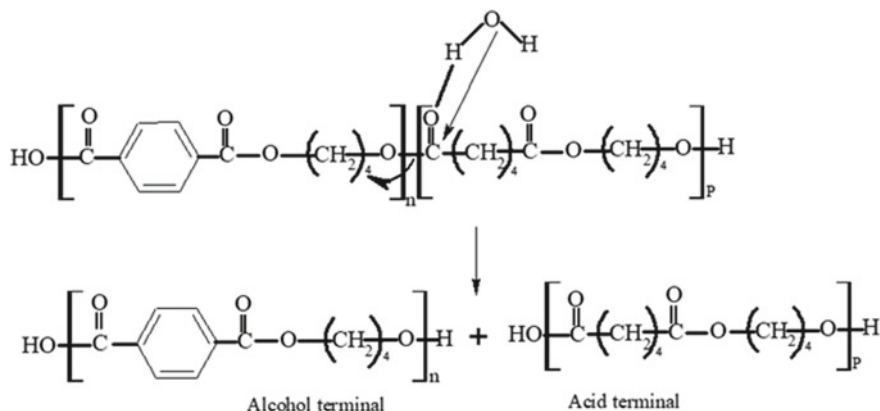
In case of polyesters and copolyesters, which have been primarily dealt with in this work, two important biodegradation mechanisms have been found effective; see Schemes 3: and 4: [139].

I. *Hydrolytic mechanism*

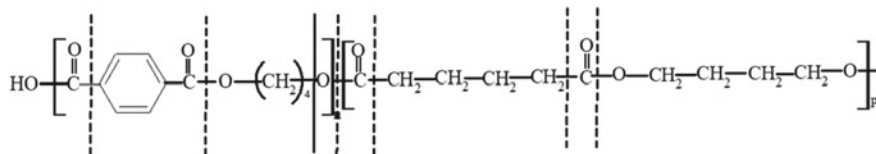
See Scheme 3.

II. *Main chain scission*

See Scheme 4.



Scheme 3 P BAT degradation *via* hydrolytic attack on carbonyl group of ester to liberate free -COOH and -OH groups; the letters “ p ” and “ n ” refer to the degree of polymerization of respective segments



Scheme 4 PBAT degradation by chain scission at different positions of the macromolecular skeleton under different conditions

5 Summary, Trends, and New Opportunities

In this chapter, we attempted to offer an overview, with recent research outputs and applications, the structure-properties correlations of biodegradable copolyesters-based polymer composites. The results can be summarized as follows.

- The lignocelluloses based micro- and nanofillers can be synthesized by various chemical, mechanical, and bioinspired (or biosynthetic) methods and be evaluated in terms of their structural and molecular characteristics via spectroscopic, microscopic, and scattering and chromatographic techniques.
- The MCC and NCC fillers can be incorporated up to a pretty high weight fraction, easily into the biodegradable copolyester matrix even without the use of compatibilizers. However, the practical applications of such composites are limited for low load objects fabrication.
- The copolyester-based composite materials undergo rapid fragmentation process under soil burial conditions leading to highly brittle materials. The molecular weight degradation has been, however, found to be not that significant within a few months duration.

There is a trend of utilizing the copolyesters and their composites for biomedical applications [9, 10, 21], for smart packaging films [14, 16, 106] and functional coatings and for flexible conducting materials [15]. These strategies are achieved by introducing different functional groups via grafting onto the natural polymer chains and then making graft and block copolymers with synthetic polymers. The challenge will be then to find suitable routes for biodegradation as the latter is a complex process and a single microbial strain would not be sufficient for the targeted biodegradation. In this case, microbial communities can be employed.

There are several biodegradation pathways for polymeric materials including degradable copolyesters which have been successfully employed. However, the routes for controlled degradation processes leading to the solution to the fundamental environmental problems are yet to evolve. In our Nepalese context, due to the presence of large microbial biodiversity in the region, and proven opportunities to design the microbial communities via uncomplicated genetic manipulation, there are unparalleled opportunities. The thermophilic and cold-loving bacteria might offer great potential in terms of degradation of the polymers, in general, which still needs to be explored.

Acknowledgements JG thanks the Indian National Science Academy (INSA) and Nepal Academy of Science and Technology (NAST) for providing the fellowship to visit IIT Guwahati and for providing PhD Research Fellowship, respectively. She further acknowledges the German Science Foundation (DFG) for providing her financial support for research stays in Germany.

References

1. Gross RA, Kalra B (2002) Biodegradable polymers for the environment. *Science* 297:803–807. <https://doi.org/10.1126/science.297.5582.803>
2. Abraham E, Elbi PA, Deepa B, Jyotishkumar P, Pothen LA, Narine SS, Thomas S (2012) X-ray diffraction and biodegradation analysis of green composites of natural rubber/nanocellulose. *Polym Degrad Stab* 97:2378–2387. <https://doi.org/10.1016/j.polymdegradstab.2012.07.028>
3. Malho JM, Laaksonen P, Walther A, Ikkala O, Linder MB (2012) Facile method for stiff, tough and strong nanocomposites by direct exfoliation of multilayered graphene into native nanocellulose matrix. *Biomacromol* 13:1093–1099. <https://doi.org/10.1021/bm2018189>
4. Cho MJ, Park BD (2011) Tensile and properties of nanocellulose-reinforced poly(vinyl alcohol) nanocomposites. *J Ind Eng Chem* 17:36–40. <https://doi.org/10.1016/j.jiec.2010.10.006>
5. Frone AN, Panaitescu DM, Donescu D (2011) *UPB Sci Bull, Ser B: Chem Mater Sci* 73:133–152. https://www.scientificbulletin.upb.ro/rev_docs_arhiva/full20599.pdf
6. Rajan KP, Veena NR, Maria HJ, Rajan R, Skrifvars M, Joseph K (2010) Extraction of bamboo microfibrils and development of biocomposites based on polyhydroxybutyrate and bamboo microfibrils. *J Comp Mater* 45:1325–1329. <https://doi.org/10.1177/0021998310381543>
7. Lee SY, Mohan DJ, Kang IA, Doh GH, Lee S, Han SO (2009) Nanocellulose reinforced PVA composite films: Effect of acid treatment and filler loading. *Fibers Polym* 10:77–82. <https://doi.org/10.1007/s12221-009-0077-x>
8. William GE, Ballerini A, Zhang J (2005) Polymer nanocomposites: synthetic and natural fillers a review. *Maderas: Clencia Technologia* 7:159–178. <https://doi.org/10.4067/s0718-221x2005000300002>

9. Morouco P, Biscaia S, Viana T, Franco M, Malca C, Mateus A, Moura C, Ferreira FC, Mitchell G, Alves NM (2016) Fabrication of poly(ϵ -caprolactone) scaffolds reinforced with cellulose nanofibers, with and without the addition of hydroxyapatite nanoparticles. *BioMed Res Int Article ID 1596157*:1–10. <https://doi.org/10.1155/2016/1596157>
10. Ozkoc G, Kemaloglu S, Quaedflieg M (2010) Production of poly(lactic acid)/organoclay nanocomposites scaffolds by microcompounding and polymer/particle leaching. *Polym Compos* 31:674–683. <https://doi.org/10.1002/pc.20846>
11. Fukushima K, Wu MH, Bocchini S, Rasyida A, Yang MC (2012) PBAT based nanocomposites for medical and industrial applications. *Mater Sci Eng C32*:1331–1351. <https://doi.org/10.1016/j.msec.2012.04.005>
12. Rasyida A, Fukushima K, Yang MC (2017) Structure and properties of organically modified poly(butylene adipate-co-terephthalate) based nanocomposites. *IOP Conf Ser Mater Sci Eng* 223:012–023. <https://doi.org/10.1088/1757-899x/223/1/012023>
13. Chivrac F, Kadlecová Z, Pollet E, Avérous L (2006) Aromatic copolyester-based nanobiocomposites: elaboration, structural characterization and properties. *J Polym Env* 14:393–401. <https://doi.org/10.1007/s10924-006-0033-4>
14. Dhar P, Bhardwaj U, Kumar A, Katiyar V (2014) Cellulose nanocrystals: a potential nanofiller for food packaging applications—food additives and packaging. In: ACS symposium series, chap 17. American Chemical Society: Washington, DC, pp 197–239. <https://doi.org/10.1021/bk-2014-1162.ch017>
15. Gopakumar DA, Pai AR, Pottathara YB, Pasquini D, Morais LCD, Luke M, Kalarikkal NK, Grohens Y, Thomas S (2018) Cellulose nanofiber-based polyaniline flexible papers as sustainable microwave absorbers in the X-band. *ACS Appl Mater Interfaces* 10:20032–20043. <https://doi.org/10.1021/acsami.8b04549>
16. Moustafa H, Kissi NE, Abou-Kandil AI, Abdel-Aziz MS, Dufresne A (2017) PLA/PBAT bionanocomposites with antimicrobial natural rosin for green packaging. *ACS Appl Mater Interfaces* 9:20132–20141. <https://doi.org/10.1021/acsami.7b05555>
17. Cotana F, Brinchi L, Gelosia M, Coccia V, Petrozzi A (2012) Nanocrystalline cellulose from lignocelluloses biomass: applications and future prospects. In: 20th European biomass conference and exhibition, Italy, pp 1182–1194. <https://doi.org/10.1016/j.carbpol.2013.01.033>
18. Grüneberger F, Künninger T, Zimmermann T, Arnold M (2014) Nanofibrillated cellulose in wood coatings: mechanical properties of free composite films. *J Mater Sci* 49:6437–6448. <https://doi.org/10.1007/s10853-014-8373-2>
19. Leung ACW, Lam E, Chong J, Hrapovic S, Luong JHT (2013) Reinforced plastics and aerogels by nanocrystalline cellulose. *J Nanoparticles Res* 15:1–24. <https://doi.org/10.1007/s11051-013-1636-z>
20. Lu Y, Tekinalp HL, Eberle CC, Peter W, Naskar AM, Ozcan S (2001) Nanocellulose in polymer composites and biomedical applications. *Tappi J Nanocellulose* 13:47–54
21. Sgarioto M, Adhikari R, Gunatillake PA, Moore T, Malherbe F, Nagel MD, Patterson J (2014) Properties and in vitro evaluation of high modulus biodegradable polyurethanes for applications in cardiovascular stents. *J Biomed Mater Res B Appl Biomater* 102B:1711–1719. <https://doi.org/10.1002/jbm.b.33137>
22. Dasaria A, Yub ZZ, Caic GP, Maic YW (2013) Recent developments in the fire retardancy of polymeric materials. *Prog Polym Sci* 38:1357–1387. <https://doi.org/10.1016/j.progpolymsci.2013.06.006>
23. Sjödin A, Carlsson H, Thuresson K, Sjölin S, Bergman A, Östman C (2001) Flame retardants in indoor air at an electronics recycling plant and at other work environments. *Environ Sci Technol* 35:448–454. <https://doi.org/10.1021/es000077n>
24. Saba N, Jawaid M, Othman YA, Paridah MT (2015) A review on dynamic mechanical properties of natural fibre reinforced polymer composites. *Const Build Mater* 106:149–159. <https://doi.org/10.1016/j.conbuildmat.2015.12.075>
25. Su SK, Wu CS (2011) Polyester biocomposites from recycled natural fibers: characterization and biodegradability. *J Appl Polym Sci* 119:1211–1219. <https://doi.org/10.1002/app.32808>

26. Chauhan YP, Sapkal RS, Sapkal VS, Zamre GS (2009) Microcrystalline cellulose from cotton rags (waste from garment and hosiery industries). *Int J Chem Sci* 7:681–688
27. Banerjee A, Chatterjee K, Madras G (2014) Enzymatic degradation of polymer: a brief review. *Mater Sci Technol* 30:567–573. <https://doi.org/10.1179/1743284713y.0000000503>
28. Leja K, Lewandowicz G (2010) Polymer biodegradation and biodegradable polymers— a review. *Polish J Environ Stud* 19:255–266. http://yunus.hacettepe.edu.tr/~damlacetin/kmu407/index_dosyalar/2.%20makale.pdf
29. Shah AA, Hasan F, Hameed A, Ahmed S (2008) Biological degradation of plastics: a comprehensive a review. *Biotechnol Adv* 26:246–265. <https://doi.org/10.1016/j.biotechadv.2007.12.005>
30. Palisikowski PA, Kuchnier CN, Pinheiro IF, Morales AR (2017) Biodegradation in soil of PLA/PBAT Blends compatibilized with chain extender. *J Polym Environ* 26:330–341. <https://doi.org/10.1007/s10924-017-0951-3>
31. Mostafa HM, Sourell H, Blockisch FJ (2010) The mechanical properties of some bioplastics under different soil type for use as a biodegradable drip tubes. *Agric Eng Int* 12:12–21. <http://cigrjournal.org/index.php/Ejournal/article/view/1497/1270>
32. Han YH, Han SO, Cho D, Kim HI (2008) Dynamic mechanical properties of natural fiber/polymer biocomposites: The effect of fiber treatment with electron beam. *Macromol Res* 16:253–260. <https://doi.org/10.1007/bf03218861>
33. Chan CH, Chia CH, Zakaria S, Ahmad I, Dufresne A (2013) Production and characterization of cellulose and nano-crystalline cellulose from kenaf core wood. *BioResources* 8:785–794
34. Vinayak DL, Guna VK, Madhavi D, Arpitha M, Reddy N (2017) *Ricinus communis* plant residues as a source for natural cellulose fiber potentially exploitable in polymer composites. *Ind Crops Prod* 100:126–131. <https://doi.org/10.1016/j.indcrop.2017.02.019>
35. Das M, Chakraborty D (2008) The effect of Alkalization and fiber loading on the mechanical properties of bamboo fiber composites, part 1: polyester resin matrix. *J Appl Polym Sci* 112:489–495. <https://doi.org/10.1002/app.29342>
36. Adhikari R, Bhandari NL, Causin V, Le HH, Radusch HJ, Michler GH, Saiter JM (2012) Study of morphology, mechanical properties, and thermal behavior of green aliphatic-aromatic copolyester/bamboo flour composites. *Polym Eng Sci* 52:2296–2303. <https://doi.org/10.1002/pen.23335>
37. Batalha LAR, Colodette JL, Gomide JL, Barbosa LCA, Maltha CRA, Gomes FJB (2012) Dissolving pulp producing from bamboo. *Bioresources* 7:640–651
38. Cherian BM, Leao AL, de Souza SF, Coata LMM, Olyveira GMd, Kottaisamy M, Nagarajan ER, Thomas S (2011) Cellulose nanocomposites with fibres nanofibres isolated from pineapple leaf fibers for medical applications. *Carbohydr Polym* 86:1790–1798. <https://doi.org/10.1016/j.carbpol.2011.07.009>
39. Morais Teixeira E, Correa AC, Manzoli A, Leite FDL, Oliveira CRD, Mattoso LHC (2010) Cellulose nanofibers from white and naturally colored cotton fibers. *Cellulose* 17:595–606. <https://doi.org/10.1007/s10570-010-9403-0>
40. Satyamurthy P, Vigneshwaran N (2013) A novel process for synthesis of spherical nanocellulose by controlled hydrolysis of microcrystalline cellulose using anaerobic microbial consortium. *Enzym Microbial Technol* 52:20–25. <https://doi.org/10.1016/j.enzmictec.2012.09.002>
41. Yu T, Li Y (2014) Influence of poly(butylenes adipate-co-terephthalate) on the properties of the biodegradable composites based on ramie/poly(lactic acid). *Composites: Part A* 58:24–29. <https://doi.org/10.1016/j.compositesa.2013.11.013>
42. Nagata M, Inaki K (2011) Biodegradable and photocurable multiblock copolymers with shape-memory properties from poly(ϵ -caprolactone) diol, poly(ethylene glycol) and 5-cinnamoyloxyisophthalic acid. *J Appl Polym Sci* 120:3556–3564. <https://doi.org/10.1002/app.33531>
43. Giri J, Adhikari R (2013) A brief review on extraction of nanocellulose and its application. *BIBECHANA* 9:81–87. <https://doi.org/10.3126/bibechana.v9i0.7179>

44. Sanjay MR, Arpitha GR, Naik LL, Gopalakrishna K, Yogesha B (2016) Applications of natural fibers and its composites: an overview. *Sci Res* 7:108–114. <https://doi.org/10.4236/nr.2016.73011>
45. Siro I, Plackett D (2010) Microfibrillated cellulose and new nanocomposite materials: a review. *Cellulose* 17:459–494. <https://doi.org/10.1007/s10570-010-9405-y2890-2895>
46. Pelissari FM, Sobral PJDM, Menegalli FC (2014) Isolation and characterization of cellulose nanofibers from banana peels. *Cellulose* 21:417–432. <https://doi.org/10.1007/s10570-013-0138-6>
47. Ibrahim NA, Hadithon KA, Abdan K (2010) Effect of fiber treatment on mechanical properties of kenaf-fiber-Ecoflex composites. *J Reinf Plast Compos* 29:2192–2198. <https://doi.org/10.1177/0731684409347592>
48. Reddy JP, Rhim JW (2014) Isolation and characterization of cellulose nanocrystals from garlic skin. *Mater Lett* 129:20–23. <https://doi.org/10.1016/j.matlet.2014.05.019>
49. Dai D, Fan M (2010) Characteristic and performance of elementary hemp fibre. *Mater Sci Appl* 1:336–342. <https://doi.org/10.4236/msa.2010.16049>
50. Rosli NA, Ahmad I, Abdullah I (2013) Isolation and characterization of cellulose nanocrystals from *Agave angustifolia* fibre. *BioResources* 8:1893–1908
51. Cesar NR, Marcelo A, da-Silva P, Botaro VR, Menezes AJD (2015) Cellulose nanocrystals from natural fiber of the macrophyte *Typha domingensis*: extraction and characterization. *Cellulose* 22:449–460
52. Yan FY, Krishniah D, Rajin M, Bono A (2009) Cellulose extraction from Palm Kernel cake using liquid phase oxidation. *J Eng Sci Technol* 1:57–68
53. Liu DY, Yuan XW, Bhattacharyya D, Eastal AJ (2010) Characterizations of solution cast cellulose nanofibre- reinforced poly(lactic acid). *eXPRESSPolym Lett* 4:26–31. <https://doi.org/10.3144/expresspolymlett.2010.5>
54. Shaheen TI, Emam HE (2018) Sono-chemical synthesis of cellulose nanocrystals from wood sawdust using acid hydrolysis. *Int J Biol Macromol* 107:1599–1606. <https://doi.org/10.1016/j.ijbiomac.2017.10.028>
55. Chen X, Kuhn E, Wang W, Park S, Flanagan K, Trass O, Tenlep L, Tao L, Tucker M (2013) Comparison of different mechanical refining technologies on the enzymatic digestibility of low severity acid pretreated corn stover. *Bioresource Technol* 147:401–408. <https://doi.org/10.1016/j.biortech.2013.07.109>
56. Stelte W, Sanadi AR (2009) Preparation and characterization of cellulose nanofibers from two commercial hardwood and softwood. *Ind Eng Chem Res* 48:11211–11219. <https://doi.org/10.1021/ie9011672>
57. Li J, Wei X, Wang Q, Chen J, Chang G, Su LKJ, Liu Y (2012) Homogeneous isolation of nanocellulose from sugarcane bagasse by high pressure homogenization. *Carbohydr Polym* 90:1609–1613. <https://doi.org/10.1016/j.carbpol.2012.07.038>
58. Oksman K, Etang JA, Mathew A, Jonoobi M (2011) Cellulose nanowhiskers separated from a bio-residue from wood bioethanol production. *Biomass Bioenergy* 35:146–152. <https://doi.org/10.1016/j.biombioe.2010.08.021>
59. Czaja W, Krystynowicz A, Bielecki S, Brownjr R (2006) Microbial cellulose—the natural power to heal wounds. *Biomaterials* 27:145–151. <https://doi.org/10.1016/j.biomaterials.2005.07.035>
60. Bielecki S, Krystynowicz A, Turkiewicz M, Kalinowska H (eds) (2005) *Bacterial cellulose: biotechnology of polymer: from synthesis to patents*. Munster, Germany. Wiley-VCH, Verlag GmbH pp 381–434
61. Iguchi M, Yamanaka S, Budhiono A (2000) Review bacterial cellulose—a masterpiece of nature’s arts. *J Mater Sci* 35:261–270
62. Mikkelsen D, Flanagan BM, Dykes GA, Gidley MJ (2009) Influence of different carbon sources on bacterial cellulose production by *Gluconacetobacter xylinus* strain ATCC 53524. *J Appl Microbiol* 107:576–583. <https://doi.org/10.1111/j.1365-2672.2009.04226.x>
63. Michler GH (2008) *Electron microscopy of polymers*. Springer, Berlin. <https://doi.org/10.1007/978-3-540-36352-1>

64. Thomas S, Chan CH, Pothen LA, Rajisha KR, Maria H (eds) (2013) Natural rubber materials. Blends and IPNs
65. Thomas S, Stephen R (eds) (2010) Rubber nanocomposites: preparation, properties, and applications. Springer Publisher, Heidelberg, Germany. ISBN 978-0-470-82345-3
66. Sawyer LC, Grubb DT, Meyers GF (eds) (2008) Polymer microscopy. Springer Publisher, Heidelberg, Germany. <https://doi.org/10.1007/978-0-387-72628-1>
67. Guo Q (2016) Polymer morphology: principles, characterization, processing. Wiley. ISBN-13: 978-1118452158
68. Grellmann W, Langer B (eds) (2017) Deformation and fracture behaviour of polymer materials. Springer, Berlin. ISBN: 978-3-319-41879-7
69. Adhikari R, Michler GH (2009) Polymer nanocomposites characterization by microscopy. *Polym Rev* 49:141–180. <https://doi.org/10.1080/15583720903048094>
70. Bandera D, Sapkota J, Josset S, Weder C, Tingaut P, Gao X, Foster EJ, Zimmermann T (2014) Influence of mechanical treatments in the properties of cellulose nanofibers isolated from microcrystalline cellulose. *React Funct Polym* 85:134–141. <https://doi.org/10.1016/j.reactfunctpolym.2014.09.009>
71. Giri J, Lach R, Sapkota J, Susan MABH, Saiter JM, Henning S, Katiyar V, Adhikari R (2019) Structural and thermal characterization of different types of cellulosic fibers. *BIBECHANA* 16:177–186. <https://doi.org/10.3126/bibechana.v16i0.21650>
72. He J, Tang Y, Wang SY (2007) Differences in morphological characteristics of bamboo fibres and other natural cellulose fibres: studies on X-ray diffraction, solid state ¹³C-CP/MAS NMR, and second derivative FTIR spectroscopy data. *Iran Polym J* 16:807–818
73. Okubo K, Fujii T, Yamamoto Y (2004) Development of bamboo-based polymer composites and their mechanical properties. *Compos Part: A* 35:377–383. <https://doi.org/10.1016/j.compositesa.2003.09.017>
74. Bozzolz JJ, Lonnie D, Jones R (1992) Electron microscopy, principals and techniques for biologists, 2nd edn. Bartlett Publish
75. Yang J, Ye DY (2012) Liquid crystal of nanocellulose whiskers grafted with acrylamide. *Chin Chem Lett* 23:367–370
76. Rosa MF, Medeiros ES, Malmonge JA, Gregorski KS, Wood DF, Mattoso LHC, Glenn G, Orts WJ, Imam SH (2010) Cellulose nanowhiskers from coconut fibers: effect of preparation conditions on their thermal and morphological behavior. *Carbohydr Polym* 81:83–92. <https://doi.org/10.1016/j.carbpol.2010.01.059>
77. Mathew AP, Oksman K, Pierron D, Harmand MF (2012) Fibrous cellulose nanocomposite scaffolds prepared by partial dissolution for potential use as ligament or tendon substitutes. *Carbohydr Polym* 87:2291–2298. <https://doi.org/10.1016/j.carbpol.2011.10.063>
78. Herrera MA, Mathew AP, Oksman K (2012) Comparison of cellulose nanowhiskers extracted from industrial bio-residue and commercial microcrystalline cellulose. *Mater Lett* 71:28–31. <https://doi.org/10.1016/j.matlet.2011.12.011>
79. Mathew AP, Oksman K, Sain M (2005) Mechanical properties of biodegradable composites from poly lactic acid (PLA) and microcrystalline cellulose (MCC). *J Appl Polym Sci* 97:2014–2025. <https://doi.org/10.1002/app.21779>
80. Maiti S, Ray D, Mitra D, Sengupta S, Kar T (2011) Structural changes of starch/polyvinyl alcohol biocomposite films reinforced with microcrystalline cellulose due to biodegradation in simulated aerobic compost environment. *J Appl Polym Sci* 122:2503–2511. <https://doi.org/10.1002/app.34377>
81. Nam JY, Ray SS, Okamoto M (2003) Crystallization behavior and morphology of biodegradable polylactide/layered silicate nanocomposite. *Macromolecules* 36:7126–7131. <https://doi.org/10.1021/ma034623j>
82. Mandal A, Chakrabarty D (2014) Studies on the mechanical, thermal, morphological and barrier properties of nanocomposites based on poly(vinyl alcohol) and nanocellulose from sugarcane bagasse. *J Ind Eng Chem* 20:462–473. <https://doi.org/10.1016/j.jiec.2013.05.003>

83. Pokhrel S, Lach R, Le HH, Wutzler A, Grellmann W, Radusch HJ, Dhakal RP, Esposito A, Henning S, Yadav PN, Saiter JM, Heinrich G, Adhikari R (2016) Fabrication and characterization of completely biodegradable copolyester-chitosan blends: I spectroscopic and thermal characterization. *Macromol Symp* 366:23–34. <https://doi.org/10.1002/masy.201650043>
84. Giri J, Lach R, Le HH, Grellmann W, Susan MABH, Saiter JM, Henning S, Adhikari R (2019) Compostable composites of wheat stalk microcrystalline cellulose and Poly(butylenes adipate-co-terephthalate): structural, thermal and mechanical properties. Submitted
85. Giri J, Lach R, Grellmann W, Susan MABH, Saiter JM, Henning S, Katiyar V, Adhikari R (2019) Compostable composites of wheat stalk microcrystalline cellulose and Poly(butylene adipate-co-terephthalate): surface properties and degradation behaviour. *J Appl Polym Sci*, Submitted
86. Lee KY, Blaker JJ, Bismarch A (2009) Improving the properties of nanocellulose/poly lactide composites by esterification of nanocellulose. Can it be done?
87. Kramer F, Klemm D, Schumann D, Heßler N, Wesarg F, Fried W, Stadermann D (2006) Nanocellulose polymer composites as innovative pool for (bio)material development. *Macromol Symp* 244:136–148. <https://doi.org/10.1002/masy.200651213>
88. Paula MPD, Larcerda TM, Frollini E (2008) Sisal cellulose acetates obtained from heterogeneous reaction. *eXPRESS Polym Lett* 2:423–428
89. Teeri TT, Brumer H, Daniel G, Gatenholm P (2007) Biomimetic engineering of cellulose-based materials. *Trends Biotechnol* 25:299–306. <https://doi.org/10.1016/j.tibtech.2007.05.002>
90. Demir H, Atikler U, Balkose D, Tihminlioglu F (2006) The effect of fiber surface treatments on the tensile and water sorption properties of polypropylene–luffa fiber composites. *Compos A* 37:447–456. <https://doi.org/10.1016/j.compositesa.2005.05.036>
91. Beg MDH, Pickering KL (2008) Mechanical performance of Kraft fibre reinforced polypropylene composites: influence of fibre length, fibre beating and hygrothermal ageing. *Compos Part A: Appl Sci Manufact* 39:1748–1755. <https://doi.org/10.1016/j.compositesa.2008.08.003>
92. Beg MDH, Pickering KL (2008) Reprocessing of wood fibre reinforced polypropylene composites. Part II: hygrothermal ageing and its effects. *Compos Part A: Appl Sci Manufact* 39:1565–1571. <https://doi.org/10.1016/j.compositesa.2008.06.002>
93. Sanadi AR, Caulfield DF, Jacobson RE, Rowell RM (1995) Renewable agricultural fibers as reinforcing fillers in plastics: mechanical properties of Kenaf fiber-polypropylene composites. *Indus Eng Chem Res* 34:1889–1896. <https://doi.org/10.1021/ie00044a041>
94. Rana AK, Mandal A, Mitra BC, Jacobson R, Rowell R, Banerjee AN (1998) Short jute fiber-reinforced polypropylene composites: effect of compatibilizer. *J Appl Polym Sci* 69:329–338. [https://doi.org/10.1002/\(sici\)1097-4628\(19980711\)69:2%3c329:aid-app14%3e3.0.co;2-r](https://doi.org/10.1002/(sici)1097-4628(19980711)69:2%3c329:aid-app14%3e3.0.co;2-r)
95. Nachtigall SMB, Cerveira GS, Rosa SML (2007) New polymeric-coupling agent for polypropylene/wood-flour composites. *Polym Test* 26:619–628. <https://doi.org/10.1016/j.polymertesting.2007.03.00>
96. Smits V, Chevalier P, Deheunynck D, Miller S (2008) A new filler dispersion technology. *Reinfor Plast* 52:37–43. [https://doi.org/10.1016/s0034-3617\(08\)70406-5](https://doi.org/10.1016/s0034-3617(08)70406-5)
97. Sanadi AR, Young RA, Clemons C, Rowell RM (1994) Recycled newspaper fibers as reinforcing fillers in thermoplastics: part i-analysis of tensile and impact properties in polypropylene. *J Reinfor Plast Compos* 13:54–67. <https://doi.org/10.1177/073168449401300104>
98. Bledzki AK, Reihmane S, Gassan J (1996) Properties and modification methods for vegetable fibers for natural fiber composites. *J Appl Polym Sci* 59:1329–1336. [https://doi.org/10.1002/\(sici\)1097-4628\(19960222\)59:8%3c1329:aid-app17%3e3.0.co;2-0](https://doi.org/10.1002/(sici)1097-4628(19960222)59:8%3c1329:aid-app17%3e3.0.co;2-0)
99. Martí-Ferrer F, Vilaplana F, Ribes-Greus A, Benedito-Borrás A, Sanz-Box C (2005) Flour rice husk as filler in block copolymer polypropylene: effect of different coupling agents. *J Appl Polym Sci* 99:1823–1831. <https://doi.org/10.1002/app.22717>
100. Yang HS, Wolcott MP, Kim HS, Kim S, Kim HJ (2006) Properties of lignocellulosic material filled polypropylene bio-composites made with different manufacturing processes. *Polym Test* 25:668–676. <https://doi.org/10.1016/j.polymertesting.2006.03.01>

101. Yang HS, Kim HJ, Son J, Park HJ, Lee BJ, Hwang TS (2004) Rice-husk flour filled polypropylene composites; mechanical and morphological study. *Compos Struct* 63:305–312. [https://doi.org/10.1016/s0263-8223\(03\)00179-x](https://doi.org/10.1016/s0263-8223(03)00179-x)
102. Ichazo M, Albano C, González J, Perera R, Candal M (2001) Polypropylene/wood flour composites: treatments and properties. *Compos Struct* 54:207–214. [https://doi.org/10.1016/s0263-8223\(01\)00089-7](https://doi.org/10.1016/s0263-8223(01)00089-7)
103. Sreekumar PA, Joseph K, Unnikrishnan G, Thomas S (2007) A comparative study on mechanical properties of sisal-leaf fibre-reinforced polyester composites prepared by resin transfer and compression moulding techniques. *Compos Sci Technol* 67:453–461. <https://doi.org/10.1016/j.compscitech.2006.08.025>
104. Satapathy A, Patnaik A, Pradhan MK (2009) A study on processing, characterization and erosion behavior of fish (*Labeo rohita*) scale filled epoxy matrix composites. *Mater Des* 30:2359–2371. <https://doi.org/10.1016/j.matdes.2008.10.033>
105. Adhikari R, Bhandari NL, Le HH, Henning S, Radosch HJ, Michler GH, Garda MR, Saiter JM (2012) Thermal, mechanical and morphological behavior of poly(propylene)/wood flour composites. *Macromol Symp* 315:24–29. <https://doi.org/10.1002/masy.201250503>
106. Pal AK, Katiyar V (2017) Thermal degradation behavior of nanoamphiphilic chitosan dispersed poly(lactic acid) bionanocomposite films. *Int J Biol Macromol* 10:1267–1279. <https://doi.org/10.1016/j.ijbiomac.2016.11.024>
107. Kitagawa K, Ishiaku US, Mizoguchi M, Hamada H (2005) Bamboo-based ecomposites and their potential applications. In: Mohanty AK, Misra M, Drzal LT (eds) *Natural fibers biopolymers, and biocomposites*. CRC Press, Boca Raton, USA
108. Lee SH, Ohkita T, Kitagawa K (2004) Eco-composite from poly(lactic acid) and bamboo fiber. *Holzforschung* 58. <https://doi.org/10.1515/hf.2004.080>
109. Pinheiro IF, Ferreira FV, Souza DHS, Gouveia RF, Lona LMF, Morales AR, Mei LHI (2017) Mechanical, rheological and degradation properties of PBAT nanocomposites reinforced by functionalized cellulose nanocrystals. *Euro Polym J* 97:356–365. <https://doi.org/10.1016/j.eurpolymj.2017.10.026>
110. Pereda M, Amica G, Racz I, Marcovich NE (2011) Structure and properties of nanocomposite films based on sodium caseinate and nanocellulose fibers. *J Food Eng* 103:76–83. <https://doi.org/10.1016/j.jfoodeng.2010.10.001>
111. Ochi S (2008) Mechanical properties of kenaf fibers and kenaf/PLA composites. *Mechan Mater* 40:446–452. <https://doi.org/10.1016/j.mechmat.2007.10.006>
112. Kabir MM, Wang H, Lau KT, Cardona F (2012) Chemical treatments on plant-based natural fibre reinforced polymer composites: an overview. *Compos Part B: Eng* 43:2883–2892. <https://doi.org/10.1016/j.compositesb.2012.04.053>
113. Novotny C, Erbanova P, Sezimova, H, Malchova K, Rybkova Z, Malinova L, Prokopova I, Brozek J (2015) Biodegradation of aromatic-aliphatic copolyesters and polyesteramides by esterase activity-producing microorganisms. *Int Biodeter Biodegrad* 97:25–30. <https://doi.org/10.1016/j.ibiod.2014.10.010>
114. Siotto M, Zoia L, Tosin M, Innocenti FD, Orlandi M, Mezzanotte V (2013) Monitoring biodegradation of poly(butylene sebacate) by gel permeation chromatography, ¹H-NMR and ³¹P-NMR techniques. *J Environ Manage* 116:27–35. <https://doi.org/10.1016/j.jenvman.2012.11.043>
115. Sharma S, Singh I, Viridi JS (2003) Apotential *Aspergillus* species for biodegradation of polymeric materials. *Curr Sci* 84:1399–1402
116. Esmaeli A, Pourbabae AA, Alikhani HA, Shabani F, Esmaeili E (2013) Biodegradation of low-density polyethylene (LDPE) by mixed culture of *Lysinibacillus xylanilyticus* and *Aspergillus niger* in soil. *PLOS One* 8:1–10. <https://doi.org/10.1371/journal.pone.0071720>
117. Carrasco GC, Miettinen A, Hendriks CLL, Gamstedt EK, Kataja M (2011) Structural characterization of Kraft pulp fibres and their nanofibrillated materials for biodegradable composite applications. In: John C (ed) *Nanocomposites and polymers with analytical methods*, chap 10, pp 243–260. ISBN: 978-953-307-352-1 <https://doi.org/10.5772/21580>

118. Saxena M, Morchhale RK, Asokan P, Prasad BK (2008) Plant Fiber- Industrial waste reinforced polymer composites as a potential wood substitute material. *J Compos Mater* 42:367–384. <https://doi.org/10.1177/0021998307087014>
119. Cho MJ, Park BD, Kadla JF (2012) Characterization of electrospun nanofibers of cellulose nanowhisker/polyvinyl alcohol composites. *Mokchae Konghak* 40:71–77. <https://doi.org/10.5658/wood.2012.40.2.71>
120. Wu CS (2012) Characterization of cellulose acetate-reinforced aliphatic-aromatic copolyester composites. *Carbohydr Polym* 87:1249–1256. <https://doi.org/10.1016/j.carbpol.2011.09.009>
121. Faguaga E, Perez CJ, Villarreal N, Rodriguez ES, Alvarez V (2012) Effect of water absorption on the dynamic mechanical properties of composites used for windmill blades. *Mater Des* 36:609–616. <https://doi.org/10.1016/j.matdes.2011.11.059>
122. Li L, Ding S, Zhou C (2003) Preparation and degradation of PLA/chitosan composite materials. *J Appl Polym Sci* 91:274–277. <https://doi.org/10.1002/app.12954>
123. Shi B, Shlepr M, Palfery D (2011) Effect of blend composition and structure on biodegradation of starch/Ecoflex-filled polyethylene films. *J Appl Polym Sci* 120:1808–1816. <https://doi.org/10.1002/app.33309>
124. Chieng BW, Ibrahim NA, Yunus WMZW (2010) Effect of organo-modified montmorillonite on poly(butylene succinate)/poly(butylene adipate-co-terephthalate) nanocomposites. *eXPRESS Polym Lett* 4:404–414. <https://doi.org/10.3144/expresspolymlett.2010.51>
125. Panaitescu DM, Frone AN, Ghiurea M, Spataru CI, Radovici C, Iorga MD (2011) Properties of polymer composites with cellulose microfibrils. In: Brahim A (ed) *Advances in composites materials-ecodesign and analysis*, vol 5, pp 103–122. ISBN: 978-953-307-150-3. <https://doi.org/10.5772/14682>
126. Cho J, Joshi MS, Sun CT (2006) Effect of inclusion size on mechanical properties of polymeric composites with micro and nano particles. *Compos Sci Technol* 66:1941–1952. <https://doi.org/10.1016/j.compscitech.2005.12.028>
127. Yang Y, Lan J, Li X (2006) Study on bulk aluminum matrix nano-composite fabricated by ultrasonic dispersion of nano-sized SiC particles in molten aluminum alloy. *Mater Sci Eng A* 380:378–383. <https://doi.org/10.1016/j.msea.2004.03.073>
128. Paul DR, Robeson LM (2008) Polymer nanotechnology: nanocomposites. *Polymer* 49:3187–3204. <https://doi.org/10.1016/j.polymer.2008.04.017>
129. Birinchi L, Cotana F, Fortunati E, Kenny JM (2013) Production of nanocrystalline cellulose from lignocellulosic biomass: technology and applications. *Carbohydr Polym* 94:154–169. <https://doi.org/10.1016/j.carbpol.2013.01.033>
130. Dhakal HN, Zhang ZY, Bennett N (2012) Influence of fibre treatment and glass fibre hybridisation on thermal degradation and surface energy characteristics of hemp/unsaturated polyester composites. *Compos Part B Eng* 43:2757–2761. <https://doi.org/10.1016/j.compositesb.2012.04.036>
131. Spiridon I, Darie RN, Kangas H (2016) Influence of fiber modifications on PLA/fiber composites: behavior to accelerated weathering. *Compos Part B Eng* 92:19–27. <https://doi.org/10.1016/j.compositesb.2016.02.032>
132. Dai X, Xiong Z, Na H, Zhu J (2014) How does epoxidized soybean oil improve the toughness of microcrystalline cellulose filled polylactide acid composites? *Compos Sci Technol* 90:9–15. <https://doi.org/10.1016/j.compscitech.2013.10.009>
133. Michler GH, Balta-Calleja FJ (2012) *Nano- and micromechanics of polymers: structure modification and improvement of properties*. Hanser Verlag Munich. ISBN-13: 978-1569904602, ISBN-10: 156990460X
134. Hassan MM, Wagner MH, Zaman HU, Khan MA (2011) Study on the performance of hybrid Jute/Betel nut fiber reinforced polypropylene composites. *J Adh Sci Technol* 25:615–626. <https://doi.org/10.1163/016942410x525858>
135. Wan YZ, Luo H, He F, Liang H, Huang Y, Li XL (2009) Mechanical, moisture absorption, and biodegradation behaviours of bacterial cellulose fibre-reinforced starch biocomposites. *Compos Sci Technol* 69:1212–1217. <https://doi.org/10.1016/j.compscitech.2009.02.024>

136. Tesfaye M, Patwa R, Dhar P, Katiyar V (2017) Nanosilk-grafted poly(lactic acid) films: Influence of cross-linking on rheology and thermal stability. *ACS Omega* 2:7071–7084. <https://doi.org/10.1021/acsomega.7b01005>
137. Singh B, Sharma N (2008) Mechanistic implications of plastic degradation. *Polym Degrad Stab* 93:561–584. <https://doi.org/10.1016/j.polymdegradstab.2007.11.008>
138. Liu Y, Li Y, Chen H, Yang G, Zheng X, Zhou S (2014) Water-induced shape-memory poly(D,L-lactide)/microcrystalline cellulose composites. *Carbohydr Polym* 104:101–108. <https://doi.org/10.1016/j.carbpol.2014.01.031>
139. Itry RA, Lamnawar K, Maazouz A (2012) Improvement of thermal stability, rheological and mechanical properties of PLA, PBAT and their blends by reactive extrusion with functionalized epoxy. *Polym Degrad Stab* 97:1898–1914. <https://doi.org/10.1016/j.polymdegradstab.2012.06.028>
140. Dvorackova M, Stloukal P, Koutny M, Gregovska M (2011) Biodegradability of aliphatic-aromatic copolyester in aqueous anaerobic and aerobic environments. In: *Recent advances in environment, energy system and naval science—Proceedings of the 4th international conference on environmental and geological science and engineering*. TBU Publications, pp 141–146. ISBN: 9781618040329
141. Giri J (2019) Wheat stalk micro- and nanocellulose based degradable polymer composites: morphology, mechanical and degradation behaviour. Ph.D. thesis submitted to Institute of Science and Technology, Tribhuvan University, Kathmandu, Nepal

Chapter 14

DSC and SWAXS Studies on the Effects of Silk Nanocrystals on Crystallization of Poly(L-Lactic Acid)



Amit Kumar Pandey, Pham Thi Ngoc Diep, Rahul Patwa, Vimal Katiyar, Sono Sasaki and Shinichi Sakurai

Abstract Poly (L-lactic acid) (PLLA) is one of the most frequently used biobased polyesters due to its favorable mechanical properties. However, some properties such as slow crystallization rate and low crystallinity restrict its commercial uses. In order to overcome these limitations, organic nanofillers are incorporated into the PLLA matrix. Herein, we report the use of silk nanocrystal (SNC) as a solid-state nucleation agent, which has been prepared in the laboratory from the wastes of the muga silk cocoon. PLLA/SNC composites with 1.0 wt% loadings of SNC have been prepared by solution casting with dichloromethane as a cast solvent. Isothermal crystallization kinetics at 110 °C has been studied by the differential scanning calorimetry (DSC) and small- and wide-angle X-ray scattering (SWAXS) upon quenching from melt (200 °C for 5 min). As a result, it is found that loading SNC with 1.0 wt% caused the reduction of the induction period, the acceleration of crystallization, the increase of the final value of the degree of crystallinity, and the acceleration of lamellar thickening. These experimental results can be explained by the fact that the regular folding of the polymer chains is attained by the loading of SNC.

Keywords Poly (L-lactic acid) · Silk nanocrystal · Small- and wide-angle X-ray scattering · Crystallization

1 Introduction

Poly(L-lactic acid) (PLLA) has received much more attention recently due to its biodegradability and high mechanical strength. However, some properties such as slow crystallization rate and low crystallinity are the main disadvantages that restrict its wider applications. To overcome these drawbacks, a number of fillers (in the solid state: talc, sodium stearate and calcium lactate, etc. [1], or small amount of

A. K. Pandey · P. T. N. Diep · S. Sasaki · S. Sakurai (✉)

Department of Biobased Materials Science, Kyoto Institute of Technology, Kyoto 606-8585, Japan
e-mail: shin@kit.ac.jp

R. Patwa · V. Katiyar

Department of Chemical Engineering, Indian Institute of Technology Guwahati, Guwahati, Assam 781039, India

© Springer Nature Singapore Pte Ltd. 2020

V. Katiyar et al. (eds.), *Advances in Sustainable Polymers*, Materials Horizons: From Nature to Nanomaterials, https://doi.org/10.1007/978-981-15-1251-3_14

plasticizer [2]) have been investigated over the past few decades to enhance the crystallization rate of PLLA. Especially, it is highly requested for manufacturers to attain the complete crystallization within the processing duration; otherwise, the gradual crystallization would take place in the processed materials which results badly in cracking or tightening of wound fibers and films due to the shrinkage of the materials. Therefore, it is very important to prevent such drawbacks by improving the crystallization abilities of PLLA. In other words, the crystallization of PLLA is desired to be completed within several seconds.

Another important aspect is that the fillers are required to be biobased and biodegradable. Very recently, some of our co-authors have reported that silk nanocrystal (SNC) can improve crystallizability of PLLA [3]. In this regard, we focus on the effects of SNC on the crystallization of PLLA in this study by conducting differential scanning calorimetry (DSC) and the time-resolved small- and wide-angle X-ray scattering (SWAXS). The SNC used for this investigation was prepared in the laboratory from the wastes of the muga silk (*Antheraea assama*) cocoon by modified acid hydrolysis process [3]. The crystalline portion (the β -sheets of the silk fibroin) was isolated, and the well-defined disklike particles were obtained. Such morphology and dimensions have been reported in the previous report [3], 20–80 nm in diameter (the average diameter of ~ 45 nm) and 2–5 nm in thickness. The degree of crystallinity in SNC was calculated from the X-ray diffraction data $\sim 93.7\%$. It is needless to say that SNC is hydrophobic and biocompostable.

It should be further noted that very quick cooling is highly required in this study in order to match the experimental condition to ordinary process condition (cooling with ~ 500 °C/min), for which a conventional DSC apparatus is useless. For such a purpose, we have utilized a special type DSC apparatus [DSC214 Polyma (NETZSCH, Germany)], which enabled us to facilitate the cooling with ~ 300 °C/min.

2 Experimental

We used a PLLA sample that was purchased from NatureWorks LLC with 0.5% D-moiety (2500 HP) (D0.5). The melt flow rate (MFR) test was conducted at 210 °C with the standard weight of 2.16 kg. The result was 8.0 g, which corresponds to the M_w (weight-average molecular weight) = 1.74×10^5 [2]. The SNC used for this investigation was prepared in the laboratory from waste muga silk (*A. assama*) by modified acid hydrolysis process [3]. The crystalline portion (the β -sheets of the silk fibroin) was isolated, and the well-defined disklike particles were obtained. Such morphology and dimensions have been reported in the previous report [3].

The isothermal crystallization process was followed by DSC and SWAXS. The DSC measurements were performed on DSC214 Polyma (NETZSCH, Germany). About 5.1–5.2 mg of the specimen was sealed in the Al pan, and it was first heated up to 200 °C with 10 °C/min from room temperature (RT), kept isothermally at 200 °C for 10 min, followed by quick cooling to 110 °C with the cooling rate of 308 °C/min for the isothermal crystallization (see Fig. 1 for the change in temperature). The

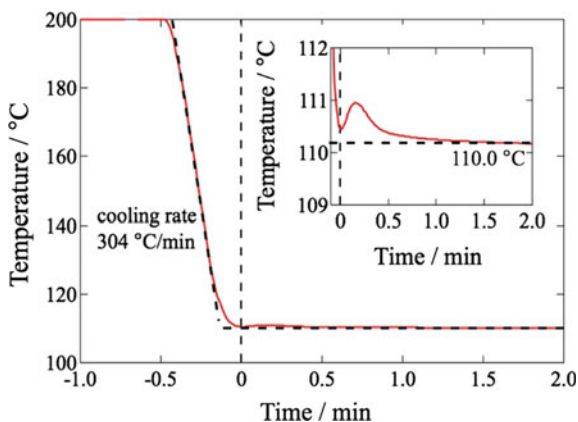


Fig. 1 Change in the temperature of DSC measurement for the isothermal crystallization upon cooling from 200 °C to 110 °C

specimen was purged with nitrogen gas (50 mL/min) during the DSC measurement.

The experimental setup of the SWAXS measurements is shown in Fig. 2. The stacked specimens with the total thickness being nearly 1 mm were sandwiched between 2 pieces of the Kapton film (thickness: 25 μm , DuPont-Toray Co., Ltd., Japan), and the sample cell was sealed. To measure the exact specimen temperature

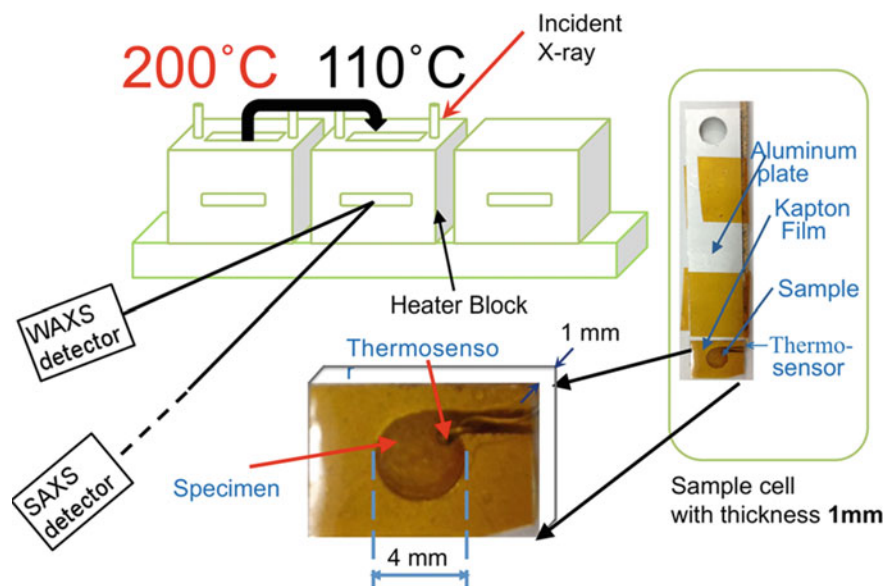
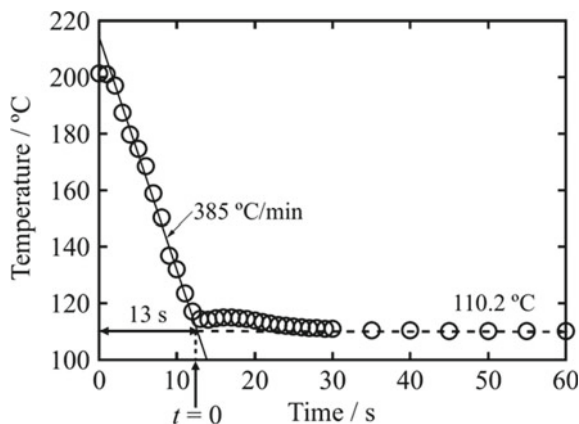


Fig. 2 Experimental setup of the time-resolved SWAXS measurements for the isothermal crystallization (adapted from reference [2] with a permission)

Fig. 3 Change in temperature of the time-resolved SWAXS measurements for the isothermal crystallization upon cooling from 200 °C to 110 °C (adapted from reference [2] with a permission)



for the T-jump from melt to the crystallization temperature for the isothermal crystallization, a thermosensor (K type) was inserted directly into the specimen. From RT, the specimen was heated to 200 °C. Then, the specimen was isothermally maintained for approximately 10 min to allow the specimen to melt completely. By quickly moving the sample cell to the SWAXS heater block maintained at 110 °C, the time-resolved measurements were started. The change in temperature of the specimen upon the T-jump from 200 to 110 °C is shown in Fig. 3 from which the cooling rate was found 385 °C/min. Thus, the cooling rates almost match each other for the DSC and SWAXS experiments. Note here that it took only 13 s to equilibrate temperature at 110 °C from melt at 200 °C.

We conducted the time-resolved SWAXS measurements to follow the isothermal crystallization with an exposure time of 5 s at BL-6A of the Photon Factory in High Energy Accelerator Research Organization, Tsukuba, Japan, using the two-dimensional detector PILATUS 100 K for WAXS and PILATUS 1 M for SAXS (DECTRIS Ltd., Baden, Switzerland). The WAXS and SAXS detectors were set at 40 mm and 2 m, respectively, from the sample position (heater block). The X-ray wavelength was 0.150 nm. Refer to the literature [4] for more details of the SAXS beamline BL-6A.

2.1 Results and Discussion

Figure 4 shows the change in the WAXS patterns with time for the D0.5 neat specimen. Here, q denotes the magnitude of the scattering vector, as defined by $q = 4\pi/\lambda \sin(\theta/2)$ with λ and θ being the wavelength of X-ray and the scattering angle, respectively. At 12 s, elapsed from $t = 0$ (shown in Fig. 3), no crystalline peak was observed and the amorphous halo peak was merely seen. This fact clearly ensures the amorphous state and the crystallization yet set in at 12 s. This further suggests that the induction period is longer than 12 s. On the contrary, after the elapse of 37 s, a

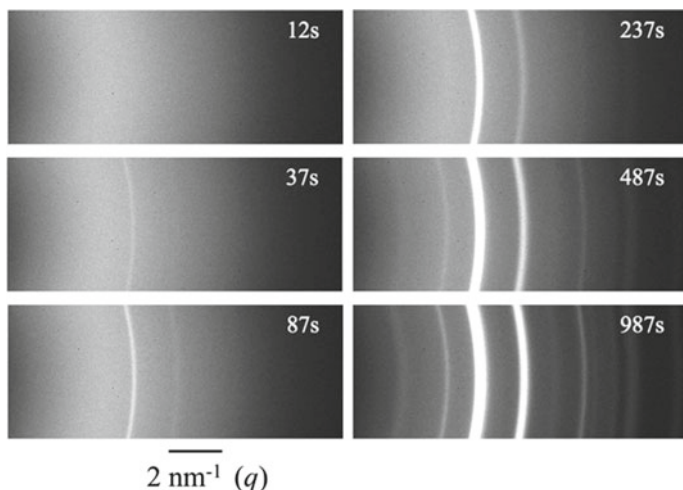


Fig. 4 Changes in the WAXS patterns with time for the D0.5 neat specimen

crystalline peak was observed, indicating that the crystallization had started. As time goes on, the intensity of the peak increased and the number of the crystalline peaks was increased. By conducting the sector average, the one-dimensional WAXS profile was obtained. A close examination of the change in the WAXS profiles revealed that the induction period for the D0.5 neat specimen was 17.5 s.

Figure 5 shows the apparent degree of crystallinity (ϕ_{WAXS}) as a function of time for the neat D0.5 and D0.5/SNC(1.0) specimens, where ϕ_{WAXS} was evaluated as:

$$\phi_{\text{WAXS}} = \frac{\sum A_c}{\sum A_c + A_a} \quad (1)$$

with A_c and A_a being the peak areas of the crystalline and the amorphous halo peaks. These peak areas were evaluated by conducting the computational peak decomposition [2, 5]. It is clear that the temporal increasing rate of ϕ_{WAXS} is much larger for the D0.5/SNC(1.0) specimen than that for the neat D0.5 specimen, indicating the acceleration ability of SNC for the PLLA crystallization. However, it is difficult, unfortunately, to make quantitative evaluation of the induction period from the plots shown in Fig. 5b.

Figure 6 shows plots of the $d_{200/110}$ spacing for the main reflection peak (200/110) as a function of time for the D0.5 neat and D0.5/SNC(1.0) specimens, where d is evaluated from the position (q^*) of the reflection peak (200/110), as $d_{200/110} = 2\pi/q^*$. It is interesting to see that the d spacing decreased with time, indicating the densification of crystallites as a function of time. In other words, this fact indicates the shrinkage of a crystalline region. This further suggests that the packing of the polymer chains is loose in the early stage, and then the loose packing becomes tight.

Figure 7 shows the DSC exothermic results as a function of time upon the isother-

Fig. 5 Plots of the apparent degree of crystallinity (ϕ_{WAXS}) as a function of time for the D0.5 neat and D0.5/SNC(1.0) specimens

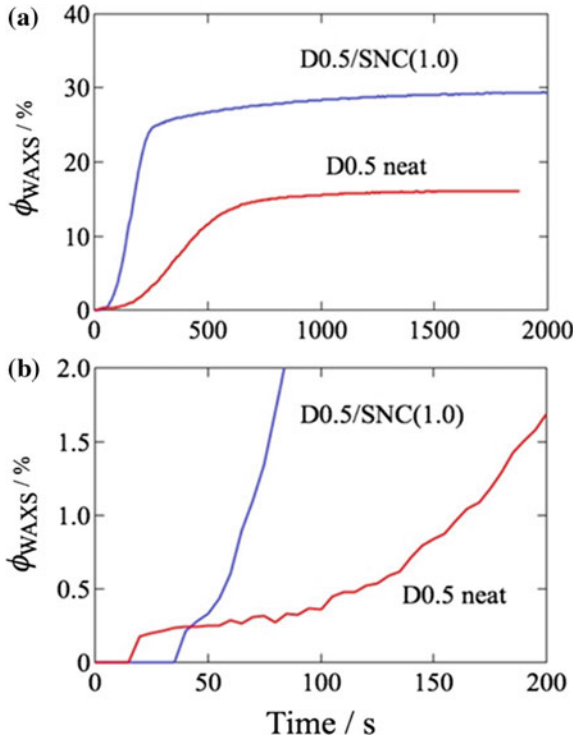
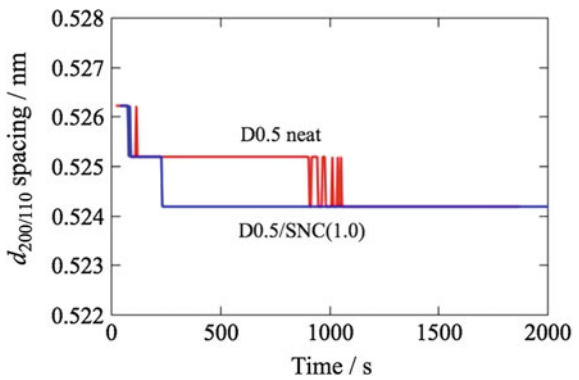


Fig. 6 Plots of the d spacing for the main reflection peak (200/110) as a function of time for D0.5 neat and D0.5/SNC(1.0) specimens



mal crystallization initiated by T-jump from 200 to 110 °C. The following facts were found: shorter induction period, faster crystallization, and the higher total exotherm (the higher final degree of crystallinity) for the D0.5/SNC(1.0) specimen as compared to the neat D0.5 specimen. These results are in good accord with the WAXS results, indicating the acceleration ability of SNC for the PLLA crystallization. Especially, it is noteworthy that such a shorter induction period was determined by our DSC

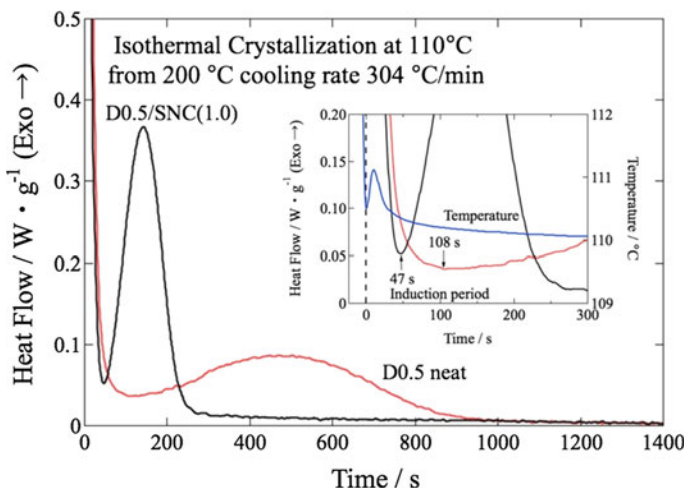


Fig. 7 DSC exothermic results as a function of time of the isothermal crystallization upon T-jump from 200 °C to 110 °C

experiments. This is because the cooling rate was available as high as 300 °C/min by using the DSC214 Polyma (NETZSCH). However, the induction period determined by DSC was longer than that evaluated by WAXS results. The reason for this discrepancy is not clear at present. Furthermore, it is important to note that the final degree of crystallinity is higher for the D0.5/SNC(1.0) specimen than for the neat D0.5 specimen. This result is noteworthy from the perspective of the shrinkage of a PLLA cup by pouring hot water which may be due to the low degree of crystallinity of the PLLA cup. The shrinkage would be prevented by increasing the degree of crystallinity by loading SNC.

Figure 8 shows the plots of the degree of crystallinity (ϕ_{DSC}) as evaluated from the DSC results as a function of time. As stated above, it was found that the crystallizability of PLLA (D0.5 specimen) has been improved by the addition of 1% SNC. Namely, the induction period was reduced, the rate of the crystallization (judging from the slope of the plot of Fig. 8, as well as from the crystallization half time) was accelerated, and the final value of the crystallinity (ϕ_{DSC}) was increased by the addition of 1% SNC.

Based on ϕ_{WAXS} and ϕ_{DSC} , it is possible to check quantitatively the crystallization behavior of PLLA by the Avrami plot, which is shown together in Fig. 9. According to the Avrami theory [7, 8], the crystallization proceeds by the following kinetic equation:

$$\phi(t) = \{1 - \exp[-(kt)^n]\} \times \phi^\infty \quad (2)$$

where $\phi(t)$ is the volume fraction of the crystalline region (the degree of crystallinity, but not in the unit of %) in the specimen as a function of time and ϕ^∞ is the degree

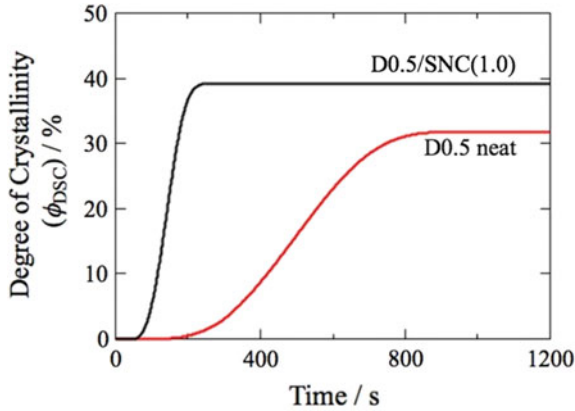


Fig. 8 Plots of the degree of crystallinity (ϕ_{DSC}) as evaluated from the DSC results as a function of time (adapted from reference [6] with a permission)

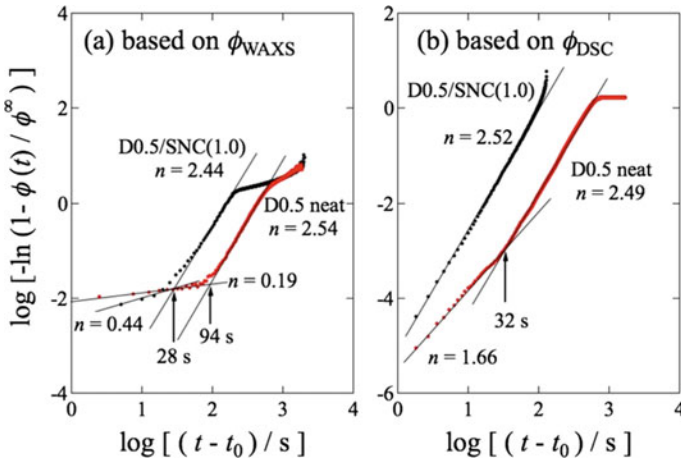


Fig. 9 Avrami plots based on **a** ϕ_{WAXS} and **b** ϕ_{DSC} for D0.5 neat and D0.5/SNC(1.0) specimens (adapted from reference [6] with a permission)

of crystallinity in the completely crystallized specimen. This equation gives

$$\log[-\ln(1 - \phi(t)/\phi^\infty)] = n[\log t + \log k] \tag{3}$$

By substituting ϕ_{WAXS} or ϕ_{DSC} into $\phi(t)$ in the Avrami equation ($\phi(t) = \phi_{WAXS}(t)/100$ or $\phi(t) = \phi_{DSC}(t)/100$), the Avrami plots as shown in Fig. 9 were demonstrated. Here, it should be noted that the induction period (t_0) is subtracted in these plots as $\log(t - t_0)$ for abscissa instead of $\log t$. In the Avrami equation, n is

the Avrami exponent, based on which the dimensionality of the crystal growth can be discussed.

The similar values of the Avrami exponent (n) and the similar tendencies of the Avrami plots are obtained in Fig. 9a (from WAXS) and 9b (from DSC). It is clearly observed that the Avrami plots are bent with a lower and a higher slope for the earlier and later stages of crystallization, except for the D0.5/SNC(1.0) specimen (DSC result). This phenomenon has been already reported in our previous publications [2, 6]. This may indicate the change in the crystallization mode during the crystallization, i.e., the lower- to higher-dimensional crystallization. Upon addition of SNC, the crystallization was accelerated. On the contrary, the Avrami exponent n is more or less unchanged upon the addition of SNC.

The changes in the Lorentz-corrected SAXS profiles upon T-jump from 200 to 110 °C are shown in Fig. 10. Here, the scattering intensity, $I(q)$, is corrected as $q^2I(q)$ by multiplying q^2 . In the initial stage, there was no peak. At the onset of crystallization, the peak appeared in the profile, which indicates the formation of the stacks of the lamellar crystallites sandwiching the amorphous layers. From the peak position, it was possible to evaluate the long period (D) of the lamellar stacks, as $D = 2\pi/q^*$ where q^* denotes the peak position. The peak is found to move toward higher q as the crystallization proceeds, which suggests a decrease in D . However, this result is strange and seemed to be opposed to the process of crystallization. In order to understand the reason, we evaluated the thickness of the crystalline lamella from the SAXS results according to the inverse Fourier transform method [2, 9].

$$\gamma(r) = \frac{\int_0^\infty I(q)q^2 \cos(qr) dq}{\int_0^\infty I(q)q^2 dq} \quad (4)$$

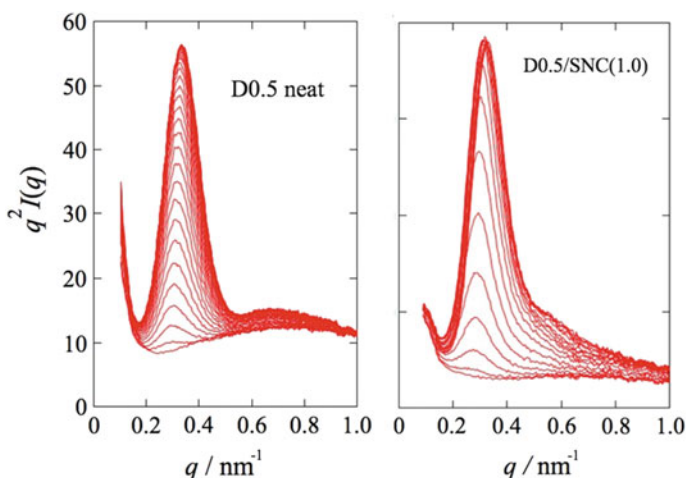


Fig. 10 Changes in the Lorentz-corrected SAXS profiles upon T-jump from 200 to 110 °C for D0.5 neat and D0.5/SNC(1.0) specimens

Here, $\gamma(r)$ is the correlation function and r is the distance in the real space. Note that to conduct the integrations in Eq. 4, the scattering intensity ($I(q)$) as a function of q should cover the whole range of q from 0 to infinity. However, the real $I(q)$ only covers the limited range. Therefore, it is required to extend the regions of smaller q toward 0 and higher q toward infinity. For the extrapolation of $I(q)$ for $q \rightarrow 0$, Guinier's law is used, i.e.,

$$I(q) = I(0) \times \exp(-k_1 q^2) \quad (5)$$

where $I(0)$ is the scattering intensity at $q = 0$ and k_1 is a constant. As for the extrapolation of $I(q)$ for $q \rightarrow \infty$, Porod's law is used, i.e.,

$$I(q) = k_2 q^{-4} \quad (6)$$

where k_2 is a constant. Using these extrapolations, the scattering function for the whole q range can be obtained as shown in Fig. 11a. Then, the correlation function $\gamma(r)$ was evaluated as shown in Fig. 11b. For comparison, the $\gamma(r)$ evaluated directly from the experimentally obtained $I(q)$ with the limited q range is shown together in Fig. 11b. It is clear that the $\gamma(r)$ shape is very much different as compared to the $\gamma(r)$ evaluated from the extrapolated $I(q)$. However, the purpose of the evaluation $\gamma(r)$ is to evaluate the thickness of the crystalline lamella (L) and the repeating distance of the lamellar stacks (D). As indicated in Fig. 11b, L is evaluated by the linear approximation of the curve of $\gamma(r)$ in the small r range where $\gamma(r)$ decreases down to the minimum point. L is the value of r at the crossing point of this approximated line with the horizontal line passing through the minimum point of $\gamma(r)$. As for D , it is straightforwardly evaluated as the value of r at the first maximum point of $\gamma(r)$. These methods are illustrated in Fig. 11b, and it is recognized that the evaluated values of L and D are almost similar to each other from the $\gamma(r)$ curve obtained by the extrapolated $I(q)$ and from that obtained by the experimentally measured $I(q)$ with the limited q range. For the sake of simple treatment of the data processing, it is not necessary to extrapolate $I(q)$ for the purpose of the evaluation of L and D .

Figure 12 shows thus evaluated L and D and the ratio (L/D) as a function of time upon T-jump from 200 to 110 °C for D0.5 neat and D0.5/SNC(1.0) specimens. As stated above, D decreased as a function of time. On the other hand, L increased with time, which is reasonable as a crystallization behavior. Therefore, the strange behavior of D decreasing with time should be considered as follows. Upon crystallization, the shrinkage takes place, as shown in Fig. 13b. The lamellar thickness increases with time, resulting in more shrinkage (Fig. 13c), and therefore the decrease in D (Fig. 13b', c') is induced. Thus, our experimental results can be accounted for.

It should be noted here that L did not monotonically increase with turning over its tendency around 650 s for the D0.5 neat specimen or around 200 s for the D0.5/SNC specimen. The reason why L decreased a bit before reaching a constant value is not clear. The d spacing for the main reflection peak (200/110) showing the decreasing tendency in Fig. 6 suggests a continuous shrinkage of the crystalline region. This fact may explain the strange tendency of L . Namely, monotonically increasing L

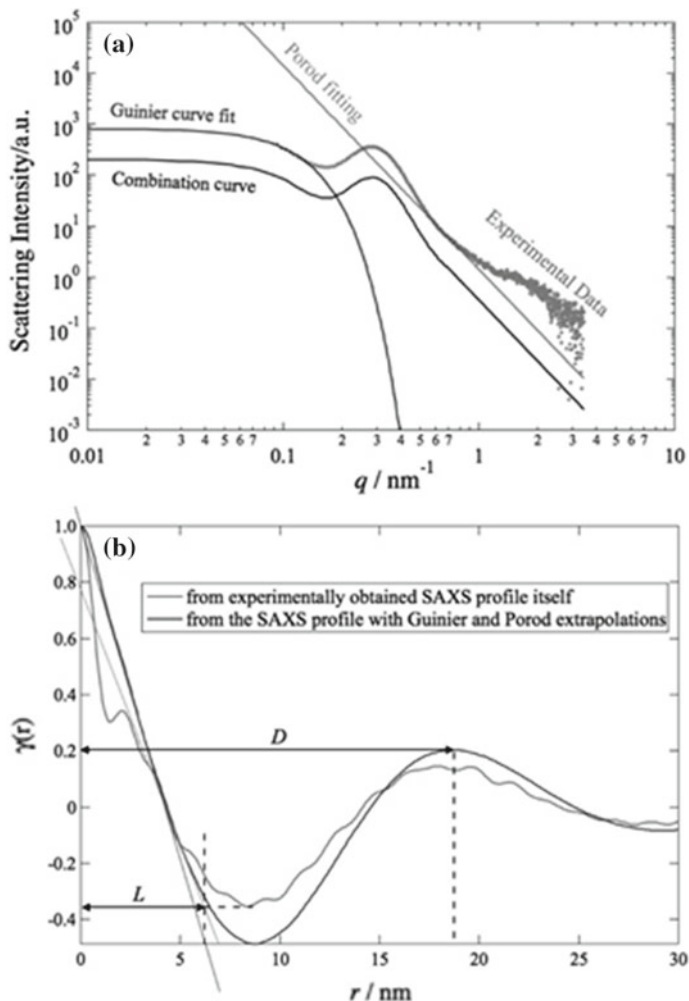
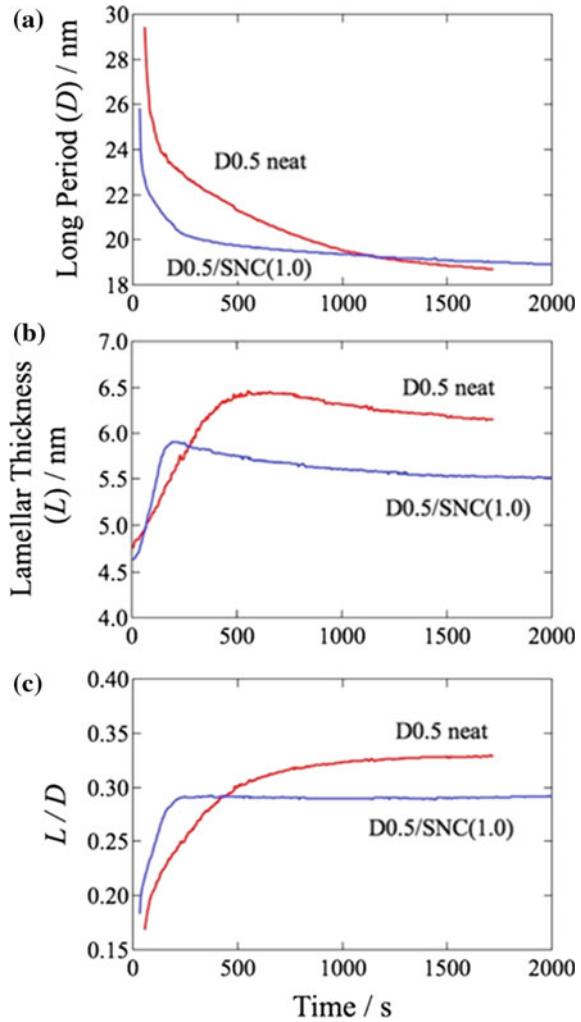


Fig. 11 **a** Guinier and Porod extrapolations for the experimentally obtained SAXS profile. **b** Correlation functions obtained with two different types of data analyses (adapted from reference [2] with a permission)

leveled off around 650 s (or 200 s), and then it turned into a bit of decreasing due to the shrinkage of the crystalline region. Unfortunately, it was found that the strange tendency of L cannot be perfectly accounted for by the effect of the shrinkage of the crystalline region. Another plausible explanation is the improvement of the chain folding in a crystalline lamella where the chain folding is less regular in the early to intermediate stage because of quick crystallization. Namely, due to quick crystallization, the polymer chains fold in irregular fashion by including many defects in the early to intermediate stages of crystallization where L increases continuously.

Fig. 12 Plots of **a** long period (D), **b** lamellar thickness (L), and **c** the ratio (L/D) as a function of time upon T-jump from 200 to 110 °C for D0.5 neat and D0.5/SNC(1.0) specimens, as analyzed by SAXS results



At the stage of the termination of the increasing L , the irregular folding of the polymer chains is improved with annihilation of defects in the lamella, which results in the reduction of L . Thus, L turns into decreasing and exhibits overshooting.

This illustrates an early stage of polymer crystallization. The ratio of L and D (L/D) can be a degree of crystallinity in a lamellar stack. The behavior of L/D as a function of time is displayed in Fig. 12, showing a monotonic increase with time, and finally leveled off. This is very much contrasted with the behavior of L which shows the overshooting. Namely, division by D changes the strange behavior of L to a reasonable behavior as a degree of crystallinity. However, the behavior of L/D is very much different from the behavior of ϕ_{WAXS} (Fig. 5) or ϕ_{DSC} (Fig. 8). The reason why L/D is larger than ϕ_{WAXS} or ϕ_{DSC} value is because the lamellar stacks are

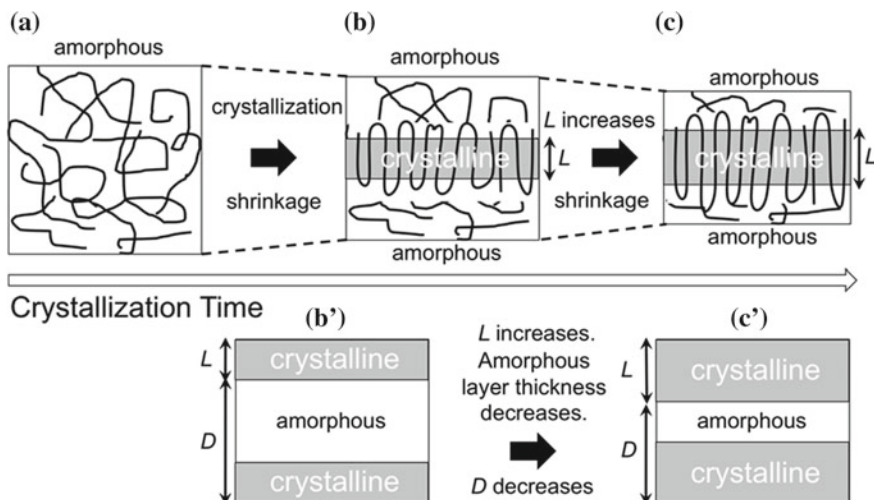


Fig. 13 Schematic illustrations showing the change in the nanostructure upon crystallization of PLLA. **a** At the amorphous state before crystallization of the polymer melt, **b** in an early stage of crystallization, and **c** lamellar thickening in the subsequent stage of the crystallization. Note the illustrations focusing on the change in the long period (D) of the lamellar stacks. **b'** and **c'** correspond to the states of **b** and **c**, respectively. The illustrations of **b'** and **c'** are intended to explain the reason why D decreases as a function of time along the proceeding of crystallization where L increases with time (adapted from reference [5] with a permission)

sparingly dispersed in the matrix of polymer melts and they do not completely fill the specimen space in the early stage. Such situation is illustrated in Fig. 14. Then, the lamellar stacks become completely filling the space in the specimen in the late stage. It is noted here that the L/D values for the D0.5/SNC(1.0) specimen in the late stage are lower than those for the D0.5 neat specimen. This result is completely opposed to the results of SWAXS and DSC. This may indicate that there are many individual crystalline regions which are not included in the stacks of lamellar crystallites in the D0.5/SNC(1.0) specimen

Finally, we try to explain the effects of SNC, which are the reduction of the induction period, the acceleration of crystallization, the increase of the final value of the degree of crystallinity, and the acceleration of lamellar thickening. Patwa et al. [3] have reported the values of the surface free energy (σ_e) of the upper and lower planes of a lamellar crystallite, which are composed of the folding of polymer chains. It is reported that the value becomes smaller upon the loading of SNC. This suggests that the chain folding becomes more regular upon the loading of SNC, as illustrated in Fig. 15. According to the Hoffman–Lauritzen theory [11], the free energy change (ΔG) upon the formation of the primary nucleus can be demonstrated as a function of the thickness of a primary nucleus (l) and the number of stems in the primary nucleus (v).

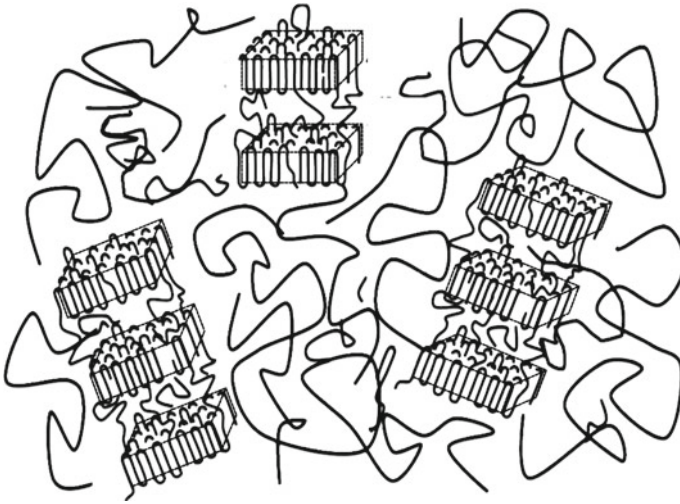


Fig. 14 Schematic illustration of the sparsely distributed lamellar stacks in the matrix of polymer melts in an early stage of polymer crystallization (adapted from reference [10] with a permission. The figure has been slightly modified)

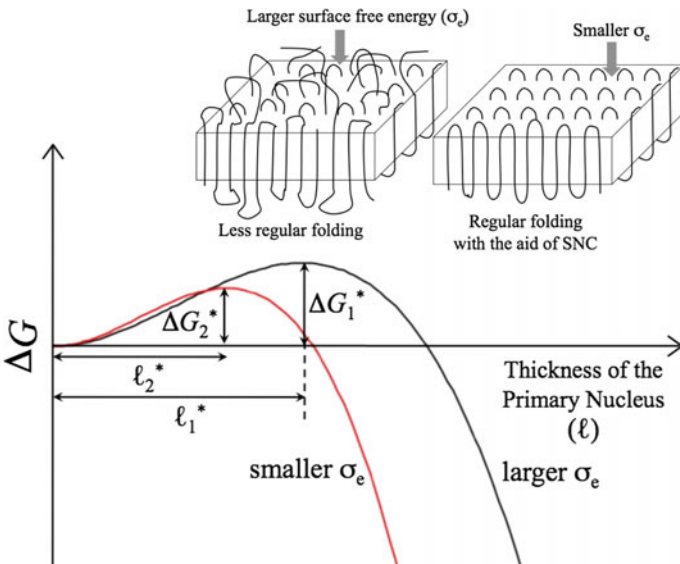


Fig. 15 Free energy change upon the formation of the primary nucleus as a function of the thickness of the primary nucleus according to the Hoffman–Lauritzen theory for cases of larger and smaller surface free energies (σ_e), which, respectively, correspond to poor regular folding and better regular folding with the aid of SNC

$$\Delta G = 2va\sigma_e + c(va)^{0.5}l\sigma_s - val\Delta g \quad (7)$$

where a denotes the cross section of the stem, c is the number of the side faces of the nucleus, σ_s is the surface free energy of the side plane of the nucleus, to which the stems are parallel, and $\Delta g (= \Delta h - T\Delta s)$ is the free energy gain upon the crystallization per unit volume. Δh , T , and Δs are the enthalpy of fusion per unit volume, the absolute temperature, and the entropy change upon crystallization per unit volume, respectively. The first term of the right-hand side of Eq. 7 is the energy increment due to the formation of the upper and lower planes of the lamellar nucleus from melt, while the second term is the energy increment due to the formation of the side planes of the lamellar nucleus from melt where $(va)^{0.5}$ stands for an edge length of the nucleus. The third term explains the energy decrement due to the formation of the crystalline region (nucleus). From Eq. 7, the following results are obtained as the thickness and the edge length of the critical nucleus:

$$l^* = 4\sigma_e/\Delta g, \quad (v^*a)^{0.5} = c\sigma_s/\Delta g \quad (8)$$

and thus,

$$(v^*a)^{0.5} = kl^* \quad (9)$$

with

$$k = c\sigma_s/(4\sigma_e) \quad (10)$$

Equation 9 suggests that the critical value l^* can be obtained from ΔG by substituting $(va)^{0.5} = kl$ into Eq. 7. Then, the following relationship for ΔG is obtained.

$$\Delta G = 2k^2l^2\sigma_e + ckl^2\sigma_s - k^2l^3\Delta g \quad (11)$$

To draw the ΔG curve, $\sigma_s = 15.4 \times 10^{-3} \text{ J/m}^2$ and $\sigma_e = 30.7 \times 10^{-3} \text{ J/m}^2$ which are reported in the literature [3] are used for modeling the PLLA neat specimen. Letting $c = 4$, then $k = 0.501$ is obtained. Furthermore, to adjust l^* at 4.8 nm (see Fig. 12) in Eq. 8, $\Delta g = 4\sigma_e/l^* = 2.56 \times 10^7 \text{ J/m}^3$ should be used and then the black curve in Fig. 15 is drawn. On the contrary, $\sigma_e = 21.4 \times 10^{-3} \text{ J/m}^2$ is reported for the PLLA/SNC(1.0) specimen in the same literature [3]. The decrease in σ_e suggests the more regular chain folding in the lamellar crystallites by loading the SNC with 1.0 wt%, as schematically shown in Fig. 15. Using $\sigma_e = 21.4 \times 10^{-3} \text{ J/m}^2$, $k = 0.720$ is obtained and these values are substituted in Eq. 11. Then, the red curve in Fig. 15 is drawn. It is found that the loading of SNC caused the reduction of the critical lamellar thickness ($l_2^* < l_1^*$), the lowering of the height of the energy barrier ($\Delta G_2^* < \Delta G_1^*$), and the slight increase of the curvature of the free energy curve beyond the critical point. Note here that from $l^* = 4\sigma_e/\Delta g$ in Eq. 8, the thickness

of the critical nucleus can be scaled as $l_1^*/l_2^* = \sigma_{e1}/\sigma_{e2}$. By substituting $l^* = 4 \sigma_e/\Delta g$ into Eq. 11, $\Delta G = 2 (c\sigma_s/\Delta g)^2 \sigma_e$ is obtained. Thus, the energy barrier also can be scaled as $\Delta G_1^*/\Delta G_2^* = \sigma_{e1}/\sigma_{e2}$. Note that $\sigma_{e1}/\sigma_{e2} = 30.7/21.4 = 1.43$. The reduction of the critical lamellar thickness results in the increase of the number of nuclei and eventually in the increase of the final crystallinity. It may also result in the reduction of the induction period. The lowering of the height of the energy barrier results also in the reduction of the induction period. Finally, the increase of the curvature of the ΔG curve beyond the critical point results in the acceleration of lamellar thickening. Thus, the lowering of σ_e upon the loading of SNC can explain all of the experimental results.

For the case of loading of the nucleation agent, the formation of nucleus seems to be different from the primary nucleation. Namely, the secondary nucleation of the Hoffman–Lauritzen theory [11] is more or less appropriate. For this case, ΔG is given by

$$\Delta G = 2 d w \sigma_e + 2 d l \sigma_s - d w l \Delta g \quad (12)$$

where d denotes the distance between the adjacent polymer chains (stems) in the nucleus in the direction perpendicular to the surface of the nucleation agent and w denotes the lateral size of the secondary nucleus (note $w \perp l$). The first term of the right-hand side of Eq. 12 is the energy increment due to the formation of the upper and lower planes of the secondary nucleus, while the second term is the energy increment due to the formation of the side planes of the secondary nucleus. The third term explains the energy decrement due to the formation of the crystalline region (nucleus). From Eq. 12, the following results are obtained as the thickness and the lateral size of the critical secondary nucleus:

$$l^* = 2 \sigma_e/\Delta g, \quad w^* = 2 \sigma_s/\Delta g \quad (13)$$

and thus,

$$w^* = (\sigma_s/\sigma_e) l^* \quad (14)$$

Equation 14 suggests that the critical value l^* can be obtained from ΔG by substituting $w = (\sigma_s/\sigma_e) l$ into Eq. 12. Then, the following relationship for ΔG is obtained.

$$\Delta G = 4 d l \sigma_s - (\sigma_s/\sigma_e) d l^2 \Delta g \quad (15)$$

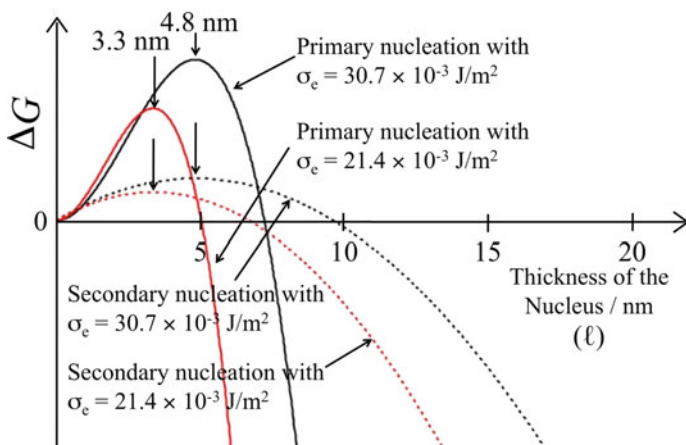


Fig. 16 Free energy change upon the formation of the primary (solid curves) or secondary (dotted curves) nucleus as a function of the thickness of the nucleus according to the Hoffman–Lauritzen theory

As for the value d , the distance between two adjacent polymer chains on a (110) plane is considered, which is identical to the unit cell b -axis length ($b = 0.615$ nm) because of the pseudo-hexagonal nature of the orthorhombic unit cell ($a = 1.07$ nm and $\gamma = 90^\circ$) [12]. It is also possible to evaluate d from the experimental result of $d_{200/110}$ spacing shown in Fig. 6 by $d = d_{200/110} \times 2/\sqrt{3}$. The initial values of $d_{200/110} = 0.526$ nm for both of the D0.5 neat and D0.5/SNC(1.0) specimens are shown in Fig. 6. Thus, we decided to use $d = 0.607$ nm. Then, the dotted curves in Fig. 16 are drawn for the case of the secondary nucleus with $\sigma_e = 30.7$ and 21.4×10^{-3} J/m² (black and red), where the two representative solid curves (black and red) for the cases of the primary nucleus ($\sigma_e = 30.7$ and 21.4×10^{-3} J/m²) are shown together for comparison. Note further that the critical thickness ($l^* = 4.8$ nm) for the black curves matches the experimental result shown in Fig. 12 (the initial value of the red curve) because of using so-adjusted value of Δg ($=2.56 \times 10^7$ for the primary nucleus and 1.28×10^7 J/m² for the secondary nucleus). Then, the red curves give the values of $l^* = 3.3$ nm. It is clear that the curves for the secondary nucleus for $l > l^*$ drop much moderately as compared to the curves for the primary nucleus. Therefore, the earlier termination of the lamellar thickening for the D0.5/SNC(1.0) specimen as shown in Fig. 12 can be accounted for by the moderate decreasing of the ΔG curves of the secondary nucleation. Thus, the secondary nucleation can be applied for the D0.5/SNC(1.0) specimen. Note here that the number of spherulites observed by the polarizing optical microscope was found to increase with time upon the isothermal crystallization for the D0.5 neat specimen [13]. However, the number of spherulites is found to be proportional to time of the power of 0.65 ($\sim t^{0.65}$). Anyway, this kind of behavior implies the homogeneous nucleation for the D0.5 neat specimen. Therefore, it is considered that the black solid curve for the D0.5 neat specimen is changed to

the red dotted curve upon the loading 1% of SNC. Thus, upon the loading of SNC, lowering of the energy barrier (ΔG^*) facilitates the acceleration of crystallization but the moderate decrease of the ΔG curve for $l > l^*$ causes the earlier termination of the lamellar thickening as compared to the D0.5 neat specimen.

3 Conclusion

The effects of loading SNC on the isothermal crystallization of PLLA at 110 °C (from 200 °C) were studied by the SWAXS and DSC measurements. It was found that loading SNC with 1.0 wt% caused the reduction of the induction period, the acceleration of crystallization, the increase of the final value of the degree of crystallinity, and the acceleration of the lamellar thickening. These experimental results can be explained by the fact that the regular folding of the polymer chains is attained by the loading of SNC.

References

1. Saeidlou S, Huneault MA, Li H, Park CB (2012) Poly (lactic acid) crystallization. *Prog Polym Sci* 37(12):1657–1677. <https://doi.org/10.1016/j.progpolymsci.2012.07.005>
2. Diep PTN, Mochizuki M, Doi M, Takagi H, Shimizu N, Igarashi N, Sasaki S, Sakurai S (2019) Effects of a special diluent as an agent of improving the crystallizability of poly(L-lactic acid). *Polym J* 51(2):283–294
3. Patwa R, Kumar A, Katiyar V (2018) Crystallization kinetics, morphology, and hydrolytic degradation of novel bio-based poly (lactic acid)/crystalline silk nano-discs nanobiocomposites. *J App Polym Sci* 135(33):46590. <https://doi.org/10.1002/app.46590>
4. Takagi H, Igarashi N, Mori T, Saijo S, Ohta H, Nagatani Y, Kosuge T, Shimizu N (2016) Upgrade of small angle X-ray scattering beamline BL-6A at the photon factory. In: AIP conference proceedings 2016 Jul 27, vol 1741, no 1. AIP Publishing, pp 030018. <https://doi.org/10.1063/1.4952841>
5. Pandey AK, Katiyar V, Takagi H, Shimizu N, Igarashi N, Sasaki S, Sakurai S (2019) Structural evolution in isothermal crystallization process of Poly(L-lactic acid) enhanced by silk fibroin nano-disc. *Materials* 12(11):1872
6. Pandey AK, Katiyar V, Sasaki S, Sakurai S (2019) Accelerated crystallization of poly(l-lactic acid) by silk fibroin nanodisc. *Polym J* 51(11):1173–1180
7. Avrami M (1939) *J. Chem. Phys.* 7:1103. *ibid.* 8 (1940) 212; *ibid.* 9 (1941) 177
8. Schultz JM (2001) Polymer crystallization: the development of crystalline order in thermo-plastic polymers. *Am Chem Soc*
9. Strobl GR, Strobl GR (1997) *The physics of polymers*, vol 2. Springer, Berlin
10. Tien ND, Hoa TP, Mochizuki M, Saijo K, Hasegawa H, Sasaki S, Sakurai S (2013) Higher-order crystalline structures of poly(oxyethylene) in poly(d,l-lactide)/poly(oxyethylene) blends. *Polymer* 54(17):4653–4659
11. Hoffman JD, Davis GT, Lauritzen JI (1976) *Treatise on solid state chemistry*, vol 3. Plenum Press, New York, pp 497

12. Fujiwara T, Miyamoto M, Kimura Y, Iwata T, Doi Y (2001) Self-organization of diblock and triblock copolymers of poly (L-lactide) and poly (oxyethylene) into nanostructured bands and their network system. Proposition of a doubly twisted chain conformation of poly (L-lactide). *Macromolecules* 34(12):4043–4050
13. Diep PTN, Takagi H, Shimizu N, Igarashi N, Sasaki S, Sakurai S (2019) Effects of Loading Amount of Plasticizers on Improved Crystallization of Poly (L-lactic acid). *J Fiber Sci Technol* 75(8):99–111

Chapter 15

Mimicking Smart Textile by Fabricating Stereocomplex Poly(Lactic Acid) Nanocomposite Fibers



Doli Hazarika, Amit Kumar and Vimal Katiyar

Abstract In the modern age, humans with their demanding nature along with comfort and fashion are also oriented toward flourishing functional textile products which have led researchers to focus toward the development of smart textiles. Scientists are now trying to introduce extraordinary properties like durable pressing performance, ultraviolet resistance, antistatic, antimicrobial and self-cleaning properties which are different from the conventional textiles. Most of the manmade fibers used in textile industry are petroleum-based which are depleting the natural resources and destructing the ecological balance at a constant rate. In this regard, the sustainable polymers for smart textiles would serve as promising candidates in solving the problem of discarding textiles. The current chapter therefore aims at providing insights about the utilization of biodegradable polymers in smart textiles. Among various biodegradable polymers, PLA has a great reputation in terms of its biodegradability, high mechanical performance and hydrophobicity. But the limitations of PLA fibers lie in its brittleness, degradation during home laundering and even storage condition. Thereby, this chapter includes the introduction of preferable and desirable approach like stereocomplexation in order to obtain a high heat stable stereocomplex PLA fiber for home laundering also. The fabrication of functional stereocomplex PLA fibers is possible by incorporating various bionanofillers which will be discussed in this chapter. Eventually, the application of such smart textile is also concerned toward the safety of human beings which will be very useful for academic and industrial use to cope up with the new concept of smart fabrics using biodegradable polymer.

Keywords Poly(lactic acid) · Stereocomplex poly (lactic acid) · Nanocomposite · Fiber spinning · Smart textile

D. Hazarika · A. Kumar · V. Katiyar (✉)

Department of Chemical Engineering, Indian Institute of Technology, Guwahati, Kamrup, Assam 781039, India

e-mail: vkatiyar@iitg.ac.in

© Springer Nature Singapore Pte Ltd. 2020

V. Katiyar et al. (eds.), *Advances in Sustainable Polymers*, Materials Horizons: From Nature to Nanomaterials, https://doi.org/10.1007/978-981-15-1251-3_15

341

1 Introduction

Fibers are the main foundation in textile industry which are spun into yarns or fabrics so as to obtain textile products. The textile fibers are classified as natural fibers (asbestos, cotton, silk, wool, etc.) and manmade fibers (polyesters, rayon, nylon, acrylic, etc.). Such fibers have various applications in the fields like geo textiles, industrial fabrics (floor mats, seat fabrics and seat cushions), wipes, clothing and home furnishing. The natural fibers which are made of cellulose and proteins have the porous structure which invites appropriate conditions for growth of bacteria and microbes, retains moisture and in turn leading to the deterioration of textiles. Enormous attention has been made to use the synthetic antibacterial agents like nitro compounds, dyes, oxidizing agents, metal-based and halogen compounds. Moreover, in the textile industry, service of laundry is consuming enough electricity as well as contaminating water resources [1]. The cultivation of natural fibers requires excessive water, land, pesticides and fertilizers, and also synthetic fibers like nylon, polyester are nonrenewable and toxicity which are obtained from polymers [2]. Polymers (repeating monomer units) are basically made up of fossil fuels, like crude oil and natural gas which are also well known as petrochemical-based polymers. They are obtained from cheap feedstock, possess low specific density, usually light in weight and are easily processable to obtain the desired complicated products to make them advantageous over other materials like metals ceramics. But excessive use of petro-based products in industries and for domestic purposes has increased their trend of demand everywhere [3]. Petrochemical-based polymers have advantageous characteristics like high strength, good oxygen barrier properties, high heat sealability, low production cost over the alternatives which is the reason for their usage in most of the industries. On the other hand, the disadvantages of petroleum-based polymers such as decline in gas oil resources, migration of toxic material while using them for packaging applications, environment pollution regarding their degradation, inflation of prices altogether prohibit them from their uses in different fields. Such issues have made technologies to deal with their recycling so that the problem is fixed, but their recycling rates remain low [4]. Green economy together with sustainable development is the only solution in solving the problem of using fossil-based resources. Bioplastics or biopolymers obtained from plants, animals and microorganisms became more popular not only because they are environment friendly but also due to their strategic nature. Release of toxic and greenhouse gases, e.g., CO₂, is in the way of reduction by use of proper agriculture-based products like cellulose, starch, wood, etc., for polymer production which confirms good impact of bioplastics on nature along with less energy consumption while producing [3]. Looking into the use of all the conventional and synthetic materials, researchers have started exploiting the sustainable resources so as to develop functional characteristics into the textile and are trying to prevent human facing severe health problems.

From centuries, human has been using the manmade fibers to make yarn and wool into textile by using handmade processes. And now in the twentieth century, polyester fiber with their low capacity production has contributed to a rapid share

production in the market. Today, almost in every sector of textile industries, the idea of potential use of nanotechnology is a growing interest. Starting from the fabrication of nanofibers using different spinning techniques to the fabrication of fiber composites using various nanomaterials is now a booming topic for the technologists. The conventional fibers used in textile industry that people have been conventionally using are facing the problem of long lasting, bacterial and microbial attack even using chemicals or detergents for removing stains which are harmful for marine animals [5]. Owing to solve such serious problems and keeping into mind the demand forgetting extraordinary functionalities into the textile industries, researchers have started thinking of impregnating nanoparticles into the fibers in order to obtain a functional composite fiber.

1.1 Smart Textile

Textile industry has given the global world a shield from cold and rain which is the main function of original textile. But recently, adapting with the environment a new discipline of interactive textile has been risen up in the textile sector. A new generation of textile has been discovered which has the potential to provide us comfort at all time together with proper protection by warning us against any danger. Such materials are termed as smart or functional textiles which are like ordinary clothes, but they provide special extraordinary functionalities for the desired application. Therefore, the smart textiles are defined as textiles which are having potential to react or sense the stimuli (mechanical, chemical, electrical, optical, biological or other sources) created by the environment in a predetermined way.

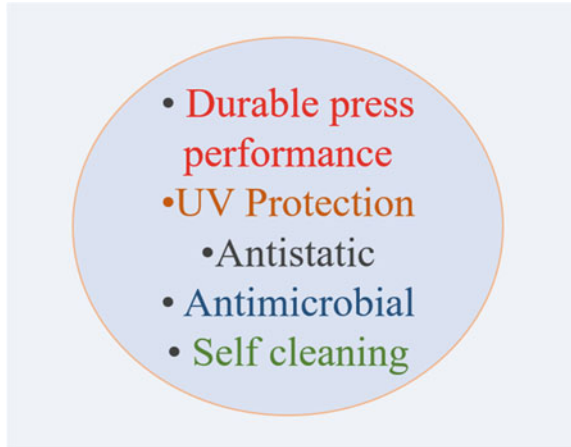
In 1968, a body covering exhibition was held in New York City where the astronaut space suits were showcased which can light up, can heat up and cool up by themselves. In 1985, Harry Wain right showed up first animated sweatshirt displaying full cartoon on its surface. In 1990, MIT researchers developed wearable computers like miniature electronic devices. Since then, many researchers have been working with smartness so as to gather an attention on smart textiles. The features of the smart textile are shown in Fig. 1.

1.1.1 Types of Smart Textiles in Terms of Different Functionalities

Passive Smart Textiles

These are the first generation of smart textiles, particularly providing various features in passive mode with the environment. As for example, if considered a highly insulating coat, it would adapt with the outside temperature and remain insulating. Antimicrobial, antiodour, antistatic and bulletproof are included in this category.

Fig. 1 Smart features of smart textiles



Active Smart Textiles

These are the second generation of smart textiles which includes actuators and sensors. These materials include new functionalities such as shape memory effect, chameleonic effect, water-resistant ability and hydrophilic/nonporous vapor permeability, heat storage, thermo regulation, vapor absorption and heat evolving fabrics and suits have electrically heated features.

Ultra Smart Textiles

These are the third generation of smart textiles which works like a brain with capacities of reasoning and activating features. They mainly involve the multidisciplinary properties such as sensing, actuation, advanced processing, provide help in communication, act as artificial intelligence for mimicking human behavior. The conductive yarns and fibers which are different in their functionalities than the natural fibers are obtained from using conducting materials into the fibers.

1.1.2 Applications of Smart Textiles

The smart components form an integrated part when incorporated into the textile structure by behaving smartly. Those are added into the substrate which may include during fiber spinning, fabric formation level or during finishing level. In terms of health, these smart fabrics act like strain fabric sensor, sensitized garment to measure heart rhythm and respiration, life belt for pregnant women to analyze vital signs at any time. The smart fabrics may be used in defense applications as they have the ability to increase the protection by alertness from environment hazard. Moreover, in fashion and entertainment world for giving dazzling effect, invisible coatings and advance fibers have been developed to get dramatic change in the textile appearance. Another important area is for the athletes or sportsman where monitoring of heartbeat,

steps count, breathing and body temperature reading are important parameters for the development of smart clothing [6].

2 Nanotechnology

Nanotechnology has come up with an idea for the researchers to assist as an environment benefiter. Nanomaterial has immense surface properties considering high surface to volume ratio which has marked them very much different from the bulky additives and materials. The relevant contribution of nanotechnology has potential applications in different sectors like packaging, textile (apparel, commodity as well as medical treatments), etc. [7]. They are classified into two class, namely organic and inorganic nanoparticle.

2.1 Organic Nanoparticle

Organic particles are solid particles which are mostly derived from natural resources. They have more reinforcing ability than inorganic fillers. They are abundantly found in nature, have low density, higher mechanical property and are also biodegradable.

Polysaccharides

Monosaccharides of same kind are called homo polysaccharides (starch, glycogen and cellulose) which are linked by glycosidic linkages, whereas the linkage that is formed by different kinds is hetero-polysaccharides (Hyaluronic acid and glucuronic acid).

Starch

Starch is a renewable source which consists of amylose and amylopectin component. Amylose consists of anhydrous units of glucose linked by α -(1-4)-d-glycoside bonds which is a linear or slightly branched macromolecule, and amylopectin is a highly branched macromolecule with α -(1-6) linkages [8]. It is in the form of concentric annular structure (onion like) consisting of both crystalline and semi-crystalline layers. Hilum, a point of initiation of the granule is encircled by alternate single chain (amorphous) and double helix (ordered) growth rings (Fig. 2). The amylopectin lamellae is a component of the crystalline region and pack together to form a crystal of double-helix structure to form a semi-crystalline region. Moreover, parallel double helical stranded is found in the crystallites in pairs, where all chains are packed together. While clustering, the amylopectin part spiral up because of stacking of nanometric subunits, to form the crystalline lamellae and then the crystalline region. The crystalline regions of starch granules can be isolated by mild acid hydrolysis using hydrochloric or sulfuric acid or by wet mashing. But mostly, the crystallinity depends on the amylose content. The more is the amylose content, more is the

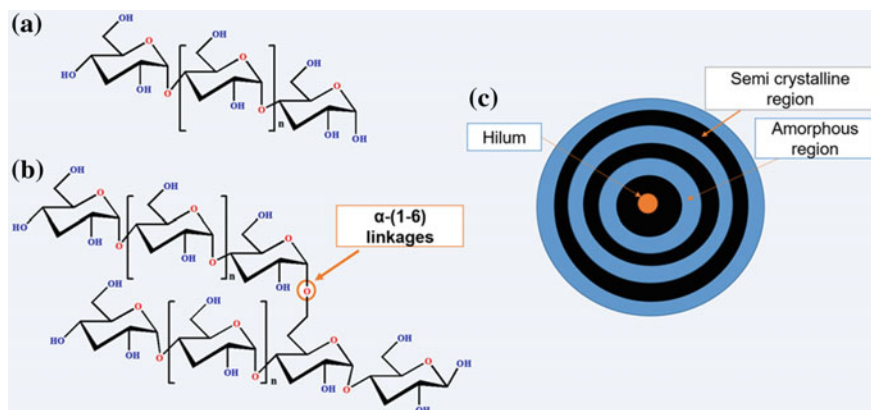


Fig. 2 Schematic representation of **a** amylose, **b** amylopectin, **c** onion-like structure with hilum

crystallinity in the nanoparticles [9]. The presence of nanometric size possesses greater surface area per mass, leading to higher self-interaction enhancing mechanical properties. Few conditions are to be followed up during hydrolysis like kind of acid, acid concentration, temperature and time which may affect the size as well as the yield of starch nanocrystals.

Cellulose Nanocrystal (CNC)

Cellulose with structure ($14 \rightarrow \beta D$ glucan) is the most abundantly found renewable biopolymer; either used in pure form or in modified form depending on its application. Cellulose has its various source of extraction like nature's wood, news-paper, filter paper, agricultural biomass (rice straw cotton stalk, pineapple leaf, flax, hemp, rice husk) marine, animals, algae and fungi [10]. It has favorable properties like hydrophilicity, chemical stability, biodegradability, which makes it to be applicable in textile applications. Cellulose exists in both amorphous and crystalline forms on the basis of its origin. The removal of amorphous region by controlled acid hydrolysis forms different size of nanocrystals, thereby improving the overall mechanical properties. Different studies have been made on the nanocellulose family that includes bacterial nanocellulose (BC), cellulose nanofibrils (CNF) and cellulose nanocrystals (CNC) derived from plants and waste [11]. The fabrication process of CNC is shown in Fig. 3. Recently, many researchers have undertaken various studies on cellulose-based nanotechnology through numerous processes. CNCs which are termed to be as promising bionanoparticles possess the unique properties like high aspect ratio, controlled morphology, specific surface area, specific strength, interesting optical properties, biodegradability and non-toxicity. Moreover, the four different morphologies of cellulose on the basis of the source extraction have been studied. Also, the discussion has been made on the difference in the relative position of oxygen atoms and rotation of the hydroxyl methyl groups which form the intermolecular hydrogen bonding [12]. CNCs usually consist of glucose repeating units (10–100 units), where each repeating units has six hydroxyl groups, which

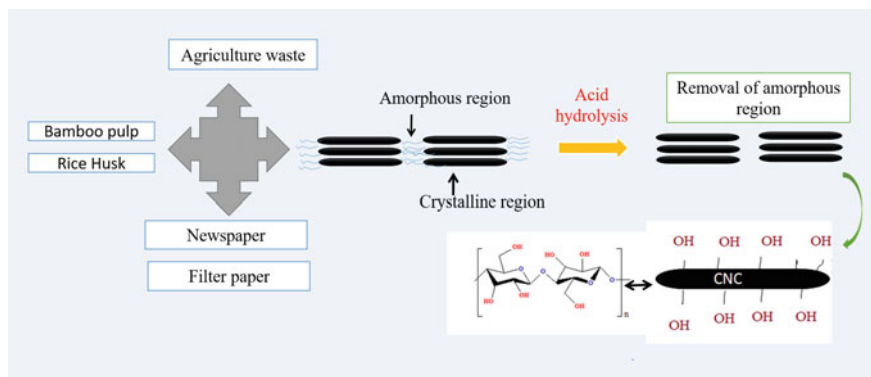


Fig. 3 Fabrication of cellulose nanocrystals from various sources

provide the improvement in functionality and reactivity of the CNC surface toward other chemical moieties. Eventually, studies have been made on introduction of high loadings of magnetic iron oxide (Fe_3O_4) nanoparticles adsorbed on the surface of CNC which led to incorporation of anisotropic mechanical, thermal and electrical properties [13].

Chitosan

Chitosan is the second most available linear polysaccharide after cellulose which is produced by the deacetylation of chitin. It is a composition of glucosamine and *N*-acetyl glucosamine units having linkage of 1–4 glucosidic bonds. They are insoluble in water, alkali and acid system but soluble in organic acid, acetic acid, lactic acid and formic acid [14]. Chitosan possesses unique properties like biocompatible, non-toxic, antifungal activity and antibacterial properties which make it an attractive choice for the functional modification of textiles. Chitosan nanoparticles are produced by the ionic gelation of chitosan with tripolyphosphate (TPP) where TPP polyanions (negative) interact with amine groups of chitosan [15]. In the textile industry, green bioactive nanochitosan has been a new concept and is gaining importance. Chitosan nanoparticles have also been known to be made by polymerization of methacrylic acid (MAA) using $\text{K}_2\text{S}_2\text{O}_8$ as initiator followed by centrifugation [16].

2.1.1 Proteins

Silk

Silk is the most precious fiber given to us by nature over the past few decades which has enormous impact in textile industry. Silk fiber structure possesses tenacity with a range from 3.5 to 5.0 g/d when in dry condition and may lose up to 20% of its strength under wet condition. Silk has no elastic behavior when it is stretched to certain amount, and it never regains to its original position. Considering the current

preferences along with the increase in demand for natural fibers, silk has made a well-known platform in textile industry due to the optimum properties in terms of human comfort and wearability because of its eco-friendly nature. Silk is the family of *Lepidoptera* and *Araeneaein* with continuous form of spun filaments having the structure of orthorhombic unit cell and high packing density [17]. Silk material is obtained from varieties of insects like silkworm and spider. The spider silk has the fibroins on inside and a protective coating of sericin with gum-like properties, wild silk like tassar, eri and muga silk which is the outer cover of silk cocoon. But the amorphous region application, i.e., sericin layer should be removed to obtain only the crystalline region, i.e., fibroin by chemical treatment (degumming process). The process continues firstly from silk to microfibrils and secondly from microfibrils to nanofibrils under proper condition. Fibroin is a component of silk fiber with repetitive and ordered structural units termed as β -sheets. The fibroin part gives strength, thereby imparting antibacterial, UV resistant, moisture regulating properties which contributes in the textile industry. Acid hydrolysis is the proper treatment which has been used by many researchers to fabricate silk nanocrystals from wild silk [18]. The sequential units in silk fibroin (SF) are glycine–alanine–glycine–alanine–glycine–serine (GAGAGS), which composes the crystal regions in SF polychain [19]. Highly crystalline region of silk provides the strength, but the presence of strong hydrogen bonding makes it insoluble in many solvents like dilute acids, alkalis and water. These sheets play an important role in strengthening and stiffening the silk fibers [20]. It has been reported that the presence of only β -sheets, i.e., crystalline region which is having ~ 50 nm diameter possesses high crystallinity, usually more than 90% [21]. The synthesis of silk nanocrystals from plant silk is shown in Fig. 4.

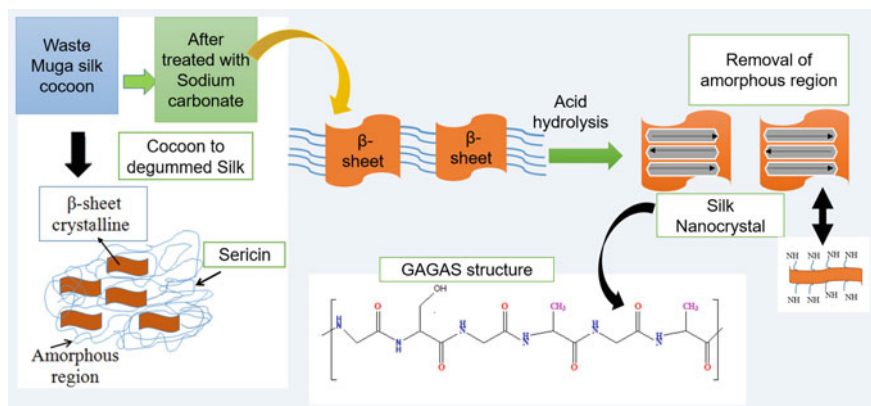


Fig. 4 Synthesis of silk nanocrystals from plant silk cocoon

2.2 Inorganic Nanoparticles

The natural or conventional fibers are more prone to staining from spilled drink, itching due to uncontrolled microbial growth, adhered micron-dust and static energy generation which have made researchers to make efforts on studying the control of human hygienic living standard to replace harmful or toxic chemicals. Introduction of new technologies by utilization of both inorganic and organic nanoparticles has delivered new opportunities for the development of improved multifunctional properties for textile applications.

The inorganic nanomaterials include metallic like silver, copper, gold, platinum, gallium and metal oxides like silver oxide, zinc oxide, titanium oxide, iron oxide, magnesium oxide, silicon oxide, zinc oxide and others such as clay nanoparticles, carbon nanotubes. A few of these inorganic nanomaterials are discussed below.

2.2.1 Titanium Oxide (TiO₂)

This nanomaterial has remarkable properties in terms of high stability, long-lasting nature, safe and antibiotic properties which have made it a promising for targeted properties like self-cleaning, antibacterial activity, UV resistance and dye degradation in textile effluents. Mainly, the photo activity effect depends on the structure, purification and its crystalline nature [22]. The three forms of TiO₂ available in nature are anatase, rutile and brookite. Table 1 highlights the important parameters of the three crystalline forms.

The anatase form is a metastable state with more photocatalytic nature than rutile, whereas rutile is more thermodynamically stable than rutile and brookite. TiO₂ when irradiated by the source of light forms electron-hole pairs which induce redox reaction over the TiO₂ surface. The active oxygen species (O²⁻) oxidize the organic compounds of bacterial cell and converts them carbon dioxide (CO₂) and water (H₂O) molecules, thereby acting as photo active agent. Different preparation techniques have been employed out of which sol-gel method is mostly applicable to obtain stable anatase form of TiO₂ [23]. The electron excitation, i.e., light absorption

Table 1 Tabulated parameters of three crystalline forms of TiO₂ [24, 25]

Sl. no.	Forms	Lattice structure	Parameters (nm)	Band gap (eV)
1	Anatase	Tetragonal	$a, b = 0.3785,$ $c = 0.2959$	3.2
2	Rutile	Tetragonal	$a, b = 0.4593,$ $c = 0.2959$	3.02
3	Brookite	Orthorhombic	$a = 0.9182,$ $b = 0.5456,$ $c = 0.5143$	2.96

range can be extended from UV (<387.5 nm) to visible light (>400 nm) by creating a local electric field using gold and silver nanomaterial, thereby increasing the photocatalytic effect.

2.2.2 Silver Nanoparticle (AgNP)

AgNPs are frequently used in many textiles, wound dressings and biomedical devices [24–26]. The functional inherent property of silver with antimicrobial property has been focused which inhibits the formation of biofilm over the substrate. Moreover, Kim et al. mentioned about the mechanism of antimicrobial activity of Ag nanoparticles which is related to free radicals formation and subsequently damages the membrane. Various parts like flower and fruits of the papaya plant also sericin extracted from the cocoons are used for the synthesis of silver nanoparticles [27]. Photo-catalytic reduction, chemical reduction, photo-chemical or radiation-chemical reduction, sono-chemical, photo-reduction, reverse micelle-based methods, metallic wire explosion and even biological synthesization have also been applied for the synthesis of silver nanoparticles [25].

2.2.3 Clay Nanoparticles

These are generally the family of inorganic layered nanomaterials or termed as aluminosilicate-based nanoparticles. They can be classified as 1:1 or 2:1 phyllosilicates owing to arrangement of the tetrahedral and octahedral sheets. Each tetrahedral sheets consists of central cation (mostly Si^{4+}), whereas each octahedral sheets consists of metal cation (M^{n+}). Depending on the metal cation, different kinds of sheet formation take place. When the metal cation is divalent such as Mg^{2+} , the sheet is termed as trioctahedral or brucite-like sheet, whereas when trivalent such as Al^{3+} creates a vacant site, it gives rise to dioctahedral or gibbsite-like sheet. For, e.g., Smectite: (Montmorillonite) $\text{Na}_m(\text{Al}_{2-m}\text{Mg}_m)\text{Si}_4\text{O}_{10}(\text{OH})_2 \cdot n\text{H}_2\text{O}$, (Laponite) $\text{Na}_h(\text{Mg}_{3-h}\text{Li}_h)\text{Si}_4\text{O}_{10}(\text{OH})_2 \cdot n\text{H}_2\text{O}$. Mlynarcikova et al. studied improvement in mechanical properties by incorporating organoclay into polypropylene to obtain high strength nanocomposite fiber [28].

2.2.4 Copper Nanoparticles

These kinds of nanoparticles are mostly implanted into submicron particles of Sepiolite particle $\text{Mg}_8\text{Si}_{12}\text{O}_{30}(\text{OH})_4(\text{H}_2\text{O})_4 \cdot 8\text{H}_2\text{O}$ and are having comparable antimicrobial activities with triclosan agent [25]. It has reported about copper nanoparticles that it has less antibacterial property than silica nanoparticles [29]. But it has less antimicrobial activity than silver nanoparticles. Magnetron sputter method was used for

deposition of Cu nanoparticles of various thickness has incorporated into polypropylene (PP), and nonwoven was used for the property improvement like antistatic, UV shielding enhancement [30].

2.2.5 Zinc Oxide Nanoparticles, ZnO

ZnO nanoparticles are more advantageous to silver nanoparticle in comparison with low cost, white in appearance also are having UV-blocking property, so as to make it useful as UV light-emitting device, sunscreens, UV absorbers and photo-catalyst [31]. Researchers have studied on potential application of ZnO nanoparticles on dye removing from when considered under UVC light from textile effluent [32]. It has been reported that with sweat concentration of 11 g/L ZnO making artificial sweat solution by considering alkaline, acidic and inorganic salt, the antibacterial activity of nanoZnO when functionalized on cotton fabric was observed better salt and alkaline resistances than acid resistances sweat solution [25]. Even more, ZnO nanorod was incorporated using dip-pad-cure process on cotton fabric samples with the addition of a hydrophobic agent to fabricate a hydrophobic fabric [33].

3 Different Preparation Techniques for Organic and Inorganic Nanomaterials

There are mainly two approaches in order to obtain nanoparticles termed as bottom up (build up) and top up (break up). The bottom-up approach is performed by the physical method like—vacuum condensation, crashing physically and ball milling, and the top-down approach is performed by chemical method like—sol-gel, precipitation, micro emulsions and hydrothermal reaction.

3.1 *Non-biodegradable Polyester as Fibers*

Synthetic fibers like polyethylene terephthalate (PET), polypropylene (PP), polyamides (PA) or polyacrylonitrile (PAN) have been widely explored in the field of textile industry, and pollution reduction in production of textile fabrics is important burning topic for the manufacturers [24, 25]. Recently, the textile industry is more focussed toward sustainable technologies to develop an era of safe environment. However, the high build up of static energy, non-biodegradability, high hydrophobicity, poor breathability, finishing resistance are some of undesirable properties found in synthetic fibers which have made researchers to think for alternative solutions. New routes have also been applied like combination of physical technologies (corona discharge, plasma functionalization, laser treatment, use of high-energy

electrons), chemical technologies (ozone gas treatment, supercritical carbon dioxide technique, vapor deposition method, surface grafting, enzyme surface modification, sol-gel technique, etc.) and nanoscience technology to overcome the difficulties associated with synthetic fibers. Moreover, the bulk modification has also been applied by blending with other polymers. But in today's world, biodegradable and biocompatible polyester fibers are very important for various applications like sutures, woven fibers, membrane, scaffolds, etc. [34].

3.2 *Natural and Synthetic Fiber Composites*

Cotton, silk and wool are termed as natural fibers along with synthetic fibers such as polyester and nylon have been most widely used from decades as fibers for apparel manufacturing. Moreover, synthetic fibers are mainly more suitable for domestic and industrial applications, such as carpets, tents, cleaning cloths and medical hygiene products [35]. Natural and synthetic fibers generally have different characteristics, which make them ideally suitable mainly for apparel applications [36]. Owing to the environmental safety and potentiality, the chemical modification processes are omitted, and the physical modification methods are used without hampering the bulk properties. Various studies have been already made using biocides like chitosan, chitosan nanoparticles and Ag-chitosan hybrid by loading into wool fabrics also wool textiles with a sulfur nanosilver colloidal solution, and it has been observed that due to such incorporation, there is an improvement in hydrophilicity, dyeability, antimicrobial, shrink proofing properties, etc. [37].

Natural cotton fabrics have perfect absorption capacity for most of the liquids than synthetic fabrics. Therefore, researchers have tried to incorporate self-cleaning property and fabricate a replicate of lotus leaf surface. MWNT has been incorporated into cotton fibers by ultrasonic irradiation procedure to fabricate a hydrophobic surface over cotton fabrics [25]. Moreover, to prevent the agglomeration of MWNT along with increasing its affinity, it has been grafted with poly (butylacrylate) (PBA) and subsequently used with cotton fabric to obtain a self-cleaning fabric by dipping–drying–curing method [38].

Report was made on magnesium oxide nanoparticles (MgO NPs) incorporated Nylon-6 solutions which were electrospun to produce nanofiber mats. The fire retardancy and antibacterial activity against bacteria *Staphylococcus aureus* and *Escherichia coli* of coated fabrics made from MgO/Nylon-6 hybrid nanofiber are better than those from Nylon-6 nanofiber [39]. The influence of nanosilver by introducing into poly (styrene-co-acrylic acid) copolymer has made on antibacterial activity which is due to presence of carboxylic groups of acrylic acid [40]. A platinum-loaded titanium dioxide nanohybrid (Pt/TiO₂) was fabricated and incorporated into cotton fabrics to explore a superior nanocomposite with self-cleaning and antibacterial properties [41].

4 Poly(Lactic Acid) (PLA)

PLA is observed to be as a linear thermoplastic polyester derived from 100% renewable and degradable resources (corn, sweet potato and starch-rich product like rice) by fermentation that can help to mitigate the energy crisis together with the reduction of CO₂. In 1932, Carothers (DuPont) produced a low molecular weight PLA only by heating lactic acid under vacuum condition [42]. In 1954, Du Pont obtained higher molecular weight PLA. Moreover, poly(lactic acid) is biodegradable and compostable but under standard condition only [43]. PLA may be amorphous or semi-crystalline in solid state, which depends on the stereochemistry and the thermal history. The polymerization of PLA takes place by either direct polycondensation of lactic acid under certain conditions like using high vacuum and high temperature or by ring-opening polymerization of lactide which is due to opening of dimer rings under mild conditions. The direct polycondensation technique uses solvent to extract the water and obtain low to an polymer of intermediate molecular weight [44]. Another polymerization method is ring-opening polymerization performed under mild conditions via opening of lactide rings resulting in high molecular weight polymer (Fig. 5). The direct condensation technique is often accompanied by several drawbacks such as the formation of low molecular weight polymer, use of large reactors, use of solvent and evaporation and problem of solvent recovery. Therefore, the most industrially acceptable method as per the reports may be the ring-opening mechanism of lactide by two step process: (a) Oligomerization of lactic acid of molecular weight approximately 1–4 kDa which is depolymerized to obtain lactide. (b) Production of high molecular weight PLA by ring-opening polymerization. During the polymerization of PLA, different types of catalysts like metal, cationic and organic (stannous octoate, dibutyltin methoxide, zinc stearate and one co-initiator, triphenylphosphine)

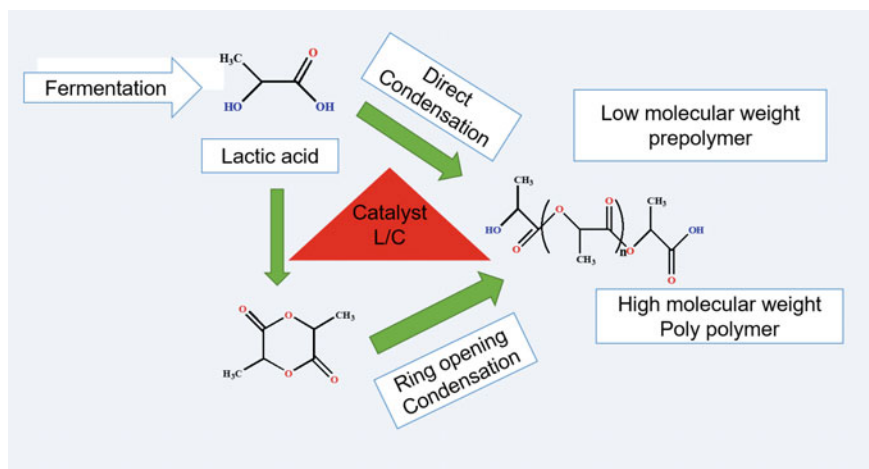


Fig. 5 Schematic diagram of synthesis of poly(lactic acid)

were used and as reported high molecular weight, and also, high optical purity was achieved [45]. The polymerization reaction was mostly carried out by preferring stannous octoate as it provides high reaction rate, high conversion rate, together with high molecular weights, just using mild polymerization conditions [45].

4.1 PLA as Composite Fibers

In 1932, Staudinger postulated the basic requirements to obtain high strength and high modulus synthetic fiber, where all molecular chains should be extended perfectly and aligned along the direction of fiber axis. The fully extended with proper oriented polymer chains provide ultimate stiffness to the fiber. Moreover, little chain end defects when considered in high molecular weight polymers provide high tenacity, thereby obtaining an ideal fiber, where tensile strength is determined by secondary bonds rather than primary bonds. Possible production processes were discussed for PLA fibers like melt spinning, dry-spinning, wet-spinning and dry-jet-wet-spinning. However, for industrial applications, mainly melt spinning is applied, as it is a solvent free and economic process.

Poly(lactic acid) (PLA) fiber along with biodegradability has better hydrophilicity, ease handle and better drapability compared to polyester polyethylene terephthalate (PET) fiber. Commonly, PLA fiber only can be dyed light color under ordinary conditions of 100 °C using disperse dyes [46], but higher temperature is required for dark dyeing. Since then PLA fiber will shrink having low melting point and low heat resistance which is a serious problem under process condition, thereby making PLA over PET for obtaining dyed fabrics. Furthermore, for its poor heat resistance, common PLA fiber products cannot be ironed in order to avoid accident which causes increase in its finishing costs and limits its popularization and application in textile field. Thus, modification for improving heat resistance of PLA fiber is very important to broaden the application. Regarding this, various studies have already made on addition of plasticizer and adding nucleating agent to lower the energy required during the crystallization phase of the folding of chains so as in enhancement of the crystallization rate [47]. Few reported plasticizers are like citrate esters, triacetate, poly(ethylene glycol) (PEG), poly(propylene glycol) (PPG), tributyl citrate and triphenyl phosphate (TPP), and nucleating agents like talc, nanoclay, carbon nanotube, exfoliated grapheme, zincphenyl phosphonate, tetramethylene dicarboxylic dibenzoyl hydrazide (TMC-306), etc., have been used to increase the chain mobility and impact of the PLA chain [48]. PLA can be spanned into fiber with distinct fiber properties via different spinning techniques like melt spinning, solution spinning and electrospinning although the solvent-free melt spinning technique is more suitable than others and also an environmental friendly process [49]. Introduction of additives has enabled to offer improved properties to polymeric fibers such as flame retardancy, heat stability, mechanical performance and also electrical and thermal conductivity properties [50]. Spinning and drawing of the fibers during melt extrusion are referred as melt draw ratio (MDR) or after solidification, another drawing

stage which is termed as solid-state drawing (SSD). The increase in the drawing ratio leads to polymer chain to a high orientation which may result in high fiber tenacity [51]. In addition to its biodegradability and renewability, a new era of using PLA fibers in textile application has been in mention. But few characteristic features prohibit its use in textile finishing like having poor resistance alkali causes strength loss when conventional disperse dye was used. Moreover, it has low melting temperature leads to low temperature while ironing and thereby may degrade the fiber. An introduction of new approach by stereocomplexation of PLA has been suggested in this chapter in order to tackle such problem for utilizing PLA in textile industry without any finishing problem. Few reported work was made on PLA composite fibers for improvement in properties which have been tabulated (Table 2).

Table 2 Reported studies on PLA composite fibers using different spinning techniques

Sl. no.	Composite	Filler content	Technique	Properties	References
1	PLLA/chitosan	No content has reported	Dry-wet-spinning method	Increase in the degradation rate	[59]
2	PLA/CNC	1 wt%	Melt spinning by twin screw micro-compound	Mechanical performance improves at high draw ratio	[49]
3	PLA/HA	5–20 wt%	Melt spinning	High thermal stability and mechanical strength	[51]
4	PLA/MWCNT	0.5 and 5.0 wt%	Melt spinning	Liquid sensing properties	[60]
5	PLA/CNW and PLA/MCC	1 and 3 wt%	Melt spinning	Thermal heat stability, flame retardancy and better tensile properties	[50]
6	PLA/ZnO	1–3 wt%	Melt spinning	Mechanical performance improves thermal stability and antimicrobial properties	[61]
7	PLA/ZnO	Up to 5 wt%	Melt spinning	UV protection, antibacterial, gas barrier and self-cleaning	[62]

4.2 Stereocomplex PLA Fibers

Considering more than over past 50 years, human has been using synthetic petroleum-derived non-biodegradable polymers which sparked the scientists to focus more on biomass-derived poly(lactic acid). Researchers have taken innovative initiation to enhance the thermal stability, thereby decelerating the hydrolytic degradation of PLA. PLA consists of asymmetric carbon atoms where two optically active enantiomers exist in its skeletal chain, namely poly(*L*-lactic acid) (PLLA) and poly(*D*-lactic acid) (PDLA). In 1987, it has been first reported by Ikada et al. that melt and solution blending of homocrystals of PLLA and PDLA in equal (1:1) molar ratio stereocomplex PLA was formed [52]. The structure of PDLA, PLLA and sc-PLA is shown in Fig. 6. Also, the lattice arrangement of *D* and *L* units in sc-PLA is shown in Fig. 7. However, improvement in crystallization rate and heat stability of sc-PLA is basic requirement for some application, and when all these were considered, then nanomodification is to be an effective method. It was also reported that PDLA with low molecular weight cannot form stereocomplex crystallites as they cannot act as a nucleation site due to large surface area, whereas when middle or high molecular weight PDLA chain with increased content were added into PLLA chain with annealing temperature, then pure and high-oriented stereocrystallites were found to be formed without any formation of homocrystallites [53]. Various reports have been made on formation of stereocomplexation using external solvent for blending use of nano-sized nucleating agent which may cost higher for industrial purposes. During the stereocrystals formation, both the PLLA and PDLA chains force a larger diffusion path than that of conventional folding crystallization mechanisms conditions. The formation of high crystallites in stereocomplex PLA (SC) is due to strong hydrogen

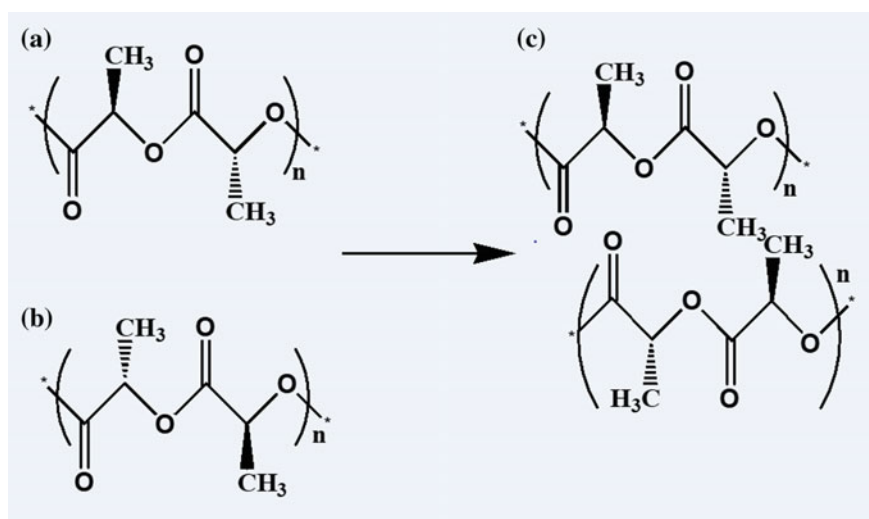


Fig. 6 Structure of **a** Poly(*L*-lactic acid), **b** Poly(*D*-lactic acid), **c** Stereocomplex PLA

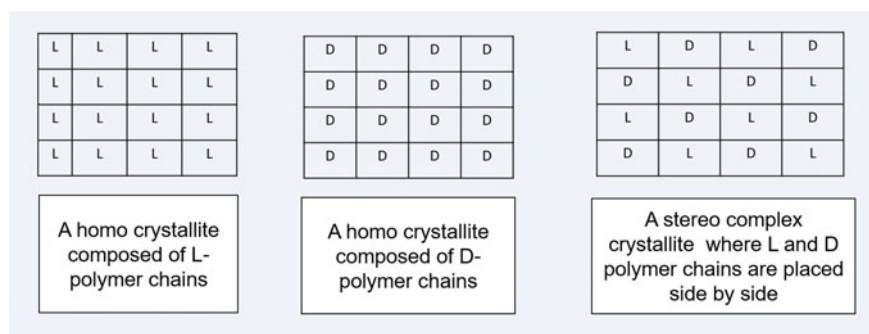


Fig. 7 Lattice arrangement of *L* and *D* units in the stereocomplex PLA

bonds and dipole–dipole interactions among the enantiomeric PLA chains which are the major reason behind enhancement of thermal stability [52]. Those formed are results of helical chain structures forming tie chains between the crystallites which also enhance packing density of the chains and enhanced better hydrolytic degradation compared to plain PLLA chains [54]. Tsuji et al. have tried wet and dry spun stereocomplex PLA by mixing it with chloroform and then studied the stereocomplex crystallites formation using differential scanning calorimeter without formation of any homocrystallites when they are hot drawn and spun into fibers. They also reported the enhancement of stereocomplex crystallization by hot drawing to high ratio which was due to chain expansion and interaction between PLLA and PDLA [55–57]. Moreover, Takasaki et al. reported hot drawing of the equal molar PLLA-PDLA mixture with high take-up velocity, lower throughput rate and lower extrusion temperature enhance the orientation of fibers [58]. Also, various reports have been made by utilizing natural fibers like flax, wood, hemp, jute reinforced with PLA composites for better improvement in mechanical and biodegradability. Melt blending of flax fiber-reinforced sc-PLA has enhanced mechanical as well as heat stability when compared with neat sc-PLA. Even fabrication of hydroxyapatite with stereocomplex PLA by grafting hydroxyapatite with PDLA by in situ polymerization was made to improve mechanical properties by blending hydroxyapatite-grafted-PDLA and PLLA chain using twin screw extruder [57]. The enhanced formation of sc-PLA via melt spinning of PDLA and PLLA blend at 230–250 °C has also been reported [58]. These authors showed that by drawing and annealing of the as-spun fibers, with certain amount of initial sc-PLA, fibers containing mainly sc-PLA could be obtained. Tsuji has also reviewed various methods for PLA stereocomplexation, its structural formation, properties, degradation for applications purposes and some of its comparative properties with PLA are listed in Table 3 [63].

Table 3 Comparison table of PLA and stereocomplex PLA [63]

Sl. no	Physical properties	PLA	Stereocomplex PLA
1.	T_m ($^{\circ}\text{C}$)	170–190	220–230
2.	T_g ($^{\circ}\text{C}$)	50–65	65–72
3.	HDT ($^{\circ}\text{C}$)	55	160–170
4.	ΔH_m (100%) Jg^{-1}	93–142	142–146
5.	Tensile strength (GPa) ^(a)	0.12–2.3	0.88
6.	Young's modulus (GPa) ^(a)	7–10	8.6
7.	Elongation at break (%) ^(a)	12–26	30

Note T_m = Melting temperature, T_g = glass transition temperature, HDT = heat distortion temperature (ASTM D648), (a) = oriented fiber

5 Conclusion and Future Scope

Since the textile industry is one of the major contributors to environment pollution, thereby sustainability has become vital reason in textile industries toward production of environmental friendly and sustainable products. From decades, increase in environment awareness, oil prices, greenhouse gases, reduction in oil feedstocks has led researchers to focus on development of materials that to from renewable resources present in natural. Earlier enhancement in functional properties for having smartness into textile was very rare, but scientists nowadays started using nanotechnology for making commercial products. Even proper control and care should be taken while synthesizing nanoparticles so as to overcome the problem of nanoparticles aggregation. Moreover, compatibility should be there between the reinforcing agent and polymer matrix. The nanobiocomposite has created a new path to produce an eco-friendly biodegradable textile fiber to tackle the major problems of using non-biodegradable environment degraded petrochemicals for textile applications. Thus, in recent years, scientists have given a major thrust so that we can rely on renewable polymers toward developing biobased materials for better environment.

A tremendous challenge for the textile industry has been made by scientists by utilization of renewable biomass so that there is minimization of carbon footprint in the environment while taking into consideration mostly in the areas which include production of fiber, yarn and fabric, textile chemical processing, from making of garments to its recycling and also the disposal of clothing. The insights gained are for better consideration of the future development production and use of nanocomposite-based textiles industry to optimize processes and products. Thereby utilization of biodegradable polymer for fiber improvement properties can be a new future development for high-performance textile applications. Relying on biodegradable PLA will eventually give better applications as huge as petroleum-derived polymers like

PET, nylon and polypropylene though they have better breathability, higher UV rays resistance, low smoke production, better hydrophilic properties and flammability. In such manner, tuning and mimicking smart by incorporating functional properties and biodegradability by proper biocatalyst optimization will guide for the development of new effective composite for commercializing smart natured textile fabrics. Nevertheless, keeping into disadvantageous features like low melting and low heat stability, nature of PLA and introduction of stereocomplexation have made regardless efforts to handle such drawbacks along with incorporation of smart nanofillers to fabricate a smart functional textile so that along with comfort, public will enjoy the impact of high technology.

References

1. Shahid-ul-Islam, Butola BS (2019) Recent advances in chitosan polysaccharide and its derivatives in antimicrobial modification of textile materials. *Int J Biol Macromol* 121:905–912. <https://doi.org/10.1016/j.ijbiomac.2018.10.102>
2. Busi E, Maranghi S, Corsi L, Basosi R (2016) Environmental sustainability evaluation of innovative self-cleaning textiles. *J Clean Prod* 133:439–450. <https://doi.org/10.1016/j.jclepro.2016.05.072>
3. Ahmed T, Shahid M, Azeem F, Rasul I, Shah AA, Noman M, Hameed A, Manzoor N, Manzoor I, Muhammad S (2018) Biodegradation of plastics: current scenario and future prospects for environmental safety. *Environ Sci Pollut Res* 25:7287–7298. <https://doi.org/10.1007/s11356-018-1234-9>
4. Chemwiki UCD, Alike CCA, License US (2017) First-Order Reactions, 1–6
5. Walser T, Demou E, Lang DJ, Hellweg S (2011) Prospective environmental life cycle assessment of nanosilver T-shirts. *Environ Sci Technol* 45:4570–4578. <https://doi.org/10.1021/es2001248>
6. Syduzzaman M, Patwary SU et al (2015) Smart textiles and nano-technology: a general overview. *J Text Sci Eng* 5. <https://doi.org/10.4172/2165-8064.1000181>
7. Rivero PJ, Urrutia A, Goicoechea J, Arregui FJ (2015) Nanomaterials for functional textiles and fibers. *Nanoscale Res Lett* 10:1–22. <https://doi.org/10.1186/s11671-015-1195-6>
8. Lin N, Huang J, Chang PR, Anderson DP, Yu J (2011) Preparation, modification, and application of starch nanocrystals in nanomaterials: a review. *J Nanomater* 2011. <https://doi.org/10.1155/2011/573687>
9. Pérez S, Baldwin PM, Gallant DJ (2019) Structural features of starch granules I, 3rd edn. Elsevier Inc., Amsterdam
10. Rajinipriya M, Nagalakshmaiah M, Robert M, Elkoun S (2018) Importance of agricultural and industrial waste in the field of nanocellulose and recent industrial developments of wood based nanocellulose: a review. *ACS Sustain Chem Eng* 6:2807–2828. <https://doi.org/10.1021/acssuschemeng.7b03437>
11. Lu Y, Cueva MC, Lara-Curzio E, Ozcan S (2015) Improved mechanical properties of polylactide nanocomposites-reinforced with cellulose nanofibrils through interfacial engineering via amine-functionalization. *Carbohydr Polym* 131:208–217. <https://doi.org/10.1016/j.carbpol.2015.05.047>
12. Dhar P, Kumar A, Katiyar V (2016) Magnetic cellulose nanocrystal based anisotropic polylactic acid nanocomposite films: influence on electrical, magnetic, thermal, and mechanical properties. *ACS Appl Mater Interfaces* 8:18393–18409. <https://doi.org/10.1021/acsami.6b02828>

13. Dhar P, Tarafder D, Kumar A, Katiyar V (2015) Effect of cellulose nanocrystal polymorphs on mechanical, barrier and thermal properties of poly(lactic acid) based bionanocomposites. *RSC Adv* 5:60426–60440. <https://doi.org/10.1039/c5ra06840a>
14. Homayoni H, Ravandi SAH, Valizadeh M (2009) Electrospinning of chitosan nanofibers: processing optimization. *Carbohydr Polym* 77:656–661. <https://doi.org/10.1016/j.carbpol.2009.02.008>
15. Koukaras EN, Papadimitriou SA, Bikiaris DN, Froudakis GE (2012) Insight on the formation of chitosan nanoparticles through ionotropic gelation with tripolyphosphate. *Mol Pharm* 9:2856–2862. <https://doi.org/10.1021/mp300162j>
16. Hebeish A, Sharaf S, Farouk A (2013) Utilization of chitosan nanoparticles as a green finish in multifunctionalization of cotton textile. *Int J Biol Macromol* 60:10–17. <https://doi.org/10.1016/j.ijbiomac.2013.04.078>
17. Wang Y, Guo J, Zhou L, Ye C, Omenetto FG, Kaplan DL, Ling S (2018) Design, fabrication, and function of silk-based nanomaterials. *Adv Funct Mater* 1805305:1805305. <https://doi.org/10.1002/adfm.201805305>
18. Patwa R, Soundararajan N, Mulchandani N, Bhasney SM, Shah M, Kumar S, Kumar A, Katiyar V (2018) Silk nano-discs : a natural material for cancer therapy. <https://doi.org/10.1002/bip.23231>
19. Jae LJ, Yamane H (2010) Role of the stereocomplex crystallites in the PLLA/PDLA mixed spinning dope on the stereocomplex formation in the wet-spun fibers. *Sen-I Gakkaishi* 66:236–242
20. Liu L, Yang X, Yu H, Ma C, Yao J (2014) Biomimicking the structure of silk fibers via cellulose nanocrystal as β -sheet crystallite. *RSC Adv* 4:14304–14313. <https://doi.org/10.1039/c4ra01284d>
21. Patwa R, Soundararajan N, Mulchandani N, Bhasney SM, Shah M, Kumar S, Kumar A, Katiyar V (2018) Silk nano-discs: a natural material for cancer therapy. *Biopolymers* 109:e23231. <https://doi.org/10.1002/bip.23231>
22. Ahmari H, Heris SZ, Khayyat MH (2018) The effect of titanium dioxide nanoparticles and UV irradiation on photocatalytic degradation of Imidaclopride, 3330. <https://doi.org/10.1080/09593330.2017.1306115>
23. Gupta SM, Tripathi M (2012) A review on the synthesis of TiO₂ nanoparticles by solution route, 10. <https://doi.org/10.2478/s11532-011-0155-y>
24. Rosenthal SB (2016) Changing the wetting properties of titanium dioxide surfaces with visible and near infrared light, 155
25. Dastjerdi R, Montazer M (2010) A review on the application of inorganic nano-structured materials in the modification of textiles: focus on anti-microbial properties. *Colloids Surf B Biointerfaces* 79:5–18. <https://doi.org/10.1016/j.colsurfb.2010.03.029>
26. Li C, Zhang Y, Wang M, Zhang Y, Chen G, Li L, Wu D, Wang Q (2014) In vivo real-time visualization of tissue blood flow and angiogenesis using Ag₂S quantum dots in the NIR-II window. *Biomaterials* 35:393–400. <https://doi.org/10.1016/j.biomaterials.2013.10.010>
27. Gokarneshan N, Velumani K (2017) Application of nano silver particles on textile materials for improvement of antibacterial finishes, 2:1–4. <https://doi.org/10.19080/gjn.2017.02.555586>
28. Mlynářčková Z, Borsig E, Legéň J, Marcinčin A, Alexy P (2005) Influence of the composition of polypropylene/organoclay nanocomposite fibers on their tensile strength. *J Macromol Sci A—Pure Appl Chem* 42:543–554. <https://doi.org/10.1081/ma-200056322>
29. Vijayakumar PS, Prasad BLV, Stewart NG, Kong H, Chi F, Lau N, Us CA, Ryan DJ, Pape HL, Solano-Serena F, Contini P, Devillers C, Maftah A, Lepape H, Solanoserena F, Leprat P, Myong NJ, Kawase et al, Kawase M, Kawase Y, Yamada K, Kobayashi K, Suzuki Y, Hutton IM, Holmes M, Chou SJ, Blucher HV, BioFriend, BIEDERMANN, Arnould, Ferrera, Andrea S, Jack T (2009) Handbook of nonwoven filter medium, 363. *Carbon N Y* 111111:11741–11747. <https://doi.org/10.1021/la901024p>
30. Qufu W, Yu L, Ning W, Shanhu H (2008) Preparation and characterization of copper nanocomposite textiles. *J Ind Text* 37:275–283. <https://doi.org/10.1177/1528083707083794>

31. Becheri A, Dürr M, Lo Nostro P, Baglioni P (2008) Synthesis and characterization of zinc oxide nanoparticles: application to textiles as UV-absorbers. *J Nanoparticle Res* 10:679–689. <https://doi.org/10.1007/s11051-007-9318-3>
32. Behnajady MA, Modirshahla N, Hamzavi R (2006) Kinetic study on photocatalytic degradation of C.I. acid yellow 23 by ZnO photocatalyst. *J Hazard Mater* 133:226–232. <https://doi.org/10.1016/j.jhazmat.2005.10.022>
33. Xu B, Cai Z (2008) Fabrication of a superhydrophobic ZnO nanorod array film on cotton fabrics via a wet chemical route and hydrophobic modification. *Appl Surf Sci* 254:5899–5904. <https://doi.org/10.1016/j.apsusc.2008.03.160>
34. El-Ola SMA (2008) Recent developments in finishing of synthetic fibers for medical applications. *Des Monomers Polym* 11:483–533. <https://doi.org/10.1163/156855508X363816>
35. Wong YWH, Yuen CWM, Leung MYS, Ku SKA, Lam HLI (2006) Selected applications of nanotechnology in textiles. *Autex Res J* 6:1–8
36. Joshi M, Bhattacharyya A (2011) Nanotechnology—a new route to high-performance functional textiles. *Text Prog* 43:155–233. <https://doi.org/10.1080/00405167.2011.570027>
37. Ki HY, Kim JH, Kwon SC, Jeong SH (2007) A study on multifunctional wool textiles treated with nano-sized silver. *J Mater Sci* 42:8020–8024. <https://doi.org/10.1007/s10853-007-1572-3>
38. Liu Y, Tang J, Wang R, Lu H, Li L, Kong Y, Qi K, Xin JH (2007) Artificial lotus leaf structures from assembling carbon nanotubes and their applications in hydrophobic textiles. *J Mater Chem* 17:1071–1078. <https://doi.org/10.1039/b613914k>
39. Dhineshbabu NR, Karunakaran G, Suriyaprabha R (2014) Electrospun MgO/nylon 6 hybrid nanofibers, 6:46–54
40. da Silva Paula MM, Franco CV, Baldin MC, Rodrigues L, Barichello T, Savi GD, Bellato LF, Fiori MA, da Silva L (2009) Synthesis, characterization and antibacterial activity studies of poly-(styrene-acrylic acid) with silver nanoparticles. *Mater Sci Eng C* 29:647–650. <https://doi.org/10.1016/j.msec.2008.11.017>
41. Derakhshan SJ, Karimi L, Zohoori S, Davodi-roknabadi A, Lessani L (2018) Antibacterial and self-cleaning properties of cotton fabric treated with TiO₂/Pt, 43:344–351
42. Chapter 1 introduction (1991). *Nord J Int Law* 60:115–127. <https://doi.org/10.1163/157181091x00278>
43. Lim LT, Auras R, Rubino M (2008) Processing technologies for poly(lactic acid). *Prog Polym Sci* 33:820–852. <https://doi.org/10.1016/j.progpolymsci.2008.05.004>
44. Ahmed J, Varshney SK (2011) Polylactides-chemistry, properties and green packaging technology: a review. *Int J Food Prop* 14:37–58. <https://doi.org/10.1080/10942910903125284>
45. Blackburn RS (2005) Poly (lactic acid) fibers. *Biodegradable Sustainable Fibres*. https://doi.org/10.2115/fiber.59.p_329
46. Cicero JA, Dorgan JR (2001) Physical properties and fiber morphology of poly(lactic acid) obtained from continuous two-step melt spinning. *J Polym Environ* 9:1–10. <https://doi.org/10.1023/A:1016012818800>
47. Gao X-R, Niu B, Hua W-Q, Li Y, Xu L, Wang Y, Ji X, Zhong G-J, Li Z-M (2018) Rapid preparation and continuous processing of polylactide stereocomplex crystallite below its melting point. *Polym Bull*. <https://doi.org/10.1007/s00289-018-2544-2>
48. Tu C, Cao X, Zhang R, Wang D, Cui L (2019) Effects of posttreatment on the properties of modified PLLA/PDLA fibers. *Polym Adv Technol* 1–10. <https://doi.org/10.1002/pat.4460>
49. Mujica-Garcia A, Hooshmand S, Skrifvars M, Kenny JM, Oksman K, Peponi L (2016) Poly(lactic acid) melt-spun fibers reinforced with functionalized cellulose nanocrystals. *RSC Adv* 6:9221–9231. <https://doi.org/10.1039/c5ra22818b>
50. Aouat T, Kaci M, Devaux E, Campagne C, Cayla A, Dumazert L, Lopez-Cuesta JM (2018) Morphological, mechanical, and thermal characterization of poly(lactic acid)/cellulose multifilament fibers prepared by melt spinning. *Adv Polym Technol* 37:1193–1205. <https://doi.org/10.1002/adv.21779>
51. Persson M, Lorite GS, Cho SW, Tuukkanen J, Skrifvars M (2013) Melt spinning of poly(lactic acid) and hydroxyapatite composite fibers: Influence of the filler content on the fiber properties. *ACS Appl Mater Interfaces* 5:6864–6872. <https://doi.org/10.1021/am401895f>

52. Bai H, Deng S, Bai D, Zhang Q, Fu Q (2017) Recent advances in processing of stereocomplex-type polylactide. *Macromol Rapid Commun* 38:1–12. <https://doi.org/10.1002/marc.201700454>
53. Zhang J, Tashiro K, Tsuji H, Domb AJ (2007) Investigation of phase transitional behavior of poly(L-lactide)/poly(D-lactide) blend used to prepare the highly-oriented stereocomplex. *Macromolecules* 40:1049–1054. <https://doi.org/10.1021/ma061693s>
54. Andersson SR, Hakkarainen M, Inkinen S, Södergård A, Albertsson AC (2010) Polylactide stereocomplexation leads to higher hydrolytic stability but more acidic hydrolysis product pattern. *Biomacromol* 11:1067–1073. <https://doi.org/10.1021/bm100029t>
55. Tsuji H, Ikada Y (1999) Stereocomplex formation between enantiomeric poly(lactic acid)s. XI. Mechanical properties and morphology of solution-cast films. *Polymer (Guildf)* 40:6699–6708. [https://doi.org/10.1016/S0032-3861\(99\)00004-X](https://doi.org/10.1016/S0032-3861(99)00004-X)
56. Tan BH, Muiruri JK, Li Z, He C (2016) Recent progress in using stereocomplexation for enhancement of thermal and mechanical property of polylactide. *ACS Sustain Chem Eng* 4:5370–5391. <https://doi.org/10.1021/acssuschemeng.6b01713>
57. Gupta A, Prasad A, Mulchandani N, Shah M, Ravi Sankar M, Kumar S, Katiyar V (2017) Multifunctional nanohydroxyapatite-promoted toughened high-molecular-weight stereocomplex poly(lactic acid)-based bionanocomposite for both 3D-printed orthopedic implants and high-temperature engineering applications. *ACS Omega* 2:4039–4052. <https://doi.org/10.1021/acsomega.7b00915>
58. Takasaki M, Ito H, Kikutani T (2003) Development of stereocomplex crystal of polylactide in high-speed melt spinning and subsequent drawing and annealing processes. *J Macromol Sci Part B* 42:403–420. <https://doi.org/10.1081/MB-120021570>
59. Zhang X, Hua H, Shen X, Yang Q (2007) In vitro degradation and biocompatibility of poly(l-lactic acid)/chitosan fiber composites. *Polymer (Guildf)* 48:1005–1011. <https://doi.org/10.1016/j.polymer.2006.12.028>
60. Pötschke P, Andres T, Villmow T, Pegel S, Brünig H, Kobashi K, Fischer D, Häußler L (2010) Liquid sensing properties of fibres prepared by melt spinning from poly(lactic acid) containing multi-walled carbon nanotubes. *Compos Sci Technol* 70:343–349. <https://doi.org/10.1016/j.compscitech.2009.11.005>
61. Murariu M, Doumbia A, Bonnaud L, Dechief AL, Paint Y, Ferreira M, Campagne C, Devaux E, Dubois P (2011) High-performance polylactide/ZnO nanocomposites designed for films and fibers with special end-use properties. *Biomacromol* 12:1762–1771. <https://doi.org/10.1021/bm2001445>
62. Pantani R, Turng L-S (2015) Manufacturing of advanced biodegradable polymeric components. *J Appl Polym Sci* 132:n/a–n/a. <https://doi.org/10.1002/app.42889>
63. Tsuji H (2005) Poly (lactide) stereocomplexes: formation, structure, properties, degradation, and applications. *Macromol Biosci* 5(7):569–597. <https://doi.org/10.1002/mabi.200500062>

Chapter 16

Life Cycle Assessment of Chitosan



Tabli Ghosh and Vimal Katiyar

Abstract Life cycle assessment (LCA) is a standardized practice to assess the life cycle of a product for regulating the environmental impacts of a product life. LCA is a significant entity to maintain the quality and ecological integrity for determining the optimal product and processes in terms of their novel growths. The chapter aims to discuss the LCA of chitosan-based materials with strategies to control the impacts on environment. Chitosan is the second most abundantly available polysaccharides, which are widely used for its biodegradable, biocompatible, non-toxic, and antimicrobial nature and several other properties. The deacetylation of chitin yields chitosan, which can be tailored in different forms and geometry to achieve an extensive demand in the form of powders, films, tablets, particles, composites, etc. Further, the development of chitosan-based active materials having enormous properties can potentially replace the fossil-based materials for stringent food packaging applications, tissue engineering, drug delivery, therapeutics, adhesives, etc. The presence of functional groups such as primary amine and primary and secondary hydroxyl groups in chitosan provides an opportunity for regulating its properties in terms of formulating functional agents. In addition, chitosan can form cross-links and multi-networks through the presence of functional groups, pH, electro response, etc., which may be desired for developing materials with tuned properties. In this context, an understanding regarding the environmental impact of chitosan during its whole life cycle is needed. In this chapter, the discussion on LCA of chitosan and related approaches from available resources for tailor-made properties is made including various design parameters, environmental impacts, product formulation steps, use of different agents, and so on. Additionally, the chapter presents the importance of chitosan in day-to-day life along with its environmental impact for various applications such as food packaging films, edible coatings, flocculants, adhesives, and others.

Keywords Life cycle assessment · Chitosan · Environment · Application

T. Ghosh · V. Katiyar (✉)
Department of Chemical Engineering, Indian Institute of Technology Guwahati, Guwahati,
Assam 781039, India
e-mail: vkatiyar@iitg.ac.in

© Springer Nature Singapore Pte Ltd. 2020
V. Katiyar et al. (eds.), *Advances in Sustainable Polymers*, Materials Horizons: From
Nature to Nanomaterials, https://doi.org/10.1007/978-981-15-1251-3_16

363

1 Introduction

Life cycle assessment (LCA) is a unique strategy to investigate the ecological influences caused by a product during its life, from basic material collection to its end use [1]. A product has multiple stages of life where every stage provides a significant effect on the ecosphere. A general product life cycle includes various stages which begin from the raw material collection followed by processing, product fabrication, packaging, transportation, use, maintenance, disposing, and recycling as represented in Fig. 1, where every stage of a product life may induce hazardous matters, disposable matters, toxicological stress on human health, water resources, air, etc., which delivers a need for an intensive study for LCA of a product. Additionally, throughout the life of a product, numerous resources are required for obtaining targeted products, in terms of raw ingredients (water, chemicals), relevant energy use, and release materials which need to be optimized for its cost-effective use (Fig. 1). In this regard, the product life cycle management helps in maintaining an ecological balance by adjusting material, energy use (fuels), and reducing environmental hazards [2]. The practice can help to quantify the use of energy, materials used for production, developed product, and the impact of individual processes on the environment. It also includes the interpretation of outcomes and related data to make an optimized

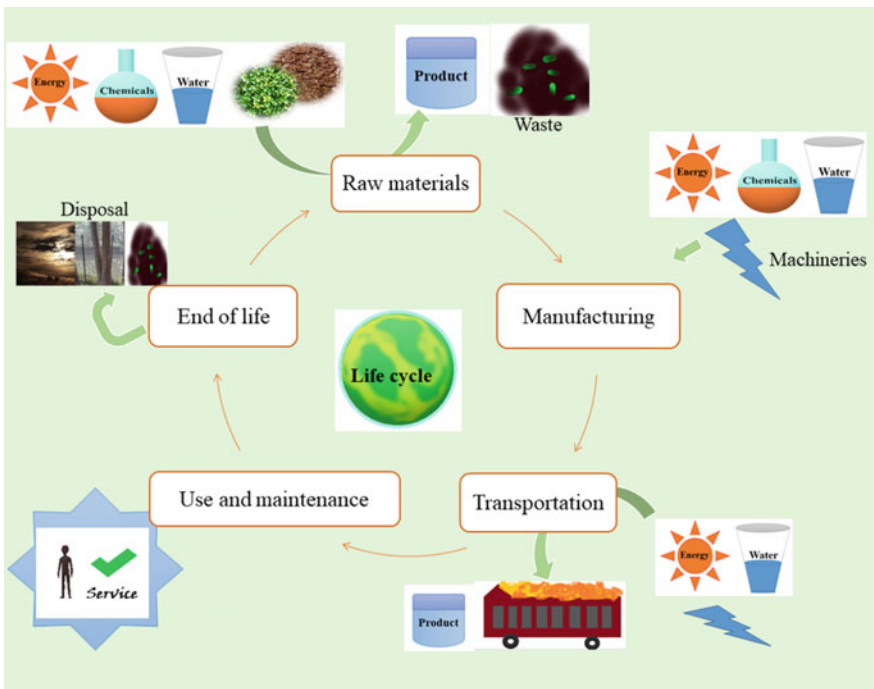


Fig. 1 Life cycle of a product

process for efficient ecobalance. Thus, LCA helps to optimize and make a decision for an optimum use of environmental resources or manmade sources for obtaining the targeted product (Fig. 1) [3]. The important features of LCA are quantity (in terms of mass), capacity (in terms of volume), energy, and other physical units, connecting physical life of the product cycle and interrelated units [4]. Considering these aspects, a discussion has been made based on the intended purpose, phases, and uses of LCA in the below sections.

2 Intended Purpose, Methods, and Variants of LCA

The use of LCA was initiated in 1960s, where the resource and energy limitations became a reason for creating a well-defined way to optimize the process for the use of resource and fuels [5]. In 1969, Coca-Cola company started an in-house study for various beverage products, which created a basis for the present approaches of inventory assessment in the USA. Further, in the USA, the measurement, use of resource, and output of release materials (solid waste, gas materials, energy use) of a product began with a system known as Resource and Environmental Profile Analysis (REPA), and the same process began as ecobalance in Europe. REPA is used as a decision-making tool for private industries, developing public policy, worldwide policy, etc. Additionally, REPA is a well-known practice applied for environmental assessment of products for release materials, procedures, resources used, energy used, discharge products, and others [6]. In later days, the United Nations Environment Programme (UNEP) and Society of Environmental Toxicology and Chemistry (SETAC) joined their hands to organize and promote product cycle initiatives for LCA.

There are various routes of LCA involving process environmental LCA, economic LCA, and society-based LCA. Thus, the assessment analysis for sustainability measurement can be related to the environment, economic, and social factors which can be termed as LCA, life cycle costing (LCC), and social life cycle assessment (SLCA) [7]. LCC deals with the economic upbringing of a process life cycle, where any hidden cost and overall cost determination of a process life cycle are involved. On the other hand, SLC inspects the impact of social and societal features of a produce and related positive and negative perspectives of a product life cycle. In comparison, the flows in LCA involves contaminants, the resource used, interprocessing flows, and energy use, whereas LCC involves the economic analysis in the process flows with an interrelated effect which directly affects decision making [4]. Thus, the complete life cycle sustainability assessment study consists of LCA, LCC, and SLCA. In this chapter, a detailed discussion for the process LCA will be done where the inclusion of LCA expresses a board view on the environmental impact analysis by various ways such as material inputs, energy recovery and production, exergy analysis, and product discharge as discussed earlier. Furthermore, the assessment of the influence of product life on the environment and GHG emission, and finally, the interpretation of outcomes have been made to derive conclusions out of it. In this regard, to maintain sustainability of the atmosphere, LCA is an elementary practice as various processes

evolve various materials, i.e., wastewater treatment plant may produce hazardous elements as waste, the extraction, and processing of polymers may induce air pollution and water pollution, and mostly the industry-based waste has a connection to rivers and other water sources, which has a very hazardous impact on society, living species as detailed in Fig. 2.

LCA of a product is mainly performed in four discrete phases, viz. goal and scope, life cycle inventory (LCI), life cycle impact assessment (LCIA), and interpretation, where each phase is interrelated among each other as represented in Fig. 2b [1]. Among these, methods for LCA analysis of sustainability are generally executed based on ISO 14040 and ISO 14044. However, LCA is considered as an entity of ISO 14000, an environmental management standard (ISO 14040 and ISO 14044) [8]. Greenhouse gas-based product analysis and measurement of an LCA can be done following the publicly available specification 2050 (PAS 2050) and Greenhouse gas (GHG) Protocol Life Cycle Accounting and Reporting Standard [9, 10]. Additionally, ISO 14040:2006 details about the principles and framework of LCA with the inclusion of goal and scope, LCI, LCIA, interpretation phase, reporting and critical review of LCA, and boundaries [11]. Further, ISO 14040:2006 discusses the relationship between phases of LCA and situations of using choices and optional elements. However, ISO 14040:2006 does not detail the LCA techniques and does not specify the methodologies for the individual phases of LCA. On the other hand, ISO 14044:2006 provides requirements and guidelines of LCA including four phases of LCA and reports the critical review of LCA, relationship among each other, conditions of choices, etc. [12]. The Technical Committee ISO/TC 207, Environmental Management, Subcommittee SC 5, and LCA prepared ISO 14040 and ISO 14044:2006. Moreover, ISO 14040 and ISO 14044:2006 replaced ISO 14040:1997, ISO 14041:1998, ISO 14042:2000, and ISO 14043:2000. Thus, the environmental analysis of a product stage can be done by following the reported rules and regulations, where any new product should be examined for its effect on the environment in comparison to an existing product for ecological wellbeing.

2.1 Phases of LCA

Goal and scope. LCA of any product should have a distinct scope of the work with determined focus. The first phase of LCA is considered as a basic step that is necessary for tailoring the process with the aid of LCA. The first phase helps in determining various work bodies such as functional units, system boundaries, assumption, allocation method, and effect on surroundings and living agents. The goal and scope of LCA methods define the functional units (input, processes, and output), which provide complete functions of a process. The goal and scope of every LCA system have some boundaries, limitations, and assumptions, which should be clearly defined to make a strategic plan in the LCA process. The distribution method of LCA is another factor in goal and scope defining the extension, division, and replacement of any entity for easy product development process. In addition,

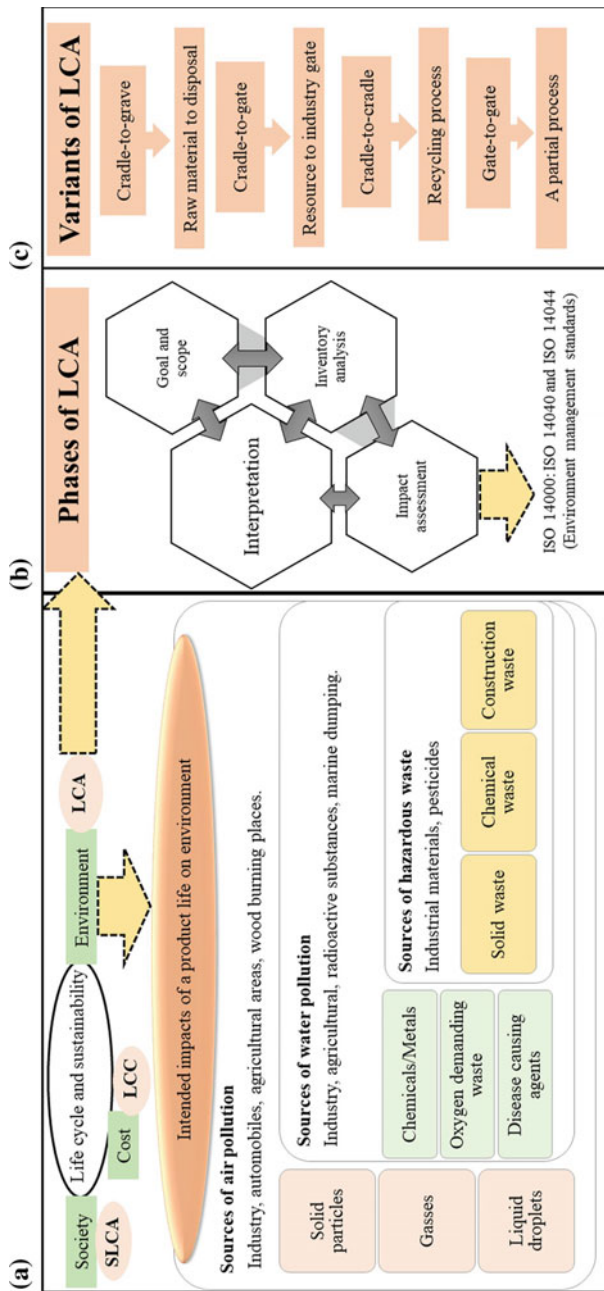


Fig. 2 a Intended environmental hazards from life cycle of a product; b phases of a life cycle based on LCA terms [SLCA: social life cycle assessment, LCC: life cycle costing; LCA: life cycle assessment]

the goal and scope should describe the impact of a process creating environmental hazards such as air pollution, water pollution, and global warming by increasing carbon footprint. The development of a product should not be toxic to human health, animals, water bodies, and others.

LCI. LCI method is a collection of materials needed for the fabrication of a specific product. As already mentioned in Fig. 1, inventory for the fabrication of any product needs raw ingredients, water, energy (for running machinery and transportation purpose), and others. The production system and disposal or reuse of the product may evolve various materials which release to the environment (Fig. 2a). By considering all these cases, LCI is a flow-through system, where an optimum graphic of a process flowchart is described.

LCIA. LCIA phase aims toward the impact assessment of the process on the environment. The process detects control categories, indicators, models, etc. However, the life cycle impacts can be classified depending on manufacture, usage, and dumping of a product, where the impacts of a product life cycle can be categorized as initial, use, and disposal impacts, respectively. The initial impacts of a product mainly include the extraction, fabrication, packaging, and transportation of the product; the use impact includes the effects of the product during its use, maintenance, and repairs; and the impact of end life depends on the discard, waste processing, and recycling of the product.

Interpretation. Interpretation of a product life cycle is a standardized technique used to recognize, quantify, and estimate the information and data values obtained during assessment and inventory analysis. The final phase mainly deals with the concise information on assessment and inventory analysis. The interpretation phase defines the significant issues related to the consequences of assessment and inventory phases; estimation of the specificity, sensitivity, limitation, and recommendations of the product life cycle.

In this way, LCA of a product is done based on the four phases as described above; however, LCA may be conducted in a different section of the product life. The process may vary depending on variants of LCA.

2.2 *Process Variants of LCA*

LCA can be applied in various sections as a functional body in a product life to determine the impact of the product (Fig. 2c). A product has various series of processes for developing the final product, where LCA may involve in a significant portion of the product or in the whole life cycle. Based on this, the variants of LCA are categorized into various processes such as cradle-to-grave [13], cradle-to-gate [13], cradle-to-cradle [14], and gate-to-gate [13]. The variant cradle-to-grave generally includes LCA from the collection of raw material to dumping of the product (end life), where the assessment of the product will be done till the end of life of the product (product stage, usage, and end of life). The cradle-to-gate variant involves the LCA of a product from raw material extraction to factory gate; it does not involve

the transportation or end life of the product, use, and maintenance of the product. Further, cradle-to-cradle variant is a closed-loop system or recycling process, where LCA is done in a closed loop without breaking the product cycle. The gate-to-gate process is a value-added process, where a step in the process involves LCA analysis, not the whole process. In this chapter, cradle-to-gate LCA of chitosan will be detailed. However, various gate-to-gate analyses for the application of chitosan as film, waste management will be discussed. This chapter deals with the life cycle assessment (LCA) of chitosan and related modifications from available renewable resource along with the details about LCA of chitosan production and its related applications.

3 Origin of Chitosan: A Class of Polysaccharides

Polysaccharides are agro-based biopolymers consisting of long chains of monosaccharide units linked together by glycosidic linkages. These are commonly a complex branch of carbohydrates, where more than ten units of monosaccharides are bound together to form a polysaccharide unit. However, polysaccharides have various structures ranging from linear to highly branched, where the properties of particular polysaccharide unit vary depending on the type, modification of monosaccharide units, etc. Polysaccharides are classified into homopolysaccharides (branched and unbranched) and heteropolysaccharides (branched and unbranched). Homopolysaccharides are composed of long chains of similar repeating units, whereas heteropolysaccharides contain different kinds of monosaccharide units. Homopolysaccharides can be regarded as storage or structural polysaccharides. The role of storage polysaccharides generally is to store energy in plants and animals, and structural polysaccharides generally supply stiffness to the plants and insects. The available storage polysaccharides in plants include amylose, amylopectin, and starch, and those in animals generally include glycogen. The structural polysaccharides are cellulose, chitosan, pectin, and arabinoxylans which serve to maintain the structure in plants. The examples of heteropolysaccharide generally include hyaluronic acid, dermatin sulfate, keratin sulfate, heparin, etc. The polysaccharide-based biopolymers have wide applications in various sectors including food packaging and biomedical [15, 16].

3.1 Storage Polysaccharides

Storage polysaccharides generally work to store energy in plants and animals. The storage polysaccharide starch is composed of amylose and amylopectin [16, 17]. Amylose is a linear storage polysaccharide having $\alpha(1 \rightarrow 4)$ glucose unit, and amylopectin is a branched storage polysaccharide consisting $\alpha(1 \rightarrow 4)$ glucose unit as a linear chain and $\alpha(1 \rightarrow 6)$ glucose as a branching unit [18]. The vegetable potato,

rice, maize, wheat, rye, and barley are renewable and available sources of starch in the human diet [17]. Starches are used for the preparation of packaging material for a biodegradable use, edible films, coatings, foams, and others [19–22]. In addition, glycogen is a storage polymer in animal cells as deposited in adipose tissue. Glycogen has a similar structure as amylopectin with a more branched and compact structure. Glycogen is generally a primary form of carbohydrate stored in the animal body [23]; however, unlike starch, it is soluble in water. The common disorder related to glycogen is glycogen metabolism, glycogen depletion, and others [24–26]. It has a special role in the glucose cycle, and the amount of presence of glycogen in the body depends on various factors including physical exercise, metabolic rates, eating habits, etc.

3.2 *Structural Polysaccharides*

The structural polysaccharides deliver stiffness to the plant and living species. Among available structural polysaccharides, cellulose is the main material for maintaining the structural integrity in plants. Cellulose is a biopolymer mainly formed by repeating units of β -glucose units and has a remarkable property with application in various fields [16, 27, 28]. Cellulose and its various derivatives provide an emerging application in the field of packaging as edible and non-edible materials for advanced applications [16, 29]. Furthermore, chitosan, a derivative of chitin, helps in maintaining the stiffness in insect, seafood such as crabs and shrimps, which are the available resources of chitin [29, 30]. Chitosan is extensively used as an antimicrobial, antibacterial, and antifungal agent in the development of active packaging in both edible and non-edible forms. Some enzymes can degrade chitin such as chitinases, which is a product of some bacteria, fungi, some plants, human, etc. [31, 32]. The other structural polysaccharide is pectin, a complex polysaccharide, which constitutes 1,4-linked α -D-galactosyl uronic acid. Some plants have pectin in addition to acetylated galacturonic acid and methyl esters. Pectin is generally obtained from citrus fruits and has a wide application in food as a gelling agent for preparing jam and jellies, and in the biomedical sector for drug delivery, gene delivery, and wound healing [33–36]. Further, it is used as an ingredient to improve the packaging property as edible and non-edible packaging. The other type of arabinoxylans is a copolymer of arabinose and xylose and available in cell walls of plants having a beneficial effect on human health. Various structural polysaccharides are available and have a beneficial effect to human; however, the chapter will widely discuss the chitosan extraction and its LCA as a guide for making an optimized decision.

4 History Outline of Chitosan

In 1811, chitin was first discovered in mushroom by Henri Braconnot, a French scientist [37]. After some 20 years later, chitin was noted to be present in the structure of insects and plants. The word chitin is derived from “chiton” (a Greek word) which has the meaning “coat of mail” [38]. The other meaning of the word is termed as “tunic” or “envelop.” In 1843, the presence of nitrogen in chitin was found by Lassaigne [39]. In 1859, chitosan was first observed by Rouget, when he observed that chitin can be modified by chemical and temperature treatment and is found to be soluble [40]. In later days, chitosan was named by Hoppe-Seyler [40, 41]. The research on chitin and chitosan was conducted since the early twentieth century from crab and fungi. Now, chitosan has become the second most abundantly available polysaccharide being used in various fields due to its biodegradable, biocompatible, non-toxic nature, and many beneficial properties [42, 43]. Chitosan is considered as an agro-based biopolymer, consisting of an acetylated unit and deacetylated unit of β -(1 \rightarrow 4)-D-glucosamine and *N*-acetyl-D-glucosamine, respectively [42, 43]. As mentioned in earlier section, chitosan is a derivative of chitin obtained generally from crabs, algae, shrimp, fungi, protozoa, etc. [44]. Every year, there is a generation of waste from sea products, which can be used for chitosan production. Table 1 shows the generation of various sea-based waste globally. Thus, the formulation of chitosan from various resources is a useful technique for waste reduction. The consumer need for chitosan is increasing day by day, where according to the Grand View Research Report (January 2017), it was announced that the market size of chitosan is 1.06 billion, which was raised to 3.19 billion by 2015. It is expected that the chitosan market size will reach USD 17.84 billion by 2025 [45]. According

Table 1 Global sea-waste generation: a source for chitosan production

S. no.	Sources of waste	Waste generation per year	Reference
1.	Crab, shrimp, lobster shell (globally)	6–8 million ton	[73]
2.	Crab, shrimp, lobster shell (Southeast Asia)	1.5 million ton	[73]
3.	Malaysian fishery industry	70,000 ton	[74]
4.	Crustacean waste (Chile, 2001)	526 ton	[75]
5.	Fish processing plants waste (five coastal cities in Argentina, 1989–2001)	49786 ton	[76]
6.	Mississippi shrimp industry (1998)	6277 ton	[76]
7.	Crab, lobster, shrimp, krill, clam/oyster shell (global production)	1.44 million metric ton	[77, 78]
8.	Global shellfishery waste	6–8 million metric ton	[79]
9.	Chitinous waste (India)	60,000–80,000 ton	[80]
10.	Mushroom-based waste	50,000 metric ton	[81]

to a market survey in 2010, the USA and Japan provide the major market size of chitin and chitosan. The chitin and chitosan production industries are located in Japan in a majority, among which shells of shrimps and crabs become a major resource for chitosan production [46]. In Japan, more than 100 billion tons of chitosan are produced annually from shrimp and crab shells annually [46]. In the European Union, the development of biopolymers including chitin and chitosan is around EUR 433 million in 2007, whereas in 2006, it was around EUR 385.5 million [47].

4.1 Routes of Chitosan Fabrication

The general process for the extraction of chitin from various resources includes chemical and enzymatic treatment. Chitosan is available from various resources such as crustaceans, insects, mollusks, and fungi. The process of chitin and chitosan fabrication mainly involves the removal of protein, calcium carbonate, magnesium carbonate, and other minerals from the specific resources. The chemical method for the extraction of chitosan includes the following steps: (1) washing and crushing of available chitosan resource, (2) deproteinization using alkali (NaOH) to remove proteins from available sources, (3) demineralization by acidic treatment (HCl, HNO₃, H₂SO₄, CH₃COOH) to remove minerals including calcium carbonate, calcium phosphate, and others, (4) discoloration, and (5) deacetylation of obtained chitin to fabricate chitosan molecule using NaOH or KOH [42, 48, 49]. The steps washing, crushing, deproteinization, demineralization, and discoloration provide chitin, and finally, the deacetylation of chitin provides chitosan. On the other hand, the extraction of chitosan by biological treatment involves (1) washing and crushing of available source, (2) deproteinization by proteolytic microorganisms or proteolytic enzymes (proteases) to remove protein, (3) demineralization can be done enzymatically (alcalase) or microbially [48, 49], and (4) deacetylation of obtained chitin to fabricate chitosan molecule using chitin deacetylase. Interestingly, the mechanical processes can also be applied for the deproteinization treatment. Chitosan can be well utilized for many beneficial properties in various fields as discussed in the later sections. Further, the development of chitosan can help to reduce sea-based waste material, which is forecasted to become the same as plastic waste in the future if not utilized properly.

4.2 Properties of Chitosan

Additionally, chitosan can be functionalized and modified for wide application due to the presence of reactive groups such as amino and primary and secondary hydroxyl groups [38]. Though the use of unmodified form of chitosan in various field has been extended throughout the world, the presence of functional groups (primary amine, primary and secondary hydroxyl groups) provides an opportunity for tailoring the

properties in the applied field through forming self-cross-linking networks or with other molecules and multi-network, where the reactivity of chitosan can be improved by the addition of a chemical group through ionic, covalent bonding (grafting). Further, the pH, temperature, and ionic sensitivity of chitosan offer an effectiveness on chitosan use. Chitosan is generally modified by targeting reactive amino groups for altered functional properties such as hydrophilicity, compatibility, and others. Thus, chitosan is well utilized in various forms and geometry according to the mode of application such as powders, films, tablets, hydrogel, capsules, particles, and composites, achieving a great application in various fields of day-to-day life. Nowadays, chitosan is considered to be a dietary supplement for weight reduction and is widely used in Japan and Europe. The general property of chitosan includes antioxidant, antibacterial, anti-inflammatory, body weight reducer, fat binder, adsorption enhancer, emulsifier, thickener, stabilizer, cholesterol-lowering property, antidiabetic property, etc., as shown in Fig. 3. The details of some of the properties of chitosan are discussed in Table 2. The antioxidant property of chitosan is varied based on the chitin source, and processing conditions such as time for alkaline deacetylation [50, 51]. As detailed in Table 2, the antioxidant property can be measured in terms of phenolics, scavenging, reducing, chelating, and other activities. In this regard, chitosan can be used as food supplements for delivering antioxidant activity to human health. Chitosan offers antibacterial and antimicrobial activity in food products. However, chitosan is more effective for gram-positive bacteria than gram-negative bacteria. The antibacterial effect of chitosan is varied depending on the concentration and

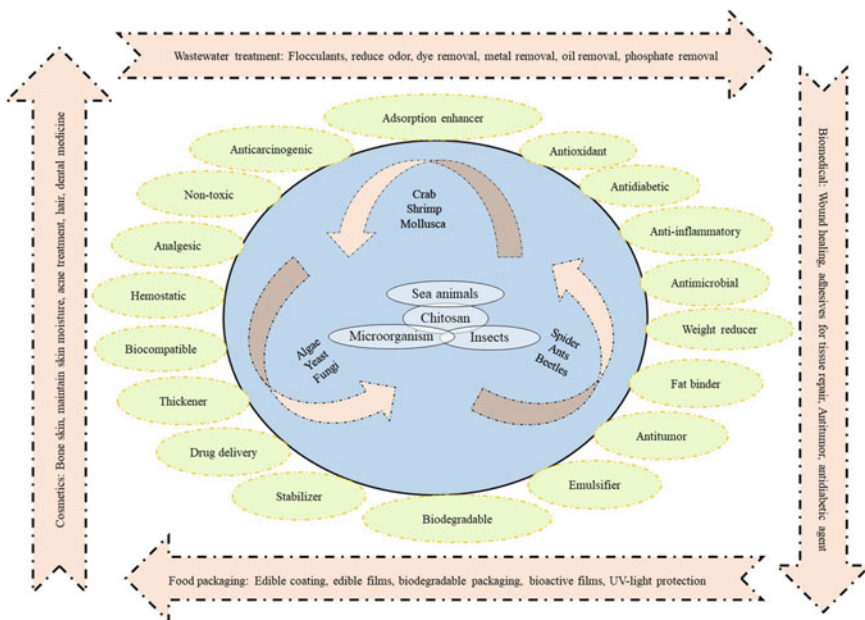


Fig. 3 Chitosan resources and its application

Table 2 Properties of chitosan and its derivatives

Form of chitosan	Properties	Effect	Reference
Chitosan (crab shell)	Antioxidant specification:(0.1–10 mg/mL (0.2% acetic acid)	Antioxidant property: 58.3–70.2% (1 mg/mL) 79.9–85.2% (10 mg/mL) Scavenging activity: 62.3–77.6% (0.1 mg/mL) 28.4% (10 mg/mL) Chelating ability: 82.9–96.5% (1 mg/mL) 97.9% (0.1 mg/mL, EDTA)	[50]
Fungal chitosan (Shiitake stipes)	Antioxidant	Antioxidant activity: 61.6–82.4% (1 mg/ml) Reducing power: 0.42–0.57 (10 mg/mL) Scavenging ability: 28.4–31.3% (10 mg/mL) Chelating ability: 88.7–90.3% (1 mg/mL)	[51]
Chitosan and chitosan oligomers (crab shell) Chitosan MW: 28, 224, 470, 746, 1106, 1671 kDa	Antibacterial (Gram-positive bacteria)	Stronger effect for all MWs chitosan Stronger effect at 0.1% chitosan Effective MW chitosan oligomers : 2, 4 kDa	[52]
Chitosan and chitosan oligomers (crab shell) Chitosan MW: 224, 470, 746, 1106 kDa	Antibacterial property (Gram-negative bacteria)	<u>Most effective</u> <i>Escherichia coli</i> , 746 kDa <i>Pseudomonas fluorescens</i> , 746 kDa <u>Less effective</u> <i>S. typhimurium</i> , <i>V. parahaemolyticus</i> , 470 kDa <u>Weak or no antibacterial activity</u> <i>Salmonella typhimurium</i> , 1106 and 224 kDa	[52]
Chitosan oligosaccharides	Anti-inflammatory	Effective against – Lipopolysaccharide-induced inflammation – Allergic inflammation and asthma – Lipopolysaccharide-mediated macrophages	[82–84]
Chitosan	Body weight and cholesterol-lowering property	– Control obesity and lipoprotein balance – Lower serum cholesterol by 5.8–42.6%. – Lower low-density lipoprotein by 15.1–35.1%	[85, 86]
Chemically modified chitosan	Antidiabetic property	<u>Chitosan–gallic acid conjugate</u> – Improved α -glucosidase activity – Improved α -amylase activity <u>Catechin-grafted chitosan</u> – Improve antidiabetic activity due to phenolic group	[87, 88]

molecular weight. Oligomers of chitosan have less antibacterial effect than chitosan [52]. Further, zinc-crystallized, insulin-loaded, glycol-loaded chitosan nanoparticle helps in controlling blood glucose and is effective in type 1 diabetes [53]. Chitosan and its derivatives also help in treating various age-related diseases such as diabetes, cancer, hypercholesterolemia, and other age-related dysfunction [54].

4.3 Applications of Chitosan

Chitosan has enormous properties and potential to replace fossil-based materials in the fields of stringent food packaging, tissue engineering, drug delivery, and therapeutic, medicinal, and commercial applications. Various applications with its added advantages and properties in various sectors are represented in Table 3. Chitosan is majorly used in the fields of food packaging, biomedical application, wastewater treatment, and cosmetics as discussed in Fig. 3.

Chitosan for Food Packaging. Chitosan is extensively used in food packaging application for the properties of biodegradability, biocompatibility, non-toxicity, etc. The properties of chitosan can be tuned in terms of formulating blends and composites with other polymers. Chitosan and oligomers of chitosan have antioxidant, antimicrobial, antibacterial, and cholesterol-lowering activity properties that could help to act as edible coating materials to deliver added advantages to human health and shelf-life extension of food products. The formulation of the edible coating accommodates a simple process of preparing coating materials which is applied on food products by dipping or spray coating. The preparation of chitosan-based coating material involves the stirring of materials in an acid solution (acetic acid solution). Additionally, chitosan is also used with other polymers and bioactive agents for additional benefits [55]. The application of chitosan as an edible coating on strawberry fruit helps in maintaining the strawberry quality in terms of bioactive compounds such as phenolic, flavonoids, and antioxidant enzyme activity [56]. Moreover, the use of bilayer coating of carboxymethyl cellulose and chitosan on fruit products can help to avoid the commercial wax-based coating to maintain fruit gloss and water resistance and maintain fruit stability during cold storage [57]. Chitosan is mixed with other polymeric materials with improved polymer–polymer interaction than water–polymer interactions to be used in food packaging and advanced industrial applications. Hydrogel of chitosan with other polymeric materials is used as a time–temperature indicator for active food packaging [58]. However, hydrogel can be considered as a perfect material for preparing better water containing materials through various cross-linking networks with other polymers. The other biopolymers such as cellulose are used as food packaging materials [16], but the use of chitosan hydrogel as food packaging materials is restricted. Thus, various design parameters of chitosan can be tailored which may affect the property of physical and chemical hydrogel. The formulation of chitosan with other materials help in improving its properties as food packaging film in terms of better mechanical properties, plasticizing effect,

Table 3 Application of chitosan as green replacement and its importance

Material	Form	Application	Reference
Chitosan Glycerol Trisodium citrate dehydrate	Adhesive	<u>Chitosan-based adhesive for wood bonding</u> – Bond strength: 6.0 MPa (dry condition) – Bond strength: 1.6 MPa (wet condition)	[63]
Chitosan	Adhesive	<u>Chitosan-based adhesive for tissue repair</u> – Flexible and insoluble strips – Elastic modulus: 6.8 MPa <u>Repair condition of intestine tissue (Upon infrared laser activation)</u> – Tensile strength: 14.7 kPa at 60–65 °C	[59]
Chitosan Dopamine Quinone	Adhesive	Quinone-tanned chitosan – Water-resistant adhesive – Analogous to mussel glue – Improve viscosity – Shear strength: 400 kPa	[60]
Chitosan Konjac glucomannan	Adhesive	– Good water resistance – Low cost – Used for plywood production	[64]
Chitosan	Edible coatings	– Maintains fruit quality – Maintains antioxidant property – Controls the decay of fruit products – Applied for strawberry	[56]
Chitosan Carboxymethyl cellulose	Bilayer edible coating	– Improves fruit gloss – Does not improve weight loss – Homogeneous and stable coating – Applicable for citrus fruits	[57]
Chitosan 1-methylcyclopropene	Edible coating	– Extends the product life of banana – Improved appearance – Improved texture	[89]

(continued)

Table 3 (continued)

Material	Form	Application	Reference
Chitosan	Edible film Vacuum packaging	<ul style="list-style-type: none"> – Reduced chemical spoilage – Reduced growth of microorganism – Improved shelf life of sea bass fillets 	[90]
Chitosan Thyme oil	Wound healing	<ul style="list-style-type: none"> – Antibacterial film – Permeable film – Improved wound healing property 	[91]
Chitosan	Coagulation and flocculation	<ul style="list-style-type: none"> – Dye removal by 99% – Recycling is possible – Flocculation of kaolinite suspension 	[92, 93]

etc. The rising importance and reasons behind designing and developing biodegradable packaging materials make chitosan a remarkable component in comparison to conventional polymers in food packaging sector.

Chitosan for Biomedical Application. In biomedical application, chitosan being a biocompatible material provides opportunities to be used in the preparation of bone and scaffold materials. Chitosan has antidiabetic, anticancer, anti-tumor, and anti-inflammatory activity which helps to gain a wide enthrallment in the area of tissue engineering (Fig. 3). Chitosan is used as an adhesive material for tissue repair (such as intestine tissue) and bonding and has the potential to mimic mussel glue in the human body [59, 60]. The infrared laser activation process helps chitosan adhesives to adhere on the tissue [59]. Chitosan forms an insoluble, flexible, water-resistant material and provides other remarkable properties, which make it a significant adhesive material [59]. Chitosan has potential to be used in antibacterial, non-toxic, and controlled drug delivery applications, so the biopolymer is used for wound healing and as drug delivery agent in human health. Chitosan with adsorbed iron in the form of magnetic chitosan can be used as an identical agent for tissue engineering and drug delivery. The chitosan-based hydrogel is extensively used in a biomedical application for the control drug delivery, skin scaffolds, wound healing, etc. [61, 62]. Chitosan with different biopolymers can be prepared through different techniques such as blending and composite formulations with available biomaterials including cellulose, starch, and chitosan for biomedical application.

Other Applications of Chitosan. Chitosan has wide application in the field of wastewater treatments such as textile wastewater, vegetable wastewater, steel industry, pulp mill wastewater, etc. Chitosan can be used for wastewater treatment such as adsorbent, flocculants, membrane, hydrogel, etc. As adsorbents, magnetic chitosan acts as an ideal agent, which forms a metal complex with the metals present in the water. The general mechanism involves the adsorption of the metal component present in water, which are further removed as solid waste. Besides, chitosan is used

as adhesive materials in biomedical application, wood bonding, and plywood production [63, 64]. Moreover, chitosan is widely used for producing health products such as hair care products, skin moisturizer, acne treatment, dental medicines, etc. (Fig. 3).

5 LCA of Chitosan and Related Products

The environmental impacts of chitosan and related products are due to the collection, extraction, production, treatment, transfer of materials, waste disposal, etc. In this section, the factors affecting the production of chitosan, and its application in the edible coating, films as adhesive materials and flocculants will be discussed. The LCA analysis can be implemented in LCA software such as SimaPro.

The chitosan and related products should be tested for the followings:

- **Raw materials:** The extraction and processing of raw materials are analyzed by LCA. The useful path for raw material extraction in terms of chitosan yield, low toxicity, and environmental impact is determined for environmental impact analysis. Further, the damage of chitosan-related products such as packaged food is reduced by taking special care and are measured in the LCA process.
- **Water:** The used water during processing is treated for reuse with proper technique. The environmental impacts on wastewater, treated wastewater, and sludge are included in an LCA process. The wastewater and separated sludge consist of heavy metals such as arsenic, fluorides, cadmium, dissolved solids, biological oxygen demand, chemical oxygen demand, phenols, oils, fats, etc. The water-based waste consists of chemicals such as herbicides and pesticides, which are removed for reuse water and avoiding pollution of water resources.
- **Energy:** The energy sources are from coal, natural gas, petroleum, etc. In addition, wood, natural gas, oils, and electricity are a source of energy needed for product processing. Transportation energy includes energies required for transporting to the customer using truck, ships, pipelines, and trains (cradle-to-grave analysis).
- **Waste generation:** The atmospheric emission of a process includes particulates, carbon sources, nitrogen, sulfur oxides, organic compounds, and others.
- **Solid waste:** Municipal solid waste, residues
- **Maintenance and recycling:** LCA for cradle-to-grave and cradle-to-cradle includes the testing of environmental effectiveness for maintenance and recycling of a product.

5.1 LCA of Chitosan Production

As discussed in the earlier section, the production of chitin from shrimp shell is done following the processes: washing of extracted shrimp shell, drying of shrimp shell,

deproteinization, demineralization, and discoloration. The LCA process of chitosan production is given in Fig. 4. The goal of the process is to determine the environmental effect of producing chitosan. The LCI includes waste chemicals, wastewater, greenhouse gas emission, and increase in carbon footprint. The main environmental burden for producing chitosan is the production of acid effluents that is used for the demineralization process. As discussed in Fig. 4, the ingredients required for chitosan production are chemicals, water, electricity, fuel, etc. In this section, the LCA of chitosan is done by analyzing chitin and chitosan production from shrimp shell. In 2017, Muñoz [65] discussed the production of 1 kg of chitin from shrimp shell. For the production, fresh weight of shrimp shell (33 kg) is required, which undergoes demineralization using dilute HCl solution (32% and 8 kg), deproteinization using NaOH solution (98%, 1.3 kg), and can fabricate 1 kg of chitin with the specified amount of shrimp shell [65]. The detailed process of chitin production (1 kg) needs 1.3 kWh of electricity, 167 L of water, and others [65]. The process of chitin production produces protein sludge as fertilizer (4 kg), calcium waste (1.5 kg), CO₂ (0.7 kg per kg chitin), and wastewater (167 L) [65]. Further, the chitosan production from chitin includes the use of NaOH, water, energy in the form of electricity and fuel. The production of 1 kg chitosan required 1.4 kg of chitin, which is fabricated following deacetylation process, where NaOH (98%, 5.18 kg) is used for deacetylation of chitin (1 kg) [65]. The process is used 250 L of water, electricity of 1.06 kWh, wood fuel (31 MJ), and others. The outlet of chitosan production includes chitin/chitosan, carbon sources, nitrogen fertilizer, wastewater, and salts. The produced nitrogen fertilizer can be used in the agricultural field, and salts of chemicals can be disposed

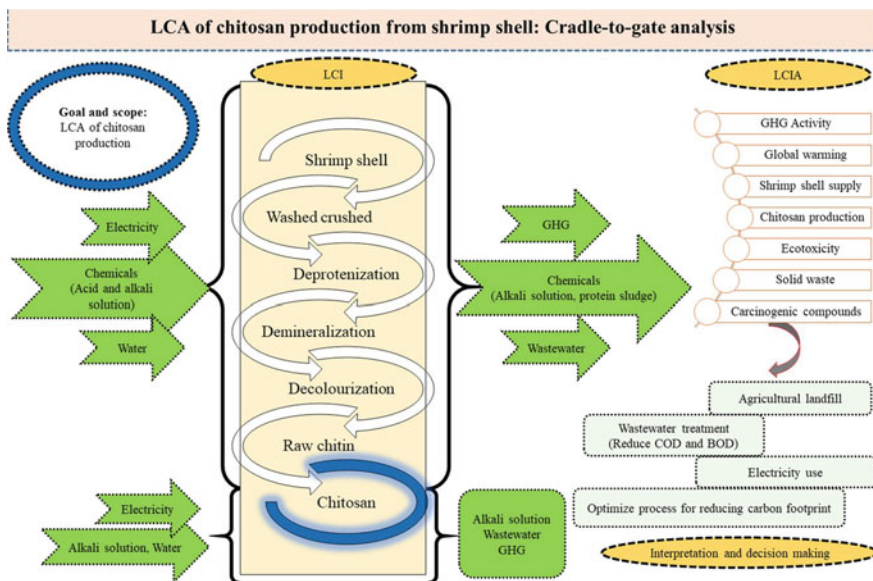


Fig. 4 LCA of chitosan production

in the landfill. The strategies for the disposal generation during chitosan production include neutralization of acid/base water for optimizing organic emission, chemical, and biological oxygen demand [66]. The fermentation of carcinogens reagents and other components helps in reducing living species, toxicity, and soil quality. Further, the wastewater management should be done properly, where management of separated sludge is also an important part. The wastewater should not be thrown to water resources, which create another reason for water pollution. The protein sludge can be reused as animal feed. The observation data for LCA of chitosan include resource available, electricity requirement, fuels, waste generation, and maintenance.

5.2 LCA of Chitosan as Edible Coatings and Films

Chitosan is extensively used as edible film and coating materials for its varied properties. Generally, fruits and vegetables respire, where the respiration rate of fruits and vegetables is directly related to the metabolic rate and senescence of fruit and vegetables. The respiration of fruits and vegetables mainly depends on storage temperature, time, and gas concentration [67]. In this regard, the use of edible films and coatings can help in reducing the respiration rate of fruits and vegetables by acting as a barrier against environment. Moreover, the use of edible coatings and films help in reducing the plastic-based waste generated by food packaging industry. The plastics used in food packaging in market are equal to the food packaging-based plastic waste due to the short life span of food products. Interestingly, bio-based products have less impact on the environment in comparison to fossil-based products [68, 69]. Further, the combined use of films and coatings with modified atmospheric packaging can help in reducing the respiration rate of fruits and vegetables with improved shelf life. There is an increasing use of edible coatings and films for maintaining the nutrient content of food products with the delivery of nutrients. The available biopolymer-based materials for edible coatings include cellulose, chitosan, starch, pectin, and others. Among available biopolymers, chitosan is one of the mostly used biopolymers as edible coating materials with added agents.

The LCA of chitosan coating for fresh-cut fruit products is found to be effective for the environment (Fig. 5). The goal of LCA for chitosan-based edible coating includes environmental influence of using chitosan. The environmental assessment of edible coating on fruit products can be measured in terms of abiotic depletion potential, global warming potential, human toxicity potential, and others. The principal component of edible coating is toxicity toward human, water, and global warming. The usage of electricity is a critical factor for the LCA of edible coating of papaya. Further, the impact of 2% chitosan to provide a coating on papaya in terms of abiotic depletion, global warming, ozone layer depletion, human toxicity, freshwater aquatic ecotoxicity, marine aquatic ecotoxicity, terrestrial ecotoxicity, photochemical oxidation, acidification, eutrophication are 0.008 kg Sb, 0.664 kg CO₂, 0.000 kg CFC-11, 0.094 kg 1,4 DB, 0.019 kg 1,4 DB, 126.592 kg 1,4 DB, 0.001 kg 1,4 DB, 0.001 kg C₂H₄, 0.007 kg SO₂ eq, and 0.000 kg PO₄ eq, respectively [70]. As shown in

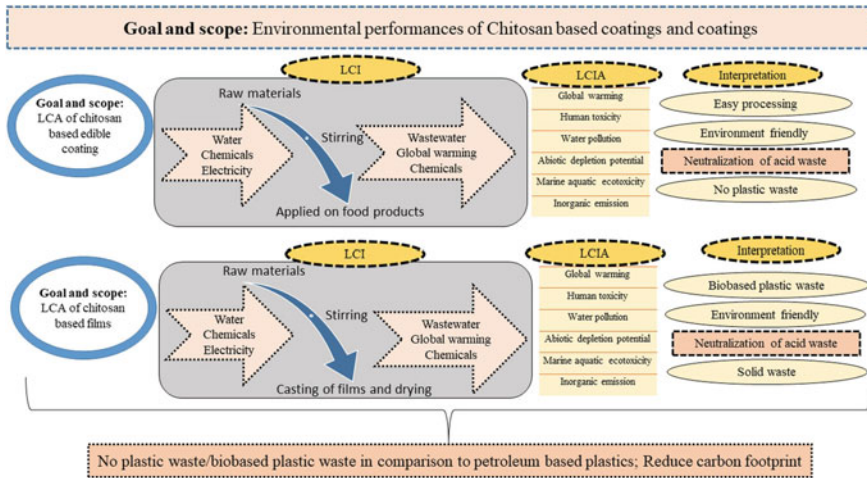


Fig. 5 LCA of chitosan-based coatings and films in comparison to petroleum-based films

Fig. 5, the impact analysis of LCA of chitosan-based coatings and films are detailed with their boundary conditions. According to various reports, it has been shown that the fossil-based films have more environmental impacts in terms of raw material extraction and producing carcinogens than biodegradable materials. The impact of packaging films can be determined in terms of carcinogens, respiratory organics/inorganics, climate change, radiation, ecotoxicity, and others. The end of life cycle of petroleum-based films causes a great environmental impact than biodegradable polymers. In this regard, the sustainable production of edible films can help to reduce the environmental impacts caused by end of life cycle.

5.3 LCA of Chitosan as Flocculation and Adhesives

As discussed in the earlier sections, chitosan is used as adhesive material for tissue repairing and wood bonding. Chitosan is a specific material to be used as adhesive materials in comparison to other available materials for its biodegradable nature [71]. Chitosan-based adhesive provides less environmental impacts in comparison to the other materials. Moreover, the development of adhesive materials should be tested based on the adhesive properties and environmental impacts for analyzing the impacts. Chitosan is also used as a flocculant for harvesting algae, where chitosan flocculants offer the least environmental impacts in comparison to centrifugation and filter/press processes [72]. The harvesting of algal biomass (*Neochloris oleoabundans*) using chitosan as flocculants (200 g) for 2.11 m³ volume processed has 95% of recovery efficiency, where 0.3 kWh electricity is needed [72]. On the other hand, the harvesting of algal biomass (*Neochloris oleoabundans*) using ferric sulfate as

flocculants (800 g) for 8.11 m³ volume processed has 25% of recovery efficiency, where 1 kWh electricity is needed [72]. Use of chitosan in various application tends to be efficient in terms of required energy and biodegradability.

6 Conclusion

LCA is considered as a standard practice used for analyzing the effect of a product life cycle on environment. LCA is also used as a process to determine the effectiveness in terms of product yield, energy efficiency, and environmental impacts. Chitosan is a popular biopolymer for its unique properties and wide applications in various sectors such as food packaging, biomedical, wastewater treatment, and commercial application. The biopolymer is an available source which is extracted from sea-based waste, where sea waste may become equal to the plastic-based waste in coming years. The use of chitosan helps in decreasing the environmental effect and optimum resource use. Chitosan consists of reactive groups which provide an extensive way to be used in various fields. However, the use of chitosan can help to reduce environmental impacts after end of use in comparison to the petroleum-based materials. The use of chitosan can help in decreasing global warming by decreasing carbon footprint. Chitosan-based coatings and films provide another way to decrease solid waste and carbon footprint, where petroleum-based packaging creates a lot of plastic waste in day-to-day life. Further, the LCA of chitosan showed that use of chitosan helps in reducing the environmental impact in comparison to the available used entity.

References

1. Kloepffer W (2008) Life cycle sustainability assessment of products. *Int J Life Cycle Assess* 13:89–95. <https://doi.org/10.1065/lca2008.02.376>
2. Groot WJ, Borén T (2010) Life cycle assessment of the manufacture of lactide and PLA biopolymers from sugarcane in Thailand. *Int J Life Cycle Assess* 15:970–984. <https://doi.org/10.1007/s11367-010-0225-y>
3. Shen L, Patel MK (2010) Life cycle assessment of man-made cellulose fibres. *Lenzinger Ber* 88:1–59
4. Norris GA (2001) Integrating life cycle cost analysis and LCA. *Int J Life Cycle Assess* 6:118–120. <https://doi.org/10.1007/BF02977849>
5. Scientific Applications International Corporation (SAIC), Curran MA (2006) *Life-cycle assessment: principles and practice*. Cincinnati, Ohio. National Risk Management Research Laboratory, Office of Research and Development, US Environmental Protection Agency, pp 1–18
6. Hunt RG, Sellers JD, Franklin WE (1992) Resource and environmental profile analysis: a life cycle environmental assessment for products and procedures. *Environ Impact Assess Rev* 12:245–269. [https://doi.org/10.1016/0195-9255\(92\)90020-X](https://doi.org/10.1016/0195-9255(92)90020-X)
7. Martínez-Blanco J, Lehmann A, Muñoz P, Antón A, Traverso M, Rieradevall J, Finkbeiner M (2014) Application challenges for the social Life Cycle Assessment of fertilizers within life

- cycle sustainability assessment. *J Clean Prod* 69:34–48. <https://doi.org/10.1016/j.jclepro.2014.01.044>
8. Finkbeiner M, Inaba A, Tan R, Christiansen K, Klüppel HJ (2006) The new international standards for life cycle assessment: ISO 14040 and ISO 14044. *Int J Life Cycle Assess* 11:80–85. <https://doi.org/10.1065/lca2006.02.002>
 9. Finkbeiner M (2009) Carbon footprinting—opportunities and threats. *Int J Life Cycle Assess* 14:91–94. <https://doi.org/10.1007/s11367-009-0064-x>
 10. Sinden G (2009) The contribution of PAS 2050 to the evolution of international greenhouse gas emission standards. *Int J Life Cycle Assess* 14:195–203. <https://doi.org/10.1007/s11367-009-0079-3>
 11. ISO (2016) Environmental management—life cycle assessment-principles and framework. ISO 14040:2006
 12. ISO (2016) Environmental management—life cycle assessment-requirements and guidelines. ISO 14044:2006
 13. Liu G, Müller DB (2012) Addressing sustainability in the aluminum industry: a critical review of life cycle assessments. *J Clean Prod* 35:108–117. <https://doi.org/10.1016/j.jclepro.2012.05.030>
 14. Braungart M, McDonough W, Bollinger A (2007) Cradle-to-cradle design: creating healthy emissions—a strategy for eco-effective product and system design. *J Clean Prod* 15:1337–1348. <https://doi.org/10.1016/j.jclepro.2006.08.003>
 15. Borkotoky SS, Ghosh T, Bhagabati P, Katiyar V (2018) Poly (lactic acid)/modified gum arabic (MG) based microcellular composite foam: Effect of MG on foam properties, thermal and crystallization behavior. *Int J Biol Macromol* 125:159–170. <https://doi.org/10.1016/j.ijbiomac.2018.11.257>
 16. Ghosh T, Katiyar V (2018) Cellulose-based hydrogel films for food packaging. In: Mondal M (eds) Cellulose-based superabsorbent hydrogels. polymers and polymeric composites: a reference series. Springer, Cham, pp 1–25. https://doi.org/10.1007/978-3-319-76573-0_35-1
 17. Fredriksson H, Silverio J, Andersson R, Eliasson AC, Åman P (1998) The influence of amylose and amylopectin characteristics on gelatinization and retrogradation properties of different starches. *Carbohydr Polym* 35:119–134. [https://doi.org/10.1016/S0144-8617\(97\)00247-6](https://doi.org/10.1016/S0144-8617(97)00247-6)
 18. Miles MJ, Morris VJ, Orford PD, Ring SG (1985) The roles of amylose and amylopectin in the gelation and retrogradation of starch. *Carbohydr Res* 135:271–281. [https://doi.org/10.1016/S0008-6215\(00\)90778-X](https://doi.org/10.1016/S0008-6215(00)90778-X)
 19. Avérous L (2004) Biodegradable multiphase systems based on plasticized starch: a review. *J Macromol Sci Polymer Rev* 44:231–274. <https://doi.org/10.1081/MC-200029326>
 20. Parra DF, Tadini CC, Ponce P, Lugão AB (2004) Mechanical properties and water vapor transmission in some blends of cassava starch edible films. *Carbohydr Polym* 58:475–481. <https://doi.org/10.1016/j.carbpol.2004.08.021>
 21. García MA, Pinotti A, Martino MN, Zaritzky NE (2009) Characterization of starch and composite edible films and coatings. In: Huber K, Embuscado M (eds) Edible films and coatings for food applications. Springer, New York, NY, pp 169–209. https://doi.org/10.1007/978-0-387-92824-1_6
 22. Carr LG, Parra DF, Ponce P, Lugao AB, Buchler PM (2006) Influence of fibers on the mechanical properties of cassava starch foams. *J Polym Environ* 14:179–183. <https://doi.org/10.1007/s10924-006-0008-5>
 23. Zawadzki KM, Yaspelkis BB 3rd, Ivy JL (1992) Carbohydrate-protein complex increases the rate of muscle glycogen storage after exercise. *J Appl Physiol* 72:1854–1859. <https://doi.org/10.1152/jappl.1992.72.5.1854>
 24. Rosai J, Lascano EF (1970) Basophilic (mucoid) degeneration of myocardium: a disorder of glycogen metabolism. *Am J Pathol* 61:99–116
 25. Chou J, Matern D, Mansfield BC, Chen YT (2002) Type I glycogen storage diseases: disorders of the glucose-6-phosphatase complex. *Cur Mol Med* 2:121–143. <https://doi.org/10.2174/1566524024605798>

26. Greene HL, Wilson FA, Hefferan P, Terry AB, Moran JR, Slonim AE, Burr IM (1978) ATP depletion, a possible role in the pathogenesis of hyperuricemia in glycogen storage disease type I. *J Clin Invest* 62:321–328. <https://doi.org/10.1172/JCI1109132>
27. O'sullivan AC (1997) Cellulose: the structure slowly unravels. *Cellulose* 4:173–207. <https://doi.org/10.1023/A:1018431705579>
28. Morán JI, Alvarez VA, Cyras VP, Vázquez A (2008) Extraction of cellulose and preparation of nanocellulose from sisal fibers. *Cellulose* 15:149–159. <https://doi.org/10.1007/s10570-007-9145-9>
29. Varma AJ, Deshpande SV, Kennedy JF (2004) Metal complexation by chitosan and its derivatives: a review. *Carbohydr Polym* 55:77–93. <https://doi.org/10.1016/j.carbpol.2003.08.005>
30. Younes I, Rinaudo M (2015) Chitin and chitosan preparation from marine sources. Structure, properties and applications. *Mar Drugs* 13:1133–1174. <https://doi.org/10.3390/md13031133>
31. Paoletti MG, Norberto L, Damini R, Musumeci S (2007) Human gastric juice contains chitinase that can degrade chitin. *Ann Nutr Metab* 51:244–251. <https://doi.org/10.1159/000104144>
32. Roberts WK, Selitrennikoff CP (1988) Plant and bacterial chitinases differ in antifungal activity. *Microbiology* 134:169–176. <https://doi.org/10.1099/00221287-134-1-169>
33. May CD (1990) Industrial pectins: sources, production and applications. *Carbohydr Polym* 12:79–99. [https://doi.org/10.1016/0144-8617\(90\)90105-2](https://doi.org/10.1016/0144-8617(90)90105-2)
34. Munarin F, Tanzi MC, Petrini P (2012) Advances in biomedical applications of pectin gels. *Int J Biol Macromol* 51:681–689. <https://doi.org/10.1016/j.ijbiomac.2012.07.002>
35. Kopjar M, Pilizota V, Tiban NN, Subaric D, Babic J, Ackar D, Sajdl M (2009) Strawberry jams: influence of different pectins on colour and textural properties. *Czech J Food Sci* 27:20–28
36. Apsara M, Pushpalatha PB (2002) Quality upgradation of jellies prepared using pectin extracted from fruit wastes. *J Trop Agric* 40:31–34
37. Alishahi A, Aider M (2012) Applications of chitosan in the seafood industry and aquaculture: a review. *Food Bioprocess Technol* 5:817–830. <https://doi.org/10.1007/s11947-011-0664-x>
38. Shahidi F, Arachchi JKV, Jeon YJ (1999) Food applications of chitin and chitosans. *Trends Food Sci Technol* 10:37–51. [https://doi.org/10.1016/S0924-2244\(99\)00017-5](https://doi.org/10.1016/S0924-2244(99)00017-5)
39. Karthik N, Akanksha K, Binod P, Pandey A (2014) Production, purification and properties of fungal chitinases—a review. <http://hdl.handle.net/123456789/29743>
40. Van der Lubben IM, Verhoef JC, Borchard G, Junginger HE (2001) Chitosan and its derivatives in mucosal drug and vaccine delivery. *Eur J Pharm Sci* 14:201–207. [https://doi.org/10.1016/S0928-0987\(01\)00172-5](https://doi.org/10.1016/S0928-0987(01)00172-5)
41. Hoppe-Seyler F (1894) Ueber chitin und cellulose. *Ber Dtsch Chem Ges* 27:3329–3331. <https://doi.org/10.1002/cber.189402703135>
42. Kumar Pal A, Das A, Katiyar V (2016) Chitosan from Muga silkworms (*Antheraea assamensis*) and its influence on thermal degradation behaviour of poly (lactic acid) based biocomposite films. *J Appl Polym Sci*, vol 133. <https://doi.org/10.1002/app.43710>
43. Pal AK, Katiyar V (2017) Thermal degradation behaviour of nanoamphiphilic chitosan dispersed poly (lactic acid) bionanocomposite films. *Int J Biol Macromol* 95:1267–1279. <https://doi.org/10.1016/j.ijbiomac.2016.11.024>
44. Kurita K (2006) Chitin and chitosan: functional biopolymers from marine crustaceans. *Mar Biotech* 8:203–226. <https://doi.org/10.1007/s10126-005-0097-5>
45. Ugraskan V, Toraman A, Yoruç ABH (2018) Chitosan: structure, properties and applications. *Chitosan-Based Adsorbents Wastewater Treat* 34:1–28
46. Palpandi C, Shanmugam V, Shanmugam A (2009) Extraction of chitin and chitosan from shell and operculum of mangrove gastropod *Nerita* (*Dostia*) *crepidularia* Lamarck. *Int J Med Sci* 1:198–205
47. Wysokińska Z (2010) Market for starch, hemicellulose, cellulose, alginate, its salts and esters, and natural polymers, including chitin and chitosan: analysis results. *Fibres Text East Eur* 18:83
48. de Queiroz Antonino RSCM, Lia Fook BRP, de Oliveira Lima VA, de Farias Rached RÍ, Lima EPN, da Silva Lima RJ, Lia Fook MV (2017) Preparation and characterization of chitosan obtained from shells of shrimp (*Litopenaeus vannamei* Boone). *Mar Drugs* 15:141. <https://doi.org/10.3390/md15050141>

49. Arbia W, Arbia L, Adour L, Amrane A (2013) Chitin extraction from crustacean shells using biological methods—a review. *Food Technol Biotech* 51:12–25. <https://hrcak.srce.hr/99743>
50. Yen MT, Yang JH, Mau JL (2008) Antioxidant properties of chitosan from crab shells. *Carbohydr Polym* 74:840–844. <https://doi.org/10.1016/j.carbpol.2008.05.003>
51. Yen MT, Tseng YH, Li RC, Mau JL (2007) Antioxidant properties of fungal chitosan from shiitake stipes. *LWT-Food Sci Technol* 40:255–261. <https://doi.org/10.1016/j.lwt.2005.08.006>
52. No HK, Park NY, Lee SH, Meyers SP (2002) Antibacterial activity of chitosans and chitosan oligomers with different molecular weights. *Int J Food Microbiol* 74:65–72. [https://doi.org/10.1016/S0168-1605\(01\)00717-6](https://doi.org/10.1016/S0168-1605(01)00717-6)
53. Jo HG, Min KH, Nam TH, Na SJ, Park JH, Jeong SY (2008) Prolonged antidiabetic effect of zinc-crystallized insulin loaded glycol chitosan nanoparticles in type 1 diabetic rats. *Arch Pharmacol Res* 31:918–923. <https://doi.org/10.1007/s12272-001-1247-9>
54. Kerch G (2015) The potential of chitosan and its derivatives in prevention and treatment of age-related diseases. *Mar Drugs* 13:2158–2182. <https://doi.org/10.3390/md13042158>
55. Elsabee MZ, Abdou ES (2013) Chitosan based edible films and coatings: a review. *Mater Sci Eng, C* 33:1819–1841. <https://doi.org/10.1016/j.msec.2013.01.010>
56. Wang SY, Gao H (2013) Effect of chitosan-based edible coating on antioxidants, antioxidant enzyme system, and postharvest fruit quality of strawberries (*Fragaria x ananassa* Duch.). *LWT-Food Sci Technol* 52:71–79. <https://doi.org/10.1016/j.lwt.2012.05.003>
57. Armon H, Zaitsev Y, Porat R, Poverenov E (2014) Effects of carboxymethyl cellulose and chitosan bilayer edible coating on postharvest quality of citrus fruit. *Postharvest Biol Tech* 87:21–26. <https://doi.org/10.1016/j.postharvbio.2013.08.007>
58. Pereira VA Jr, de Arruda INQ, Stefani R (2015) Active chitosan/PVA films with anthocyanins from *Brassica oleracea* (Red Cabbage) as time–temperature indicators for application in intelligent food packaging. *Food Hydrocoll* 43:180–188. <https://doi.org/10.1016/j.foodhyd.2014.05.014>
59. Lauto A, Hook J, Doran M, Camacho F, Poole-Warren LA, Avolio A, Foster LJR (2005) Chitosan adhesive for laser tissue repair: in vitro characterization. *Laser Surg Med* 36:193–201. <https://doi.org/10.1002/lsm.20145>
60. Yamada K, Chen T, Kumar G, Vesnovsky O, Topoleski LT, Payne GF (2000) Chitosan based water-resistant adhesive. Analogy to mussel glue. *Biomacromolecules* 1:252–258. <https://doi.org/10.1021/bm0003009>
61. Bhattarai N, Gunn J, Zhang M (2010) Chitosan-based hydrogels for controlled, localized drug delivery. *Adv Drug Deliv Rev* 62:83–99. <https://doi.org/10.1016/j.addr.2009.07.019>
62. Yang C, Xu L, Zhou Y, Zhang X, Huang X, Wang M, Li J (2010) A green fabrication approach of gelatin/CM-chitosan hybrid hydrogel for wound healing. *Carbohydr Polym* 82:1297–1305. <https://doi.org/10.1016/j.carbpol.2010.07.013>
63. Patel AK, Michaud P, Petit E, de Baynast H, Grédiac M, Mathias JD (2013) Development of a chitosan-based adhesive. Application to wood bonding. *J Appl Polym Sci* 127:5014–5021. <https://doi.org/10.1002/app.38097>
64. Wang Y, Guo KQ, Li JN, Duan XF, Li YJ (2009) Konjac glucomannan/chitosan based adhesive for plywood production. *China Wood Industry* 23(2):13–15
65. Muñoz I, Rodríguez C, Gillet D, Moerschbacher BM (2017) Life cycle assessment of chitosan production in India and Europe. *Int J Life Cycle Assess*, pp 1–10. <https://doi.org/10.1007/s11367-017-1290-2>
66. Orrego CE, Salgado N (2014) Green logistics in chitin/chitosan industry. *Appl Agroindustries* 1400000:1200000
67. Ghosh T, Dash KK (2018) Respiration rate model and modified atmosphere packaging of bhimkol banana. *Eng Agric Environ Food* 11:186–195. <https://doi.org/10.1016/j.eaef.2018.04.004>
68. Leceta I, Guerrero P, Cabezudo S, de la Caba K (2013) Environmental assessment of chitosan-based films. *J Clean Prod* 41:312–318. <https://doi.org/10.1016/j.jclepro.2012.09.049>
69. Madival S, Auras R, Singh SP, Narayan R (2009) Assessment of the environmental profile of PLA, PET and PS clamshell containers using LCA methodology. *J Clean Prod* 17:1183–1194. <https://doi.org/10.1016/j.jclepro.2009.03.015>

70. Suwanmanee S, Lertworasirikul, S (2015) Environmental impact assessment of coating fresh-cut papaya Cv. Holland with chitosan. In: Proceedings of 35th the IIER international conference, Bangkok, Thailand. ISBN 978-93-85465-89-5
71. Mati-Baouche N, Elchinger PH, De Baynast H, Pierre G, Delattre C, Michaud P (2014) Chitosan as an adhesive. *Eur Polym J* 60:198–212. <https://doi.org/10.1016/j.eurpolymj.2014.09.008>
72. Beach ES, Eckelman MJ, Cui Z, Brentner L, Zimmerman JB (2012) Preferential technological and life cycle environmental performance of chitosan flocculation for harvesting of the green algae *Neochloris oleoabundans*. *Bioresour Technol* 121:445–449. <https://doi.org/10.1016/j.biortech.2012.06.012>
73. Yan N, Chen X (2015) Don't waste seafood waste: turning cast-off shells into nitrogen-rich chemicals would benefit economies and the environment. *Nature* 524:155–158
74. Balakrishnan M, Batra VS, Hargreaves JSJ, Pulford ID (2011) Waste materials—catalytic opportunities: an overview of the application of large scale waste materials as resources for catalytic applications. *Green Chem* 13:16–24. <https://doi.org/10.1039/C0GC00685H>
75. Cárdenas G, Cabrera G, Taboada E, Miranda SP (2004) Chitin characterization by SEM, FTIR, XRD, and 13C cross polarization/mass angle spinning NMR. *J Appl Polym Sci* 93:1876–1885. <https://doi.org/10.1002/app.20647>
76. Islam MS, Khan S, Tanaka M (2004) Waste loading in shrimp and fish processing effluents: potential source of hazards to the coastal and nearshore environments. *Marine Poll Bull* 49:103–110. <https://doi.org/10.1016/j.marpolbul.2004.01.018>
77. Shahidi F, Synowiecki J (1991) Isolation and characterization of nutrients and value-added products from snow crab (*Chionoecetes opilio*) and shrimp (*Pandalus borealis*) processing discards. *J Agric Food Chem* 39:1527–1532. <https://doi.org/10.1021/jf00008a032>
78. Rødde RH, Einbu A, Vårum KM (2008) A seasonal study of the chemical composition and chitin quality of shrimp shells obtained from northern shrimp (*Pandalus borealis*). *Carbohydr Polym* 71:388–393. <https://doi.org/10.1016/j.carbpol.2007.06.006>
79. Gao X, Chen X, Zhang J, Guo W, Jin F, Yan N (2016) Transformation of chitin and waste shrimp shells into acetic acid and pyrrole. *ACS Sustain Chem Eng* 4:3912–3920. <https://doi.org/10.1021/acssuschemeng.6b00767>
80. Suresh PV, Chandrasekaran M (1998) Utilization of prawn waste for chitinase production by the marine fungus *Beauveria bassiana* by solid state fermentation. *World J Microbiol Biotechnol* 14:655–660. <https://doi.org/10.1023/A:1008844516915>
81. Wu T, Zivanovic S, Draughon FA, Sams CE (2004) Chitin and chitosan value-added products from mushroom waste. *J Agric Food Chem* 52:7905–7910. <https://doi.org/10.1021/jf0492565>
82. Yoon HJ, Moon ME, Park HS, Im SY, Kim YH (2007) Chitosan oligosaccharide (COS) inhibits LPS-induced inflammatory effects in RAW 264.7 macrophage cells. *Biochem Biophys Res Commun* 358:954–959. <https://doi.org/10.1016/j.bbrc.2007.05.042>
83. Yang EJ, Kim JG, Kim JY, Kim SC, Lee NH, Hyun CG (2010) Anti-inflammatory effect of chitosan oligosaccharides in RAW 264.7 cells. *Cent Eur J Biol* 5:95–102. <https://doi.org/10.2478/s11535-009-0066-5>
84. Chung MJ, Park JK, Park YI (2012) Anti-inflammatory effects of low-molecular weight chitosan oligosaccharides in IgE-antigen complex-stimulated RBL-2H3 cells and asthma model mice. *Int Immunopharmacol* 12:453–459. <https://doi.org/10.1016/j.intimp.2011.12.027>
85. Ylitalo R, Lehtinen S, Wuolijoki E, Ylitalo P, Lehtimäki T (2002) Cholesterol-lowering properties and safety of chitosan. *Arzneimittelforschung* 52:1–7. <https://doi.org/10.1055/s-0031-1299848>
86. Ausar SF, Morcillo M, Leon AE, Ribotta PD, Masih R, Vilaro Mainero M, Beltramo DM (2003) Improvement of HDL- and LDL-cholesterol levels in diabetic subjects by feeding bread containing chitosan. *J Med Food* 6:397–399. <https://doi.org/10.1089/109662003772519985>
87. Liu J, Lu JF, Kan J, Jin CH (2013) Synthesis of chitosan-gallic acid conjugate: structure characterization and in vitro anti-diabetic potential. *Int J Biol Macromol* 62:321–329. <https://doi.org/10.1016/j.ijbiomac.2013.09.032>
88. Zhu W, Zhang Z (2014) Preparation and characterization of catechin-grafted chitosan with antioxidant and antidiabetic potential. *Int J Biol Macromol* 70:150–155. <https://doi.org/10.1016/j.ijbiomac.2014.06.047>

89. Baez-Sañudo M, Siller-Cepeda J, Muy-Rangel D, Heredia JB (2009) Extending the shelf-life of bananas with 1-methylcyclopropene and a chitosan-based edible coating. *J Sci Food Agric* 89:2343–2349. <https://doi.org/10.1002/jsfa.3715>
90. Günlü A, Koyun E (2013) Effects of vacuum packaging and wrapping with chitosan-based edible film on the extension of the shelf life of sea bass (*Dicentrarchus labrax*) fillets in cold storage (4 C). *Food Bioprocess Technol* 6:1713–1719. <https://doi.org/10.1007/s11947-012-0833-6>
91. Altıok D, Altıok E, Tihminlioglu F (2010) Physical, antibacterial and antioxidant properties of chitosan films incorporated with thyme oil for potential wound healing applications. *J Mater Sci Mater Med* 21:2227–2236. <https://doi.org/10.1007/s10856-010-4065-x>
92. Szyguła A, Guibal E, Palacín MA, Ruiz M, Sastre AM (2009) Removal of an anionic dye (Acid Blue 92) by coagulation–flocculation using chitosan. *J Environ Manage* 90:2979–2986. <https://doi.org/10.1016/j.jenvman.2009.04.002>
93. Divakaran R, Pillai VS (2001) Flocculation of kaolinite suspensions in water by chitosan. *Water Res* 35:3904–3908. [https://doi.org/10.1016/S0043-1354\(01\)00131-2](https://doi.org/10.1016/S0043-1354(01)00131-2)

Chapter 17

Recent Trends and Advances in the Biodegradation of Conventional Plastics



Naba Kumar Kalita, Ajay Kalamdhad and Vimal Katiyar

Abstract With the increasing use of fossil-based plastics worldwide, the need for proper disposal of plastic waste has become a menace for developing countries as well as the developed world. The overuse of plastic and its improper disposal system in many countries of the world has led to severe environmental concerns. Disposal system and methods of plastic through various chemical and physical processes are very expensive which also produces organic pollutants, resulting in environmental deterioration. Recent trends suggest the biodegradation of conventional plastics like polyethylene terephthalate (PET), polyethylene (PE), and polystyrene (PS) under different environments like using enzymes and microbes for disintegration and assimilation, respectively, as a viable bioremediation. Among enzymes, lipases, cutinases, and PETase has been identified as potential fossil-based plastic degrader as viable solution. This chapter aims to provide a broader aspect of conventional plastic biodegradation and its degradation mechanisms, providing an overview on viable bioremediation of plastic waste. This chapter also discusses the current status of the techniques used for degradation, characterizing degraded plastics and factors affecting their biodegradation.

Keywords Biodegradation · Enzymes · Conventional plastics · Mechanism

1 Introduction

In recent years, the severe effects caused by the persistent accumulation of plastics in the environment have led the scientific community to develop and utilize proper waste management system and regulatory conditions. However, the proper waste disposal and landfilling might be the short-term solutions for maintaining the plastic

N. K. Kalita · V. Katiyar (✉)
Department of Chemical Engineering, Indian Institute of Technology Guwahati, Guwahati,
Assam 781039, India
e-mail: vkatiyar@iitg.ac.in

A. Kalamdhad
Department of Civil Engineering, Indian Institute of Technology Guwahati, Guwahati, Assam,
India

waste. The long-term solution for this problem is still lacking scientific attention or study or policies. Although certain conventional plastics get decayed during longer time under landfill conditions, its intermediates are very harmful for the environment which often leads to the soil and water pollution. Plastics are a global commodity of synthetic materials having a long chain of polymeric molecules possessing excellent all-round properties having wide range of application. They are very easy to mold and manufacture. Generally, the conventional plastics have stable carbon-based backbone which makes them resistant to degradation under various environmental conditions. This property makes conventional plastics non-degradable which are one of the most used commodity materials in the current world [1]. The waste generation estimated in Europe is around 25.8 million ton per year. In India, 15,342 ton of plastic waste is generated per day, but the per capita usage of plastics is much lower than the world average. India consumes 11 kg of plastics per capita as compared to the total consumption of plastics 28 kg globally. As per the Central Pollution Control Board (CPCB) reports 2015–16, plastic contributes to 8% of the total solid waste, although 60% is recycled still 40% is clogging India's cities leading to flood and other environmental disasters. Biodegradation is the only solution to deal with this plastic waste studied worldwide currently. Commodity plastic waste recycled or recovered is 69% according to 2014 plastics data in Europe, whereas 31% still ends up in landfills. To counter the environmental problems caused by the conventional plastics, researchers have developed plastics which are biodegradable and cause no or little impact on the environment [2–7]. Biodegradable plastics are used in many fields like medicine, agriculture, building materials, food packaging industry, biomedical implants, and devices [8]. But these plastics are very costly and certain properties like durability and matching of the materials with the present equipments, and its end-of-life management systems are an issue which resists its application commercially [9]. Thermal degradation is another option of waste management, but it releases harmful metals and generates toxic gases like CO and dioxin. Incineration process operates according to the principle of thermal degradation which causes heavy air and soil pollution which ultimately pollutes the groundwater. In order to overcome such issues, scientists/researchers are putting their efforts toward developing methods of degrading conventional plastics like PET and LDPE using various microbes and enzymes. Studies showed that *Aspergillus niger*, *Papthnutius ostentus*, *Gloeophyllum trabeum*, etc., have the capacity to completely degrade conventional polymers [10]. Although, active research in manufacturing biodegradable plastics like PLA and PVA which can decompose in composting and landfill environments are also in effect, but its high restricts its use globally [11, 12]. These plastics under various regulated conditions can degrade completely under various environments without causing any pollution. Large quantities of conventional polymers like PET as well as polyethylene and polystyrene have been introduced into the environment through its production and disposal, resulting in the accumulation of these materials in ecosystems across the globe [13–15].

This chapter summarizes recent studies and advances in the biodegradation and enzymatic degradation of the widely used petroleum-based plastics like polyethylene (PE), polystyrene (PS), polyurethane (PUR), and polyethylene terephthalate (PET),

Table 1 Types of biopolymers (from various sources)

Microorganism-based	Biotechnology-based	Agro-based	
Polyhydroxyalkanoates (mcl-PHA, PHB, PHB-co-V)	Poly lactides, PBS, PE, PTT, PPP	Polysaccharides and lipids (starch, cellulose, alginates)	Proteins—animal proteins (casein, whey, collagen/gelatin), plant protein (zein, soya, gluten)

and the pros and cons faced for designing potential microbes or enzymes that can degrade these plastics in a proper waste disposal system will be presented.

2 Types of Plastics

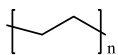
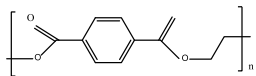
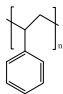
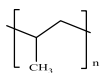
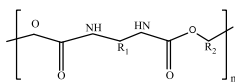
2.1 Natural Plastics

Plastics which are derived from plants and are easily biodegradable are known as natural plastics [5]. Table 1 shows the list of the biopolymers. With the changing composition of the lignocellulosic biomass, the constituents of the plant cell also differ [1]. Lignocelluloses constitute the major developing part of the plant biomass, which contains cellulose, hemicellulose, and lignin. Among all natural plastics, poly(lactic acid) (PLA), polyvinyl alcohol (PVA), cellulose, chitosan, and gum are the most widely used natural plastics for various purposes [3, 4, 16].

2.2 Synthetic Plastics

Plastics are basically divided into two types namely thermoplastics and thermosets which differ according to their manufacturing process. Table 2 shows some of the most commonly used conventional plastics. The production of thermoplastics involves polymerization which proceeds by breaking of double bonds in the original olefin forming new carbon–carbon bonds. The production of thermosets involves the elimination of water between a carboxylic acid and an alcohol or amine to form polyester or polyamide. Thermoplastics can be hardened or softened by repeated heating and cooling processes. Thermosets are synthesized such that after melting, these plastics are solidified. Thermoplastics have linear structure, whereas thermosets contain crosslinked structures [1, 15, 17]. The most widely used polymers are listed in Table 2.

Table 2 Some of the most commonly used conventional polymers and their application

Polymer	Structure	Application
Polyethylene (PE)		Films and packaging
Polyethylene terephthalate (PET)		Bottles, tubes, pipes, insulation molding
Polystyrene (PS)		Tanks, jugs, containers
Polypropylene (PP)		Disposable plates, foams, etc.
Polyurethane (PUR)		Coating, insulation, paints, packing

3 Biodegradation of Plastics

Degradation of polymer refers to complete de-polymerization, mineralization, pyrolysis, etc. Degradation properties are not desirable for any model polymer for engineering applications except biodegradation or lowering the molecular weight of a polymer for recycling polymers under certain induced or natural environmental conditions undergoing degradation resulting in lowering of physical and chemical properties as shown in Fig. 1. This kind of induced processes helps in studying polymer aging, which mainly sheds light on polymer end-of-life or after end-use properties and conditions.

Biodegradation is the assimilation of carbon or nitrogen fixation by bacteria or by other biological means. Biodegradation of a material will involve microbes possessing typical resistance to different environments. Biodegradation of polymers takes place in two sequential steps namely, chemical degradation followed by microbial assimilation using enzymes. The first step proceeds via abiotic reactions resulting in fragmentation of the polymers into lower molecular mass intermediates, like chemical hydrolysis, oxidation, and or photo-oxidation. This step is followed by mineralization or microbial assimilation. Biodegradation of polymers depends upon various factors like the availability of intermediates for microbial assimilation, types of polymers, and environmental conditions applied for biodegradation, [18]. Mechanism of biodegradation is shown in Fig. 2.

Polymer biodegradation mechanism involves microbial attachment to the polymer substrate either on the surface or bulk, or by the formation of biofilms, thereby utilizing the carbon source present in the polymer resulting in ultimate degradation. Figure 3 shows various analytical techniques used during biodegradation or to ana-

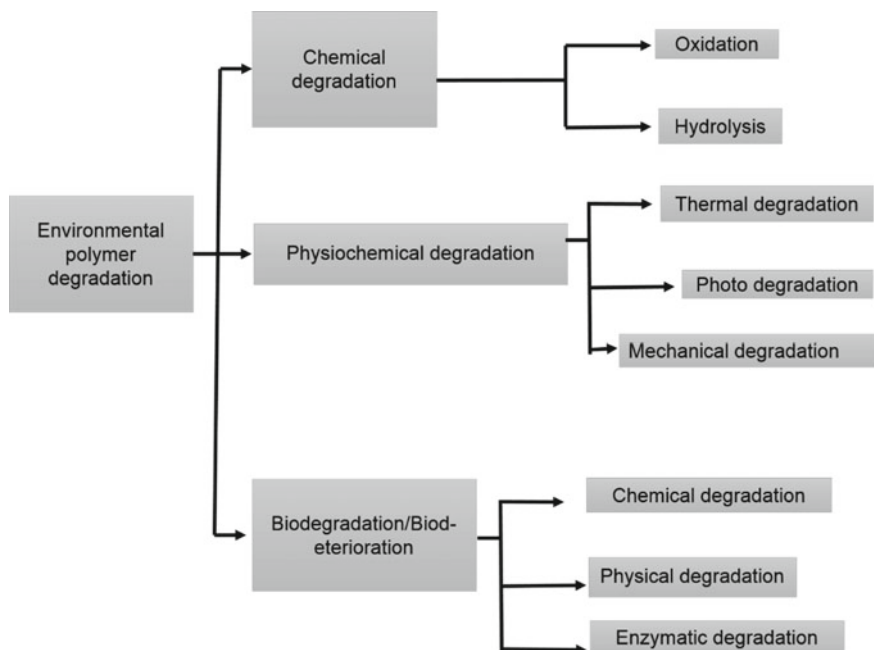


Fig. 1 Different routes of polymer degradation under various environmental conditions

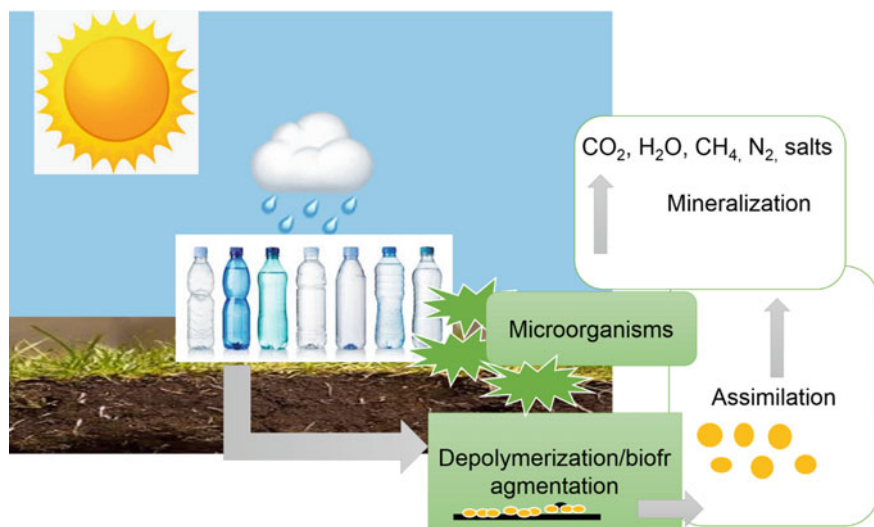


Fig. 2 Polymer biodegradation mechanism

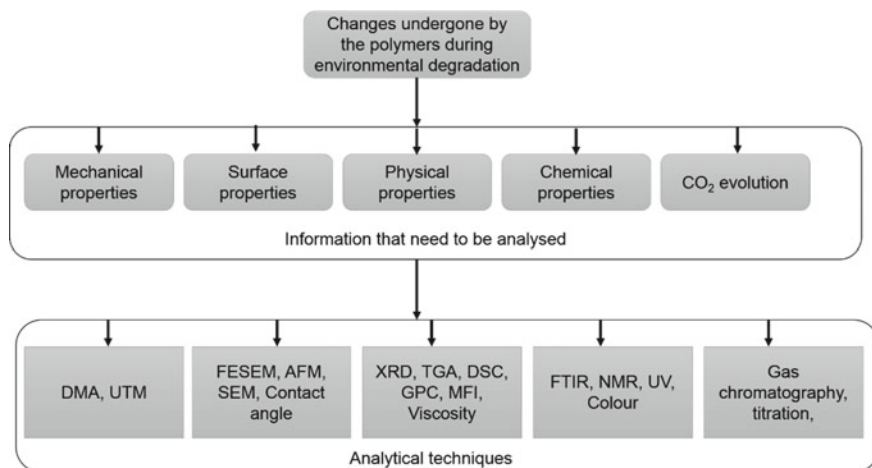


Fig. 3 Analytical techniques used for the evaluation of biodegradation of polymers

lyze biodegradation. Enzymes play the most vital role during biodegradation which are released or produced by microorganism's in vitro or in vivo known exo-enzymes or endo-enzymes, respectively. This process can prove to be a prolific environmental approach for waste management. Mineralization of polymers is done under both aerobic and anaerobic conditions. In the aerobic condition, CO_2 and H_2O are formed, while under anaerobic conditions, CH_4 , CO_2 , and H_2O are produced [18].

3.1 Factors Affecting Plastic Biodegradation

Various factors affecting the biodegradation process include moisture, enzyme property, and polymer property as well as exposure conditions. Moisture is an utmost property which influences biodegradation in various ways. The moisture facilitates microbial growth along with inducing chemical hydrolysis of the polymer [1] and thereby facilitates chain scission reaction. pH and temperature are another factors which influence biodegradation by changing the acidic and basic conditions. Temperature plays a crucial role in the enzymatic degradation of polymers [19]. The characteristics of enzyme also influence polymer degradation at various temperature and pH. It is reported that the linear chain polymers obtained from diacid monomers tend to degrade more quickly by enzymes of fungal origin of *A. niger* and *Aspergillus flavus* [20]. Molecular weight also plays a crucial role in determining the degradability of a polymer. Higher the molecular weight, lower the accessibility of the polymer chains for the microbes to assimilate. Properties like shape and size play an important role in the degradation of polymers. There is a standard criterion of shape and size for the biodegradation of various kinds of plastics. Sometimes, non-polymeric

elements such as dyes, moisture, or catalysts used for polymerization can influence the degradability of the polymer [21, 22].

4 Recent Advances in Biodegradation of Plastics

The biodegradation of conventional or petroleum-based plastics has become a focused area of research [1, 23–27]. Biodegradation process of conventional plastics is very complex due to the various biotic and abiotic factors. The fragmentation of the bulk polymer under biological attack is displayed in Fig. 2. Extracellular enzymes either induced or released by microbes play an important role in plastic biodegradation [26, 28, 29]. The polymers consisting of linear (C–C) bonds are more difficult to degrade than heteroatomic backbone polymers (structures displayed in Fig. 4). Degrading (C–C) bonds or finding microbes that can degrade the (C–C) bond of the polymers will prove to be a boon for the environment.

Studies show that the polymers extracted from plants form the most suitable substrates for the key enzymes for attacking the synthetic polymer backbone. Such studies showed that cutinase can hydrolyze cutin which is an aliphatic polyester [30]. These findings opened the door for PET and PUR degradation using the cutinase enzyme [32]. Various researchers also modified this cutinase enzyme and created mutant cutinases or cutinase like enzymes for the degradation of PET [14, 31]. Researchers also found several enzymes which are involved in the metabolism of plant lignin that can degrade thermoplastic PE [28, 32]. Synthetic polymer characteristics also play a major role in their resistance to degradation behavior like crystallinity, surface morphology, and hydrophobicity molecular weight [19, 32, 33].

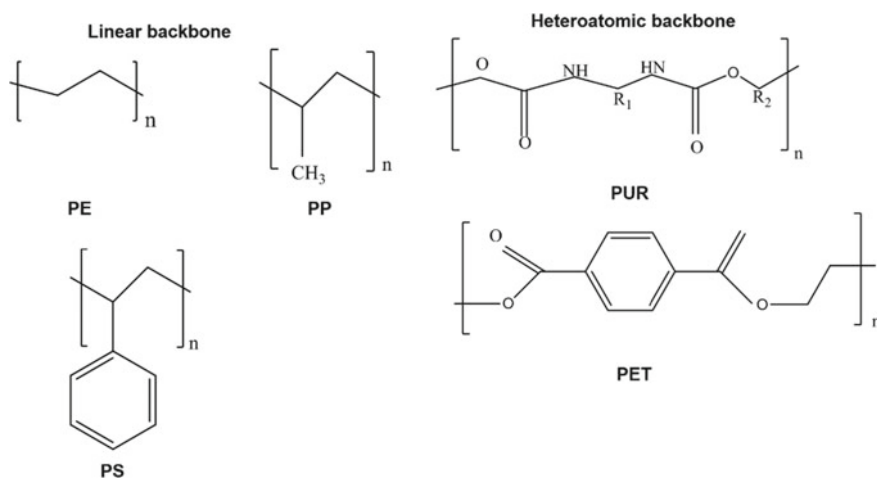


Fig. 4 Some of the commonly used conventional polymers grouped according to their structures

Certain widely used polymers like PET and PUR are more susceptible to biodegradation than PE, PS, and PP. This is mainly due to their chemical structure having hydrolysable bonds in their backbones [33] and PUR [1, 19, 25, 34]. PE, PP, and PS have highly stable (C-C) bonds which are very resistant to any kind of degradation under normal environment. Studies showed that prior to biodegradation, these polymers having (C-C) bonds have to be oxidized for de-polymerization or fragmentation by considering various abiotic factors [1, 32]. Abiotic environments consist of factors like UV radiation, photo-oxidation, and oxidation and play a crucial role in the biodegradation of PE, PP, and PS using certain categories of microbes [35–37]. Mechanism of PE degradation is shown in Fig. 5.

The synthetic polymers widely used are of high molecular weight with very high hydrophobicity. These two characteristics hinder the microbial assimilation either slowly or rapidly underwater or substrates containing higher moisture [1, 25, 32, 38]. Various studies showed that the degradation of synthetic polymers like PE and PS by enzymes and microbes is mainly a surface erosion process and depends upon the polymer application and chemical structure [26, 39, 32]. Further, several studies confirmed that hydrophobicity and smooth surface restrict the growth of microbial biofilms on the polymer surface by microorganisms which are normally capable of degrading synthetic polymers under certain environments [26, 32, 34, 40]. Hydrophobicity also restricts the catalytic activity of enzymatic degradation of synthetic polymers [41–43]. Surface-to-volume ratio plays a crucial role during the enzymatic biodegradation of polymers. In a study by Gamerith et al. [44], PET was micronized to 0.25–0.5 mm, wherein the authors proved that the bacterial polyester degraded

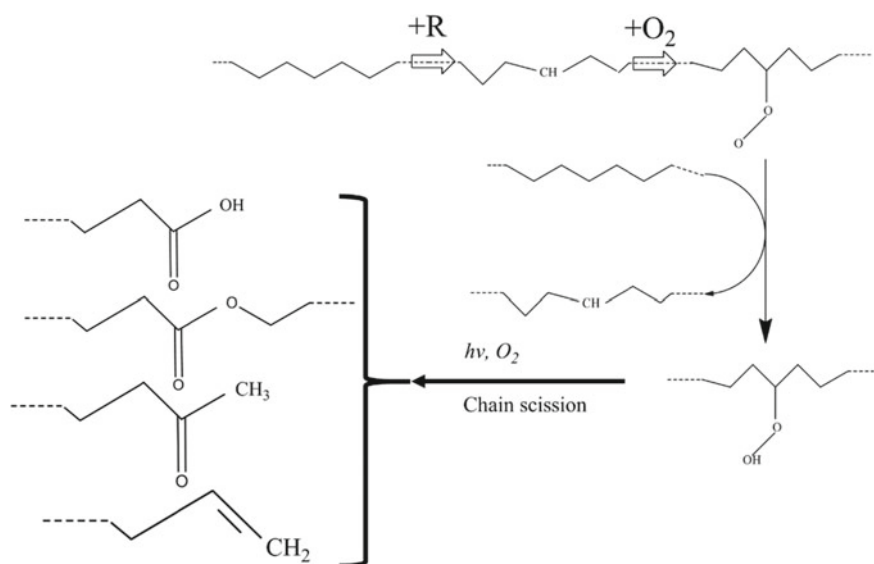
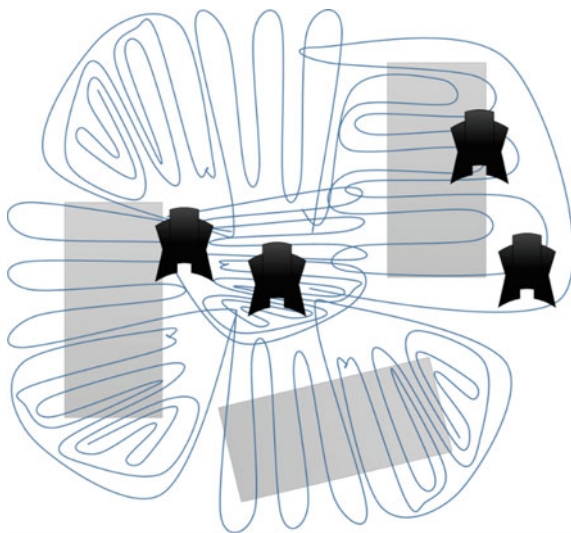


Fig. 5 Mechanism of PE degradation

Fig. 6 Schematic illustration of a semicrystalline polymer containing both amorphous and crystalline regions (gray areas)



micronized PET more rapidly which might be due to low surface-to-volume ratio which increased the assessable area of the enzyme.

Biodegradation of petroleum-based plastics is a complex process to execute and administer. However, most of the plastics are semicrystalline in nature containing a crystalline as well as amorphous phases. The microbes are known to attack the amorphous region first as the amorphous region is more susceptible to microbial attack as shown in Fig. 6. Hence, the degree of crystallinity influences the biodegradability of the polymers [45]. However, studies by Restrepo-Flórez et al. [32] and Manzur et al. [46] showed that crystalline portion can also be degraded by using enzymes.

Although several conducted showed that semicrystalline as well as low crystalline PET is easier to degrade, the mechanism reaction of PET degradation is shown in Fig. 7.

The complete decomposition of PET having very low crystalline portion was degraded using fungal polyester hydrolases and concluded that linear degradation occurred which also suggests degradation of the crystalline portion by the enzyme [44].

From the various reports mentioned above, it can be concluded that both fungal and bacterial hydrolases can be utilized to carry on degradation of semicrystalline PET. Further, researches may be conducted on understanding the degradation of crystalline portion of the conventional plastics. Identifying microbes and enzymes or by modifying their genes which can either degrade semicrystalline or highly crystalline parts can be a great tool for degradation of petroleum-based plastic and reduce the carbon footprint of the current world.

However, most of the studies and experiments were conducted at higher temperature. Yoshida et al. [13] conducted experiments with an enzyme collected from microbe (*Ideonella sakaiensis* 201-F6) present in a PET recycling bottling plant.

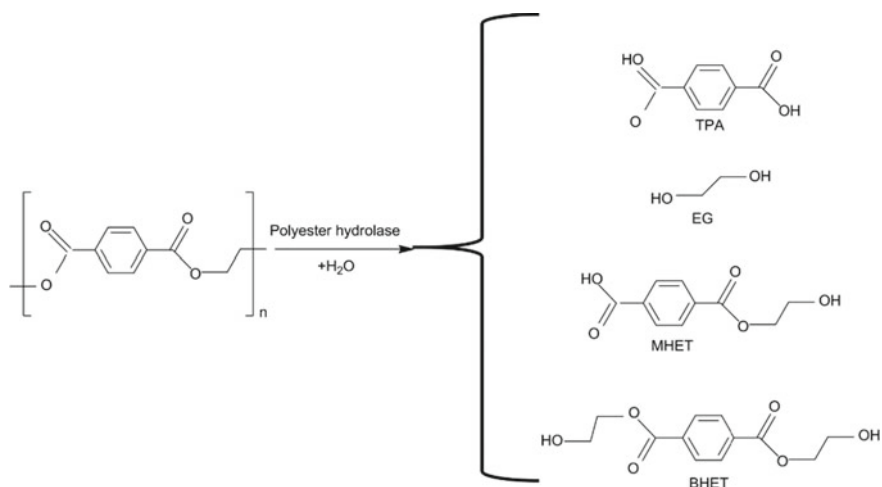


Fig. 7 Mechanism of PET degradation [9, 13]

The PETase enzyme was able to degrade semicrystalline PET at lower temperature ~ 40 °C.

As discussed earlier in the chapter, degradation of (C–C) backbone is the most difficult task and the lack of various hydrolysable bonds also leads to their resistance to degradation using microbes as well as enzymes [19, 25, 32]. Studies concluding initial fragmentation or breakdown of polymers in the environment are the result of the synergy between various biotic and abiotic factors [23, 32, 35, 36]. Since various pretreatments are needed for the degradation of PE, PP, and PS like UV radiation, and oxidation these pretreatments lead to various oxidizing agents as well as carbonyl groups which are more susceptible to biodegradation [47–50]. Plant lignin also contains (C–C) backbone, but researchers have found or developed enzymes to degrade lignin. These enzymes can also degrade PE, PS, and PP at certain levels as reported by [25, 32]. PE is the most common plastic with C–C backbone and is one of the widely studied materials for biodegradation using various enzymes as well as microbes [51, 52]. Another study showed that laccase extracted from *Rhodococcus ruber* C208 degraded pretreated PE films both in culture media and in the cell-free extracts in the presence of copper [53]. They reported that the degradation mainly happened due to pretreatment with which resulted in formation of carbonyl groups and reduction of molecular weight after 2 weeks of incubation with the enzyme extracted. The laccase enzyme has been studied by various researchers and is found to degrade PE under certain environment. *Bacillus cereus* is found to have degraded UV-irradiated PE. The report concluded the association of the microbes with a pronounced extracellular production of both laccases and MnP. Two potential fungal strains, namely *Penicillium oxalicum* NS4 (KU559906) and *Penicillium chrysogenum* NS10 (KU559907), had been isolated and identified to have plastic degrading abilities [52].

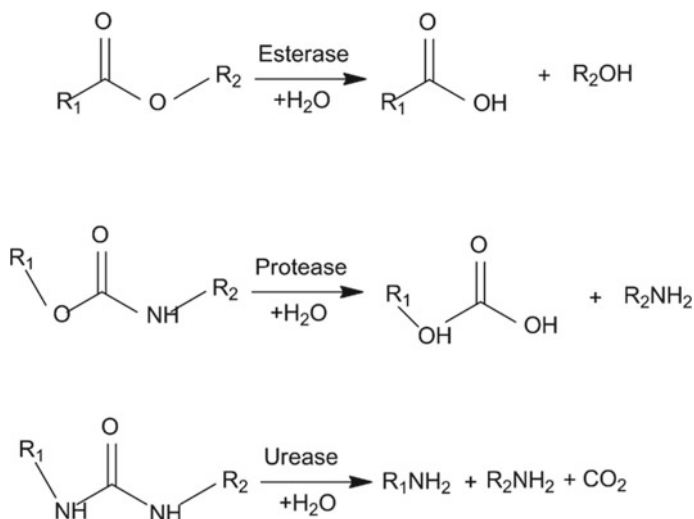


Fig. 8 Mechanism of PUR degradation

Recent trends in studies also suggested that the utilization of mixed cultures have shown to improve the degradation of PE and PS than single strain study [54–56]. However, various studies showed that in case of (C–C) backbone polymers, the whole cell has proven to degrade the polymer more rather than the enzyme alone and this strategy has been reported for both PE and PS by various researchers [22, 56].

PUR is another commonly used polymer consisting of di- or polyisocyanate and polyols linked by urethane bonds. This polymer can be tuned according to the polyols used during the polycondensation reaction having different characteristics properties [57]. Reports suggested de-polymerization of PUR using microbial enzymes. Enzymes are extracted either from fungi or from bacteria mainly hydrolyse the ester linkages which is a major mechanism of degradation as shown in Fig. 8 for PUR [27, 32, 58–60]. However, a fungal isolate is found to degrade PUR with 60% weight loss without showing the enzymes [32]. Previous studies suggest that PUR degrading enzymes have low catalytic activity or efficiency, which can be upgraded by using the whole microbial cell as a potential degrader of the PUR samples [34].

5 Challenges and Future Directions

Bio-degradable plastics are considered as sustainable polymers due to their potential to reduce the fossil fuel consumption. However, waste disposal and high production cost related to biodegradable polymers are one of the major limitations which are restricting their mass production and limiting their potential from replacing conventional plastics.

Product cost At present, the cost of bioplastics is higher than that of the conventional polymers. As an example, the cost of PLA is 3–5 times more than the cost of PET. It is obvious that the other advantages of bioplastics are meaningless if the material is too expensive. So, the prospects of biocatalytic recycling or waste management through biodegradation are immense for conventional plastics. Recycling as well as biodegradation will shape the future of the plastic world which is creating havoc in terms of environmental degradation. Increasing research on the microbial enzymes which are capable of degrading conventional polymers will promote the development of environmental friendly waste recycling processes associated with plastics. Although several enzymes have been found to contribute to the degradation of PE, PS, and PP, the degradation of the (C–C) backbone has not been demonstrated by any researcher till date. Therefore, extensive studies are necessary for identifying enzymes and microbes which can degrade PE, PP, and PS without any pretreatment and better understanding of the degradation mechanism is the utmost necessity. The single strain or mixed culture of strains like bacteria/fungi might prove instrumental in degrading (C–C) backbone of PE, PS, and PP. Extensive research has been done to degrade PET which is one of the most used polymers. Various kinds of enzymes and microbes have been utilized and identified which can degrade PET. PET is found to degrade using PETase and cutinase enzyme but mainly the semicrystalline PET or low crystalline PET has been reported wherein most of them have been mutated for better and faster degradation. These enzymes are thermostable, and the degradation condition of higher temperature also plays a crucial role during the degradation of PET. Research in the direction of developing better degradation system for low-temperature degradation of PET may be carried out. Studies are also required to identify microbes and enzymes which can degrade PET or other conventional plastics at a linear rate throughout the degradation process. Although there are few reports indicating degradation of crystalline portion of PET, the process is too slow for application in recycling plants or at pilot scale. Certain simulation strategies can be applied for the identification of the mutation sites which can help in optimization of the mutation spots in polyester hydrolyses which would give insights for enzyme mutation for degradation of polymers [14, 31, 61]. This chapter illustrated the current advances and trends in the occurrence and usage of polymer degrading microbes and enzymes. Further, the extensive screening of the effective polymer degrading enzymes and whole cell is necessary for the lower polymer carbon footprint on the present and future world and to develop a proper biocatalytic recycling system for the present class of conventional polymers.

References

1. Zheng Y, Yanful EK, Bassi AS (2005) A review of plastic waste biodegradation. *Crit Rev Biotechnol* 25:243–250. <https://doi.org/10.1080/07388550500346359>
2. Valapa RB, Pugazhenth G, Katiyar V (2016) Hydrolytic degradation behaviour of sucrose palmitate reinforced poly(lactic acid) nanocomposites. *Int J Biol Macromol* 89:70–80. <https://>

- doi.org/10.1016/j.ijbiomac.2016.04.040
3. Dhar P, Bhasney SM, Kumar A, Katiyar V (2016) Acid functionalized cellulose nanocrystals and its effect on mechanical, thermal, crystallization and surfaces properties of poly (lactic acid) bionanocomposites films: a comprehensive study. *Polymer (UK)* 101:75–92. <https://doi.org/10.1016/j.polymer.2016.08.028>
 4. Gupta A, Pal AK, Woo EM, Katiyar V (2018) Effects of amphiphilic chitosan on stereocomplexation and properties of poly(lactic acid) nano-biocomposite. *Sci Rep* 8:1–13. <https://doi.org/10.1038/s41598-018-22281-1>
 5. Pal AK, Katiyar V (2016) Nanoamphiphilic chitosan dispersed poly (lactic acid) bionanocomposite films with improved thermal. *Mech Gas Barrier Prop.* <https://doi.org/10.1021/acs.biomac.6b00619>
 6. Pradhan R, Misra M, Erickson L, Mohanty A (2010) Compostability and biodegradation study of PLA-wheat straw and PLA-soy straw based green composites in simulated composting bioreactor. *Bioresour Technol* 101:8489–8491. <https://doi.org/10.1016/j.biortech.2010.06.053>
 7. Kalita NK, Nagar MK, Mudenur C et al (2019) Biodegradation of modified Poly(lactic acid) based biocomposite films under thermophilic composting conditions. *Polym Test.* <https://doi.org/10.1016/j.polymertesting.2019.02.021>
 8. Gupta A, Mulchandani N, Shah M et al (2018) Functionalized chitosan mediated stereocomplexation of poly(lactic acid): influence on crystallization, oxygen permeability, wettability and biocompatibility behavior. *Polymer (UK)* 142:196–208. <https://doi.org/10.1016/j.polymer.2017.12.064>
 9. Wei R, Zimmermann W (2017) Microbial enzymes for the recycling of recalcitrant petroleum-based plastics: how far are we? *Microb Biotechnol* 10:1308–1322. <https://doi.org/10.1111/1751-7915.12710>
 10. Vimal Kumar R, Kanna GR, Elumalai S (2017) Biodegradation of polyethylene by green photosynthetic microalgae. *J Bioremediat Biodegrad* 8:1–8. <https://doi.org/10.4172/2155-6199.1000381>
 11. Valapa RB, Pugazhenthai G, Katiyar V (2016a) Hydrolytic degradation behaviour of sucrose palmitate reinforced poly(lactic acid) nanocomposites. *Int J Biol Macromol* 89:70–80. <https://doi.org/10.1016/j.ijbiomac.2016.04.040>
 12. Pradhan R, Reddy M, Diebel W et al (2010b) Comparative compostability and biodegradation studies of various components of green composites and their blends in simulated aerobic composting bioreactor. *Int J Plast Technol* 14. <https://doi.org/10.1007/s12588-010-0009-z>
 13. Yoshida S, Hiraga K, Takanaha T et al (2016) A bacterium that degrades and assimilates poly(ethyleneterephthalate). *Science* (80)351:1196–1199. <https://doi.org/10.1126/science.aad6359>
 14. Kitadokoro K, Thumarat U, Nakamura R et al (2012) Crystal structure of cutinase Est119 from *Thermobifida alba* AHK119 that can degrade modified polyethylene terephthalate at 1.76 Å resolution. *Polym Degrad Stab* 97:771–775. <https://doi.org/10.1016/j.polymdegradstab.2012.02.003>
 15. Gnanavel G, Mohana Jeya Valli VP, Thirumarimurugan Kannadasan T (2012) Degradation of plastics using microorganisms. *Int J Pharm Chem Sci* 1:1040–1043
 16. Tripathi N, Katiyar V (2017) Poly (lactic acid)/modified gum arabic based bionanocomposite films: thermal degradation kinetics. <https://doi.org/10.1002/pen>
 17. Kale SK, Deshmukh AG, Dudhare MS, Patil VB (2015) Microbial degradation of plastic: a review. *J Biochem Technol* 6:952–961. <https://doi.org/10.5897/AJMR2016.8402>
 18. Singh B, Sharma N (2008) Mechanistic implications of plastic degradation. *Polym Degrad Stab* 93:561–584. <https://doi.org/10.1016/j.polymdegradstab.2007.11.008>
 19. Tokiwa Y, Calabia BP, Ugwu CU, Aiba S (2009) Biodegradability of plastics. *Int J Mol Sci* 10:3722–3742. <https://doi.org/10.3390/ijms10093722>
 20. Kale (2015) Microbial degradation of plastics: a review. *J Biochem Technol* 6:952–961. <https://doi.org/10.1504/ijep.2008.016895>
 21. Yang J, Yang Y, Wu WM et al (2014) Evidence of polyethylene biodegradation by bacterial strains from the guts of plastic-eating waxworms. *Environ Sci Technol* 48:13776–13784. <https://doi.org/10.1021/es504038a>

22. Yang Y, Yang J, Wu WM et al (2015) Biodegradation and mineralization of polystyrene by plastic-eating mealworms: part 2. role of gut microorganisms. *Environ Sci Technol* 49:12087–12093. <https://doi.org/10.1021/acs.est.5b02663>
23. Eubeler JP, Bernhard M, Knepper TP (2010) Environmental biodegradation of synthetic polymers II. Biodegradation of different polymer groups. *TrAC Trends Anal Chem* 29:84–100. <https://doi.org/10.1016/j.trac.2009.09.005>
24. Gu JD (2003) Microbiological deterioration and degradation of synthetic polymeric materials: Recent research advances. *Int Biodeterior Biodegrad* 52:69–91
25. Krueger MC, Harms H, Schlosser D (2015) Prospects for microbiological solutions to environmental pollution with plastics. *Appl Microbiol Biotechnol* 99:8857–8874. <https://doi.org/10.1007/s00253-015-6879-4>
26. Lucas N, Bienaime C, Belloy C et al (2008) Polymer biodegradation: mechanisms and estimation techniques—a review. *Chemosphere* 73:429–442. <https://doi.org/10.1016/j.chemosphere.2008.06.064>
27. Shah AA, Hasan F, Hameed A, Ahmed S (2008) Biological degradation of plastics: a comprehensive review. *Biotechnol Adv* 26:246–265. <https://doi.org/10.1016/j.biotechadv.2007.12.005>
28. Sivan A (2011) New perspectives in plastic biodegradation. *Curr Opin Biotechnol* 22:422–426. <https://doi.org/10.1016/j.copbio.2011.01.013>
29. Bhardwaj H, Gupta R, Tiwari A (2013) Communities of microbial enzymes associated with biodegradation of plastics. *J Polym Environ* 21:575–579. <https://doi.org/10.1007/s10924-012-0456-z>
30. Heredia A (2003) Biophysical and biochemical characteristics of cutin, a plant barrier biopolymer. *Biochim Biophys Acta Gen Subj* 1620:1–7. [https://doi.org/10.1016/S0304-4165\(02\)00510-X](https://doi.org/10.1016/S0304-4165(02)00510-X)
31. Thumarat U, Nakamura R, Kawabata T et al (2012) Biochemical and genetic analysis of a cutinase-type polyesterase from a thermophilic *Thermobifida alba* AHK119. *Appl Microbiol Biotechnol* 95:419–430. <https://doi.org/10.1007/s00253-011-3781-6>
32. Restrepo-Flórez JM, Bassi A, Thompson MR (2014) Microbial degradation and deterioration of polyethylene—a review. *Int Biodeterior Biodegrad* 88:83–90. <https://doi.org/10.1016/j.ibiod.2013.12.014>
33. Webb HK, Arnott J, Crawford RJ, Ivanova EP (2013) Plastic degradation and its environmental implications with special reference to poly(ethylene terephthalate). *Polymers (Basel)* 5:1–18. <https://doi.org/10.3390/polym5010001>
34. Cregut M, Bedas M, Durand MJ, Thouand G (2013) New insights into polyurethane biodegradation and realistic prospects for the development of a sustainable waste recycling process. *Biotechnol Adv* 31:1634–3647. <https://doi.org/10.1016/j.biotechadv.2013.08.011>
35. Bonhomme S, Cuer A, Delort AM et al (2003) Environmental biodegradation of polyethylene. *Polym Degrad Stab* 81:441–452. [https://doi.org/10.1016/S0141-3910\(03\)00129-0](https://doi.org/10.1016/S0141-3910(03)00129-0)
36. Hakkarainen M, Karlsson S, Albertsson A (2000) Rapid (bio) degradation of polylactide by mixed culture of compost microorganisms—low molecular weight products and matrix changes. *Polymer (Guildf)* 41:2331–2338
37. Arkatkar A, Juwarkar AA, Bhaduri S et al (2010) Growth of *Pseudomonas* and *Bacillus* biofilms on pretreated polypropylene surface. *Int Biodeterior Biodegrad* 64:530–536. <https://doi.org/10.1016/j.ibiod.2010.06.002>
38. Arutchelvi J, Sudhakar M, Arkatkar A et al (2008) Biodegradation of polyethylene and polypropylene. *Indian J Biotechnol* 7:9–22
39. Mueller RJ (2006) Biological degradation of synthetic polyesters—enzymes as potential catalysts for polyester recycling. *Process Biochem* 41:2124–2128. <https://doi.org/10.1016/j.procbio.2006.05.018>
40. Loredó-Treviño A, Gutiérrez-Sánchez G, Rodríguez-Herrera R, Aguilar CN (2012) Microbial enzymes involved in polyurethane biodegradation: a review. *J Polym Environ* 20:258–265. <https://doi.org/10.1007/s10924-011-0390-5>

41. Espino-Rammer L, Ribitsch D, Przylucka A et al (2013) Two novel class ii hydrophobins from *Trichoderma* spp. Stimulate enzymatic hydrolysis of poly(ethylene terephthalate) when expressed as fusion proteins. *Appl Environ Microbiol* 79:4230–4238. <https://doi.org/10.1128/AEM.01132-13>
42. Ribitsch D, Acero EH, Przylucka A et al (2015) Enhanced cutinase-catalyzed hydrolysis of polyethylene terephthalate by covalent fusion to hydrophobins. *Appl Environ Microbiol* 81:3586–3592. <https://doi.org/10.1128/AEM.04111-14>
43. Sammond DW, Yarbrough JM, Mansfield E et al (2014) Predicting enzyme adsorption to lignin films by calculating enzyme surface hydrophobicity. *J Biol Chem* 289:20960–20969. <https://doi.org/10.1074/jbc.M114.573642>
44. Gamerith C, Herrero Acero E, Pellis A et al (2016) Improving enzymatic polyurethane hydrolysis by tuning enzyme sorption. *Polym Degrad Stab* 132:69–77. <https://doi.org/10.1016/j.polyimdegradstab.2016.02.025>
45. Sarkar S, Singha PK, Dey S et al (2006) Synthesis, characterization, and cytotoxicity analysis of a biodegradable polyurethane. *Mater Manuf Process* 21:291–296. <https://doi.org/10.1080/10426910500464727>
46. Manzur A, Cuamatzi F, Favela E (1997) Effect of the growth of *Phanerochaete chrysosporium* in a blend of low density polyethylene and sugar cane bagasse. *J Appl Polym Sci* 66:105–111. [https://doi.org/10.1002/\(SICI\)1097-4628\(19971003\)66:1%3c105:AID-APP12%3e3.3.CO;2-3](https://doi.org/10.1002/(SICI)1097-4628(19971003)66:1%3c105:AID-APP12%3e3.3.CO;2-3)
47. Albertsson AC, Andersson SO, Karlsson S (1987) The mechanism of biodegradation of polyethylene. *Polym Degrad Stab* 18:73–87. [https://doi.org/10.1016/0141-3910\(87\)90084-X](https://doi.org/10.1016/0141-3910(87)90084-X)
48. Koutny M, Sancelme M, Dabin C et al (2006) Acquired biodegradability of polyethylenes containing pro-oxidant additives. *Polym Degrad Stab* 91:1495–1503. <https://doi.org/10.1016/j.polyimdegradstab.2005.10.007>
49. Li YF, Wu CJ, Sheng YJ, Tsao HK (2015) Facile manipulation of receding contact angles of a substrate by roughening and fluorination. *Appl Surf Sci* 355:127–132. <https://doi.org/10.1016/j.apsusc.2015.07.078>
50. Fontanella S, Bonhomme S, Koutny M et al (2010) Comparison of the biodegradability of various polyethylene films containing pro-oxidant additives. *Polym Degrad Stab* 95:1011–1021. <https://doi.org/10.1016/j.polyimdegradstab.2010.03.009>
51. Kumar Sen S, Raut S (2015) Microbial degradation of low density polyethylene (LDPE): A review. *J Environ Chem Eng* 3:462–473. <https://doi.org/10.1016/j.jece.2015.01.003>
52. Ojha N, Pradhan N, Singh S et al (2017) Evaluation of HDPE and LDPE degradation by fungus, implemented by statistical optimization. *Sci Rep* 7:1–13. <https://doi.org/10.1038/srep39515>
53. Santo M, Weitsman R, Sivan A (2013) The role of the copper-binding enzyme—laccase—in the biodegradation of polyethylene by the actinomycete *Rhodococcus ruber*. *Int Biodeterior Biodegrad* 84:204–210. <https://doi.org/10.1016/j.ibiod.2012.03.001>
54. Roy PK, Titus S, Surekha P et al (2008) Degradation of abiotically aged LDPE films containing pro-oxidant by bacterial consortium. *Polym Degrad Stab* 93:1917–1922. <https://doi.org/10.1016/j.polyimdegradstab.2008.07.016>
55. Esmaeili A, Pourbabaee AA, Alikhani HA et al (2013) Biodegradation of low-density polyethylene (LDPE) by mixed culture of *Lysinibacillus xylanilyticus* and *Aspergillus niger* in soil. *PLoS One* 8. <https://doi.org/10.1371/journal.pone.0071720>
56. Mukherjee S, Roy Chowdhuri U, Kundu PP (2016) Bio-degradation of polyethylene waste by simultaneous use of two bacteria: *Bacillus licheniformis* for production of bio-surfactant and *Lysinibacillus fusiformis* for bio-degradation. *RSC Adv* 6:2982–2992. <https://doi.org/10.1039/c5ra25128a>
57. Seymour RB, Kauffman GB (1992) Polyurethanes: a class of modern versatile materials. *J Chem Educ* 69:909. <https://doi.org/10.1021/ed069p909>
58. Nakajima-Kambe T, Shigeno-Akutsu Y, Nomura N et al (1999) Microbial degradation of polyurethane, polyester polyurethanes and polyether polyurethanes. *Appl Microbiol Biotechnol* 51:134–140. <https://doi.org/10.1007/s002530051373>

59. Howard G (2011) Microbial biodegradation of polyurethane. *Recent Dev Polym Recycl* 661:215–238
60. Stern RV, Howard GT (2000) The polyester polyurethanase gene (*pueA*) from *Pseudomonas chlororaphis* encodes a lipase. *FEMS Microbiol Lett* 185:163–168. [https://doi.org/10.1016/S0378-1097\(00\)00094-X](https://doi.org/10.1016/S0378-1097(00)00094-X)
61. Kawai F, Oda M, Tamashiro T et al (2014) A novel Ca²⁺-activated, thermostabilized polyesterase capable of hydrolyzing polyethylene terephthalate from *Saccharomonospora viridis* AHK190. *Appl Microbiol Biotechnol* 98:10053–10064. <https://doi.org/10.1007/s00253-014-5860-y>